



Abstracts

5367

CHARACTERIZATION OF ASTEROIDAL BASALTS THROUGH REFLECTANCE SPECTROSCOPY AND IMPLICATIONS FOR THE DAWN MISSION

P. A. Abell¹, D. W. Mittlefehldt¹, and M. J. Gaffey². ¹Astromaterials Research and Exploration Science, NASA Johnson Space Center, Houston, Texas 77058, USA. ²Department of Space Studies, University of North Dakota, Grand Forks, North Dakota 58202, USA

Introduction: There are currently five known groups of basaltic achondrites that represent material from distinct differentiated parent bodies. These are the howardite-eucrite-diogenite (HED) clan, mesosiderite silicates, angrites, Ibitira, and Northwest Africa (NWA) 011 [1]. Spectroscopically, all these basaltic achondrite groups have absorption bands located near 1 and 2 microns due to the presence of pyroxene. Some of these meteorite types have spectra that are quite similar, but nevertheless have characteristics (e.g., spectral slope, band depths, etc.) that may be used to differentiate them from each other.

Spectral Characteristics: Laboratory analysis of spectral features from meteorites and terrestrial samples has been used in the past to help make connections to various bodies located among the asteroid population [2–4]. Based on similar techniques, analyses of various spectra of basaltic achondrites have demonstrated clear distinctions between some of these groups. In particular, the spectral signatures of such basaltic achondrites as Ibitira, NWA 011, and HEDs are quite different when various spectral parameters such as band area ratio (BAR) and band centers are identified and compared. Although band centers for Ibitira and NWA 011 are the same as those of basaltic eucrites, the former two achondrites have distinctly lower BAR. On a diagram of band center versus BAR, Ibitira and NWA 011 plot outside the field of basaltic eucrites. Stannern-trend basaltic eucrites are compositionally distinct from the majority of eucrites [5], but seem to be indistinguishable from them on a band center versus BAR plot.

Implications: The revitalized Dawn mission is now scheduled for launch sometime between June and August 2007 [6]. Its first target is the asteroid Vesta, which is often thought to be the parent body of the HEDs [7, 8]. Given the various distinct terrains previously discovered across the surface of Vesta [9, 10], preliminary results from this study suggest that Dawn should be able to obtain spectra of sufficient quality to constrain the possible types of basaltic achondrites that exist on the surface of Vesta. Since no single petrogenesis scheme is capable of explaining the formation of all basaltic eucrites, the identification of one or more of these meteorites on Vesta will provide an important constraint on eucrite petrogenesis.

Acknowledgments: Various portions of this work were supported by the NASA Cosmochemistry and the NASA Planetary Geology and Geophysics programs.

References: [1] Mittlefehldt D. W. 2005. *Meteoritics & Planetary Science* 40:655–677. [2] Gaffey M. J. 1976. *Journal of Geophysical Research* 81:905–920. [3] Cloutis E. M. et al. 1986. *Journal of Geophysical Research* 91:11,641–11,653. [4] Gaffey M. J. et al. 1993. *Icarus* 106:573–602. [5] Mittlefehldt D. W. and Lindstrom M. M. 2003. *Geochimica et Cosmochimica Acta* 67:1911–1935. [6] Russell C. T. et al. 2004. *Planetary and Space Science* 52:465–489. [7] McCord T. B. et al. 1970. *Science* 168:1445–1447. [8] Drake M. J. 2001. *Meteoritics & Planetary Science* 36:501–513. [9] Gaffey M. J. 1997. *Icarus* 127:130–157. [10] Binzel R. P. 1997. *Icarus* 128:95–103.

5372

ONSET OF AQUEOUS ALTERATION IN PRIMITIVE CR CHONDRITES

N. M. Abreu and A. J. Brearley. Department of Earth and Planetary Sciences, University of New Mexico, Albuquerque, New Mexico 87131, USA. E-mail: abreu@unm.edu

Introduction: Although some CR chondrites show evidence of significant aqueous alteration [1], our studies [2] have identified CR chondrites that exhibit only minimal degrees of aqueous alteration. These meteorites have the potential to provide insights into the earliest stages of aqueous alteration and the characteristics of organic material that has not been affected by aqueous alteration, i.e., contains a relatively pristine record of carbonaceous material present in nebular dust. The CR chondrites are of special significance in this regard, because they contain the most primitive carbonaceous material currently known [3].

Results: Matrix and fine-grained rims in CR chondrites MET 00426 and QUE 99177 were examined by TEM, focusing particularly on EFTEM (energy filtered TEM) and EFTEM spectral imaging (EFTEM SI) to locate and characterize carbonaceous material in situ. Our new observations are consistent with earlier HRTEM and EFTEM studies, but we have made a number of significant new observations. As previously reported [2], abundant amorphous silica-bearing material and μm to nm-sized, well-faceted Fe sulfides containing variable amounts of Ni were identified in the matrix and fine-grained rims of both meteorites. In addition, carbonaceous material is widespread in all regions and is often associated with sulfides. However, isolated, rounded, nm-sized C-rich hotspots were also common. The electron energy loss spectra (EELS) of this material are most consistent with amorphous C or carbonaceous phases. EFTEM spectral maps served to unequivocally establish a spatial relationship between C and N. The one example of a fine-grained rim studied to date in QUE 99177 is more complex than the matrices documented above. This rim contains abundant fine-grained (few unit cells) phyllosilicates and wispy and rounded Fe sulfides. Rare olivines and low-Ca pyroxenes (cpx-opx intergrowths) were also observed. The low-Ca pyroxenes are embedded within a groundmass of nanocrystalline phyllosilicates, but show only very limited evidence of alteration.

Discussion: In general, our TEM observations of MET 00426 and QUE 99177 show that aqueous alteration of matrix was extremely limited and localized. However, the one fine-grained rim studied so far in QUE 99177, appears to have experienced more extensive aqueous alteration with comparatively extensive development of phyllosilicates. Both these meteorites are breccias, so this phenomenon could be the result of regolith mixing of materials with variable degrees of alteration. Alternatively, it is possible that under fluid-limited conditions, at the onset of aqueous alteration, hydration occurs heterogeneously within the fine-grained material. Factors such as the local porosity and permeability of the fine-grained material will be important factors in controlling the extent of aqueous alteration. Observations of minimal replacement of anhydrous phases supports the assertion that fluid alteration proceeded by replacement of metastable, amorphous material first, followed by replacement of crystalline grains as alteration became more advanced [4].

References: [1] Weisberg M. K. et al. 1995. *Proceedings of the NIPR Symposium on Antarctic Meteorites* 8:11–32. [2] Abreu N. M. and Brearley A. J. 2006. Abstract #2395. 37th Lunar and Planetary Science Conference. [3] Ash R. D. et al. 1993. *Meteoritics* 28:318. [4] Nuth J. et al. 2005. *In Chondrites and the protoplanetary disk*. 675 p.

5125

Pb-Pb SYSTEMATICS OF MARTIAN METEORITES AND THE DIFFERENTIATION HISTORY OF MARS

F. Albarède¹, A. Bouvier^{1, 2}, J. Blichert-Toft¹, and J. D. Vervoort³. ¹Ecole Normale Supérieure, 69007 Lyon, France. E-mail: al-barede@ens-lyon.fr. ²Department of Geosciences, University of Arizona, Tucson, Arizona 85721, USA. ³Department of Geology, Washington State University, Pullman, Washington 99164, USA

Our new Pb isotope analyses of basaltic shergottites, in combination with literature data, suggest that their ancient ~4.1 Ga Pb-Pb isochron age reflects the magmatic emplacement of these rocks [1]. This age, however, is in apparent conflict with much younger ages of ~180 Ma of U-Pb, Rb-Sr, Sm-Nd, and Lu-Hf mineral isochrons. We have argued that these younger ages record the last disturbance of disseminated phosphates by acidic brines percolating beneath the Martian surface. The counter suggestion that the old Pb-Pb age reflects contamination by terrestrial Pb [2] has been dismissed in [1] and conflicts with two additional observations: a) shergottite Pb does not lie between modern terrestrial (SKE) and 180 Myr old radiogenic Pb in ²⁰⁷Pb/²⁰⁶Pb-²⁰⁴Pb/²⁰⁶Pb space, b) SKE Pb plots well off the 1.3 Gyr nakhlite isochron; given the low Pb contents of nakhlites, they should be far more susceptible to terrestrial contamination than more Pb-rich shergottites. Furthermore, U-Pb Concordia plots are prone to severe artifacts and it is well established that U-Pb systematics in silicate rocks are disrupted by recent sub-surface processes and laboratory leaching procedures.

Here we use the principle of intersecting secondary isochrons developed for terrestrial Pb [3] to suggest that Pb isotopes in SNCs portray a rather simple account of Mars' differentiation. The present-day Pb isotopic composition of the common source of SNCs (SKM) lies at the intersection between the two isochrons of nakhlites and basaltic shergottites. Within error, SKM plots off the geochron, but on the primary growth curve for a broad range of ²³⁸U/²⁰⁴Pb (μ) ratios. The low μ value of SKM [2, 4] is inconsistent with extraction of Pb into the core. Rather, together with Hf/Sm ratios, which are subchondritic in nakhlites and superchondritic in shergottites [5], it signals extraction of the Martian lithosphere and ilmenite fractionation during the waning stages of magma ocean solidification. We speculate that basaltic shergottites formed at 4.1 Gyr from the ilmenite-rich residual mush, whereas the parent melts of nakhlites formed at 1.3 Gyr as melts from the KREEP-like part of the upper mantle rich in heat-producing elements. The ilmenitic shergottites, plotting across both isochrons, may represent different melts forming over most of the planet's history from various sources.

The history emerging from the present re-interpretation of SNC chronology solves the longstanding conundrum of multiple exposure ages for these samples. It also provides a straightforward explanation for the existence of variable extinct radioactive nuclide anomalies (¹⁸²Hf, ¹⁴⁶Sm) with implications for Martian mantle convection. It further removes the need for complex scenarios of meteorite extraction, thereby potentially improving the understanding of Martian cratering chronology.

References: [1] Bouvier A. et al. 2005. *Earth and Planetary Science Letters* 240:221–233. [2] Borg L. E. et al. 2005. *Geochimica et Cosmochimica Acta* 69:5819–5830. [3] Stacey J. S. and Kramers J. D. 1975. *Earth and Planetary Science Letters* 26:207–221. [4] Jagoutz E. 1991. *Space Science Reviews* 56:13–22. [5] Blichert-Toft J. et al. 1999. *Earth and Planetary Science Letters* 173:25–39.

5098

THE REGOLITH PORTION OF THE LUNAR METEORITE SAYH AL UHAYMIR 169

A. Al-Kathiri^{1, 2}, E. Gnos¹, and B. A. Hofmann³. ¹Institut für Geologie, Universität Bern, Baltzerstrasse 1, CH-3012 Bern, Switzerland. ²Directorate General of Commerce and Industry, Ministry of Commerce and Industry, Salalah, Oman. ³Naturhistorisches Museum der Burgergemeinde Bern, Bernstrasse 15, CH-3005 Bern, Switzerland

Introduction: Sayh al Uhaymir (SaU) 169 is a complete, light gray-greenish stone (70 × 43 × 40 mm) with a mass of 206.45 g found in the Sultanate of Oman in January 2002. The rock consists of two contrasting lithologies. Approximately 87 vol% consists of a holocrystalline, fine-grained poikilitic polymict KREEP-rich impact melt breccia, the other 13 vol% is shock-lithified regolith [1].

Discussion: The regolith shows two formation stages and contains the following clasts: Ti-poor to Ti-rich basalts, gabbros to granulites, and regolith breccias. The younger regolith additionally contains a highland gabbro-norite clast with anorthite (An₉₆₋₉₇), forsteritic (Fo₈₅), and fayalitic (Fo₁₂) mineral clasts, and impact melt glass shards. The average regolith bulk chemical composition and its REE content lie between the soil and regolith breccias of Apollo 12 and 14, with more affinity with Apollo 14 [2, 3, 4]. The largest KREEP breccia clast in the regolith is identical in its chemical composition and total REE content to the ITE-rich high-K KREEP rocks of the Apollo 14 landing site, pointing to a similar source. The regolith shows characteristic lunar ratios of Fe/Mn (74–80) and K/U (535–1682). The Sc content, the Sm versus Al₂O₃ and the La/Yb values show that the SaU 169 average regolith is very similar to the Apollo 14 regolith breccias but different to regoliths from other Apollo landing sites and lunar far side highland regolith. All data point to a regolith origin at the lunar front side with strong influence from Procellarum terrane KREEP rocks.

References: [1] Gnos E., Hofmann B., Al-Kathiri A., Lorenzetti S., Eugster O., Whitehouse M. J., Villa I. M., Jull A. J. T., Eikenberg J., Spettel B., Krähenbühl U., Franchi I. A., and Greenwood R. C. 2004. *Science* 305:657–659. [2] Jolliff B. L. 1998. *International Geology Review* 40:916–935. [3] Warren P. H. and Wasson J. T. 1979. *Reviews of Geophysics and Space Physics* 17:73–88. [4]

5056

EXTRATERRESTRIAL CHROMITE IN THE ORDOVICIAN LOCKNE IMPACT STRUCTURE, CENTRAL SWEDEN

C. Alwmark and B. Schmitz. Department of Geology, Lund University, SE-22362 Lund, Sweden. E-mail: carl.alwmark@geol.lu.se; birger.schmitz@geol.lu.se

Introduction: More than 170 impact craters are known on Earth, but only a fraction of the impactors have been identified. This is mainly due to the low survival rate of projectile material. Physical pieces of projectile material have, with a few exceptions, only been found at small (<1.5 km in diameter) impact craters. Larger projectiles are believed to be totally vaporized upon impact, leaving only a small amount of recondensed projectile vapor, generally less than 1% [1], mixed in with the target rocks. In this study a sample of the resurge deposit of the mid-Ordovician Lockne impact structure in central Sweden has been searched for chromite (FeCr_2O_4), a common accessory mineral in many meteorites [2]. Chromite has a high resistance against weathering and diagenesis and is often the only mineral surviving in fossil meteorites [3]. Chromite is also a good petrogenetic indicator; extraterrestrial chromite (EC) has a characteristic composition that differs from the terrestrial equivalent, with typically higher TiO_2 content (2.0–3.5 wt%) and Cr/(Cr + Al) ratio (>0.8) and a narrow span of V_2O_3 (0.6–0.9 wt%) [4–5]. Furthermore, the compositions within the EC vary with type of host meteorite [6].

Results and Discussion: We studied a sample of 1.1 kg of resurge deposit, the so called Loftarstone, from the central part of the Lockne crater. The sample is extremely rich in chromium spinels, mainly chromite (125 grains kg^{-1}). Due to post-depositional alterations coupled to the hydrothermal system induced by the impactor, the origin of several of the grains is dubious, although it is clear that the major part of the chromites are of extraterrestrial origin (>75 grains kg^{-1}), most likely derived from the impactor. A comparison of Cr/(Cr + Al) and TiO_2 with analyses of recent and fossil chondrites implies that the impactor was an ordinary chondrite of the L group [5, 7]. The impactor being an L chondrite concurs well with the theory that the influx of asteroids to earth was increased during the mid-Ordovician because of the disruption of the L chondrite parent body at ~470 Ma [5].

Survival of Extraterrestrial Material: It is clear that the general assumption that physical fragments of the impactor are not to be expected at craters larger than ~1.5 km does not hold for the Lockne impact structure. The fact that the impact was oblique and that the target was overlain by water, has probably increased the extent to which impact material has survived [8]. If further studies of other impact craters reveal that survival of chromite is not unique for the Lockne impact structure, extraterrestrial chromite becomes a powerful instrument in the identification of other chromite-bearing projectiles that have struck our planet.

References: [1] Koeberl C. 1998. Geological Society of London Special Publication 140, pp. 133–153. [2] Rubin A. E. 1997. *Meteoritics & Planetary Science* 32:231–247. [3] Thorslund P. et al. 1984. *Lithos* 17:87–100. [4] Nyström J. O. et al. 1988. *Nature* 336:572–574. [5] Schmitz B. et al. 2001. *Earth and Planetary Science Letters* 194:1–15. [6] Bunch T. E. et al. 1967. *Geochimica et Cosmochimica Acta* 31:1569–1582. [7] Schmitz B. and Häggström T. 2006. *Meteoritics & Planetary Science* 41:455–466. [8] Pierazzo E. and Melosh H. J. 2000. *Meteoritics & Planetary Science* 35:117–130.

5328

Ne-E(L) ACCOMPANIED BY ^{40}K

S. Amari. Laboratory for Space Sciences and the Physics Department, Washington University, Saint Louis, Missouri 63130, USA. E-mail: sa@wuphys.wustl.edu

Introduction: Presolar graphite carries Ne-E(L) [1], the component highly enriched in ^{22}Ne . This huge excess prompted the idea that the ^{22}Ne is from the decay of radiogenic ^{22}Na ($T_{1/2} = 2.6$ a) produced in novae [2]. Amari et al. [3] analyzed noble gases in the four graphite separates, KE1, KFA1, KFB1, and KFC1 with a range of density (1.6–2.2 g/cm^3) extracted from the Murchison meteorite [4], and concluded that the ^{22}Ne in KE1 and KFA1 (1.6–2.05 and 2.05–2.10 g/cm^3) is mostly ($\geq 90\%$) from the decay of ^{22}Na . Low-density graphite grains (1.65–1.72 g/cm^3) are characterized by ^{18}O excesses, Si isotopic anomalies (mainly in the form of ^{28}Si excesses), and high $^{26}\text{Al}/^{27}\text{Al}$ ratios (up to 0.1), indicating they formed in type II supernovae [5]. From noble gas analyses of bulk samples [3] and of single grains [6] from the Murchison separates, Amari et al. [7] concluded that ^{22}Ne in low-density grains is from ^{22}Na produced in supernovae and is not from ^{22}Ne that was directly implanted onto the grains. Sodium-22 is synthesized during hydrostatic burning by $^{21}\text{Ne}(p,\gamma)^{22}\text{Na}$, where ^{21}Ne is produced by $^{20}\text{Ne}(n,\gamma)^{21}\text{Ne}$ and protons are produced by $^{12}\text{C}(^{12}\text{C},p)^{23}\text{Na}$ in the O/Ne zone [8].

Discussion: In the O/Ne zone, isotopes that have a similar first ionization potential as that of Na (5.203 eV) include K (4.34 eV). Potassium-40 ($T_{1/2} = 1.27$ Ga) decays to ^{40}Ar (11.16%) and ^{40}Ca (88.84%). Predicted $^{22}\text{Na}/^{40}\text{K}$ ratios are 3.40 [9] and 9.77 [8] in the O/Ne zone of $25M_{\text{sun}}$ stars with the solar metallicity. If non-radiogenic ^{40}Ca and ^{40}Ar are not overwhelmingly abundant and ^{40}K was incorporated along with ^{22}Na , elevated ^{40}Ca and ^{40}Ar abundances are expected in ^{22}Ne -rich low-density grains. In graphite bulk analysis, the lighter noble gases were released in lower temperature steps than the heavier noble gases (Fig. 2 in [3]), indicating noble gases were released by diffusion. In the figure below (data are from [3]), where ^{22}Ne , ^{40}Ar , and s-process Kr concentrations are plotted against temperatures for KE1 and KFA1, the ^{40}Ar release peaks are observed between the ^{22}Ne and the Kr-S release peaks. A similar release pattern is also observed in KFB1 (2.10–2.15 g/cm^3). Argon-40 must be from the graphite grains and is most likely from the decay of ^{40}K .

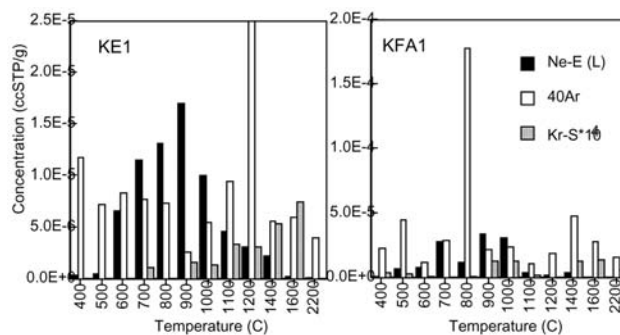


Fig. 1.

References: [1] Amari S. et al. 1990. *Nature* 345:238–240. [2] Clayton D. D. 1975. *Nature* 257:36–37. [3] Amari S. et al. 1995. *Geochimica et Cosmochimica Acta* 59:1411–1426. [4] Amari S. et al. 1994. *Geochimica et Cosmochimica Acta* 58:459–470. [5] Travaglio C. et al. 1999. *The Astrophysical Journal* 510:325–354. [6] Nichols R. H., Jr. et al. 1994. *Meteoritics* 29:510–511. [7] Amari S. et al. 2006. Abstract #2409. 37th Lunar and Planetary Science Conference. [8] Chieffi A. and Limongi M. Forthcoming. [9] Heger A. et al. 2006. <http://www.icolick.org/~alex/nucleosynthesis>.

5188

COSMOGENIC PRODUCTION RATES IN IRON METEORITES

K. Ammon¹, J. Masarik², and I. Leya¹. ¹University of Bern, Sidlerstrasse 5, CH-3012 Bern, Switzerland. E-mail: katja.ammon@space.unibe.ch. ²Department of Nuclear Physics, Komensky University, Mlynska dolina F/1, SK-842 48 Bratislava, Slovakia

Introduction: In contrast to stony meteorites, which have exposure ages usually not higher than a few tens of million years, most iron meteorites exhibit cosmic-ray exposures of hundreds of million years. Consequently, iron meteorites have collected information about the solar system, encoded in so-called “cosmogenic nuclides,” for much longer than stony meteorites. Therefore, iron meteorites are indispensable for long-term studies of solar system dynamics. For example, the still open question of whether there has been a long-term change in the galactic cosmic-ray (GCR) intensity is only accessible using iron meteorites. For such studies a consistent database of cosmogenic nuclides in iron meteorites, together with physical model calculations for understanding their production mechanisms, are mandatory.

Experiments: After having demonstrated the reliability and reproducibility of our measurements, we recalibrated the preatmospheric center of Grant (IIIAB). The depth profiles thus obtained enable us to evaluate physical model calculations for cosmogenic production rates in iron meteorites. We also studied whether the production rates are affected by trace elements, e.g., sulfur and phosphorous. Finally, we started to measure a complete and consistent cross section database for the proton-induced production of He, Ne, and Ar isotopes from iron and nickel. Such data are necessary for reliable physical model calculations.

Results: To determine shielding depths in iron meteorites, the ratios ⁴He/²¹Ne and ³⁶Ar/³⁸Ar can be used. While ³⁶Ar/³⁸Ar is lowest at the preatmospheric center, ⁴He/²¹Ne reaches a maximum value [3]. We measured four depth profiles for Grant and found a clearly different location of the preatmospheric center than previously assumed [1, 2]. Interesting new results are also obtained for the influence of trace elements on the production rates. Based on our new experimental data (depth profiles, cross-sections) and new Monte Carlo calculations for the spectra of primary and secondary particles new sophisticated physical model calculations for cosmogenic production rates in iron meteorites are established. The new results will be compared to results from earlier semi-empirical models [1, 2]. Based on the new model calculations the basic assumptions of the ³⁹K-⁴⁰K-⁴¹K dating technique will be discussed and the system will be re-evaluated.

References: [1] Signer P. and Nier A. O. 1960. *Journal of Geophysical Research* 65:2947–2964. [2] Voshage H. 1984. *Earth and Planetary Science Letters* 71:181–194. [3] Wieler R. 2002. In *Noble gases*. Washington, D.C.: Mineralogical Society of America. pp. 125–170.

5257

Ar-Ar AGE AND HALOGEN CHARACTERISTICS OF NAKHLITE MIL 03346: RECORDS OF CRUSTAL PROCESSES ON MARS

M. Anand^{1, 2}, R. Burgess³, V. Fernandes⁴, and M. M. Grady¹. ¹Centre for Earth, Planetary, Space and Astronomical Research (CEPSAR), The Open University, Milton Keynes, UK. E-mail: m.anand@open.ac.uk. ²Department of Mineralogy, The Natural History Museum, London, UK. ³Department of Earth Sciences, University of Manchester, Manchester, UK. ⁴Instituto Geofísico, Universidade de Coimbra, Portugal

Introduction: MIL 03346 is one of the seven members of the nakhlite group of Martian meteorites. The texture and mineralogy of this rock distinguishes it from other nakhlites [1]. Almost complete absence of crystalline plagioclase and ferro-hedenbergitic rim on pyroxene phenocrysts are some of the unique characteristics of this sample. Previous Ar-Ar age study of MIL 03346 reported a total Ar-Ar age of 1.37 Ga [2]. Recent reports have also highlighted presence of exotic minerals such as K-Cl-rich amphibole in melt inclusions in pyroxenes and olivines in MIL 03346 [3]. The non-chondritic halogen ratios in nakhlites have been interpreted as a result of fluid activity on Mars [4]. In the present study we have combined measurements of step-heating Ar-Ar ages with that of halogen contents. The work was conducted on ~12 mg whole-rock sample, sliced out from 1g allocation of MIL 03346,37 from the MWG to the senior author.

Results: The total Ar-Ar age is 1360 ± 2 Ma, similar to that reported by [2]. The main release of K is between 600–900 °C, and there is a clear decrease in age with temperature, most likely recoil-related. The major Cl release occurs at around 1000 °C, is therefore separate from K release, and accompanies the release of Ca from pyroxene. The measured halogen contents in MIL 03346 are high relative to other SNC meteorites, only lower than Nakhla [4]. The halogen data for MIL 03346 are Cl = 156 ppm, Br = 0.41 ppm, I = 0.014 ppm. The halogen ratios of Nakhla are slightly higher than MIL (Br/Cl = 0.002; I/Cl = 6×10^{-5}) but this may be explained by high Br/Cl and I/Cl ratios of Martian weathering components in alteration veins in Nakhla olivines [5]. For comparison, the Martian regolith Br/Cl = 0.007 and I/Cl = 16×10^{-5} [6], while shergottites are more similar at Br/Cl = 0.005; I/Cl = 3×10^{-5} .

The presence of K-Cl-rich amphibole in melt inclusions in pyroxene could explain the major Cl release at high temperature and some of the recoil effect if ³⁹Ar_K moves from the melt inclusions into the pyroxene. Alternatively, ³⁹Ar_K may also be released from the mesostasis glass, but then we would also expect to see major Cl release at the same time. Between 600–850 °C 73% of total K and 26% of total Cl are released; >900 °C the values are 21% and 67%; so the majority of halogen release presumably comes from the melt inclusions. This indicates that the Br/Cl and I/Cl are representative of the melt (although they may originate from a soil contaminated melt).

References: [1] Anand M. et al. 2005. Abstract #1639. 36th Lunar and Planetary Science Conference. [2] Bogard D. D. and Garrison D. H. 2006. Abstract #1108. 37th Lunar and Planetary Science Conference. [3] Sautter V. et al. 2006. Abstract #1318. 37th Lunar and Planetary Science Conference. [4] Dreibus et al. 2006. Abstract #1180. 37th Lunar and Planetary Science Conference. [5] Sutton S. R. et al. 2002. Abstract #1278. 33rd Lunar and Planetary Science Conference. [6] Rao M. N. et al. 2002. *Icarus* 156:352–372.

5009

MODELING THERMAL REDUCTION OF CHONDRITIC MELTS PRODUCING METALLIC IRON AND RESIDUAL SILICATE SYSTEMS

Ariskin A. A.¹, Yakovlev O. I.¹, Barmina G. S.¹, and Bychkov K. A.²
¹Vernadsky Institute of Geochemistry and Analytical Chemistry, Kosygin Str. 19, Moscow, 119991, Russia. E-mail: ariskin@geokhi.ru. ²Division of Geology, Moscow State University, Vorob'evy gory, Moscow, 119992, Russia

Introduction: In the early 1980s, Elbert King performed a series of vertical access solar furnace experiments with meteoritic and terrestrial bulk rock samples [1, 2]. Fast heating in vacuum resulted in the formation of large-size, immiscible metal droplets and spherules by in situ reduction of iron from silicate melts. Similar process was observed during experimental melting and vaporization of Krymka, Saratov, and Murchison samples [3–5]. This allowed the authors to state that temperature increase may be considered as the leading factor driving chondritic melts to metal precipitation, a process that may be called by thermal reduction [4].

Genetic Implications: Recognizing importance of the mechanism results in a fundamental conclusion that differences in nebular or planetary redox conditions may play a subordinate role in the formation of metal. At a flush heating up to 1600–1800 °C the presence of a reducing agent (carbon, hydrogen gas) in a primordial system is not necessary to produce metallic iron from silicates. As far as the reaction $2\text{FeO} = 2\text{Fe} + \text{O}_2$ is highly endothermic, a large “amount of heat” absorbed into a super-liquidus chondritic melt may serve as the major agent initiating the iron reduction process and responsible for its completeness.

Computer Modeling: These thermodynamic principles are accounted in the METEOMOD phase equilibria model [6]. A distinguished feature of this program is its ability to calculate Fe-Ni metal reduction in two ways. 1) In parallel to the IW buffer conditions one can simulate metal precipitation during cooling a parental chondritic melt, including crystallization of $\text{Metal} \pm \text{Ol} \pm \text{Opx} \pm \text{Cpx} \pm \text{Pl}$ assemblages. 2) At low values of $f\text{O}_2$'s = const the separation of metal is simulated as the system is heated up from the silicate liquidus to higher temperatures.

Results: Using the new version of METEOMOD [6, 7], we have carried out a series of calculations simulating thermal reduction of LL chondritic melts with variable NiO contents in the parent. These simulations cover the temperature range of 1550–2100 °C, producing liquid residues of low FeO to iron-free compositions and a complimentary increase in SiO_2 . Both metal and residual liquid compositions are compared in terms of the amount of metallic iron separated. The effect of $f\text{O}_2$'s is also considered.

References: [1] King E. A. 1982. *Journal of Geophysical Research* 87: A429–434. [2] King E. A. 1983. In *Chondrules and their origin*. pp. 180–187. [3] Yakovlev et al. 1985. 16th Lunar and Planetary Science Conference. pp. 928–929. [4] Yakovlev et al. 1987. *Meteoritics* 46:104–118. In Russian. [5] Yakovlev et al. 2003. *Geochemistry International* 41:417–430. [6] Ariskin A. A. et al. 1997. *Meteoritics & Planetary Science* 32:123–133. [7] Bychkov K. A. et al. 2006. Abstract #5010. *Meteoritics & Planetary Science* 41. This issue.

5066

SIZE AND VELOCITY OF CANYON DIABLO METEORITE—MODELS COMPARISON

N. A. Artemieva. Institute for Dynamics of Geospheres, Moscow. E-mail: artemeva@psi.edu

Introduction: About 50 kyr ago, an impact of an iron meteoroid excavated Meteor crater in Arizona, the first terrestrial structure recognized as a meteorite impact crater. Its mass and impact velocity estimates varied widely, starting from the historical Barringer's hypothesis of a huge body comparable to the crater size buried beneath the crater floor [1] to modern scaling law values [2] giving rather modest diameter of ~40 m for an 18 km/s impact. However, iron bodies larger than a meter are subjected to strong disruption and deceleration while traveling through the atmosphere [3]. Using the pancake approximation this predicts a low-velocity, strongly deformed Meteor crater impactor [4]. Here we compare various models of atmospheric disruption to provide more reliable estimates of the final projectile velocity and amount of meteorite material lost during atmospheric passage (part of it has been found scattered on the plains around the crater and has become known as the Canyon Diablo meteorites).

Models in Use: Atmospheric entry of the cosmic body can be described by differential equations for a point mass without disruption, with a simplified treatment of disruption—namely separated fragments (SF) model [5–6] and pancake model [7]. Alternatively, full-scale hydrodynamic models can be applied, in which the projectile is treated as strengthless or ductile material [8–9], or as a cloud of fragments [10]. The 3-D SOVA hydrocode [11] with particles is used here for numerical modeling.

Results: The minimum (non-realistic) projectile mass estimate of 3×10^8 kg ($D_0 = 42$ m) corresponds to a non-disrupted projectile, which loses 4% of its initial velocity and 5% of its mass by ablation. The pancake model with restriction of projectile expansion (flattening) to $4 \times D_0$ (similar to [4]) leads to a rather low final impact velocity of 11 km/s for initial projectile mass of 7.8×10^8 kg ($D_0 = 57$ m). A more realistic projectile expansion to $2 \times D_0$ (also supported by numerical modeling) results in a higher final velocity of 15 km/s (for a pre-atmospheric diameter of ~46 m). The SF model provides a variety of final outcomes depending on projectile strength and mass (see [12] for more details).

Finally, the numerical modeling with SOVA shows that a strengthless body is disrupted and dispersed even at large pre-atmospheric masses, while a reasonable strength provides a scenario similar to the Pancake $2 \times D_0$ model. Catastrophic disruption into a swarm of interacting fragments (unlike SF) seems to be the most realistic yet most complex description of Canyon Diablo projectile.

References: [1] Barringer D. M. 1909. Paper read before the National Academy of Science. [2] Schmidt R. M. and Housen K. R. 1987. *International Journal of Impact Engineering* 5:543–560. [3] Bland P. and Artemieva N. 2003. *Nature* 424: 288–291. [4] Melosh H. J. and Collins G. S. 2005. *Nature* 434:157. [5] Passey Q. R. and Melosh H. J. 1980. *Icarus* 42: 211–233. [6] Artemieva N. and Shuvalov V. 2001. *Journal of Geophysical Research* 106:3297–3309. [7] Chyba C. F. et al. 1993. *Nature* 361:40–44. [8] Crawford D. A. et al. 1995. 26th Lunar and Planetary Science Conference. pp. 291–292. [9] Ivanov B. A. et al. 1997. *Planetary and Space Science* 45: 993–1007. [10] Svetsov V. et al. 1995. *Icarus* 116:131–153. [11] Shuvalov V. 1999. *Shock Waves* 9:381–390. [12] Pierazzo E. and Artemieva N. 2005. Abstract #2325. 36th Lunar and Planetary Science Conference.

5053

METEORITICAL AND PLANETOLOGICAL CONSEQUENCES OF “HIT AND RUN” NON-ACCRETIONARY GIANT IMPACTS

E. Asphaug¹, C. B. Agnor¹, E. R. D. Scott², and Q. C. Williams¹. ¹Center for the Origin, Dynamics and Evolution of Planets, University of California, Santa Cruz, California 95064, USA. ²University of Hawai‘i at Manoa, Honolulu, Hawai‘i 96822, USA. E-mail: asphaug@pmc.ucsc.edu

Introduction: The origin of terrestrial planetary systems is believed to conclude with a series of major collisions between similarly sized planetary embryos formed after oligarchic growth (e.g., [1]). This giant impact stage, plausibly lasting about 30 Ma, involves Moon- to Mars-sized embryos growing over time in cataclysmic event into terrestrial planets. Recently it has been shown [2, 3] that giant impacts do not usually result in efficient mass accretion and that their consequences are not limited to shock effects. About half the time [2] giant impacts are “hit and run” [3], where the smaller planet bounces off, severely altered and sometimes stripped of its atmosphere, hydrosphere, and upper mantle, and in severe cases ripped into a handful of smaller iron-enriched planets plus debris. The combined effects of shocks, tides, mechanical shears, and gravitational torques, as well as whole-planet pressure unloading, must be explored.

Context: A surprising number of metal-rich meteorites show metal-silicate textures and/or thermal histories incompatible with melting and cooling in isolated bodies. Formation of differentiated meteorites close to the terrestrial planets helps explain the lack of complementary olivine-rich meteorites and asteroids and differentiated asteroid families [4] and offers an environment in which hit and run collisions would be frequent during the first few Ma. Such collisions might produce metallic asteroids that cooled with little or no silicate insulation such as the IVA iron body [5], mix molten metal with basaltic surfaces forming mesosiderites, distort partly molten asteroidal bodies generating pallasites at core-mantle interfaces, and generate Ge-poor iron meteorites with 1000-fold depletions of volatile siderophiles.

Modeling: Here we explore the consequences of typical giant impacts, making an effort to relate such events to the origin of meteorites. One process we explore is the pressure unloading of planetary materials during hit and run events, which can unload deep pressures by 50% or more for hours throughout an impactor which loses only a fraction of its mass, and which can unload pre-impact (hydrostatic) pressures entirely in severely disruptive collisions. We examine specific effects of mechanical shears and pressure unloading, as a complement to shocks. We also make a novel attempt to explain the “oddball” planet Mercury, for which we present a model based on the stripping of a Mars-like planet’s mantle during a low-velocity grazing collision with a larger planet, for example the proto-Venus. In the course of such a collision we show that the larger planet can be donated some of the lower density exterior (e.g., atmosphere) that is stripped from the smaller planet, while the impactor planet becomes significantly iron enriched. The process is efficient at low impact velocities.

Acknowledgements: This research is sponsored by NASA’s Planetary Geology and Geophysics Program, “Small Bodies and Planetary Collisions.”

References: [1] Goldreich P., Lithwick Y., and Sari R. 2004. *The Astrophysical Journal* 614:497–507. [2] Agnor C. B. and Asphaug E. 2004. Accretion efficiency during planetary collisions. *The Astrophysical Journal* 613:L157–L160. [3] Asphaug E., Agnor C. B., and Williams Q. 2006. Hit and run planetary collisions. *Nature* 439:155–160. [4] Bottke W. F. et al. 2006. *Nature* 439:821–824. [5] Yang J., Goldstein J. I., and Scott E. R. D. 2006. Abstract #5146. *Meteoritics & Planetary Science* 41. This issue.

5391

THE BIRTH ENVIRONMENT OF PLANETARY SYSTEMS

John Bally. Department of Astrophysical and Planetary Sciences, University of Colorado, Boulder, Colorado, USA. E-mail: John.Bally@colorado.edu

Introduction: Observations demonstrate that most stars in the sky are born in short-lived clusters or multiple star systems. Many form within a few parsecs of massive stars that produce intense UV radiation, powerful stellar winds, and die in supernova explosions. Thus, during the first few million years, forming planetary systems are likely to experience dynamical perturbations from passing sibling stars, become exposed to intense UV radiation fields, and be peppered by supernova ejecta containing short-lived radioactive species. I will review the observational evidence and the theoretical basis for the emerging view that planetary systems form in dynamically complex and radiation-rich environments.

The Orion Nebula, the nearest site of both low- and high-mass star formation, has spawned a cluster of several thousand low-mass stars along with a handful of massive ones within the last 1 to 2 million years. UV radiation from nearby massive stars erodes the outer parts of protoplanetary disks beyond a radius of about 5 AU (for a 1 solar mass central star), preferentially removing gas and small entrained particles. In disks which have experienced grain growth and sedimentation to the disk mid-plane, UV radiation selectively removes metal-depleted material from the disk surface layers and leaves behind ices and solids. Increased metallicity drives the disk towards gravitational instability and prompt formation of kilometer-sized planetesimals [1].

Massive stars end their lives in supernova explosions within 3 to 40 million years of their formation, the time-interval of during which planetary systems form and mature. Protoplanetary disks can either inherit supernova-enriched debris from their natal clouds, or become polluted after formation by grains ejected by nearby supernovae formed from the same parent cloud. Either mechanism can inject large amounts of short-lived radioactive species such as ⁶⁰Fe or ²⁶Al.

References: [1] Throop H. and Bally J. 2005. *The Astrophysical Journal* 623:149–152.

5281

MICROSTRUCTURE AND CRYSTAL PREFERRED ORIENTATION OF THE BASALTIC ACHONDRITE NWA 4269

J. Bascou¹, C. Maurice², B. Moine¹, A. Sedikki³, and J. Y. Cottin¹. ¹Equipe Transferts Lithosphériques, UMR-CNRS 6524, Université de St-Etienne, France. ²UMR-CNRS 5146, Ecole Nationale Supérieure des Mines de Saint-Etienne, France. ³Laboratoire de Magmatisme et Géodynamique des Bassins Algériens, Université d'Oran, Algérie

Petrostructural investigations were realized on a high metamorphic Fe-rich, silica-rich eucrite. This meteorite presents microstructure variation characterized by both coarse-grained regions (subophitic texture) constituted by pigeonite and plagioclase minerals, and fine grained recrystallized regions, which contain silica, clinopyroxene, orthopyroxene with ilmenite, troilite, and Fe metal in minor proportion. Moreover, fine-grained zone is generally located close to large elongated iron grains (up to a mm size). Crystal preferred orientation (CPO) analysis of minerals allows to obtain new information on relationships between crystallography and microstructure and leads to a better understanding of the deformation and thermal history of the sample.

CPO of minerals was measured using the electron backscattered diffraction (EBSD) technique in a field emission scanning electron microscope (FE SEM). Indexed diffraction patterns are generated by interaction of a vertical incident electron beam with a carefully polished flat surface of the sample tilted to a high angle (70°) to the electron beam. Typical working conditions were 17 kV acceleration voltage, 140 µA beam current, and 18 mm working distance.

Preliminary CPO analysis of the fine-grained areas allows to bring out several interesting crystallographic features. SiO₂ phase is identified as α quartz polymorph. Moreover, in spite of the undisturbed appearance of the fine-grained regions, EBSD orientation mapping leads to distinct areas (up to several hundreds micrometers in size) characterized by high maximum density (MD) in pole figure projections of quartz crystallographic axes (for example, MD of [0001] > 30 m.u.d.). Orthopyroxene CPO presents similar characteristics. In addition, relationships between quartz and orthopyroxene CPO are observed: [0001] maximum density (MD) of quartz is close to the [010] MD of orthopyroxene, and the first and second prism of the quartz are close to the [001] and the [100] maximum density of orthopyroxene.

In the eucrite NWA 4269, evidence for thermal metamorphism (around 900 °C) is indicated by the existence of equilibrated pyroxenes (clinopyroxene and orthopyroxene). Microstructure analysis suggests that the thermal event was accompanied and followed by a complex recrystallization history including syn- and post-deformation processes. Alternative formation mechanisms of observed microstructures are discussed in the light of the last EBSD data on silicate and iron phases.

5389

PHYSICAL AND CHEMICAL CHARACTERISTICS OF APOLLO 16 LUNAR HIGHLAND SOIL 64500

M. M. Battler and J. G. Spray. Planetary and Space Science Centre, Department of Geology, 2 Bailey Drive, University of New Brunswick, Fredericton, NB, E3B 5A3, Canada. E-mail: melissa.battler@unb.ca

Introduction: Apollo 16 lunar soil sample 64500 is an example of lunar highland-type regolith. It was collected at Apollo 16 station 4A, just northwest of Stone Mountain, near the Cinco B crater [1]. Most soil samples collected during Apollo 16 have very similar chemical compositions [2], and therefore sample 64500 can be viewed as representative of the Descartes region of the Moon, and perhaps of other highland regions, as well. The average regolith thickness over the Descartes region is 6–10 m, and the average regolith chemical composition is quite consistent, indicating a local source for the parent bedrock [2]. Apollo 16 regolith samples contain large amounts of anorthosite and anorthositic gabbro-based lithic and mineral fragments, and varying amounts of breccias, glasses, and agglutinates. Relative to typical anorthositic gabbro, the Apollo 16 soils are slightly enriched in Al and Ca, and depleted in Mg [3].

Scanning Electron Microscopy (SEM): Sample 64500 was examined as gold-coated soil grains mounted on a gold-coated glass slide, under a JEOL 6400 analytical SEM.

Observations: Sample 64500 consists of several components, ranging from rock and mineral fragments to glasses and agglutinates. All particles show evidence of repeated micro-bombardment, in the form of fused melt droplets, pits, and fractured edges. Rock and mineral particles show varying degrees of degradation, although they are all very angular, typically with jagged, fractured edges and faces. Glass particles range from fairly smooth, unfractured spheres, to highly vesicular, conchoidally fractured particles with fused melt droplets occurring on the exterior (Fig. 1). These latter particles may be agglutinates. Particles observed so far range in size from <1 µm to 100 µm.

Energy Dispersive X-ray Spectrometry (EDS): Qualitative EDS analysis reveals high concentrations of Si, O, and Al, with varying low to high concentrations of Ca and Mg, and low to medium concentrations of Fe and Na. These compositions can be equated with plagioclase and pyroxene fragments or their melted equivalents.

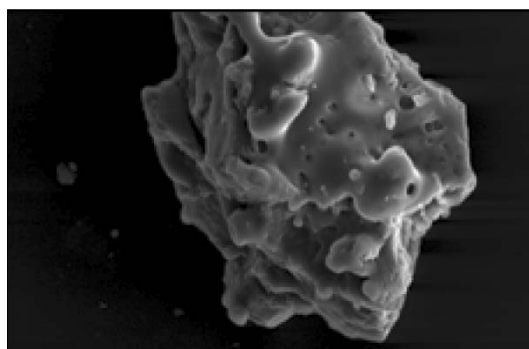


Fig 1. An SEM image of glass from lunar soil 64500; 30 µm.

References: [1] Graf J. C. 1993. *Lunar soils grain size catalog*. Houston, Texas: National Aeronautics and Space Administration. pp. 286–288. [2] Ulrich G. E., Hodges C. A., and Muehlberger W. R. 1981. *Geology of the Apollo 16 area, central lunar highlands*. Washington, D.C.: National Aeronautics and Space Administration. [3] Heiken G. et al. 1991. *Lunar source book*. 736 p.

5392

THE FORMATION OF TERRESTRIAL PLANETS: WHAT DO THE EXTRA-SOLAR PLANETS TELL US?

W. Benz. Physikalisches Institut, University of Bern, Switzerland

The number of discovered extra-solar giant planets (over 180 at the time of this writing) is growing rapidly. While very little information is available for most of these planets on an individual basis (essentially a minimum mass and orbital parameters), together they begin to provide a large enough sample to allow for a meaningful statistical analysis of their properties. In addition, statistical comparisons with populations of synthetic planets have emerged as a powerful tool to constrain planet formation theories. We shall discuss some of these constraints with a particular focus on their implications for the formation of terrestrial planets. Among others, we shall show that the current population of detected extra-solar planets is actually probably only the tip of the iceberg as the models predict that by far the largest fraction of planetary embryos do not accrete sufficient gas to become giant planets. Moreover, the relation between the time scale required to form planetary embryos and the lifetime of the proto-planetary accretion disk is also an important factor which determines in part the final mass a giant planet can reach.

5208

COMBINED ELEMENTAL AND TEXTURAL STUDIES OF FOUR IAB IRON METEORITESG. K. Benedix¹ and D. J. Prior². ¹IARC, Department of Mineralogy, The Natural History Museum, Cromwell Road, London, SW7 5BD UK. E-mail: g.benedix@nhm.ac.uk. ²Department Earth and Ocean Sciences, University of Liverpool, Liverpool L69 3GP, UK

Introduction: Iron meteorites offer important information about differentiation processes on small bodies in the early solar system [1, 2]. They are classified into one of 13 groups on the basis of trace element chemistry. The majority of these groups are thought to have formed by fractional crystallization during core formation. Although containing abundant Fe,Ni metal, implying that a significant amount of melting occurred on the parent asteroids, some iron meteorite groups (IAB/IIICD and IIE) have trace element trends inconsistent with core formation.

Most studies of iron meteorites have focused on their chemistry (e.g., [3]). Macrottextures (i.e., Widmännstatten patterns) in iron meteorites are related to the bulk chemistry and cooling rate. EBSD studies of the textures of iron meteorites have focused on fine-grained microtextures (e.g., [4]). We present preliminary data from a combined elemental and textural study of macro-textures in four IAB iron meteorites.

Analytical Techniques: We studied four IAB iron meteorites using X-ray mapping (JEOL 5900LV SEM at the Natural History Museum) and electron backscatter diffraction (CamScan X500 FEG-SEM at University of Liverpool).

Results and Discussion: Campo del Cielo (CdC) and Canyon Diablo (CD) have bulk Ni compositions less than 7 wt% and are classified as coarse octahedrites. Mundrabilla (Mun) and Four Corners (FC) have > 7 wt% Ni and are medium octahedrites [5].

X-ray maps of CdC show metal dominated by the low-Ni iron kamacite, with minor troilite, schreibersite, and taenite found at what appear to be grain boundaries. EBSD in both CdC and CD shows a recrystallized texture of coarse kamacite grains with random orientations. Kamacite grains contain up to 2 sets of Neumann bands that have boundary traces consistent with {211} and misorientations of 60° around <111>. These grains also show significant crystal plastic deformation and limited recovery.

In hand sample, Mun exhibits textures in metal/sulfide consistent with rapid crystallization from a melt [6]. Element maps of FC reveal that it also likely experienced rapid cooling at the solidus. EBSD of both samples reveals that high-Ni areas comprise 2 phases: a single orientation of taenite (fcc) with variably oriented kamacite (bcc) grains that all have a {110}_{bcc}/{111}_{fcc} orientation relationship indicating an interesting cooling history for both of these meteorites' sub-solidus.

Use of EBSD to look at macrottextures combined with elemental mapping of iron meteorites offers an innovative way to explore these meteorites. Future work includes investigation of the structure of silicate in these enigmatic iron meteorite groups.

References: [1] Haack H. and McCoy T. J. 2005. In *Meteorites, comets, and planets*, edited by Davis A. M. Amsterdam: Elsevier. pp. 1151–1154. [2] Buchwald V. F. 1975. *Handbook of iron meteorites*. Berkeley, California: University of California Press. 1418 p. [3] Scott E. R. D. and Wasson J. T. 1975. *Reviews in Geophysics and Space Physics* 13:527–546. [4] Goldstein J. I. and Michael J. R. 2006. *Meteoritics & Planetary Science* 41:553–570. [5] Wasson J. T. and Kallemeyn G. W. 2002. *Geochimica et Cosmochimica Acta* 66:2445–2473. [6] Scott E. R. D. 1982. *Geochimica et Cosmochimica Acta* 46:813–823.

5347

DISENTANGLING THE DIVERSITY OF BULK CHONDRULE COMPOSITIONS: DID CO CHONDRITES SAMPLE TWO VERY DISTINCT CHONDRULE POPULATIONS?

J. Berlin, R. H. Jones, and A. J. Brearley. Department of Earth and Planetary Sciences, University of New Mexico, Albuquerque, New Mexico 87131, USA. E-mail: jberlin@unm.edu

Introduction: Isotopic, chemical, and petrographic differences recorded in the major components of chondrites imply that they must have formed under very different conditions in different regions of the solar nebula, and/or at different times, before they mixed and accreted to asteroidal bodies [1]. We want to address the question of whether or not primitive chondrites sampled distinct chondrule populations that were later recycled. Available data sets for bulk chemical compositions of chondrules show a continuum in compositions for ordinary chondrites [2], but a noticeable gap between Fe-rich and Fe-poor compositions in CO chondrites ([2]; Fig. 1). We are studying a suite of Kainsaz (CO3.2) chondrules and, so far, determined 12 bulk compositions by electron microprobe using modal recombination (see [3] for details). We also conducted broad beam (10 μm) EPMA analyses of Kainsaz matrix in order to examine the question of chemical complementarity between chondrules and matrix [4].

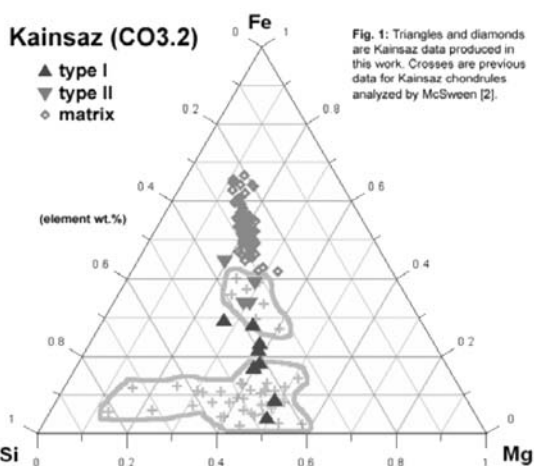


Fig. 1.

Results and Discussion: Our data for Kainsaz chondrules (Fig. 1) show a continuum of compositions, rather than the bimodality seen in previous data sets. Type II chondrules are at the Fe-rich end of the continuous trend, and matrix compositions lie on an extension of the chondrule trend. For type I chondrules, a correlation between Fe content of the chondrule, which varies from 2 to 16 vol%, and metal/sulfide abundance is evident. Differences in Fe content among type I chondrules could be largely the result of physical metal loss, e.g., while the chondrule was spinning. We have not yet studied the Si-rich group of RP chondrules included in Fig. 1. If we only consider the silicate portion of the chondrules, there are two distinct populations: FeO-rich type II chondrules and FeO-poor type I chondrules. Therefore, two chondrule populations were indeed sampled in CO chondrites, but the bimodality is in oxidation states (oxidized type II versus reduced type I chondrules) rather than in bulk Fe content.

References: [1] Zanda and Hewins. 2006. Abstract #2199. 37th Lunar and Planetary Science Conference. [2] Jones et al. 2005. In *Chondrites and the protoplanetary disk*. San Francisco: Astronomical Society of the Pacific. pp. 251–285. [3] Berlin et al. 2006. Abstract #2370. 37th Lunar and Planetary Science Conference. [4] Huss et al. 2005. In *Chondrites and the protoplanetary disk*. San Francisco: Astronomical Society of the Pacific. pp. 701–731.

5217

NICKEL ISOTOPE ANOMALIES IN METEORITES

M. Bizzarro, D. Ulfbeck, A. Trinquier¹, K. Thrane, and J. N. Connelly. Geological Institute, University of Copenhagen, Copenhagen, Denmark. E-mail: bizzarro@geol.ku.dk

With a half-life of 1.49 Myr, the ^{60}Fe - ^{60}Ni decay scheme is ideally suited for dating meteorites and planetary processes that occurred in the first 10 Myr of the early solar system (ESS). Ni has two neutron-rich isotopes, ^{62}Ni and ^{64}Ni , produced through nuclear statistical equilibrium processes occurring in neutron-rich supernova ejecta. Excesses and deficits have been documented for neutron-rich isotopes from iron group elements (^{48}Ca , ^{50}Ti , ^{54}Cr , ^{62}Ni , and ^{64}Ni) in normal and FUN calcium-aluminium-rich inclusions (CAIs) as well as primitive and differentiated meteorites, providing information on the scale and extent of isotopic heterogeneity in the ESS.

We have developed analytical protocols for high-precision Ni isotope measurements in metal and silicate materials by MC-ICPMS, enabling typical external reproducibilities of 0.010‰ and 0.015‰ for $\delta^{60}\text{Ni}^*$ and $\delta^{62}\text{Ni}$ values, respectively [1]. Two terrestrial rock standards (BHVO-1 and DTS-2b) have $\delta^{60}\text{Ni}^*$ and $\delta^{62}\text{Ni}$ identical within analytical uncertainty to the Ni standard solution, thus validating our approach. One enstatite chondrite (Qingzhen) and a Martian dunite (NWA 2737) yielded $\delta^{60}\text{Ni}^*$ and $\delta^{62}\text{Ni}$ values identical to the terrestrial average. Three carbonaceous chondrites (Murchison, Orgueil, and Renazzo) have average $\delta^{60}\text{Ni}^*$ and $\delta^{62}\text{Ni}$ values of $0.0012 \pm 0.0057\%$ and $0.0341 \pm 0.0025\%$, respectively. One ordinary chondrite (Bjurbole) has $\delta^{60}\text{Ni}^*$ and $\delta^{62}\text{Ni}$ values of $-0.0052 \pm 0.0081\%$ and $-0.0201 \pm 0.0161\%$, respectively. These results suggest that if ^{60}Fe was present in the ESS when these bodies formed, it was homogeneously distributed ($\pm 20\%$) within the accretion region of the terrestrial planets and chondrites. Seven iron meteorites show resolvable uniform deficits in $\delta^{60}\text{Ni}^*$ and $\delta^{62}\text{Ni}$ of $0.0233 \pm 0.0071\%$ and $0.0409 \pm 0.0213\%$, respectively. Although $\delta^{60}\text{Ni}^*$ deficits in irons are consistent with Fe/Ni fractionation during the life span of ^{60}Fe , a whole-rock fragment and olivine separate from the 4.566 Gyr old angrite SAH 99555 as well as a chondrule and CAI from Allende with supracanonical $^{26}\text{Al}/^{27}\text{Al}$ yielded identical deficits in $\delta^{60}\text{Ni}^*$, not correlated with their Fe/Ni ratios. We suggest that irons, SAH 99555 and the Allende chondrule and CAI analyzed here formed in the absence of ^{60}Fe , at a time when ^{26}Al was widespread within ESS solids, reflecting a late injection of ^{60}Fe in the ESS. Injection of ^{60}Fe occurred after accretion of the angrite parent body, $\sim 600,000$ yr after CAI formation, but was homogeneously distributed within the ESS at the time of accretion of chondrite parent bodies ~ 2 Myr after CAI formation. Observed excesses and deficits in ^{62}Ni are correlated with ^{54}Cr anomalies. These results provide important constraints regarding the origin of short-lived nuclides in the ESS, and demonstrate the presence of large-scale coupled Cr and Ni isotopic heterogeneity in ESS materials.

Reference: [1] Ulfbeck D. et al. 2006. Abstract. 16th Annual Goldschmidt Conference.

5246

VOLATILE DEPLETION: CONSTRAINTS FROM DIFFERENTIATED METEORITES

P. A. Bland^{1, 2} and G. K. Benedix². ¹Impacts and Astromaterials Research Centre, Department of Earth Science and Engineering, Imperial College London, SW7 2AZ, UK. E-mail: p.a.bland@ic.ac.uk. ²IARC, Department of Mineralogy, Natural History Museum, London SW7 5BD, UK

Recent Hf-W and Al-Mg ages for irons and achondrites (e.g., [1–3]) constrain the timing of other processes in addition to differentiation. ¹⁶O-depletion in angrites, IIIAB, and IVA inclusions [4] suggests rapid modification of solar system oxygen. In addition, most irons show volatile-depletion, plausibly inherited from precursor materials (e.g., [5]), to levels not seen in chondrites.

The principal theories that have sought to explain volatile depletion are incomplete condensation (e.g., [6, 7]) and the two-component model (e.g., [8, 9]) where bulk depletion is related to chondrule depletion. A problem for the latter model is that many differentiated objects (e.g., Earth [10]) are more volatile-depleted than chondrules. But the Hf-W data raises another issue. Initial W isotopic compositions for magmatic irons are indistinguishable from CAI [2]. Chondrule formation ~2 Ma after CAI (e.g., [11]) therefore postdates core formation in planetesimals. If chondrites are not the precursor for differentiated asteroids [1], then chondrule formation is not responsible for volatile depletion.

A problem for incomplete condensation is that depletion does not clearly correlate with heliocentric distance [12]. The main belt contains 4 Vesta (similar depletion to the Moon) and probably the parent bodies of highly depleted irons. A possible solution comes from a recent model which suggests that differentiation occurred in the terrestrial planet region [13]. Differentiated planetesimals evolved collisionally, with some survivors scattering into the main belt: 4 Vesta may be an interloper [13].

The Bottke model [13] is a partial solution to the depletion-gradient problem. Further modelling is required to assess whether extreme depletion is possible at small heliocentric distances, but we might also consider another mechanism. Impact-generated vapor of ~solar composition would allow for local incomplete condensation. A variety of evidence supports an origin for highly depleted CB chondrites as condensates from an impact-generated vapor plume (e.g., [14–16]). Giant impacts should be common in the early solar system [17]. Given short accretion times (e.g., [18]) and plausible impact velocities (Bottke, personal communication), high energy impacts may have occurred within 1 Ma of CAI. Although degassing might chemically fractionate elements, incomplete condensation of impact-generated vapor would produce a volatility-controlled depletion and should be considered as a general mechanism for extreme volatile depletion.

References: [1] Kleine T. et al. 2005. *Geochimica et Cosmochimica Acta* 69:5805. [2] Markowski A. et al. 2006. *Earth and Planetary Science Letters* 242:1. [3] Baker J. et al. 2005. *Nature* 436:1127. [4] Clayton R. N. and Mayeda T. K. 1996. *Geochimica et Cosmochimica Acta* 60:1999. [5] Campbell A. J. and Humayun M. 2005. *Geochimica et Cosmochimica Acta* 69:4733. [6] Wasson J. T. and Chou C.-L. 1974. *Meteoritics* 9:69. [7] Cassen P. 1996. *Meteoritics & Planetary Science* 31:793. [8] Anders E. 1964. SSR 3: 583. [9] Alexander C.M.O'D. 2005. *Meteoritics & Planetary Science* 40:943. [10] McDonough W. F. and Sun S.-S. 1995. *Chemical Geology* 120: 223. [11] Amelin Y. et al. 2002. *Science* 297:1678. [12] Palme H. 2000. SSR 192:237. [13] Bottke W. F. et al. 2006. *Nature* 439:821. [14] Campbell A. J. et al. 2002. *Geochimica et Cosmochimica Acta* 66:647. [15] Rubin A. E. et al. 2003. *Geochimica et Cosmochimica Acta* 67:3283. [16] Krot A. N. et al. 2005. *Nature* 436:989. [17] Asphaug E. et al. 2006. *Nature* 439:155. [18] Weidenschilling S. J. et al. 1997. *Icarus* 128:429.

5227

WHY ASTEROIDAL ALTERATION WAS ISOCHEMICAL: HIGH POROSITY ≠ HIGH PERMEABILITY

P. A. Bland^{1, 2}, M. D. Jackson¹, R. F. Coker³, B. A. Cohen⁴, and G. K. Benedix². ¹Impacts and Astromaterials Research Centre (IARC), Department Earth Science and Engineering, Imperial College London, SW7 2AZ, UK. E-mail: p.a.bland@ic.ac.uk. ²IARC, Department of Mineralogy, Natural History Museum, London SW7 5BD, UK. ³Los Alamos National Laboratory, Los Alamos, New Mexico 87545, USA. ⁴Institute of Meteoritics, University of New Mexico, Albuquerque, New Mexico 87131, USA

Carbonaceous chondrites (CCs) are among the most primitive materials available to us. However, it has become clear that their mineralogy is highly altered. A range of evidence indicates that alteration occurred within CC parent asteroids (e.g., [1, 2]). Solar abundances for soluble elements show that aqueous alteration was isochemical, with negligible fluid flow (even over sub-millimeter distances [3, 4]). Hydration models (which assume zero flow) based on O isotopes indicate that water:rock ratios were high [5].

Numerous studies have modelled asteroidal aqueous and thermal alteration [6–12]. In each case, large-scale fluid flow was observed, frequently over tens of km [6–9, 12]. But whether flow is observed as a single pass “exhalation” [8] or in convecting cells [6, 12], the movement of liquid water through rock would fractionate aqueous species. The modelling results directly contradict the meteorite data—the one indicates that alteration occurred in an open system with large-scale fluid-flow; the other that alteration was isochemical, with minimal flow.

How to resolve this paradox? Permeability is fundamental to flow. Initial permeability estimates of 10⁻¹¹–10⁻¹³ m² for chondritic asteroids [6] (based on suggested terrestrial and lunar analogs), were adopted in all subsequent studies [7–12]. But is this permeability appropriate for CC precursors? Matrix grain size in the least altered CCs is ~200 nm [13, 14], far lower than in the analog materials. Using the Blake-Kozeny-Carman equation [15] to predict permeability for grain sizes of this order (given reasonable estimates of the hydraulic tortuosity coefficient) yields values ranging from 10⁻¹⁶–10⁻¹⁹ m², even in high-porosity matrix. Matrix grain size dictates mean pore-throat diameter, so is a key control on permeability (which scales as grain size squared). This observation may reconcile compositional data indicating minimal fluid flow and oxygen isotope studies suggesting high water:rock ratios. Preliminary modelling using lower permeability [16] now appears consistent with the meteorite data.

References: [1] Zolensky M. E. and McSween H. Y., Jr. 1988. In *Meteorites and the early solar system*. Tucson, Arizona: The University of Arizona Press. p. 115. [2] Brearley A. J. In *Meteorites and the early solar system II*. Tucson, Arizona: The University of Arizona Press. p. 587. [3] Wulf A. V., Palme H., and Jochum K. P. 1995. *Planetary and Space Science* 43:451. [4] Bland P. A. et al. 2005. *Proceedings of the National Academy of Sciences* 102:13,755. [5] Clayton R. N. and Mayeda T. K. 1999. *Geochimica et Cosmochimica Acta* 63:2089. [6] Grimm R. E. and McSween H. Y., Jr. 1989. *Icarus* 82:244. [7] Cohen B. A. and Coker R. F. 2000. *Icarus* 145:369. [8] Coker R. F. and Cohen B. A. 2001. *Meteoritics & Planetary Science* 36:A43. [9] Young E. D. et al. *Science* 286:1331. [10] McSween H. Y., Jr. et al. 2002. In *Asteroids III*. Tucson, Arizona: The University of Arizona Press. 559 p. [11] Young E. D., Zhang K. K., and Schubert G. 2003. *Earth and Planetary Science Letters* 213:249. [12] Travis B. J. and Schubert G. 2005. *Earth and Planetary Science Letters* 240:234. [13] Greshake A. 1997. *Geochimica et Cosmochimica Acta* 61:437. [14] Nuth J. A. III, Brearley A. J., and Scott E. R. D. 2005. In *Chondrites and the protoplanetary disk*. San Francisco: Astronomical Society of the Pacific. 675 p. [15] Dullien F. A. L. 1992. *Porous media: Fluid transport and pore structure*. San Diego: Academic Press. 574 p. [16] Coker et al. 2006. Abstract #5278. *Meteoritics & Planetary Science* 41. This issue.

5197

FIRST LIGHT FOR THE DESERT FIREBALL NETWORK

P. A. Bland^{1,2}, P. Spurny³, A. W. R. Bevan⁴, M. C. Towner⁵, T. McClafferty⁶, and G. Deacon⁴. ¹Impacts and Astromaterials Research Centre (IARC), Department of Earth Science and Engineering, Imperial College London, SW7 2AZ, UK. E-mail: p.a.bland@imperial.ac.uk. ²IARC, Department of Mineralogy, Natural History Museum, London SW7 5BD, UK. ³Ondrejov Observatory, Astronomical Institute, Academy of Sciences of the Czech Republic, 251 65 Ondrejov, Czech Republic. ⁴Department of Earth and Planetary Science, Western Australian Museum, Francis Street, Perth, Western Australia 6000, Australia. ⁵PSSRI, The Open University, Milton Keynes MK7 6AA, UK. ⁶Western Australian Museum, Kalgoorlie-Boulder, 17 Hannan Street, Kalgoorlie, Western Australia 6433, Australia

Introduction: There are over 30,000 meteorites in collections worldwide. However, although we can analyze these samples to gain clues to the origins of our solar system, we only have an approximate knowledge of where they come from. Camera networks, designed to observe fireballs, calculate orbits, triangulate fall positions, and recover meteorites, have been set up in several nations at various times in the past e.g., [1]. Although a primary motive behind most of these projects was the recovery of meteorites with orbital information, only four samples have been obtained. The reason is related to the chosen field areas: any vegetation makes looking for small meteorites extremely difficult. We are building a network in a desert that has proved eminently suitable for locating meteorites. The aim is to deliver numbers of samples with accurate orbits, providing a spatial context to aid in interpreting meteorite composition.

The Project: Our preliminary autonomous fireball camera network has now been established in the Nullarbor region of Western Australia. Three cameras designed to operate in deserts have been developed, and were deployed in late 2005. First light for our first camera was on December 3, 2005. Operations are monitored via a satellite link. Orbits are calculated from observed fireballs, and meteorite fall positions will be determined for later recovery by field parties. The network will detect meteorites falling over an area of approximately $0.3\text{--}0.4 \times 10^6$ km².

Results: The first fireball for which we were able to derive an orbit occurred on December 7, 2005, during the initial deployment of the cameras. The object may have been a small comet fragment. The fireball started at 103.92 km, and terminated very high at 72.76 km. It traveled 60.29 km along its luminous trajectory in 1.8 seconds, with an initial velocity of 35.31 km/s. Its heliocentric orbit is typical for short period comets: semimajor axis 24.4 AU, eccentricity 0.960, perihelion distance 0.97801 AU, argument of perihelion 350.14 degrees, ascending node 75.41934 degrees, and inclination 51.74 degrees. Radiant position: right ascension 111.02 degrees, declination -68.75 degrees.

Future Work: A number of technical issues have been overcome, and testing (and observing) continues. Routine operations are scheduled from September 2006. Based on estimated fall rates [1, 2], we hope to observe at least one meteorite fall by the end of the year. Recovery of meteorites during the grant period would prove our concept and open the way for funding of a full network. Our current detection area is approximately 25% that of previous networks. The final Desert Fireball Network will have an area of 1.5×10^6 km², and will be capable of recovering significant numbers of meteorites per year.

References: [1] Halliday I. et al. 1996. *Meteoritics & Planetary Science* 31:185. [2] Bland P. A. et al. 1996. *Monthly Notices of the Royal Astronomical Society* 283:551.

5311

SHOCK METAMORPHIC STATE OF THE CHASSIGNITE NORTHWEST AFRICA 2737

U. W. Bläss¹, F. Langenhorst¹, T. Frosch², M. Schmitt², and J. Popp². ¹Institute for Geosciences, University of Jena, Germany. E-mail: Ulrich.Blaess@uni-jena.de. ²Institute for Physical Chemistry, University of Jena, Germany.

The achondrite Northwest Africa 2737 (NWA 2737) is besides Chassigny the second known member of the chassignite subgroup of SNC meteorites, which are assumed to originate from Mars. The meteorite has been recovered from the Moroccan desert in 2000. Both chassignites are cumulate dunites with similar modal and REE abundances, which suggests a genetic relationship between both rocks and offers the opportunity for a better understanding of the formation of Martian magmas and therefore also for basaltic SNC meteorites [1, 2]. For both chassignites similar Sm-Nd crystallization ages of ~ 1.38 Ga have been obtained [3], pointing to a common origin of chassignites. However, NWA 2737 is slightly more enriched in magnesium, indicating a crystallization from a less evolved parent melt. Its mineralogy has been previously determined, showing the predominance of olivine over subordinate augite, spinel, analbite, orthopyroxene, pigeonite, and phosphates [2]. Whereas olivine (Fo_{78.7}) and chromite rich spinels are cumulus phases, pyroxenes, analbitic maskelynites and phosphates occur in interstitial areas between olivine crystals or as melt inclusions in olivine.

In this study a 400 μ m large melt area with adjacent olivine crystals has been analyzed by polarizing light microscopy and Raman spectroscopy in order to study the petrology of the crystallized melt areas and superimposed shock damage. Raman measurements are performed using a 244 nm UV-laser excitation in order to avoid fluorescence effects.

As a result of strong shock metamorphism, olivine crystals show an intense brown staining, parallel planar fractures and are penetrated by two perpendicular sets of colorless lamellae. Raman spectra indicate that both lamellae and the brownish host crystal are made of olivine. The brownish olivine host, however, shows a band broadening compared to the bright lamellae. In addition second order bands are more expressed in the spectra of the brownish olivine. The lamellae could therefore be formed due to olivine recrystallization. Transmission electron microscopy will be applied to examine the formation of olivine lamellae in detail and to determine shock related features of crystals within the melt area, resulting in an estimate of shock conditions for NWA 2737. The relatively large melt area is predominantly composed of deformed augite and zoned orthopyroxene, an opaque spinel, and a maskelynite glass, containing eventually a second generation of pyroxene crystals.

Altogether, using the recent shock classification [4], the aforementioned observations allow us to provide an estimate of shock pressure. Staining in olivine and the transformation of analbitic feldspar to maskelynite indicates minimum shock pressures of about 40 GPa.

References: [1] Mikouchi T. 2005. Abstract. *Meteoritics & Planetary Science* 40:A102. [2] Beck P. et al. 2006. *Geochimica et Cosmochimica Acta* 70: 2127–2139. [3] Misawa K. et al. 2005. Abstract. *Meteoritics & Planetary Science* 40: A104. [4] Stöffler D. et al. 1991. *Geochimica et Cosmochimica Acta* 55: 3845–3867.

5043

SOLAR NEON ABUNDANCE INFERRED FROM APOLLO FOIL EXPERIMENTS

P. Bochsler. Physikalisches Institut, University of Bern, Switzerland. E-mail: bochsler@soho.unibe.ch

Neon and helium with first ionization potentials (FIP) of 21.6 and 24.6 eV, respectively, are elements which are generally depleted with respect to hydrogen in the solar wind. Coulomb friction with protons in the inner corona tends to discriminate helium and, to some extent, also neon. Whereas the FIP-related discrimination has at most a weak effect on isotopic abundances, inefficient Coulomb friction is probably the main cause of isotopic fractionation effects in the solar wind. Inspection of the photoionization cross sections of helium and neon indicates that elemental fractionation in the solar chromosphere is probably of minor importance and that the variability of He/Ne in the solar wind must mainly be attributed to variable Coulomb drag. From a theoretical model on Coulomb drag and a fit to the data of the Apollo Foil measurements (Geiss et al. 1972), we derive a He/Ne ratio of 720 for the outer convective zone of the Sun and a value for the solar neon abundance of 8.09 ± 0.15 in the logarithmic dex units ($[H] = 12.00$). In view of the anticipated results from the Genesis mission, we make a new attempt to estimate the magnitude of isotopic fractionation effects in the solar wind.

5234

EFFECTS OF SECONDARY PROCESSES ON THE ISOTOPIC COMPOSITION OF INSOLUBLE ORGANIC MATTERL. Bonal¹, E. Quirico¹, and J. Aléon². ¹Laboratoire de Planétologie de Grenoble, Université Joseph Fourier, Bât. D de Physique, 38041 Grenoble Cedex 9, France. E-mail: lydie.bonal@obs.ujf-grenoble.fr. ²CRPG 15, rue Notre-Dame des Pauvres, BP20, 54501 Vandoeuvre les Nancy, France

Isotopic anomalies (IOM) in H and N suggest that the chondritic insoluble organic matter has an interstellar origin [e.g., 1]. However, the D/H ratio in IOM remains much lower than those measured in the organic molecules commonly observed in the dense interstellar medium [2]. Process in protosolar cloud, in planetary disk, and in the parent bodies of meteorites may have altered the initial isotope signatures of interstellar IOM. In particular, aqueous alteration (AA) and thermal metamorphism (TM) on the parent body have modified the structure of the IOM [5, 6, 7]. Thus, these secondary process may have modified the isotopic composition, too. So, in the present study, we are interested by the influence of AA and TM on D and ¹⁵N. We used isotopic data available in the literature [e.g., 1–4] and acquired by ourselves; the metamorphic grade of the objects was provided by the structural grade of the organic matter attempted by Raman spectroscopy [5, 6, 7].

Discussion: Oxidized CV chondrites have significantly lower D values (194–239‰) than reduced (500–1360‰) [4]. CV_{Ox} have suffered from more AA than CV_{Red}, with a comparable metamorphic grade for some objects [5]. The organic precursor of the IOM of the CV seems to be structurally and chemically comparable [5]. Thus, it seems reasonable to suppose an same initial isotopic composition for the whole CV chondrites [3]. Thus, it appears that AA would perturb the D/H composition to a larger extent than TM. This trend is confirmed by the D enrichment in CI/CM, in comparison with UOC. Indeed, CI/CM have suffered from a large extent of AA, their D values (D 1460‰) are lower than those of UOC (until 5484‰), that have suffered from minor AA.

On the other hand, the N isotopic composition appears to be very sensitive to TM: the CI/CM are slightly more enriched ($6 < ^{15}\text{N} (\text{‰}) < 29$ [3, 4]) than type 3 chondrites ($^{15}\text{N}_{\text{max}} = 9\text{‰}$; Semarkona is an exception with $^{15}\text{N} = 56\text{‰}$ [3]). The CR chondrites are the unique chondrites with high ¹⁵N enrichment (until 233‰ [8]). Thus, carrier of the N isotopic enrichment appears to be a labile organic phase sensitive to heating and maybe, to a lesser extent, to AA.

Thus, the effects induced by secondary process on the isotopic composition appear to be different on D and ¹⁵N. They should not be underestimated and must be taken into account in a model of formation and evolution of IOM. This study confirms that structurally and isotopically [3, 8], CR chondrites are the most primitive chondrites. This study is consistent with an interstellar origin of the organic matter, initially enriched in D and N.

References: [1] Yang J. and Epstein S. 1983. *Geochimica et Cosmochimica Acta* 47:2199–2216. [2] Robert F. 2002. *Planetary and Space Science* 50:1227–1234. [3] Alexander C. M. O'D. et al. 1998. *Meteoritics & Planetary Science* 33:603–622. [4] Alexander C. M. O'D. et al. 2005. Abstract #5289. 35th Lunar and Planetary Science Conference. [5] Bonal L. et al. 2006. *Geochimica et Cosmochimica Acta* 70:1849–1863. [6] Bonal L. et al. 2005. Abstract #1699. 35th Lunar and Planetary Science Conference. [7] Quirico E. et al. 2003. *Meteoritics & Planetary Science* 38:795–811. [8] Busemann H. et al. 2006. *Science* 312:727:730.

5085

SPECTROSCOPIC ANALYSIS OF GEMINID METEORS

J. Borovicka. Astronomical Institute of the Academy of Sciences, 251 65 Ondrejov, Czech Republic. E-mail: borovic@asu.cas.cz

Introduction: The Geminid meteor shower is one of the most intense annual meteor showers. The parent body of the shower is asteroid 3200 Phaeton. The orbit of the shower and its parent body is notable by the short period (~1.5 yr) and small perihelion distance (0.14 AU). Since Phaeton's discovery in 1983, the question has arisen whether it is a regular asteroid or a dormant comet. Detailed observations have shown no sign of cometary activity on Phaeton [1]. The activity profile of the shower suggests an age of several thousand years for the meteoroid stream. The stream was possibly formed within one orbital revolution of Phaeton around the Sun [2]. Geminids produce no meteorites because of their large entry speed (36 km/s), nevertheless, their strength and density was found to be closer to stony meteorites than cometary meteoroids [3]. On the other hand, our recent work on sporadic meteors [4] has shown that solar heating at small perihelion distances leads to the loss of volatile sodium and to general compaction of meteoroids. In this paper we study the chemical composition of Geminids from video and photographic spectroscopy.

Results: We analyzed 79 video spectra and 2 photographic spectra of Geminid meteors. The Mg/Fe ratio was found to be 1.5–3 times larger than the chondritic value. Similar values were earlier found for other cometary showers, the Leonids and the Perseids [5]. The Na abundance in the Geminids is generally low, but shows large variations among the meteors. The Na/Mg ratio is always lower than chondritic. The Na/Fe ratio varies from chondritic to 10 times lower than chondritic. There is a weak trend of increasing Na abundance with increasing meteoroid mass; nevertheless, the spread of values is large for each mass interval within the range of 10^{-6} to 3×10^{-4} kg. There is a hint that the average Na abundance is lower in the outlying parts of the shower, several days before maximum.

Discussion: The high Mg/Fe ratio suggests cometary origin of the Geminids. The depletion of Na was evidently caused by thermal desorption in the vicinity of the Sun. The large variations in Na abundance need, nevertheless, an explanation. One possibility is that the meteoroids are of different ages, i.e., that they were released from the parent body at different times. Younger meteoroids suffered less Na loss because they were shielded inside the parent body before their ejection. This scenario would imply that Phaeton was an active comet over a long period of time. Alternatively, if the period of activity was short, different depths of meteoroid material inside the parent body could perhaps explain the differences in the Na content. The study of the Quadrantid meteors showed that partial Na loss can occur also on the surface of the parent body [6].

Acknowledgements: This work was supported by GA CR grant no. 205/05/0543.

References: [1] Hsieh H. H. and Jewitt D. 2005. *The Astrophysical Journal* 624:1093–1096. [2] Ryabova G. O. 2006. *Proceedings of the International Astronomical Union* 229:229–247. [3] Borovicka J. 2006. *Proceedings of the International Astronomical Union* 229:249–271. [4] Borovicka J. et al. 2005. *Icarus* 174:15–30. [5] Borovicka J. 2005. *Earth, Moon, and Planets* 95:245–253. [6] Koten P. et al. 2006. *Monthly Notices of the Royal Astronomical Society* 366:1367–1372.

5014

SPATIAL HETEROGENEITY OF SHORT-LIVED AND STABLE ISOTOPES IN THE SOLAR NEBULA

A. P. Boss. Department of Terrestrial Magnetism, Carnegie Institution, 5241 Broad Branch Road NW, Washington, D.C. 20015, USA. E-mail: boss@dtm.ciw.edu

Introduction: The short-lived radioisotope (SLRI) ^{60}Fe must have been synthesized in a supernova [1] and then injected into the presolar cloud [2]. The same nucleosynthetic event is likely to have been the source of the bulk of the solar nebula's ^{26}Al . This injection occurred through narrow Rayleigh-Taylor (R-T) fingers [2] that peppered the solar nebula's surface with highly non-uniform doses of SLRIs. After the arrival of each R-T finger, the nebula must have been strongly spatially heterogeneous in terms of the abundances of those isotopes, possibly explaining some of the observed range of $^{26}\text{Al}/^{27}\text{Al}$ ratios. The wide range in stable oxygen isotope abundances, on the other hand, is attributed to self-shielding of molecular CO gas from UV photodissociation at the cool surface of the outer solar nebula [3] where water ice is stable. This scenario would thus lead to significant oxygen anomalies at the surface of the outer solar nebula, again a highly spatially heterogeneous starting point.

Results: Previous 3-D disk models [4] have shown that a marginally gravitationally unstable (MGU) disk of the type required to form gas giant planets is able to transport tracers over distances of ~10 AU in ~1000 yr, implying a similar time scale for mixing and an approach to spatial homogeneity. We quantify here the evolution of the dispersion of the abundance ratio (e.g., $^{26}\text{Al}/^{27}\text{Al}$) from its mean value at each time in these same models. Each injection event led to a high initial dispersion that decreased over a time scale of ~2000 yr and approached a steady state level of ~10% in these dynamically evolving, chaotic MGU disks.

Conclusion: Components of primitive meteorites have a scatter in initial $^{26}\text{Al}/^{27}\text{Al}$ ratios ranging from values of ~0 to $\sim 4.5 \times 10^{-5}$ or to even higher values ($\sim 7 \times 10^{-5}$; [5]). The scatter around the peak value [6] of $^{26}\text{Al}/^{27}\text{Al}$ ratios of $\sim 4.5 \times 10^{-5}$ is about 10%. This scatter is entirely consistent with the dispersion expected from spatial heterogeneity of injected SLRIs in the solar nebula. Such a low level of spatial heterogeneity implies that larger variations in initial $^{26}\text{Al}/^{27}\text{Al}$ ratios must be due primarily to temporal heterogeneity, preserving the role of SLRIs as accurate chronometers for the solar nebula. An ~10% level of heterogeneity is also roughly consistent with the preservation of oxygen isotope anomalies produced by self-shielding at the outer disk surface [3] followed by transport inward to regions of the disk where such anomalies could not have been sustained because disk surface temperatures were too high for stability of water ice. MGU disk models thus are capable of solving the puzzle of nebular spatial heterogeneity presented by SLRIs and oxygen isotope anomalies.

References: [1] Mostefaoui S., Lugmair G., and Hoppe P. 2005. *The Astrophysical Journal* 625:271–277. [2] Vanhala H. A. T. and Boss A. P. 2002. *The Astrophysical Journal* 575:1144–1150. [3] Lyons J. R. and Young E. D. 2005. *Nature* 435:317–320. [4] Boss A. P. 2004. *The Astrophysical Journal* 616:1265–1277. [5] Young E. D. et al. 2005. *Science* 308:223–227. [6] MacPherson G., Davis A. M., and Zinner E. K. 1995. *Meteoritics* 30:365–386.

5262

AMINO ACIDS AND POLYCYCLIC AROMATIC HYDROCARBONS IN METEORITES AND ICE SAMPLES FROM LA PAZ ICE FIELD, ANTARCTICA

O. Botta¹, Z. Martins², C. Emmenegger³, J. P. Dworkin¹, D. P. Glavin¹, R. P. Harvey⁴, R. Zenobi³, and P. Ehrenfreund². ¹Goddard Center for Astrobiology, NASA Goddard Space Flight Center, Greenbelt, Maryland 20771, USA. E-mail: Oliver.Botta.1@gssc.nasa.gov. ²Astrobiology Laboratory, Leiden Institute of Chemistry, RA 2300 Leiden, The Netherlands. ³Department of Chemistry and Applied Biosciences, ETHZ Höggerberg, 8093 Zürich, Switzerland. ⁴Department of Geology, Case Western Reserve University, Cleveland, Ohio 44106, USA

Introduction: We report on further progress on a systematic study of the contribution of amino acids and polycyclic aromatic hydrocarbons (PAHs) of Antarctic meteorites from terrestrial sources [1]. In order to investigate the relationship between the meteorite and its surrounding ice with respect to the organic composition, meteorite and ice samples were collected at the same time and location.

The meteorites samples LAP 03624 (LL5), LAP 03573 (LL5), LAP 03637 (LL5), LAP 03784 (CK5) were obtained from the NASA JSC Antarctic meteorite collection. For each specimen, one surface sample and three interior samples representing different distances from the surface were analyzed. The corresponding ice samples (~4 kg each) were collected during the 2003–2004 ANSMET expedition to the La Paz ice field, Antarctica.

Sample Preparation and Analysis: PAHs were analyzed using two-step laser mass spectrometry (L2MS) [2]. The meteorite chips were analyzed directly without further sample preparation. The ice samples were evaporated and filtered, and the extracted using PVC membranes. Both filters and membranes were analyzed with L2MS. Amino acids analysis was carried out by hot water extraction of a crushed meteorite samples followed by 6 M HCl hydrolysis and desalting. Evaporated ice samples were analyzed without acid hydrolysis. Detection and quantification was carried out using the LC-UVF-ToF-MS system at NASA GSFC [3].

Results and Discussion: The PAHs in the particulate matter shows extensive alkylation, indicating a terrestrial origin of these molecules. The PAH concentrations in the membrane extracts of the ice samples indicate concentrations of below 10–80 pg/l, depending on the concentration factors of the individual samples and the m/z signal. The L2MS spectra of the meteorites depict similar overall characteristics, although the signal intensities vary between the different specimens.

The concentration levels of the amino acids in the ice samples are found to be close to blank levels. However, some variability between the ice samples with regard to their amino acid composition could be observed. Most importantly, the signals corresponding to α -amino-isobutyric acid (AIB), an extremely rare compound on Earth, and its co-eluting homolog β -AIB were found to correspond to concentration levels between 1.5 ± 0.3 and 33.1 ± 10.6 ppt in four of the ice samples. No AIB could be detected in any of the meteorite samples. However, a new family of peaks of mass m/z 409 was detected that are not found in other Antarctic meteorites such or the ice samples.

References: [1] Botta O. et al. 2006. Abstract #1464. 37th Lunar and Planetary Science Conference. [2] Emmenegger C. et al. 2003. *Analytical Chemistry* 75:4508–4513. [3] Glavin D. P. et al. 2006. *Meteoritics & Planetary Science* 41:889–903.

5263

KINETIC FRACTIONATION OF NICKEL AND IRON BETWEEN KAMACITE AND TAENITE: INSIGHTS INTO COOLING RATES OF IRON METEORITES

B. Bourdon¹, G. Quitté¹, and A. N. Halliday². ¹IGMR, ETH Zurich, Switzerland. E-mail:bourdon@erdw.ethz.ch. ²Department of Earth Sciences, Oxford University, UK

Introduction: Fractionation of stable isotopes provides new insights into the differentiation processes of iron meteorites; in particular, stable isotopes are generally sensitive to crystallization, cooling and phase exsolution. Most iron meteorites are characterized by an intergrowth of two Fe-Ni alloys, Ni-poor kamacite and Ni-rich taenite. Here, we present Ni isotopic data for a whole set of iron meteorites from different groups, for sulfide inclusions, and for coexisting taenite and kamacite.

Results: It has been previously shown that iron meteorites display no anomaly in radiogenic ⁶⁰Ni [1]; all isotopes can therefore be used for studying mass dependent fractionation. All bulk metal phases show enrichment in heavy isotopes relative to the terrestrial standard, in good agreement with data reported by [2]. Variations of 0.3‰ per mass unit are observed. The range in Ni isotope composition is much wider for sulfides than for metals (2‰ per mass unit). In all magmatic iron meteorites, the sulfide yields a heavier Ni isotopic composition than the metal or a composition similar to the metal. We also observed that the Ni-poor kamacite is isotopically heavier than the Ni-rich taenite. Contrary results are obtained for Fe isotopes [3, 4].

Interpretation and Model: During cooling, the growth of kamacite exsolved from taenite depends on the diffusion rate of Ni from kamacite to taenite. The rate limiting parameter is in fact the Ni diffusion coefficient in taenite and the light Ni isotope is enriched in the taenite. We modeled this process over the temperature range 700–350 °C, with a temperature-dependent diffusion coefficient and a moving boundary between kamacite and taenite phases. Concentration profiles were calculated in the taenite for two Ni isotopes and the isotopic fractionation factor was then inferred. Input parameters for the model—such as the diffusion coefficient as a function of the Ni and P concentration, or the relative diffusion coefficients for two isotopes in the solid metal—are poorly constrained. However, we demonstrated that the precise cooling rate of the meteorite can be deduced from the isotopic fractionation measured between kamacite and taenite, once the diffusion coefficients are better determined. This kinetic process can also explain the Fe isotopic data: Fe isotopes are fractionated with an opposite sign relative to Ni because of the reverse diffusion fluxes. Such a diffusion-related mass dependent isotopic fractionation may also be responsible for the Ni fractionation between metal and sulfides.

References: [1] Quitté G. et al. 2006. *Earth and Planetary Science Letters* 242:16–25. [2] Moynier F. et al. 2005. Abstract #1593. 36th Lunar and Planetary Science Conference. [3] Poitrasson F. et al. 2005. *Earth and Planetary Science Letters* 234:151–164. [4] Williams H. et al. *Earth and Planetary Science Letters*. Forthcoming.

5348

EFFECTS OF IMPACTS ON SM-ND AND LU-HF INTERNAL ISOCHRONS OF EUCRITES

A. Bouvier^{1, 2}, J. Blichert-Toft², J. D. Vervoort³, and F. Albarède². ¹The University of Arizona, Department of Geosciences, USA. E-mail: abouvier@geo.arizona.edu. ²Ecole Normale Supérieure de Lyon, France. ³Washington State University, Pullman, Washington, USA

Eucrites are among the most ancient basalts of the solar system, thus bearing witness to its earliest episodes of planetary differentiation. Previous studies (i.e., [1–3]) have yielded scattered ages at 3.0–4.5 Ga, indicating that impacts may have disturbed the isotopic systems in these rocks. In order to shed new light on the apparent differences between terrestrial and meteoritic $\gamma^{176}\text{Lu}$ determinations [4–6], we examined the combined Sm-Nd and Lu-Hf isotope systematics in one cumulate (Moama) and five basaltic (Béréba, Bouvante, Juvinas, Millbillillie, and Stannern) eucrites. These samples yield relatively imprecise ages for whole-rock (WR) and internal (WR, pyroxene PX, and plagioclase PL) isochrons for both Sm-Nd and Lu-Hf systems. The WR isochrons yield a Sm-Nd age of 4559 ± 150 Ma and a Lu-Hf age of 4637 ± 86 Ma. Individual Sm-Nd and Lu-Hf internal isochrons also give imprecise ages. Of these, Moama and Juvinas yield Sm-Nd ages of 4520 ± 33 Ma and 4532 ± 53 Ma, respectively, and Millbillillie and Juvinas yield the least scattered Lu-Hf results, with ages of 4566 ± 93 Ma and an impossibly old 4697 ± 35 Ma, respectively, when using $\gamma^{176}\text{Lu} = 1.867 \times 10^{-11} \text{ y}^{-1}$ [7, 8].

The most probable explanation for these inconsistent results is open-system behavior in the eucrites. Sm-Nd and Lu-Hf data for the 6 PX-PL pairs do not consistently plot on their respective WR isochrons. The Sm-Nd PX data alone define two separate trends corresponding to 3.4 ± 0.5 Ga ($n = 4$) and 0.92 ± 0.06 Ga ($n = 2$), while the Lu-Hf PX data form a single trend corresponding to 3.8 ± 0.6 Ga ($n = 6$). We suggest that these ages correspond to two major episodes of bombardment in the solar system, both previously recognized on the basis of Rb-Sr and Ar-Ar chronometry of HEDs and chondritic meteorites [1, 3]. While the Lu-Hf isotope system appears to have been reset only during the first event, the Sm-Nd isotope system in some eucrites indicates two major events.

If we use the internal Lu-Hf isochrons for Millbillillie and Juvinas to determine $\gamma^{176}\text{Lu}$ by age comparison [9, 10], we obtain values of approximately 1.87×10^{-11} and $1.92 \times 10^{-11} \text{ y}^{-1}$, respectively. The former value is consistent with the terrestrial $\gamma^{176}\text{Lu}$ value [7, 8], while the latter is consistent with the extraterrestrial value [4–6]. The reasons for these complexities are not completely understood [11], but constraining the isotopic systematics of individual meteorites, such as these eucrites, will ultimately help explain the discrepancy between the terrestrial and meteoritic $\gamma^{176}\text{Lu}$ decay constant determinations.

References: [1] Birck J.-L. and Allègre C. J. 1978. *Earth and Planetary Science Letters* 39:37–51. [2] Tera F. et al. 1997. *Geochimica et Cosmochimica Acta* 61:1713–1731. [3] Bogard D. D. 1995. *Meteoritics* 30: 244–268. [4] Patchett P. J. and Tatsumoto M. 1980. *Nature* 288:571–574. [5] Blichert-Toft J. et al. 2002. *Earth and Planetary Science Letters* 204:167–181. [6] Bizzarro M. et al. 2003. *Nature* 421:931–933. [7] Scherer E. et al. 2001. *Science* 293:683–687. [8] Söderlund U. et al. 2004. *Earth and Planetary Science Letters* 219:311–324. [9] Miura Y. N. et al. 1998. *Geochimica et Cosmochimica Acta* 62:2369–2387. [10] Lugmair G. W. and Shukolyukov A. 1998. *Geochimica et Cosmochimica Acta* 62:2863–2886. [11] Albarède F. et al. 2006. *Geochimica et Cosmochimica Acta* 70:1261–1270.

5351

ELEMENTAL MAPS OF MARS FROM THE MARS ODYSSEY GAMMA-RAY SPECTROMETER

W. V. Boynton¹, R. C. Reedy², G. J. Taylor³, and the GRS team. ¹Lunar and Planetary Laboratory, The University of Arizona, Tucson, Arizona 85721, USA. E-mail: wboynton@lpl.arizona.edu. ²Institute of Meteoritics, MSC03-2050, University of New Mexico, Albuquerque, New Mexico 87131, USA. ³Hawai'i Institute of Geophysics and Planetology, University of Hawai'i, Honolulu, Hawai'i 96822 USA

Introduction: Gamma rays that were measured by an advanced Ge spectrometer on the polar-orbiting Mars Odyssey spacecraft [1] have been used to map the distribution of H, Si, Cl, K, Fe, and Th. These gamma rays are emitted from depths to tens of centimeters and are used to infer elemental abundances over footprints with radii of ~500 km or more.

Spectra from June 2002 have been accumulated, processed, and sorted into spatial bins. Many corrections are applied to the data. The final count rates for gamma rays from specific elements are compared to theoretical values to get elemental abundances. Only decay data are needed to model abundances for the naturally radioactive elements K and Th. Computer codes that model the production and transport of neutrons are needed for interpreting the measurements for other elements, with absolute abundances normalized to the silicon abundances measured by Mars Pathfinder [2]. To date for cosmic-ray-produced gamma rays, only regions within about 45° of the equator have been analyzed to avoid regions with high concentrations of H that complicate data analysis. Details on the data processing and many results and interpretations are in a series of papers to be published in *Journal of Geophysical Research*.

Elemental Results: The maps of elemental abundances for H, Si, Cl, K, Fe, and Th all show variations. There are two regions with high abundances of H (about 7% of hydrogen, equivalent to water) near the equator, in Arabia Terra and around Gusev crater. There is a region of low Si abundance west and south of Olympus Mons. Iron tends to be higher in the northern lowlands. Chlorine varies by a factor of ~4 with the highest values in the Medusae Fossae formation west of Tharsis. K and Th correlate well and vary by factors of ~5 and ~10, with most higher abundances in regions of the northern lowlands.

These elemental abundances show some spatial clustering. About 8 regions account for most of the variations [3, 4]. Except for K and Th, these elements do not have strong correlations among themselves. These element abundances do not correlate significantly with geology or other mapped data for Mars.

Future Work: The gamma rays for Ca, Al, S, and U are weak and often have interferences, but some elemental abundances should be obtainable. Analyses of spectra further poleward will involve modeling high H concentrations in wet layers below dry layers. Work will continue on mapping seasonal variations near the poles of enhancements of Ar in the atmosphere and thicknesses of the carbon dioxide caps.

References: [1] Boynton W. V. et al. 2004. *Space Science Reviews* 110: 37–83. [2] Wänke H. et al. 2001. *Space Science Reviews* 96:317–330. [3] Taylor G. J. et al. 2006. Abstract #1981. 37th Lunar and Planetary Science Conference. [4] Gasnault O. 2006. Abstract #2328. 37th Lunar and Planetary Science Conference.

5133

UNUSAL WEATHERING EFFECTS IN THE EL6 CHONDRITE NORTHWEST AFRICA 4282

F. Brandstätter and G. Kurat. Naturhistorisches Museum, Burgring 7, A-1010, Vienna, Austria. E-mail: franz.brandstaetter@nhm-wien.ac.at; gero.kurat@univie.ac.at

Introduction: NWA 4282 is a recently described EL6 chondrite that exhibits some unusual weathering features. One rock fragment (mass ~1.5 kg) purchased in Morocco was partly covered by a brownish-black to light brown crust. A cut through the fragment (polished plate) revealed that the crust has an average thickness of ~1–2 mm. Parallel to the surface and along cracks some brownish staining is visible. However, the interior of the meteorite consists of a light-grey to medium-grey groundmass and looks fresh without any indication of weathering. Surprisingly, it turned out that the apparently unweathered interior has weathering grade W5 [1].

Results: Microscopically, the overall texture of the meteorite is characterized by i) a strongly recrystallized silicate matrix with crystals of enstatite and plagioclase of about 20–200 μm in size, ii) the presence of numerous empty “holes” resulting in a porous appearance, iii) the low abundance of opaque phases which comprise mainly daubreelite, minor troilite and metal, iv) occurrence of relic chondrules and v) the absence of metal grains >10 μm in size and of other sulfides typical for EL chondrites such as oldhamite and alabandite, e.g., [2]. In places, a yellow-brownish, yet unidentified (Na, Cr, Fe) sulfate is present. This phase, apparently being a terrestrial alteration product, occurs as aggregates up to 200 μm in size. Compositions of enstatite (in wt%: <0.05 FeO, 0.2 CaO, 0.8 Al₂O₃) and plagioclase (Ab₈₂An₁₅Or₃) are quite similar to the composition of these phases reported for the Neuschwanstein EL6 chondrite [3]. Silicon contents of kamacite (1.2 wt% Si) are within the compositional range reported for equilibrated EL chondrites [4]. SEM investigations revealed that many enstatite crystals in the interior of the meteorite contain narrow (<10–20 μm) silica-bearing veins which are connected to each other. The veins have a “zig-zag” boundary to the surrounding enstatite host which apparently is the result of corrosion. Mostly, silica forms a seam attached to the enstatite whereas the central part of the veins is empty.

Discussion: The interior part of NWA 4282 has weathering grade W5 without exhibiting a corresponding Fe staining. This indicates an unusual weathering process for this meteorite. The presence of numerous empty holes and the low abundance of opaque phases, especially the lack of large metal grains and the absence of oldhamite and alabandite, suggest that these phases were dissolved and removed from the meteorite’s interior. The presence of silica-bearing veins in enstatite indicate that aqueous alteration of enstatite took place under acidic conditions—as is also supported by experiments [5] which revealed that only under acidic conditions enstatite alters to silica whereas under alkaline conditions phyllosilicates are formed. The missing Fe staining indicates metal dissolution at moderate O fugacity.

References: [1] Wlotzka F. 1993. *Meteoritics* 28:460. [2] Brearley A. J. and Jones R. H. 1998. *Planetary materials*. Washington, D.C.: Mineralogical Society of America. pp. 3-1–3-398. [3] Bischoff A. and Zipfel J. 2003. Abstract #1212. 34th Lunar and Planetary Science Conference. [4] Zhang Y. et al. 1995. *Journal of Geophysical Research* 100:9417–9438. [5] Ohnishi I. and Tomeoka K. 2005. Abstract. *Meteoritics & Planetary Science* 40:A118.

5361

EXPERIMENTAL HYDROTHERMAL ALTERATION OF KAINSAZ (CO3) UNDER ANOXIC CONDITIONS: CONSTRAINTS ON AQUEOUS ALTERATION IN CARBONACEOUS CHONDRITES

Adrian J. Brearley and Paul V. Burger. Department of Earth and Planetary Sciences, University of New Mexico, Albuquerque, New Mexico 87131, USA. E-mail: brearley@unm.edu

Introduction: To gain further insights into aqueous alteration processes that affected carbonaceous chondrites, we have carried out a series of hydrothermal experiments to investigate the alteration behavior of Kainsaz (CO3) under anoxic conditions. This study, carried out using uncrushed samples, extends our previous work using Allende [1] to protolith materials that contain significant amounts of Fe,Ni metal. Two sets of experiments have been performed at temperatures of 100 and 200 °C for time periods of 7, 28, 90, and 180 days. The experiments were carried out in Parr reaction vessels in an inert atmosphere of nitrogen. These conditions are much more reducing than our Allende experiments. Rather than being immersed in the aqueous fluid, the samples were suspended above the fluid reservoir and interacted with water vapor. After the experimental runs the samples were examined by optical microscopy, SEM, and TEM.

Results: Irrespective of experimental conditions, all the samples show evidence of alteration. The sample surfaces exhibit a red-brown coloration and crystals of white secondary phases are apparent on the sample surfaces. At both experimental temperatures and for all run times, SEM studies show that the dominant alteration phase on the sample surfaces are calcite grains with grain sizes ranging between 5–100 μm . There is no systematic variation in the grain size of the calcites as a function of run time or experimental temperature. The sample surfaces show variable development of bulbous to fibrous Fe oxide, whose abundance is a function of both temperature and run time. TEM studies of samples removed from the surfaces of the samples show that magnetite is present and also show that fine-grained fibrous phyllosilicates with compositions and d-spacings consistent with Mg-rich serpentine are common.

Discussion: Like our experiments using Allende, alteration occurs extremely rapidly even at 100 °C and the reaction products bear close similarities to those that occur in altered carbonaceous chondrites. However, there are notable differences compared with our Allende experiments, which we attribute to the more reducing conditions. In particular, Ca sulfates are absent in these new experiments, with carbonate dominating the alteration assemblage. This observation indicates that oxidation of sulfides in the protolith material has not occurred. In addition, the development of Mg-rich phyllosilicates on the sample surfaces appears to have occurred much more rapidly than in our Allende experiments. Although the experiments were carried out in the presence of water vapor rather than liquid water, the presence of abundant Ca carbonate on the sample surfaces indicates that mass transfer of soluble material was still highly effective. It seems probable that even under these conditions, a film of liquid water must still have been present along grain boundaries within the sample and possibly along the sample surfaces that acted as a mass transfer medium. Further characterization studies are in progress, but these data indicate that these experiments closely approximate the alteration assemblage found in CM chondrites.

References: [1] Jones C. L. and Brearley A. J. 2006. *Geochimica et Cosmochimica Acta* 70:1040–1058.

5365

TRACE ELEMENT ZONING IN CM CHONDRITE CARBONATES: INSIGHTS FROM COMPOSITIONAL MAPPING USING NANOSIMS

Adrian J. Brearley¹, Peter Weber², and Ian D. Hutcheon². ¹Department of Earth and Planetary Sciences, University of New Mexico, Albuquerque, New Mexico 87131, USA. E-mail: brearley@unm.edu. ²Lawrence Livermore National Laboratory, P. O. Box 808, L-231, Livermore, California 94551-0808, USA

Introduction: Carbonates have been widely recognized in CM carbonaceous chondrites and have the potential to constrain conditions and processes of aqueous alteration in this complex group of meteorites. SEM and CL studies show that carbonate grains in CM chondrites exhibit complex zoning that is a function of minor or trace element contents [1]. However, the distribution of minor and trace elements in these grains is not well understood. To address this problem, we have used the Cameca NanoSIMS at LLNL to study the distribution of a suite of trace elements (Mg, Mn, Fe, Cu, Ba, Sr, Pb, Cr) in calcite grains in the Y-791198 CM chondrite. We are particularly interested in the distribution of Mn in calcites for studies of the Mn-Cr systematics of CM carbonates to extend our previous work [1, 2].

Results: These studies have been highly successful at revealing complex trace element zoning in calcites that generally correlates well with the zoning observed by CL investigations. A common feature of many of the carbonate grains is the presence of distinct, localized regions within the grains that are enriched in Mn. These regions vary in size and shape, but are typically less than 5 μm in size and generally correlate reasonably well with regions of high CL. Without exception in the grains studied so far, the enrichments in Mn are never at the center of the grains, but are usually present in zones close to the grain edges. In several grains, Sr/Ca ratios are spatially anticorrelated with Mn/Ca ratios and many grains show an increase in the Sr/Ca ratio at their rims. In addition, in some grains we have observed distinct hot spots with extremely high Sr/Ca or Ba/Ca ratios, whose origin is currently obscure.

Discussion: The NanoSIMS trace element maps confirm that there is remarkable diversity in zoning behavior from one calcite grain to another. Although some grains appear to share common zoning characteristics (e.g., increased Sr at grain edges), many do not. We suggest that the diversity in zoning is a reflection of variations in the trace element chemistry of the fluid as a function of both space and time. We have recently suggested that some of the textural characteristics of CM chondrites, particularly the spatial distribution of carbonates and phosphates, could be explained by the presence of localized variations in fluid chemistry (i.e., microchemical environments)[3]. These variations in fluid chemistry are controlled by alteration reactions on a highly localized scale (tens of microns). The zoning in the carbonates appears to be compatible with such a scenario. In this model, specific trace elements are enriched in the fluid depending on what primary minerals are being altered locally at a particular time. Changes in fluid chemistry will occur as particular phases are consumed or trace elements are fractionated into new alteration phases.

References: [1] Brearley A. J. and Hutcheon I. D. 2002. Abstract. *Meteoritics & Planetary Science* 37:A23. [2] Brearley A. J. and Hutcheon I. D. 2000. Abstract #1407. 31st Lunar and Planetary Science Conference. [3] Brearley A. J. 2006. Abstract #2074. 37th Lunar and Planetary Science Conference.

5192

TEMPERATURE AND PRESSURE DEPENDENT FORMATION OF RINGWOODITE ALONG A MELT VEIN IN DAR AL GANI 650 (L6).

P. C. Buchanan¹, K. Wünnemann¹, and W. U. Reimold¹. ¹Museum für Naturkunde (Mineralogie), Humboldt-Universität, Invalidenstrasse 43, D-10115 Berlin, Germany. E-mail: Paul.Buchanan@museum.hu-berlin.de

Introduction: The L6 ordinary chondrite Dar al Gani 650 contains relatively thick (up to 1 mm) melt veins. During analysis by SEM and Raman spectroscopy, we identified a 5 μm wide layer of ringwoodite that runs along both edges of one of these veins for up to several mm. Such layers are also present along thinner veins that represent injection of melt from the main vein into surrounding host rock. These textures suggest that the olivine-ringwoodite transformation was controlled by increased temperature associated with the melt [see discussions in 1 and 2]. Kerschhofer et al. [3] determined that this transformation requires temperatures 900 °C and pressures 18 GPa. The present study is an attempt to use the width of these ringwoodite layers, the probable time available for transformation, and the thermal conductivity of olivine to determine the initial temperature of the melt.

Modeling of Impact: In order to estimate the time this chondritic material experienced pressures great enough to transform olivine to ringwoodite, we first modeled the pressure and temperature as a function of time at a point immediately below the crater formed by the impact of a 10 km diameter object on a much larger ordinary chondrite asteroid. Velocity of the impactor was assumed to be 10 km/s, and both impactor and target were approximated as dunite with 5% porosity. Maximum calculated shock pressure was slightly greater than 120 GPa (in contrast to [2], who assumed that maximum pressure was approximately 25 GPa). The time between completion of melting and decay of shock pressure to 18 GPa was approximately 1 s.

Modeling of Olivine-Ringwoodite Transformation: We used this time and the equation for conduction of heat from a vein through an olivine host [4] to determine the temperature within the vein required to develop a 900 °C isotherm 5 μm from the vein edge. Considering the lack of ringwoodite at significant distances from the veins, we assumed a host rock temperature of 500 °C [2]. Further, we ignored anisotropy of olivine thermal properties and, instead, used an average value for conductivity. These calculations suggest that the required temperature is close to 4800 °C. Considering the assumptions employed, this is relatively similar to the numerically calculated maximum temperature at the point below the crater (slightly under 4000 °C).

Conclusions: The high pressure and melt temperature suggested by these layers of ringwoodite indicate that these veins were principally formed by shock melting with minor or negligible influence of frictional melting. Large variations in temperature and pressure within short distances in these shocked chondritic materials emphasize the heterogeneous character of hypervelocity impact.

References: [1] Langenhorst F. and Poirier J.-P. 2000. *Earth and Planetary Science Letters* 184:37–55. [2] Sharp T. G. et al. 2003. Abstract #1278. 34th Lunar and Planetary Science Conference. [3] Kerschhofer L. et al. 2000. *Physics of the Earth and Planetary Interiors* 121:59–76. [4] Carslaw H. S. and Jaeger J. C. 1959. *Conduction of heat in solids*, 2nd ed. Oxford: Clarendon Press. 510 p.

5126

MAPPING METEORITE DISTRIBUTION AS A FUNCTION OF SOIL CHARACTERISTICS, CENTRAL OMAN DESERT

J. Bühler¹, E. Gnos¹, B. A. Hofmann², A. J. T. Jull³, and A. Al-Kathiri⁴.
¹Institut für Geologie, Universität Bern, Baltzerstrasse 1, CH-3012 Bern, Switzerland. E-mail: 2B-WAVE@schweiz.com. ²Naturhistorisches Museum der Burggemeinde Bern, Bernstrasse 15, CH-3005 Bern, Switzerland. ³NSF–University of Arizona Accelerator Mass Spectrometer Laboratory, The University of Arizona, 1118 East Fourth Street, Tucson, Arizona 85721, USA. ⁴Directorate General of Commerce and Industry, Ministry of Commerce and Industry, Salalah, Sultanate of Oman

Introduction: During the fourth Omani-Swiss meteorite search campaign in 2005, two target areas of ~20 km² each were selected for detailed mapping of rock and soil types in order to test influences of surface types on meteorite abundance and to date young geological deposits with meteorites.

Mapping Area 1: This area is centered about 15 km E of Haima at 20°0'N, 56°24'E. Surfaces are characterized by soils consisting of cm-size limestone fragments mixed with wind-blown silt, with shallow outcrops of limestone belonging to the Early to Middle Miocene Dam formation in between. Mapping area 1 is characteristic for typical meteorite recovery areas in the central Oman deserts.

Mapping Area 2: This area is located 50 km east of Ghaba centered at 21°20'N, 57°45'E. It is located on alluvial fans derived from the Oman Mountains with surfaces consisting of relatively dark gravel with more fine-grained areas between channels. This area is also characterized by a relief inversion (channels facies modelled out to elongated hills). The age of the alluvial fan sediments assigned to the Barzaman formation is uncertain (Pliocene/Pleistocene). Here we wanted to test the idea to date sediments indirectly by obtaining terrestrial ages of meteorites that fell on them.

Meteorite Finds, Area 1: >100 meteorites (not corrected for pairing) were found in and near the mapping area, including overlapping strewn fields of a mesosiderite and of a Rumuruti chondrite. The process of classification of all finds and sorting out pairings is still in progress. Meteorite find locations are generally correlated with the less sandy areas.

Meteorite Finds, Area 2: Mapping area 2 yielded only a single 7 kg LL meteorite. Due to the predominance of dark-colored rocks systematic searches are very difficult, and surface dating with meteorites depends on accidental finds. The low ¹⁴C age of 6.3 ± 1.3 kyr of the single find only puts a lower limit to the age of the formation.

Conclusions: The combination of satellite image based mapping of soil surfaces with a systematic search for meteorites is found very promising to better understand the processes of meteorite accumulation on the desert surfaces in Oman. Whether this approach will allow predictions about the meteorite abundance on certain surfaces will be a subject of testing during future searches.

5088

HIGH-PRECISION ⁴⁰Ar-³⁹Ar DATING OF DIFFERENT RUMURUTI LITHOLOGIES

A. I. Buikin^{1,2}, M. Trieloff¹, E. V. Korochantseva^{1,2}, J. Hopp¹, J. Berlin^{3,4}, and D. Stöffler⁴. ¹Mineralogisches Institut, Ruprecht-Karls-Universität Heidelberg, Im Neuenheimer Feld 236, D-69120 Heidelberg, Germany. ²Vernadsky Institute of Geochemistry, Kosygin St. 19, 119991 Moscow, Russia. ³Department of Earth and Planetary Sciences, University of New Mexico, Northrop Hall, Albuquerque, New Mexico 87131, USA. ⁴Museum für Naturkunde, Invalidenstr. 43, 10115 Berlin, Germany

R chondrites have highly oxidized mineral assemblages [1, 2] and contain, with decreasing abundance, olivine, plagioclase, Ca-rich pyroxene, low-Ca pyroxene, minor phases such as pyrrhotite, pentlandite, chromian spinel, and traces of metallic FeNi. Most R chondrites are light/dark structured regolith breccias consisting of highly recrystallized fragments as well as unequilibrated lithologies and contain solar-wind-implanted rare gases [3]. The meteorite Rumuruti is the only fall of the highly oxidized R chondrite group. Previous studies performing ⁴⁰Ar-³⁹Ar dating on Rumurutiites yielded complex age spectra disturbed by both diffusive ⁴⁰Ar loss and ³⁹Ar recoil redistribution [4]. This hampers conclusions on the early thermal history of Rumuruti and its parent body. Realizing that Rumuruti is a complex breccia containing fragments of petrologic type 3, 4, 5, and 6 and “shock-blackened” [5] lithologies, we applied ⁴⁰Ar-³⁹Ar dating to different lithologies. A light clast of type 5/6 (Rumuruti B), a sample of clastic matrix type 3.8 (Rumuruti C), and a type 3 clast (Rumuruti A).

The age spectra show partial degassing and diffusive ⁴⁰Ar loss as low apparent ages in the first argon extractions, plateau segments and age drop-offs at high degassing temperatures due to ³⁹Ar recoil redistribution into pyroxene and/or olivine. The disturbing features increase in the order Rumuruti B → C → A and correlate with decreasing grain size of plagioclase (glass) which is the major carrier of K and radiogenic ⁴⁰Ar. In fragments of petrologic type 3, feldspar-normative glass can be found within chondrules and also in the fine-grained, porous matrix. In type 4 plagioclase crystals form large isolated intergrowths (up to 200 μm) which seem to develop into networks in type 5 and 6. The feldspars of type 4, 5, and 6 have a composition of Ab₇₄₋₉₀An₅₋₂₃Or₂₋₉. Age plateaus are best preserved for the coarse grained equilibrated type 5/6 lithology, defining an age of 4.53 ± 0.01 Ga. We interpret the different lithologies to have the same thermal history, but with different response to thermal events due to different plagioclase (glass) grain size. This implies a very short metamorphic history of the R chondrite parent body and very early breccia formation, probably within a few Ma after R chondrite parent body formation.

References: [1] Schulze H. et al. 1994. *Meteoritics* 29:275–286. [2] Kallemeyn G. W. et al. 1996. *Geochimica et Cosmochimica Acta* 60:2243–2256. [3] Weber H. W. and Schultz L. 2001. Abstract #1500. 32nd Lunar and Planetary Science Conference. [4] Dixon E. T., Bogard D. D., and Garrison D. H. 2003. *Meteoritics & Planetary Science* 38:341–355. [5] Stöffler D. et al. 1991. *Geochimica et Cosmochimica Acta* 55:3845–3867.

5254

PETROLOGY AND COMPOSITION OF LUNAR FELDSPATHIC BRECCIAS NWA 2995, DHOFAR 1180 AND DHOFAR 1428

T. E. Bunch¹, J. H. Wittke¹, and R. L. Korotev². ¹Department of Geology, Northern Arizona University, Flagstaff, Arizona. E-mail: tbear1@cableone.net. ²Earth and Planetary Sciences, Washington University, St. Louis, Missouri

A feldspathic breccia from Algeria and two mingled highlands + mare lunar breccias found recently in Oman bring the total number of unpaired lunar meteorites to more than 40.

Northwest Africa 2995 is a very fresh feldspathic fragmental breccia that contains many highlands fine-grained lithologies: norite (orthopyroxene $Fs_{26.4}Wo_4$, FeO/MnO = 66), olivine basalt (olivine $Fa_{87.2}$, FeO/MnO = 95; plagioclase $An_{84.7}$), subophitic basalt (augite $Fs_{25-48}Wo_{37.1-25.9}$; pigeonite $Fs_{27.8-31.7}Wo_{15.4-9.3}$, FeO/MnO = 53; olivine $Fa_{36.3}$, FeO/MnO = 90; plagioclase An_{97}), gabbro (olivine $Fa_{34.7}$, FeO/MnO = 95; pigeonite $Fs_{28.2}Wo_{8.9}$, FeO/MnO = 67; plagioclase An_{94}), KREEP-like basalt (plagioclase $Ab_{50}Or_{17.4}$; K-feldspar $Ab_{14.3}Or_{83.6}$; silica, phosphate and Fe-rich pyroxenes), troctolite (olivine $Fa_{30.8}$, FeO/MnO = 94; plagioclase $An_{94.7}$), granulitic impact melts (olivine Fa_{31} ; orthopyroxene $Fs_{25.2}Wo_{3.4}$; plagioclase An_{95}); anorthosite ($An_{92.7-96.8}$), glassy impact melts, coarse-grained mineral fragments, and a 0.35 mm-size grain of meteoritic NiFe metal (Ni = 6.3 wt%, Co = 1.0 wt%).

Dhofar 1180 and Dhofar 1428 are clast-rich, crystalline melt breccias that do not appear to be paired stones. Dhofar 1180 is largely populated with anorthositic lithologies, including ferroan anorthosite (plagioclase An_{95} with up to 1.1 wt% FeO), anorthositic gabbro (olivine Fa_{39} , FeO/MnO = 96–101), norite (olivine Fa_{18}), troctolite, minor amounts of ophitic to subophitic basalts (evidently with mare affinities) and impact melt breccias. Dhofar 1428 is dominated by plagioclase and xenolithic breccia clasts with subordinate amounts of norite (olivine Fa_{36} , FeO/MnO = 104; plagioclase $An_{96.4}$; orthopyroxene $Fs_{28.4}Wo_{4.1}$, FeO/MnO = 51), troctolite (plagioclase $An_{95.5}$; olivine $Fa_{25.8}$, FeO/MnO = 89), and subophitic basalts that contain highly zoned pyroxenes ($Fs_{14.9}Wo_{5.1}$ to $Fs_{41.2}Wo_{15.2}$).

Bulk Compositions: Dhofar 1180 contains 22.6 wt% Al_2O_3 , 9.3 wt% FeO and 0.9 ppm Th, and plots at the feldspathic end of the field for mingled highlands + mare lunar breccias [1]. It does not appear to be paired with any other of the known Omani lunar meteorites, and shows compositional similarities to Calalong Creek and Yamato-983885, but with a lower bulk Mg/Fe ratio and lower concentrations of incompatible elements. Analyses of NWA 2995 and Dhofar 1428 are in progress.

References: [1] Korotev R. L. 2005. *Chemie der Erde* 65:297–346.

5252

NORTHWEST AFRICA 2968: A DUNITE FROM 4 VESTA

T. E. Bunch¹, J. H. Wittke¹, D. Rumble III², A. J. Irving³, and B. Reed. ¹Department of Geology, Northern Arizona University, Flagstaff, Arizona, USA. E-mail: tbear1@cableone.net. ²Geophysical Laboratory, Carnegie Institution, Washington, D.C. ³Department of Earth and Space Sciences, University of Washington, Seattle, Washington, USA

Discovery: A total of 268 grams of blocky, dark brown fragments (17–25 mm across) collected by nomads in Algeria in 2004 appear to be from the first recognized coarse-grained olivine-rich rock with affinities to the HEDO meteorites.

Petrography: The original grain size is unknown because of a tendency to fracture on curved to linear compression and shear fractures subparallel to one of the extinction directions in olivine, but it must have been in excess of 20 mm. Olivine ($Fa_{7.5±0.2}$; FeO/MnO = 48; both Cr_2O_3 and NiO < 0.03 wt%) is predominant (>95 vol%), and exhibits large domain offset, isolated mosaicism and undulatory extinction. Tiny grains (<0.03 mm) of orthopyroxene ($Fs_{6.7}Wo_{1.5}$, FeO/MnO = 26), metal (kamacite, Ni = 4.7–6.8; taenite, Ni = 39.1–50.7 wt%), troilite (Ni = 0.36 wt%) and pyrrhotite (Ni = 1.7–4.7 wt%) occur commonly within fractures (see BSE image below) and as rare inclusions.

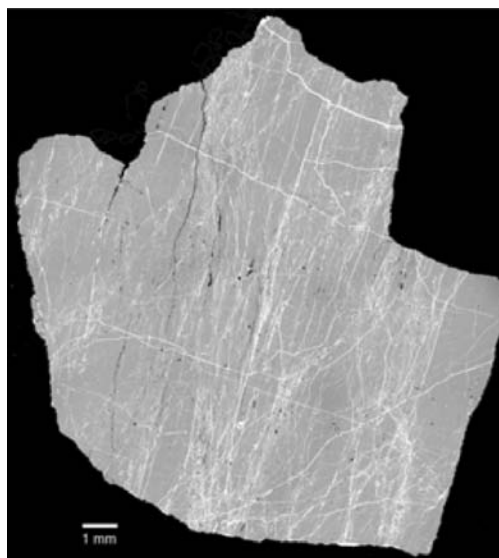


Fig. 1.

Oxygen Isotopic Composition: Replicate analyses of an acid-washed and metal-free sample by laser fluorination gave, respectively: $\delta^{17}O = +1.44$, $+1.48$, $\delta^{18}O = +3.08$, $+3.22$, $\Delta^{17}O = -0.178$, -0.212 per mil (for $m_{TFL} = 0.526$).

Conclusions: On the basis of FeO/MnO ratios [1] and oxygen isotopic compositions [2], NWA 2968 has affinities with the HEDO meteorites and by inference 4 Vesta. Olivine is much more magnesian than in the six known olivine diogenites (Fa_{28-36} [3]), and thus NWA 2968 may represent a cumulate from a very primitive Vestan magma.

References: [1] Papike J. et al. 2003. *American Mineralogist* 88:469–472. [2] Wiechert U. et al. 2004. *Earth and Planetary Science Letters* 221: 373–382; Greenwood R. et al. 2005. *Nature* 435:916–918. [3] Irving A. et al. 2003. Abstract #1502. 36th Lunar and Planetary Science Conference. Irving A. et al. 2005. Abstract #2188. 36th Lunar and Planetary Science Conference.

5301

HOW DOES THE MINERALOGY OF VESTOIDS VARY WITH EJECTION VELOCITY FROM 4 VESTA?

T. H. Burbine¹, R. P. Binzel², P. C. Buchanan³, T. J. McCoy⁴, J. M. Sunshine⁵, and A. S. Rivkin⁶. ¹Department of Astronomy, Mount Holyoke College, South Hadley, Massachusetts 01075, USA. E-mail: tburbine@mholyoke.edu. ²Department of Earth, Atmospheric, and Planetary Sciences, Massachusetts Institute of Technology, Cambridge, Massachusetts 02139, USA. ³Museum für Naturkunde (Mineralogie), Humboldt-Universität, Invalidenstrasse 43, D-10115 Berlin, Germany. ⁴Department of Mineral Sciences, National Museum of Natural History, Smithsonian Institution, Washington, D.C. 20560-0119, USA. ⁵Department of Astronomy, University of Maryland, College Park, Maryland 20742, USA. ⁶Johns Hopkins University Applied Physics Laboratory, Laurel, Maryland 20723, USA

Introduction: Vestoids [1] are relatively small objects, usually with estimated diameters of 10 km or less, that have reflectance spectra similar to the ~500 km-diameter asteroid 4 Vesta and the HEDs (howardites, eucrites, and diogenites). Approximately seventy vestoids have been identified in the main belt and approximately fifteen in the near-Earth asteroid population on the basis of visible and/or near-infrared reflectance spectra.

Near-infrared spectra of vestoids taken using the SpeX instrument at the NASA Infrared Telescope Facility (IRTF) allow for average pyroxene mineralogies to be estimated for these objects [2] since the SpeX spectra encompass both the 1 and 2 μm absorption features. SpeX spectra have currently been obtained on Vesta, fifteen main-belt vestoids, and nine near-Earth vestoids. These spectra are currently being analyzed to try to determine their mineralogies and the minimum ejection velocities from Vesta needed for these objects to reach their present orbits.

Method: Minimum theoretical ejection velocities are calculated from the escape velocity (~360 m/s) needed to escape Vesta's gravitational field and the estimated minimum velocity needed to change the vestoid's orbital elements from Vesta's orbital elements [3]. Possible compositional trends versus ejection velocity from Vesta will be identified by looking at variations in the wavelength positions of the 1 and 2 μm band minima and calculated relative abundances of low- and high-Ca pyroxenes, which can be estimated using Modified Gaussian Modeling (MGM) [4, 5]. No trend may exist since cratering studies [6] have found that the largest fragments ejected at any velocity are spalls that originate from the target planet's surface. The mineralogy of the km-size Vestoids would then be only a function of where on Vesta's surface that they originated from.

Results: Approximately 90% of observed main-belt vestoids have calculated ejection velocities from Vesta of ~1 km/s or smaller. A few vestoids have ejection velocities between 1 and 2 km/s. Excluding 1459 Magnya, which is located at 3.15 AU, the only known vestoid with a minimum ejection velocity from Vesta greater than 2 km/s is 1468 Zomba (2.20 AU). We are currently determining if the composition of the vestoids varies with minimum ejection velocity from Vesta and if all vestoids have mineralogies consistent with being derived from Vesta.

References: [1] Binzel R. P. and Xu S. 1993. *Science* 260:186–191. [2] Kelley M. S. et al. 2003. *Icarus* 165:215–218. [3] Zappalà V. et al. 1996. *Icarus* 124:156–180. [4] Sunshine J. M. et al. 1990. *Journal of Geophysical Research* 95:6955–6966. [5] Sunshine J. M. and Pieters C. M. 1993. *Journal of Geophysical Research* 98:9075–9087. [6] Melosh H. J. 1984. *Icarus* 59: 234–260.

5081

THERMOMETRY OF LANDES SILICATE INCLUSIONS AND ACAPULCOITES BASED ON IN SITU TRACE ELEMENT ANALYSES

C. Burkhardt, G. Witt-Eickschen, and H. Palme. Institut für Geologie und Mineralogie, Zülpicherstr. 49b 50674 Köln. E-mail: christoph.burkhardt@uni-koeln.de

Trace elements in ol, opx, cpx, and plag from the Landes IAB silicate-inclusions (La-sil-inc) and two acapulcoites, Acapulco and Dhofar 125 were determined by LA-ICP-MS (ANU-Canberra), major elements by electron microprobe. Results are compared with corresponding data on terrestrial spinel-peridotites (sp-per) [1], equilibrated at temperatures ranging from 1145 K to 1489 K (calculated at an assumed pressure of 15 kbar with the Ca-in-opx thermometer). The mineral chemistry of meteorite assemblages is with fa4 to fa11 and equilibration temperatures of 1170 K to 1230 K, as determined by Ca in opx-cores (<1 kbar), very similar to that of sp-per. acapulcoites and sil-incl in IABs differ from sp-per in having plag, metal and low Al in opx and cpx.

Cpx/opx ratios of Ga, Y, Yb and Lu are similarly good temperature indicators in the meteorites as in sp-per. The cpx/opx ratios of Zr, Hf, Sc and V are higher in meteorite samples than in the sp-per, probably caused by lower Al in the meteoritic opx. Minor Ca-zoning in opx and Ca-in-olivine temperatures of ~910 K in the equilibrated meteorites reflect slow cooling [2], in contrast to the sp-per samples analyzed by [1] where zoning is absent.

The distributions of trace elements among mineral phases are apparently independent of pressure. This is also true for ol/opx ratios of Fe, Ni, Co, and Ga, which are very similar in sp-per and Acapulcoites, despite 300 times lower Ni in meteoritic olivine, confirming the validity of Henry's law of up to 0.4% Ni in ol. In La-sil-incl all four elements are lower in ol than predicted by the sp-per data, reflecting decreasing $f\text{O}_2$ with cooling and simultaneous diffusion of Fe, Ni, Co, and Ga from olivine into metal. Lower FeO than expected from opx-ol equilibrium distribution [3] is typical of many sil-incl in IAB iron meteorites [4]. The late reducing event in IABs could be the result of collisional disruption of the IAB-parent body. If $f\text{O}_2$ in IAB silicate inclusions is determined by the C-CO-CO₂ buffer a sudden pressure release caused by the disruption would lead to a strong decrease in $f\text{O}_2$ [5].

References: [1] Witt-Eickschen G. and O'Neill H. St. C. 2005. *Chemical Geology* 221:65–101. [2] Köhler T. et al. 1991. *Neues Jahrbuch Mineralogie Monatshefte* H9:423–431. [3] von Seckendorff V. and O'Neill H. St. C. 1993. *Contributions to Mineralogy and Petrology* 113:196–207. [4] von Seckendorff V. et al. 1992. *Meteoritics* 27:288. [5] Brett R. and Sato M. 1984. *Geochimica et Cosmochimica Acta* 48:111–120.

5270

THE SOLAR WIND FE/MG RATIO

D. S. Burnett¹, A. J. G. Jurewicz², Y. Guan², D. S. Woolum³, and K. McKeegan⁴. ¹Geological and Planetary Sciences, Caltech, Pasadena, California, 91125, USA. ²Department of Geology, Arizona State University, Arizona, USA. ³Department of Physics, California State University, Fullerton, California, USA. ⁴Department of Earth and Space Sciences, University of California–Los Angeles, Los Angeles, California, USA

To meet the Genesis mission goal for improved solar elemental abundances, we need to address the issue of fractionation of the abundances of elements in the solar wind compared to the solar photosphere. There is a well-established depletion of elements in the solar wind with high first ionization potential (FIP > 9eV) compared to lower FIP elements, but there is no evidence for fractionation between lower FIP elements.

Using secondary ion mass spectrometry, we have measured the fluences of Fe and Mg for the “bulk” collector of the Genesis mission. Excellent solar wind depth profiles were obtained for Fe in diamond-like-carbon collector materials. Reasonable fluence agreement is found in replicate analyses among different samples. Integration of the depth profiles and comparison with an implant standard of known fluence yields an Fe fluence of $1.4 \times 10^{12}/\text{cm}^2$.

Excellent depth profiles for Mg in diamond-like-C are also obtained, but there are problems with fluence reproducibility, so at present, we base a Mg fluence on profiles measured in Si substrates. The profiles at shallow depths (<40 nm) appear to depend on whether a low pressure O₂ flood is used. Although additional study is required, the O₂ flood appears to significantly reduce problems due to Mg surface contamination. However, at depths than about 40 nm the flood and no-flood profiles are in good agreement, as are the derived fluences. Fourteen profiles in four different Si samples are consistent with a Mg fluence of $1.8 \times 10^{12}/\text{cm}^2$.

Thus, the present Genesis solar wind Fe/Mg ratio is 0.78, which is in good agreement with both spacecraft data and the abundance ratio derived from photospheric absorption line spectra. Our ultimate goal is to obtain Genesis abundance ratios accurate to ~5% two sigma for major elements, whose photospheric abundances are also well known.

5384

SPECTRO-DYNAMICAL ASTEROID FAMILIES

S. J. Bus. University of Hawai'i, Institute for Astronomy, Hilo, Hawai'i 96720, USA. E-mail: sjb@ifa.hawaii.edu

Asteroid families are normally identified through similarities in proper orbital elements that are shared among the members of each family. It is commonly believed that asteroid families consist of remnants from the collisional disruptions of once larger parent bodies, and thus the members of each family should be genetically related, and their range in compositions should make cosmochemical sense.

Recent studies have tested the genetic reality of dynamical asteroid families through analyses of the spectral reflectance colors or taxonomic classifications of family members [1, 2]. While these studies have typically reported significant similarities in color between members of each family, these results are somewhat limited by their reliance on family memberships defined solely on orbital elements.

A new method of searching for asteroid families was proposed that combines both orbital and spectral information as part of the clustering process [3]. The initial application of this procedure focused on families in the middle of the main belt, using visible-wavelength spectra for 465 asteroids with semi-major axes between 2.7 and 2.8 AU. We now extend this method to cover the entire main belt, utilizing data for 2074 asteroids obtained during three major spectroscopic surveys: the first and second phases of the Small Main-belt Asteroid Spectroscopic Survey (SMASS) [4, 5] and the Small Solar System Objects Spectroscopic Survey (S3OS2) [6].

The clustering algorithm involves identifying pairs of objects with small differences (dissimilarities) in both orbital element and spectral component spaces. The well-established dynamical families are all confirmed using this approach, and several new families have been identified.

Results: The combination of both orbital and spectral information in the search for asteroid families has several advantages over previous studies that focus primarily on the distributions of orbital elements. By including spectral parameters in the cluster analysis, boundaries of known families can be more accurately determined, close or overlapping families in orbital element space can be separated, interlopers can be identified, and older, more diffuse families that might otherwise be missed can now be recognized. Preliminary results from this work show that, aside from variations in spectral slope, nearly every family appears to be spectrally homogeneous. There is no indication that we have sampled different lithologies within a single family that might be attributed to layering of a differentiated body (iron core, olivine-rich mantle, silicate crust). These results will help place important constraints on collisional models and on the processes of family formation.

References: [1] Ivezić Z. et al. 2002. *The Astronomical Journal* 124: 2943–2948. [2] Mothe-Diniz T. et al. 2005. *Icarus* 174:54–80. [3] Bus S. J. 1999. Ph.D. thesis, MIT, Cambridge, Massachusetts, USA. [4] Xu S. et al. 1995. *Icarus* 115:1–35. [5] Bus S. J. and Binzel R. P. 2002. *Icarus* 158:106–145. [6] Lazzaro D. et al. 2004. *Icarus* 172:179–220.

5327

CORRELATED ANALYSES OF D- AND ¹⁵N-RICH CARBON GRAINS FROM A CR2 CHONDRITE EET 92042

H. Busemann¹, C. M. O'D. Alexander¹, L. R. Nittler¹, T. J. Zega², R. M. Stroud², S. Baji³, G. D. Cody⁴, and H. Yabuta⁴, ¹DTM, Carnegie Institution of Washington, Washington, D.C., USA. ²Naval Research Laboratory Washington, D.C., USA. ³Lawrence Livermore National Laboratory, Livermore, California. ⁴GL, Carnegie Institution of Washington, Washington D.C., USA. E-mail:busemann@dtm.ciw.edu

Introduction: Insoluble organic matter (IOM) and matrix from primitive carbonaceous chondrites carry isotope enrichments ($\delta D \leq 20000\%$, $\delta^{15}N \leq 3200\%$) that are comparable to those in interplanetary dust particles [1, this work]. Hence, primitive organics that formed in the protosolar cloud (PSC)—or maybe in the cold outer regions of the protoplanetary disk—survived accretion and planetary processing on the asteroids, the parent bodies of the chondrites. Most D and ¹⁵N anomalies are spatially uncorrelated, indicating that distinct processes produced them. While various reactions in the PSC can account for the D enrichments [2], the ¹⁵N anomalies cannot be explained by existing models [3]. Alternative mechanisms, possibly within the solar system [4], have to be considered. Identifying the isotopically anomalous carriers will help to understand the earliest evolution of organic matter from PSC to the solar system.

Results: SIMS analyses of CR2 chondrite Elephant Moraine (EET) 92042 IOM [5] revealed two isotopically anomalous, micron-size discrete carbon grains (“A” with $\delta^{13}C \sim -113\%$ and $\delta^{15}N \sim 1150\%$; “B” with $\delta D \sim 6000\%$, Fig. 1). Grains and intermediate IOM ($\delta D \sim 2200\%$) were thinned and extracted by FIB-SEM [6] and examined by transmission electron microscopy (Fig. 1). EDS and electron diffraction patterns show that all analyzed matter is C-rich and amorphous. ¹⁵N-rich grain A is monolithic C with trace Si; D-rich grain B is porous organic C with traces of Si and S. The intermediate IOM is also porous organic C and contains nm-size Fe-Ni, chromite and Ca-rich grains. C- and N-XANES spectroscopy proves the hydro-carbonaceous, non-graphitic character of the IOM and indicates distinct N bonding states for grains A and B. On-going EELS, NanoSIMS, and synchrotron IR micro-spectroscopic analyses will characterize the isotopic compositions of additional elements, and the chemical structural variation and bonding states of the C-bearing molecules.

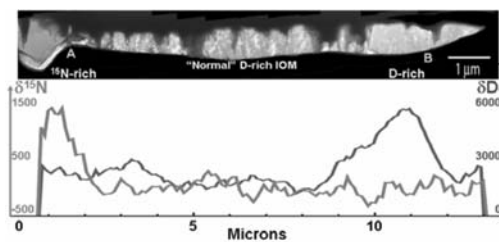


Fig. 1.

Acknowledgements: Part of this work was performed under the auspices of the U.S. DoE by the University of California Lawrence Livermore National Laboratory under contract No. W-7405-ENG-48. The Advanced Light Source is supported by the Director, Office of Science, Office of Basic Energy Sciences, Materials Sciences Division, of the U.S. DoE under contract No. DE-AC03-76F00098 at Lawrence Berkeley National Laboratory.

References: [1] Busemann H. et al. 2006. *Science* 90:1151–1154. [2] Sandford S. A. 2001. *Meteoritics & Planetary Science* 36:1117–1133. [3] Charnley S. B. and Rodgers S. D. 2002. *The Astrophysical Journal* 569: L133–L137. 27th Lunar and Planetary Science Conference. [4] Marty B. 2006. *Science* 90:706–707. [5] Busemann H. et al. 2006. Abstract #2005. 37th Lunar and Planetary Science Conference. [6] Zega T. J. and Stroud R. M. 2006. Abstract #1441. 37th Lunar and Planetary Science Conference.

5141

CONSTRAINING THE Pu/U RATIO OF THE EARLY SOLAR SYSTEM

A. Busfield, S. Crowther, G. Turner and J. D. Gilmour SEAES, University of Manchester, Manchester M13 9PL, UK. E-mail: a.busfield@manchester.ac.uk

Introduction: The initial Pu/U ratio of the solar system is an important parameter in models of nucleosynthesis, cosmochronology and development of the terrestrial mantle and atmosphere. Previous estimates of this ratio are based on analyses of the St. Severin chondrite and the angrite Angra dos Reis. Results are poorly constrained, ranging from 0.004 to 0.008. Estimation of this parameter for the Earth is complicated by the short half-life of ²⁴⁴Pu (82 Ma), meaning it was effectively extinct by 3.9 Ga ago. Ancient detrital zircons from Jack Hills, Australia are up to 4.4 Ga in age, providing a possible window on the Hadean Earth when ²⁴⁴Pu was still live and providing an opportunity to determine the initial Pu/U ratio. We have previously reported analyses of fission xenon in individual zircons ranging in age from 4.1–4.2 Ga, which showed evidence for plutogenic xenon [1]. The (Pu/U)₀ inferred from these results varied from essentially zero to 0.0066 for individual zircons, indicating either metamorphic loss of Xe or igneous fractionation of Pu and U. Here we report results from a larger zircon suite and address the question of Xe loss.

Experimental: Individual zircons are minute, weighing only a few micrograms, and as such the expected amount of xenon in these grains is only $\sim 10^{-15}$ cc STP. In order to measure this Xe we have utilized the highly sensitive RELAX laser resonance ionization mass spectrometer. To investigate Xe loss, 17 zircons were neutron-irradiated to generate fission xenon from ²³⁵U. Measurement of ¹³¹Xe/¹³⁴Xe and ¹³²Xe/¹³⁴Xe ratios allows us to calculate the relative contributions from spontaneous fission of ²⁴⁴Pu and ²³⁸U and neutron fission of ²³⁵U and hence compare Pu/U and Xe retention ages.

Results: Measured Pu/U ratios (back calculated to 4.56 Ga on the basis of Pb-Pb ages) range from zero to 0.012. U-Xe ages indicate that xenon loss is common and occurred typically between 3 and 4 Ga ago. It has been suggested that LREE, such as Nd [2], and Pu behave similarly during fractionation. We are currently attempting to investigate the additional effects of geochemical fractionation of Pu from U by comparing Xe isotopes with REE/U abundance ratios.

References: [1] Turner G, Harrison T. M., Mojzsis S., Holland G, and Gilmour J. 2004. *Science* 306:89–91. [2] Jones J. H. 1982. *Geochimica et Cosmochimica Acta* 46:1793–1804.

5010

THERMODYNAMIC MODELING OF PRECIPITATION OF Fe-Ni METAL IN SUPER-LIQUIDUS CHONDRITIC SYSTEMS

K. A. Bychkov¹, A. A. Ariskin², and A. A. Borisov³. ¹Division of Geology, Moscow State University, Vorob'evy gory, Moscow, 119992, Russia. E-mail: kbs@na.ru. ²Vernadsky Institute of Geochemistry and Analytical Chemistry, Kosygin Str. 19, Moscow, 119991, Russia. ³Institute of Geology of Ore Deposits, Petrography, Mineralogy and Geochemistry, Staromonetnyi Str. 35, Moscow, 109017, Russia

Introduction: In the scope of our efforts to include the metallic phase into computer models simulating the melting-crystallization relationships in sub-chondritic systems [1, 2], a new version of the METEOMOD program [3] is presented. It is designed to study the effect of Fe-Ni metal precipitation on the evolution of high-temperature chondritic melts and partially molten meteoritic materials.

Approach: To develop a model simulating equilibrium of Fe-Ni alloys with chondritic liquids, we used two empirical equations of the Fe and Ni solubilities in silicate melts at 1 atm pressure [2], the metal stoichiometry equation ($X_{Ni} + X_{Fe} = 1$) and thermodynamic relations describing activities of Fe and Ni in the metallic phase as a function of composition [4]. These relations have been combined in the SILMET program designed to calculate equilibrium temperature and composition of Fe-Ni metal at given fO_2 's and liquid composition [1]. Now this code is incorporated into the METEOMOD program that can be applied to a variety of meteoritic systems to study the effects of oxygen fugacities and melt composition on the precipitation temperatures and composition of metal equilibrated with sub-chondritic melts and mineral assemblages ($Ol \pm Opx \pm Pig \pm Aug \pm Pl$).

Testing METEOMOD-2006: The proposed model have been applied to two melts produced by melting of the Saint Severin LL chondrite at 1 atm and equilibrated with Metal+ Ol+Opx at 1200 °C ($\log fO_2 = -12.9$) and 1300 °C ($\log fO_2 = -11.70$) [5]. While the authors have not analyzed the experimental glasses for Ni, they found 33 and 39 mole% Ni in the metal at 1200 °C and 1300 °C, respectively. A series of isobaric calculations at variable Ni contents in the melts (10–100 ppm with 5 ppm increment) allowed us to obtain the metal containing 31.5 mole% Ni at 30 ppm Ni in the “1200 °C” melt. Similar calculations for the “1300 °C” composition produced the metal with 35.5 mole% Ni at 65 ppm Ni in the melt.

Other Results: Additional calculations were carried out at different NiO contents in the bulk Saint Severin melt and variable $\log fO_2$'s (from -7 to -15) to constrain fields of stability of high-temperature “taenite” and “kamacite.” An important conclusion is that even low NiO contents of 0.01–0.02 wt% may result in precipitation of metallic iron at $\log fO_2$'s approximately one unit higher as compared to those of Ni-free system [6].

References: [1] Ariskin A. A. et al. 1996. 27th Lunar and Planetary Science Conference. pp. 37–38. [2] Borisov A. A. and Ariskin A. A. 27th Lunar and Planetary Science Conference. pp. 133–134. [3] Ariskin A. A. et al. 1997. *Meteoritics & Planetary Science* 32:123–133. [4] Tomiska J. and Neckel A. 1985. *Berichte der Bunsen Gesellschaft für Physikalische Chemie* 89:1104–1109. [5] Jurewicz A. J. G. et al. 1995. *Geochimica et Cosmochimica Acta* 59:391–408. [6] Ariskin A. A. et al. 2006. Abstract #5009. *Meteoritics & Planetary Science* 41. This issue.

5096

HYDRATION STATE OF LHERZOLITIC SHERGOTTITE ALH 77005: EVIDENCE FROM REHOMOGENIZED MELT INCLUSIONS

C. Calvin¹ and M. Rutherford¹. ¹Brown University. E-mail: Christina_Calvin@Brown.edu

Introduction: Several lines of evidence suggest that water was once abundant on the surface of Mars. There are broad implications to the discovery of water that include the search for Martian life and the evolution of the Martian surface. However, the source of surficial Martian water is less clear. [1] discusses models where surficial Martian water originated from impacts. However, studies of Martian meteorites suggest that some of the surficial water may have originated within the Martian mantle [2, 3, 4]. This study examined rehomogenized, olivine-hosted melt inclusions in lherzolitic shergottite ALH 77005 [5] to assess the hydration state of the parental melt. Because rehomogenization of these samples was performed using a graphite buffer, H₂O would have partitioned into the CO phase generated during the experiment. Therefore, we have used other lines of evidence to discuss the hydration state of ALH 77005.

The Partitioning of Chlorine into a Vapor Phase: Chlorine strongly partitions into a water rich vapor or fluid phase [6, 7]. We examined the chlorine content of our rehomogenized melt inclusions and found that chlorine increases by two orders of magnitude from the early crystallizing olivine (100 ppm) to the later crystallizing low-Ca pyroxene (10,000 ppm). This indicates several things. 1) If there was H₂O in the melt inclusions chlorine should have partitioned into the vapor phase generated during the experiment. As the chlorine contents of the melt inclusions remain high, it is unlikely there was any water-bearing vapor generated during the experiment. 2) The increase in chlorine has two likely origins. Chlorine could have increased during crystallization of the rock. However, P₂O₅ was high in the melt and therefore chlorine may have behaved compatibly during crystallization of phosphate phases. The other alternative is that chlorine was added through addition of new magma or through a metasomatizing agent.

The Role of Water in Plagioclase Crystallization: Plagioclase crystallization is particularly sensitive to the water content of the magma. At low water contents, the crystallization of plagioclase occurs at lower Al₂O₃ content. This is because H₂O depolymerizes the melt, inhibiting plagioclase nucleation. In crystallization experiments on the parental melt composition of Chassigny, [8] showed that plagioclase crystallization in a hydrous magma occurred at higher Al₂O₃ and that the onset of plagioclase crystallization was delayed, changing the crystallization sequence of the rock. Through our rehomogenization experiments, we determined that plagioclase crystallization occurred at ~3 wt% MgO. Crystallization experiments are in progress to determine the implications of this Al₂O₃ concentration for a hydrous parental magma.

References: [1] Owen T. 1992. In *Mars*. pp. 818–834. [2] Dann J. C. et al. 2001. *Geochimica et Cosmochimica Acta* 36:793–806. [3] Watson L. L. et al. 1994. *Science* 265:86–90. [4] Lentz et al. 2001. 65:4551–4565. [5] Calvin C. and Rutherford M. J. 2005. Abstract #1697. 37th Lunar and Planetary Science Conference. [6] Mathez E. A. and Webster J. D. 2005. *Geochimica et Cosmochimica Acta* 69:1275–1286. [7] Metrich N. et al. 2001. *Journal of Petrology* 42:1471–1490. [8] Minitti M. E. and Rutherford M. J. 2000. *Geochimica et Cosmochimica Acta* 64:2535–2547.

5006

INTRACRYSTALLINE TRANSFORMATION OF OLIVINE TO RINGWOODITE IN THE SIXIANGKOU METEORITE

M. Chen¹, H. Li², A. El Goresy³, J. Liu², and X. Xie¹. ¹Guangzhou Institute of Geochemistry, CAS, 510640 Guangzhou, China. E-mail: mchen@gig.ac.cn. ²Institute of High Energy Physics, CAS, 100039 Beijing, China. ³Bayerisches Geoinstitut, Universität Bayreuth, D-95440 Bayreuth, Germany

Introduction: The transformation of olivine to ringwoodite can proceed by incoherent intercrystalline diffusion-controlled [1] or interface-controlled [2] mechanism, as well as coherent intracrystalline martensitic transformation [3] or a nucleation and growth mechanism [4]. Natural ringwoodite found in shocked meteorites occurs mainly as fine-grained polycrystalline aggregates formed through a phase transition of olivine [5]. Recently, we found natural occurrence of lamellar ringwoodite in olivine of the Sixiangkou L6 chondrite.

Meteorite: Sixiangkou meteorite contains a number of shock veins up to several millimeters in thickness. The veins contain abundant high-pressure minerals including ringwoodite, majorite, majorite-pyropo garnet, and magnesio-wüstite, for which the shock-produced pressure and temperature of about 20 GPa and 2000 °C were inferred.

Results and Discussion: In addition to polycrystalline aggregate of ringwoodite inside the shock veins, we found the lamellar ringwoodite in olivine within and neighboring the shock veins. Three kinds of lamellar ringwoodite were identified in some olivine grains by Raman spectroscopy: a) the lamellae occurring in the {101} planes of olivine inside the shock veins, b) the lamellae occurring in the (100) plane of olivine outside the shock veins, c) the lamellae occurring in planar and irregular fractures of olivine outside the shock veins. Widths of ringwoodite lamellae are mostly from 0.1 to 2 µm. FeO content of lamellae is a few percent higher (22.51 wt%) than that of olivine matrix (21.86 wt%).

The compositional difference between the lamellae and olivine matrix indicating that the Mg-Fe interdiffusion should have taken place between olivine and crystallizing ringwoodite at high pressures and high temperatures. Formation of these lamellae shows a diffusion-controlled nucleation and growth of ringwoodite along deformation-produced planar defects including stacking faults and fractures in olivine. It appears that lamellar ringwoodite have incoherently nucleated and grew along all kinds of planar defects in olivine.

Our results indicate that the P-T condition available for an intracrystalline olivine-ringwoodite transformation during the shock metamorphism of this meteorite might last from seconds to minutes, a time much longer than previously assumed duration of high pressure and temperature locally prevailed in the shocked meteorite, especially along the shock veins. These new data should bring new insight into mechanisms of olivine-ringwoodite phase transitions in the lower mantle and subducting lithosphere.

Acknowledgements: The author gratefully acknowledges the support of K. C. Wong Education Foundation, Hong Kong.

References: [1] Sung C. M. and Burns R. G. 1976. *Earth and Planetary Science Letters* 32:165–170. [2] Mosenfelder J. L. et al. 2001. *Physics of the Earth and Planetary Interiors* 127:165–180. [3] Poirier J. P. 1981. *Physics of the Earth and Planetary Interiors* 26:179–187. [4] Kerschhofer L. et al. 1996. *Science* 274:79–81. [5] Price G. D. et al. 1979. *Contributions to Mineralogy and Petrology* 71:211–218.

5214

POST STISHOVITE IN SHERGOTTITES NWA 856 AND ZAGAMI: A CATHODOLUMINESCENCE STUDY

H. Chennaoui Aoudjehane^{1, 2} and A. Jambon². ¹Université Hassan II Aïn Chock, Faculté des Sciences, Equipe Géoresources, BP 5366 Maârif Casablanca, Morocco. E-mail: chennaoui_h@yahoo.fr. ²Université Pierre et Marie Curie-Paris6 Laboratoire MAGIE, Case 110, 4 place Jussieu, 75252 Paris France. E-mail: jambon@ccr.jussieu.fr

The physical state of silica is a very useful index of shock in meteorites. Its study has been revived by the discovery of high pressure silica in Shergottites of the αPbO_2 and ZrO_2 structure [1–4]. Shergottites usually contain a few percent of silica with varied textures depending on their location in the rock.

Cathodoluminescence (CL) imaging and spectroscopy is a powerful technique which enables easy identification of tridymite, cristobalite, quartz, coesite, stishovite and high/low pressure silica glass [5]. This was cross checked previously by Raman spectroscopy on reference samples and shergottites [5]. According to its textural signature we suspected the presence of post stishovite as described previously [1, 2], but we were unable to collect unambiguous CL spectra with the additional difficulty that Raman spectroscopy is destructive to this phase.

The strong luminescence of stishovite enables easy collection of its CL spectra. In addition, imaging at the maximum wavelength of stishovite permits to locate this phase rapidly and efficiently even when small grains are present and throughout a polished section. The luminescence of high-pressure silica glass is weaker but the large number of areas with pure HP silica glass and their significant size permitted to record its spectrum without difficulty.

The problem with post stishovite is of another kind. The only way to recognize post stishovite was from its textural aspect; Raman spectroscopy must be avoided and all grains for which electron or X-ray diffraction patterns had been obtained were all extracted previously from the sections. After a systematic survey of the putative grains we could distinguish between stishovite, HP glass and spectra differing from all the silica phases studied so far. Such CL spectra are weaker than those of either HP glass or stishovite. It also appears that post stishovite does never occur alone, but always mixed with HP glass or Stishovite blurring its specific luminescence. Using this procedure, we could detect the presence of post stishovite in two shergottites NWA 856 and Zagami where it was not recognized previously [6].

CL appears an easy and powerful technique for identifying silica and particularly post stishovite in shocked meteorites. Unlike Raman spectroscopy it remains harmless to the samples. It is far more practicable than X-ray or electron diffraction patterns. The presence of post stishovite in all shergottites investigated so far is a strong argument to suggest a shock intensity of at least 40 GPa.

References: [1] Sharp T. G. et al. 1999. *Science* 284:1511–1513. [2] El Goresy A. et al. 2000. *Science* 288:632–634. [3] Malavergne V. et al. 2001. *Meteoritics & Planetary Science* 36:1297–1305. [4] El Goresy A. et al. 2004. *Journal of Physics and Chemistry of Solids* 65:1597–1608. [5] Chennaoui Aoudjehane H. et al. 2005. *Meteoritics & Planetary Science* 40:967–979. [6] Chennaoui Aoudjehane H. et al. 2006. Abstract #1036. 37th Lunar and Planetary Science Conference.

5220

A CATHODOLUMINESCENCE STUDY OF CRISTOBALITE AND K-FELDSPAR IN THE NAKHLITE MIL 03346

H. Chennaoui Aoudjehane^{1,2}, A. Jambon², and O. Boudouma³. ¹Université Hassan II Aïn Chock, Faculté des Sciences, Equipe Géoresources, BP 5366 Maârif Casablanca, Morocco. E-mail: chennaoui_h@yahoo.fr. ²Université Pierre et Marie Curie-Paris6 Laboratoire MAGIE, Case 110, 4 place Jussieu, 75252 Paris, France. E-mail: jambon@ccr.jussieu.fr. ³Université Pierre et Marie Curie-Paris6 Service de microscopie électronique à balayage, Case 110, 4 place Jussieu 75252 Paris, France. E-mail: boudouma@ccr.jussieu.fr

Shock intensity in Martian meteorites has been actively studied in recent years to understand their formation and ejection from their parent body. The analysis of high-pressure phases like stishovite, post-stishovite, majorite, hollandite, or maskelynite in shergottites permits to constrain the intensity of the shock between 30 and 90 GPa [1–4]. Nakhilites are definitely less shocked and none of them contain high-pressure minerals.

Cathodoluminescence (CL) spectroscopy is an easy approach for determining which polymorphs of silica or other silicates are present in thin or polished sections of meteorites [5]. We applied this technique to the determination of silica and feldspar speciation in the nakhilite MIL 03346. Notice that a previous CL study of MIL 03346, with a comparison to Lafayette, was restricted to imaging [6].

CL images and spectra have been recorded by the cathodoluminescence system in the scanning electron microscope (SEM) of the UPMC (Université Pierre et Marie Curie Paris VI), a detailed description of which can be found in [5]. Backscattered electron (BSE) images of the mesostasis have been collected first. Mineralogy and texture are in agreement with previous results obtained on different sections [7–10]. Details of the images show subhedral grains of silica, euhedral grains of pyroxene, and dendritic oxides. The strong luminescence of the K-FP irradiates the whole mesostasis of CL images, hiding the weaker luminescence of silica. CL spectra restricted to much smaller areas permit to identify cristobalite [11].

The shock intensity in MIL 03346 is low in agreement with that of other nakhilites, much weaker in comparison to shergottites [11]. The presence of cristobalite confirms that it is undoubtedly less than 0.1 GPa. Statistical considerations on the number of nakhilites compared to shergottites suggest that either, their number is unreasonably above the statistical expectation or more likely that the shock recorded in shergottites is not related to their ejection from their parent body.

References: [1] Stöffler D. 2000. Abstract #1170. 31st Lunar and Planetary Science Conference. [2] Malavergne V. et al. 2001. *Meteoritics & Planetary Science* 36:1297–1305. [3] El Goresy A. et al. 2000. *Science* 288: 632–634. [4] Beck P. et al. 2005. Abstract #1333. 36th Lunar and Planetary Science Conference. [5] Chennaoui Aoudjehane H. et al. 2005. *Meteoritics & Planetary Science* 40:967–979. [6] Rost D. and Vincenzi E. P. 2005. Abstract. *Meteoritics & Planetary Science* 40:A130. [7] McKay G. A. and Schwandt C. 2005. Abstract #2351. 36th Lunar and Planetary Science Conference. [8] Rutherford M. J. et al. 2005. Abstract #2233. 36th Lunar and Planetary Science Conference. [9] Stopar J. D. et al. 2005. Abstract #1547. 36th Lunar and Planetary Science Conference. [10] Sautter V. et al. 2005. Abstract. *Meteoritics & Planetary Science* 40:A134. [11] Chennaoui Aoudjehane H. et al. 2006. Abstract #1037. 37th Lunar and Planetary Science Conference.

5166

KINETICS OF PHYLLOSILICATE FORMATION IN HYDRATED MAGNESIOSILICATE SMOKES

L. J. Chizmadia^{1,2} and J. A. Nuth III³. ¹Institute for Astronomy, University of Hawai'i, Honolulu, Hawai'i 96822, USA. E-mail: lchiz@ifa.hawaii.edu. ²Hawai'i Institute for Geophysics and Planetology, Honolulu, Hawai'i 96822. ³Astrochemistry Laboratory, NASA Goddard Space Flight Center, Greenbelt, Maryland 20771, USA

Introduction: Amorphous non-stoichiometric silicate smokes produced by combustion from gas-phase precursors have similar infrared spectra as the materials observed in circumstellar and cometary dust [1]. In addition, amorphous silicate materials have been reported in the matrices of several primitive carbonaceous chondrites [e.g., 2–4]. TEM characterization of these smokes revealed chains of rounded amorphous particles 10–50 nm in size [5–6]. In a continued effort to explore the possibility that the matrices of chondritic meteorites could have contained an amorphous, non-stoichiometric component similar to the smokes, we have set up a series of hydration experiments at temperatures consistent with the oxygen isotope studies of CM2 chondrites [e.g., 7]: room temperature (~22 °C) and refrigerated at 5 °C.

Results: The Mg smokes react immediately with H₂O to form a hydrated amorphous gel [8]. After 2 days, TEM characterization of samples at both temperatures show incipient nanocrystals [8]. These results are consistent with hydration experiments performed at 84 °C and 150 °C [9]. We have tracked the rate of growth of the incipient crystals during hydration experiments at 5 °C and 22 °C. The phyllosilicates are first detectable at 2 days and show elongated shapes with lattice fringes, which are highly sensitive to the electron beam. The first observed crystals have an average length of 92 ± 33 and 103 ± 66 nm (at 5 °C and 22 °C, respectively) and their growth is linear until 56 days (260 ± 57 and 218 ± 54 nm at 5 °C and 22 °C, respectively). At 73 days, the 5 °C samples exhibit large blocky crystals that are an order of magnitude larger than the elongated phyllosilicates in the previous time step. Interestingly, the phyllosilicates in the samples run at 22 °C continue their linear growth to an average size of 328 ± 123 nm at 112 days, with no sign of the larger blocky crystals seen in the 5 °C samples.

Discussion: The similarity in crystal sizes between the batches run at 5 °C and 22 °C does not offer a way to distinguish between the two temperatures; the phyllosilicates from both temperatures are similar to those observed in primitive chondrites. However, the blocky crystals observed in the samples hydrated at 5 °C for >73 days have not been reported. This may indicate that the alteration of chondritic matrices occurred at higher temperatures and/or for a shorter time period. One caveat is that these experiments involved an excess of water compared to silicate and this extra room may have allowed the formation of the large blocks observed. More experiments are needed where more confined matrices are explored.

References: [1] Nuth J. A. et al. 2002. *Meteoritics & Planetary Science* 37:1579–1590. [2] Barber D. J. 1981. *Geochimica et Cosmochimica Acta* 45: 945–970. [3] Brearley A. J. 1993. *Geochimica et Cosmochimica Acta* 57: 1521–1550. [4] Greshake A. 1998. *Geochimica et Cosmochimica Acta* 61: 437–452. [5] Rietmeijer F. J. M. et al. 1986. *Icarus* 66:211–222. [6] Fabian D. et al. 2000. *Astronomy and Astrophysics* 364:282–292. [7] Clayton R. N. and Mayeda T. K. 1984. *Earth and Planetary Science Letters* 67:151–161. [8] Chizmadia L. J. et al. 2006. Abstract #2187. 37th Lunar and Planetary Science Conference. [9] Rietmeijer F. J. M. et al. 2004. *Meteoritics & Planetary Science* 39:723–746.

5158

EXPERIMENTS ON OXYGEN ISOTOPE EXCHANGES BETWEEN SILICATE MELT AND O₂ GAS DURING BRIEF MELTING USING CO₂ LASER AND THEIR IMPLICATIONS TO OXYGEN ISOTOPIIC HETEROGENEITY

B.-G. Choi¹ and M. Kusakabe². ¹Department of Earth Science Education, Seoul National University. E-mail: bchoi@snu.ac.kr. ²ISEI, Okayama University, Okayama, Japan

Introduction: Oxygen isotopic heterogeneity preserved especially in primitive meteorites is interpreted as results of mixing between two or more oxygen reservoirs that had existed prior to or during the formation of chondritic materials [1]. Many models have been proposed for the nature of the reservoirs, including recent models of CO self shielding [2–4]. However, there are few experimental and theoretical studies for O isotope exchanges between oxygen-bearing phases in the nebula [e.g., 5]. Here we report preliminary results on O isotope exchange reactions between silicate melts and O₂ gas during brief heating using an on-line CO₂ laser-BrF₅ fluorination system [6].

Experiments: Olivine grains of the Eagle Station pallasite, bulk samples of Allende (CV3), Kainsaz (CO3), Duwun (L6) were used as starting materials. About 1–4 mg of these samples were placed in Ni holder and briefly (30 s to 10 min) heated with defocused CO₂ laser while the chamber was filled with small amount of O₂ gas (OKAO; $\delta^{18}\text{O} = 17.5\text{‰}$ and $\Delta^{17}\text{O} = -0.3\text{‰}$), where $P_{\text{O}_2} = \sim 10\text{--}50$ mbar (the amounts of OKAO gas are a few times those in silicates). Every O₂ gas after exchange reaction was recovered at molecular sieve and measured for O isotope composition, followed by measurements of reacted silicates using the standard BrF₅ method with CO₂-laser heating [6]. Some silicate runs were saved for petrological studies and future ion microprobe works.

Results and Discussion: Since we used relatively small amount of O₂ gas, isotopic compositions of both gas and solid changed after experiments. At high temperature equilibrium process, one can expect the reactants approaching to each other along near the mixing line connecting the initial compositions on a three-isotope plot, for example, slope ~ 0.75 for Kainsaz and OKAO. However, run products of Allende, Kainsaz, and the Eagle Station pallasite moved with much steeper slopes than those expected from a simple mixing. Compositions of the reacted OKAO gas fall on the right side of the mixing line: in many case the $\delta^{18}\text{O}$ values even increased. Similar results have been observed for ordinary chondrite samples. These behaviors can be explained by kinetic processes (evaporation and condensation) + mixing between liquid and gas. We suspect, during brief heating, some evaporated metallic irons recondensed as oxides preferentially with lighter oxygen in the gas. As a result, the reacted gas became heavier in its composition and the run products moved with much steeper slope than that of simple mixing. During chondrule and CAI forming heating events in the nebula, similar processes might have occurred to produce the chondritic mixing line.

References: [1] Clayton R. N. 1993. *Annual Review of Earth and Planetary Science* 21:115–149. [2] Clayton R. N. 2002. *Nature* 415:860–861. [3] Lyons J. R. and Young E. D. 2004. *Nature* 435:317–320. [4] Yurimoto H. and Kuramoto K. 2004. *Science* 305:1763–1766. [5] Yang Y. et al. 1995. *Geochimica et Cosmochimica Acta* 59:2095–2104. [6] Kusakabe M. et al. 2004. *Journal of Mass Spectrometry* 52:205–212.

5151

TRANSPORT IN THE SOLAR NEBULA: IMPLICATIONS FOR THE DEPLETION OF MODERATELY VOLATILE ELEMENTS IN CHONDRITIC METEORITES

F. J. Ciesla. Carnegie Institution of Washington, Department of Terrestrial Magnetism, 5241 Broad Branch Road NW, Washington, D.C. 20015, USA. E-mail: ciesla@dtm.ciw.edu

Introduction: The bulk abundances of moderately volatile elements (MOVEs, those elements that condense between $\sim 650\text{--}1300$ K) decrease with condensation temperature in many chondritic meteorites. Over the last 3+ decades, there have been two major theories for explaining this depletion trend: a two-component mixing model where volatile-rich and volatile-depleted materials were combined to form the chondritic meteorites [1] and an incomplete condensation model where solar nebular gas was continuously removed as the disk cooled [2]. As discussed in [3], the incomplete condensation model has gained favor, in part, due to the fact that astrophysical models of the solar nebula have been able to roughly reproduce the depletion trend [4, 5]. Here I am using a more detailed model of transport in the solar nebula to evaluate whether such trends are still reproduced.

Previous Work: Cassen demonstrated that the incomplete condensation model could reproduce the MOVE-depletion observed in some chondrites [4, 5]. In these models, the solar nebula was allowed to evolve, losing mass to the sun and expanding in radial extent to account for angular momentum transport. The nebula cooled as a result of its mass loss and coagulation of dust to form larger bodies. During this evolution, dust was transported through the disk by the net flow of the gas and was accreted by immobile planetesimals.

This Work: I have developed a model to re-examine whether incomplete condensation is consistent with astrophysical models of the solar nebula. In particular, I am focusing on the importance of those solids that are subjected to gas-drag migration, and therefore moved rapidly through the solar nebula. Cassen's models assumed that some fixed fraction of these bodies were lost to the Sun [4, 5]. However, recent work has shown that such bodies were either incorporated into planetesimals at heliocentric distances that differ from where these bodies formed or crossed evaporation fronts and lost their mass to the gas [6, 7]. In either scenario, this transport led to spatial and temporal variations in the abundances of elements throughout the solar nebula. In addition, I also allow for the outward diffusion of MOVEs in the vapor phase. This work is based on a modified version of the transport model developed in [7].

New Results: Preliminary runs show that the redistribution of vapor by diffusion can lead to different results than those found in Cassen's models. For example, the outward diffusion of vapor can result in the enhancement relative to Si of MOVEs immediately outside the corresponding condensation front. This could imply that certain conditions were necessary for the incomplete condensation model to work or other processes are responsible for the observed MOVE depletions [3, 8].

References: [1] Anders E. 1964. *Space Science Reviews* 3:583–714. [2] Wasson J. T. and Chou C.-L. 1974. *Meteoritics* 9:69–84. [3] Bland P. A. et al. 2005. *Proceedings of the National Academy of Sciences* 102:13,755–13,760. [4] Cassen P. 1996. *Meteoritics & Planetary Science* 31:793–806. [5] Cassen P. 2001. *Meteoritics & Planetary Science* 36:671–700. [6] Cuzzi J. N. and Zahnle K. J. 2004. *The Astrophysical Journal* 614:490–496. [7] Ciesla F. J. and Cuzzi J. N. 2006. *Icarus* 181:178–204. [8] Alexander C. M. O'D. 2005. *Meteoritics & Planetary Science* 40:943–966.

5272

MULTIVARIATE ANALYSIS OF IN SITU AND EX SITU MARTIAN IMPACT GLASS

B. A. Cohen, Institute of Meteoritics, University of New Mexico, Albuquerque, New Mexico 87131, USA. E-mail: bcohen@unm.edu

Introduction: On the West Spur of Husband Hill, the Mars Exploration Rover Spirit encountered a class of rocks (Clovisclass) thought to be extensively altered clastic rocks of possible impact origin, having high Ni/Cr ratios, and miniTES analyses distinguished by a component consistent with basaltic glass [1–4]. I am using multivariate analysis (multi-element correlations and principal component analysis) to try to determine whether a unique impact glass component can be characterized in these rocks, using the impact-generated Martian glass Elephant Moraine (EET) A79110 Lithology C as an analog. EETA79001 Lithology C: Lith C consists of pods of impact glass in a basaltic (Lith A) host and has been modeled as a mixture of 85% Lith A + 7% plagioclase + 8% Martian soil [5]. I used microprobe X-ray maps (Si, Mg, Ca, Ni, and S) of two Lith C pods. Principal component analysis shows that both pods have constant amount of S, regardless of Mg or Ca content, implying that S was introduced independently, not by specific sulfate or silicate phases. A weak anticorrelation of S with Si may reflect mechanical mixing of a small amount of soil (low Si) with the silicate minerals of Lith A (low S), as modeled by [5]. There was too much noise in the Ni element maps to make meaningful relationships with Ni; a longer integration time will be used to reduce noise in future efforts. A positive correlation between Mg and Ca (Principal Component 1) and a weak anticorrelation between Si and S (Principal Component 2) describe 55% of the total variation. Gusev rocks: Analyses using the same element set were performed using Athena APXS data (molar basis) of as-is, brushed, and RATted analyses of Adirondack- and Clovis-class rocks. Adirondack rocks are relatively unaltered basalts where RAT grinds penetrated thin weathering rinds. Analysis of the Adirondack class (n = 17) shows that both S and Ni are strongly anticorrelated with Si, Ca, and Mg, showing that the components carrying these elements are distinguishable from the basalt. One principal component describes 80% of the variability among analyses, mainly describing an array with the RATted basaltic compositions at one end and a mix of brushed and as-is analyses along a trajectory enriched in Sand Ni, as has been shown in [6], confirming these techniques. Preliminary analyses of the Clovis class (n = 22) show that, unsurprisingly, this class of rocks is not as easily interpreted. Among these elements, Ca and S have the strongest positive correlation, demonstrating that S is carried in a sulfate phase [4] rather than primarily in an impact glass. However, in contrast to Adirondack rocks, Ni is positively correlated with Ca and anticorrelated with Si and Mg. Such a relationship might be expected if the precursor to the altered phases was an impact glass high in Ni. Such glasses may easily alter to phyllosilicates in the presence of water, as might be seen in the Clovis-class rock Woolly Patch [7]. Further analysis of the Clovis-class components is ongoing.

References: [1] Squyres S. W. et al. 2006. *Journal of Geophysical Research* 111, doi:10.1029/2005JE002562. [2] Gellert R. et al. 2006. *Journal of Geophysical Research* 111, doi:10.1029/2005JE002555. [3] Ruff S. W. et al. Forthcoming. [4] Ming D. W. et al. 2006. *Journal of Geophysical Research* 111, doi:10.1029/2005JE002560. [5] Rao M. N. et al. 1999. *Geophysical Research Letters* 26:3265. [6] McSween H. Y., Jr. et al. 2004. *Science* 305:842. [7] Wang A. et al. 2006. *Journal of Geophysical Research* 111, doi:10.1029/2005JE002516.

5278

THE EFFECTS OF PERMEABILITY-DRIVEN WATER TRANSPORT ON THE EVOLUTION OF CM PARENT BODIESR. F. Coker¹, B. A. Cohen², and P. A. Bland³. ¹Los Alamos National Laboratory, Los Alamos, New Mexico 87545, USA. E-mail: robc@lanl.gov. ²University of New Mexico, Albuquerque, New Mexico 87131, USA. ³Imperial College London, SW7 2AZ, UK

Introduction: A range of numerical models of asteroid thermal evolution [1–4] predict large-scale movement of water on chondrite parent bodies. However, aqueous alteration in carbonaceous chondrites was likely isochemical [5], implying that little fluid flow occurred (see also Bland et al., this issue). To resolve this contradiction, we have modelled the thermal evolution of CM parent bodies using three different expressions for permeability (k).

We present models of CM parent bodies using a constant permeability of 10^{-13} m^2 (representing lunar regolith) and two versions of the Blake-Kozeny-Carman (BKC) equation [6]. The first [7], based on micro-gravity experiments using mm-size balls, is valid only for small porosities and uses $k = a^2/150 \times \phi^3/(1-\phi)^2$, where a is the grain size (in μm) and ϕ is the total porosity (the sum of voids and any liquid water). The second [8], based on experiments with calcite aggregates with a grain size of 5 μm , uses $k = a^2/2200 \times \phi^3$.

Results: Since the unaltered matrix grain size for CCs is $\sim 1 \mu\text{m}$ [9], we show in Fig. 1 the amount of H_2O moved upward through a given radius (compared to its initial H_2O mass) for a = 0.5 and 5 μm . This model is for a 20 km diameter parent body that formed at 3 AU 1.5 Myr after the collapse of the solar nebula (CAI formation). The asteroid starts with 7% void space and 18% ice and a composition that results in 50% serpentine (by volume) after complete alteration. With a maximum total porosity of less than 30%, using the BKC expressions, the permeability for even a = 5 μm is everywhere always less than 10^{-13} m^2 . As a result, both water liquid and vapor transport is greatly reduced from previous models; in the models shown in Fig. 1, all H_2O transport is by water vapor. We discuss these and other results and their implications for CM parent body modeling.

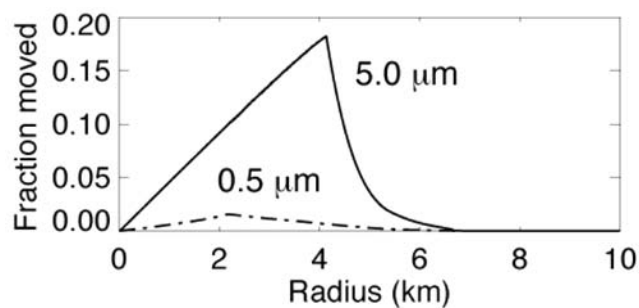


Fig. 1. Fraction of H_2O moved upward through each radius.

References: [1] Grimm R. E. and McSween H. Y., Jr. 1989. *Icarus* 82: 244. [2] Travis B. J. and Schubert G. 2005. *Earth and Planetary Science Letters* 240:234. [3] Coker R. F. and Cohen B. A. 2001. *Meteoritics & Planetary Science* 36:43. [4] McSween H. Y., Jr. et al. 2002. In *Asteroids III*, Tucson, Arizona: The University of Arizona Press. 559 p. [5] Hanowski N. P. and Brearley A. J. 2001. *Geochimica et Cosmochimica Acta* 65:495. [6] Dullien F. A. L. 1992. *Porous media*. San Diego: Academic Press. 574 p. [7] Yendler B. and Webbon B. 1993. *Capillary movement of liquid in granular beds*. Washington, D.C.: SAE. [8] Zhang S. et al. 1994. *Journal of Geophysical Research* 99:15,741–15,760. [9] Greshake A. 1997. *Geochimica et Cosmochimica Acta* 61:437.

5113

RUBBLE PILES OR PLANETS? IMPLICATIONS FOR METEORITE PARENT BODIES

G. J. Consolmagno SJ¹ and D. T. Britt². ¹Specola Vaticana, V-00120, Vatican City State. E-mail: gjc@specola.va. ²University of Central Florida, Orlando, Florida, USA

Introduction: Most meteorites show at least some degree of thermal, and in some cases aqueous, processing that presumably occurred on their parent bodies before they were ejected into Earth-crossing orbits. However, a detailed analysis of small bodies in the solar system indicates that virtually all bodies with masses less than 10²⁰ kg are today significantly porous, with many of them showing extensive macroporosity (>40%). It is not clear they could provide the physical environment needed to produce the observed degrees of metamorphism.

Small Body Macroporosity: Our previous work [1] has compared the densities of asteroids inferred via a number of methods to the densities of meteorites that are reasonable analogues to the surfaces of asteroids as inferred from their spectral features. The general trend is that all but the largest asteroids appear to be 20% to 50% or more macroporous, with a suggestion that C type asteroids tend to be more macroporous than S types. (Macroporosity here signifies the void spaces larger than the microcrack porosity seen in meteorite hand samples.) Data from recent spacecraft missions and new observations have allowed this analysis to be extended to cometary nuclei, additional small asteroids, planetary satellites, (especially using Cassini measurements of the densities of Saturn's moons), and Centaurs and Transneptunian objects, where we have estimated densities from their shape and spin characteristics [2]. From this analysis we find a general trend that, regardless of composition, bodies larger than 10²⁰ kg mass tend to be well-compacted objects while smaller bodies, down to fragments much smaller than a few hundred meters diameter, are either extensively fragmented or loose piles of rubble. The universal nature of this size limits suggests that it may reflect an underlying physics, either that such-sized bodies are able to withstand catastrophic disruptions or that they are able to reshape themselves after such disruptions.

Implications for Meteorite Parent Bodies: Much of the new data included in this analysis comes from recent spacecraft missions, which allow us not only to measure the bodies' densities but also inspect images of their surfaces. Not surprisingly, the rubble pile surfaces are characterized primarily by dust, rubble, and impact features; even their occasional tectonic features appear to be related to impact or accretion events. On the other hand, more complex geologic processes (including heating and alteration of surface materials) can be seen on larger icy moons and inferred for larger asteroids like Ceres and Vesta [3, 4]. This suggests that either only large meteorite parent bodies are capable of producing metamorphosed meteorites and aqueous alteration, or that such metamorphism occurred very early in solar system history before smaller coherent bodies were fragmented and reaccreted.

References: [1] Britt D. T. et al. 2002. *Asteroids III*. Tucson, Arizona: The University of Arizona Press. pp. 485–500. [2] Britt D. T. et al. 2006. Abstract #2214. 37th Lunar and Planetary Science Conference; Consolmagno G. J. et al. 2006. Abstract #1222. 37th Lunar and Planetary Science Conference. [3] Thomas et al. 2006. Abstract #1639. 37th Lunar and Planetary Science Conference. [4] Thomas P. et al. 2005. *Nature* 437:224.

5167

MASS-DEPENDENT FRACTIONATION OF NICKEL ISOTOPES IN IIIAB IRON METEORITES

D. L. Cook^{1, 2, 3}, M. Wadhwa^{2, 3}, R. N. Clayton^{1, 2, 4}, P. E. Janney^{2, 3}, N. Dauphas^{1, 2, 4}, and A. M. Davis^{1, 2, 4}. ¹Department of the Geophysical Sciences, University of Chicago, Chicago, Illinois 60637, USA. E-mail: davecook@uchicago.edu. ²Chicago Center for Cosmochemistry, Chicago, Illinois 60637, USA. ³Department of Geology, The Field Museum, Chicago, Illinois, 60605, USA. ⁴Enrico Fermi Institute, The University of Chicago, Chicago, Illinois, 60637, USA

Introduction: Studies of the mass-dependent fractionation of stable isotopes of light elements have been a useful tool for investigating early solar system processes operating in the nebula and on parent bodies. The advent of multi-collector ICPMS has expanded the range of elements now available for such investigations. Studies of Fe, Cu, and Zn isotopes in meteorites [e.g., 1, 2] show that the transition metals underwent mass-dependent fractionation during processes occurring in the early solar system. Additionally, Ni isotopes in metal from various meteorite groups follow a mass-dependent fractionation trend [3]. Nevertheless, the mass-dependent fractionation of Ni isotopes in natural samples remains largely unexplored. We have chosen to examine the possible effects on the isotopic composition of Ni due to fractional crystallization of a liquid Fe-Ni alloy during core formation by investigating a suite of the magmatic IIIAB iron meteorites.

Samples: Relatively large (~1 g) pieces of IIIAB metal were digested by [4] for their Fe isotope study. Thus, digested but chemically unprocessed solutions remained for many samples, and aliquots of these solutions were used to investigate Ni isotopic fractionation in IIIAB irons. Samples were chosen to represent a wide range in Ni content, which is considered a proxy for the degree of fractional crystallization. Specifically, Fe-Ni metal from the following IIIAB irons was analyzed: Avoca, Augustinovka, Bald Eagle, Bella Roca, Henbury, Nova Petropolis, Orange River Iron, and Welland.

Results and Discussion: Five of the IIIAB irons investigated here (Avoca, Augustinovka, Henbury, Nova Petropolis, and Orange River Iron) have similar Ni isotopic compositions and yield a weighted average value of $0.48 \pm 0.12 \text{ ‰}$ per a.m.u. relative to the SRM 986 Ni standard. The other three samples (i.e., Bald Eagle, Bella Roca and Welland) are enriched in the heavy isotopes of Ni and have compositions ranging from 1.44 to 2.93 ‰ per a.m.u. However, the degree of mass fractionation of Ni isotopes does not correlate with the Ni content ($r^2 = 0.11$). This suggests that if all IIIAB irons originated in a single parent body, core formation and crystallization did not mass fractionate Ni isotopes in a systematic way. In fact, fractionation of Ni isotopes in different IIIAB iron meteorites may be the result of a combination of factors including partitioning between metal and silicate during core segregation and the interaction of a metallic melt with a sulfide melt during core crystallization.

Acknowledgements: We thank E. Mullane for generously providing digested aliquots of the IIIAB samples studied here.

References: [1] Zhu X. K. et al. 2001. *Nature* 412:311–313. [2] Luck J.-M. et al. 2005. *Geochimica et Cosmochimica Acta* 69:5351–5363. [3] Moynier F. et al. 2004. Abstract #1286. 35th Lunar and Planetary Science Conference. [4] Mullane E. et al. 2005. Abstract. *Meteoritics & Planetary Science* 40:A108.

5309

Mg ISOTOPES FRACTIONATION IN MELILITE IN AN ALLENDE TYPE A INCLUSION: A HIGH-PRECISION, HIGH-SPATIAL RESOLUTION APPROACH

M. Cosarinsky¹, K. D. McKeegan¹, I. D. Hutcheon², and S. Fallon².
¹Department of Earth and Space Sciences, University of California–Los Angeles, Los Angeles, California 90095–1567, USA. ²Chemical Biology and Nuclear Science Division, Lawrence Livermore National Laboratory, Livermore, California 94551–0808, USA. E-mail: mariana@ess.ucla.edu

Introduction: Type A CAIs are coarse-grained, melilite-rich inclusions common in CV chondrites. The irregular and nodular structures of some of these CAIs, in addition to their chemical compositions, suggest an origin by condensation and aggregation rather than melting [1]. Previous isotopic studies have shown that these objects are highly heterogeneous in their stable Mg isotope records [2]. In order to better understand the microdistribution of Mg isotopes in these samples we performed coordinated high precision (ims1270) and high spatial resolution (NanoSIMS) ion microprobe analyses on melilite and spinel in an Allende type A CAI.

Results and Discussion: Allende TS25 is a large (15 × 5 mm), oblong, coarse-grained type A CAI consisting of reversely zoned melilite crystals (Åk₋₂₅ in the core to Åk₋₁₀ near the rim) with inclusions of spinel, hibonite, and perovskite. Spinel grains are mostly euhedral, 10–15 μm in size, and sometimes occur grouped in clusters. Alteration minerals are abundant, especially around the perimeter of the CAI or where it is fractured. A well-developed and continuous Wark-Lovering rim (WLR, [3]) surrounds the inclusion [2]. The same WLR sequence also occurs inside the inclusion as “enclosed” features, usually lining interior cavities or brecciated fragments. The enclosed WLRs are usually less altered as is the melilite right below these rims. Mg isotope analyses show large ranges in fractionation in melilite (²⁵Mg = –2.5 to +16.4 ‰, 1 ± 0.3) and spinel (²⁵Mg = –1.4 to +23.7‰, 1 ± 0.1). NanoSIMS data yield consistent ranges in ²⁵Mg values. The data are correlated in the sense that the most fractionated spinel grains occur within fractionated melilite and those interior melilite grains that do not show isotopic enrichments contain inclusions of isotopically normal spinel. Analyses of these phases near the WLR yield ²⁵Mg compositions closer to normal (unfractionated). In particular, melilite adjacent to WLR spinel is the lightest. High spatial resolution analyses show a progressive variation in ²⁵Mg towards the rim of the order of 14‰ over 100 μm, with only a slight chemical gradient of decreasing Mg contents (Åk₈₋₁).

Our data suggest that Allende TS-25 formed by the aggregation of grains with different nebular histories that then underwent minor melting or solid-state recrystallization without major isotopic equilibration. The petrographic correlation between isotopically heavy spinel and melilite indicates that some diffusive exchange from spinel into melilite occurred [4]. In addition, the strong compositional gradient observed close to the WLR suggests that isotopically heavy melilite exchanged with the ambient nebular gas, but the preservation of the fine-scale isotopic heterogeneities implies that heating was brief followed by cooling rates sufficient to allow for some diffusive transport of Mg between spinel and melilite and between melilite and the gas.

References: [1] MacPherson G. J. and Grossman L. 1984. *Geochimica et Cosmochimica Acta* 48:29–46. [2] Cosarinsky et al. 2005. Abstract #2105. 36th Lunar and Planetary Science Conference. [3] Wark D. and Boynton W. V. 2001. *Meteoritics & Planetary Science* 36:1135–1166. [4] Sheng et al. 1992. *Geochimica et Cosmochimica Acta* 56:2535–2546.

5157

THERMAL PROCESSES OF THE 4 Kyr BP OCEANIC IMPACT BASED ON CARBON AND MINERAL PHASE ASSOCIATION IN MELT PRODUCTS

M.-A. Courty¹, B. Deniaux¹, A. Crisci², K. Grice³, P. Greenwood³, M. Mermoux², D. Smith⁴, and M. Thiemens⁵. ¹UMR 5198, CERP 66720 Tautavel, France. E-mail: courty@tautavel.univ-perp.fr. ²LEPMI-ENSEEG, University Grenoble, 38042 Saint-Martin d’Hères, France. ³Curtin University Technology, Perth, Western Australia, 6845, Australia. ⁴MNHN-Minéralogie, 59 rue Buffon, 75005 Paris, France. ⁵Chemistry and Biochemistry, University of California–San Diego, San Diego, California 92093, USA

Introduction: Impact events into crystalline targets are known to generate high-pressure shock and large volumes of melt rocks and glasses [1]. In contrast, impacts into volatile-rich soft sediments lead to minor melt formation, weak shock effects and high ejecta dispersion [2]. Thus, the related impact signature mainly results from thermal effects during collision and ejecta redistribution [3]. The well-preserved worldwide ejecta-strata horizon of the 4 kyr B.P. impact [4] provides a unique opportunity to understand impact-thermal processes.

Methods: The 4 kyr B.P. impact products from marine and terrestrial records were compared. The key association of nanodiamonds, graphite, and hydrocarbons in melt clasts and in the host materials was studied using an environmental SEM/EDAX microprobe, Raman microspectrometry, electron microprobe, TEM, GC-IR-MS, and isotope analysis (C, O, S, Pb, Fe, Cr).

Results and Discussion: The ~7 m-thick sequence in deep sea cores along the Antarctica coast showing impact-melt clasts with heated marine sediments provides stratigraphic and geochemical signatures to identify the proximal ejecta from an oceanic impact. The impact debris show devitrified melt clasts with crystalline defects due to hydrocarbon incorporation before quenching. Metallic droplets associated to high temperature graphite and clusters of nanodiamonds form splash mounds on the melt clasts and on heated marine particles. In contrast, the distal impact-ejecta debris display sharp contact of weakly heated marine clasts with vesicular flow-textured glass derived from marine sediments. Thermal transformations of the host soil surface splashed by the distal impact-ejecta express pulverization of a volatile-rich carbonaceous melt. Metal-rich clasts with a banded texture formed of graphitic and alumino-silicate sheets are fragments of the projectile, possibly a CV3 carbonaceous chondrite. Metallic mounds in the distal impact glass formed in situ from local vaporization of the projectile fragments. Clusters of HT graphite, nanodiamonds and hydrocarbons coating voids in the impact glass are also vaporization residues of the projectile. Absence of projectile clasts in the proximal ejecta debris would result from its total vaporization in the collision zone. In contrast, preservation of projectile clasts in the distal dispersion area would express its fragmentation while crossing the Earth atmosphere and block entrainment after the collision by the impact ejecta while rising.

References: [1] Dressler B. O. and Reimold W. U. 2001. *Earth Science Reviews* 56:205–284. [2] Kieffer S. W. and Simons C. H. 1980. *Reviews of Geophysics and Space Physics* 18:143–181. [3] Wasson J. T. 2003. *Astrobiology* 3:163–179. [4] Courty M. A. et al. 2006. *Geophysical Research Abstracts* 8:A01812.

5058

A SEARCH FOR EXTRATERRESTRIAL CHROMITE ACROSS THE CRETACEOUS-PALEOGENE BOUNDARY AT GUBBIO, ITALY

A. Cronholm and B. Schmitz. Department of Geology, Lund University, SE-22362 Lund, Sweden. E-mail: Anders.Cronholm@geol.lu.se; Birger.Schmitz@geol.lu.se

The distribution of sediment-dispersed extraterrestrial chromite (EC) grains ($>63 \mu\text{m}$) has been studied in marine, condensed limestone across the Cretaceous-Paleogene (K-P) boundary in the Bottaccione Gorge section at Gubbio, Italy. Chromite is a common accessory mineral in ordinary chondrites [1] and is highly resistant to weathering. Hence, chromite is often the only surviving mineral of decomposed meteorites, making it useful for assessing the accretion rates of extraterrestrial material in ancient sediments [2, 3]. The EC can be readily distinguished from terrestrial chromite based on its element composition, including specific ranges of TiO_2 (2.0–3.5 wt%) and V_2O_5 (0.6–0.9 wt%) [4]. The aim of this study is to determine if the K-P boundary asteroid impact was associated with an enhanced influx to Earth of ordinary chondritic meteorites.

Six limestone samples of 28 kg each and one of 14 kg were collected from 7.2 m below the K-P boundary clay to 17.2 m above it. Three of the samples were taken at or close to the K-P boundary, while the remaining constituted background material. The samples were leached in HCl and HF. Chromite grains ($>63 \text{m}$) were picked from the residues and analyzed by EDS methods [2, 3].

In a total of 182 kg of limestone only four EC grains were found ($0.022 \text{ EC grains kg}^{-1}$). Based on estimated sedimentation rates for the Gubbio section [5], we calculate a flux of $\sim 0.23 \text{ EC grains m}^{-2} \text{ kyr}^{-1}$. The four grains were found throughout the section, and no increase of EC grains could be observed in the samples from the K-P boundary. The absence of EC grains at the K-P boundary is not surprising considering that the K-P impactor probably was a carbonaceous chondrite low in chromite [6, 7]. Our results give no support for the K-P impactor being related to perturbations of the asteroid belt during chaotic transitions in the motion of the inner planets, see [8].

The content of EC grains in the Gubbio limestone is very low compared to Middle Ordovician limestone from Kinnekulle, southern Sweden. The latter sediment contains 1–3 EC grains per kg, which has been interpreted as a two orders of magnitude increase in the influx of ordinary chondrites to Earth following the disruption of the L chondrite parent body $\sim 470 \text{ Ma}$ [2–4]. Sedimentation rates of the limestones at Kinnekulle and Gubbio lie at the same order of magnitude [3, 5], i.e., a few mm per thousand years. At Kinnekulle condensed limestone that formed prior to the L chondrite disruption event show similarly low EC content (5 EC grains 379 kg^{-1} or $0.013 \text{ EC grains kg}^{-1}$) as the Gubbio limestone [3]. These low concentrations of EC grains probably reflect the normal flux of ordinary chondrites to Earth.

References: [1] Rubin A. E. 1997. *Meteoritics & Planetary Science* 32: 231–247. [2] Schmitz B. et al. 2003. *Science* 300:961–964. [3] Schmitz B. and Högström T. 2006. *Meteoritics & Planetary Science* 41:455–466. [4] Schmitz B. et al. 2001. *Earth and Planetary Science Letters* 194:1–15. [5] Mukhopadhyay S. et al. 2001. *Geochimica et Cosmochimica Acta* 65:653–669. [6] Shukolyukov A. and Lugmair G. W. 1998. *Science* 282:927–930. [7] Kyte F. T. 1998. *Nature* 396:237–239. [8] Varadi et al. 2003. *The Astrophysical Journal* 592:620–630.

5260

FIRST SYSTEMATIC TEM/NANOSIMS COORDINATED STUDY OF CRYSTAL STRUCTURE AND ISOTOPIC COMPOSITION OF PRESOLAR SILICON CARBIDE

T. L. Daulton^{1, 2}, F. J. Stadermann^{2, 3}, T. J. Bernatowicz^{2, 3}, S. Amari^{2, 3}, and R. S. Lewis⁴. ¹Center for Materials Innovation, Washington University in Saint Louis, Saint Louis, Missouri 63130, USA. ²Physics Department, Washington University in Saint Louis, Saint Louis, Missouri 63130, USA. ³Laboratory for Space Sciences, Washington University in Saint Louis, Saint Louis, Missouri 63130, USA. ⁴Enrico Fermi Institute, University of Chicago, Chicago Illinois 60637, USA

Introduction: Submicron- to micron-sized presolar grains of SiC are ubiquitous in the matrices of primitive chondrites. While numerous studies have measured the isotopic compositions in primary and trapped elements of individual presolar SiC grains [1], providing information on their stellar sources, there have been few detailed studies of their microstructure. Grain microstructures provide important information on mechanisms of grain formation, physical conditions at sources of formation, and metamorphic processing subsequent to formation. The value of isotopic and microstructural measurements on presolar SiC grains would be increased if those data sets were correlated to one another on an individual grain basis.

Results: Suspensions of SiC isolated by acid dissolution from Murchison (KJB residue) [2] were deposited on transmission electron microscopy (TEM) grids. Crystal structure of randomly selected grains was determined by TEM; three SiC polytypes or stacking sequences (cubic 3C, hexagonal 2H, and disordered) along with their intergrowths and a range of defect and twin microstructures were identified [3, 4]. The locations on the TEM grid of 48 TEM-characterized grains of the following structure types—hexagonal 2H SiC (3% of Murchison SiC population), intergrowths of cubic 3C and hexagonal 2H SiC (17% of population), and disordered SiC (1% of population)—were determined for use in subsequent isotopic measurement by NanoSIMS.

Forty randomly selected grains on the TEM mount, presumably mostly 3C SiC (79% of population), were analyzed by NanoSIMS as a control, and they exhibited a range of isotopic compositions similar to those measured in far larger presolar SiC populations [1]. As a group, the 2H, 2H/3C intergrowth, and disordered SiC structure types are isotopically anomalous and exhibit a greater scatter in both $\delta^{29}\text{Si}$ and $\delta^{30}\text{Si}$ in comparison to the predominantly 3C SiC set of randomly selected grains. All three measured 2H grains are isotopically mainstream. Of the 42 SiC 2H/3C intergrowth grains analyzed, one has $^{12}\text{C}/^{13}\text{C} = 8.7 \pm 0.8$ (i.e., <10) and is identified as type A + B; two exhibit small enrichments in ^{28}Si and are possibly type X; one has $^{12}\text{C}/^{13}\text{C} = 110.3 \pm 2.3$ (i.e., >100) with Si isotopes on the ^{30}Si -enriched side of the mainstream distribution and is identified as type Y; two have mainstream $^{12}\text{C}/^{13}\text{C}$ with Si isotopes on the ^{30}Si -enriched side of the mainstream distribution as well as $\delta^{29}\text{Si} < 0$ and are identified as type Z. We also confirm our earlier inference that one-dimensionally disordered SiC [3, 4] is a presolar grain type. Interestingly, all three disordered grains analyzed have very similar isotopic compositions in $\delta^{29}\text{Si}$ (46 to 63‰), $\delta^{30}\text{Si}$ (34 to 57‰), and $^{12}\text{C}/^{13}\text{C}$ (51 to 60). Although the statistics are limited, the probability of three disordered grains clustering as observed in Si isotopes is $< \sim 3\%$, suggesting disordered SiC might be associated with a specific type of stellar source.

References: [1] Meyer B. S. and Zinner E. 2006. In *Meteorites and the early solar system II*. Tucson, Arizona: The University of Arizona Press. 942 p. [2] Amari S. et al. 1994. *Geochimica et Cosmochimica Acta* 58:459–470. [3] Daulton T. L. et al. 2002. *Science* 296:1852–1855. [4] Daulton T. L. et al. 2003. *Geochimica et Cosmochimica Acta* 67:4743–4767.

5162

THEORY OF ISOTOPIC FRACTIONATION DURING PHASE GROWTH IN A DIFFUSION-LIMITED REGIME

N. Dauphas. Origins Laboratory, Department of the Geophysical Sciences and Enrico Fermi Institute, The University of Chicago, 5734 South Ellis Avenue, Chicago Illinois 60637, USA. E-mail: dauphas@uchicago.edu

Introduction: Phase growth in a diffusion-limited regime is a ubiquitous process in planetary sciences. It may, for instance, apply to growth of hematite spherules from an aqueous fluid on Mars. Such a process can affect isotopes in two ways: i) Phase growth creates a concentration gradient between the surface and the surrounding medium. Different isotopes have slightly different diffusion coefficients. They therefore can be supplied at different rates to the surface of the growing phase. ii) If there is any equilibrium or kinetic isotope fractionation at the interface between the two phases, diffusion will control whether this fractionation is expressed in the fluid or in the solid. Frank [1] and Berner [2] evaluated the influence of supersaturation at infinity on the rate of crystal and concretion growth in a diffusion-limited regime. Recently, Dauphas and Rouxel [3] extended this work to calculate isotopic fractionation in the growing phase.

Results: The intuitive idea regarding the dynamic of this process might be that when the system has reached steady state, the interface grows linearly with time and there can be no isotopic fractionation because whatever comes in must be incorporated in the growing phase. This picture is flawed, however, because what governs the supply of elements to the growing phase is diffusion. If the concentration of an element is to remain constant at the interface (at saturation), then the interface must move as \sqrt{t} [1, 2]. The differential equations governing diffusion transport of elements towards a growing sphere or an infinite plate can be solved analytically when the interface moves as \sqrt{t} (quasi-stationary solution). The transient state for an initial step-function in concentration was calculated by numerical integration using the front-tracking fixed finite-difference grid method described by Crank [4]. The degree of supersaturation at infinity compared to the surface ($C_{\text{sat}}^* = C_{\text{sat}}/C_{\infty}$) is a convenient nondimensional variable to describe the system. When C_{sat}^* is close to 1, then the concentration gradient is small, the phase grows slowly, there is no isotopic fractionation due to diffusion, but the fractionation at the interface is expressed in the growing phase. When C_{sat}^* is close to 0, the phase grows rapidly, the isotopic fractionation due to diffusion is maximal, but the fractionation at the interface is expressed in the source medium.

Conclusions: Phase growth in a diffusion-limited regime can fractionate isotopes. At high growth rates, isotope fractionation will occur because of differences in diffusivities of different isotopes. At low growth rates, kinetic or equilibrium isotope fractionation at the interface will be expressed in the growing phase. The formalism described here may be useful for understanding and predicting isotopic fractionation measured in a variety of planetary materials, including terrestrial analogues of Martian blueberries [5].

References: [1] Frank F. C. 1950. *Proceedings of the Royal Society of London A* 201:586–599. [2] Berner R. A. 1968. *Geochimica et Cosmochimica Acta* 32:477–483. [3] Dauphas N. and Rouxel O. 2006. *Mass Spectrometry Reviews* 25:515–550. [4] Crank J. 1984. *Free and moving boundary problems*. Oxford: Oxford University Press. [5] Busigny V. and Dauphas N. *Earth and Planetary Science Letters*. Forthcoming.

5354

QUANTITATIVE MAPPING OF MELILITE ELEMENTAL COMPOSITION IN REFRACTORY INCLUSIONS

A. M. Davis. Department of the Geophysical Sciences, Enrico Fermi Institute and Chicago Center for Cosmochemistry, The University of Chicago, Chicago, Illinois 60637, USA. E-mail: a-davis@uchicago.edu

Introduction: Compositional variations in minerals in rocks are typically depicted in a qualitative way through X-ray maps and in a quantitative way through plots of concentration versus distance along linear profiles. The utility of X-ray maps has been improved in recent years through the application of combined color elemental maps [e.g., 1]. Modern X-ray microanalysis hardware and software also allow quantitative mapping to be done. Here, an X-ray spectrum is collected at each pixel and reduced to provide a chemical analysis. The information from quantitative maps can be extracted and manipulated so that maps of mole% of mineral components in solid solutions series can be produced. Several such maps for melilite have been published recently, but the methods used have not been described in detail.

Methods: All maps were collected using a JEOL JSM-5800LV SEM with an Oxford Link ISIS-300 microanalysis system. Maps are collected at a beam current high enough to produce ~40,000 counts per second on the detector, typically 10 nA, with a dwell time of 1–2 s per pixel. For mapping melilite, quantitative maps of wt% MgO, Al₂O₃, SiO₂ and CaO are needed. The Oxford software allows export of the data in each of these elemental maps as a grid of concentrations, along with grids of the 1 uncertainty for each element. After conversion of each grid to a column of numbers, plots of uncertainty versus concentration are used to eliminate pixels that are in cracks or on epoxy. Such data points will have anomalously high uncertainties. Once errant data points are eliminated, the mole percent åkermanite is calculated for each spot. Spots that are not melilite can easily be recognized and eliminated, as the Åk content based on Mg will not agree with that based on Al or Si. After culling of data in cracks and for minerals other than melilite, the mole% Åk data is transformed back to grid form and plotted as a color intensity map using the software package Igor. Collection and treatment of data using methods described here gives precision of ~1 mole% Åk.

Applications: Åk mapping led to the discovery of extreme variations in melilite composition in the unusual Allende inclusion Golfball, where the entire range of melilite composition from Åk₂ to Åk₇₂ can be found only μm apart [2]. A recent study of experimental crystallization of melilite from CAI melts led to the discovery of sector-zoned melilite [3]. Sudden jumps of a few mole% Åk along linear profiles through melilite in natural CAIs may be due to sector-zoning rather than complicated growth history. Given the bulk compositions of Type B CAIs in CV chondrites, the most Åk-poor melilite expected to crystallize contains 15–25 mole% Åk. However, most type B CAIs have more gehlenitic compositions, sometimes as low as Åk₁, within 100 μm of the rim. This has been known in a qualitative way from polarized light microscopy for some time, but Åk mapping makes this very easy to see. This unusual zoning feature likely results from a heating event subsequent to crystallization and may be related to Wark-Lovering rim formation.

References: [1] Krot A. N. et al. 2003. In *Meteorites, Comets, and Planets*. Amsterdam: Elsevier. pp. 407–430. [2] Simon S. B. et al. 2005. *Meteoritics & Planetary Science* 40:461–475. [3] Mendybaev R. A. et al. 2006. *Geochimica et Cosmochimica Acta* 70:2622–2642.

5182

THERMAL ANNEALING OF AMORPHOUS SILICATES: THE BEHAVIOR OF SILICATE DUST IN PROTOPLANETARY DISCS

C. Davoisne¹, Z. Djouadi², H. Leroux¹, L. d'Hendecourt², A. P. Jones², and D. Deboffle². ¹Laboratoire de Structure et Propriétés de l'Etat Solide (LSPES) USTL, 59655 Villeneuve d'Ascq, France. E-mail: carine.davoisne@ed.univ-lille1.fr. ²Institut d'Astrophysique Spatiale (IAS), Bâtiment 121, F-91405 Orsay, Université Paris-Sud 11-CNRS (UMR 8617) France

Introduction: In protoplanetary discs, the infrared spectra from ISO have shown evidence for crystalline silicate features [1], whereas in the interstellar medium, all the silicate dust is detected in an amorphous state [2]. To explain the presence of crystalline silicates in protoplanetary discs, condensation and thermal annealing are frequently invoked [3, 4]. In this study, we explore the behavior of amorphous ferromagnesian-silicates under annealing at controlled atmosphere with the aim to define the microstructural evolution of the interstellar precursors in the inner protoplanetary disc.

Experimental Procedure: The amorphous silicate precursor (olivine composition $Mg_{1.8}Fe_{0.2}SiO_4$) was obtained by electron beam evaporation as 100 nm-thick films onto different substrates [5]. The thin films were then submitted to thermal annealing in situ in a transmission electron microscope (TEM) or in a furnace under vacuum at controlled atmosphere (O_2 , CO/CO_2 and C/CO buffers).

Results: Under reduced conditions we have observed the formation of spherical iron metallic precipitate near 600 °C and their development at higher temperature. A progressive recrystallization of the silicate film into Mg-rich silicates (forsterite and enstatite) is obtained for temperature above 700 °C.

The investigation of microstructure after thermal annealing under oxidized conditions shows the formation of an Mg-Fe oxide (magnesioferrite) at 700 °C. The matrix recrystallizes progressively for temperature above 700 °C into Mg-rich silicate (forsterite and enstatite).

Conclusion: These results demonstrate that the microstructural evolution under thermal annealing is strongly dependent on the gas composition in which the silicate dust recrystallizes.

The crystalline phases formed are in strong agreement with those (principally Mg-rich silicate) observed by ISO in the protoplanetary discs and some of the microstructures can be related to those in IDPs, the so-called GEMS. Our results suggest a formation of these different phases in reduced conditions and are compatible with the scenario of a recrystallization of interstellar dust by thermal effect in protoplanetary discs. By means of a turbulent effect the annealed silicates can then be redistributed in the region of formation of comets and meteorites [6, 7].

References: [1] Malfait et al. 1998. *Astronomy and Astrophysics* 332: L25–L28. [2] Li A. and Draine B. T. 2001. *The Astrophysical Journal* 550: L213–L217. [3]. Rietmeijer F. J. M. 2004. Abstract #1960. 35th Lunar and Planetary Science Conference. [4] Keller L. P. and Messenger S. 2004. Abstract #1985. 35th Lunar and Planetary Science Conference. CD-ROM. [5] Djouadi Z. et al. 2005. *Astronomy and Astrophysics* 440:179–184. [6] Bockelée-Morvan D. et al. 2002. *Astronomy and Astrophysics* 384:1107–1118. [7] Davoisne C. et al. 2006. *Astronomy and Astrophysics* 448: L1–L4.

5163

CALCULATIONS OF HEATING CAUSED BY IMPACTS OF POROUS BODIES IN THE EARLY SOLAR SYSTEM

Paul S. De Carli¹ and John Wasson². ¹SRI International, Menlo Park, California 94025, USA. E-mail: paul.decarli@sri.com. ²University of California–Los Angeles, Los Angeles, California 90095, USA

Introduction: Wasson, Rubin, and others have suggested that shock compression provided a significant source of heating for planetesimals in the early solar system. It seems reasonable to assume that early planetesimals comprised porous aggregates of mm-size grains. Here we present calculations of heating due to impacts between porous bodies.

Method: The Autodyn wave propagation code was used to calculate the impact of a 1 km radius projectile on a 20 km radius target body. These calculations scale for any projectile mass, provided that the target dimensions are at least an order of magnitude greater than the projectile. Both bodies were modeled as chondritic with volume fractions of .38 pyroxene, .39 olivine, .07 albite, .06 troilite, and .1 Fe-10Ni. Compression and thermal data for the mineral constituents served as the basis for construction of a synthetic Hugoniot for the solid and for construction of a synthetic heat capacity versus temperature table. We constructed a P-alpha equation of state for a 50% porous initial material (1.84 g/cc), compressing to the appropriate solid compression curve at 5 GPa. To date, calculations have been carried out for impact velocities of 5 km/s, 7 km/s, and 10 km/s. Pressure histories were recorded at up to 150 stations in the target volume of interest. The peak pressure at each station was equated to the increase in internal energy due to shock compression followed by adiabatic pressure release. We then calculated the mass of target material relative to the projectile mass, Mp, in each of 4 post-shock temperature bins. Bin 1, 1500–2100K, corresponds to internal energy increases in the range of 1.4–2.3 kJ/g and peak pressures in the range of 10.2 GPa to 16.6 GPa. Bin 2, 2100–2400 K (complete melting), corresponds to internal energy increases in the range of 2.3–3.5 kJ/g and peak pressures in the range of 16.6–25.4 GPa. Bin 3, 2400–>3000K (incipient/partial vaporization), internal energy increase 3.5–5 kJ/g and peak pressures in range of 25.4–36.2 GPa. Bin 4 covers the internal energy range from 5 kJ/g up to about 12 kJ/g, still in the partial vaporization regime >3000K.

Table 1.

	Bin 1, 1500– 2100 K	Bin 2, 2100– 2400 K	Bin 3, 2400– >3000 K	Bin 4, >3000 K, <12 kJ/g
10 km/s	3 Mp	1 Mp	0.98 Mp	1.74 Mp
7 km/s	1.13 Mp	1.3 Mp	0.44 Mp	0.8 Mp
5 km/s	0.66	0.2	0	0

Results: Preliminary results show that impact velocities in excess of 5 km/s are required for substantial melt production in the case of impacts between 50% porous bodies of chondritic composition.

5015

CAN THE WATER PRESSURE IN THE ACCRETION DISK SUSTAIN WATER ADSORPTION ON OLIVINE?

N. H. de Leeuw¹, M. Stimpfl², C. R. A. Catlow¹, M. J. Drake², P. A. Deymier³, and A. W. Walker⁴. ¹Department of Chemistry, University College London, UK. ²Lunar and Planetary Laboratory, The University of Arizona, Tucson, Arizona, USA. ³Department of Material Science and Engineering, The University of Arizona, Tucson, Arizona, USA. ⁴University of Cambridge, Cambridge, UK

Introduction: In the accretion disk, gases coexist with solid particles for long periods. According to thermodynamic calculation, the H₂O/H₂ ratio in the accretion disk was about 5×10^{-4} , [1] which correspond to a p_{H₂O} of $\sim 10^{-8}$ bar. Note that the equilibrium partial pressure is probably a lower limit [2–3]. Astronomical observations show that dust clouds consist of Mg-rich olivine (Mg₂SiO₄, aka forsterite), pyroxenes, and other refractory minerals with radii <1 μm [4]. Several authors [5–7] suggest that these refractory minerals should coalesce during the early stage of planet formation by means of low-velocity impacts that would create low-density, irregularly shaped fractal structures. The concomitant presence of small fractal particulates with high surface area and of water gas in an environment of low-energy impacts raises the overlooked question of the role of adsorption of water into the building blocks of the rocky planets.

Methods: We have employed atomistic simulation techniques (program GULP [8–9]), to study the interaction between selected forsterite surfaces and water gas. We simulated associative adsorption, which entails molecular adsorption of a water molecule over olivine surfaces [10] while [11] simulated dissociative adsorption of water (adsorption of dissociated water molecules) over the same surfaces and investigated the energetic for both partial and total coverage.

The process of adsorption can be described according to the following equation: Surface + H₂O(g) ↔ Surface*(H₂O), where the left hand side of the equation represents water adsorbed on the surface. Once the thermodynamic properties of the reaction are known, the p_{H₂O} required to adsorb water on the forsterite surfaces at the T of interest can be obtained.

Results: Our calculations show that adsorption of water can take place on perfect forsterite surfaces at temperatures consistent with the inner accretion disk. In particular, associative adsorption on the {100} surface can begin at ~700K, while dissociative adsorption can take place on several surfaces at temperatures as high as 1000 K. Our investigation shows that adsorption of water gas onto forsterite grains is consistent with temperatures in the accretion disk. Next, we will explore the effect of olivine composition on the efficiency of adsorption and the kinetics of such reaction by means of molecular dynamic calculation.

References: [1] Lodders K. 2003. *The Astrophysical Journal* 591: 1220–1247. [2] Clayton R. N. 2004. Abstract #3020. Workshop on Oxygen in the Terrestrial Planets. [3] Cuzzi J. N. et al. 2004. Workshop on Chondrites and the Protoplanetary Disk. [4] Boekel R.V. et al. 2004. *Nature* 432:479–481. [5] Weidenschilling S. J. et al. 1999. *Protostar and planets III*. Tucson, Arizona: The University of Arizona Press. pp. 1031–1060. [6] Blum J. et al. 2000. *Icarus* 143:138–146. [7] Fogel M. et al. 1998. *The Astrophysical Journal* 501:175–191. [8] Gale J. D. et al. 2003. *Molecular Simulation* 29: 219–314. [9] Gale J. D. 1997. *Journal of the Chemical Society Faraday Transactions* 93:629–637. [10] Stimpfl M. et al. *Journal of Crystal Growth*. Forthcoming. [11] de Leeuw N.H. et al. 2000. *Physics and Chemistry of Minerals* 27:332–341.

5380

INDUCTION HEATING IN ASTEROIDS PART 1: OBSERVATIONS AND THEORY

D. N. Della-Giustina, C. A. Marsh, J. Giacalone, and D. S. Lauretta. Lunar and Planetary Laboratory, The University of Arizona, Tucson, Arizona 87521, USA. E-mail: dellagiu@email.arizona.edu

Introduction: Induction heating, or Joule heating, is the release of thermal energy within a body due to the resistance of that material to a current passing through it. Electromagnetic induction by the T Tauri solar winds has been proposed as a heating mechanism in the early solar system, and could have contributed to the thermal metamorphism and melting in planetesimals [1]. In order for electromagnetic induction to occur, a magnetic field of sufficient strength must sweep through a finitely conductive planetesimal inducing a current. Such a magnetic field would originate in the T Tauri sun and propagate through the early solar winds. In recent years, the induction heating theory has lost favor as a viable mechanism because the estimated T Tauri solar wind flux along the ecliptic was thought to be too weak to produce significant heating in planetesimal bodies [2].

Recently, the Chandra X-ray observatory completed a 13-day observation in the Orion Cluster of Young Stellar Objects (YSOs) comparable in mass to the early Sun [3]. Twenty-eight of these YSOs, located in the COUP field, emitted intense X-ray flares an average of 1.5 times over a 9 day interval of observation. The average flare luminosity of these objects was calculated to be $10^{3.8}$ ergs/s [4]. Using the characteristics of the X-ray flares Favata et al. [3] measured the minimum magnetic field necessary to confine the flaring plasma in the stellar corona of these objects. Results yielded a wide range of magnetic field strengths that range between 12 and 3480 Gauss with flare lengths of 0.002 to 0.216 AU. In contrast, the magnetic field strength in the modern solar corona is on the order of milliGauss [5]. The data derived from [3] demonstrate that the magnetic structures around these YSOs are in many cases significantly larger than the objects themselves. The presence of such extended magnetic fields suggest that they connect the stellar photosphere with the inner rim of a protoplanetary disk [3].

Conclusions: These magnetic field strength measurements indicate that the fields around these objects maintain enough intensity to validate the induction heating model. Although this evidence does not provide the direct magnetic field measurements in the estimated region of planetesimal formation, it does prompt the feasibility of electromagnetic induction to be re-evaluated as a viable heating mechanism in the early solar system [4]. We are re-evaluating this theory with a larger magnetic field strength using mathematic modeling and the magnetic field strength around the COUP field YSOs. We determine that field strengths in the region of the modern asteroid belt were on the order of 10–20 Gauss. These values inform the experimental simulation of this process [6].

References: [1] Sonett C.P. et al. 1968. *Nature* 219. [2] Wood J. A. and Pellas P. 1991. The sun in time, <http://science.nasa.gov/ssl/pad/solar/suntime/suntime.stm>. [3] Favata F. et al. 2005. *The Astrophysical Journal* 160:469–502. [4] Marsh C. A. et al. 2006. Abstract #2078. 37th Lunar and Planetary Science Conference. [5] Mancuso S., Spangler S. R. 2000. *The Astrophysical Journal* 539:480. [6] Marsh C. A. et al. 2006. Abstract #5318. *Meteoritics & Planetary Science*. This issue.

5168

MANGANESE-RICH PHASES IN CM CHONDRITES: Mn-Cr SYSTEMATICS OF CARBONATES AND SILICATES

Simone de Leuw, Alan E. Rubin, and John T. Wasson. Institute of Geophysics and Planetary Physics, University of California–Los Angeles, Los Angeles, California 90095–1567, USA. E-mail: sdeleuw@ucla.edu

Introduction: CM carbonaceous chondrites record a variety of nebular and parent-body processes. An important process that affected CM chondrites is aqueous alteration. This process resulted in the formation of secondary phases [1, 2]. Little is known about the time scale and locations of these alteration processes. Models range from progressive alteration within a parent-body environment [1, 3, 4] to the possibility that significant alteration occurred in small precursor planetesimals prior to the formation of the CM asteroid [5]. It is important to determine where and when the alteration took place. It is possible that the time scale of alteration is comparable to the ^{53}Mn half-life (3.7 Ma).

Observations: We studied several CM chondrites of different petrographic subtypes (e.g., CM2.0 LAP 02277, CM2.1 QUE 93005, CM2.2 Cold Bokkeveld, CM2.4/2.5 Murray, CM2.5 Murchison). We used SEM techniques (EDX element maps) as well as electron-probe studies (wavelength-dispersive element maps and quantitative analyses). Element maps show Mn-rich carbonates in QUE 93005 and LAP 02277 as well as Mn-bearing silicates in Murchison. Carbonates are relatively abundant (~2–3 vol%) and randomly distributed in the thin sections of QUE 93005 and LAP 02277. The carbonates occur as individual crystals as well as irregularly shaped aggregates in QUE 93005 and as single crystals in LAP 02277. We analyzed 25 different carbonate crystals from QUE 93005 by electron-probe. QUE 93005 contains both calcite and/or aragonite (CaCO_3) and dolomite ($\text{CaMg}(\text{CO}_3)_2$). Dolomites typically occur as single crystals within larger calcite crystals. Most calcite crystals range between 50 and 100 μm , dolomite grains are typically 10–30 μm . The analyses show enrichments of Mn in several carbonate grains, indicating their suitability for Mn-Cr isotopic studies. MnO contents in calcites range between 0.05 and 0.86 wt% with an average of 0.19 wt%. Dolomites are characterized by higher MnO contents, ranging between 1.8 and 4.5 wt% with an average content of 3.4 wt%.

Discussion and Future Work: In order to constrain the timing of carbonate formation, we will use the CAMECA ims 1270 ion microprobe at UCLA to study the Mn-Cr systematics of Mn-rich phases in CM chondrites that have undergone different degrees of aqueous alteration. We will focus our study on large carbonate and silicate grains with high Mn/Cr ratios, two important prerequisites for the search for radiogenic ^{53}Cr formed from the decay of ^{53}Mn . Published data for CM chondrites show initial $^{53}\text{Mn}/^{55}\text{Mn}$ ratios of $(5.0 \pm 1.5) \cdot 10^{-6}$ for ALH 84034 [6], and $(1.31 \pm 0.6) \cdot 10^{-5}$ for Y-791198 [7]. Our new data for CM chondrites will help constrain the time scale of aqueous alteration.

References: [1] Zolensky M. E. and McSween H. Y., Jr. 1988. In *Meteorites and the early solar system*. Tucson, Arizona: The University of Arizona Press. pp. 114–143. [2] Brearley A. J. and Jones R. H. 1998. *Reviews in Mineralogy* 36:398. [3] McSween H. Y., Jr. 1987. *Geochimica et Cosmochimica Acta* 51:2469–2477. [4] Rubin A. E. et al. *Geochimica et Cosmochimica Acta*. Forthcoming. [5] Bischoff A. 1998. *Meteoritics & Planetary Science* 33:1113–1122. [6] Brearley A. J. and Hutcheon I. 2000. Abstract #1407. 31st Lunar and Planetary Science Conference. [7] Brearley A. J. and Hutcheon I. 2002. Abstract. *Meteoritics & Planetary Science* 37: A23.

5147

IDENTIFICATION OF A COMMON R CHONDRITE IMPACTOR ON THE UREILITE PARENT BODY

H. Downes^{1, 2} and D. W. Mittlefehldt³. ¹Birkbeck University of London, Malet St. London, WC1E 7HX, UK. E-mail: h.downes@ucl.ac.uk. ²Lunar and Planetary Institute, Houston, Texas 77054, USA. ³Johnson Space Center, Nasa Road 1, Houston, Texas, USA

Introduction: Polymict ureilites are brecciated ultramafic meteorites that contain a variety of single mineral and lithic clasts [1]. They represent the surface debris from a small, differentiated asteroid. We are continuing a detailed petrological study of several polymict ureilites including EET 87720, EET 83309 and FRO 93008 (from Antarctica), North Haig, Nilpena (Australia), DaG 976, DaG 999, DaG 1000, and DaG 1023 (Libya). The latter four stones are probably paired. Clast sizes can be 10 mm in diameter, so a thin-section can consist of a single lithic clast.

Clast Types and Compositions: The most common clast-types are ureilitic olivines and pyroxenes that cover the range of mg# (74–96) and Fe/Mn values observed in monomict ureilites [2]. Among the non-ureilitic mineral clasts are a variety of olivine and pyroxene grains with variable mg#s and distinct minor element contents, some of which may represent as-yet unsampled chondritic bodies. Among the lithic clasts is a type dominated by ferroan olivine (mg# = 59–65), with subordinate sodic plagioclase, orthopyroxene, chromite and pyrrhotite. These clasts have variable recrystallized metamorphic textures, ranging from fine to medium grained and generally lack chondrules. We have found them in EET 87720, EET 83309 and DaG 999/DaG 1000. Similar ferroan olivines were previously described in polymict ureilites DaG 319 [3], FRO 93008 [4] and DaG 164 [5] and they likely represent a common impactor on the ureilite parent body.

R Chondrite Origin of Impactor Clasts: Clasts in DaG 319 were suggested to be derived from an R chondrite, but oxygen isotope data on one of these resembled ordinary chondrites [6]. The olivines in these clasts clearly differ from those in the ureilites, not only in their low mg#s but also in their low Cr and Ca and high Ni contents. Their compositions very closely resemble those of olivines in R chondrites such as Rumuruti [7], Acfer 217 [8], PCA 91002 [9], Carlisle Lakes and ALH 85151 [10]. Furthermore, the presence of chromite and pyrrhotite and the absence of metal also suggest a strong similarity to R chondrites. Similar R chondrite lithic clasts have also been reported from Weatherford [11] and Kaidun [12], suggesting that R chondrite projectiles may have been common impactors on carbonaceous clan asteroids in the early solar system.

References: [1] Goodrich C. A. et al. 2004. *Chemie der Erde* 64:283–327. [2] Downes H. and Mittlefehldt D. W. Abstract #1150. 37th Lunar and Planetary Science Conference. [3] Ikeda Y. et al. 2000. *Antarctic Meteorite Research* 13:177–221. [4] Fioretti A. M. and Goodrich C. A. 2001. Abstract #5003. *Meteoritics & Planetary Science* 36:A58. [5] Cohen B., Goodrich C. A., and Keil K. 2004. *Geochimica et Cosmochimica Acta* 68:4249–4266. [6] Ikeda Y. et al. 2003. *Antarctic Meteorite Research* 16:105–127. [7] Schulze H. et al. 1994. *Meteoritics* 29:275–286. [8] Bischoff A. et al. 1994. *Meteoritics* 29:264–274. [9] Rubin A. E. and Kallemeyn G. W. 1994. *Meteoritics* 29:255–264. [10] Rubin A. E. and Kallemeyn G. W. 1989. *Geochimica et Cosmochimica Acta* 53:3035–3044. [11] Prinz et al. 1993. *Meteoritics* 28:419. [12] Zolensky M. and Ivanov A. 2003. *Chemie der Erde* 63:185–246.

5060

ORIGIN OF THE HALOGENS IN THE DARK MATRIX OF RUMURUTI

G. Dreibus, W. Huisl, B. Spettel, and R. Haubold, Max-Planck-Institut für Chemie, P.O. Box 3060, D-55020 Mainz, Germany. E-mail: dreibus@mpch-mainz.mpg.de

Introduction: Rumuruti is a regolith breccia with typical light-dark structure and has solar-wind-implanted gases [1, 2]. The first analyses with INAA of two whole rock samples from a large light-colored clast (110 mg) and from the dark matrix (90 mg) gave identical compositions of both lithologies, except for the enrichment of C, Br, and Hg in the dark matrix. The other halogens could not be measured [1]. In a new aliquot of the dark matrix, all halogens were measured by RNAA and an ionselective electrode, and compared with the gas-rich H5-chondrite regolith breccia Pantar.

Results: Measured halogens and other volatile and moderately volatile elements are as follows:

Table 1.

	Rum.	Rum.	Rum.	CM	H3	H5	H5
*	1	2	3	4	5	6	7
wt. (mg)	90	113	110	207	129	102	101
S (%)	4.1		3.99	3.07	2.2		
F (ppm)	4	<30		38	13	8	8
Cl		282		180	303	119	75
Br	1.2	1.19	0.41	0.75	1.15	0.79	0.25
J		0.22		0.19		0.21	0.03
C	740		420	17100			
Se	14.4	14	14.7	12.9	7.9	8.5	9.3
Zn	165	157	160	180	44	54	50
Na	6900	6790	6780	1740	6760	5900	5700
K	693	816	820	310	505	790	
Mn	2270	2230	2270	1560	2420	2300	2300

*1: Rumuruti, dark matrix [1]; 2: Rumuruti, dark matrix, this work; 3: Rumuruti, light clast [1]; 4: Murchison, this work; 5: Tieschitz, this work and [3]; 6: Pantar dark, this work and [4]; 7: Pantar light, this work and [4].

The concentrations of Cl, Br, and J in the dark matrix of Rumuruti are similar to carbonaceous chondrites (CM), Tieschitz (H3), and the dark matrix of Pantar. The abundances of the moderately volatiles S, Se, and Zn are similar to CM and show no variations between dark and light matrix in Rumuruti as also found in ordinary chondrites (see Table 1). Br is enriched in the dark matrix relative to the light clast by a factor of 3 which we also found for both components in the gas-rich regolith breccia Pantar. The heterogeneous distribution of the highly volatile halogens in the gas-rich regolith breccias Rumuruti and ordinary chondrites could be caused by redistribution processes during thermal metamorphism or by interaction with fluid phases on their parent bodies.

References: [1] Schulze H. et al. 1997. *Meteoritics* 29:275–286. [2] Weber H. W. and Schultz L. 1995. Abstract. *Meteoritics* 30:A596. [3] Kallemeyn G. W. et al. 1989. *Geochimica et Cosmochimica Acta* 53:2747–2781. [4] Lipschutz M. E. et al. 1983. *Geochimica et Cosmochimica Acta* 47: 169–181.

5008

IS MARTIAN SURFACE TYPE 1 MILDLY ALKALINE? RESULTS FROM NEW LINEAR DECONVOLUTIONS OF SURFACE TYPES 1 AND 2

T. L. Dunn and H. Y. McSween, Jr. Department of Earth and Planetary Sciences, University of Tennessee, Knoxville, Tennessee 37996, USA. E-mail: tdunn@utk.edu

Introduction: The Thermal Emission Spectrometer (TES) uses thermal infrared energy emitted from the Martian surface to identify rock compositions and surface lithologies [1]. TES analyses have identified two compositionally distinct surface types on Mars [2, 3]. Surface type 1 is basalt, and surface type 2 has been suggested to be either andesite [2, 3] or partially weathered basalt [4, 5]. Both of these volcanic surface compositions are subalkaline, but evidence from Gusev crater rocks analyzed by the Spirit Rover suggests alkalic magmatism may also have occurred on Mars [6]. This assertion is also supported by evidence from SNC meteorites. For example, mineral assemblages and LREE enriched signatures of the Chassigny meteorite are comparable to those of some terrestrial alkalic magmas, prompting [7] to propose that Chassigny may have formed from an alkalic magma. Also, fractional crystallization modeling [8] of a parental magma composition for Nakhla produces an alkaline liquid line of descent [9]. These observations suggest that Martian volcanism may not have been strictly subalkaline, as current remote sensing data would suggest.

Methodology: To test the validity of the assessment of surface type 1 and 2 as subalkaline rocks, ST1 and ST2 were linearly deconvolved [10] using an end-member suite tailored for mildly alkaline volcanic rocks. Modal mineralogies were determined directly from the linear deconvolution algorithm, and bulk rock chemistries were derived from modeled mineralogies by combining endmember compositions in proportion to their abundances and recalculating to wt%. Our modeled modal mineralogies and derived bulk rock chemistries were then compared to previous deconvolutions of surface types 1 and 2 [2, 3, 4].

Results: Deconvolution of surface types 1 and 2 spectra using an end-member set tailored for alkalic rocks produces modal mineralogies that are distinct from previous deconvolutions using subalkaline end-member sets [2, 3, 4]. Derived chemical compositions of surface type 2 are similar to previous estimates, confirming that surface type 2 is subalkaline. Surface type 1, however, is more alkaline than previous results. Using [11], surface type 1 is classified as a basaltic trachyandesite rather than a basalt. Combined with evidence from Gusev crater rocks and SNC meteorites, this may suggest that some surface type 1 regions could contain alkalic rocks. The average surface type 1 spectrum, however, is not definitive.

References: [1] Christensen P. R. et al. 2000. *Journal of Geophysical Research* 106:23,823–23,871. [2] Bandfield J. L. et al. 2000. *Science* 287: 1626–1630. [3] Hamilton V. E. et al. 2001. *Journal of Geophysical Research* 106:14,733–14,746. [4] Wyatt M. B. and McSween H. Y., Jr. 2002. *Nature* 417:263–266. [5] Michalski J. R. et al. 2005. *Icarus* 174:161–177. [6] McSween H. Y., Jr. et al. 2006. Abstract # 1120. 37th Lunar and Planetary Science Conference. [7] Nekvasil H. 2003. Abstract #3041. 6th Mars Conference. [8] Ghiorso M. S. and Sack R. O. 1995. Contributions to Mineralogy and Petrology 119:197–212. [9] Stockstill K. R. et al. 2005. *Meteoritics & Planetary Science* 40:377–396. [10] Ramsey M. S. and Christensen P. R. 1998. *Journal of Geophysical Research* 103:577–596. [11] Le Bas M. J. et al. 1986. *Journal of Petrology* 27:745–750.

5239

THE MICROMETEORITE MASS FLUX AS RECORDED IN DOME C CENTRAL ANTARCTIC SURFACE SNOW

J. Duprat¹, C. Engrand¹, M. Maurette¹, F. Naulin¹, G. Kurat², and M. Gounelle³. ¹CSNSM, Bat.104, 91405 Orsay, France. ²University Wien, Inst. Geol. Wissenschaft., A-1090 Vienna, Austria. ³MNHN, 57 rue Cuvier, 75231 Paris, France

Introduction: We used the unique characteristics of central Antarctic surface snow to revisit the issue of the extraterrestrial (ET) dust flux reaching the Earth's surface. Marine osmium isotopic data indicate an average flux of ET material of 30×10^3 tons/yr [1], in agreement with flux of micrometeoroids before atmospheric entry [2]. On short time scales (<Myr), the bulk of ET material comes from dust with sizes $\sim 200 \mu\text{m}$ [2]. Still a challenging issue is to estimate the fraction of this flux that actually reaches the Earth surface as particles (i.e., micrometeorites) from the one that it vaporized during atmospheric entry.

Experimental Procedure and Results: The evaluation of the micrometeorite (MM) flux requires an accurate control on several critical parameters: i) the equivalent exposition surface, S, (in m^2/yr), ii) the collection efficiency, iii) the potential statistical biases. In January 2002, we collected MMs at CONCORDIA station at Dome C (75°S - 123°E). A total of 10 m^3 of snow were manually extracted in a clean trench at a depth of 4 m, corresponding to $S \sim 100 \text{ m}^2/\text{yr}$. This snow was melted and sieved down to $30 \mu\text{m}$ in a dedicated ultra-clean stainless steel snow smelter allowing us to measure, for each melt, the collection efficiency in two size ranges (30 – $100 \mu\text{m}$ and $>100 \mu\text{m}$). Dome C snow is well protected from terrestrial dust within the $>30 \text{ m}$ size range allowing the analysis of all the particles contained in the filters. The collection technique used and the unique conditions of Dome C snow allow recovering of all types of ET particles, i.e., both melted and unmelted. We identified by SEM imaging and EDX analysis a total of 500 MMs. The accumulation rate at Dome C is low and regular [3], thus the S parameter can be deduced accurately for each melt. The 10 consecutive melts yielded 10 independent flux values ranging from 3×10^3 up to 10×10^3 tons/yr. The large variations of these values can be understood as resulting from statistical sampling. Following [1], we developed a Monte Carlo numerical code simulating the expected flux. We find an average MM flux at Dome C of 5300 tons/yr. The flux of MMs at Earth surface represent no more than one-third of the total incoming flux of particles before atmospheric entry, in agreement with recent studies conducted in Antarctic snow [4] and ice [5]. We will discuss the various sources of uncertainties for all these different studies and emphasize the assets of the present work as well as the corrections that have to be applied to both CONCORDIA flux and to values determined before atmospheric entry [1, 6]. Finally, we will present the high statistics MMs collection we performed at CONCORDIA in January 2006.

Acknowledgements: We thank IPEV and PNRA for funding and logistical support to the CONCORDIA micrometeorite collection at Dome C.

References: [1] Peucker-Ehrenbrink B. and Ravizza G. 2000. *Geochimica et Cosmochimica Acta* 64:1965–1970. [2] Love S. G. and Brownlee D. E. *Science* 1993. 262:550–553. [3] Petit J.-R. et al. 1982. *Journal of Raman Spectroscopy* 87:4301–4308. [4] Taylor S. et al. *Science* 1998. 392:899–903. [5] Yada T. et al. *Earth and Planetary Science Letters* 2004. 56: 67–79. [6] Grün E. et al. 2001. *Interplanetary dust*. Berlin: Springer.

5352

LAYERED CHONDRULES IN CARBONACEOUS AND ORDINARY CHONDRITES

D. S. Ebel¹ and M. K. Weisberg^{1, 2}. ¹Department of Earth and Planetary Sciences, American Museum of Natural History, New York, New York 10024, USA. E-mail: debel@amnh.org. ²Department of Earth and Planetary Sciences, Kingsborough College CUNY, Brooklyn, New York 11235, USA

Introduction: Chondrules with sharp concentric layers are reported from CV [2], CR [1–3], CM [4], and ordinary chondrites (OC) [5, 6]. Layers vary in texture, mineralogy, and composition. CAIs, and AOs (transitional to chondrules) also exhibit concentric layers in whole or in parts [7, 8]. Many hypotheses exist for layering [1–4, 6–9], and different types of layering may form by different processes. The relative abundances and 3-D structures of concentric layered chondrules are unknown. Few are described in detail. We identified layered chondrules in Renazzo (CR2), Allende (CV3), Semarkona (LL3), Bjurböle (L/LL4), Karoonda (CK4), and Chainpur (LL3) in 3-D images of $\sim 1 \text{ cm}^3$ pieces from the AMNH collection, using synchrotron X-ray tomographic reconstructions [10], and 2-D elemental mapping and spot analyses of slices that were cut guided by 3-D images. Layering provides clues to chondrule source materials, crystallization and accretion environments, and possible heating mechanisms.

Results: Types of layering include, from inside to outside: 1) ol-rich to opx-rich; 2) metal-poor to metal-rich; 3) barred ol to coarse ol; 4) metal-rich to ol-rich; 5) coarse metal to fine metal; 6) opx-rich to ol-rich (rare); 7) silicate to metal-rich “dust”; and 8) CAI-like to ol-rich, in AOs. Layered objects appear to be more common in the CR than in the CV, and rare in OC [1, 3]. Tomography, however, allowed location of, for example, a rare layered chondrule in Semarkona with multiple type 2 layers.

Discussion: Each meteorite class displays chondrule layering of different kind and extent. The heating process for chondrule formation probably differed in intensity or efficiency in the region from which each class formed. Unlike OC and CV chondrules, many CR chondrules have metal, Mg silicate, and Ca-, Al-rich components in distinct layers. The OC appear more thoroughly converted from dust into chondrules, by higher degrees of melting and/or remelting, whereas in CV, CR, and CK the chondrule rims are sintered into layers to varying extents, preserving earlier growth cycles. In the perhaps most primitive chondrites, CR [12], metal-silicate fractionation occurred very early, recorded in type 2 layering, and rim accretion and re-heating followed chondrule collisions. Some layered chondrules suggest open-system olivine-vapor reaction to form pyroxene, others suggest sintering of lower-temperature, pyroxene-normative dusty rims.

References: [1] Prinz M. et al. 1985. Abstract. 16th Lunar and Planetary Science Conference. pp. 677–678. [2] Metzler K. et al. 1988. Abstract. 19th Lunar and Planetary Science Conference. pp. 772–773. [3] Weisberg M. K. et al. 1993. *Geochimica et Cosmochimica Acta* 57:1567–1586. [4] Metzler K. et al. 1992. *Geochimica et Cosmochimica Acta* 56: 2873–2897. [5] Jones R. and Scott E. R. D. Proceedings of the 19th Lunar and Planetary Science Conference. pp. 523–536. [6] Krot A. N. and Wasson J. T. 1995. *Geochimica et Cosmochimica Acta* 59:4951–4966. [7] Weisberg M. K. et al. 2004. *Meteoritics & Planetary Science* 39:1741–1753. [8] Ruzicka A. 1997. *Journal of Geophysical Research* 102:13,387–13,402. [9] Trigo-Rodríguez et al. 2006. *Geochimica et Cosmochimica Acta* 70:1271–12909. [10] Ebel D. S. et al. *Meteoritics & Planetary Science*. Forthcoming. [12] Wood J. A. 1963. *Icarus* 2:152–180. (NASA Cosmochemistry NAG5-12855 (DSE); DOE, Basic Energy Sciences, W-31-109-ENG-38 (APS/GSECARS); NASA Astrophysics Data System Bibliographic Services).

5012

MATHEMATICAL MODEL AND IMPACT CONDITIONS FOR WETUMPKA IMPACT CRATER, ALABAMA, USAJ. C. Echaurren¹, D. T. King, Jr.², L. W. Petruny³, and M. C. L. Rocca⁴.¹Codelco Chuquicamata, Chile. E-mail: jecha001@codelco.cl. ²Department of Geology, Auburn University, Auburn, Alabama 36849-5305, USA.³AstraTerra Research, Auburn, Alabama 36831 USA. ⁴Mendoza 2779-16A, Ciudad de Buenos Aires, Argentina

Synopsis: Wetumpka impact structure, located in Elmore County, Alabama, USA (centered at 32°31.3'N, 86°10.4'W), is a locally prominent, semi-circular, rimmed feature with a structural diameter of 7.6 km and a modern rim height of as much as 120 m [1, 2]. This impact structure is composed of relatively highly indurated crystalline rock, which forms the impact-structure rim, and an unconsolidated mélange of resedimented and (or) deformed Upper Cretaceous sedimentary formations comprising two impact-structure related sedimentary terrains: a) within the crystalline rim (interior unit), and b) directly outside the crystalline rim on the southern side (extra-structure or deformed unit) [1, 2]. Both the marine target setting and composite target stratigraphy had a profound effect upon the shape and sedimentology of this impact structure [3, 4]. In marine setting, which was less than 100 m deep, a water crater was opened and then collapsed with a violent resurgence. The inability of the missing southern rim to withstand this resurgence is interpreted to be the origin of an early modification stage rim collapse event.

Analytical Method and Results: According to this model [5], the asteroid diameter is ~246.5 m, with a velocity and impact angle of ~18.46 km/s and 43.18°, respectively. The number of rings are calculated in ~0.84 with a initial crater profundity of ~572.68 m, this quantity could be altered across the passage of time to ~353.03 m, the melt volume is ~2.2E10 m³ or ~22.03 km³. The number of ejected fragments are estimated in ~2.55E6 with average sizes of ~1.81 m, and a cloud of dust with diameter of ~9,498 km. The total energy in the impact is calculated in ~7.7E25 Ergs, i.e., ~1,833 megatons. Before of the erosion effects the transient crater is estimated in ~4.29 km, the hydrothermal zone (hydrothermal systems) is of ~338.08 m to 2.15 km from the nucleus of impact. The lifetimes estimated are of ~37,077 years to 57,874 years with uncertainties of ~±0.67% to ±3.00%, i.e., from ±249 years to ±1,737 years. Hydrothermal temperatures from 0.25 years to 1,400 years are estimated in ~158.14 °C to 61.35 °C, respectively. The fragments are ejected to ~87.74 km from the impact center, with a velocity of ejection of ~2.2 km/s, ejection angle of ~5.14° and maximum height of ~1.97 km. The density of the asteroid is calculated in ~4.97 g/cm³ and the combined density (maximum and minimum) for the ejected fragments is estimated in ~2.08 g/cm³. The maximum height of Tsunami for 400 m and 7.5 km from the source is ~414 m and 22 m, respectively. The seismic shock-wave magnitude is calculated in ~8.1 in the Richter scale. The maximum time of permanency for the cloud of both dust and acid in the atmosphere is ~28 days and 4.6 months, respectively. The temperature peak in the impact is calculated in ~1.17E3 times the temperature of the solar nucleus, by a space of time of ~1.16 ms. The pressure to 1.01 km of the center of impact is ~4.18 Gpa.

References: [1] King D. T., Jr. et al. 2002. *Earth and Planetary Science Letters* 202:541–549. [2] King D. T., Jr. et al. 2003. In *Impact markers in the stratigraphic record*. Berlin: Springer. pp. 97–112. [3] King D. T., Jr. et al. 2004. *GSA Abstracts with Program* 36:266–267. [4] King D. T., Jr. et al. 2005. Abstract. *Meteoritics & Planetary Science* 40:A81. [5] Echaurren J. and Ocampo A. C. 2003. Abstract. EGS-AGU-EUG Joint Assembly, Nice, France.

5335

PETROPHYSICAL AND ROCK MAGNETIC PROPERTIES OF IMPACTITES FROM DEEP DRILL CORES OF BOSUMTWI IMPACT STRUCTURE

T. Elbra and L. J. Pesonen. Division of Geophysics, University of Helsinki, Helsinki, Finland. E-mail: tiu.elbra@helsinki.fi

Introduction: We are reporting petrophysical and rock magnetic data from deep drill cores of Bosumtwi impact structure. Several measurements (e.g., magnetic susceptibility and its temperature dependence, intensity of natural remanent magnetization, density, porosity) were carried out in order to better understand the formation of Bosumtwi impact structure and to improve the geophysical modellings. Special attention was drawn to core BCDP-8A and its interval of 300–400 m. Lithologically this interval consists of breccias inter-layered with greywacke and dark shale.

Results: Results of magnetic susceptibility show that although most of the samples hold relatively low ferromagnetic component of magnetic susceptibility (200–500 E⁻⁶ SI) there are present few magnetic susceptibility highs. These highs are present in above mentioned interval 300–400 m and pinpoint toward greywacke. In order to find out what is causing enhanced susceptibilities more detailed rock magnetic measurements were carried out. Even though greywacke shows higher susceptibilities, the values are still too small to explain the aeromagnetic anomalies. Density results show that in case of drill core BCDP-8A average density (2350–2750 kg/m³) is lower in upper part of the core and increases with depth. Densities from BCDP-7A are in general much lower (1900–2700 kg/m³) and do not show depth dependence. Both drill cores show high porosity values.

5059

INTRACRYSTALLINE AND GRAIN-BOUNDARY OLIVINE-RINGWOODITE (-WADSLLEYITE) PHASE TRANSITIONS IN SHOCKED L6 CHONDRITES: EVIDENCE FOR DIFFUSION CONTROLLED PHASE TRANSITION MECHANISMS INVOLVING Fe AND Mn

A. El Goresy¹, T. Ferroir², Ph. Gillet², M. Chen³, L. Dubrovinsky¹, and A. Simionovici². ¹Bayerisches Geoinstitut, Universität Bayreuth, 95447 Bayreuth, Germany. E-mail: ahmed.elgoresy@uni-bayreuth.de. ²Ecole Normale Supérieure de Lyon, 69364 Lyon Cedex 07, France. ³Guangzhou Institute of Geochemistry, CAS, Wushan, Guangzhou 510640, China

Introduction: Two coexisting different olivine-ringwoodite phase transition mechanisms in shocked L6 chondrites were first reported by [1, 2]: 1) phase transition commencing at grain boundaries only in olivine grains <100 μm in melt veins leading to polycrystalline ringwoodite aggregates, and 2) intracrystalline ringwoodite lamellae along {101} and (100) planes of large olivine single crystals inside and outside the melt veins, respectively [1, 2]. We conducted a detailed survey of both phase transition mechanisms in the shocked chondrites Sixiangkou and Peace River by reflected-light microscopy, laser microRaman mapping, SEM, combined synchrotron microbeam X-ray diffraction and X-ray fluorescence mapping and electron microprobe microanalysis to determine the fine-scale mineral inventory, mineral compositions, interface relationships and to elucidate the phase transformation mechanisms, both prograde and retrograde.

Results: Olivine single grains (Fa₂₂₋₂₅) entrained in the melt veins depict phase transformation to both ringwoodite and wadsleyite with stark contrasting compositions and unique spatial arrangements. 1) Ringwoodite (Fa₃₂₋₃₆) in the polycrystalline aggregates occupies the major outer portions of the original olivine grains, whereas wadsleyite (Fa₁₂₋₁₄), along with residual olivine (Fa₁₈₋₂₀) occupy the cores of the original individual grains. 2) Large olivines depict spectacular ringwoodite-wadsleyite textures and compositions not encountered before. Olivines are intersected by two sets of thick ringwoodite lamellae (≥12 μm; Fa₃₀₋₃₉), the latter overgrown by large wadsleyite patches (<8 μm; Fa₁₇₋₁₉). Residual olivine (Fa₁₈₋₂₀) islands display in their interiors two sets of well-oriented wadsleyite lamellae. Synchrotron X-ray fluorescence mapping revealed depletion of both ringwoodite and wadsleyite in Mn due to diffusion to olivine during their growth. There is Raman and synchrotron X-ray ample evidence for partial back transformation of ringwoodite lamellae to secondary wadsleyite and olivine, respectively. Remarkably, both less dense secondary polymorphs inherited the ringwoodite compositions (Fa₃₀₋₃₉) thus negating back interdiffusion of Fe and Mn.

Conclusions: The results unambiguously indicate that both olivine-ringwoodite (-wadsleyite) phase transition mechanisms encountered are diffusion controlled leading to enrichment of ringwoodite in Fe and depletion in Mn. In contrast, the resulting primary wadsleyite is exceedingly depleted in fayalite. These findings are in contrast to [3] and hence suggest that the crystallizing ringwoodite may have acquired additional FeO from the melt vein. Ringwoodite lamellae are strongly zoned (Fa₃₅₋₃₉) thus confirming the diffusion-controlled phase transition mechanism.

References: [1] Chen M. et al. 2004. *Proceedings of the National Academy of Sciences* 101:15,033–15,037. [2] El Goresy A. et al. 2005. Abstract. *Meteoritics & Planetary Science* 40:A43. [3] Akaogi M. et al. 1996. *Journal of Geophysical Research* 94:15,671–15,685.

5022

STAR FORMATION IN A TURBULENT INTERSTELLAR MEDIUM

Bruce G. Elmegreen. IBM Research Division, T. J. Watson Research Center. E-mail: bge@watson.ibm.com

The interstellar medium is a highly dissipative, fractal gas that is stirred constantly on many scales by a variety of energy sources. Stars and star clusters form in the dense regions where gravity overcomes the turbulent and thermal motions. In this talk, the general properties of star formation will be reviewed, along with specific properties most relevant to elemental enrichment and the formation of the Sun.

5031

THE UNIQUE BUSHVELD COMPLEX: SUPERHEAT-DOMINANT IMPACT PROCESSES BEYOND SUDBURY

W. E. Elston. Department of Earth and Planetary Sciences, University of New Mexico, Albuquerque, New Mexico 87131, USA. E-mail: welston@unm.edu

Stages beyond Sudbury: The >400 km multiring Bushveld Complex is reinterpreted in terms of two catastrophes separated by relative quiescence: Multiple impacts, mantle upwelling, and caldera-like collapse. Impacts resulted in two magma suites: 1) a Sudbury-type superheated melt pool [1], which overflowed into lobate outer ring basins (lower 1200 m of the Rooiberg Group, a pseudovolcanic suite new to petrology); 2) decompression melts of upper mantle (Rustenburg Layered Suite) and crust (Lebowa Granite Suite, RLS), generated at the head of upwelling mantle [2] and emplaced as multiple sills beneath the Rooiberg overflow. Marginal to the upwelling, subsidence of the outer ring basin [3] allowed >10 km of Rooiberg, RLS, and LGS to accumulate at the surface, without collapse. Of all proposed terrestrial impacts, the Bushveld alone had the force to trigger mantle upwelling and voluminous melts (10^6 km^3 , ~90% of the Bushveld Complex).

Additional LGS plutons and younger sediments conceal the Sudbury-type melt pool, except for massive granophyre at the Rooiberg. More evidence for its existence comes from a) textures in overflow-facies Rooiberg, explicable as viscous emulsion segregations [1] in superheated inflated flows and surges, b) a lower Rooiberg sequence from mafic to siliceous, with Fe-Ti-P enrichment at the interface [1, 4], and c) from Sudbury-type Ni-Cu-Pt "offset" ores, unlike Cr-Pt ores of RLS.

Lower Rooiberg outflow is dominated by superheat, not shock. Quench-textured high-T polymorphs of SiO_2 (e.g., quartz paramorphs after tridymite needles, as known elsewhere from the basal breccia of the Onaping Fm. [5]), take the places of high-P phases. Deformation twins take the place of PDFs in annealed quartz. Rare shock features (high-relief diaplectic glass, kink bands, mosaics) occur in relatively "cool" paleochannels.

Water influxes triggered later explosive overflows from the melt pool, evidenced by tsunami deposits between high-T Rooiberg melt rocks. Melt pool equilibrated with the upper crust; the top ~3 km of the Rooiberg converged with invading LGS in composition [6] and with conventional rhyolite in petrography.

The Second Catastrophe: Crustal melting culminated in caldera-like catastrophic collapse. The Bushveld Complex assumed the present enlarged four-basin configuration by collapse of the lobate outer ring. Previously horizontal ring-basin fill assumed its basinward tilt, consistent with the "dipping sheets" modeled by geophysics [7]. A tuff breccia-megabreccia-ash fall zone in upper Rooiberg marks this event. Peripheral to the entire Bushveld Complex [4], it proves the Rooiberg Group to be a single 10^5 km^3 stratigraphic package. It is not a composite erupted from many centers, as in siliceous volcanic fields of similar volume.

References: [1] Zieg M. J. and Marsh B. D. 2005. *Geological Society of America Bulletin* 117:1427–1450. [2] Jones A. P. et al. 2002. *Earth and Planetary Science Letters* 202:551–556. [3] Marsh B. D. 1982. *American Journal of Science* 282:808–855. [4] Schweitzer J. K. et al. 1995. *South African Journal of Geology* 98:245–255. [5] Stevenson J. S. 1963. *Canadian Mineralogist* 7:413–419. [6] Schweitzer et al. 1997. *Journal of African Earth Sciences* 24:95–104. [7] Meyer R. and de Beer J. H. 1987. *Nature* 325:610–612.

5237

COMPARISON OF ANHYDROUS MINERALS OF CONCORDIA AND CAP-PRUDHOMME ANTARCTIC MICROMETEORITES. PREDICTIONS FOR WILD-2 COMETARY PARTICLESC. Engrand¹, J. Duprat¹, M. Maurette¹, G. Kurat², and M. Gounelle^{1, 3}. ¹CNSM-CNRS, Bat. 104, F-91405 Orsay, France. E-mail: engrand@cnsm.in2p3.fr. ²University Wien, Inst. Geol. Wissenschaft., 1090 Vienna, Austria. ³LEME-MNHN, 75005 Paris, France

Introduction: We compare the abundance and composition of anhydrous minerals in Cap Prud'homme Antarctic micrometeorites (CP-AMMs) with that of Concordia-Dome C AMMs (DC-AMMs, see [1]) to investigate the prediction of a possible link between cometary matter and AMMs [2].

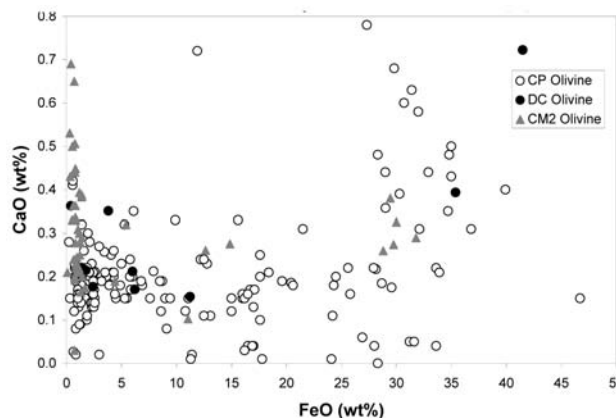


Fig. 1.

Results and Discussion: On this CaO versus FeO plot, the olivines found in CM2 chondrites show two distinct clusters with $\text{FeO} < 5 \text{ wt}\%$ and CaO up to $0.7 \text{ wt}\%$, and $27 < \text{FeO} < 33 \text{ wt}\%$, respectively, which are connected by a sparsely populated gap. The distribution of FeO contents in CP-AMMs shows the same clusters with a more densely populated gap. Although the statistics for DC-AMM olivines is limited, there is a hint that the distribution of their FeO contents is comparable to that of CP-AMM olivines.

The pyroxene/olivine abundance ratio in CP-AMMs is about 1 (i.e., 165 pyroxenes for 179 olivines) whereas it reaches about 3 (38 pyroxenes for 12 olivines) in the DC collection. The ratio of 1 found for CP-AMMs was already much higher than that found in CM chondrites and was compared to that observed in CR chondrites [3]. The higher value found in the DC-AMMs is possibly related to the new population of friable grains found in this collection [4].

It will be interesting to check how the characteristics of olivine and pyroxene grains in anhydrous IDPs and in Wild-2 particles returned by Stardust will compare with that of CP- of DC-AMMs. All these olivines might originate from a common locale in the early solar nebula. They were possibly generated during the collisional fragmentation and/or abrasion of chondrules in the hot inner solar system. Then, only the finest fragments could be fired on ballistic trajectory, by X-wind [5], to the distant and cold formation regions of cometary ices.

References: [1] Duprat J. et al. ASR. Forthcoming. [2] Maurette M. 1998. In *The molecular origin of life*. Cambridge: Cambridge University Press. pp. 147–186. [3] Kurat G. et al. 1994. *Geochimica et Cosmochimica Acta* 58:3879–3904. [4] Duprat J. et al. 2005. Abstract #1678. 37th Lunar and Planetary Science Conference. [5] Shu F. et al. 1996. *Science* 271:1545–1552.

5275

THERMAL OUTGASSING OF ORDINARY CHONDRITIC MATERIAL—I. NOMINAL MODEL RESULTS

B. Fegley, Jr. and L. Schaefer. Washington University in Saint Louis, Saint Louis, Missouri 63130, USA. E-mail: bfegley@wustl.edu; laura_s@wustl.edu

Introduction: Outgassing of ordinary chondritic (H, L, LL) material as a function of T (300–1200 K), P (1–100 bars), and bulk composition was modeled with chemical equilibrium calculations. Our results are fundamentally important for outgassing of asteroids, planets and satellites, metamorphic reactions on ordinary chondrite parent bodies, survival of presolar grains in meteorites, and the origin of life on Earth.

Methods: The thermodynamic calculations include ~1000 solids and gases of Si, Ti, Al, Cr, Fe, Mn, Mg, Ca, Na, K, P, Ni, Co, H, C, N, O, S, Cl, and F. We averaged analyses of meteorite falls in [2] to compute mean compositions of H, L, and LL chondritic material. We used radial temperature profiles for 6 Hebe, the putative H-chondrite parent body. Lithostatic pressures were calculated with depth using $\rho = 3.7 \text{ g cm}^{-3}$ for 6 Hebe. All models are below the Fe-FeS eutectic melting point (~1260 K). Our nominal (closed system) model chemically equilibrates all phases at a given P, T level. The effects of large changes in P and T, variable abundances of H, C, N, O, and S kinetic inhibition of mineral and metallic solid solutions, C and N dissolution in metal, and open versus closed system behavior on our results are described in our companion abstract [1] and preprint [3].

Nominal Results: The major outgassed volatiles are CH_4 , H_2 , H_2O , N_2 , and NH_3 (the latter at T and P where hydrous minerals form). Contrary to widely held assumptions, CO is never the major C gas during ordinary chondrite metamorphism. The figure shows results for average H chondritic material along the hottest thermal profile we used. The calculated oxygen fugacity f_{O_2} of H and L chondritic material is close to the QFI buffer. LL chondritic material is slightly more oxidized.

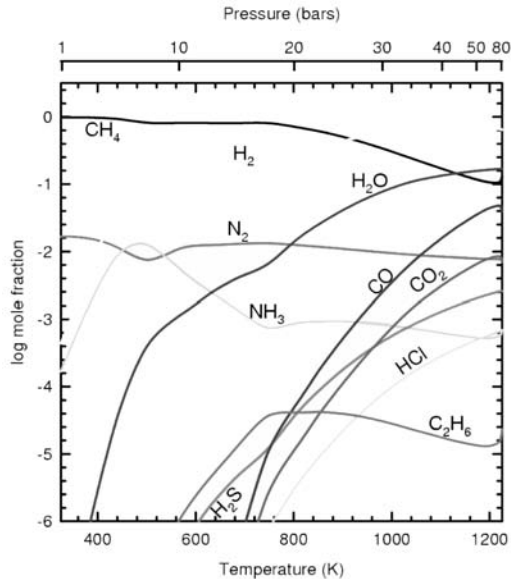


Fig. 1. Outgassed volatiles as a function of P and T from average H chondritic material.

Acknowledgments: This work was supported by the NASA Astrobiology, Origins, and Outer Planets Research Programs. We thank K. Lodders for helpful discussions.

References: [1] Schaefer L. and Fegley B., Jr. 2006. Abstract #5277. *Meteoritics & Planetary Science*. This issue. [2] Metbase 7.2. [3] Schaefer L. and Fegley B., Jr. *Icarus*. Forthcoming.

5222

UV/VIS SPECTROSCOPY OF STARDUST

C. D. Fernandes¹, D. Johnson¹, and M. M. Grady^{1, 2}. ¹Open University, PSSRI, MK7 6AA, UK. E-mail: c.d.fernandes@open.ac.uk. ²The Natural History Museum, Department of Mineralogy, London SW7 5BD, UK

Introduction: Cometary material from the Stardust mission has been distributed to Preliminary Examination Teams. This abstract describes the techniques that we are applying to cometary particles, captured in aerogel and aluminium foil. We will measure the UV/Vis spectra of returned Stardust materials. Visible reflectance spectroscopy is a useful technique that has been applied to IDPs [1] in order to compare them with primitive meteorites. The [1] study only considered spectral wavelengths >400 nm, and so could not investigate features for organic molecules that frequently occur below 300 nm. The aims of our study are to observe whether or not there is an absorbance present that can be compared with the 217.5 nm interstellar absorption band, make qualitative analyses of the presence (or otherwise) of organic molecules in the grains and assign bond identities, assess the relative abundances of hydrated and anhydrous minerals within grains on the basis of OH features.

Techniques: UV/Vis spectroscopy is a technique that utilizes the excitation of valence electrons within an atom as a tracer of atomic or molecular bonds. We are using a Craic optical microspectrophotometer system fitted with xenon lamps (wavelength range 200–950 nm). The instrument can acquire data by transmission and reflectance, and is able to measure spectra from powders, discrete grains or from polished mounts.

Results: As part of a long-term project to compare the spectra of meteorite grains (measured in the laboratory) with spectra from astrophysical dust (from telescope observations), and also serving as a framework for the analysis of Stardust grains, UV/Vis spectra have been measured on a range of standard materials. We have measured the spectra of discrete grains of minerals and polished mounts of carbonaceous chondrites in order to provide a library of spectra against which the Stardust particles may be compared.

Acknowledgements: This work was financed by grants from the PPARC and the OU.

References: [1] Bradley J. P. et al. 1996. *Meteoritics & Planetary Science* 31:394–402.

5308

Ar COMPOSITION OF THE MELT LITHOLOGY WITHIN THE NWA 2457 BRECCIA

V. A. Fernandes^{1,2,3}, R. Burgess², A. Bischoff⁴, and K. Metzler⁴. ¹University Coimbra, Portugal. ²University of Manchester, Manchester, UK. ³University College London, London, UK. E-mail: veraafernandes@yahoo.com. ⁴Institut für Planetologie, Münster, Germany

NWA 2457 is a single stone of 172 g. It has been classified as an impact-melt breccia containing cm-sized H5/6 fragments (Fa₁₈). The rock consists of two different lithologies: a) ~80% olivine-rich (mean Fa: 10.5 ± 3 mol%), metal-poor melt, and b) ~20% H-chondrite clasts. The host is the melt, in which the clasts are embedded. The bulk rock has been very weakly shocked (S2); shock veins are visible within the H5/6 fragments, but not within the melt portions. Heavy calcite veining is due to terrestrial alteration. The bulk composition of the NWA 2457 melt portion is extremely depleted in metal (and thus Fe, Ni) compared with "normal" bulk compositions of ordinary chondrites; roughly in wt% (EDS-analysis): Na₂O 1.3, MgO 27.5, Al₂O₃ 3.4, SiO₂ 49.7, SO₃ 1.1, K₂O 0.16, CaO 2.6, Cr₂O₃ 0.6, MnO 0.4, FeO 13.2 and NiO <0.05. Based on this compositional estimate, this sample is richer in plagioclase than normal H chondrites.

Ar-Ar a total of 17 heating steps were performed on the melt portion of NWA 2457 covering temperatures from 200 to 1600 °C. As typical of breccias, NWA 2457 shows a disturbed age spectrum (Fig. 1) with the age of disturbance being a maximum of 2.5 Ga ago. At intermediate temperature release there is an increase in apparent ages up to 4.503 ± 0.012 Ga (2σ) at 850 °C. For the remainder of the heating steps, from 900 to 1600 °C, the release is characterized by a decrease in apparent ages correlated by a lowering in the K/Ca × 1000 from 97 to 14. Considering that this sample mainly comprises fine-grained matrix of plagioclase and olivine it is likely that ³⁹Ar recoil from the relatively K-rich phase (e.g., plagioclase) to a K-poor phase (i.e., olivine) during irradiation has resulted in the artificially low apparent ages at high temperature. The maximum apparent age observed at intermediate temperature, 4.503 ± 0.012 Ga, may correspond either to the minimum crystallization age of the melt portion, or it may reflect the age of metamorphism of the H5/6 clasts in this meteorite. However, this age is well within the overall formation ages reported previously for ordinary chondrites [1 and refs. therein]. The suggested impact age of 2.5 Ga is also comparable with other impact ages reported previously [2, 3]. The 4π CRE age is 91 ± 1 Ma.

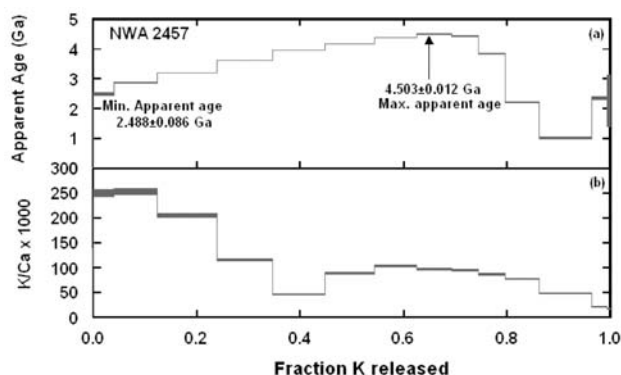


Fig. 1. Ar-Ar step heating results for ordinary chondrite 2457: a) age spectrum versus % K release; b) K/Ca × 1000 versus % K.

References: [1] Dalrymple B. 1991. *The age of the Earth*. Stanford: Stanford University Press. 474 p. [2] Bogard D. 1995. *Meteoritics* 30:244–268. [3] Swindle T. et al. 2006. Abstract #1454. 37th Lunar and Planetary Science Conference.

5297

LUNAR VOLCANISM DURING THE ERASTOTHEAN I: KALAHARI 009

V. A. Fernandes^{1, 2, 3}, R. Burgess², A. Bischoff⁴, and A. K. Sokol⁴. ¹University Coimbra, Portugal. ²University of Manchester, Manchester, UK. ³University College London, UK. E-mail: veraafernandes@yahoo.com. ⁴Institut für Planetologie, Wilhelm-Klemm-Str. 10, 48149 Münster, Germany

Kalahari 009 was found in the Kalahari desert, in Botswana, as a single grey rock of about 13.5 kg [1] and is compatible with a VLT lunar mare basalt [2]. It is a breccia consisting of fragments of basaltic lithologies embedded in a fine-grained matrix. The basaltic clasts have a coarse-grained subophitic texture. Clasts and matrix display the same composition. The main constituent minerals are pyroxene and plagioclase, with lesser olivine. Accessory minerals are ilmenite, chromite, troilite, ulvöspinel, and Fe,Ni metal (having about 0.6 wt% Ni). Pyroxene grains are zoned and have compositions of pigeonite and augite (En₁₄₋₄₆ Fs₄₂₋₇₆ Wo₇₋₄₄) and display exsolution lamellae of <5 µm. On a Mn versus Fe plot the pyroxenes plot along the lunar fractionation line. Kalahari 009 is significantly shocked, suggesting pressures of at least 15–20 GPa [1] according to the calibration scheme of Stöffler et al. [3] for ordinary chondrites (S4). Veins are present and contain up to ~4.3 wt% K₂O.

The Ar-Ar spectrum (Fig. 1a) shows a disturbed Ar release indicating that a significant disturbance occurred at ~0 Ma ago. This minimum apparent age is associated with Ar release from a high K/Ca component (Fig. 1b), likely the K-rich veins and related with terrestrial contamination. At intermediate and high temperature Ar release apparent ages range between 1.4–2.7 Ga. The highly disturbed Ar release of Kalahari 009 means that the minimum crystallization age of the lunar basalt is estimated from the highest apparent age of 2.67 ± 0.06 Ga (2σ). Also, it may have undergone an impact on the lunar surface at 1.40 ± 0.01 Ga (?). Integrating the age and composition of this meteorite with crater counting ages by [4, 5] and chemical maps by [6, 7], the likely source area is within the Mare Imbrium.

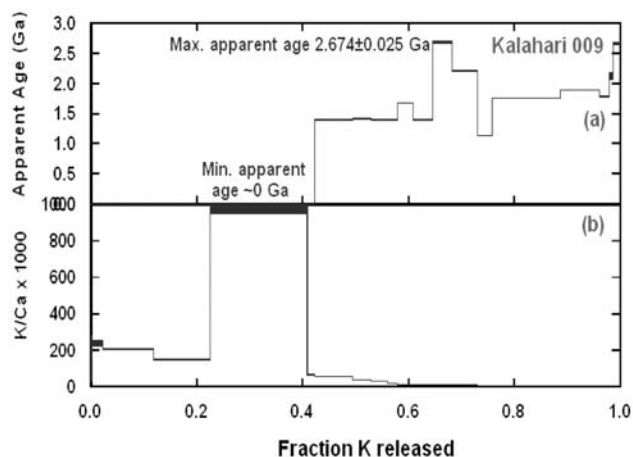


Fig. 1. Ar-Ar step heating results for lunar basalt Kalahari 009: a) age spectrum versus % K release; b) K/Ca × 1000 versus % K.

References: [1] Russell S. S. et al. 2005. *The Meteoritical Bulletin* No. 89. *Meteoritics & Planetary Science* 40:A201–A263. [2] Sokol A. K. and Bischoff A. 2005. *Meteoritics & Planetary Science* 40:A177–A184. [3] Stöffler, Keil, and Scott. 1991. *Geochimica et Cosmochimica Acta* 55:3845–3867. [4] Hiesinger et al. 2000. *Journal of Geophysical Research* 105: 29,239–29,275. [5] Hiesinger H. et al. 2003. *Journal of Geophysical Research* 108, doi:10.1029/2002JE001985. [6] Elphic et al. 2002. *Journal of Geophysical Research* 107, doi:10.1029/2000JE001460. [7] Gillis et al. 2004. *Geochimica et Cosmochimica Acta* 68:3791–3805.

5312

LUNAR VOLCANISM DURING THE ERASTOTHENIAN II: NWA 479

V. A. Fernandes^{1, 2, 3} and R. Burgess². ¹University Coimbra, Portugal. ²University of Manchester, Manchester, UK. ³University College, London, UK. E-mail: veraafernandes@yahoo.com

NWA 479 is paired with NWA 032 [1], and both were found in the Sahara Desert on the Morocco/Libya border in 2000 and 1999. While the petrology of NWA 479 has not been published, Fagan et al. [2] reported a comprehensive chemical and petrologic study of NWA 032. NWA 032/479 is an unbrecciated mare basalt containing phenocrysts of olivine, pyroxene, and chromite in a matrix of radiating pyroxene and feldspar crystals. The olivine phenocrysts make up ~12 vol% of the meteorite and are up to 300 μm in size and the pyroxene phenocrysts comprise ~5 vol%. Accessory phases include ilmenite, troilite, and trace Fe metal. High-silica glass is present in abundant shock veins that permeate the meteorite crystals [2]. Shock pressures greater than 25 GPa are indicated by the presence of melt veins, maskelynitized feldspar, and mosaicism in olivine crystals [2]. Terrestrial weathering caused only minor alteration seen as reddish to orange coloration due to the presence of ferric oxide or oxyhydroxide. Low-Ti composition, lower MgO and higher olivine phenocryst abundance than other mare basalt samples (this sentence does not make sense). The bulk composition of NWA 032 does not overlap that of any known mare basalts, but is similar to Apollo 15 olivine basalt, and the olivine phenocrysts abundance is similar to that in Apollo 12 olivine basalts [2].

The Ar-Ar spectrum for NWA 479 (Fig. 1) completely overlaps that of NWA 032 (the scale seems odd going up to 7.5 Ga—better if you limit it to 4.5 Ga). There is evidence for a disturbance event occurring at 1.96 Ga. Argon released between 400–750 °C shows increasing apparent ages reaching a maximum of 3.208 ± 0.012 Ga. Following the interpretation of Ar data for NWA 032 [3], the age spectrum of NWA 479 shows evidence of ³⁹Ar-recoil. On this basis a total age of 2.734 ± 0.01 Ga (2 σ error) is calculated over the intermediate and high-temperature steps comprising ~90% K release. This age is indistinguishable from the weighted mean age obtained from three samples of NWA 032 2.779 ± 0.028 [3]. An age of ~2.8 Ga is within the range of the second lunar volcanism peak, e.g., Erastothian flows within the Mare Imbrium or Mare Serenitatis [4, 5] and its chemical composition indicates possible source areas in the Imbrium Basin (chemical maps by [6, 7]). The CRE-age is 275 ± 4 Ma, which is slightly higher than that obtained for NWA 032 (212 ± 11 Ma, [3]) suggesting a relative position of NWA 479 closer to the lunar surface.

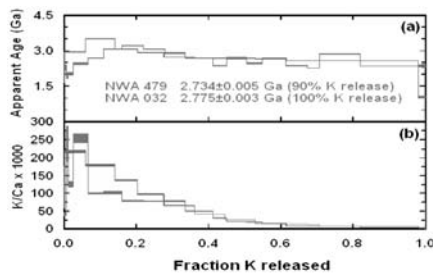


Fig. 1. Ar-Ar step heating results for lunar basalts NWA 479 and NWA 032: a) age spectrum versus % K release; b) K/Ca \times 1000 versus % K.

References: [1] Grossman J. N. and Zipfel J. 2001. The Meteoritical Bulletin No. 85. *Meteoritics & Planetary Science* 36:A293–A32. [2] Fagan T. J. et al. 2002. *Meteoritics & Planetary Science* 37:371–394. [3] Fernandes V. A., Burgess R., and Turner G. 2003 *Meteoritics & Planetary Science* 38: 555–564. [4] Hiesinger et al. 2000. *Journal of Geophysical Research* 105: 29,239–29,275. [5] Hiesinger et al. 2003. *Journal of Geophysical Research* 108:5065. [6] Elphic et al. 2002. *Journal of Geophysical Research* 107, doi: 10.1029/2000JE001460. [7] Gillis et al. 2004. *Geochimica et Cosmochimica Acta* 68:3791–3805.

5097

BALLEN QUARTZ IN IMPACT GLASS FROM THE BOSUMTWI IMPACT CRATER, GHANA

L. Ferrière¹, C. Koeberl¹, and W. U. Reimold². ¹Department of Geological Sciences, University of Vienna, Althanstrasse 14, A-1090 Vienna, Austria. (ludovic.ferriere@univie.ac.at). ²Mineralogy, Museum of Natural History, Humboldt University, Invalidenstrasse 43, D-10115 Berlin, Germany

Introduction: The 1.07 Ma old Bosumtwi impact crater in Ghana is a well-preserved complex impact crater [1]. Suevites occur outside the crater rim, to the north and southwest of the crater [2]. Recent work on breccia samples from the ICDP boreholes LB-O7A and LB-O8A, which were drilled into the deep crater moat and the central uplift, respectively, confirmed the presence of glass and melt particles [3–4]. Here, we study the presence of ballen quartz in suevitic breccia at Bosumtwi. Ballen quartz (Fig. 1) has been observed in impact glass from many other impact structures, but its formation mechanism [5–6] is still unresolved.

Results: Diaplectic quartz glass is abundant in suevite deposits outside the northern crater rim [2]. Ballen quartz is however restricted to samples from drill hole BH1 [2]. In contrast, diaplectic quartz glass is rare, and ballen quartz is absent, in samples from drillcores LB-O7A and LB-O8A. Ballen in the few grains observed display varied shapes (circular to oval or crescent), sizes (8 to 214 μm , with an average of 50 μm ; 471 ballen measured in 14 quartz grains within suevite samples BH1-0790 and BH1-0800) and distribution density from grain to grain.

Discussion: This study shows that: i) ballen quartz is irregularly distributed in the breccia deposits at the Bosumtwi crater, and ii) ballen size and shape vary from grain to grain. The heterogeneous distribution and sizes of the ballen must have implications regarding ballen quartz formation and preservation.

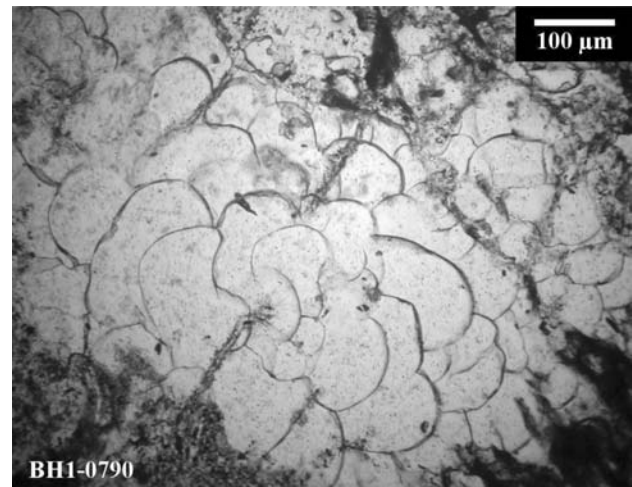


Fig. 1. Thin section microphotograph (plane-polarized light) of ballen quartz in suevite from Bosumtwi impact crater (sample BH1-0790).

References: [1] Koeberl C. and Reimold W. U. 2005. *Jb. Geol. B.-A. Austria* 145:31–70. [2] Boamah D. and Koeberl C. 2003. *Meteoritics & Planetary Science* 38:1137–1159. [3] Coney L. et al. 2006. Abstract #1279. 37th Lunar and Planetary Science Conference. [4] Ferrière L. et al. 2006. Abstract #1845. 37th Lunar and Planetary Science Conference. [5] Carstens H. 1975. *Contributions to Mineralogy and Petrology* 50:145–155. [6] Bischoff A. and Stöffler D. 1984. *Journal of Geophysical Research* 89: 645–656.

5048

ZONATIONS IN SPINEL FROM METEORITE FUSION CRUSTS AND THEIR RELEVANCE TO IMPACT SPINEL FORMATION

L. Ferrière¹ and E. Robin². ¹Department of Geological Sciences, University of Vienna, Althanstrasse 14, A-1090 Vienna, Austria. E-mail: ludovic.ferriere@univie.ac.at. ²LSCE, CEA, 91198 Gif sur Yvette, France

Introduction: Ni-rich spinel present in K/T boundary clays [1, 2] is a cosmic event marker, but its formation is still controversial [3–6]. K/T spinel is characterized by a high Ni²⁺ and Fe³⁺ content involving formation in an oxygen-rich environment [5–7]. Some of these crystals show a compositional zoning from core to rim, with a core depleted in Fe, Ni, and Ti, and enriched in Cr, Al, and Mg [8, 9]. Similar zonations have been reported in spinel from meteorite fusion crusts [5, 10], but these have never been studied in detail.

We report here SEM observations and EDS analyses of zoned spinel crystals from various meteorite fusion crusts (Orgueil, Murchison, Krymka, Bruderheim and Beni M'hira) and two K/T boundary sites (Bidart in France and Caravaca in Spain).

Results: Spinel from meteorite fusion crusts occurs mostly as small (0.5–1 µm), chemically homogeneous, dendritic crystals. Rare large euhedral crystals (up to 3 µm) with skeletal and well-developed octahedral morphologies are observed, however. Some of them display a compositional zoning with a decrease in Cr and an increase in Fe and Ni toward the margin. The Cr-rich core also contains variable amounts of V, the abundance of which (up to 1.5 wt%) is positively correlated with the Cr content of the core. The highest V concentrations are observed in primary chromite grains present in both the fusion crust and the unmelted core of the meteorites.

Discussion: The compositional similarity between the Cr-rich spinel cores and the primary chromite grains suggests that spinel zonation originates from incomplete equilibration of primary spinel crystals at subliquidus temperatures. Incomplete equilibration results from the pulse heating experienced by the meteorite during atmospheric entry and is shown by the occurrence in the fusion crust of i) dendritic crystals; and ii) relic chromite grains. A similar origin can be invoked for the compositional zonations observed in impact spinel from the K/T boundary. If so, this excludes a formation by condensation in the impact plume.

References: [1] Smit J. and Kyte F. T. 1984. *Nature* 310:403–405. [2] Kyte F. T. and Smit J. 1986. *Geology* 14:485–487. [3] Robin E. et al. 1992. *Earth and Planetary Science Letters* 108:181–190. [4] Kyte F. T. and Bostwick J. A. 1995. *Earth and Planetary Science Letters* 132:113–127. [5] Gayraud J. et al. 1996. *The Cretaceous-Tertiary event and other catastrophes in Earth history*. Boulder, Colorado: Geological Society of America. pp. 425–443. [6] Ebel D. S. and Grossman L. 2005. *Geology* 33:293–296. [7] Toppani A. and Libourel G. 2003. *Geochimica et Cosmochimica Acta* 67: 4621–4638. [8] Ferrière L. and Robin E. 2005. *Meteoritics & Planetary Science* 40:A47. [9] Preisinger A. et al. 1997. Abstract #1694. 28th Lunar and Planetary Science Conference. [10] Genge M. J. and Grady M. M. 1999. *Meteoritics & Planetary Science* 34:341–356.

5280

I-Xe AND THE CHRONOLOGY OF SOLAR SYSTEM FORMATION

M. J. Filtness, A. C. Busfield, and J. D. Gilmour. School of Earth, Atmospheric and Environmental Sciences, University of Manchester, Manchester M13 9PL, UK. E-mail: michal.filtness@postgrad.manchester.ac.uk

I-Xe: Iodine-129 was the first extinct radioisotope demonstrated to be present in the early solar system [1]. In spite of this, chronological evidence based on its decay is often overlooked when the chronology of solar system formation is discussed [e.g., 2]. This is unfortunate, since I-Xe data has foreshadowed discoveries based on the decay of other extinct radioisotopes. Notably, the first suggestion that processes on differentiated bodies (as dated by igneous clasts in the Barwell meteorite) were contemporaneous with chondrule formation came from the I-Xe system and from comparison between the I-Xe system and other chronometers [3]. This view is becoming widely accepted following Hf-W analyses of iron meteorites [4, 5]. In addition, since there is no reason to suspect that ¹²⁹I was distributed heterogeneously in the protoplanetary disk, comparisons between I-Xe and other extinct radioisotopes can allow proposed heterogeneities to be assessed [6,7].

I-Xe and Hf-W: We have previously produced comparisons among the I-Xe, Mn-Cr, Al-Mg and Pb-Pb chronometers and shown that they plausibly tell a consistent story in the region of the protoplanetary disk sampled by ordinary chondrites [3, 6, 7]. Although data are limited, possible points of comparison between this candidate chronology and the Hf-W system exist in CAIs, Ste Marguerite, the HED parent body and IAB iron meteorites. Kleine et al. [4] noted that the Hf-W intervals among CAI formation, mantle differentiation of the eucrite parent body and closure of Ste Marguerite are consistent with data from the Mn-Cr and Pb-Pb systems. A further datum can be found in the I-Xe age for silicates from the IAB iron Caddo County [8], which was found to be the equivalent of 4558.9 ± 0.4 Ma and compares well with the estimated from Hf-W systematics of 5–11 Ma after formation of Allende CAIs.

Chondrules: Interpretation of chondrule I-Xe data is controversial. Data from suites of chondrules from Semarkona and Chainpur are consistent with the data from the Al-Mg system [9]. This suggests that further examination of chondrules from primitive LL chondrites may be profitable. Such studies are under way and we plan to present data at the meeting.

References: [1] Jeffrey P. M. and Reynolds J. H. 1961. *Journal of Geophysical Research* 66:3582–3583. [2] Kita N. et al. 2005. In *Chondrites and the Protoplanetary Disk*. San Francisco: Astronomical Society of the Pacific. pp. 558–587. [3] Gilmour J. 2000. *Space Science Reviews* 92:123–132. [4] Kleine T. et al. 2005. *Geochimica et Cosmochimica Acta* 69:5805–5818. [5] Markowski et al. 2006. *Earth and Planetary Science Letters* 242:1–15. [6] Gilmour J. et al. 2000. *Meteoritics & Planetary Science* 35:445–455. [7] Gilmour J. et al. 2006. *Meteoritics & Planetary Science* 41:19–31. [8] Bogard D. et al. 2005. *Meteoritics & Planetary Science* 40:207–224. [9] Hutchison R. et al. 2005. In *Chondrites and the Protoplanetary Disk*. San Francisco: Astronomical Society of the Pacific. pp. 933–948.

5153

TRACE ELEMENT TRENDS IN WINONAITE PYROXENES: EQUILIBRATION OF HETEROGENEOUS PRECURSORS

C. Floss¹, G. Benedix², B. Jolliff³, G. Crozaz³, and S. Colton⁴. ¹Physics Department, Washington University, Saint Louis, Missouri 63130, USA. ²The Natural History Museum, London SW7 5BD, UK. ³Department of Earth and Planetary Sciences, Washington University, Saint Louis, Missouri 63130, USA. ⁴Southwest Research Institute, San Antonio, Texas 78238, USA. E-mail: floss@wustl.edu

Introduction: Winonaites and silicate inclusions from IAB iron meteorites formed on a common parent body that may have undergone partial melting and incomplete differentiation, followed by impact breakup and reassembly of the debris [1, 2]. We are studying the trace element distributions of individual minerals from these meteorites to evaluate the roles that silicate partial melting and metamorphism played in their formation.

Results: The meteorites we have studied to date span the range of grain sizes seen in winonaites, from Pontlyfni, which has a fine-grained (~75 µm) equigranular texture, to HaH 193, which consists of very coarse-grained (up to 5 mm) poikilitic orthopyroxene grains enclosing smaller grains of olivine, plagioclase and clinopyroxene [3, 4]. Although variable REE patterns in apatite, similar to those seen in some lodranites [5], may suggest redistribution of the REE, trace element abundances in pyroxenes define distinct uniform groups within a given meteorite. Among the winonaites, however, some systematic trends are evident. Abundances of Ti, Zr, Mn, Y, Cr, Sc and V are lowest in both clino- and orthopyroxene from Pontlyfni and are highest in the pyroxenes from Winona. Mount Morris and HaH 193 pyroxenes have intermediate abundances of these elements. While depletions of highly incompatible trace elements such as Ti, Zr, and Y, suggest melt removal [e.g., 5], the concurrent depletions in Mn, Cr, Sc, and V (elements that are more compatible in pyroxene) suggest more complex processes. Moreover, pyroxenes from NWA 1463, the most primitive winonaite [6], and Tierra Blanca are similar to those of Mount Morris and HaH 193 for most trace elements, but have distinctly higher Mn, Cr, and V.

Discussion: The distinct trace-element groupings in winonaite pyroxenes suggest equilibration of minerals with initially heterogeneous and distinct compositions, rather than partial melting of a compositionally homogeneous precursor. In addition, the systematic trends among the winonaites are decoupled from their mineralogies. Whereas the lodranites exhibit mineralogical indications of silicate melt removal (e.g., depletion of plagioclase) consistent with their incompatible trace element depletions [5], the winonaites studied here all have approximately chondritic silicate mineral abundances [4]. Moreover, Pontlyfni, with the lowest incompatible trace element abundances, contains plagioclase- and clinopyroxene-enriched areas that have been interpreted as silicate partial melts [1], whereas the trace element-rich Winona contains coarse olivine that could represent a partial melt residue [1]. Impact brecciation and mixing of lithologies, followed by varying degrees of metamorphism in different parts of the parent body, may have obscured early partial melting trends.

References: [1] Benedix G. K. et al. 1998. *Geochimica et Cosmochimica Acta* 62:2535. [2] Benedix G. K. et al. 2000. *Meteoritics & Planetary Science* 35:1127–1141. [3] Floss C. et al. 2003. Abstract. *Meteoritics & Planetary Science* 38:A22. [4] Floss et al. *American Mineralogist*. Forthcoming. [5] Floss C. 2000. *Meteoritics & Planetary Science* 35:1073–1085. [6] Benedix et al. 2003. Abstract. *Meteoritics & Planetary Science* 38:A70.

5201

COSMIC SPHERULES FROM FRONTIER MOUNTAIN (ANTARCTICA)

L. Folco¹, P. Rochette², C. Suavet², and J. Gattacceca². ¹Museo Nazionale dell'Antartide, Siena, Italy. E-mail: folco@unisi.it. ²CEREGE, Aix en Provence, France

Introduction: A new type of micrometeorite trap was discovered by a PNRA party in 2003 on top of Frontier Mountain (~2800 m a.s.l. and ~600 m above ice level) in northern Victoria Land, Antarctica [1]. Thousands of extraterrestrial particles in the 100–800 µm size range were found within fine-grained bedrock detritus accumulated along joints and in decimetric-sized sink-hole cavities of flat, glacially eroded, granitic surfaces. The collection includes both unmelted micrometeorites (fine-grained and coarse-grained particles) and cosmic spherules. Field data suggest that the traps collect only infalling micrometeorites. Cosmogenic nuclide concentrations of two samples of the glacially eroded surface indicate a minimum exposure age of ~2 Myr. As such, Frontier Mountain micrometeorites may represent an ancient collection that could be of significant value for studying the long-term flux of extraterrestrial matter accreting on Earth.

Size Distribution: The cumulative size distribution of spherules from a sink-hole cavity (sample 3) of the granitic surface was determined under SEM. A linear fit in log-log scale for sample 3 above 200 µm yields an exponent of -4.9, which is indistinguishable from the -5.2 ± 0.5 obtained by [2] for the South Pole Water Well collection (depositional age 1100–1500 A.D.).

Frequency by Type: A set of 265 spherules in the 200–650 µm size range representative of samples 2 and 3 were sectioned and investigated under SEM-EDS and electron microprobe. The set consists of 3% of I type spherules, 1% G type spherules, 76% S type spherules (with porphyritic, barred olivine and cryptocrystalline textures, including one CAT type) and 20% spherules consisting of glass (V type). The statistics by type is therefore similar to the South Pole Water Well and Greenland collections [2, 3, 4] Maurette et al. 1987; Taylor and Brownlee 1991; Taylor et al. 2000).

Weathering: The external surface of the spherules may be fresh or covered by a thin crust of weathering products (mostly sulphates and carbonates). The interior of the sectioned particles show evidence indicating null to moderate terrestrial weathering, allowing definition of textural types and compositions in all cases. The range of weathering levels attests for varying terrestrial residence times for the different particles.

Conclusions: The size distribution and the frequency by type of the Frontier Mountain collection are indistinguishable from those of the Greenland and South Pole collections, which are considered the least biased collections so far known. This implies that no significant bias is introduced by the accumulation mechanism and weathering at Frontier Mountain.

References: [1] Rochette et al. 2005. Abstract #1315. 37th Lunar and Planetary Science Conference. [2] Taylor S. et al. 1998. *Nature* 392:899–903. [3] Maurette M. et al. 1987. *Nature* 328: 699–702. [4] Taylor S. and Brownlee D. E. 1991. *Meteoritics* 26:203–211.

5298

LAYERED MATRIX IN THE NWA 2364 CV3 CHONDRITE

J. M. Friedrich¹, M. K. Weisberg^{1, 2}, D. S. Ebel¹, and K. P. Jochum³.
¹American Museum of Natural History, New York, New York 10024, USA.
²Department of Physical Sciences, Kingsborough College, CUNY, Brooklyn, New York 11235, USA. ³Department of Geochemistry, Max Planck Institute for Chemistry, Joh.-Joachim-Becher-Weg 27, D- 55128, Mainz, Germany

We report on the textural, mineralogical, and chemical characteristics of an unusual layered matrix phenomenon in the NWA 2364 CV3 chondrite. The layers are enclosed within a cup-shaped CAI [1] and suggest a temporally distinct collection process followed by parent body modification.

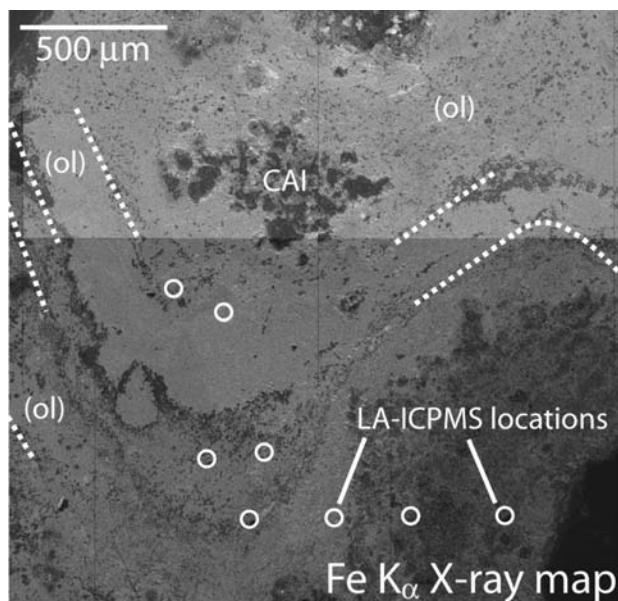


Fig. 1.

We used SEM, EMPA, and LA-ICPMS to characterize layered regions. The layers are porous aggregates of olivine (labeled ol above) with minor to trace awaruite and Ca pyroxene. Each layer has a distinct porosity and texture and they vary from fine (<5 μm) olivine grains to mixtures of fine olivine and coarser grains up to 20 μm. Slight compositional differences between the olivine in the layers was noted, and additional EMPA work is in progress. A border material (dark boundaries and indicated by dashed lines) of hedenbergite composition separates the olivine layers. Trace elemental analyses using LA-ICPMS show varying enrichments of up to 5 × CI in Cu, Co, As, Se, Mo, and Sn across all layers. Analyses of other matrix regions in NWA 2364 do not show these elemental signatures. Enrichments of these elements suggest unusual redox conditions within this region. The layered regions share textural and compositional features with dark inclusions (DI) in CV3s [2] and bear some similarity to crossbedded layers in Vigarano DIs, interpreted to have formed in asteroidal ponds by seismic shaking [3, 4]. The layered matrix regions clearly provide clues to compaction, deformation, and alteration in an asteroidal setting.

References: [1] Friedrich J. M. et al. 2005. Abstract #1756. 35th Lunar and Planetary Science Conference. [2] Johnson C. A. et al. 1990. *Geochimica et Cosmochimica Acta* 54:819–830. [3] Zolensky M. E. et al. 2002. Abstract #1593. 33rd Lunar and Planetary Science Conference. [4] Zolensky M. E. et al. 2004. Abstract #1332. 35th Lunar and Planetary Science Conference.

5306

SHOCK PRESSURE AND ORBITAL EVOLUTION OF LUNAR AND MARTIAN METEORITES

J. Fritz¹. Museum für Naturkunde (Mineralogie), Humboldt-Universität, Invalidenstrasse 43, 10115 Berlin, Germany. E-mail: joerg.fritz.1@rz.hu-berlin.de

Impact ejection and the subsequent transfer of rocks from Mars and Moon to Earth is documented by ~35 Martian and ~40 lunar meteorites, which are all unpaired. This process involves 1) impact ejection from the parent body; 2) transport through interplanetary space, and 3) landing on Earth. These stages can be investigated by considering petrology and geochemistry of the delivered meteorites and comparing these results with theoretical predictions derived from numerical models of impact events and orbital evolution of the escaping fragments [1–7].

A comparison of shock pressures with ejection and terrestrial ages of Martian meteorites supports theoretical predictions that, on average, the highest shocked fragments escape at highest velocities from Mars and, thus, acquire Earth-crossing orbits in the shortest time [7]. In contrast to Martian meteorites, which are weakly to strongly shocked [7], it appears that almost all lunar meteorites are weakly shocked, as plagioclase was not transformed to maskelynite in the ejection event(s). These differences in shock pressures can be explained by considering the orbital evolution of fragments which escaped from Mars and Moon.

The probability that fragments that escape Mars eventually impact on Earth was calculated to range from ~2 to 8% and only slightly varies with their departure velocity [2]. However, the probability that fragments that escape Moon will hit Earth is about 25 to 50% and strongly depends on their departure velocity (relative to the motion of the Moon) [1]. Three different scenarios can be discriminated: 1) direct collision with Earth for fragments departing from the Moon at various velocities; 2) fragments with departure velocities of 2.4–3.0 km/s travel in geocentric orbits towards Earth; and 3) fragments with departure velocities >3.0 km/s escape into heliocentric orbits [1]. The highest probability for Earth impacts have fragments that travel in geocentric orbits [1–2]. Thus, the lack of recovered highly shocked lunar meteorites can be explained by the following conclusion: generally, the most highly shocked fragments escape with highest velocities, are preferably transferred into heliocentric orbit, and thus have a lower probability to impact Earth compared to weakly shocked fragments which travel on geocentric orbits. Thus, it appears plausible that no shock-melted lunar impact ejecta have been recovered so far, although there could be a small amount.

Additionally, the equal number of lunar and Martian meteorites document that no moderate to large lunar impact occurred in the last few Myr. However, it is tempting to speculate whether the Giordano Bruno crater (22 km Ø), which appears to be the youngest lunar impact of this size [8] ejected the lunar highland breccias Y-82192/Y-82193 and Y-86032 at 8 ± 3 Myr ago [4].

References: [1] Gladman B. et al. 1995. *Icarus* 118:302–321. [2] Gladman B. 1997. *Icarus* 130:228–246. [3] Eugster O. et al. 2002. *Meteoritics & Planetary Science* 37:1345–1360. [4] Thalmann C. et al. 1996. *Meteoritics & Planetary Science* 31:857–868. [5] Head J. N., Melosh H. J., and Ivanov B. 2002. *Science* 298:1752–1756. [6] Artemieva N. A., Ivanov B. A. 2004. *Icarus* 171:84–101. [7] Fritz J., Artemieva N. A., and Greshake A. 2005. *Meteoritics & Planetary Science* 40:1393–1411. [8] Withers P. 2001. *Meteoritics & Planetary Science* 36:525–529.

5304

DATING LARGE LUNAR IMPACTS BY HELIUM-3 IN MARINE SEDIMENTS

J. Fritz¹, R. Tagle², and N. A. Artemieva³. ¹Museum fuer Naturkunde. E-mail: joerg.fritz.1@rz.hu-berlin.de. ²Vrije Universiteit Brussel, B-1050 Brussels, Belgium. ³Russian Academy of Science, 119334 Moscow, Russia

The transfer of rocks from Mars and Moon to Earth is documented by about 40 lunar and 35 Martian meteorites, which are all unpaired. The increasing amount of those meteorites recovered from hot and cold deserts lead to a change in the opinion of the meteoritic community from: "It is practically impossible" to "It is practically easy" to eject solid matter from Moon and Mars [e.g., 1]. Recent numerical simulations of impacts on the Moon showed that a given impacting projectile ejects about 1 to 5 times its mass from the Moon, and even in the case of small impacting projectiles (10–30 m diameter) the Moon is losing mass [2].

Here we discuss the possibility to geochemically identify large lunar impact events in terrestrial sediments. Lunar composition does not allow tracing lunar impact layers in terrestrial sediments by conventional impact indicators such as platinum group element enrichments or shocked quartz. However, the surface of the Moon accumulated helium-3 (³He) over billions of years with concentrations ranging from 5 to 50 ppb [3], and represents the largest (except the sun) reservoir for ³He in the inner solar system. Thus, a rather small amount (~40–50 t) of average lunar regolith (15 ppb) on the Moon contain the current annual/global average volume of ³He delivered by 40,000 t of IDPs to Earth [4].

The mass of lunar ejecta transferred to Earth's atmosphere can be calculated by considering that a projectile ejects about 1 to 5 times its mass from the Moon [2] and ~one-third of the escaping mass eventually hits Earth after a few million years (most arrives in <10⁴ years) [5]. About 0.15–0.20 times the projectile mass is ejected from the Moon without experiencing shock pressures in excess of 20 GPa and, thus, can retain >40% of the initial ³He during impact ejection [6, 7] (Note that lunar meteorites appear to be exclusively weakly shocked). During the Moon-Earth transit especially the fine grained fraction accumulates additional ³He.

Finally, the ³He-delivery through Earth's atmosphere implies that the very fine grained dust enters a peak-temperatures below the ³He release temperature. For a given particle friction, heating is controlled by entry angle and velocity [8]. Thus lunar dust on geocentric orbits (11.1 km/s; entry angle mostly >45° [5]) is highly favored for delivering ³He compared to asteroidal (12.1 km/s) or cometary dust (14.1 km/s), which enter along the full capture cross section of Earth [8]. Additionally, lunar dust on geocentric orbits which enter at grazing angles have a high probability for aerobreaking and, hence, soft deceleration. Therefore, we propose that large lunar impact events may be recorded by a pronounced ³He-*oa* in marine sediments.

References: [1] Artemieva N. A. and Ivanov B. A. 2004. *Icarus* 171: 84–101. [2] Shuvalov V. V. and Artemieva N. A. 2006. Abstract #1168. 37th Lunar and Planetary Science Conference. [3] Cameron E. N. 1992. 2nd Conference on Lunar Bases and Space Activities. pp. 189–197. [4] Farley K. A., Love S. G., and Patterson D. B. 1997. *Geochimica et Cosmochimica Acta* 61:2309–2316. [5] Gladman et al. 1995. *Icarus* 118:302–321. [6] Stöffler D., Keil K., and Scott E. R. D. 1991. *Geochimica et Cosmochimica Acta* 55: 3845–3867. [7] Schwenzer et al. 2004. *Meteoritics & Planetary Science* 39: A96. [8] Flynn G. J. 2001. In *Accretion of extraterrestrial matter throughout Earth's history*. New York: Kluwer Academic. pp. 107–126.

5032

NUCLEAR FIELD SHIFT EFFECT AS AN ORIGIN OF ISOTOPIC ANOMALIES IN THE EARLY SOLAR SYSTEM

T. Fujii¹, F. Moynier², and F. Albarède². ¹Research Reactor Institute, Kyoto University, 2-1010, Asashiro Nishi, Kumatori, Sennan, Osaka 590-0494, Japan. E-mail: tosiyuki@HL.rri.kyoto-u.ac.jp. ²Laboratoire de Sciences de la Terre, UMR 5570 CNRS, Ecole Normale Supérieure de Lyon, 46, Allée d'Italie, 69364 Lyon Cedex 7, France

Introduction: Most of the isotopic variability in the solar system is accounted for by four types of processes: mass-dependent thermodynamic fractionation, radioactive decay, spallation by cosmic rays, and incomplete mixing in the solar nebula. Isotopic anomalies for Mg, Si, Ca, Ti, Cr, Sr, Ba, Nd, Sm, and so on, which have been found in the unusual CAIs in Allende (so-called FUN inclusions) (see references in [1]), epitomize the occurrence of isotopic anomalies in early nebular condensates. Some isotopic anomalies cannot, however, be accounted for by nucleosynthetic processes and we therefore explore the possibility that they may instead be due to mass-independent isotope fractionation induced by nuclear field shift.

Discussion: The theory of first-order mass-dependent fractionation has been revised to include the mass-independent isotope effect, i.e., so-called nuclear field shift effect [2]. The spatial distribution of protons in the nucleus, which impacts the charge distribution interacting with electronic shells, obeys symmetry requirements that in turn cause the nuclear charge radii to vary unevenly with the number of neutrons characterizing the different isotopes of a same element [3]. The ensuing shift of the nuclear field imparts a mass-independent character to the electric field around the nucleus of the different isotopomers and therefore to mass fractionation among coexisting species.

We tested that the isotopic anomalies observed in FUN inclusions can be explained by the nuclear field shift effect by using the following equation [4]:

$$\epsilon_{m_i} = \left(\delta \langle r^2 \rangle_{m_i, m_1} - \frac{m_2 (m_i - m_1)}{m_1 (m_2 - m_1)} \delta \langle r^2 \rangle_{m_1, m_2} \right) \times a \quad (1)$$

where m_1 , m_2 , and m_i ($i = 3, 4, \dots, i$) are masses of isotopes, in which an isotope pair m_1 and m_2 is used for normalization. $\delta \langle r^2 \rangle$ is isotopic difference in nuclear charge radius and a adjustable parameter. Isotope anomalies observed for alkaline earth elements (Mg, Ca, Sr, and Ba) would simply be explained by the nuclear field shift effect. Those observed for transition metals (Ti and Cr) may partly be explained by the nuclear field shift effect. Hence, a whole class of isotopic heterogeneities is considered to reflect evaporation/condensation processes in the solar nebula rather than nucleosynthetic effects. We speculate that the current estimates of the r -process component of the normal solar material may be affected by non-mass dependent fractionation effects.

References: [1] Birck J. L. 2004. In *Geochemistry of non-traditional stable isotopes*. Washington, D.C.: Mineralogical Society of America. pp. 25–64. [2] Bigeleisen J. 1996. *Journal of American Chemical Society* 118: 3676–3680. [3] King W. H. 1984. *Isotope shifts in atomic spectra*. New York: Plenum Press. 208 p. [4] Fujii T., Moynier F., and Albarède F. *Earth and Planetary Science Letters*. Forthcoming.

5033

ANALYSES OF STABLE CHLORINE ISOTOPES IN CHONDRITES (2): CHARACTERISTIC ISOTOPE COMPOSITIONS OF C, E, AND O CHONDRITES

T. Fujitani^{1, 2} and N. Nakamura^{1, 3}. ¹Graduate School of Science and Technology, Kobe University, Nada, Kobe 657-8105, Japan. E-mail: fujitani@mail.mtc.ac.jp. ²Marine Technical College, Ashiya 659-0026, Japan. ³Department of Earth and Planetary Science, Kobe University, Kobe 657-8501, Japan

Introduction: Chlorine is one of the mobile elements and highly diffusive among vapor, fluids, and solids during geochemical processes. Due to a large relative mass difference between two stable isotopes (³⁵Cl and ³⁷Cl), natural variations in ³⁷Cl/³⁵Cl ratio are expected for planetary materials, which might provide useful natural tracers to investigate evolution processes of planetary materials. Due to analytical difficulties, the isotopic studies on stable Cl isotopes in planetary materials are limited, particularly for rare cosmic materials with low-Cl concentrations, like meteorites. In order to examine Cl isotope variations for chlorinated compounds related to environmental problems, we have developed an analytical technique by thermal ionization mass spectrometry (TIMS) using Cs₂Cl⁺ ion mode [1, 2]. Extending our earlier works, we have newly established precision techniques, which is applicable to small silicate materials [3, 4]. Except for a few cases [5–7], analyses of Cl isotopes for meteorites have rarely been reported and thus general isotopic features of chlorine in the early solar system have not been well understood. In order to examine possible characteristic variations of Cl isotopes, we have initiated systematic Cl isotopic analysis for different kinds of chondrites. Here we report preliminary results for 24 chondrite samples including bulk samples of 6 C, 3 E, and 12 O chondrites. A part of results for O chondrites has been reported in [8].

Results and Discussion: The Cl concentrations obtained by N-TIMS ID range from 44 (Allegan, H5) to 632 ppm (Boriskino, CM2), indicating that the Cl concentration decreases, in general, from low metamorphic grade to higher grade in the same group. The isotopic composition defined by $\delta^{37}\text{Cl}_{\text{SMOC}} [\text{‰}] (\equiv \{ [^{37}\text{Cl}/^{35}\text{Cl}]_{\text{sample}} / [^{37}\text{Cl}/^{35}\text{Cl}]_{\text{SMOC}} - 1 \} \times 1000)$ ranges from –0.6 (Kobe, CK4) to +4.4‰ (Boriskino, CM2) for C, from +3.0 (Abee, EH4) to +5.2‰ (Hvittis, EL6) for E, from –0.6 (Tahara, H5) to +5.0‰ (Allegan, H5) for H, from –4.6 (Y-74191, L3) to –0.7‰ (Homestead, L5) for L, and from –3.2 (Parnallee, LL4) to +2.2‰ (ALHA77304, LL3) for LL chondrites.

It is remarkable that bulk chondrites show relatively limited range within a group but display significantly large variations (up to 10‰) for whole groups in Cl isotopic composition, indicating that several characteristic Cl reservoirs with even larger range of isotopic compositions existed in the early solar system materials.

References: [1] Numata M. et al. 2001. *Geochemistry Journal* 35:89–100. [2] Numata M. et al. 2002. *Environmental Science & Technology* 36: 4389–4394. [3] Fujitani T. and Nakamura N. *Geostandard and Geoanalysis Research*. Forthcoming. [4] Fujitani T. et al. 2005. 6th Int. Natl. Sympos. Appl. Isotope Geochem. 79–80. [5] Magenheim A. J. et al. 1994. *Geochimica et Cosmochimica Acta* 58:3117–3121. [6] Magenheim A. J. et al. 1995. *Earth and Planetary Science Letters* 131:427–432. [7] Bridges J. C. et al. 2004. *Meteoritics & Planetary Science* 39:657–666. [8] Fujitani T. and Nakamura N. 30th Symposium on Antarctic Meteorites. Forthcoming.

5388

DEVELOPMENT OF INSTRUMENTAL NEUTRON ACTIVATION ANALYSIS FOR μg-SIZE OF MICROMETEORITE SAMPLES

T. Fukuoka¹, Y. Fukushi^{1, 4}, N. Hoshi¹, Y. Tazawa², and Y. Saito³. ¹Department of Environmental Systems, Faculty of Geo-Environmental Science, Rissho University, Kumagaya 360-0194, Japan. E-mail: tfukuoka@ris.ac.jp. ²Department of Physics and Astrophysics, Graduate School of Science, Kyoto University, Kyoto 606-8502, Japan. ³Radio Isotope Laboratory, College of Science and Engineering, Aoyama Gakuin University, Sagamiyama 229-8551, Japan. ⁴Present address: Department of Earth and Planetary Science, Tokyo Institute of Technology, Tokyo 182-8551, Japan

A large quantity of micrometeorites has been collected from Antarctic ice by the Japanese Antarctic Research Expedition teams. Chemical data of micrometeorites are important to discuss their nature and origin. Instrumental neutron activation analysis (INAA) is the most important analytical technique to obtain chemical data of micrometeorites. Mineralogical, petrological data, etc., can be obtained from same micrometeorite sample after INAA, because INAA is a nondestructive technique. More than 15 elemental abundances can possibly be analyzed from μg-size micrometeorites by INAA. However, because of tiny sample size, there are many problems (e.g., handling of samples, homogeneity of standard samples).

In this paper, we introduce a recently developed INAA technique for μg-size micrometeorite samples.

Sample micrometeorites, JB-1 glass chip (standard for lithophiles) and metal wire (Al-Au (IRMM-530) and Pt (SRM-680a)) for siderophiles (Au, Ir etc.) are heat-sealed individually into ~3 × 3 mm size of ultra pure polyethylene bag for easy handling, and they are activated with thermal neutron for 10 min at 20 MW (~2 × 10¹³n/cm²s) in the pneumatic tube of the JRR-3M reactor of the Japan Atomic Energy Research Institute (JAERI). The activated samples and standards with polyethylene bags are counted to determine Al, Ti, Mg, Ca, V, Na, and Mn. After removal of polyethylene bag, the samples and standards are put in a ultra pure synthetic quartz vessel, individually. They are activated again with thermal neutrons for 100 h at 20 MW (1 × 10¹⁴n/cm²s) in the hydraulic rabbit irradiation facility of the JRR-3M reactor of the JAERI. The activated samples and standards without quartz vessel are counted repeatedly to determine Na, Cr, Fe, Sc, REE, Co, Ir, Au, etc.

JB-1 glass standard was made by fusion of the GSJ standard rock powder JB-1. Chemical homogeneity of the JB-1 glass chip was checked on the chips of crushed glass standard. The homogeneity (standard deviation) for 5–20 μg chips of these standards were 3–4% which are similar to practical INAA precision (3–5%).

5326

IRON AND NICKEL IN UREILITE SILICATES-CHEMISTRY AND ISOTOPES

A. Gabriel¹, G. Quitté², R. Schönberg¹, J. Schüssler¹, and A. Pack¹. ¹Institut für Mineralogie, Universität Hannover, Callinstrasse 3, D-30167 Hannover, Germany. ²Institute of Isotope Geochemistry and Mineral Resources, ETH Zentrum, Clausiusstrasse 25, CH-8092 Zürich, Switzerland. E-mail: a.gabriel@mineralogie.uni-hannover.de

Introduction: Ureilites are ultramafic rocks composed of olivine, low- and high-Ca pyroxene and C-rich material that occurs along grain boundaries [1]. Their formation is usually attributed to asteroidal differentiation [1], but a nebular setting has also been proposed [2].

Results: We have begun our study with ICP-OES (University of Hannover) trace element analyses (Fe, Co, Ni, Mn, Ca) of inclusion free silicate separates of the Kenna ureilite. We have estimated the ol composition (we have separated a mixture with ~13% px and ~87% ol) using the Fe/Ni ol-opx-partitioning data by [3] and FeO electron microprobe data to 18.8 ± 0.3 wt% FeO and 350 ± 11 $\mu\text{g/g}$ Ni (67 ± 17 $\mu\text{g/g}$ Co). Based on the ol-metal partitioning data by [4], our data suggest that metal coexisting with Kenna ol should contain ~20–60 wt% Ni (2000 K > T > 1000 K). If we assume a chondritic Kenna parent asteroid (bulk) with ~20 wt% FeO and negligible Ni in the mantle, the Fe,Ni core should contain only ~10 wt% Ni. The discrepancy between the two approaches can be explained in terms of Fe/Ni distribution between ultramafic rocks (ureilites) and basalt after core separation during partial mantle melting or subsequent fractional crystallization.

The iron isotope composition of the Kenna silicates (MC-ICPMS, University of Hannover) is $\delta^{56/54}\text{Fe} = +0.035 \pm 0.049\text{‰}$ (2σ). Within uncertainty this value is indistinguishable to the mean of 14 bulk chondrite analyses ($\delta^{56/54}\text{Fe} = -0.015 \pm 0.020\text{‰}$ [5]), the mean magmatic iron meteorite composition ($\delta^{56/54}\text{Fe} = +0.047 \pm 0.016\text{‰}$; N = 8 [5]) and the mean composition of non-cumulate and polymict eucrites ($\delta^{56/54}\text{Fe} = -0.001 \pm 0.017\text{‰}$; N = 8 [5]). More data will be provided to obtain information about the Fe-isotope composition of the reservoir from which ureilites formed and its relation to other achondrites.

The ⁶⁰Fe-⁶⁰Ni short-lived isotope chronometer ($t_{1/2} = 1.5$ Ma) is well suited to precisely date the formation of ureilites. Ni isotope analyses were conducted at ETH Zürich for an olivine fraction. Our very preliminary data suggest a ⁶⁰Ni excess of +0.5‰. If true, this would correspond to an initial ⁶⁰Fe/⁵⁶Fe $\approx 3 \times 10^{-7}$ and a time interval of ~3 Ma after the start of the solar system (initial ⁶⁰Fe/⁵⁶Fe taken from [6]). This is higher than ⁶⁰Fe/⁵⁶Fe < 1.2×10^{-7} as reported by [7].

We will obtain more data on different ureilites to discuss the chronological issue in more detail.

References: [1] Goodrich C. A. 1992. *Meteoritics* 27:327. [2] Clayton R. N. and Mayeda T. K. 1988. *Geochimica et Cosmochimica Acta* 52:1313. [3] Witt-Eickschen G. and O'Neill H. St. C. 2005. CG 22165. [4] Seifert S. et al. 1988. *Geochimica et Cosmochimica Acta* 52:603. [5] Schoenberg R. and von Blanckenburg F. *Earth and Planetary Science Letters*. Forthcoming. [6] Mostefaoui S. et al. 2004. NAR 48:155. [7] Kita N. T. et al. 1997. Abstract #1052. 28th Lunar and Planetary Science Conference.

5357

SPECTROSCOPY AND THE ASTEROID-METEORITE LINK: A PERSPECTIVE AFTER THREE DECADES

M. J. Gaffey. Department of Space Studies, Odegard School of Aerospace Sciences, University of North Dakota, Grand Forks, North Dakota 58202–9008, USA. E-mail: gaffey@space.edu

Introduction: The “holy grail” of asteroid spectral studies has been to identify the specific parent bodies of the meteorites in order to place the detailed compositional, genetic and temporal data from meteorite studies into a spatial context in the early solar system. In the early 1970s, when asteroid spectroscopy was in its infancy, most of us naively assumed that the asteroid-meteorite linkages would quickly reveal themselves. The identification of asteroid 4 Vesta as the probable parent body of the HED meteorites encouraged this optimistic outlook. However, failures to quickly identify other probable meteorite parent bodies—and the failure of many of the early identifications to survive subsequent scrutiny—led to disillusionment for many in the asteroid spectroscopy community. Even three decades into the effort, the probable parent bodies of only four meteorite types (HEDs, H chondrites, IIE irons, and aubrites—making up ~40% of all meteorite falls) have been identified.

Meteoritics and Dynamics: Steady progress has been made over the past two decades across a broad range of disciplines which allows a much more optimistic outlook for our future understanding of the asteroid-meteorite link. Advances in meteorite science have brought both subtlety and nuance to many of our simplistic early models of meteorite formation and relationships; models which govern much of our thinking about asteroids. Advances in the dynamical studies of asteroids have provided a better understanding of the evolution of the asteroid population, and of the mechanisms that deliver meteorites to the Earth. Dynamical studies have increased our understanding of the general linkages between asteroids and meteorites (such as the central importance of proper motion and secular resonances) while simultaneously challenging our ability to link meteorites to specific parent bodies (e.g., the Yarkovsky effect delivering meteoroids into resonances from relatively distant parent bodies).

Advances in Asteroid Spectroscopy: Our ability to obtain robust and sophisticated asteroid mineralogical characterizations suitable for comparison to meteoritic data has advanced ever more rapidly in the past two decades. The initial very limited techniques of curve matching have increased given way to the use of spectral parameters which are diagnostic of the presence, abundance and composition of a number of cosmically important mineral species. Combined with improvements in telescopic instrumentation, observing protocols, data reduction methodologies and interpretive calibrations the quality of asteroid mineralogical characterizations has increased dramatically. Space weathering—one of the great bugaboos of asteroid spectroscopy—has yielded to detailed study. While still not completely understood, the effects of space weathering can now be effectively eliminated in asteroid mineralogical characterizations.

Conclusions: We stand on the threshold of a golden age in our understanding of the origin and early evolution of the inner solar system from the asteroid-meteorite relationship. In addition to significantly enhancing our ability to identify plausible and probable meteorite parent bodies, the newer asteroid spectroscopic capabilities also provide information on bodies that are not represented in the meteorite collections enhancing our understanding of the late solar nebula and early solar system.

5152

PETROLOGY AND GEOCHEMISTRY OF THE NWA 3368 EUCRITE

K. G. Gardner¹, D. S. Lauretta¹, D. H. Hill¹, J. S. Goreva¹, K. J. Domanik¹, I. A. Franchi², and M. J. Drake¹. ¹Lunar and Planetary Laboratory, The University of Arizona, Tucson, Arizona, USA. ²Planetary and Space Sciences Research Institute, Open University, UK. E-mail: kgardner@lpl.arizona.edu

Introduction: A considerable amount of debate exists on the petrogenesis of eucrites, basaltic meteorites believed to have originated on 4 Vesta [1]. Many scientists have speculated on the formation event, supplementing ideas to Mason's fractional crystallization model and Stolper's partial melting model ([2–5]). Thus, an understanding of major and trace element compositions of all eucrites is imperative. Here, we report the petrology and trace element geochemistry of NWA 3368.

Methods: Two thin sections and one 20.5 gram polished slab were studied using a Cameca SX-50 electron microprobe. Six sub-samples including four clasts, a section of light-colored matrix, and a section of dark-colored matrix were extracted from the polished slab, and each piece was analyzed by both INAA and ICP-MS using the UA Nuclear Reactor Laboratory-LPL Gamma Ray Analysis Facility and the LPL ICP-MS facility, respectively [6]. A series of custom-made solutions of basaltic composition and the Geological Society of Japan standard basalt JB-2 were used as standards. Two small chips of NWA 3368 were sent to Open University to determine oxygen isotope composition.

Results: NWA 3368 has a variety of dark and light angular clasts that range in size from several millimeters to a couple of centimeters in length. They range in texture from coarse- to fine-grained. The fine-grained texture is composed of abundant plagioclase and lamellae-free pyroxene, while the coarse-grained texture contains abundant pyroxenes with varying degrees of exsolution lamellae. Electron microprobe analyses yielded pyroxene compositions of $Wo_5En_{36}Fs_{59}$ for low-Ca pyroxene and $Wo_{43}En_{30}Fs_{27}$ for high-Ca pyroxene. Plagioclase has a composition of $An_{90}Ab_{10}Or_{0.4}$. Ilmenite and troilite grains are abundant, along with chromite containing 5 to 27% TiO_2 and ~5% Al_2O_3 . Other phases include iron metal and silica. All Fe/Mn ratios lie between 28 and 32, typical for eucrites. Trace element data reveal a flat REE pattern with a slightly negative Eu anomaly. Sm versus Sc, La, and Eu plots all reveal a pattern normal to eucrites. Similarly, O-isotope data are consistent with other HEDs [7].

Conclusions: NWA 3368 is a non-cumulate, monomict eucrite breccia related to known eucrites. The two separate lithologies, particularly the pyroxene exsolution, probably represent two separate thermal events that may be either metamorphic or primary igneous in origin. The REE abundances and patterns, as well as other trace element abundances, are typical of normal or main group eucrites.

Acknowledgements: This work was supported by NASA grant NAG 12795 to M. J. Drake. Special thanks go to William Boynton for use of the LPL Gamma Ray Analysis Facility.

References: [1] Consolmagno G. J. and Drake M. J. 1977. *Geochimica et Cosmochimica Acta* 41:1271–1282. [2] Stolper E. M. 1977. *Geochimica et Cosmochimica Acta* 41:587–611. [3] Mason B. 1962. *Meteorites*. New York: Wiley. 274 p. [4] Ikeda Y. and Takeda H. 1985. Proceedings, 15th Lunar and Planetary Science Conference. pp. C649–C663. [5] Righter K. and Drake M. J. 1997. *Meteoritics & Planetary Science* 32:929–944. [6] Gardner K. G. et al. 2006. Abstract #2389. 37th Lunar and Planetary Science. [7] Mittlefehldt D. W. et al. 1998. *Planetary materials*. Washington, D.C.: Mineralogical Society of America. pp. 4–103–130.

5134

COMPOSITION IN THE PROTOSOLAR AND LOCAL INTERSTELLAR CLOUDS—IMPLICATIONS FOR THE CHEMICAL EVOLUTION IN THE GALAXY DURING THE LAST 5 Gyr

J. Geiss¹ and G. Gloeckler². ¹International Space Science Institute, Bern, Switzerland. ²Department of Atmospheric, Oceanic and Space Sciences, University of Michigan, Ann Arbor, Michigan, USA

Our concepts of nucleosynthesis, as well as what we know about the origin of the elements and their isotopes are largely based on abundance measurements in the solar system. We know the relative abundance of nearly 300 nuclear species in the Protosolar Cloud (PSC), a sample of Galactic matter frozen-in (in terms of nuclear evolution) 4.6 Gyr ago. In meteorites, we also have measurements of isotopic ratios in stellar grains that were included in asteroids at the time of solar system formation. These grains have preserved the isotopic signature of matter released from stellar sources, such as AGB stars or supernovae.

Although we have a large body of spectroscopic composition data from galactic and extra-galactic objects, missing until recently was a sample of the present-day Galaxy with reliable observations of a number of elemental and isotopic abundance ratios, all measured in one and the same sample. Investigation of the composition in the local interstellar cloud (LIC) is beginning to fill this gap.

Elemental and isotopic abundances in the LIC, obtained so far by in situ ion mass spectrometry, ACR measurements and remote spectroscopy will be summarized. Also, methods of deriving PSC abundances from solar wind composition measurements will be discussed.

By comparing abundances in the LIC and in the PSC, we have investigated the galactic evolution during the last 5 Gyr, using the mixing model introduced by Geiss, Gloeckler, and Charbonnel (*The Astrophysical Journal* 578:862). The effect of “infall” on the evolution of chemical and isotopic abundances in the galaxy and the source of the infalling matter will be discussed.

5070

EQUILIBRATED ORDINARY CHONDRITE-LIKE MICROMETEORITES

M. J. Genge. Impact and Astromaterials Research Centre (IARC), Imperial College London and the Natural History Museum, Exhibition Road, London SW7 2AZ, UK. E-mail: m.genge@imperial.ac.uk

Introduction: Among unmelted micrometeorites (MMs) recovered from Antarctic ice are coarse-grained particles dominated by pyroxene, olivine, and glass, that usually have igneous textures. On the basis of the mineral chemistries, textures and the presence of small amounts of fine-grained matrix Genge [1] has suggested these are mainly fragments of chondrules. Mineral chemistries, furthermore, suggest that ~70% of coarse-grained MMs are derived from ordinary chondrite-like parent bodies. The majority of such particles are unequilibrated, however, 7 particles (9%) have been reported that have olivine and pyroxene major and minor element compositions within the restricted range of the equilibrated ordinary chondrites [2].

In this study the chemistry, texture and mineralogy of equilibrated particles is examined to confirm their EOC origin.

Samples and Methods: The 7 equilibrated cgMMs were identified among a collection of 77 cgMMs collected from Antarctic ice. Selection and analytic techniques are described in Genge et al. [1]

Results: The EOC-like particles are dominated by olivine and pyroxene with homogeneous major and minor element compositions within the range of H and L4–6 chondrites. Five particles have granular textures and lack significant mesostasis. Accessory phases in the granular particles are taenite, albitic feldspar and Cr spinel. Two particles have porphyritic textures and have vesicular mesostases dominated by pyroxene and olivine dendrites within aluminosilicate glass. One of these particles contains Ni-bearing sulfides in the mesostasis and one albitic feldspar. Both porphyritic particles have rounded particle shapes implying melting during atmospheric entry. One of the granular cgMMs also has a small area of compositionally variable vesicular glass containing partially melted feldspar.

Discussion: The reported particles have mineral compositions that are consistent with an EOC origin. The occurrence of albitic feldspar (An_{13–20}) in combination with the olivine and pyroxene minor elements is in particular strong evidence for an EOC origin [3]. Cr-bearing spinels are unfortunately too small for quantitative analysis.

The presence of glass within the mesostases of three of the particles, however, is not compatible with an EOC origin. The generation of compositionally variable, vesicular glass, often containing partially melted albitic glass, however, is observed in the thermally altered substrates of EOC fusion crusts [4]. The formation of vesicles, presumably occurring due to degassing of sulfides under oxidizing conditions. Considering the evidence for surface correlated melting in these particles, the presence of mesostasis probably represents the overprint of entry heating.

Due to their small size, it is difficult to apply petrologic grade criteria to MMs. Chromite-olivine geothermometry may offer a method by which this can be evaluated for selected particles.

References: [1] Genge M. J. et al. 2005. *Meteoritics & Planetary Science* 40:255–238. [2] Genge M. J. 2006. Abstract #1759. 37th Lunar and Planetary Science Conference. [3] Brearley A. J. and Jones R. H. 1998. *Planetary materials*. Washington, D.C.: Mineralogical Society of America. pp. 120–518. [4] Genge M. J. and Grady M. M. 1999. *Meteoritics & Planetary Science* 34:341–356.

5284

STABLE IRON ISOTOPE ANALYSES OF METAL GRAINS IN ORDINARY CHONDRITES BY MC-ICP-MS

K. J. Gildea¹, R. Burgess¹, I. Lyon¹, and D. W. Sears². ¹School of Earth, Atmospheric and Environmental Sciences, The University of Manchester, Oxford Road, Manchester, M13 9PL, UK. E-mail: karen.j.gildea-1@student.manchester.ac.uk. ²Arkansas Center for Space and Planetary Science, University of Arkansas, Fayetteville, Arkansas 72701, USA

Introduction: Stable iron isotope analyses of meteorites are being studied to help determine the processes involved in their formation, the source of their materials and subsequent surface alteration. Variation in iron isotope fractionation may be influenced by metal/silicate fractionation, metamorphism, aqueous alteration, chondrule formation and terrestrial weathering. The aim of this study is to assess whether the effects of these processes can be distinguished by analyzing separated iron metal grains from 25 ordinary chondrites consisting of different classes (H, L, and LL), different petrographic types (3–6) and different terrestrial weathering status (falls and finds).

Equipment: Analysis was by Nu Instruments multi-collector ICP-MS. Isobaric interferences were reduced by the introduction of samples via a DSN-100 Desolvating Nebuliser and by running the ICP in medium resolution mode to ensure that the Fe isotopes were sufficiently resolved to show a flat topped peak with “iron shoulder” [1].

The reproducibility and accuracy of the ICP-MS was determined by measuring the “in-house” Johnson-Matthey standard against the IRMM014 iron isotope standard using the sample/standard bracketing method to give $\delta^{56}\text{Fe} = 0.33 \pm 0.06\text{‰}$ and $\delta^{57}\text{Fe} = 0.5 \pm 0.07\text{‰}$ (to 1 standard deviation).

Samples and Sample Preparation: Samples were crushed and separated [2]. The magnetic separates were re-crushed and metal grains hand picked for HNO₃ dissolution using a microscope.

Results:

Table 1.

	$\delta^{56}\text{Fe}$	s.e.	$\delta^{57}\text{Fe}$	s.e.
Bremervörde (H3)	−0.01	0.04	−0.02	0.05
Beaver Creek (H4)	0.08	0.04	0.12	0.08
Elm Creek (H4)	0.13	0.02	0.26	0.02
Acme (H5)	0.19	0.05	0.27	0.06
Crumlin (L5)	0.19	0.02	0.36	0.06
Etter (L5)	0.19	0.02	0.36	0.02
Aldsworth (LL5)	0.24	0.04	0.42	0.04
Barwell (L6)	0.33	0.02	0.55	0.08

When plotted, these results trend along a mass fractionation line with $\delta^{56}\text{Fe}$ and $\delta^{57}\text{Fe}$ increasing with petrographic order. Further results will be presented at the meeting along with discussion and conclusion.

Acknowledgements: This work was supported by PPARC and by the University of Manchester through SRIF funding for the Nu Plasma MC-ICP-MS.

References: [1] Weyer S. and Schweiters J. B. 2003. *International Journal of Mass Spectrometry* 226:355–368. [2] Sears D. W. and Axon H. J. 1976. *Nature* 260:34–35.

5150

IRON OXIDATION STATE IN AUSTRALASIAN MICROTEKTITES BY HIGH-RESOLUTION XANES SPECTROSCOPY AND K-DETECTED XANES SPECTROSCOPY

Gabriele Giuli¹, Sigrid Griet Eeckhout², Christian Koeberl³, Eleonora Paris¹, and Giovanni Pratesi^{4,5}. ¹Dip. Scienze della Terra, Università di Camerino, Italy. E-mail: gabriele.giuli@unicam.it. ²European Synchrotron Radiation Facility (ESRF), Grenoble, France. ³Department of Geological Sciences, University of Vienna, Austria. ⁴Museo di Storia Naturale, Università di Firenze, Italy

We examined the iron oxidation state and coordination number in 6 microtektites from the Australasian strewn field by a combination of high-resolution X-ray absorption near edge structure (XANES) and X-ray emission spectroscopy (XES). The latter technique (K_{β} -detected XANES spectroscopy) has the advantage of displaying sharper peaks in the pre-edge region, thus allowing a better resolution and a more straightforward way of decomposing the pre-edge features into its components. The spectra have been collected at ID26 beamline of the ESRF storage ring (Grenoble, France). The X-ray beam (size = $30 \times 80 \mu\text{m}$) has been monochromatized with two Si (220) crystals. XANES and XES spectra consistently show small variations in the energy and intensity of the pre-edge peaks. Comparison with Fe model compounds with known Fe oxidation state and coordination number allowed us to estimate the Fe oxidation state for the microtektites under study.

Within experimental reproducibility, all the pre-edge peak energies of the microtektite samples plot very close to the divalent Fe model compounds. $\text{Fe}^{3+}/(\text{Fe}^{2+} + \text{Fe}^{3+})$ are estimated to be in the 0 to 0.1 range.

Comparison with literature data on splash form tektites from all four known strewn field [1] and impact glass from a K/T boundary layer [2] allows us to confirm that, as for the Fe oxidation state, Australasian microtektites are indistinguishable from splash form tektites. On the other hand, noticeable differences are observed with K/T impact glasses, which in the view of these data should not be considered as microtektites.

References: [1] Giuli G. et al. 2002. *Geochimica et Cosmochimica Acta* 66:4347–4353. [2] Giuli G. et al. 2005. *Meteoritics & Planetary Science* 40: 1575–1580.

5149

IRON OXIDATION STATE IN IMPACT GLASS FROM THE CRETACEOUS/TERTIARY BOUNDARY AT BELOC (HAITI) BY HIGH-RESOLUTION XANES SPECTROSCOPY: IMPLICATIONS ON THE FORMATION CONDITIONS

Gabriele Giuli¹, Sigrid Griet Eeckhout², Christian Koeberl³, Giovanni Pratesi^{4,5}, and Eleonora Paris¹. ¹Dip. Scienze della Terra, Università di Camerino, Italy. E-mail: gabriele.giuli@unicam.it. ²European Synchrotron Radiation Facility (ESRF), Grenoble, France. ³Department of Geological Sciences, University of Vienna, Austria. ⁴Museo di Storia Naturale, Università di Firenze, Italy

We examined the iron oxidation state and coordination number in five yellow impact glasses from the Cretaceous-Tertiary (K/T) boundary section at Beloc, Haiti, which formed as the result of impact melting during the Chicxulub impact event. The samples have been analyzed by Fe K-edge high-resolution X-ray absorption near edge structure (XANES) spectroscopy, and the resulting data on Fe oxidation state and coordination number have been compared with literature data on 9 black impact glasses and 1 high Si-K impact spherule from the same impact layer.

Although there are several studies on the chemical and isotopic composition of these impact glasses, very few studies on the Fe coordination number and oxidation state have been reported [1]. Such studies are, however, of utmost importance to reconstruct the oxygen fugacity conditions prevailing during impact melt formation.

The Fe K-edge high-resolution X-ray absorption near edge structure (XANES) spectra have been recorded at the ID26 beamline of the ESRF storage ring (Grenoble, F). The pre-edge peaks of our XANES spectra display noticeable variations in intensity and energy, which are indicative of significant changes in the Fe oxidation state, spanning a wide range from about 20 to 100 mole% trivalent Fe. All data plot along a trend, falling between two mixing lines joining a point calculated as the mean of a group of tektites studied so far (consisting of 4- and 5- coordinated Fe^{2+}) to $^{44}\text{Fe}^{3+}$ and $^{55}\text{Fe}^{3+}$, respectively. Thus, the XANES spectra can be interpreted as a mixture of $^{44}\text{Fe}^{2+}$, $^{55}\text{Fe}^{2+}$, $^{44}\text{Fe}^{3+}$, and $^{55}\text{Fe}^{3+}$. There is no evidence for six-fold coordinated Fe, however, its presence in small amounts cannot be excluded from XANES data alone. Yellow glasses display clearly higher $\text{Fe}^{3+}/(\text{Fe}^{2+} + \text{Fe}^{3+})$ ratios (from 75 to 100 mole% trivalent Fe [3]) when compared to black impact glasses (from 20 to 75 mole% trivalent Fe [2]) and high Si-K glass (20 mole% trivalent Fe). Our observations are explained by a very large variety of oxygen fugacity conditions prevailing during melt formation. Furthermore, there is a clear positive relationship between the $\text{Fe}^{3+}/(\text{Fe}^{2+} + \text{Fe}^{3+})$ ratio and the Ca content of the studied glasses, suggesting that the Fe oxidation state was affected by a variable contribution of the Ca sulfate-bearing sedimentary rocks overlying the target rock at the impact site.

References: [1] Oskarsson N. et al. 1996. In *New developments regarding the KT event and other catastrophes in Earth history*. Boulder, Colorado: Geological Society of America. pp. 445–452. [2] Giuli G. et al. 2005. *Meteoritics & Planetary Science* 40:1575–1580. [3] Giuli G. et al. Forthcoming.

5148

DIVALENT VANADIUM IN VIGARANO CV3 METEORITE CHONDRULE

Gabriele Giuli¹, Giovanni Pratesi², Sigrid Griet Eeckhout³, and Eleonora Paris¹. ¹Dip. Scienze della Terra, Università di Camerino, Italy. E-mail: gabriele.giuli@unicam.it. ²Museo di Storia Naturale, Università di Firenze, Italy. ³European Synchrotron Radiation Facility (ESRF), Grenoble, France

A chondrule of the CV3 Vigarano carbonaceous chondrite has been studied by high-resolution XANES spectroscopy in order to get accurate information on the V oxidation state. Comparison of the experimental spectrum with those of V model compounds with known oxidation state and coordination number provided strong evidence of the presence of divalent vanadium in the chondrule examined.

In the aim of establishing the location of V in the minerals making up the chondrule, experimental spectra have been calculated for a set of mineral structures possibly hosting vanadium. For each mineral, theoretical spectra have been calculated and this for each crystallographic site possibly hosting V, and the results have been summed with different weights in order to better reproduce the experimental spectrum.

A comparison with the experimental spectrum rules out preferential incorporation of V in magnetite, whereas forsterite, enstatite, and diopside can all be accounted for as possible hosts for V.

The presence of divalent vanadium in a chondrule of a CV3 chondrite has never been reported in the literature and bears important consequences on the formation conditions of this class of meteorites.

5112

THE JaH 091 STREWN FIELD

E. Gnos¹, M. Eggimann², A. Al-Kathiri³, and B. A. Hofmann². ¹Institut für Geologie, Universität Bern, Baltzerstrasse 1, 3012 Bern, Switzerland. E-mail: gnos@geo.unibe.ch. ²Naturhistorisches Museum der Burgergemeinde Bern, Bernstrasse 15, 3005 Bern, Switzerland. ³Directorate General of Commerce and Industry, Ministry of Commerce and Industry, Salalah, Oman

Introduction: Initial finds of two paired large masses of an L5 meteorite in 2002 (JaH 090, 92.7 kg; JaH 091, 123.7 kg; ~5.7 km distance between the two localities) suggested the presence of a large meteorite strewn field in Oman. Additional stones recovered in 2003 yielded the orientation of the strewn field. We were able to extend the strewn field length to >40 km in spring 2005, and additional systematic searches for larger masses so far yielded ~2300 kg of material. Searches at the smaller mass end of the strewn field confirmed the field over a length of 49 km × 9 km making it one of the largest meteorite strewn fields known, comparable to Jilin and Allende. JaH 091 is moderately weathered (W2-W3), its shock grade is S2 and mineral compositions are $Fa_{25.0}Fs_{21.3}Wo_{1.6}$. The material characteristically shows half to >1 cm-sized olivine chondrules at its surface. Larger stones commonly show small holes on its lower side in the soil.

Relations with JaH 055: As the published JaH 055 (L4-5) coordinate fell in the area of another well-searched strewn field (JaH 073) we were amazed to learn that we should have missed such a large mass. Further searches around the published coordinates and in our JaH 073 collection confirmed the absence of any L4-5 stones such as JaH 055. Meteorites seized by the Omani police from illegal meteorite collectors in 2005 were labeled JaH 055 and associated coordinates were close to JaH 091. This material is >700 kg and includes large fragments. The finding of similar large masses within the JaH 091 strewn field sparked the idea that an error in the published coordinate could solve the discrepancy. From the finders of JaH 055 we were informed that the JaH 055 coordinate is indeed in error, and we thus think that JaH 091 and JaH 055 are in fact paired. This would bring the total mass known to ~3200 kg.

Possible Connection to Locality Name: It is interesting to note that according to a Bedouin legend an area near the JaH 091 strewn field is called "Lahoob" meaning "Big Fire." Qualitative age estimates using weathering grade and other weathering proxies [2] indicate that the JaH 091 fall occurred <15,000 years ago. This may well be within human tradition. The ¹⁴C age of JaH 091 (19.3 ± 1.3 kyr [2]) may be strongly influenced by shielding.

References: [1] Russell S. et al. 2004. The Meteoritical Bulletin, No. 88. *Meteoritics & Planetary Science* 39:A215-A272. [2] Al-Kathiri A. et al. 2005. *Meteoritics & Planetary Science* 40:1215-1239.

5111

THE KREEP-RICH IMBRIUM IMPACT MELT BRECCIA OF THE LUNAR METEORITE SAYH AL UHAYMIR 169

E. Gnos¹, B. A. Hofmann⁴, A. Al-Kathiri³, and M. J. Whitehouse⁴. ¹Institut für Geologie, Universität Bern, Baltzerstrasse 3, 3012 Bern, Switzerland. E-mail: gnos@geo.unibe.ch. ²Naturhistorisches Museum der Burgergemeinde Bern, Bernastrasse 15, 3005 Bern, Switzerland. ³Directorate General of Commerce and Industry, Ministry of Commerce and Industry, Salalah, Oman. ⁴Laboratory for Isotope Geology, Swedish Museum of Natural History, Box 50007, SE-104 05, Stockholm, Sweden

Introduction: The dominant lithology (87 vol%) of the unique lunar meteorite Sayh al Uhaymir (SaU) 169 from Oman consists of an extremely KREEP-rich polymict, crystalline impact-melt breccia interpreted to be derived from the Imbrium impact melt sheet [1]. This lithology is now assigned together with a few mm-sized rock fragments from the Apollo 12 and 14 landing sites to a group called “high-Th impact melt group” [2].

Results and Interpretation: The impact melt contains 25–40 vol% of shocked plutonic (gabbro-noritic to noritic) Procellarum-Terrane clasts characterized by the absence of anorthosites. Many plagioclase clasts show a high albite content reaching An₅₇. The crystalline impact melt between the clasts consists mainly of low-Ca pyroxene, plagioclase intergrown with Ba-bearing K-spar, and smaller amounts of merrillite, zircon, olivine, troilite and kamacite. The SaU 169 impact melt bulk composition shows a strong enrichment in Th (32.7 µg/g), U (8.6 µg/g), K₂O (0.54 wt%), REE (~1330 µg/g), P₂O₅ (1.14 wt%), and Zr (2835 µg/g) [1]. LREE-enriched merrillite is the main REE carrier containing 4–9 wt% REE oxides. Zircon is characterized by HREE-enriched patterns with a negative Eu anomaly. Application of Ti thermometer for zircon [3] yielded a minimum crystallization temperature of 1168 ± 33 °C. SaU 169 impact melt ilmenites are characterized by containing ~0.6 wt% Nb₂O₅. The detailed analysis of all phases crystallized from the impact melt, in combination with its modal abundance and calculated mineral densities allows to estimate the “pure clast-free Imbrium KREEP melt” composed of: ~2.0 wt% P₂O₅, 44.4 SiO₂, 4.9 TiO₂, 10.9 Al₂O₃, 14.0 FeO, 12.2 MgO, 7.4 CaO, 0.8 Na₂O, 0.4 K₂O, ~380 Nb, ~1250 Ba, and ~3400 REEs. This indicates that highly evolved differentiates were present at the Imbrium impact site.

References: [1] Gnos E. et al. 2004. *Science* 305:657–659. [2] Zeigler R. A. 2006. Abstract #2366. 37th Lunar and Planetary Science Conference. [3] Watson E. B. and Harrison T. M. 2005. *Science* 308:841–844.

5073

EFFECTS OF FALLING IMPACT EJECTA ON THE POST-CHICXULUB ATMOSPHERE

T. J. Goldin^{1, 3} and H. J. Melosh^{2, 3}. ¹Department of Geosciences, The University of Arizona, Tucson, Arizona 85721, USA. E-mail: tgoldin@geo.arizona.edu. ²Lunar and Planetary Laboratory, The University of Arizona, Tucson, Arizona 85721. ³Bayerisches Geoinstitut D-95440 Bayreuth, Germany.

Introduction: The mechanics of impact ejecta deposition are not well understood, especially for planets with atmospheres, where complex interactions occur between the ejected particles and the surrounding atmosphere. Studying the interactions between the ejecta from large terrestrial impacts and the atmosphere is particularly important for understanding the environmental effects of such events.

The K/T boundary ejecta layer, linked to the 65 Ma Chicxulub impact, is found worldwide. This study focuses on the 2–3 mm thick [1] distal ejecta, which consists of densely packed spherules 250 µm in average diameter [2]. Additionally, a global soot layer has been identified at the K/T boundary [3], suggesting the impact triggered global wildfires.

Modeling: KFIX-LPL is a version of the KFIX code [4], which has been modified to suit the problem of impact sedimentation. KFIX is based on the original KACHINA code [5]. The finite-difference code models two-dimensional, two-phase fluid flow allowing us to examine the interactions between the atmosphere and ejected spherules.

We modeled a simplified Chicxulub scenario with the injection of uniform 250 µm diameter spherules into the atmosphere at 8 km/s, at an altitude of 200 km and with a variable inflow density consistent with the volume of spherules observed and models of mass deposition rates [6]. The initial mesh approximates the Earth’s atmosphere. Air is modeled as a perfect gas and the spherules are modeled as a simple incompressible fluid with the properties of basaltic glass. We modeled both a vertical injection angle and a more realistic angle of 45 degrees. The particles fall through the thin upper atmosphere, pushing the atmosphere downwards until the particles decelerate due to drag and increasing atmospheric pressure. The particles accumulate at ~100 km altitude and the deceleration heats the atmosphere around the particles (>2500 K), causing expansion of the atmosphere and creating a sharp transition between hot dense atmosphere below the deceleration boundary and cool thin atmosphere above.

Discussion: These models provide important insight into the state of the atmosphere after the Chicxulub impact. It has been proposed that thermal energy radiated from ejecta reentering the atmosphere caused global wildfires [6] and our models provide support for significant atmospheric heating and thus the delivery of significant thermal radiation to the Earth’s surface. Additionally, our results provide the starting conditions and time frames for chemical models examining the environmental consequences of Chicxulub, such as acid rain and sulfate aerosol formation.

References: [1] Smit J. et al. 1992. Proceedings, 22nd Lunar and Planetary Science Conference. pp. 87–100. [2] Smit J. 1999. *Annual Review of Earth and Planetary Science* 27:75–113. [3] Wolbach W. et al. 1985. *Science* 208:1095–1108. [4] Rivard W. C. and Torrey M. D. 1977. Los Alamos National Laboratory Report #LA-NUREG-6623. Los Alamos, New Mexico. 125 p. [5] Amsden A. A. and Harlow F. H. 1974. Los Alamos Scientific Laboratory Report #LA-5680. Los Alamos, New Mexico. [6] Melosh H. J. et al. 1990. *Nature* 343:251–253.

5213

CONSTRAINING VOLATILE ABUNDANCE IN CHONDRITIC COMPONENTS

S. H. Gordon^{1, 2}, P. A. Bland^{1, 2}, S. J. Hammond^{1, 3}, and N. W. Rogers³.
¹Impact and Astromaterials Research Centre (IARC), Imperial College London, South Kensington Campus, London SW7 2AZ, UK. E-mail: s.h.gordon@imperial.ac.uk. ²Department of Mineralogy, The Natural History Museum, Cromwell Road, London, SW7 5BD, UK. ³Department of Earth Sciences, The Open University, Walton Hall, Milton Keynes MK7 6AA, UK

Introduction: Volatile depletion was the fundamental chemical process occurring in the early solar system, but has yet to be fully explained. Proposed models include the two-component model (e.g., [1, 2]), incomplete condensation (e.g., [3, 4]), evaporative fractionation prior to chondrule formation [5] and inheritance of a depletion from the interstellar medium [6]. These hypotheses are largely based on bulk compositional data from chondrites. A knowledge of the variation in composition of chondritic components (e.g., matrix and chondrules) may provide some useful constraints on the mechanism for volatile depletion.

In addition, an improved knowledge of their trace and minor element composition may help to clarify chondrule:matrix complementarity. Some models (e.g., [2]) call for chondrule formation close to the young Sun, with chondrules being added to chemically unrelated matrix at asteroidal distances. Complementarity between chondrules and matrix in siderophile and chalcophile elements (e.g., [7, 8]) casts doubt on this scenario.

The relatively sparse data for many elements in chondrules and matrix is related to the difficulty in acquiring precise separates. The current study is intended to overcome this obstacle.

Method: Modal recombination analysis (MRA) [9] and electron probe microanalysis (EPMA) are used to determine the bulk composition of individual chondrules. A micromill is then used to drill precise volumes of material from a pre-specified area. Solution and LA-ICP-MS is subsequently employed to determine the chemistry of these separates. The ICP-MS data are then combined with major element data determined by MRA and EMPA.

Results: CV3 chondrites Allende and Vigarano were investigated initially, as chondrules are large and easily defined. In addition, Allende is one of the few meteorites for which chondrule minor and trace element data are available [10]. Data gained via MRA and EPMA fall within the compositional parameters defined in the literature. Solution ICP-MS will allow for the determination of a wider range of minor and trace elements than in previous INAA studies.

Conclusions: Matrix and chondrules have been analyzed to investigate the extent of chemical complementarity between these two components, and to constrain mechanisms for volatile depletion. Results will be presented at the meeting.

References: [1] Anders E. 1964. *Space Science Reviews* 3:583. [2] Shu F. H. et al. 1996. *Science* 271:1545. [3] Wasson J. T. and Chou C.-L. 1974. *Meteoritics* 9:69. [4] Cassen P. 1996. *Meteoritics & Planetary Science* 31: 793. [5] Huss G. R. et al. 2003. *Geochimica et Cosmochimica Acta* 67:4283. [6] Yin Q. 2005. *Chondrites and the protoplanetary disk*. San Francisco: Astronomical Society of the Pacific. 675 p. [7] Bland P. A. et al. 2005. *Proceedings of the National Academy of Sciences* 102:13755. [8] Kong P. and Palme H. 1999. *Geochimica et Cosmochimica Acta* 63:3673. [9] Berlin J. et al. 2006. Abstract #2370. 37th Lunar and Planetary Science Conference. [10] Rubin A. E and Wasson J. T. 1988. *Geochimica et Cosmochimica Acta* 52:425.

5342

Li-Be ISOTOPE SYSTEMATIC IN EFREMOVKA CAIs

J. N. Goswami and M. P. Deomurari. Physical Research Laboratory, Ahmedabad, 380009, India. E-mail: goswami@prl.res.in

The presence of excess ¹⁰B from in situ decay of ¹⁰Be (half-life = 1.5 Ma) in CAIs is well established [1–4]. Energetic particle interactions as well as ¹⁰Be of galactic cosmic ray origin, trapped within the protosolar cloud, are considered as potential sources of this nuclide in the early solar system [1–5]. A hint for the presence of the short-lived nuclide ⁷Be (half-life = 53 days) at the time of formation in an Allende CAI (3529-41) has been claimed recently [6]. Disturbance in the Al-Mg isotope system in this CAI is well documented [7], and an attempt was made to avoid this problem by accepting Li-Be isotope data for only those analyses where Be concentration was compatible with the expected fractionation trend during magmatic differentiation of CAI melt [6]. The presence of ⁷Be in early solar system, if confirmed, will uniquely identify local production of this nuclide via interactions of energetic particles from the early Sun. We have initiated a study of Efremovka CAIs to look for possible presence of ⁷Li at the time of their formation. Petrographic characteristics and Al-Mg isotope systematics do not suggest presence of any post-magmatic perturbation in almost all Efremovka CAIs [8].

We have analyzed melilite in the Efremovka CAIs E-2 and E-40 for Li-Be isotope records using a Cameca ims-4f ion microprobe. Both these CAIs have well-behaved Al-Mg isotope systematics with initial ²⁶Al/²⁷Al ratios of $(5.64 \pm 0.97) \times 10^{-5}$ and $(3.4 \pm 1.0) \times 10^{-5}$, respectively [8, 9]. The isotopic studies were carried out at a mass resolution (M/ΔM) of ~1500, sufficient to remove all the molecular interferences at the masses of interest. We use GB-4 glass as a standard to correct for instrument mass fractionation as well as to infer the relative ion yields and absolute concentration of Li, Be, and B in the analyzed phases. Our study confirms the dependence of Li ion yield, relative to Be, as a function of energy of the secondary ions accepted for analysis [6]. Li concentrations in the analyzed melilite from E-2 are ≤0.06 ppm, while Be contents are ≤0.2 ppm.

The results obtained so far do not provide any indication for the presence of resolved excess of ⁷Li in E-2 melilite. Further, the inferred initial ⁷Li/⁶Li at the time of formation of E-2 is lower than the reference value. We note that multiple sources are needed for explaining the natural abundance of ⁷Li [10]. Thus, the lower initial ⁷Li/⁶Li in the early formed refractory phases may imply heterogeneity in Li isotopic composition within the proto-solar cloud that did not undergo complete mixing and homogenization by the time of CAI formation. We made a similar suggestion to explain variations in the initial boron isotopic composition in CAIs [11].

References: [1] McKeegan K. D. et al. 2000. *Science* 289:1334–1337. [2] Sugiura N. et al. 2001. *Meteoritics & Planetary Science* 36:1397–1408. [3] MacPherson G. J. et al. 2003. *Geochimica et Cosmochimica Acta* 67: 3165–3179. [4] Marhas K. K. et al. 2002. *Science* 298:2182–2185. [5] Desch S. J. et al. 2004. *The Astrophysical Journal* 602:528–542. [6] Chaussidon M. et al. 2006. *Geochimica et Cosmochimica Acta* 70:224–245. [7] Podosek F. A. et al. 1991. *Geochimica et Cosmochimica Acta* 55:1083–1110. [8] Goswami J. N. et al. 1994. *Geochimica et Cosmochimica Acta* 58:431–447. [9] Fahey et al. 1987. *Geochimica et Cosmochimica Acta* 51:3215–3229. [10] Walker T. P. et al. 1985. *The Astrophysical Journal* 299:745–751. [11] Goswami J. N. 2003. Abstract. *Meteoritics & Planetary Science* 38:A48.

5279

A ¹⁶O-RICH CAI-LIKE PARTICLE AMONG ANTARCTIC MICROMETEORITES

M. Gounelle^{1,2,3}, M. Chaussidon⁴, C. Engrand³, J. Duprat³, and H. Leroux⁵.
¹LEME-MNHN, CP52, 57 rue Cuvier, 75005 Paris, France. E-mail: gounelle@mnhn.fr. ²IARC, NHM London SW7 5BD, UK. ³CSNSM, Bât. 104, 91405 Orsay Campus, France. ⁴CRPG-CNRS, BP20, 54501 Vandoeuvre les Nancy, France. ⁵LSPES, 59655 Villeneuve d'Ascq, France

Introduction: Antarctic micrometeorites (AMMs) are interplanetary dust particles collected in the Antarctic ice cap, and belonging to the size range 25–400 μm [1]. They might represent the bulk of extraterrestrial matter accreting on Earth today [2]. They bear strong resemblances with low petrographic type, hydrous carbonaceous chondrites [1]. Compared to IDPs they lack chondritic porous particles [3]. Antarctic micrometeorites might be of cometary or asteroidal origin, or a mixture thereof. Given the discovery of calcium-aluminium-rich (CAI) particles among the Stardust samples [4], we have characterized a CAI-like particle among the AMMs collection.

Results: Micrometeorite 98-03-04 was collected at the Astrolabe glacier during the field season 1997–1998 [5]. After extraction under a binocular microscope, it was embedded in epoxy and polished. SEM examination has revealed an elongated, 100 μm across, compact particle with some holes, probably due to loss of grains. It is made of diopside (En_{53–60}Wo_{39–50}), spinel and other Ca-Al-rich minerals too small to be analyzed with the electron microprobe, all set up in a phosphorus-rich chondritic matrix and surrounded by a partial magnetite rim. Pyrrhotite is present at the boundary of the Ca-Al-rich minerals and the chondritic matrix. In a previous polishing plan, olivine (Fo_{68–97}) was also found. The bulk oxygen isotopic composition, measured at the CRPG Nancy with the CAMECA 1270 ion probe, and expressed relative to the Standard Mean Ocean Water, is δ¹⁷O = –36.6 ± 0.1 ‰, δ¹⁸O = –32.3 ± 0.4 ‰, i.e., Δ¹⁷O = –19.9 ± 0.5 ‰.

Discussion: The compact nature and mineralogy of micrometeorite 98-03-04 sets it apart from others CAI-like micrometeorites which are usually made of spinel (±perovskite) and iron-rich phyllosilicates [6, 7], or of isolated spinel and hibonite [8]. Though it lacks anorthite, it is reminiscent of the CAI particle found among Stardust samples. The oxygen isotopic composition of 98-03-04 is similar to other CAIs among Antarctic micrometeorites [6, 7, 9] or in carbonaceous chondrites [10], suggesting the existence of one common reservoir for all CAIs, possibly close to the Sun [11]. In this context, it will be of uttermost importance to measure the oxygen isotopic composition of CAI-like particles among Stardust samples.

References: [1] Engrand C. and Maurette M. 1998. *Meteoritics & Planetary Science* 33:565–580. [2] Duprat J. et al. 2006. Abstract #5279. *Meteoritics & Planetary Science*. This issue. [3] Gounelle M. et al. 2005. *Meteoritics & Planetary Science* 40:917–932. [4] Zolensky M. E. et al. Abstract #1203. 37th Lunar and Planetary Science Conference. [5] Gounelle M. et al. 1999. Abstract. *Meteoritics & Planetary Science* 34:A46. [6] Hoppe P. et al. 1995. 26th Lunar and Planetary Science Conference. pp. 623–624. [7] Kurat G. et al. 1994. Abstract. *Meteoritics & Planetary Science* 29:487–488. [8] Gounelle M. 2000. Ph.D. thesis, Université Paris, Paris, France. [9] Engrand C. et al. 1999. *Geochimica et Cosmochimica Acta* 63:2623–2636. [10] Clayton R. N. 1993. *Annual Review of Earth and Planetary Science* 21: 115–149. [11] Shu F. H. et al. 2001. *The Astrophysical Journal* 548:1029–1050.

5187

DEPTH-DEPENDENT FRACTIONATION OF LIGHT SOLAR WIND NOBLE GASES IN A GENESIS TARGET

A. Grimberg¹, F. Bühler², P. Bochsler², D. S. Burnett³, H. Baur¹, and R. Wieler¹. ¹Isotope Geology, ETH Zürich, Switzerland. E-mail: grimberg@erdw.ethz.ch. ²Physikalisches Institut, University of Bern, Bern, Switzerland. ³GPS, CalTech, Pasadena, California, USA

We analyzed light noble gases in a bulk metallic glass (BMG) that was exposed to solar wind (SW) irradiation on Genesis for its total exposure time and all SW regimes [1]. The BMG was especially designed to look for a putative solar energetic particle (SEP) component, reported to be present in lunar soils [2], by using the closed system stepwise etching (CSSE) technique. Here we present the depth distribution of He and Ne isotopes and discuss different processes leading to the observed fractionation patterns. Moreover, this will be compared with measurements of Ar isotopes that are actually in progress.

The Ne isotope depth distribution measured in the BMG resembles a fractionation pattern that follows a mass dependant fractionation line. Lighter isotopes are enriched at shallow depth with initial ²⁰Ne/²²Ne higher than the bulk SW value, whereas the heavier isotopes are enriched in deeper layers. This distribution is fully consistent with model calculations using the SRIM code [3] of an isotopically uniform SW that fractionates within the BMG upon implantation, assuming a velocity distribution as measured by Genesis. From this it follows that there is no evidence for a distinct isotopic fractionation of Ne among the different SW regimes. Most importantly, the use of BMG data in combination with SRIM simulations, which allow for surface sputtering and cosmogenic Ne production in lunar grains, shows that no “SEP-Ne” component, that would be isotopically heavier than the SW-Ne, is needed to explain the lunar soil data.

The measured He isotopic distribution in the BMG is very different from the Ne fractionation pattern and also from the He distribution as simulated with SRIM for the same SW conditions applied for Ne. The ³He/⁴He ratios released from shallow depth first increase by 10% and later drop to almost constant values 13% lower than the initial in all remaining steps. This is in contrast to SRIM simulations that predict a steep decrease of ³He/⁴He with depth by more than a factor of 6. A diffusional loss, which in turn would have led to a smearing of the He isotope distribution, is unlikely. Bulk analyses show no difference of the He abundance compared to other Genesis targets [4] or in situ spacecraft measurements. On the other hand, it is well conceivable that the SRIM code overestimates the fractionation with depth for very light elements as He. However, the largely different isotope pattern between He and Ne suggests that the trapped solar He suffered an additional fractionation process not yet identified.

References: [1] Grimberg A. et al. 2006. Abstract #1782. 37th Lunar and Planetary Science Conference. [2] Wieler R. et al. 1986. *Geochimica et Cosmochimica Acta* 50:1997–2017. [3] Ziegler J. F. 2004. *Nuclear Instruments and Methods in Physics Research* 219/220:1027–1036. [4] Hohenberg C. M. et al. 2006. Abstract #2439. 37th Lunar and Planetary Science Conference.

5231

OSBORNITE IN CB/CH-LIKE CARBONACEOUS CHONDRITE ISHEYEVO

V. I. Grokhovsky. Physico-Technical Department, Ural State Technical University, UPI, Ekaterinburg 620002, Russian Federation. E-mail: grokh47@mail.ru

Introduction: Recently discovered metal-rich primitive meteorite Isheyevu genetically links CH and CB carbonaceous chondrites [1]. As with other meteorites of the CR clan, the unique mineralogical and textural data of Isheyevu are being widely discussed [1–4]. Both nebular and asteroidal models have been proposed to explain this data [6]. Here we report the first discovery of the osbornite refractory mineral for the CR clan in the Isheyevu chondrite.

Results and Discussion: Optically, SEM/EDX and element X-ray mapping detected the large (~100 μm) grain of osbornite TiN in the area of the CB lithology by the so-called border between CB and CH chondrite in Isheyevu. Single crystal of osbornite (Fig. 1) with Ti, N stoichiometric contents contacts both metal and silicates (olivine, pyroxene). The phase boundaries of these minerals are marked by thin secondary minerals. The osbornite possesses characteristic yellow color and is subject to low roughening in course of sample preparation.

TiN is a very refractory mineral. It is condensed at high temperatures under highly reducing conditions. Rare grains of osbornite occur in few EH and EL chondrites and aubrites. Besides that, TiN was found in the ALH 85085 reduced carbonaceous chondrite [5] and, recently, the osbornite inclusion was observed in CAIs from Isheyevu [6]. It is concluded that there is no simple equilibrium process which can explain all peculiarities of texture in the Isheyevu meteorite, but it is clear that observed osbornite was among the first crystals that condensed from gaseous phase in the solar nebula.

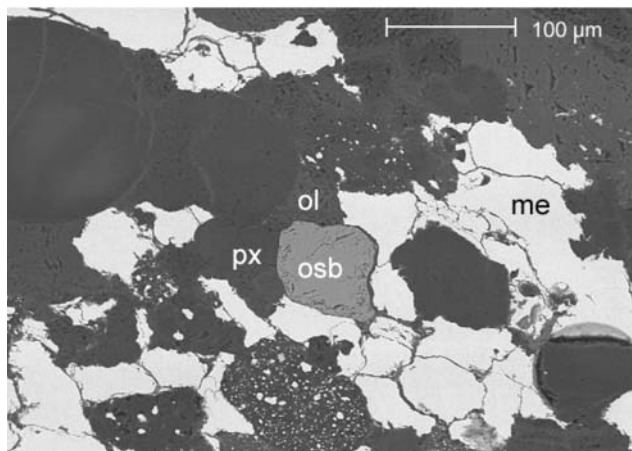


Fig. 1. A BSE image of the osbornite from Isheyevu. osb = osbornite TiN; me = Fe(Ni)-metal; px = pyroxene; ol = olivine.

References: [1] Ivanova M. A. et al. 2006. Abstract #1100. 37th Lunar and Planetary Science Conference. [2] Krot A. N. et al. 2006. Abstract #1224. 37th Lunar and Planetary Science Conference. [3] Perron C. et al. 2004. *AMSM* 67: #5041. [4] Righter K. et al. 2003. Abstract #1373. 34th Lunar and Planetary Science Conference. [5] Bischoff A. et al. 1993. *Geochimica et Cosmochimica Acta* 57:2631–2648. [6] Krot A. N. 2006. Personal communication.

5276

IN SITU Fe-XANES STUDY OF GRAINS TRAPPED IN AEROGEL: AN ANALYTICAL TEST FOR THE INTERPRETATION OF STARDUST SAMPLES ANALYSES

F. Grossemy¹, J. Borg¹, and A. Simonovici². ¹Institut d'Astrophysique Spatiale, CNRS, University Paris-Sud, UMR8617, Orsay Cedex, F-91405. E-mail: faustine.grossemy@ias.u-psud.fr. ²Laboratoire des Sciences de la Terre, ENS Lyon, France

Introduction: In January 2006, the Stardust mission of the NASA brought back to Earth aerogel collectors, in which grains of the comet Wild-2 as well as interstellar grains have been trapped [1]. Here we report on an experiment carried out to study the slowing down of hypervelocity particles into aerogel. Micrometer-sized grains trapped inside pieces of aerogel, a few hundreds of microns large, were analyzed. They originate either from the Orbital Debris Collection Experiment (ODCE) of the NASA exposed outside the Mir station from 1997 to 1998, or from gas gun shots in Stardust's aerogel of grains from the Allende meteorite. Micro-fluorescence mappings and XANES spectra at the iron K-edge have been performed on these samples using the X-ray Microscopy beamline ID21 at the ESRF, Grenoble (France).

Results: From the micro-fluorescence mappings, both the trapped grain and its penetration track were identified. It can be concluded from the Fe "hot spots" found along the track that the incident grain broke up into many fragments while entering and slowing down in the aerogel in spite of its very low density.

XANES spectra at the Fe K edge were then acquired in hotspot regions. For each spectrum, the energy of the absorption edge and the centroid energy of the pre-edge were used to determine the Fe redox states following [2]. The edge and the pre-edge centroid are indicative of an evolution from a Fe³⁺ form at the track entrance to a more reduced form along the track and in the final grain. Beam-induced photoreduction was checked for by acquiring several spectra on the same points and seeing no shift towards lower energies.

Discussion: Given the observed Fe redox state of the particles in the aerogel, several mechanisms can be inferred. Based on the results for the Allende sample, known to be Fe²⁺ rich [3, 4], the most probable one is the following. Incident grains of 2+ oxidation state undergo rapid oxidation to 3+ at the entrance of the track, due to high temperature slowing down from the initial velocity of a few km/s⁻¹ in the presence of the aerogel oxygen. The shell of oxidized iron is lost at the track entrance by the grain that remains in the 2+ oxidation state at the end of the track. This suggests that the final grain has the same mineralogy as the incident one, which is crucial for current and upcoming Stardust analyses.

References: [1] Tsou P. et al. 2006. Abstract #2189. 37th Lunar and Planetary Science Conference. [2] Wilke M. et al. 2001. *American Mineralogist* 86:714–730. [3] Olivier F. W. et al. 1984. *Meteoritics* 19:25–27. [4] Hoffman E. et al. 2000. *Meteoritics & Planetary Science* 35:431–434.

5283

A SPECTACULAR COMPOUND CHONDRULE-CAI IN NORTHWEST AFRICA 2918, A NEW CO_{3.1} CHONDRITE

J. N. Grossman¹, G. J. MacPherson², E. P. Vicenzi², and C. M. O'D. Alexander³. ¹U.S. Geological Survey, Reston, Virginia 20192, USA. E-mail: jgrossman@usgs.gov. ²Department of Mineral Sciences, Smithsonian Institution, Washington, D.C. 20560-0119, USA. ³Carnegie Institution of Washington, Washington, D.C. 20015-1305, USA

Introduction: Northwest Africa (NWA) 2918 was recently classified as a very primitive, type 3.0, CO chondrite [1]. Our analysis of the Cr content of ferroan olivine using the method of [2] shows a distribution very similar to that in DOM 03238 [3], lacking a prominent mode near 0.4 wt% Cr₂O₃ as in type 3.0; mean Cr₂O₃ = 0.24 ± 0.12 wt%. Both meteorites are probably type 3.1 and have experienced very light thermal metamorphism.

Optical examination of a 2 cm² thin section of NWA 2918 revealed a typical CO chondrite texture, with an abundance of small chondrules and Ca-Al-rich inclusions (CAIs). A deep blue, circular object 170 μm in diameter was conspicuous in transmitted light. This object is a CAI partially enveloped by a type I, porphyritic pyroxene (PP) chondrule. Compound objects consisting of CAIs and ferromagnesian chondrules are extremely rare [4], and this one has many unusual properties worthy of study.

Mineralogy/Petrology: The chondrule portion of the compound object is unremarkable in mineralogy. Low-Ca pyroxenes, Fs_{1.5}Wo_{1.5} are richer in refractory elements than is normal for PP chondrules (2.4% Al₂O₃, 0.4% TiO₂), and poikilitically enclose olivine (Fa₂). Abundant oxidized grains, formerly rich in Fe metal are present. Mesostasis is anorthite or anorthitic glass, richest in TiO₂ near the CAI and Na₂O away from it. Ca-rich pyroxene is also abundant.

The core of the CAI is dominantly a deep blue colored spinel that has 2.0 wt% TiO₂, 0.6 wt% Cr₂O₃, and 0.6 wt% FeO. Spinel near the rim of the CAI has 1.3 wt% TiO₂ and is nearly colorless. A pale blue spinel grain previously extracted from Murchison [5] was not rich in TiO₂. The outer portion of the CAI is mostly anorthite or anorthitic glass. Like the spinel, anorthite is high in TiO₂ near the CAI core (0.4 wt%) and has approximately half as much near the rim. Several crystals of an unidentified Ti-rich oxide phase occur in the CAI core, with 85% TiO₂, 10% MgO, and 4% Al₂O₃. Nepheline and Ca-rich pyroxene are present in the outer part of the CAI, but only on the surface away from the chondrule. Tiny metal grains rich in Fe, Ru, and Mo are also present in the CAI.

Discussion: This compound object formed by the collision of an unusual Ti-rich CAI with a molten or partially molten chondrule. The absence of perovskite is puzzling; there is no evidence that the Ti-rich oxide is secondary after perovskite. The chondrule minerals experienced chemical exchange with those in the CAI, leading to zoning and refractory enrichment. Entry of alkalis occurred after the compound object solidified, resulting in sodic plagioclase in the chondrule far from the CAI and nepheline in the CAI far from the chondrule. Isotopic studies are underway to determine the chronology of the events leading to the formation of the object as well as the origin and nature of the minerals in the strange CAI.

References: [1] Connolly H. C., Jr. et al. *Meteoritics & Planetary Science*. Forthcoming. [2] Grossman J. N. and Brearley A. J. 2005. *Meteoritics & Planetary Science* 40:87-122. [3] Grossman J. N. and Rubin A. E. 2006. Abstract #1383. 27th Lunar and Planetary Science Conference. [4] Krot A. N. et al. 2006. *The Astrophysical Journal* 639:1227-1237. [5] MacPherson G. et al. 1983. *Geochimica et Cosmochimica Acta* 47:823-839.

5103

IDENTIFICATION OF REIDITE FROM THE RIES IMPACT CRATER USING MICRORAMAN SPECTROSCOPY: A REVIEW

A. Gucsik. University of West Hungary, Bajcsy-Zs. u. 4., Sopron, Hungary. E-mail: ciklamensopron@yahoo.com

Introduction: The phase transformation from the zircon crystal structure (ZrSiO₄) to a scheelite (CaWO₄)-structure phase (reidite) was described in shock-metamorphosed zircon by Kusaba et al. [1] to begin at about 30 GPa and to be complete at around 53 GPa. These observations were confirmed by Leroux et al. [2] through their TEM investigations of experimentally shocked zircon. More recently, according to Scott et al. [3] the high-pressure X-ray data show that a small amount of residual zircon-structured material remained at 39.5 GPa. Glass et al. [4] found the scheelite-type phase in zircon samples from marine sediments from an upper Eocene impact ejecta layer sampled near New Jersey and Barbados. They named this mineral phase "reidite" after Alan F. Reid, who first produced this high shock-pressure polymorph of zircon [4]. The purpose of this investigation is to further investigate the capability of the Raman spectroscopy to document shock deformation and to determine whether specific Raman effects in zircon/scheelite-structure can be utilized to determine particular shock stages.

Experimental Procedure: Raman spectra were obtained on shocked single zircon grains from the Ries impact structure with a Renishaw RM1000 confocal microRaman spectrometer with a 20 mW, 632 nm He-Ne laser excitation system and a thermo-electrically cooled CCD detector. The power of laser beam on sample was approximately 3 mW. Spectra were obtained in the range 100-1200 cm⁻¹ with approximately thirty seconds total exposure time. The spectral resolution (apparatus function) was 4 cm⁻¹.

Results and Discussion: The Raman spectra of the naturally shock-deformed zircon samples from the Ries crater (Stage II: 35-45 GPa, Stage III: 45-50 GPa, Stage IV: >50 GPa) cut parallel and perpendicular to their crystallographic c-axis do not exhibit significant differences from each other. Stage II samples are characterized by five peaks at 224, 356, 439, 974, and 1007 cm⁻¹. Addition Raman spectrum of the Stage III (45-50 GPa) sample (parallel) shows eleven peaks at 202, 224, 327, 356, 404, 439, 465, 558, 845, 974 and 1007 cm⁻¹, which indicate the presence of the scheelite-type phase among predominant zircon-type material. In general, the fluorescence background in the parallel-sample is considerably higher than in the perpendicular-sample. In both cases, the peak intensities are similar. The spectra of the Stage IV samples (parallel- and perpendicular-samples) are characterized by seven peaks at 202, 215, 225, 356, 439, 974, and 1007 cm⁻¹.

Conclusion: Raman spectroscopy is a potentially useful tool that can be used to characterize the shock stages of zircon from impactites. These results also give new insight into the structural changes that occur in zircons during shock metamorphism, and the pressures associated with these changes.

Acknowledgements: This work has been partly supported by Hungarian Space Office (TP-293).

References: [1] Kusaba K. et al. 1985. *Earth and Planetary Science Letters* 72:433-439. [2] Leroux H. et al. 1999. *Earth and Planetary Science Letters* 169:291-301. [3] Scott H. P. et al. 2002. *Physical Review Letters* 88: 015506-1-015506-4. [4] Glass B. P. et al. 2002. *American Mineralogist* 87: 562-565.

5099

THE HIGH-ENERGY VIEW OF STAR FORMATION

M. Güdel, Paul Scherrer Institut, Würenlingen and Villigen, CH-5232 Villigen PSI, Switzerland. E-mail: guedel@astro.phys.ethz.ch

Although stars form in very cold, molecular environments, observations with X-ray satellites reveal stellar environments rich in high-energy radiation (X-rays). X-ray luminosities up to four orders of magnitude above solar levels are common in protostars and T Tauri stars. Most of this emission is thought to originate from heated plasma trapped in a corona or magnetosphere around the stars, although alternative X-ray generation mechanisms have been proposed, such as shock-heating in accretion columns [1] or shocks in outflows and jets [2, 3]. It is likely that X-ray emission is, like in the case of the Sun, accompanied by high-energy particle streams ejected in particular during magnetic energy release events. Non-thermal radio emission has indeed provided spectacular evidence for the presence of relativistic electrons around some systems.

High-energy radiation and particle beams have a profound impact on the stellar environment, in particular on circumstellar disks in which planets eventually form. They heat disk surfaces, partly ionize the disk gas, and induce chemistry at various locations in the stellar environment (e.g., [4]).

Furthermore, high-energy, ionizing radiation is important in the process of planet formation and the buildup of planetary atmospheres. This may be of particular relevance to our understanding of the early evolution of the inner planets in our solar system [5].

This presentation will summarize selected aspects of high-energy emission and magnetic fields around young, forming stars, addressing i) the origin and characteristics of high-energy radiation and particles around forming stars, ii) the role of magnetic fields around young stars, iii) the potential impact of high-energy radiation (+particles) on the stellar environment, and iv) evidence for a violent environment of the young Sun.

References: [1] Kastner J. H. et al. 2002. *The Astrophysical Journal* 567:434. [2] Bally J. et al. 2003. *The Astrophysical Journal* 584:843. [3] Güdel M. et al. 2005. *The Astrophysical Journal* 626:L53. [4] Glassgold A. E. et al. 2004. *The Astrophysical Journal* 615:972. [5] Ribas I. et al. 2005. *The Astrophysical Journal* 622:680.

5223

WATER IN BENCUBBIN

N. Guilhaumou¹, C. Fiéni¹, C. Perron¹, B. Ghazharova², and Y.-L. Mathis². ¹Museum National d'Histoire Naturelle, 75005 Paris, France. E-mail: guilhau@mnhn.fr. ²Institute for Synchrotron Radiation, 76021 Karlsruhe, Germany

Introduction: The origin of Bencubbin and its few siblings (hereafter CB chondrites) is still controversial, and we have no clear explanation for some of their most intriguing properties. CB chondrites have suffered at least one shock event in their parent body, as testified by the metal-silicate melt that fills all spaces between large grains. In Bencubbin, vesicles containing ¹⁵N-rich nitrogen gas were found in glassy phases [1, 2]. We have extended this work and find that water also is present in the vesicles, in the phases in which these are set, and in the impact melt.

Experimental: Self-supporting, doubly-polished sections, 70–140 μm thick, were prepared in anhydrous conditions from the MNHN Bencubbin specimen. They were studied by micro-infrared spectroscopy, using the synchrotron source at the ANKA facility, Karlsruhe. The phases studied include the silicate portion of the impact melt and phases in which bubbles were observed, namely the mesostasis in large silicate grains and the chondrule mesostasis in an ordinary chondrite (OC) inclusion.

Results: Water was detected in bubbles both in the mesostasis in the host and in the chondrule mesostasis in the OC inclusion, by means of the two bands of the bending and stretching modes of molecular H₂O, respectively centered at 1634 and 3567 cm⁻¹. It was also detected in the two bubble-bearing mesostases themselves and in the silicate portion of the impact melt. Slight differences in the shape and position of the band of the stretching mode, and maps of IR absorbance in the range 3200–3600 cm⁻¹ allowed us to distinguish water vapor in the bubbles from water in the glassy phases.

The water content of the glasses was estimated by comparison with glasses of known water contents. It varies from 2500 to 4500 ppm, with no significant differences between the different phases studied. The main uncertainty on these values results from the uncertainty on the thickness of the studied phases, taken as one half that of the thin section. In the host mesostasis bubbles are present only in some parts. In the parts with no bubbles that we studied, water was below detection limit (i.e., <100 ppm).

Discussion: Our interpretation is that water (and ¹⁵N-rich nitrogen) was degassed during a shock event in the Bencubbin parent body. At the same time, in addition to the impact melt, some phases with low melting temperatures (mesostasis in the host, mesostasis of chondrules in the OC inclusion) were also partially melted, at least in the part of Bencubbin we studied. Water (and N₂) dissolved in the liquids, then partially degassed when pressure and temperature decreased, leading to the formation of vesicles. Where did water come from? Hydrated matrix lumps have been observed in some CB chondrites and in the related CH chondrites [3]. It has been suggested that this sort of material was the precursor of the impact melt [4]. Our findings support this hypothesis and suggest that this hydrated matrix was initially abundant in Bencubbin.

References: [1] Marty B. et al. 2000. Abstract #1489. 31st Lunar and Planetary Science Conference. [2] Perron C. et al. 2001. Abstract. *Meteoritics & Planetary Science* 36:A160. [3] Greshake A. et al. 2002. *Meteoritics & Planetary Science* 37:281–293. [4] Meibom A. et al. 2005. *Meteoritics & Planetary Science* 40:1377–1391.

5124

EXPERIMENTS ON CHONDRULE FORMATION BY "LIGHTNING"

C. Güttler¹, T. Poppe¹, J. Blum¹, T. Springborn¹, and J. Wasson². ¹Institut für Geophysik und extraterrestrische Physik, Technische Universität Braunschweig, Mendelssohnstr. 3, 38106 Braunschweig, Germany. E-mail: C.Guettler@TU-Braunschweig.de. ²Institute for Geophysics and Planetary Physics, University of California, 405 Hilgard Avenue, Los Angeles, California 90095-1567, USA

Introduction: Chondrules are generally assumed to have formed in the early solar system from macroscopic dust agglomerates largely composed of micrometer-sized grains. One hypothesis concerning the heating mechanism assumes that electrical discharges in the solar nebula transformed the dust into melt spherules. There is one single experiment reported [1], in which ground meteoritic material was exposed to a 5 kJ discharge. Most material was dispersed, some spherules up to 200 μm in diameter were found, which, unlike meteoritic chondrules, were porous.

We are presently conducting an experimental study to tackle the question whether and under which conditions a discharge can transform a sample of micrometer-sized grains into chondrule-like spherules. Thus we exposed samples of silica, iron, fayalite, albite and peridot agglomerates of micrometer-sized dust grains to a 500 J electric discharge between two electrodes of 3 mm distance. The ambient air pressure was between 0.1 mbar and atmospheric pressure. The objects are analyzed by optical microscopy and with scanning electron microscopy.

First Results: Largely independent of the nature of the sample and the gas pressure, the dust was instantly dispersed by the discharge, but a small part was thermally processed. Together with unprocessed dust, we found different types of large objects, among them spherules, depending on the material: iron built many hollow spheres of all sizes up to 300 μm in diameter, whereas fayalite formed only a few spherules of about 50 μm in diameter and clusters of sizes up to 200 μm consisting of crystals and original grains. Similar clusters were also found with albite, peridot and silica precursors, which formed no spherules. A few typical spherules were embedded in epoxy resin for sectioning. Under the microscope, they revealed bubbles to a varying extent (fayalite) or were even completely hollow (iron). The fraction of material converted into spherules was in general extremely low. Assuming that 2 kJ/kg is necessary for melting [2], the energetic efficiency (energy for melting/electrical energy) of lightning heating is less than 10^{-5} .

Summary: We transformed dust agglomerates of micrometer-sized grains into spherules containing molten material by a gas discharge. The spherules are quite small, although some are of chondrule size. However, in contrast to chondrules, the spherules had bubbles or even were hollow. Also, the energetic efficiency of our discharge heating is extremely low. Extrapolating to solar nebular conditions, chondrule formation by lightning is inconsistent with any reasonable assumptions on the energy of possible nebular lightning strokes, although it is an open issue whether the energetic efficiency might be higher under different conditions, e.g., a different linear scale.

References: [1] Wdowiak T. J. 1983. In *Chondrules and their origins*. p. 279–283. [2] Wasson J. T. 1996. In *Chondrules and the protoplanetary disk*. p. 45–54.

5334

TITANIUM ISOTOPIC RATIOS IN KJG PRESOLAR SiC GRAINS FROM MURCHISON

F. Gyngard¹, S. Amari¹, M. Jadhav¹, K. Marhas¹, E. Zinner¹, and R. S. Lewis². ¹Laboratory for Space Sciences and Department of Physics, Washington University, Saint Louis, Missouri 63130, USA. E-mail: fmgyngar@wustl.edu. ²Enrico Fermi Institute, University of Chicago, Chicago, Illinois 60637, USA

Introduction: Thousands of individual presolar SiC grains have been measured for their C and Si isotopic compositions [1–3]. Despite the fact that Ti is one of the most abundant trace elements in SiC, only approximately 110 SiC grains have had their Ti isotopic compositions determined [1, 4–7], but most analyses suffer from selection effects. Specifically, the Ti data for mainstream SiC, thought to have formed in the outflows of low-mass (1–3 M_{\odot}) C-rich asymptotic giant branch (AGB) stars [8], have not been obtained from a representative sample of the larger population. The grains analyzed have been chosen either for their high Ti concentrations [4] or their large ²⁹Si and ³⁰Si excesses [1]. To rectify this situation, we report here the Ti isotopic composition of 75 of the 247 SiC grains we have randomly selected for these measurements.

Experimental: Energy Dispersive X-ray (EDX) analysis was performed on grains from a Murchison KJG separate (diameter 2–4.5 μm) [9] dispersed on gold foil. After identification as SiC, 247 grains of size roughly $\geq 2.5 \mu\text{m}$ were randomly selected for isotopic measurement in the Washington University NanoSIMS, with this lower limit on grain size in place only to ensure suitably precise Ti results. Carbon, N, and Si isotopic ratios were measured first and the Ti isotopes for 75 of the grains measured afterwards by a combination of peak jumping and multidetection. Signals from ⁴⁴Ca, ⁵¹V, ⁵²Cr, and ⁵³Cr were also monitored in order to correct for Ca interferences at masses 46 and 48 and Cr and V interferences at mass 50.

Results: The $\delta^{46,47,49,50}\text{Ti}/^{48}\text{Ti}$ values measured cover a range comparable to what has been seen previously [1, 4], and plot along correlation lines in Ti 3-isotope plots. The data also exhibit a linear correlation between Si and Ti isotopic ratios, similar to what has been previously observed, indicative of a galactic chemical evolution component in the grains' Si and Ti compositions [10–12]. Hoppe et al. [1] observed that Ti in SiC is usually characterized by enrichments in the minor isotopes relative to ⁴⁸Ti, resulting in a V-shaped pattern; here, we have found that roughly 40% of the grains measured so far exhibit this pattern, while about 55% have irregular patterns and the rest (5%) have an inverted pattern. The grains of this study can be grouped into three broad categories based on the Ti concentration as a function of depth: those with very negligible amounts of Ti, virtually at the limit of sensitivity ($\sim 10\%$); those with relatively uniform Ti concentration ($\sim 40\%$); and those with marked variation—often orders of magnitude changes—in Ti concentration, likely due to the presence of Ti subgrains ($\sim 50\%$).

References: [1] Hoppe P. et al. 1994. *The Astrophysical Journal* 430: 870–890. [2] Hoppe P. et al. 1996. *Geochimica et Cosmochimica Acta* 60: 883–907. [3] Nittler L. R. and Alexander C. M. O'D. 2003. *Geochimica et Cosmochimica Acta* 67:4961–4980. [4] Alexander C. M. O'D. and Nittler L. R. 1999. *The Astrophysical Journal* 519:222–235. [5] Amari S. et al. 2001. *The Astrophysical Journal* 546:463–483. [6] Amari S. et al. 2001. *The Astrophysical Journal* 559:248–266. [7] Zinner E. et al. 2005. Abstract #1691. 36th Lunar and Planetary Science Conference. [8] Hoppe P. and Ott U. 1997. In *Astrophysical Implications of the Laboratory Study of Presolar Material*. New York: American Institute of Physics. pp. 27–58. [9] Amari S. et al. 1994. *Geochimica et Cosmochimica Acta* 58:459–470. [10] Lugaro M. et al. 1999. *The Astrophysical Journal* 527:369–394. [11] Lugaro M. and Gallino R. 2001. Abstract. *Meteoritics & Planetary Science* 36:A118. [12] Nittler L. R. 2005. *The Astrophysical Journal* 618:281–296.

5199

FROM SIZE SORTING OF CHONDRULES TO ACCRETION OF PARENT BODIES—THE EFFECTS OF PHOTOPHORESIS

H. Haack¹, O. Krauss², and G. Wurm². ¹Natural History Museum of Denmark, Øster Voldgade 5-7, DK-1350 Copenhagen K, Denmark. E-mail: hh@snm.ku.dk. ²Institute for Planetology, Wilhelm-Klemm-Str 10, D48149 Münster, Germany

Introduction: Recent evidence based on ²⁶Al chronology suggest that the differentiated asteroids accreted ~0.7 Myr after CAI formation, while chondrules were still forming in the nebula [1]. Chondrules appear to have been size-sorted prior to accretion [2], suggesting that physical processes allowed rapid accretion of some asteroids while components of other asteroids formed and were being size-sorted at the same time. Observations of asteroids and theoretical models suggest that the differentiated asteroids formed closer to the Sun than primitive asteroids, possibly in the terrestrial planet forming region [3]. We believe that several of these observations could be attributed to photophoresis, which have recently been shown to be of significance while gas and dust coexisted in the solar nebula [4].

Chondrule and CAI-Based Constraints: Several clues to the sorting and concentration processes come from the observations of chondrules and CAIs in chondrites. 1) Chondrules are better sorted than CAIs [5]. If the sorting process was operating on a small scale we should expect that all of the locally available components were equally well sorted. We thus infer that the sorting process was operating on a large scale. 2) Chondrules are common in all types of equilibrated chondrites whereas CAIs are only common in carbonaceous chondrites, 3) CAIs apparently formed close to the Sun but are mainly found in carbonaceous chondrites believed to originate in the outer part of the asteroid belt. 4) Differences in oxygen isotope signatures show that the source regions for ordinary, enstatite, and carbonaceous chondrites were separated from each other in space and/or time.

Photophoresis and Size Sorting in the Nebula: We suggest that photophoresis could have two significant effects on the particle motion in the solar nebula. In the early stages while the nebula was still optically thick photophoresis would help concentrate particles at the inner edge of the disk leading to enhanced accretion rates here [6]. As the nebula became optically thin photophoresis pushed chondrules and CAIs out to the point where inward motion caused by gas drag is balanced by the outward motion caused by photophoresis and radiation pressure. The particles will drift toward the radial distance where the forces balance and since the photophoresis is a size dependent force, different size ranges of chondrules and CAIs will accumulate and subsequently accrete at different heliocentric distances. As the gas gets thinner and thinner the accumulation point will move inward [7]. The first chondritic bodies will therefore accrete in the outer parts of the belt and probably include the majority of the remaining CAIs. As the accumulation point moves inward, later generations of chondrules will be incorporated in chondrite parent bodies largely devoid of CAIs, in the inner part of the asteroid belt.

References: [1] Bizzarro M. et al. 2005. *The Astrophysical Journal* 632:L41–L44. [2] Kuebler K. E. et al. 1999. *Icarus* 141:96–106. [3] Bottke W. F. et al. 2006. *Nature* 439:821–824. [4] Wurm G. and Krauss O. 2006. *Icarus* 180:487–495. [5] May C. et al. 1999. Abstract #1688. 30th Lunar and Planetary Science Conference. [6] Wurm G. et al. 2006. *Meteoritics & Planetary Science* 41. This issue. [7] Petit J.-M. et al. 2006. Abstract #1558. 37th Lunar and Planetary Science Conference.

5314

MASS-FRACTIONATION INDUCED BY THE GENESIS SOLAR WIND CONCENTRATOR: ANALYSIS OF NEON ISOTOPES BY UV LASER ABLATION

V. S. Heber¹, R. C. Wiens², C. Olinger², D. S. Burnett³, H. Baur¹, U. Wiechert⁴, and R. Wieler¹. ¹Isotope Geology, NW C85, ETH, CH-8092 Zürich, Switzerland. E-mail: heber@erdw.ethz.ch. ²LANL, Space and Atmospheric Science, Los Alamos, New Mexico 87544, USA. ³CalTech, JPL, Pasadena, California 91109, USA. ⁴AG Geochemie, FU Berlin, 12249 Berlin, Germany

The solar wind (SW) concentrator, a key instrument onboard the Genesis mission, was designed to provide larger fluences of implanted SW for precise isotope analyses of oxygen and nitrogen [1]. SW ions in the mass range 4–28 amu were accelerated and focused on a “concentrator target” by an electrostatic mirror. This concentration process caused some instrumental mass fractionation of the implanted SW ions as function of the radial position on the target. Correction of this fractionation will be based on a combination of the measured radial fractionation of Ne isotopes with results of simulations of the implantation process using the actual performance of the concentrator and the SW conditions during exposure. Here we present He and Ne abundance and Ne isotopic composition data along one arm of the gold cross that framed the 4 concentrator subtargets.

He and Ne were released from pits ~120 µm in diameter by UV laser ablation using a 248 nm Eximer laser [2]. In the first 34 analyses, He and Ne were analyzed together at constant analytical conditions. In a second set of 16 analyses, He and Ne were separated to protect the mass spectrometer from solar ³He. In total, 12 positions along the arm (30 mm long) were analyzed, each with 1 to 6 single analyses. He and Ne abundances increase from the edge (at 30 mm) towards the center of the concentrator cross, He from 5.3E+15 ions/cm² (at 20.5 mm) to 1.8E+16 ions/cm² (at 2.9 mm) and Ne from 3.5E+12 ions/cm² (at 29.4 mm) to 3.4E+13 ions/cm² (at 1 mm). Thus, the concentration factor increases by about a factor of 10, similar to expected values from post-flight models for oxygen. Applying a simplified backscatter correction measured and expected Ne abundances agree within 20%. The measured Ne isotopes show a large mass fractionation as function of the target radius. The ²²Ne values (relative to SW ²⁰Ne/²²Ne of 13.75, [3]) range from –19‰ (at 26 mm) to +40‰ (at 2.9 mm), reflecting a preferential implantation of the heavier isotopes towards the center of the concentrator target. Precision of the ²⁰Ne/²²Ne ratios, expressed as error of the mean, is on average 4‰ (2σ) for the analyses in which He and Ne were not separated. More work is needed to reduce the considerably larger scatter observed so far in the analyses where He and Ne were separated. The obtained Ne isotope fractionation curve resembles, in shape and extent of fractionation, the post-flight modeled δ¹⁸O curve. The two curves are offset by about 10%. This is probably to be explained by the missing backscatter correction for the measured Ne isotopes. At the conference we will compare measured Ne data with simulated results of Ne implantation at SW conditions prevalent during Genesis collection period.

References: [1] Wiens R. C. et al. 2003. *Space Science Reviews* 105: 601–625. [2] Heber V. S. et al. 2006. Abstract #2175. 37th Lunar and Planetary Science Conference. [3] Grimberg A. et al. 2006. Abstract #1782. 37th Lunar and Planetary Science Conference.

5054

RARE PRESOLAR SILICON CARBIDE GRAINS FROM NOVAE: AN AUTOMATED SEARCH BY NANOSIMS

Ph. R. Heck¹, P. Hoppe¹, E. Gröner¹, K. K. Marhas^{1, 2}, H. Baur³, and R. Wieler³. ¹MPI für Chemie, Partikelchemie, Becherweg 27, D-55128 Mainz, Germany. E-mail: heck@mpch-mainz.mpg.de. ²Washington University, CB 1105, 1, Brookings Dr., Saint Louis, Missouri 63130-4899, USA. ³ETH Zürich, Isotopengeologie, NW C84, CH-8092 Zürich, Switzerland

Introduction: The very rare nova grains were traditionally attributed to condense in the ejecta of ONe novae, based on the qualitative agreement of their isotopic composition with models [1, 2]. However, we recently reported grain data, which are qualitatively consistent with CO nova model predictions [3]. Another recent study of putative nova grains found supernova-only-produced nuclides and hereby excluding a nova origin [4].

Our main goal is to examine the general validity of these findings by applying an automated grain search and analysis technique on a large number of presolar SiC with the NanoSIMS ion microprobe combined with noble gas analyses. C and N isotopes are used to identify nova grain candidates, while Ne-isotopes can be used to discern between CO and ONe nova grains. The presence of radiogenic supernova isotopes would exclude a nova origin. At the conference, we will present results of this ongoing study of so far 1089 analyzed presolar SiC grains.

Samples and Experimental: Using a standard procedure [5] SiC was extracted from Murchison. The sample preparations and NanoSIMS setup is described elsewhere [3]. Our automated procedure [3, 6] primarily consists of the following steps: presputtering to remove surface contamination, raster image (50 × 50 μm²) acquisition, particle recognition, single grain analysis. Grains of interest will be analyzed manually for radiogenic supernova isotopes and/or He and Ne isotopes. SiC from Murchison and Murray from our first study [7] are also included in the data set.

Results: We have found 979 SiC grains from a total of more than 1000 automatically recognized particles. The ¹²C/¹³C and the ¹⁴N/¹⁵N ratios span the range from 3.7 to 420 and from 26 to 1400, respectively. We classify 19 grains as type A/B, 3 of them having very low ¹²C/¹³C ratios (<5). Our manual study of 110 presolar SiC grains revealed 5 A/B type grains, with 1 grain having a ¹²C/¹³C ratio < 5. This gives us 4 out of 1089 grains with particularly low ¹²C/¹³C ratios, which have ¹⁴N/¹⁵N ratios > 200.

Discussion and Conclusion: The C- and N-isotopic compositions of these 4 grains are qualitatively consistent with a CO nova model prediction. For grain SiC070 also the Ne- and Si-isotopic compositions agree qualitatively with this prediction. The analysis of Ne, Mg, and Ca isotopes will be diagnostic for the determination of the stellar sources of the grains.

The study of a large number of presolar SiC with our automated search and analyses technique turned out to be efficient. We are confident to discover more nova grain candidates and elucidate their true origin.

Acknowledgements: We thank A. Besmehn, S. Merchel, and U. Ott for preparing the Murchison residue, and J. Huth for his help with the SEM.

References: [1] Amari S. et al. 2001. *The Astrophysical Journal* 551: 1065. [2] José et al. 2004. *The Astrophysical Journal* 612:414. [3] Heck P. R. et al. 2006. Abstract #1355. 37th Lunar and Planetary Science Conference. [4] Nittler L. R. and Hoppe P. 2005. *The Astrophysical Journal* 631:L89. [5] Besmehn A. and Hoppe P. 2003. *Geochimica et Cosmochimica Acta* 67: 4693. [6] Gröner E. and Hoppe P. 2006. SIMS 15. Forthcoming. [7] Heck P. R. et al. 2005. Abstract #1938. 36th Lunar and Planetary Science Conference.

5055

SOLAR NOBLE GASES IN 470 Myr OLD FOSSIL MICROMETEORITES

Ph. R. Heck^{1, 2}, B. Schmitz³, H. Baur², and R. Wieler². ¹Max-Planck Institut für Chemie, Partikelchemie, Becherweg 27, D-55128 Mainz, Germany. E-mail: heck@mpch-mainz.mpg.de. ²ETH Zürich, Isotopengeologie, NW C84, CH-8092 Zürich, Switzerland. ³University of Lund, Department of Geology, Sölvegatan 12, SE-22362 Lund, Sweden

Introduction: A large abundance of fossil meteorites [1] and sediment-dispersed extraterrestrial chromite grains (SEC grains) [2] have been found in ~470 Myr old marine sediments [3] in quarries in southern Sweden. Cosmic-ray exposure ages of the fossil meteorites are very short (~0.1–1 Myr) and increase in younger sediments [4]. The breakup of the L-chondrite parent body is thought to be responsible to have caused the high concentration of extraterrestrial matter [1–6]. Since SEC grains are less difficult to find than the fossil meteorites [2, 6], our main motivation was to try to determine the exposure ages of the grains.

Samples and Experimental: The chromites were extracted from large (10–30 kg) limestone samples with acids, yielding up to a maximum of ~3 grains per kg of rock [2]. Grains were hand-picked and identified as extraterrestrial with SEM/EDS (L/LL chondrite composition). Batches of 4–6 chromite grains were weighted (4–8 μg ± 10%) and noble gases were extracted with an IR laser and analyzed in an ultra-high sensitivity mass-spectrometer equipped with a compressor ion source [7].

Results and Discussion: The SEC grains contain very high concentrations (⁴He: 1.4–9.4 10⁻³ cm³/g; ²²Ne: 4.9–17 10⁻⁶ cm³/g) of trapped He and Ne. Therefore, the determination of cosmic ray-exposure ages as done for the fossil meteorites [4] was not possible. However, the trapped gases provide clues about the nature of SEC grains. The He- and Ne-isotopic composition of the SEC grains is consistent with solar composition, and noble gas data from stratospheric IDPs [8] and recently fallen micrometeorites [9]. This strongly suggests that also the SEC grains were IDPs and came to Earth as micrometeorites. As we find solar noble gases in all SEC grains from different sediment beds, it is highly unlikely that the grains are fragments of regolith breccias, since only a few percent of all L and LL chondrites are regolith breccias [10]. Model calculations predict that large collisions in the asteroid belt produce so much dust, that the influx of material on Earth increases by two orders of magnitude [11]. Using a simple estimate of the dynamical lifetime (t) of dust based on P-R-drag [12] we estimate t = 0.6 to 1 Myr for 100 μm chromite grains. This is consistent with the delivery times of the fossil meteorites in the same sediment beds [4].

Acknowledgements: We thank B. Bottke for helpful discussions and M. Tassinari for participation in the fossil meteorite search. This project has been partly funded by ETH Zürich. Field work was funded by the National Geographic Society.

References: [1] Schmitz B. et al. 2001. *Earth and Planetary Science Letters* 194:1–2. [2] Schmitz B. et al. 2003. *Science* 300:961–964. [3] Trierloff M. et al. 2006. ESA Special Publication #612. [4] Heck P. R. et al. 2004. *Nature* 430:323–325. [5] Heck P. R. 2005. Ph. D. thesis, ETH Zürich, Zürich, Switzerland. [6] Schmitz B. and Häggström T. 2006. *Meteoritics & Planetary Science* 41:455–466. [7] Baur H. 1999. *EOS* 46:F1118. [8] Nier A. O. and Schlutter D. J. 1990. *Meteoritics* 25:263–267. [9] Olinger C. T. et al. 1990. *Earth and Planetary Science Letters* 100:77–93. [10] Bischoff A. and Schultz L. 2004. *Meteoritics & Planetary Science* 39:5118. [11] Dermott et al. 2000. In *Asteroids III*. pp. 423–442. [12] Burns et al. 1979. *Icarus* 40:1–48.

5027

AN OCCURRENCE OF JAROSITE IN MIL 03346: IMPLICATIONS FOR CONDITIONS OF MARTIAN AQUEOUS ALTERATION

C. D. K. Herd. Department of Earth and Atmospheric Sciences, University of Alberta, Edmonton, Alberta, Canada. E-mail: herd@ualberta.ca

Introduction: Knowledge of the geochemical behavior of K, U, and Th is essential in the application of natural gamma-ray spectrometry techniques to Mars exploration. Whereas K, U, and Th are expected to behave incompatibly during igneous crystallization, it is difficult to predict whether aqueous alteration will cause fractionation, as it depends on a number of variables such as pH, T, water/rock ratio, etc. This study examines the distribution of K, U, and Th between igneous and aqueous alteration phases within a Martian meteorite to gain insights into the geochemical behavior of these elements under Martian conditions.

Techniques: Polished thin sections of MIL 03346 (.93 and .165) from the Antarctic Meteorite Collection were examined using optical, electron microprobe and Synchrotron X-ray methods. A JEOL JXA-8900 electron microprobe (EMP) was used for quantitative (WDS) analysis and X-ray mapping of Fe, Si, S, Al, and K using a spot size of 1 μm . Synchrotron X-ray microprobe mapping failed to detect U and Th, although the technique yielded maps of K, Rb, Sr, Zn, Zr and Fe with an $\sim 4 \mu\text{m}$ spot size.

Results: Iddingsite alteration in olivine, typical for the nakhlites [1], was identified near the edge of an olivine phenocryst and within skeletal olivine in the mesostasis. In both cases, K, S, and Fe are enriched and Si is depleted along fractures and grain boundaries associated with the alteration. Preliminary EMP analysis of this material gives $\sim 5 \text{ wt\% K}_2\text{O}$, $1 \text{ wt\% Na}_2\text{O}$, $2 \text{ wt\% Al}_2\text{O}_3$, 26 wt\% SO_3 , $50 \text{ wt\% Fe}_2\text{O}_3$ and a low total consistent with the presence of OH. Reduction results in a formula broadly consistent with jarosite, $\text{KFe}_3(\text{SO}_4)_2(\text{OH})_6$.

Discussion: Jarosite has been identified on the Martian surface by the Mars Exploration Rover instrument package [2]. Its presence constrains the conditions under which aqueous alteration occurred: jarosite forms in a highly oxidized, acidic ($\text{pH} < 4$) environment [3]. Notably, the jarosite-rich alteration crosscuts the more typical iddingsite alteration, which presumably formed under more neutral conditions. These relationships suggest that the conditions of aqueous alteration changed from neutral to acidic as the hydrothermal system evolved.

Acidic conditions of aqueous alteration favor the mobilization of Th [4]; on this basis the alteration products should have a higher K/Th than the igneous minerals. The crystal structure of jarosite is likely to exclude U and Th [3], and the jarosite in MIL 03346 should therefore have a higher K/U ratio than the igneous minerals. Work is underway to test these hypotheses.

Acknowledgements: This study is funded by a Canadian Space Agency contract to MDA Space Missions as part of a Mars Borehole Gamma Ray Spectrometer Concept Study.

References: [1] Treiman A. H. 2005. *Chemie der Erde* 65:203–270. [2] Klingelhofer G. et al. 2004. *Science* 306:1740–1745. [3] Papike J. J. et al. 2006. *Geochimica et Cosmochimica Acta* 70:1309–1321. [4] Fanghaenel Th. and Neck V. 2002. *Pure & Applied Chemistry* 74:1895–1907.

5362

SOME METHODS TO SYSTEMATICALLY DOCUMENT THE COMPONENTS OF CHONDRITES

R. K. Herd, P. A. Hunt, and K. E. Venance. Geological Survey of Canada, Natural Resources Canada, 601 Booth Street, Ottawa, Ontario K1A 0E8, Canada. E-mail: herd@nrcan.gc.ca; pahunt@nrcan.gc.ca; kvenance@nrcan.gc.ca

Introduction: We have recently studied and discussed the textures and mineralogy of recrystallized ordinary chondrites, a carbonaceous chondrite, and primitive ordinary chondrites. We have proposed an atlas of chondrule textures [1, 2], to stimulate community interest in the textures of all meteorites and in what they reveal. We here present a framework for precisely locating features within any sample, and we outline an approach to systematically documenting the components of chondrites and their textures, in order to interpret their petrogenesis more rigorously.

Framework for Locations: An adaptation of a common and simple means of locating areas of interest in prepared thin sections of rocks is recommended. The lower left-hand corner of a section, photo, or field of view becomes the origin, allowing a cm-, mm-, or μm -scale grid to be superimposed on the whole area. Positions of objects or areas of interest can be noted in (x, y) coordinates. During scanning electron microscope or electron microprobe studies, the positions of analytical points can be noted within detailed grids related to less detailed ones. For “mapping,” e.g., of backscattered electron photomosaics, the positions of all components selected for more detailed imaging and analysis can be recorded, along with their dimensions, and their areas can be calculated. The availability of easily reproducible digital images means that basic documentation of this kind should be the first step in examining any prepared materials. The location of objects in 3-D within samples can be recorded using an additional coordinate (z), representing e.g., the position of a slice of a sample. Thus coordinates (1, 1, 1) represent an area of interest within a slice 1 cm. from the end of a sample, and 1 cm. from the origin along each axis in the prepared section. The equivalent position in mm. is (10, 10, 10), and in μm . (10000, 10000, 10000).

Systematic Documentation: The above framework allows us to “leave a trail.” Chondrites of all kinds are complex, and analogous to variably melted and recrystallized agglomerations of igneous, sedimentary and metamorphic Earth rocks, each component of which may represent an early Solar System process. We recommend the following: 1) identify lithologies within the section(s) and record their nature, dimensions and position within a grid; 2) treat each lithology as a separate entity, and for each record its components; 3) record the components’ size range, modality and primary aspects, e.g., for chondrules, size range and average size, whether certain sizes are predominant, and whether they are rounded, multiple, zoned, fragmental or partial; 4) record the nature of the matrix, and the fusion crust if present (treat as a derivative lithology); 5) use a grid to estimate the percentages of components and matrix; 6) examine e.g., intrachondrule textures, and contained phases; 7) divide e.g., chondrules into petrographic types, based on contained phases and their textures, presence/absence of mesostasis, and detailed examination of any reaction textures preserved; 8) interpret the textures as results of processes that may have formed or altered the chondrules and other components; 9) test interpretations with appropriate analyses; 10) preserve all data.

References: [1] Herd R. K. et al. 2005a. Abstract #2241. 36th Lunar and Planetary Science Conference. [2] Herd R. K. et al. 2005b. Abstract. *Meteoritics & Planetary Science* 40:A65.

5374

HISTORY OF METAL VEINS IN ACAPULCOITE-LODRANITE CLAN METEORITE GRA 95209

J. S. Herrin¹, D. W. Mittlefehldt¹, and M. Humayun². ¹NASA Johnson Space Center, Houston, Texas 77058, USA. E-mail: jason.s.herrin1@jsc.nasa.gov. ²National High Magnetic Field Laboratory and Department of Geological Sciences, Florida State University, Tallahassee, Florida 32306, USA

Graves Nunataks (GRA) 95209 has been hailed as the “missing link” of core formation processes in the acapulcoite-lodranite parent asteroid because of the presence of a complex cm-scale metal vein network. Because the apparent liquid temperature of the metal vein (~1500 °C) is higher than inferred for the metamorphic grade of the meteorite, questions regarding the vein’s original composition, temperature, and mechanism of emplacement have arisen [1, 2]. We have determined trace siderophile element compositions of metals in veins and surrounding matrix in an effort to clarify matters.

We analyzed metals in GRA 95209 in a portion of thick metal vein and adjacent metal-rich (30–40 modal%), sulfide-poor (<1%) matrix by EPMA and LA-ICP-MS for major and trace siderophile elements using methods described by [3]. We also examined metals from a metal-poor (~15 modal%) and relatively sulfide-rich (2–5 modal%) region of the sample.

Kamacite is the dominant metal phase in all portions of the sample. In comparison to matrix metal, vein metal contains more schreibersite and less tetraenaite, and is less commonly associated with Fe,Mn,Mg-bearing phosphates and graphite [2, 4]. Vein kamacite contains higher Co, P, and Cr and lower Cu and Ge. These minor variations aside, all metal types in GRA 95209 are fairly homogeneous in terms of their levels of enrichment of compatible siderophile elements (e.g., Pt, Ir, Os) relative to incompatible siderophile elements (e.g., As, Pd, Au), consistent with the loss of metal-sulfide partial melt that characterizes much of the clan. Whatever compositional differences between matrix and vein metal that may have originally existed, they have since largely coequilibrated to similar restitic trace element compositions.

We agree with [2] that metal veins, in their present state, do not represent a liquid composition. The original vein liquid was much more S-rich and emplaced at correspondingly lower liquid temperatures. Much of the Fe,Ni component solidified in cm-scale conduits while S-rich melts were expelled and continued to migrate by percolation. The higher troilite content in metal-poor regions of the sample results mostly from trapping of a small portion of these melts. The troilite is not remnant primary sulfide.

Strong depletions of W, Mo, and especially Ga (>50%, >60%, and >90% depletion, respectively) in metals of the metal-poor GRA 95209 lithology are localized at scales of 10–100 μm in the vicinity of graphite spherules. These depletions must have occurred below the temperatures at which cm-scale equilibration occurred, and future work will seek to determine their cause.

References: [1] Mittlefehldt D. W. and Lindstrom M. M. 1998. Abstract. *Meteoritics & Planetary Science* 33:A111. [2] McCoy T. J. et al. 2006. *Geochimica et Cosmochimica Acta* 70:516–531. [3] Campbell A. J. et al. 2002. *Geochimica et Cosmochimica Acta* 66:647–660. [4] Floss C. 1999. *American Mineralogist* 84:1354–1359.

5131

LABORATORY ADSORBED NITROGEN AND NOBLE GASES—ARE WE ON THE SAFE SIDE?

S. Herrmann, S. P. Schwenzer, and U. Ott. Max-Planck-Institut für Chemie, Joh.-J. Becherweg 27, D-55128 Mainz, Germany. E-mail: herrmann@mpch-mainz.mpg.de

Noble gas measurements are usually carried out using stepwise degassing protocols, whereby the lowest T step(s) are aimed to remove (and quantify) terrestrial contamination. The influence of grinding [1–3] and acid treatment [4] has already been demonstrated. Further, natural weathering processes are capable of introducing fractionated air into the rocks [5, 6]. To our knowledge no investigation of “pure” adsorption during sample handling has been done. Here we present results from an experiment on San Carlos olivine where we determined the amounts of adsorbed nitrogen and noble gases. We compare these to noble gases found in Martian meteorites.

Experiment: A sample of San Carlos olivine was mildly crushed to reduce the grain size, resulting in a range of 0.01 to 1.5 mm. The sample was handled and measured according to our usual procedures: 99.56 mg were wrapped in Pt foil, loaded into the sample holder and degassed for 24 h at 130 °C under vacuum. In a first run, the sample was measured at 250, 400, and 800 °C, after which it was removed from the system. The temperature was low enough to avoid any melting of olivine. The Pt foil was opened carefully on one side and stored—with the sample inside—in an open sample container. After three weeks the Pt foil was closed, again loaded into the sample holder, degassed and measured at 250, 400, 600, and 800 °C.

Results: The intention was to obtain a sample degassed at the temperatures of interest and to quantify the amount and elemental ratios of nitrogen and noble gases adsorbed during re-exposure to air in the short time span of three weeks.

Helium and Neon: The light noble gases are at blank level in all temperature steps of both experiments.

Nitrogen and Argon: In the analysis of the re-exposed sample, 55% of ³⁶Ar (corresponding to 9⁺10⁻¹¹ ccSTP/g) and 68% of N₂ (corresponding to 1.3 ppm) are released in the 600 °C step. Compared to ³⁶Ar and N₂ concentrations in Martian meteorites, the amounts are small and not expected to compromise the interpretation of bulk sample data.

Krypton and Xenon: 75% and 85% of ⁸⁴Kr and ¹³²Xe, respectively, are released in the 600 °C step of the re-exposed sample. In contrast to nitrogen and argon, the released amounts are only by factor of 5 lower than amounts found in Martian meteorites, thus an influence on bulk measurements cannot be ruled out. However, the adsorbed gas is found in the lower T step(s) only. Fractionation of ⁸⁴Kr/¹³²Xe is observed to values lower than in water [7] but not as low as elementally fractionated air found in desert weathering products [5, 6].

References: [1] Srinivasan B. et al. 1978. *Geochimica et Cosmochimica Acta* 42:183–198. [2] Niemeyer S. and Leich D. A. 1976. Proceedings, 7th Lunar Science Conference. pp. 587–597. [3] Niedermann S. and Eugster O. 1992. *Geochimica et Cosmochimica Acta* 56: 493–509. [4] Schwenzer S. P. et al. 2005. Abstract. *Meteoritics & Planetary Science* 40: A137. [5] Mohapatra R. K. et al. 2002. Abstract #1532. 33rd Lunar and Planetary Science Conference. [6] Schwenzer S. P. et al. 2003. Abstract #1694. 34th Lunar and Planetary Science Conference. [7] Ozima M. and Podosek F. A. 2002. *Noble gas geochemistry*. Cambridge: Cambridge University Press. 286 p.

5303

BULK COMPOSITION OF CHONDRULES IN CARBONACEOUS CHONDRITES

D. C. Hezel, H. Palme, and R. Kiesswetter. Universität zu Köln, Institut für Geologie und Mineralogie, Zülpicherstr. 49b, 50674 Köln, Germany. E-mail: d.hezel@uni-koeln.de

Introduction: The formation conditions and the precursor material of chondrules are still a matter of debate. It is not clear whether chondrules formed as open or closed systems, whether they were molten dust balls or condensed as liquids from a gas or whether and/or to what extent their precursor material was presolar, early solar system processed [e.g., 1], derived from earlier chondrules [e.g., 1] or even from differentiated bodies [e.g., 2, 3].

Chondrule bulk compositions provide information about chondrule precursors and are essential for understanding chondrule formation. There is only a limited number of bulk chondrule data available from the literature [e.g., 1, 4, 5]. We have started a project to determine bulk chondrule compositions with improved accuracy in all types of carbonaceous chondrites (e.g., Efremovka, Allende, Renazzo, Acfer 209, Karoonda, Kainsaz, Vigarano, Acfer 182, Hammadah al Hamra 207, Ishiyev and a variety of Antarctic meteorites) to further constrain chondrule formation and the nature of precursor material.

Technique: Bulk chondrule data are obtained by modal recombination of thin section EPMA analyses. Using the procedure of [6, 7] allows to quantify uncertainties associated with the analyses.

Results: So far we analyzed chondrules in five meteorites; data for 8 Efremovka (CV3) chondrules are fully reduced. Efremovka chondrules have Mg/Si ratios between 0.77 and 1.49. The mean of all 8 chondrules is with an Mg/Si ratio of 0.99 superchondritic (CI Mg/Si ratio is 0.91). Matrix varies in Mg/Si ratio between ~0.55 and ~0.90 and has a subchondritic mean Mg/Si ratio of 0.74. Modal abundance of Efremovka matrix is ~39 vol% and of chondrules ~61 vol%. This is used to calculate the bulk Mg/Si ratio of Efremovka with 0.89, which agrees within analytical errors to the literature data of 0.91 [8]. The superchondritic Mg/Si ratio of the chondrules is thus balanced by the subchondritic Mg/Si ratio of the matrix. Similar complementary relationships between chondrules and matrix have been previously described for Renazzo (CR2) [9]. This chondrule-matrix relationship has important implications for chondrule formation models. The chemically complementary system of chondrules and matrix requires that both components formed in the same nebula compartment [10]. This nebula compartment either consisted of physically separate chondrule and matrix precursors, which had their matrix and chondrule specific chemical compositions; or, more probable, this nebula compartment consisted of a homogenous dust from which homogenous dust balls formed, which served as precursors for chondrules. During chondrule formation chondrules then acted as open systems and by exchange with the surrounding gas developed their high Mg/Si ratios.

At the conference we will present a comprehensive set of chondrule data of all types of carbonaceous chondrites.

References: [1] Jones R. H. et al. 2005. In *Chondrites and the protoplanetary disk*. San Francisco: Astronomical Society of the Pacific. pp. 251–285. [2] Bridges J. C. et al. 1995. *Meteoritics & Planetary Science* 30: 715:727. [3] Libourel G. and Krot A. N. 2006. Abstract #1334. 37th Lunar and Planetary Science Conference. [4] Hezel D. C. et al. 2006. *Geochimica et Cosmochimica Acta* 70:1548–1564. [5] Russell S. S. et al. 2005. In *Chondrites and the protoplanetary disk*. San Francisco: Astronomical Society of the Pacific. pp. 317–350. [6] Hezel D. C. 2006. Abstract #1668. 37th Lunar and Planetary Science Conference. [7] Hezel D. C. Forthcoming. [8] Klerner S. 2001. Ph.D. thesis. 119 p. [9] Klerner S. and Palme H. 1999. *Meteoritics & Planetary Science* 34:A64–A65. [10] Huss G. et al. 2005. In *Chondrites and the protoplanetary disk*. San Francisco: Astronomical Society of the Pacific. pp. 701–731.

5169

NEODYMIUM, SAMARIUM, AND GADOLINIUM ISOTOPIC STUDIES OF LUNAR METEORITES DHOFAR 489 AND NWA 032

H. Hidaka¹ and S. Yoneda². ¹Department of Earth and Planetary Systems Science, Hiroshima University, Higashi-Hiroshima 739-8526, Japan. E-mail: hidaka@hiroshima-u.ac.jp. ²Department of Engineering and Science, National Science Museum, Tokyo 169-0073, Japan

Introduction: Geochemical studies of lunar meteorites are expected to offer new information that has not been known from the Apollo and Luna missions samples. We report here isotopic compositions of Nd, Sm, and Gd of two lunar meteorites, NWA 032 and Dhofar 489, and compare the data with those of lunar soils and rocks. Isotopic determination of Nd leads to ¹⁴⁷Sm-¹⁴³Nd and ¹⁴⁶Sm-¹⁴²Nd chronometry to consider early differentiation of the samples from lunar mantle. Isotopic compositions of Sm and Gd are used to characterize exposure history of the samples from isotopic shifts on ¹⁴⁹Sm-¹⁵⁰Sm and ¹⁵⁷Gd-¹⁵⁸Gd due to neutron capture effect.

Samples and Experiments: NWA 032 is a crystalline mare basalt [1]. Dhofar 489 is an anorthositic breccia with magnesian mafic silicates [2]. Besides two lunar meteorites, two soils, 70002 and 70004, and two rocks, 60626 and 77017, were also used for this study. Each sample weighing 20–80 mg was decomposed by HF + HClO₄. After evaporation to dryness, the sample was redissolved in 2M HCl. Conventional ion exchange techniques using two column procedures were carried out to chemically separate Nd, Sm, and Gd [3]. A Micro-mass VG 54-30 thermal ionization mass spectrometer equipped with seven Faraday cup collectors was used for the isotopic measurements.

Results and Discussion: Sm and Gd isotopic shifts provide neutron fluences of $\psi = 0.53 \times 10^{16}$ and 2.58×10^{16} n cm⁻² for Dhofar 489 and NWA 032, respectively. Small fluence of Dhofar 489 suggests short exposure time and/or deep ejection depth, which is consistent with low concentrations of cosmogenic ¹⁰Be and ⁴¹Ca [4]. On the other hand, large fluence of NWA 032 is consistent with long CRE ages of 226–227 Ma supported by ³⁸Ar production rate [5].

Dhofar 489 shows a small enrichment of ¹⁴²Nd ($\epsilon_{142\text{Nd}} = +0.24 \pm 0.19$), even considering neutron capture effect on Nd isotopes. Therefore, the ¹⁴²Nd isotopic excess of Dhofar 489 is concluded to be due to decay from ¹⁴⁶Sm. Although the Nd isotopic data of other lunar samples are in progress, ¹⁴⁷Sm-¹⁴³Nd and ¹⁴⁶Sm-¹⁴²Nd systematics of a suit of data from lunar materials may put constraints to construct the model of early differentiation and evolution of lunar mantle and crust [6].

References: [1] Fagan et al. 2002. *Meteoritics & Planetary Science* 37: 371–394. [2] Takeda et al. 2003. Abstract #1284. 34th Lunar and Planetary Science Conference. [3] Hidaka et al. 1995. *Analytical Chemistry* 67:1437–1441. [4] Nishiizumi et al. 2004. Abstract #1130. 35th Lunar and Planetary Science Conference. [5] Fernandes et al. 2001. *Meteoritics & Planetary Science* 36:A57. [6] Nyquist et al. 1995. *Geochimica et Cosmochimica Acta* 59:2817–2837.

5378

A POSSIBLE METEORITE LAG DEPOSIT AFTER CONTINENTAL GLACIATION IN SOUTHEASTERN MANITOBA

A. R. Hildebrand¹, M. Beech², S. A. Kissin³, and G. B. Quade¹. ¹Department of Geology and Geophysics, University of Calgary, 2500 University Drive NW, Calgary, Alberta, Canada T2N 1N4. E-mail: ahildebr@ucalgary.ca. ²Campion College, The University of Regina, 3737 Waskana Parkway, Regina, Saskatchewan S4S 0A2. ³Department of Geology, Lakehead University, Thunder Bay, Ontario, Canada P7B 5E1

Introduction: Since the discovery that meteorites are concentrated near margins of the Antarctic ice sheet (where stagnation of ice flow occurs due to topographic obstacles and deflation of the ice surface occurs from ablation), many have wondered if other continental glaciers (particularly the large ice masses of the northern hemisphere) produced similar concentrations. Both extant ice caps and the much larger, now-melted Pleistocene continental ice sheets have been considered; no similar situation has yet been found, and the occurrence frequency of sufficient flow stagnation and deflation conditions is unknown.

Iron Meteorite Recoveries in Southeastern Manitoba: In Canada surface conditions and recent glacial history have resulted in relatively few meteorite recoveries (68), mostly by farmers on cultivated land. However, extraordinarily, a single individual, Derek Erstelle, has found three weathered iron meteorites in the forested area of southeastern Manitoba (from 1998 to 2005). The three meteorites have been recovered in a triangular area with sides of 30 to 40 km. The meteorites are moderately to heavily weathered (most weathered has portions that are >50% oxide). Two individual meteorites were recovered at one locality, but proved to be petrographically identical. The three specimens from the different localities represent different falls: a coarsest octahedrite of chemical group IAB (kamacite bandwidth 4.3 ± 1.3 mm, $n = 19$), a medium octahedrite (kamacite bandwidth 1.16 ± 0.28 mm, $n = 15$), and a severely deformed octahedrite. The third meteorite recovered was the result of a dedicated search of ~10 days duration.

Glacial History of Southeastern Manitoba: Manitoba was entirely covered by the Laurentide ice sheet during the Pleistocene; ice withdrew northwards across southern Manitoba ~11,500 years ago [1]. The glacially shaped bedrock surface is covered with subglacial and periglacial deposits, including basal and ablation tills, outwash sand and gravels, and lacustrine sediments [2]. No topography exists in the region that might have blocked ice flow to create a meteorite concentration analogous to the Antarctic case. However, southeastern Manitoba was the site of a right angle collision of two ice lobes. In the west the Koochiching Lobe flowed SE-wards from the Keewatin dispersal center to collide with the possibly slower-moving Rainy Lobe flowing SW-wards from a dispersal center in the vicinity of the Hudson Bay [1, 2].

Possible Meteorite Concentration Mechanism: That meteorites can be found in forested land with modest searching indicates a concentration mechanism operated in southeastern Manitoba. The damming of the Rainy Lobe against the Koochiching Lobe may have created a meteorite concentration. The recovered meteorites were all found near to, but east of the line of collision.

References: [1] Fullerton D. S. et al. 2000. Misc. Invest. Ser. Map I-1420 (NM-14). [2] Sado E. V. et al. 1995. Misc. Invest. Ser. Map I-1420 (NM-15).

5319

WHY DOES ANGRA DOS REIS HAVE AN ANOMALOUS (TYPE B) NIR SPECTRUM?

E. J. Hoffman. Physics Department, Morgan State University, Baltimore, Maryland 21251, USA. E-mail: ehoffman@morgan.edu

Burbine et al. [1] presented near infrared (NIR) spectra for three angrites, meteorites containing pyroxenes with large abundances of Ca, Ti, and Al, noting that of the three, Angra dos Reis gives an anomalous ("Type B") NIR spectrum [2], similar to patterns that appear almost at random in spectra of some terrestrial high-Ca pyroxenes (clinopyroxenes) [3, 4].

Mössbauer spectroscopy, an additional method sensitive to the Fe ions responsible for the pertinent absorption bands, turned up yet another anomalous result for almost all NIR Type B samples among some 40 terrestrial high-Ca pyroxenes: a signature suggesting ferric-ion levels beyond those of chemical analysis [5 and references therein]. A mechanism for this correlation remains elusive, however, and Angra dos Reis does not show this Mössbauer anomaly [5, 6]. Its Mössbauer pattern does suggest Fe²⁺ in the octahedral M2 site, though, and Hazen and Finger [7] deemed this fact consistent with the small amount of Fe²⁺ placed in that site by their structure refinement (Table 1, AR). Perhaps this 0.018 ions per 6 oxygens is sufficient also to cause the Type B absorption at 2 μ m.

To test this hypothesis I am trying to collect other high-Ca pyroxene samples for which an X-ray diffraction structure refinement exists and subject them to NIR spectroscopy. Best would be those with high Ti and Al (fassaïtes) like the principal phase in Angra dos Reis, perhaps the only such pyroxene for which both an NIR spectrum [2] and a structure refinement [7] have been published. I will present NIR results for several well-characterized terrestrial samples sent to the RELAB for spectroscopy, including two kindly supplied by Dr. J. De Grave, Andronondambo (Table 1, M5) and Val di Fassa RA313 (Table 1, RA) [8].

The greatest need is for samples that like Angra dos Reis have a small amount of Fe²⁺ in the M2 octahedral site, and I appeal to the mineralogical community to suggest some.

Table 1. Samples mentioned in the text.

	Cations per 6 oxygens {M2}[M1](T)	
AR	{Ca _{0.968} Na _{0.002} Mn _{0.002} Fe _{0.018} Mg _{0.010} }	[Mg _{0.568} Fe _{0.205} Cr _{0.005} Al _{1.161} Ti _{0.059}] (Si _{1.728} Al _{0.272})
M5	{Ca _{0.98} Na _{0.03} }	[Mg _{0.68} Fe ²⁺ _{0.07} Fe ³⁺ _{0.03} Al _{1.16} Ti _{0.04}] (Si _{1.77} Al _{0.23})
RA	{Ca _{0.98} }	[Mg _{0.77} Fe _{0.21} Al _{0.04}] (Si _{1.65} Al _{0.15})

References: AR [7]; M5 and RA [8]; neither AR nor RA showed the presence of ferric ion in chemical analysis.

References: [1] Burbine T. H. et al. 2001. Abstract #1857. 32nd Lunar & Planetary Science Conference. [2] Gaffey M. J. 1976. *Journal of Geophysical Research* 81:905–920; this report. [3] Cloutis E. A. and Gaffey M. J. 1991. *Journal of Geophysical Research* 96:22,809–22,826. [4] Schade U. et al. 2004. *Icarus* 168:80–92. [5] Hoffman E. J. et al. 2006. Abstract #1215. 37th Lunar and Planetary Science Conference. [6] Mao H.-K. et al. 1977. *Earth and Planetary Science Letters* 35:352–356. [7] Hazen R. M. and Finger L. W. 1977. *Earth and Planetary Science Letters* 35:357–362. [8] De Grave J. et al. 2002. *American Mineralogist* 87:132–141.

5127

NEW FINDS OF SHATTER CONES IN DISTAL RIES EJECTA, BERNHARDZELL, EASTERN SWITZERLAND

B. A. Hofmann¹ and E. Gnos². ¹Naturhistorisches Museum der Burgergemeinde Bern, Bernstrasse 15, CH-3005 Bern, Switzerland. E-mail: beda.hofmann@geo.unibe.ch. ²Institut für Geologie, Universität Bern, Baltzerstrasse 1, CH-3012 Bern, Switzerland

Introduction: A thin horizon of impact ejecta comprising angular fragments of upper Jurassic limestone (up to 30 cm in size), fragments of Triassic pelites and shocked quartz grains is known from three outcrops near St. Gallen in eastern Switzerland. The best outcrop is located on the left bank of the Sitter River near Bernhardzell. The impact horizon is hosted by Miocene marls of the Swiss Molasse basin. A zircon-bearing, 14.4 to 14.6 ± 0.06 Ma old tuff [1] stratigraphically located 70 m above the impact horizon constrains the age of the impact layer. At the time of discovery in 1945, the horizon was interpreted as volcanic [2]. The impact nature was recognized in 1973 after the discovery of a limestone block containing shatter cones [3], and a connection with the Ries was made plausible [4] after recognition of high-speed ejection processes. In recent years several blocks of limestone with shatter cones have been found in the best exposure near Bernhardzell, among the new finds is one with particularly well developed shatter cones allowing the measurement of a statistically valid number of angles between striations (V angle).

Comparison of Bernhardzell and Steinheim Shatter Cones: A well-preserved Bernhardzell shatter cone has a higher mean V angle of 32 ± 5° as compared with samples from the Steinheim basin (6 samples yielded 13 ± 2, 17 ± 4, 20 ± 5, 20 ± 2°, 16.4 ± 2.2 24.7 ± 5.5, all measurements 17 ± 5°, n = 93). Based on a model that relates the angle between shatter cone striations with increasing distance from the impact center [5], and the fact that the Steinheim shatter cones seem restricted to the central uplift close to the impact center, the larger angles in the Bernhardzell ejecta suggest a different origin. It is thus likely that these samples are derived from a larger distance from the impact center, such as a peripheral position in the Ries crater.

Ejection Processes: Located at a distance of 160 km from the center of the Ries crater, an ejection velocity of at least 1.3 kms⁻¹ is required. While this appears possible in case of limestone, processes of ejection of low-strength pelitic rock fragments up to 10 cm in size remain poorly constrained.

References: [1] Fischer et al. 1987. Annual Meeting of The Swiss Academy of Sciences. Abstract. [2] Büchi, U. and Hofmann F. 1945. *Eclogae Geologicae Helvetiae* 38:337–343. [3] Hofmann F. 1973. *Eclogae Geologicae Helvetiae* 66:83–100. [4] Hofmann B. and Hofmann F. 1992. *Eclogae Geologicae Helvetiae* 85:788–789. [5] Sagy A. et al. 2004. *Journal of Geophysical Research* 109, doi:10.1029/2004JB003016.

5128

THE TWANNBERG, SWITZERLAND IIG IRON: NEW FINDS, CRE AGES, AND A GLACIAL SCENARIO

B. A. Hofmann¹, S. Lorenzetti², O. Eugster², F. Serefidin³, D. Hu³, G. F. Herzog³, and E. Gnos⁴. ¹Naturhistorisches Museum der Burgergemeinde Bern, Bernstrasse 15, 3005 Bern, Switzerland. E-mail: beda.hofmann@geo.unibe.ch. ²Physikalisches Institut, Sidlerstr. 5, 3012 Bern, Switzerland. ³Department of Chemistry, Rutgers University, Piscataway, New Jersey 08854, USA. ⁴Institut für Geologie, Universität Bern, Baltzerstrasse 3, 3012 Bern, Switzerland

Introduction: The first mass of Twannberg (TWI; 15,915 g [1]) was found in 1984 in an area marking the limit of the Rhône Valley glacier during the last ice age. Two additional masses (TWII: 2246 g, TWIII: 2533 g) were recovered in 2000 and 2005 on the attic of an old house and in an old mineral collection, respectively. Both locations are within a few km of the original find site. After discovery of the second mass a reinvestigation and comparison with the first mass was initiated.

Mineralogy and Weathering: As the original find, the newly recovered masses consist of single crystals of kamacite with skeletal, up to 4.5 cm long and a few mm wide inclusions of schreibersite (10.5 wt% Ni). Fracturing follows a second generation of rhabditic schreibersite (17.2 wt% Ni) occurring as very large (several cm) and thin (20 µm) plates. Bulk phosphorous contents based on schreibersite abundance are 1.7 wt% (TWI) and 0.85 wt% (TWII). Troilite is rare. All three masses are covered by a thick rind of oxides containing numerous inclusions of silicate sand grains, identical to those occurring in local glacial till of the Rhône glacier. Fractures following rhabdite plates allow local deep penetration of oxidation products.

Noble Gases and CRE Ages: Noble gas analyses of TW I and II yielded similar results, confirming pairing. ⁴He/²¹Ne ratios indicate stronger shielding for TW I than for TW II. CRE ages of 14.4 ± 7.0 (TWI) and 13.0 ± 3.0 Ma (TWII) are atypically low for iron meteorites.

Cosmogenic Radionuclides: Activities of ¹⁰Be and ²⁶Al are much lower (by a factor of 40) than those typically encountered in small iron meteorites. The low values are most likely due to heavy shielding.

Discussion: Twannberg is a large meteorite with an unusually young CRE age. During weathering, different meteorite fragments resided in glacial till of the Rhône glacier, as indicated by terrestrial mineral grains in the oxide rind. The meteorite fragments were glacier transported for an unknown distance from their location of fall during one or several cold periods.

References: [1] Graham A. L. 1986. *Meteoritics* 21:309–313.

5200

PETROLOGY AND REE GEOCHEMISTRY OF THE LUNAR METEORITE SAYH AL UHAYMIR 300

Weibiao Hsu¹, Y. Guan², T. Ushikubo², R. Bartoschewitz³, A. Zhang¹, Th. Kurtz⁴, and P. Kurtz⁴. ¹Purple Mountain Observatory, Nanjing, China. E-mail: wbxu@pmo.ac.cn. ²Department of Geological Science, Arizona State University, Tempe, Arizona 85287, USA. ³Bartoschewitz Meteorite Lab, Lehmweg 53, D-38518 Gifhorn, Germany. ⁴Henckellweg 25, D-30459 Hannover, Germany

Introduction: Sayh al Uhaymir 300 (SaU 300) is a newly recovered lunar meteorite from Oman. It was classified as a feldspathic regolith [1, 2]. This meteorite has a Fe/Mn ratio of 71, Al₂O₃ content of 20.4 wt%, FeO + MgO of 16.7 wt%, and Th of 0.46 ppm [2]. Its chemical composition falls into the range of mingled basaltic-feldspathic breccias [2, 3].

Petrology: SaU 300 is predominantly composed of fine-grained matrix with abundant mineral fragments and a few polymict breccias (anorthosite, troctolitic anorthosite, noritic gabbro, and anorthositic gabbro). Numerous euhedral to subeuhedral mineral fragments (~100 µm) of olivine, anorthite, and pyroxenes are set in the fine-grained matrix. Lithic clasts appear in angular to round shapes and range in size from several hundred microns to a few mm. Glass veins (50 µm wide), FeNi and troilite grains are also observed in the section.

REE Geochemistry: REE microdistributions in SaU 300 were analyzed with the ASU Cameca 6f ion microprobe. Measurements were carried out in olivine, anorthite, pyroxenes, and apatite within lithic clasts and the fine-grained matrix. Because of the small grain size (<50 µm) and inclusion, olivine analyses are often contaminated by a small amount of anorthite. After excluding the contribution from anorthite, olivine exhibits a HREE-enriched pattern with Lu at 3–10 × CI and Gd at 0.4–0.6 × CI. Within the same clast, olivine has relatively homogeneous REEs. REEs vary by a factor of 3 in olivine from different clasts. Anorthite varies significantly in REEs both within clasts and among different clasts. It has a relatively LREE-enriched pattern with a positive Eu anomaly (~20 × CI). La varies from 0.8 to 22 × CI and Y, an analog of HREE, from 0.5 to 8 × CI. Both high-Ca and low-Ca pyroxenes were analyzed. They exhibit typical HREE-enriched pattern with a negative Eu anomaly. High-Ca pyroxene has higher REEs (La 3–25 × CI, Lu 20–50 × CI) than low-Ca pyroxene (Lu 3–10 × CI). One anorthositic clast contains an apatite grain (30 × 150 µm). Apatite has very high REEs with a relatively LREE-enriched pattern (La 2800 × CI and Lu 650 × CI) and a negative Eu anomaly (Eu 30 × CI). It is very similar to apatite from lunar highlands [4] and from the lunar meteorite EET 96008 [5]. Glass veins have homogeneous REEs with a relatively LREE-enriched (La 17 × CI, Sm 12 × CI), a positive Eu anomaly (Eu 17 × CI) and a relatively flat HREE (12 × CI) pattern. Its REEs fall into the range of lunar highlands meteorites [5, 6].

Conclusions: Petrological and geochemical signatures of SaU 300 are in many ways similar to those of lunar highlands meteorites. SaU 300 is primarily a feldspathic regolith breccia with small amounts of mare components.

References: [1] Bartoschewitz R. et al. 2005. Personal communication. [2] Bartoschewitz R. et al. 2005. Personal communication. [3] Korotev R. L. 2005. *Chemie der Erde* 65:297–346. [4] Lindstrom M. M. et al. 1985. Abstract. 16th Lunar and Planetary Science Conference. pp. 493–494. [5] Anand M. et al. 2003. *Geochimica et Cosmochimica Acta* 67:3499–3518. [6] Korotev R. L. 2003. *Geochimica et Cosmochimica Acta* 67:4895–4923.

5324

SELENIUM AND SULFUR DISTRIBUTION IN THE ANOMALOUS CK CHONDRITE EET 99430

H. Huber¹, H. A. Ishii², and S. Brennan³. ¹Institute of Geophysics and Planetary Physics, University of California, Los Angeles, California 90095–1567, USA. E-mail: hhuber@ucla.edu. ²Institute of Geophysics and Planetary Physics, Lawrence Livermore National Laboratory, Livermore, California 94550, USA. ³Stanford Synchrotron Radiation Laboratory, Stanford Linear Accelerator Center, Stanford, California 94025, USA

Introduction: Within a recent study on bulk trace elemental anomalies in carbonaceous chondrites of the Karoonda group (CK), one meteorite was found to be of specific interest [1]. EET 99430 is a CK4 with a quite low chondrule and opaque mineral abundance compared to mean CKs [2]. Still, most of the major and trace element contents show typical CK chondrite values, except for elements affected by sulfide weathering (Ni, Co, Se). It has lost most of its sulfide phases, as represented in the lack of coarse sulfides in the thin sections as well as a depletion in bulk sulfur by a factor of 10 [3]. Former sulfide veins display visible losses in one phase (presumably pentlandite, the most abundant sulfide in CKs) and only left-over grains of pyrite. Nevertheless, the abundances of several siderophile and chalcophile elements, such as Ni, Co, Au and Se were found to be enriched on average by a factor of 2. Since Se is usually considered as a proxy for sulfur contents, the question of S/Se decoupling within this meteorite arose.

Analytical Methods: We performed reflected-light optical microscopy to determine the sulfide phases. A mosaic of BSE images was made with the UCLA SEM and the phases were determined with the JEOL-superprobe at UCLA. In order to determine the Se and S (and several other elements) distribution within the sulfide-depleted parts of the thin sections EET 99430,11 and EET 99430,6 we performed micro-synchrotron radiation X-ray fluorescence (µ-SXRF) spectroscopy in two line scans [4]. The region of the former sulfide vein was scanned in steps of 25 µm and the variations of S, Se, Cu, Fe, Zn, Si, and Mn extracted from the spectra obtained.

Results and Discussion: The sulfide mineralogy in EET 99430 shows occasional occurrences of pyrites and MSS—no pentlandite, violarite or other thiospinel was found in either thin section. These minerals comprise more than 90% of average CK chondrites sulfide minerals. We chose the former sulfide vein as a potential region to explore possible S/Se decoupling, since it has apparently lost parts of its sulfides with only pyrite remaining. The µ-SXRF data show a clear trend for the elements S, Se, and Cu peaking within the sulfide region, whereas Fe shows basically a flat distribution from the olivine on the side towards the pyrite grains. S and Se are enriched by a factor of 6 compared to the surrounding olivine bearing areas.

First, the results show the versatility of µ-SXRF in determining Se and S in these low concentrations. Second, Se obviously follows sulfur within this area, so the enrichments in Se may appear within other regions of the meteorite. Further investigations on the source, or rather the reprecipitation areas, within EET 99430 have to be made.

References: [1] Huber H. et al. *Geochimica et Cosmochimica Acta*. Forthcoming. [2] Neff K. E. and Righter K. 2006. Abstract #1320. 37th Lunar and Planetary Science Conference. [3] Oura et al. 2004. *Antarctic Meteorite Research* 17:172–184. [4] Ishii et al. 2006. Abstract #2198. 37th Lunar and Planetary Science Conference.

5371

SULFIDE VARIATIONS IN CR CHONDRITES

Heinz Huber^{1,2} and Alan E. Rubin¹. ¹Institute of Geophysics and Planetary Physics, University of California, Los Angeles, California 90095–1567, USA. ²Department of Chemistry and Biochemistry, University of California, Los Angeles, California 90095, USA. E-mail: hhuber@ucla.edu

Introduction: CR chondrites are low in bulk S and Se (9.2 ± 2.2 mg/g and 5.0 ± 0.8 $\mu\text{g/g}$, respectively) relative to other carbonaceous chondrite groups (e.g., CO: ~ 22 mg/g S, 7.6 $\mu\text{g/g}$ Se; CV: ~ 22 mg/g S, 8.5 $\mu\text{g/g}$ Se; CM: ~ 31 mg/g S, 12.9 $\mu\text{g/g}$ Se). CR chondrites are also low in coarse sulfide (mainly troilite) as indicated by microscopically determined modal abundances (in vol%): CR (1.7 ± 1.0); CO (3.3 ± 1.2); CV (2.1 ± 0.8). Data from [e.g., 1–4].

A significant fraction of the S in CR chondrites occurs as fine sulfide grains in the matrix. This is indicated by the relatively high abundance of bulk S (22.6 mg/g) and Se (11.4 $\mu\text{g/g}$) in the matrix-rich CR-an chondrite Al Rais [2].

Analytical Techniques: In order to ascertain the distribution of coarse sulfides in CR chondrites we studied thin sections of 12 CR and CR-an chondrites microscopically: Acfer 097, Acfer 139, Al Rais, Dar al Gani 1004, El Djouf 001, EET 92062, LAP 02342, NWA 721, NWA 801, NWA 1083, NWA 1616, and Renazzo. We made BSE mosaic maps of the entire thin sections of Acfer 097, Al Rais, El Djouf 001, and LAP 02342. Six of the CR chondrites were also studied by electron microprobe.

Results and Discussion: Sulfide in CR chondrites occurs in three principle petrographic settings: 1) Some sulfide is present as submicrometer grains and rare isolated coarse grains ($5\text{--}40$ μm) in the matrix. 2) Approximately 10% of the porphyritic chondrules are surrounded by sulfide-rich rims. Sulfide in these rims ranges from 0.2 μm particles surrounded by fine-grained silicate to thick patches (20×200 μm) connected to thinner ($5\text{--}30$ μm thick) sulfide stringers. Sulfide-rich rims surround both low-FeO (type I) and high-FeO (type II) porphyritic chondrules; we did not find any systematic differences in mineral chemistry between chondrules that are surrounded by sulfide-rich rims and those that are not. 3) There are coarse patches (50×100 to 50×400 μm) of sulfide within rare porphyritic chondrules. In many cases, these sulfide patches are near the edges of their host chondrule.

Chondrules that contain internal sulfide grains also have sulfide-bearing rims. It seems possible that the sulfide-rich rims were formed during chondrule remelting events by the expulsion of sulfide from the chondrule interior.

The paucity of sulfide in CR chondrites may be a result of chondrule formation in the CR region having largely ceased prior to the local nebular environment cooling below the temperature (~ 670 K) where significant condensation of S commenced.

References: [1] Dreibus G. et al. 1995. *Meteoritics* 30:439–445. [2] Kallemeyn G. W. et al. 1994. *Geochimica et Cosmochimica Acta* 58:2873–2888. [3] Weisberg M. K. et al. 1993. *Geochimica et Cosmochimica Acta* 57:1567–1586. [4] McSween H. Y., Jr. 1977. *Geochimica et Cosmochimica Acta* 41:477–491.

5370

LAYERED TEKTITES AND ADJACENT SOILS FROM SE THAILAND

H. Huber¹ and J. T. Wasson^{1,2}. ¹Institute of Geophysics and Planetary Physics and Department of Chemistry and Biochemistry, University of California–Los Angeles, Los Angeles, California 90095–1567, USA. E-mail: hhuber@ucla.edu. ²Department of Earth and Space Science, University of California–Los Angeles, Los Angeles, California 90095–1567, USA

Introduction: During a field trip to SE Thailand in February 2005 we recovered a large mass of layered tektites from an area southeast of Ubon Ratchathani along the Thai-Cambodian-Laotian border. The main purpose of the expedition was to recover tektites and soils from known localities near and far from a small volcanic locality. Several soil profiles were taken for detailed studies on the soil chemistry and mineralogy and to permit a chemical and isotopic comparison with the nearby layered tektites. The goal was to test the hypothesis that the layered tektites are parts of a melt sheet formed when soils were melted [1]. Besides the chemical analysis, the soil and tektite samples will be analyzed for Sr and Nd isotopic variations by K. Mezger and T. Kleine and for ¹⁰Be by G. Herzog.

Analytical Technique: We used instrumental neutron activation analysis (INAA) to determine the major and trace element contents of tektites and soils. Tektites were sawn in solid slabs of ~ 3 mm thickness, whereas $300\text{--}500$ mg of soil samples were filled in polyethylene vials. Samples along with standard reference material were irradiated and counted in four cycles using high-resolution gamma-ray detectors. These data were combined with INAA data from previous runs [2] including a basalt sample from Ban Kaset Sombun. We then further prepared the soil samples with a 315 μm sieve and made grain mounts to permit characterization with the optical microscope.

Results and Discussion: One special focus was laid on the influence of local basaltic material from near Ban Kaset Sombun in order to attempt to determine whether there were parallel variations in tektite and soil compositions, as expected if the tektites formed at their present locations. Past studies have revealed an ultramafic component mixed within the layered tektites as described by [2–3] and also found in microtektites by [4]. Their influence on the soils is clearly visible by a distinct reddish coloring of local material. We included the westernmost layered tektite at Ban Song and a soil profile from the proximate Ban Ta Kao. From there following the major and trace element distribution of the tektites towards the NE (region near Ban Huai Sai we can clearly distinguish the samples from the basalt-rich area as being high in Co, Fe, Ba, Sc, and Sr and low in Ca, As, Hf, and to a minor extent in Na and Ga. The other elements show either high variations within (Ir, Au) are quite uniform such as the REE, Ta, and U.

For some of the layered tektites we could distinguish between the top and bottom surface. Vertical thin sections of the whole tektites reveal their internal structures and layering. The compositional differences in dark layers of $10\text{--}300$ μm thickness show distinct enrichments in the elements Fe, Mg, Mn, and Ca compared to the lighter glass. These layers do not correlate with the bubble rich and bubble poor layers.

References: [1] Wasson J. T. 2003. *Astrobiology* 3:163–179. [2] Wasson J. T. 1991. *Earth and Planetary Science Letters* 102:95–109. [3] Huber H. and Wasson J. T. 2004. Abstract #2110. 35th Lunar and Planetary Science Conference. [4] Glass W. et al. 2004. *Geochimica et Cosmochimica Acta* 68:3971–4006.

5069

THE EXPOSURE HISTORY OF THE VERY LARGE L6 CHONDRITE JaH 073

L. Huber¹, B. Hofmann², E. Gnos³, and I. Leya¹. ¹Physikalisches Institut, University of Bern, 3012 Bern, Switzerland. E-mail: liliane.huber@space.unibe.ch. ²Naturhistorisches Museum Bern, 3005 Bern, Switzerland. ³Institut für Geologie, 3012 Bern, Switzerland

Introduction: Large stony meteorites are relatively rare because, in contrast to iron meteorites, they fragment during atmospheric entry, producing large meteorite showers. Surprisingly, many of the large chondrites appear to have complex exposure histories with a first stage exposure on the parent body. In an ongoing study to answer the question whether a complex exposure history is simply more easily detected in large objects or whether they really more likely experienced a complex exposure [1, 2] we intensively studied the very large meteorite JaH 073 (L6).

Experimental: We analyzed 8 different strewn field fragments with at least two aliquots each. In addition we took 7 samples from known locations within the main mass (~80 kg) and performed 3 step-wise heating experiments. The samples consisted of one or several chips (100–150 mg), free of fusion crust and wrapped in Ni foil. Prior to analysis the samples were preheated to desorb loosely bound atmospheric contamination. We measured He, Ne, and Ar isotopic concentrations.

Results: The data for JaH 073 show some very interesting features which are worth to be discussed. First, whereas most of data measured for meteorites so far and most of the model calculations predict a lower limit for ²²Ne/²¹Ne of about 1.06, some of our data are clearly below this ratio. Second, in a plot ³He/²¹Ne versus ²²Ne/²¹Ne all our data are below the empirical correlation line [3], indicating (at first glance) ³He and/or ³H diffusive losses. However using rather qualitative arguments we suppose that the obvious ³He deficits are not due to diffusive losses (neither on earth nor in space). We instead propose that the semiempirical correlation [3] is not valid for very large meteorites. Recent model calculations for lunar surface rocks indicate that for low values of ³He/²¹Ne the ratios ²²Ne/²¹Ne start to increase (at nearly constant ³He/²¹Ne) [4]. If true, the data measured by us indicate that JaH 073 was rather a 2π than a 4π object. Plotting ²¹Ne_{cos} as a function of ²²Ne/²¹Ne for JaH 073 fragments and main mass samples indicate, despite of the low range of ²²Ne/²¹Ne, that the ²¹Ne_{cos} concentrations vary by more than a factor of 10, giving evidence of a complex exposure history. An interesting result is obtained from the samples taken from known locations of the main mass. In contrast to most model calculations and usual assumptions, which all predict decreasing ²¹Ne concentrations with decreasing ²²Ne/²¹Ne ratios (for large objects), our data clearly show increasing ²²Ne/²¹Ne ratios for decreasing ²¹Ne concentrations. A similar result has already been observed of one other meteorite, strewn field fragments from Gold Basin [1].

To summarize, the new data, together with sophisticated model calculations, indicate that the very often used correlations ²¹Ne versus ²²Ne/²¹Ne and ³He/²¹Ne versus ²²Ne/²¹Ne are ambiguous for large shielding depths. The new data from JaH 073 therefore help to better constrain physical model calculations.

References: [1] Welten et al. 2003. *Meteoritics & Planetary Science* 38:157–173. [2] Welten et al. 2004. Abstract #2020. 35th Lunar and Planetary Science Conference. [3] Nishiizumi et al. 1980. *Earth and Planetary Science Letters* 50:156–170. [4] Masarik et al. 2001. *Meteoritics & Planetary Science* 36:643–650.

5256

P-T EQUILIBRATION CONDITIONS FOR LUNAR GRANULITIC IMPACTITES: EVIDENCE FROM APOLLO 15, 16, AND 17

J. A. Hudgins and J. G. Spray. Planetary and Space Science Centre, Department of Geology, University of New Brunswick. 2 Bailey Drive, Fredericton, New Brunswick, E3B 5A3, Canada. E-mail: jillian.hudgins@unb.ca

We estimate the pressure and temperature conditions at which seven representative samples of the granulitic impactite suite last. This suite is believed to have formed between the solidification of the lunar magma ocean (~4.4 Ga) and the start of the heavy bombardment period (~4.0) [1]. Therefore, results of this study may shed light on the thermal conditions of the Moon during its first 0.5 Ga of evolution.

Lunar granulitic impactites are complex rocks and are poorly understood. These coherent crystalline rocks were derived from the recrystallization of previously brecciated rocks containing clasts from both the ferroan anorthosite and Mg suites. They are characterized by 70–80% modal plagioclase, display a clast/matrix structure, are enriched in trace siderophile elements (indicative of meteoritic contamination) and contain virtually no KREEP component. Mineral compositions are homogeneous on a cm scale and are assumed to have been re-equilibrated by the last thermal event [1].

Equilibration temperatures were determined using two-pyroxene thermometry [2] based on Ca, Na, Fe, and Mg concentrations in co-existing orthopyroxene and clinopyroxene crystals. For the seven investigated samples, equilibration temperatures were constrained to be between 850 °C and 1050 °C. These results are in accordance with previous geothermometric calculations (e.g., [3]) and correspond to the latest episode of re-equilibration between clinopyroxene and orthopyroxene (i.e., the conditions of the last episode of metamorphism and recrystallization).

The low pressure gradient on the Moon (0.05 kbar/km) [4] and the lack of phases sensitive to low pressure variations complicate pressure calculations. We estimated equilibration pressures using two monomineralic (clinopyroxene) geobarometers [5, 6]. One was based on the variation of the structural unit-cell parameters of clinopyroxene with pressure; the other considered the Jd-Di exchange reaction and equilibration temperature. We attempted to calculate pressures based on exchange reactions between mineral pairs (e.g., cpx-ol), but were not successful in obtaining viable results, perhaps because these barometers are calibrated for higher pressure assemblages and have errors of a few kbars. Pressures from the monomineralic barometers were determined to be ~1–2 kbar. These pressures correspond to depths of burial of 20 to 40 km, which represent the mid- to lower-crustal region of the Moon. Surface sampling by Apollo astronauts requires exhumation of the granulitic impactites, presumably by subsequent impact events. Our results indicate that metamorphism was due to burial rather than by juxtaposition with impact melt sheets.

References: [1] Warner J. L. et al. 1977. 8th Lunar Science Conference. pp. 2051–2066. [2] Brey G. P. and Köhler T. 1990. *Journal of Petrology* 31: 1353–1378. [3] Cushing J. A. et al. 1999. *Meteoritics & Planetary Science* 34:185–195. [4] McCallum I. S. and O'Brien H. E. 1996. *American Mineralogist* 81:1166–1175. [5] Nimis P. and Ulmer P. 1998. *Contributions to Mineralogy and Petrology* 133:122–135. [6] Ashchepkov I. V. 2001. Abstract. GSA Annual Meeting.

5028

NI-RICH OLIVINE AND A CAI WITH AI-DIOPSIDE IN NWA 2748, LL3.4 0.2

R. Hutchison and A. Kearsley. Mineralogy Department, Natural History Museum, London SW7 5BD, UK. E-mail: marobh@btopenworld.com

Introduction: Survey of a thin section of NWA 2748, using SEM with EDS, revealed two unusual objects, a 4 mm porphyritic olivine (PO) clast chondrule and a 1.4 mm CAI.

Ni-Bearing Olivines: The PO object has phenocrysts <1 mm in size. Cores are Fo_{85±2} with NiO = 0.94 ± 0.10, MnO = 0.26 and CaO = 0.17 (all wt%; means of 17 WD analyses), zoned to Fo₅₈ with decreasing NiO and increasing MnO and CaO (Table 1). Euhedral to subhedral chrome spinels, <30 µm, are set in olivine rims, rarely in mesostasis. The spinels, analyzed by EDS, have 7–8 wt% MgO and 10–13 wt% Al₂O₃, higher than the averages in ordinary chondrites [1]. Charge balance indicates that ~10% of the Fe is Fe³⁺. Mesostasis comprises augite dendrites and feldspathic material, “An₃₃.”

Discussion: The high NiO in the PO cores is unmatched, but the clast chondrule is normal in other respects. Equilibrated CK chondrites have olivines of Fo_{70–66} with NiO <0.6 wt% and Mn/Fe wt ratios of 0.006–0.010 [from ref. 2], compared with a mean of 0.018 in the olivines in the clast chondrule. The range of Mn/Fe ratios overlaps that in Martian olivines [3]. In a planetary body, several factors control the Fe/Mn ratio, including degree of oxidation, with which it should inversely correlate. The NiO content, however, indicates that the PO chondrule may be the most oxidized igneous object recognized to date, but its Fe/Mn ratios are inconsistent with this and testify to a complex origin.

Spinel-Pyroxene CAI: It lacks a rim sequence and is semicircular with abraded margins. It consists of subhedral to anhedral Al-diopside, <0.2 mm, with interstitial spinels <30 µm. Diopside has 18–25 wt% Al₂O₃, above the range in CAIs in ordinary chondrites, but low TiO₂ (Table 1) is normal [4]. FeO in spinels increases towards the margin of the inclusion. The diopside combines high Al₂O₃ typical of CAIs in carbonaceous chondrites with low TiO₂ typical of those in ordinary chondrites.

Table 1.

	1	2	3	4	5	6
SiO ₂	40.00	35.30	0.32	0.60	39.20	–
TiO ₂	–	–	0.64	1.31	1.95	0.39
Al ₂ O ₃	0.10	0.12	13.20	10.20	25.00	67.50
Cr ₂ O ₃	0.36	0.10	52.70	55.70	–	–
FeO	13.60	35.70	24.40	25.30	–	7.82
MnO	0.22	0.63	0.71	–	–	–
NiO	0.83	0.28	0.60	–	–	–
MgO	46.10	27.60	8.18	7.40	9.92	23.10
CaO	0.13	0.42	–	–	25.20	–
Sum	101.34	100.15	100.75	100.51	101.27	98.81

1–4, PO clast chondrule, 5–6, spinel-pyroxene CAI. 1 olivine core, Fo₈₆, and 2, rim, Fo₅₈, both are WD analyses. Cr-spinels, 3, in mesostasis, and 4, in olivine rim. 5, Al-diopside, 6, Fe-bearing spinel. 3–6 are ED analyses

References: [1] Wlotzka F. 2005. *Meteoritics & Planetary Science* 40: 1673–1702. [2] Noguchi T. 1993. *Proceedings of the Sixth Symposium on Antarctic Meteorites*. pp. 204–233. [3] Papike J. J. 1998. In *Planetary materials 7-1-7-11*. [4] Brearley A. J. and Jones R. H. 1998. In *Planetary materials 3-188-3-189*.

5291

FIB-TEM AND SIMS OF AEOLIAN AND GLACIAL ANTARCTIC MICROMETEORITES—EVIDENCE FOR ORIGIN OF “COPS”

K. A. Huwig and R. P. Harvey. Department of Geological Sciences, CWRU, Cleveland, Ohio 44106, USA. E-mail: huwig@case.edu

Introduction: Previous TOF-SIMS results have shown a difference in distribution and amount of S, F, H, and OH ions between the micrometeorites melted from glacial ice and those collected dry from aeolian traps [1]. The goal of this study was to determine whether the increase in F (and the differences in S, H, and OH) was consistently present in more than the one micrometeorite studied at that time and to determine what the host mineral(s) for the anomalous ions is.

Methods: The two particles are representatives for glacial (ice recovery) and aeolian trap (recovered “dry”) micrometeorites. Both particles are the same as within the study described in [1] and were chosen on the basis of least amount of melting and highest overlapping in mineralogy and appearance.

In addition to these two, ten micrometeorites on the same mount as the glacial micrometeorite and eight from the aeolian mount were analyzed using a CAMECA ims1270 ion microprobe at the IGPP, UCLA. NIST SRM 610 glass was analyzed under the same analytical conditions to record the relative sensitivities of ¹⁹F⁻ and ³⁰Si⁻.

A section from both of the previously analyzed micrometeorites was removed using the focused ion beam (FIB) technique as described in [2]. These sections were then imaged and analyzed using a 200 keV FEI TF20 XT STEM at LLNL and EDX and EELS data were collected.

Results: Ion probe analyses have shown that the aeolian micrometeorites had a fluorine content comparable to the glass standard, while the micrometeorites melted out of glacial ice varied highly in fluorine content, but were consistently one or two orders of magnitude higher than both the aeolian micrometeorites and the glass standard.

FIB-TEM analyses showed that both the aeolian and glacial particles consist of small spinel and Ol or Px grains with interstitial glass. The grains in the glacial particle were larger, ranging from about 0.1 to 1 µm across, while those in the aeolian particle typically ranged from 10 to 300 nm. Due to the similarity in mineralogy and texture, it is likely that they were very similar before atmospheric entry and experienced a slightly different amount of heating creating the disparity in grain sizes.

The glacial micrometeorite also included a beam sensitive amorphous phase that contained the S seen in [1]. This phase also included C, O, P, Fe, Si, Al, Mg, Ca, Na, Cr, and Ni in varying amounts. No crystalline portion of this phase was found, so no positive identification of the phase was possible. These spectra correspond to the “COPS” phase as described by [3]. This phase occupies limited areas around the silicate grains, apparently replacing the glass otherwise found. Also it coats the surface of most of the vesicles within the section. The aeolian particle does not contain this phase.

Acknowledgements: Thanks to J. Bradley, Z. Dai, N. Teslich, K. McKeegan, and A. Schmidt for instrument time and their expertise. The ion microprobe facility at UCLA is partly supported by a grant from the Instrumentation and Facilities Program, Division of Earth Sciences, National Science Foundation.

References: [1] Huwig K. A. et al. 2006. Abstract #2403. 37th Lunar and Planetary Science Conference. [2] Lee et al. 2003. *Mineralogical Magazine* 67:581–592. [3] Engrand C. et al. 1993. 24th Lunar and Planetary Science Conference. pp. 441–442.

5333

A TRANSMISSION ELECTRON MICROSCOPE STUDY OF INTERNAL SUBGRAINS IN SiC-X GRAINS

K. M. Hynes, T. K. Croat, S. Amari, A. F. Mertz, and T. J. Bernatowicz. Laboratory for Space Sciences and Department of Physics, Washington University, Saint Louis, Missouri 63130, USA. E-mail: khynes@hbar.wustl.edu

Introduction: SiC-X grains comprise approximately 1% of the total presolar SiC population. Based on their isotopic compositions, these rare grains are thought to have a supernova origin [1]. While over 500 SiC grains have been studied by transmission electron microscopy (TEM), these grains were primarily mainstream grains and most have not been studied for their isotopic compositions [2]. Microstructure and phase information have been obtained for only two known SiC-X grains and there have been no previous reports of internal subgrains in them [3]. Here we present preliminary results from TEM studies on four SiC-X grains.

Experimental: SiC-X grain candidates from the KJG fraction (3 μm average size) from the Murchison meteorite were located by ion imaging (with the IMS-3f) and subsequently analyzed for their C and Si isotopic ratios with the NanoSIMS to confirm their origin. Four of these grains were then selected for TEM studies. The grains were placed in resin and sliced into ≤ 100 nm sections with a diamond ultramicrotome and subsequently studied in a JEOL 2000FX TEM equipped with a NORAN Energy Dispersive X-ray Spectrometer (EDXS).

Results: The four selected grains all have large ^{28}Si excesses ($-309\% \leq \delta^{29}\text{Si} \leq -187\%$; $-436\% \leq \delta^{30}\text{Si} \leq -329\%$), as well as $^{12}\text{C}/^{13}\text{C}$ ratios greater than solar ($111\% \leq ^{12}\text{C}/^{13}\text{C} \leq 250\%$). EDXS analysis shows that three of the grains have significant amounts of Mg, with Mg/Al ratios of up to ~ 0.67 . The Mg and Al appear to be distributed uniformly, in agreement with previously studied SiC-X grains [3]. Because an insignificant amount of Mg typically condenses within SiC during formation ($\text{Mg}/\text{Al} < 0.05$ in mainstream SiCs [4]), the Mg is likely radiogenic ^{26}Mg from the decay of ^{26}Al . The polytypes observed thus far in the SiC-X grains are the same as those found in mainstream SiC [2]. Most of the crystal domains analyzed in the SiC-X grains are consistent with the 3C-SiC polytype (79% of mainstream SiC), with a preponderance of $\Sigma = 3$ twins. Also observed was one case of an intergrowth between the 3C-SiC and the 2H-SiC polytypes (17% of mainstream SiC). Unlike mainstream grains, which are predominantly single crystal domains [2], the SiC-X grains are composed of multiple small crystal domains, ranging in size from ~ 70 – 200 nm. Five subgrains were found within one of the SiC grains. Three of the subgrains are mainly Fe, with Ni/Fe ratios of 0.21 ± 0.07 , 0.19 ± 0.03 , and 0.18 ± 0.06 . Significant Ti is seen in the third subgrain, although it is unclear at this time if the Ti is uniformly distributed or is in a separate subgrain. The other two subgrains are Ni-rich, with Ni/Fe ratios of 1.889 ± 0.279 and 0.41 ± 0.05 . Preliminary TEM diffraction data from the Ni-rich subgrains do not appear to be consistent with the metal phases previously observed in subgrains found within presolar graphite [5]. Due to the SiC background, we cannot rule out the presence of Si in these subgrains, and silicides are, indeed, a possibility. Further investigation on the phases of these subgrains is ongoing.

References: [1] Amari S. et al. 1992. *The Astrophysical Journal* 394: L43–L46. [2] Daulton T. L. et al. 2003. *Geochimica et Cosmochimica Acta* 67:4743–4767. [3] Stroud R. M. et al. 2004. Abstract. *Meteoritics & Planetary Science* 39:A101. [4] Amari S. et al. 1995. *Meteoritics* 30:679–693. [5] Croat T. K. et al. 2003. *Geochimica et Cosmochimica Acta* 67:4705–4725.

5176

ISOTOPIC ANALYSIS OF THE SUN

T. R. Ireland and M. Asplund. Planetary Science Institute, The Australian National University, Canberra, Australia. E-mail: Trevor.Ireland@anu.edu.au

In order to understand the inventories of different isotopic systems in the solar system, solar isotopic compositions must be determined. Oxygen is particularly notable as there is a 5% range in $^{18}\text{O}/^{16}\text{O}$ and $^{17}\text{O}/^{16}\text{O}$ due primarily to the presence of a ^{16}O -rich reservoir in the early solar system mixing with isotopically normal (as seen from a terrestrial perspective) oxygen. Two popular models for the solar isotopic composition identify these end-members as the most appropriate. A normal composition is suggested by scaling in the solar system where increasingly large bodies (asteroids to Mars and Earth) show a similar ^{16}O abundance. On the other hand refractory inclusions from the early solar system are interpreted as solar condensates and the elevated ^{16}O abundance is taken as the solar value.

We have determined the solar oxygen isotopic composition by two means. Firstly, we have measured the isotopic composition of oxygen implanted in to Fe metal grains that have little intrinsic lunar oxygen. Secondly we have measured oxygen isotopes from the solar photosphere by observational means.

The oxygen isotopic composition measured from the lunar grains is enriched in ^{17}O and ^{18}O by 5.3 (± 0.3)% relative to terrestrial oxygen [1]. This is in good agreement with our new improved measurement of the solar photosphere that indicates $^{18}\text{O} = +4$ (± 6)% [2]. The relatively large error limits are also consistent with a normal (terrestrial) oxygen isotopic composition, but do not support a ^{16}O -rich composition for the Sun.

These observations suggest that the bulk protonebular oxygen isotopic composition differs from the composition of the residual planetary system. Such a situation will arise if there is a difference in isotopic composition between the dust and gas of the primordial molecular cloud. While the planetary system is entirely sourced from the dust component, the Sun also obtains a substantial fraction of its oxygen from carbon monoxide gas. The dust brings the refractory element inventory to the Sun, hence CI chondrites are a good representation of the solar abundances of the non-volatile elements.

References: [1] Ireland T. R., Holden P., Norman M. D., and Clarke J. 2006. *Nature* 440:776–778. [2] Scott P. C., Asplund M., Grevesse N., and Sauval A. J. *Astronomy and Astrophysics*. Forthcoming.

5264

MORE AFRICAN ENSTATITE-RICH METEORITES: AUBRITE NWA 2828, ZAKŁODZIE-LIKE NWA 4301, NWA 1840, AND EL6 CHONDRITES

A. J. Irving¹, S. M. Kuehner¹, T. E. Bunch², J. H. Wittke², D. Rumble III³, and G. M. Hupé. ¹Earth and Space Sciences, University of Washington, Seattle, Washington, USA. E-mail: irving@ess.washington.edu. ²Department of Geology, Northern Arizona University, Flagstaff, Arizona, USA. ³Geophysical Laboratory, Carnegie Institution, Washington, D.C., USA

Several very different types of enstatite-rich meteorites have been found recently in Northwest Africa.

Aubrite NWA 2828: Pale gray microbreccia composed mainly of twinned enstatite with subordinate plagioclase ($An_{13.5-15.3}Or_{3-4}$) and altered troilite (with daubreelite blades). Rare Mn alabandite, daubreelite, oldhamite, Ti-free troilite, and very rare kamacite specks are enclosed within enstatite.

Zakłodzie-Like Enstatite Achondrite NWA 4301: Mainly twinned pure enstatite with subordinate kamacite plagioclase ($An_{31-38}Or_{1.6}$) and troilite with subequigranular igneous cumulate texture (very similar to Zakłodzie [1]).

Enstatite Achondrite NWA 1840: Igneous texture with no chondrules; predominantly twinned enstatite with minor maskelynite (An_{42}), Si-bearing metal and Cr-rich troilite.

EL6 Chondrites NWA 3102 and NWA 3134: Very fresh (W0) paired specimens composed of enstatite ($En_{98.6-99.3}Wo_{1.2-0.6}$, 0.16–0.22 wt% Al_2O_3) and metal (1–2 wt% Si) with subordinate sodic plagioclase ($An_{9.9-11.9}Or_{6.0-4.7}$), troilite (Ti-poor, with rare daubreelite blebs), alabandite and fresh oldhamite. Rare partial chondrules are present.

EL6/7 Chondrite NWA 2965: Numerous small stones (probably paired with NWA 002 and NWA 1067) evidently are fragments of a very large (>100 kg), broken enstatite-rich meteorite characterized by compression fractures filled with terrestrial limonite and an overall metamorphic texture. We interpret rare round aggregates of fanning prismatic enstatite grains (in 1 out of 4 thin sections) to be recrystallized former RP chondrules. We suspect that NWA 2736 (classified as an aubrite by [2]) may be part of this same material.

Oxygen Isotopic Compositions: Means of replicate analyses by laser fluorination: NWA 2828 $\delta^{17}O = 2.895$, $\delta^{18}O = 5.530$, $\Delta^{17}O = -0.017$; NWA 1840 $\delta^{17}O = 2.793$, $\delta^{18}O = 5.229$, $\Delta^{17}O = +0.043$ per mil ($m_{TFL} = 0.526$). Analyses of NWA 2965, NWA 3134, and NWA 4301 are in progress.

Conclusions: We propose that all of these enstatite-rich meteorites originated on the same (fairly large) parent body. As we have argued for the CR parent body [3], there is evidence for a regolith which has been metamorphosed to varying degrees, as well as igneous rock bodies (NWA 011/2400 versus aubrites) produced by internal partial melting.

References: [1] Przylibski T. et al. 2005. Abstract. *Meteoritics & Planetary Science* 40:A185–A200; Grossman J. 2000. *The Meteoritical Bulletin* No. 84; Patzer A. et al. 2002. *Meteoritics & Planetary Science* 37: 823–833 [2] Lowe J. et al. 2005. Abstract #1913. 36th Lunar and Planetary Science Conference. [3] Bunch T. et al. 2005. Abstract #2308. 36th Lunar and Planetary Science Conference.

5288

OXYGEN ISOTOPES IN BRACHINA, SAH 99555, AND NORTHWEST AFRICA 1054

A. J. Irving¹ and D. Rumble III². ¹Earth and Space Sciences, University of Washington, Seattle, Washington, USA. E-mail: irving@ess.washington.edu. ²Geophysical Laboratory, Carnegie Institution, Washington, D.C., USA

Brachina: Oxygen isotope analyses by laser fluorination of two whole rock fragments (provided by M. Wadhwa) gave $\delta^{17}O = 1.59, 1.38$; $\delta^{18}O = 3.60, 3.21$; $\Delta^{17}O = -0.304, -0.307$ per mil. These $\Delta^{17}O$ values are more negative than earlier measurements ($\Delta^{17}O = -0.20$) [1], and also more negative than values for NWA 595 and NWA 3151, which have petrologic characteristics like brachinites [2]. We re-measured NWA 595 after more thorough acid-washing to remove terrestrial oxidation and obtained slightly different results from those we reported previously [2]: $\delta^{17}O = 2.11, 2.36, 2.33$; $\delta^{18}O = 4.33, 4.77, 4.78$; $\Delta^{17}O = -0.173, -0.162, -0.197$ per mil. NWA 4042 is petrologically and isotopically similar ($\Delta^{17}O = -0.154$) [3], and may be related to NWA 595 and NWA 3151 (with $\Delta^{17}O = -0.15 \pm 0.02$). However, if all these specimens (including Brachina) derive from the same parent body, then it must be isotopically quite heterogeneous.

Angrite SAH 99555: Analyses of disaggregated silicate material (provided by T. Kleine) gave $\delta^{17}O = 2.20, 2.06$; $\delta^{18}O = 4.32, 4.06$; $\Delta^{17}O = -0.077, -0.078$ per mil, which are essentially identical to results obtained for other angrites [4].

NWA 1054 is not an Acapulcoite but a Chondrite Related to Winonaites: Analyses of material (provided by M. Chinellato via N. Classen) gave $\delta^{17}O = 1.56, 1.44$; $\delta^{18}O = 3.74, 3.54$; $\Delta^{17}O = -0.408, -0.425$ per mil. We confirm that olivine is Fa_6 [5] and that chondrules definitely are present (see BSE images). Thus we infer that NWA 1054 is a Type 5 or 6 chondrite related to winonaites not acapulcoites (see [6]), and is likely paired with (or even part of the very same stone as) NWA 725, NWA 1052, NWA 1058 and NWA 1463 (which could usefully be termed “W chondrites”).

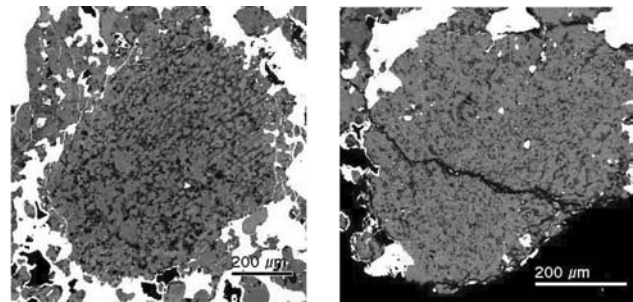


Fig. 1.

References: [1] Clayton R. and Mayeda T. 1996. *Geochimica et Cosmochimica Acta* 60:1999–2018. [2] Irving A. et al. 2005. Abstract. *Meteoritics & Planetary Science* 40:A73. [3] Connolly H. et al. Forthcoming. *Meteoritical Bulletin* No. 90. [4] Greenwood R. et al. 2005 *Nature* 435:916–918; Irving A. et al. 2005. Abstract #P51A-0898. *EOS*. [5] Moggi-Cecchi V. et al. 2005. Abstract #1808. 36th Lunar and Planetary Science Conference. [6] Rumble D. et al. 2005. *Meteoritics & Planetary Science* 40:A133.

5046

GLOBAL CATASTROPHIC CHANGES ON THE TERRESTRIAL PLANETS CAUSED BY LARGE IMPACTS: AN IMPLICATION TO THE PERMAFROST FORMATION ON MARS

Isaev V. S. and Kondrat'eva K. A. Geological Department, Moscow State University, Vorob'evy Gory, Moscow, Russia, 119899. E-mail: tpomed@rambler.ru

Introduction: A proposal of simultaneous global changing of all terrestrial planets has been made based on the hypothesis of periodical intersection of terrestrial planets in the Solar System with intergalactic asteroid flow [1] at the following periods: 3.6, 2.6, 1.65, 1.05 Gyr. This allowed us to find out some analogues between impacts on the Earth, the Moon, and Mars, as well as on Venus and Mercury and make some conclusions about the age of large impacts for the planets where direct age verification is impossible, as it was made for the Moon [2, 3, 4, 5] and the Earth [6, 1].

Discussion: The large impact craters influenced the global Earth climate by thermal regime changing, composition and intensity of sediment accumulation [9, 1]. The impactors lead first to the short-term heating of the atmosphere and the surface, then to the long-term cooling that is followed by glaciations [6]. Based on these conceptions and systematization of impacts on the Earth [7, 8], we inferred a paleotemperature curve for the Earth. Similar work was made for Mars, where the largest impacts were selected and the closest analogues on the Earth with the determined age have been found. Taking into account present environmental conditions on Mars, we made a paleoreconstruction of thermal regime on Mars through its history. Also, some particular features and common elements in the planet's evolution were defined and compared with the Earth and the Moon.

Conclusions: Due to specific conditions (thin atmosphere, low gravitation, and remote position from the Sun), we assume the next mechanism of large impacts interaction with Mars. Dust-icy material bringing by celestial bodies and icy material of the surface layers that was excavated by impacts led to the short-period formation of dense atmosphere highly saturated by water and carbonic acid on the planet. This water could be responsible for the appearance of catastrophic fluvial forms on the Martian surface. The later cooling due to the low transparency of dusty atmosphere followed by the freezing of short-term water-ice basins. Following accumulation of dust fraction covered the surface by dust layer and preserved water-ice saturated layers from evaporation.

Acknowledgements: This work is supported by fund of RFFI (# 04-05-65110).

References: [1] Barenbaum A. A. et al. 2004. Moscow University Bulletin. ser. 4, Geology, v. 3, pp. 3–16. [2] Tera F., Papanastassou D. A., and Wasserburg G. J. 1974. *Earth and Planetary Science Letters* 22:1–21. [3] Swindle T. D., Spudis P. D., Taylor G. J., Korotev R. L., Nichols R. H., Jr., and Olinger C. T. 1991. Proceedings, 21st Lunar and Planetary Science Conference. pp. 167–181. [4] Darliple G. B. and Ryder G. 1993. *Journal of Geophysical Research* 98:13,085–13,095. [5] Darliple G. B. and Ryder G. 1996. *Journal of Geophysical Research* 101:26,069–26,084. [6] Hain V. E. 2003. Second issue. Moscow Nauchnii Mir. p. 337. [7] Feldman V. I. 1987. *Meteoritika* 46:154–171. [8] Feldman V. I. 1993. *Meteoritika* 50:142–145. [9] Abbot D. H. and Isley A. E. 2002. *Earth and Planetary Science Letters* 205:53–62. [10] Boynton W. V. et al. 2002. *Science* 297:75–78.

5090

CONCENTRIC-ZONED INCLUSIONS IN THE KAUDUN METEORITE

M. A. Ivanova, N. N. Kononkova, and A. V. Ivanov. Vernadsky Institute of Geochemistry, Kosygin St, Moscow 119991, Russia. E-mail: venus2@online.ru

Introduction: The Kaidun meteorite contains a huge variety of different materials formed by multiple processes: 1) nebular condensation, gas metasomatism, agglomeration, nebular melting, 2) asteroidal impact melting, aqueous alteration, and transport of material, and 3) planetary igneous processes typical for large planets [1–3]. Here we report results from Kaidun clast #d6A, which contains many concentric-zoned inclusions formed by processes similar to terrestrial.

Results: Clast #d6A is 4 mm in size and consists of phyllosilicates, carbonates, and sulfides. It completely lacks anhydrous silicates. The clast has many inclusions with different sizes, textures and compositions. The most interesting of them are two concentric-zoned inclusions #d6Aa and #d6Ab. Both inclusions are surrounded by tiny sulfide-phyllosilicate rims. Inclusion #d6Aa consists of serpentine, replaced by talc along its periphery. In the serpentine, FeO and Al₂O₃ content increase from the center outward to the boundary with talc, while MgO and SiO₂ decrease. The talc is magnesian in composition. Inclusion #d6Ab consists of alternating zones enriched in either calcium carbonates or phyllosilicates (serpentine and chlorite) forming banded structure. The inclusions' cores are mostly carbonates with low Fe and Mg. In the central zones, serpentine and chlorite are present in equal proportions, while chlorite dominates at the periphery. Phyllosilicate compositions from different zones are quite similar.

Discussion: The sulfide rims surrounding inclusions in clast #d6A and the absence of anhydrous silicates indicate that it has experienced intense aqueous alteration. A sulfide-enstatite aggregate [4] in direct contact with #d6A suggests the alteration happened before the clast was incorporated into its current location. The serpentine-talc replacement in #d6Aa inclusion appears linked to carbonatization or silicification by Si-bearing fluids below 300 °C. The talc composition indicates silicification is more likely. Silicification is usual for contact metamorphism of large masses of ultramafic terrestrial rocks. Talc found in some thermally metamorphosed carbonaceous chondrites is enriched in Al and Na compared with common terrestrial talc. The talc of #d6Aa compositionally resembles terrestrial magnesian talc. This suggests that the altering fluid for the inclusion, whose talc is similar to terrestrial talc, probably had different composition than the fluid which produced the Al and Na talcs found in metamorphosed carbonaceous chondrites. Inclusion #d6Ab texturally resembles magnesian lime scars of progressive metamorphism and appears to have formed by metasomatic alteration of carbonates by SiO₂-Al₂O₃-bearing fluids below 400–500 °C. Given the overall characteristics of Kaidun, we suggest that objects #d6Aa and #d6Ab may have formed in a large, differentiated planet.

References: [1] Ivanov A.V. 1989. *Geochemistry International* 26:84–91. [2] Ivanov A.V. 2004. *Solar System Research* 38:150–156. [3] Zolensky M. E. and Ivanov A.V. 2003. *Chemie der Erde* 63:185–246. [4] Kurat G. et al. 2004. *Meteoritics & Planetary Science* 39:53–60.

5089

UNIQUE ZONED CHONDRULES IN THE ISHEYEVO CH/CBB-LIKE CHONDRITE AND THEIR AQUEOUS ALTERATION

M. A. Ivanova, C. A. Lorenz. Vernadsky Institute of Geochemistry, Kosygin St. 19, Moscow 119991, Russia. E-mail: venus2@online.ru

Introduction: The recently discovered Isheyevov CH/CBB-like chondrite consists of FeNi metal, chondrules, CAIs, and heavily hydrated matrix lumps which have no genetic relationships with other components [1]. The matrix lumps were the only objects in CH/CBB chondrites indicative of aqueous alteration [2]. However, we found several zoned chondrules surrounded by phyllosilicate rims. Here we report the results of studying of these chondrules and discuss their possible origin.

Results: Isheyevov contains chondrules with various textures, including several unusual zoned chondrules, 40–90 μm in size. They consist of magnesian Px or Ol cores and fayalitic rims (Fa_{60-72}), sometimes with small FeNi metal grains. Some chondrules have cryptocrystalline texture in the core and also contain two zones: magnesian in the core and ferrous in the rim with tiny FeNi blebs. Fe/Mn ratios of silicates dramatically change from the core (Fe/Mn 66–78) to the rim (Fe/Mn 141–175) of the chondrules. Similar objects were found in the CHs NWA 470 [3] and Acfer 182 [4]. The chondrule in NWA 470 had even three different zones: MgO-Opx, FeO-Opx, and FeO-Ol. Several zoned chondrules have phyllosilicate rims and magnesian Px or Ol core, sometimes with FeNi metal grains. No any relationships were observed between these phyllosilicate rims and other components of Isheyevov. Phyllosilicate compositions of the rims are in the range of the CMs but differ from the phyllosilicates of the hydrated matrix lumps, which are richer in Mg. FeO content in phyllosilicate rims is similar to that of fayalitic zones.

Discussion: The texture and mineralogy of zoned chondrules from Isheyevov, NWA 470, and Acfer 182 indicate an multistage formation. It appears that the core of MgO-rich pyroxene material formed first during condensation. Then, the pyroxene grew richer in FeO with decreasing temperature, or fayalite-rich olivine mantle condensed onto the pyroxene core in a region of highly oxidizing conditions. Thus, the zones record drastic changes in the physicochemical conditions of the environments where they formed. Phyllosilicate rims either probably were formed from the fayalitic zones of the chondrules in an icy region of the nebula by their reaction with impact-generated H_2O -vapor as proposed by Ciesla et al. (2003) [5], or the chondrules came from a different asteroid body that had experienced aqueous alteration. Phyllosilicate mantles around chondrules as found in Isheyevov have never previously been reported in CH/CBB chondrites. Regardless of the origin of zoned chondrules, their structures must have formed before final accretion of the parent body of Isheyevov as well as all CH and CBB chondrites components (matrix lumps, chondrules, CAIs, FeNi-metal grains) were formed before their accretion into the CH/CBB chondrite parent body.

References: [1] Ivanova M. A. 2006. Abstract #1100. 37th Lunar and Planetary Science Conference. [2] Krot A. N. et al. 2002. *Meteoritics & Planetary Science* 37:1452–1490. [3] Ivanova M. A. et al. 2001. Abstract. *Meteoritics & Planetary Science* 36:A88. [4] Hezel D. 2002. Abstract #1787. 33rd Lunar and Planetary Science Conference. [5] Ciesla F. J. et al. 2003. *Science* 299:549–552.

5261

NEUTRAL GAS AND ION MEASUREMENTS WITH THE REFLECTRON-TYPE TIME OF FLIGHT MASS SPECTROMETER ROSINA-RTOFA. Jäckel, M. Rubin, K. Altwegg, P. Wurz, H. Balsiger¹, U. Mall², and H. Rème³. ¹Physikalisches Institut, Universität Bern, CH-3012 Bern, Switzerland. E-mail: jaeckel@space.unibe.ch. ²Max-Planck-Institut für Sonnensystemforschung, D-37191 Katlenburg-Lindau, Germany. ³Centre d'Etude Spatiale des Rayonnements, F-31028 Toulouse, France

Introduction: On March 2, 2004, the European Space Agency (ESA) successfully launched the Rosetta spacecraft that will rendezvous with comet 67P/Churyumov-Gerasimenko (C-G) in November 2014. Onboard this spacecraft is, among other instruments, the ROSINA (Rosetta Orbiter Spectrometer for Ion and Neutral Analysis) instrument package comprising two mass spectrometers, a cometary pressure sensor, and a data processing unit [1]. The two mass spectrometers DFMS (Double Focusing Mass Spectrometer) and RTOF (Reflectron-type Time of Flight mass spectrometer) are designed to analyze the volatile material in the vicinity of C-G and to quantify the molecular and isotopic composition of C-G during the conjoint journey towards the Sun and throughout the perihelion passage. Here, we report on RTOF neutral gas measurements from space and the first RTOF ion measurements with a low energy ion source in the lab.

RTOF Characterization: The RTOF sensor consists of four different parts [2]. The first part is the source region, in which two independent ion sources are located. The electron impact ion storage source is used to store ions which are continuously produced from incoming cometary neutrals by electron bombardment. These ions are extracted by a short high-voltage pulse and are further accelerated into the time of flight system. In the second source, the orthogonal extraction ion source, the incoming primary cometary ions are directly pulsed onto the time of flight path, again by means of a high-voltage pulse. The second part of the sensor is the time of flight section, which consists of the field-free drift path (length ~ 1 m) and two ion mirrors facing each other for multiple reflections of the ion trajectories. The RTOF sensor houses two separate MCP (multi channel plate) detectors (third part), one for the cometary neutrals and one for cometary ions. The fourth part of RTOF is the electronic box that houses eight electronic boards.

Discussion: The RTOF sensor complements DFMS with an extended mass range from 1 to > 300 amu/e and a high sensitivity. An advantage of the RTOF sensor is that within 100 μs a full mass spectrum is recorded over the entire mass range. The recorded mass range is only limited by the signal accumulation memory. The mass resolution in the triple reflection mode is $m/\Delta m > 4500$ at the 50% peak height. During the calibration program we could demonstrate that RTOF has a wide dynamic range. Therefore, in the environment of C-G, RTOF will be able to cope with highly variable outgassing rates and will measure the minor constituents of the volatile material. Species with partial pressure $< 10^{-12}$ mbar are detected. Measurements in the lab with a specially constructed low energy ion source [3] have been performed in order to calibrate the ion measurements of the RTOF sensor. This source has been designed to simulate the cometary ions which have energies well below 20 eV.

References: [1] Balsiger H. et al. *Space Science Reviews*. Forthcoming. [2] Altwegg K. et al. 2004. *Astrophysics and Space Science Library*. [3] Rubin M. 2006. Ph.D. Thesis, University of Bern, Bern, Switzerland.

5323

SUPERNOVA GRAPHITE GRAINS FROM ORGUEIL

M. Jadhav, S. Amari, T. Maruoka¹, and E. Zinner. Laboratory for Space Sciences, Washington University, Saint Louis, Missouri 63130, USA. E-mail: manavjadhav@wustl.edu. ¹Present address: Graduate School of Life and Environmental Sciences, University of Tsukuba, Ibaraki 305-8572, Japan

Introduction: In previous studies [1–3], some of the graphite grains from the low-density fraction of Orgueil, ORG1d (~1.75–1.92 g cm⁻³; grain sizes > 1 μm), were found to have isotopic signatures in N, O, and Si that indicated a supernova (SN) origin. In a continued attempt to better understand SN graphite grains, we isolated ORG1d candidate grains from the large amounts (much larger than in graphite separates from Murchison) of macromolecular carbonaceous material, in which the graphite grains are often found embedded. This was done to reduce contamination from this carbonaceous material and, hence, facilitate the isotopic analyses. Here we present C, N, O, Si, and Al-Mg isotopic data obtained with the NanoSIMS, for the grains of this fraction. The same grains will be analyzed for Ti isotopes and, eventually, heavy element isotopes (Sr, Zr, Mo, Ru, Ba) by resonant ionization mass spectrometry (RIMS) with CHARISMA.

Experimental: Spherical, carbonaceous grains identified by X-ray analysis in the SEM were picked with a micromanipulator and deposited on a gold-foil mount. Isotopic analyses of these grains were carried out in the NanoSIMS. Negative secondary ions of ¹²C, ¹³C, ¹²C¹⁴N, and ¹²C¹⁵N (analysis phase 1) and ¹⁶O, ¹⁸O, ²⁸Si, ²⁹Si, and ³⁰Si (phase 2) produced by bombarding the sample with a Cs⁺ primary beam were counted in multidetection mode. In phase 3 of the analysis, positive secondary ions of ¹²C, ²⁴Mg, ²⁵Mg, ²⁶Mg, and ²⁷Al produced with an O⁻ beam were detected.

Results and Discussion: 18 of the 41 candidate carbonaceous grains were found to be presolar, as indicated by their ¹²C/¹³C ratios that vary from 6 to 910. We found 12 grains that contain ¹⁸O excesses, with ¹⁸O/¹⁶O ratios of up to 15 times the solar value. 8 of these grains also exhibit ¹⁵N excesses and 6 contain ²⁸Si excesses. These signatures indicate a SN origin for these grains [4]. In addition, 17 grains exhibit large ²⁶Al/²⁷Al ratios (up to 0.33) that were derived from ²⁶Mg excesses. In Fig. 1, we compare the ²⁶Al/²⁷Al ratios of these grains with those of graphite grains from the Murchison KE3 low-density fraction [4]. The high ²⁶Al/²⁷Al ratios we found now were probably not seen in the previous study of grains from ORG1d [3] because of the large ²⁴Mg and ²⁷Al signals obtained from the contamination present on that mount. All the grains with ¹⁸O, ¹⁵N, and ²⁸Si excesses have high ²⁶Al/²⁷Al ratios indicating that they are bona fide SN grains.

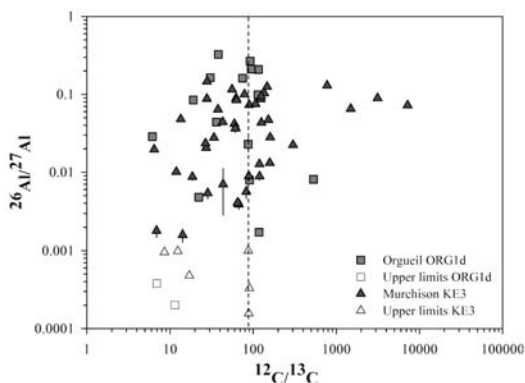


Fig. 1.

References: [1] Jadhav M. et al. 2005. Abstract #1976. 36th Lunar and Planetary Science Conference. [2] Jadhav M. et al. 2005. Abstract. *Meteoritics & Planetary Science* 40:A75. [3] Jadhav M. et al. 2006. Abstract #2177. 37th Lunar and Planetary Science Conference. [4] Travaglio C. et al. 1999. *The Astrophysical Journal* 510:325–354.

5212

U-Pb DATA ON CLEAN MINERALS FROM NAKHLITES

E. Jagoutz, G. Dreibus, R. Jotter, A. Kubny, and Zartman R. Max-Planck-Institut f. Chemie, P.O. Box 3060, D-55020 Mainz, Germany. E-mail: jagoutz@mpch-mainz.mpg.de

Introduction: Nakhilites constitute about one-fifth of about 30 known Martian meteorites. Among the finds are the recently discovered two nakhilites, Y-000593 and Y-000749, from the Yamato Mountains [1] and MIL 03346 found in the Miller Range. All nakhilites have basaltic composition and a cumulate texture. From electron microscope (EM) and microprobe imagery the olivine and augite are seen to be zoned in major and trace elements. Our Pb and Nd isotopic results have already been presented at the recent Lunar and Planetary Science Conference [2, 3], and here we report U-Pb results on ultra-clean mineral separates. Previously determined Rb-Sr and Sm-Nd mineral ages for Nakhla are about 1.3 Ga. A similar ²³⁸U-²⁰⁶Pb age was measured on a baddeleyite containing residue fraction of the leached meteorite. However, for combined leach and residue fractions have ²⁰⁷Pb-²⁰⁶Pb ages >2 Ga, and the Pb-Pb isochron plot show considerable scatter [2–5]. In this study, we try to better define the initial Pb isotopic composition of nakhilites.

Plagioclase and pyroxene separates were obtained by hand-picking under the binocular microscope. The pyroxene was then further crushed to 50 μ, and separated into high-Fe and low-Fe fractions using a magnetic separator. Pyroxene analyses were made on only optically pure grains, and both pyroxene and plagioclase were additionally acid-washed to avoid surface contamination. The same technique was then applied to other nakhilites from the Antarctic NIPR collection and NASA (MIL 03346) with similar results, indicating that all nakhilites may have the same age.

Results: An identical initial Pb isotopic composition indicates that all of these meteorites were derived from the same homogeneous source. Moreover, it is strongly suggested by their initial Pb that the “olivine shergottites,” like SaU 005, DaG 476, and Y-980459, as well as the basaltic shergottite QUE 94201 [6], likewise come from this Nakhla source. While “normal” shergottites like Shergotty and Los Angeles, for example, are from sources having a more evolved Pb isotopic composition, “olivine shergottites” are clearly younger than nakhilites. Their Sm-Nd and Rb-Sr isotopic systems are highly disturbed. Analyzing the existing data, we favor an age of 800 Myr for the “olivine shergottites,” which is also suggested by Ar-Ar systematic.

The Nakhla reservoir was sampled at least 2 times: at 1300 Myr (nakhilites) and at 800 Myr (olivine shergottites). However, the Pb isotopic composition plots close to the Geochrone at a ²³⁸U/²⁰⁴Pb of about 2. This gives interesting implications for the evolution of this reservoir and their parent body.

References: [1] Imae N. et al. 2002. Abstract #1483. 33rd Lunar and Planetary Science Conference. [2] Jagoutz E. and Jotter R. 2000. Abstract #1609. 31st Lunar and Planetary Science Conference. [3] Jagoutz E. et al. 2001. Abstract #1307. 32nd Lunar and Planetary Science Conference. [4] Chen J. H. and Wasserburg G. J. 1986. Abstract. 17th Lunar and Planetary Science Conference, pp. 113–114. [5] Nakamura N. et al. 1982. *Geochimica et Cosmochimica Acta* 46:1555–1574. [6] Gaffney A. M. et al. 2006. Abstract #1483. 37th Lunar and Planetary Science Conference.

5242

SECONDARY FAYALITE IN THE VIGARANO CV3 CARBONACEOUS CHONDRITE: OCCURRENCE AND FORMATION AGE

K. Jogo¹, T. Nakamura¹, and T. Noguchi². ¹Department of Earth and Planetary Sciences, Kyushu University, Fukuoka, Japan. E-mail: kaori@geo.kyushu-u.ac.jp. ²Department of Materials and Biological Sciences, Ibaraki University, Ibaraki, Japan

Introduction: Vigarano meteorite, classified to reduced sub-group of CV3 chondrite (CV3_{Red}) [1], is one of the most primitive solid materials in the solar system. However, it is known that Vigarano experienced very weak aqueous alteration, which resulted in the formation of secondary fayalite [2]. In the present study, we made detailed characterization of many fayalite grains in Vigarano and then determined formation age of the fayalite based on Mn-Cr system using an ion probe at Kyushu University in order to constrain the early evolution of a CV3_{Red} Vigarano asteroid.

Results and Discussion: The SEM and FE-SEM observation indicates that, among twenty-three chondrules investigated, only four POP chondrules have fayalite-magnetite-troilite veins (~10 × 100 μm in size) that extend from large troilite-magnetite inclusions at chondrule surfaces to exterior matrix. Fayalite grains in the veins are smaller than 20 μm in size. The four POP chondrules having the veins have fine-grained rims around them. The rims and the enclosing chondrules comprise discrete clasts which can be recognized by the boundary lines to Vigarano host by SEM observation. The fayalite-magnetite-troilite veins terminate at the boundary. The mineralogy of the clasts suggests that they are probably Bali-like oxidized material CV3_{OxB} [3, 4].

Within the fayalite grains iron-magnesium zoning is commonly observed: high Fa# at the center and low Fa# at the rim (Fa# = 95–72). This indicates that at the early stage of the alteration almost pure fayalite formed and later the rim of the fayalite became enriched in MgO, approaching equilibrium with matrix olivine (Fa₅₀). Ion-probe analysis was performed on an interior portion of the biggest fayalite (10 × 20 μm in size, Fa₉₅ at the center, and high MnO content of 0.6 wt%). The Mn-Cr data for the fayalite defines an initial ⁵³Mn/⁵⁵Mn ratio of (2.19 ± 0.53) × 10⁻⁶. This ratio indicates that Vigarano pure fayalite formed 3 ± 1 Ma before angrites. An absolute age was also determined to be 4561 ± 1 Ma. The obtained age corresponds to the time of pure fayalite formation induced by early aqueous alteration in a CV asteroid.

CV3_{Red} Vigarano meteorites consist of both CV3_{OxB} and CV3_{Red} materials. This implies that Vigarano is a breccia. The preferential occurrence of fayalites in the clasts of CV3_{OxB} suggests that the fayalite formation did not take place in situ in the present structure of Vigarano: the fayalites had formed in a different location of the Vigarano asteroid or in a different CV asteroid where the alteration was very active. The obtained fayalite formation age of Vigarano is identical within errors to that of CV3_{OxB} Mokoia [5] and CV3_{OxB} Kaba [6]. This identical match indicates that the CV3_{OxB} clasts in the Vigarano CV3_{Red} meteorite formed in the period same as other CV3_{OxB} meteorites.

References: [1] McSween H. Y., Jr. 1977. *Geochimica et Cosmochimica Acta* 41:1777–1790. [2] Krot A. N. et al. 2004. *Antarctic Meteorite Research* 17:153–171. [3] Krot A. N. et al. 2000. *Meteoritics & Planetary Science* 35:817–825. [4] Weisberg M. K. and Prinz M. 1998. *Meteoritics & Planetary Science* 33:1087–1099. [5] Hutcheon I. D. 1998. *Science* 282:1865–1867. [6] Hua X. et al. 2004. *Geochimica et Cosmochimica Acta* 69:1333–1348.

5210

TEXTURAL EVIDENCE FOR MELT PROCESSES ON THE PALLASITE PARENT BODY

D. Johnson¹, R. Hutchison², and M. M. Grady^{1,2}. ¹Open University, Walton Hall, Milton Keynes, MK7 6AA, UK. E-mail: D.Johnson@open.ac.uk. ²Natural History Museum, London SW7 5BD, UK

Introduction: Pallasites are generally ~50:50 mixtures of iron-nickel metal and olivine; iron sulfides are normally present only as a minor phase. We have recently described [1] a new unusually sulfide-rich pallasite. Irregular distribution of its metal, sulfide, and olivine yields clues to the origin and evolution of main group pallasites. It has been suggested [2, 3] that cooling and evolving IIIAB iron metallic melt should form two immiscible liquids when the sulfur to phosphorous ratio exceeds 25. We have observed textures that support this view.

Observations: The meteorite has marginal, olivine-rich regions composed of sub-rounded, ~cm-sized crystals forming a granular mosaic. Towards the interior, this gives way to metal-rich or sulfide-rich regions in which the olivines tend to be fragmented, angular and smaller in size. There seems little doubt that where metal is host to angular olivine, the silicate was solid and brittle when enveloped in molten metal [4]. A similar textural relationship exists between olivine and sulfide, but the latter intrudes the olivines as fracture-filling veins <1 mm thick that carry sub-rounded to angular sub-mm fragments of olivine. Sulfide veining commonly occurs to the exclusion of metal.

Discussion: The ability of sulfide to have been injected along sub-mm channels indicates that it was more fluid than metal. The tendency for metal and sulfide to be segregated is consistent with their occurrence as two immiscible liquids, as attested by the textural relationship between olivine fragments and metallic or sulfide hosts.

Conclusions: The new pallasite provides strong support for the separation of immiscible metallic and sulfide-rich liquids during pallasite genesis. Such evidence had previously been sought [3], but, until now, was lacking.

References: [1] Johnson D., Hutchison R., Grady M. M. and Kirk C. 2006. Abstract #5216. *Meteoritics & Planetary Science* 41. This issue. [2] Ulff-Møller F. 1998. *Meteoritics & Planetary Science* 33:207–220. [3] Ulff-Møller et al. 1998. *Meteoritics & Planetary Science* 33:221–227. [4] Scott E. R. D. 1977. *Geochimica et Cosmochimica Acta* 47:693–710.

5216

HAMBLETON—A NEW SULFUR-RICH PALLASITE

D. Johnson¹, R. Hutchison², C. Kirk², and M. M. Grady^{1,2}. ¹Open University, Walton Hall, Milton Keynes, MK76AA, UK. E-mail: D.Johnson@open.ac.uk. ²Natural History Museum, London, SW7 5BD, UK

Introduction: A new pallasite, a single mass of 17.6 kg, was found south of Hambleton, North Yorkshire, by R. and I. Elliott in August 2005. The mass is composed of ~60 vol% olivine, ~25 vol% metal, and ~15 vol% sulfide. The phases are irregularly distributed and highly weathered. Here we present the results of a study by optical and analytical scanning electron microscopy.

Observations: Olivine occurs as cm-sized sub-rounded crystals in a granular mosaic. Many contain sub-parallel sets of fractures, some of which are annealed, while others are filled with metal or sulfide. In metal-rich or sulfide-rich areas olivines are fragmented and angular to sub-angular and veined by metal or sulfide respectively. Some regions <5 cm in size are composed entirely of olivine crystals enclosed within troilite. Olivine is Fo_{88,3}, and together with the oxygen isotopic ratios: $\delta^{17}\text{O} = +1.383\text{‰}$; $\delta^{18}\text{O} = +3.029\text{‰}$; $\delta^{17}\text{O} = -0.187\text{‰}$, indicate that the meteorite is a main group pallasite. From the olivine-rich exterior, weathering has penetrated for 4–5 cm towards the interior of the mass. The weathered, olivine-rich outer portion is brittle and prone to disintegration. A blue secondary mineral rich in Mg, P, and Fe was shown by XRD to be baricite (Mg, Fe)₃(PO₄)_{2,8}H₂O. Much of the metal has succumbed to terrestrial oxidation, especially low-Ni phases such as kamacite, cloudy taenite, or plessite. The sulfide is more susceptible to terrestrial alteration than the metal.

Discussion: Metal rich regions are consistent with the view of Scott [1] that pallasites formed by the injection of metallic liquid into dunite. Evolved metallic melts, related to IIIAB irons, should be sulfur-rich. Paucity of sulfide in pallasites led Ulf-Møller et al [2] to suggest that either FeS-rich liquid was lost or formed pallasites that are underrepresented in our samples.

Conclusions: With Phillips County (pallasite), Hambleton is a rare FeS-rich pallasite.

References: [1] Scott E. R. D. 1977. *Geochimica et Cosmochimica Acta* 47:693–710. [2] Ulf-Møller et al. 1998. *Meteoritics & Planetary Science* 33:221–227.

5221

THE PETROGRAPHY AND GEOCHEMISTRY OF LUNAR REGOLITH BRECCIA MET 01210

K. H. Joy^{1,2}, I. A. Crawford¹, and S. S. Russell². ¹University College London, UK. E-mail: K.Joy@ucl.ac.uk. ²The Natural History Museum London, UK

Introduction: MET 01210 [1] is an anorthosite bearing basaltic lunar regolith breccia [2] that is dominated by clast and mineral fragments consolidated in a predominately mare region of the Moon [3]. The MWG sections studied in this investigation (MET 01210,21 and MET 01210,27) have vesicular fusion crusts and are composed of an immature breccia sample with rock (<4 mm) and mineral fragments (<1 mm) fused in a fine grained crystalline and glass matrix.

Analytical Methods: Mineralogical analysis was done at the NHM using a WDS Cameca SX-50A and elemental mapping was performed using a LEO 1455VP EDS SEM fitted with Oxford Instrument's INCA analysis software.

Observations: Mare basalt fragments in MET 01210 have a range of textures. Examples of mare material include rapidly crystallized fine grained clasts that have a distinctive feathery or plumose texture with a low-Ti affinity. Holocrystalline, coarser grained ferro-basalt fragments have large zoned pyroxenes (<500 μm En₁₋₄₇ Fs₂₇₋₈₆ Wo₁₀₋₃₀), evolved Low-Ti-VLT bulk compositions and some examples include small fractionated mesostasis assemblages (silica, fayalite, K feldspar, glass, apatite, whitlockite). Additional clasts of very fine-grained/granular symplectites of silica, fayalite and hedenbergite are the collective breakdown products of pyroxferroite. Mineral fragments in the matrix are predominantly associated with a fractionated mare basalt parentage.

MET 01210 also contains a non-mare anorthositic component including fragments of anorthositic norite, feldspathic meta-igneous clasts and granulites with Mg-rich mafic phases. Additional material in our sections includes small fragments of feldspathic impact melt derived rocks, glass beads (20–100 μm : including one with a HASP composition [4, 5]) and small melt veins.

Discussion: The mineralogical and clast assemblage of MET 01210 is dominated by Fe-enriched, low-Ti mare basalt material with a minor anorthositic component. The bulk rock composition was reported by [3] and is similar to typical average mare soils with elevated Al₂O₃ and depleted MgO as a consequence of additional mixing with anorthositic material. Bulk rock Th (0.86 ppm [3]) is comparatively low for mare regolith breccia material [7] suggesting that the mare components in MET 01210 did not experience KREEP assimilation and are likely to have been emplaced distally to the PKT.

References: [1] Russell S. S. et al. 2004. *The Meteoritical Bulletin* No. 88. *Meteoritics & Planetary Science* 39:A215–A272. [2] Korotev R. L. 2005. *Chemie der Erde* 65:297–346. [3] Joy K. H. et al. 2006. Abstract #1247. 37th Lunar and Planetary Science Conference. [4] Kempa M. J. and Papike J. J. 1980. Abstract. 11th Lunar and Planetary Science Conference. pp. 609–610. [5] Huber H. and Warren P. H. 2005. Abstract #2401. 36th Lunar and Planetary Science Conference. [6] Heiken et al. 1991. *The lunar sourcebook*. New York: Cambridge University Press. pp. 450–451. [7] Korotev R. L. 2001. Abstract #1234. 32nd Lunar and Planetary Science Conference.

5019

A POSSIBLE 552 A.D. COMET SIGHTING IN JAPAN AND ITS PARALLELS WITH COMETARY PHENOMENA ASSOCIATED WITH THE SARASVATI RIVER OF ANCIENT INDIA

Robert A. Juhl¹ and RN Iyengar². ¹Independent researcher, Penang, Malaysia. ²Department of Civil Engineering, Indian Institute of Science, Bangalore, India. E-mail: AD552@mac.com; rmi@civil.iisc.ernet.in

Introduction: The Enoshima Engi (EE) was written in 1047 A.D. by the Japanese monk Kokei. The narrative mentions spectacular phenomena that took place in the early summer of 552 A.D., including dark clouds covering the sea, earthquakes, the appearance of a bright goddess (Benzaiten/Sarasvati) above the clouds, boulders falling from the sky, lightning bolts, rocks and sand spurting up from the sea, flames on the water, the emergence of an island, and the descent of the goddess onto the island. In 2003, Juhl translated and studied parts of the EE [1].

The Prabhasa-ksetra-mahatmya book (PK) of the Skanda-purana contains references to similar phenomena associated with the Sarasvati River. In 2004, Iyengar published an article on comet-related phenomena in the PK [2].

Discussion: Following is a list of possible comet-related parallels in the PK. All parallels with the EE listed below are from Juhl [1].

The PK mentions objects making holes in the ground in association with a smoky demon [3]. The EE parallel is the “dark clouds covering the sea” and “great boulders descending from above the clouds.”

In one episode, the Sarasvati River, carrying fire, enters the ocean. Iyengar translates: “With fire in his hand, the ocean lit up ... Due to the gases emanating from the sea, the waters overflowed.” [4] The EE parallel is the description “flames flickered amidst the white-tipped waves.”

The level of the sea apparently rose and dropped. Iyengar writes: “after the fire started burning, initially the sea exceeded its boundaries but later the coast started receding ... In the 346th chapter, there is reference to large-scale loss of life associated most probably with a ... tsunami” [5]. The EE parallel is the loss of life as the dragon (the floodwaters) invaded the villages.

The PK has a chapter entitled Sarasvati-avatara-mahima-varnamam, meaning “description of the purpose of the avatara (descent) of Sarasvati” [6]. The EE parallel is the descent of Benzaiten from the sky.

Iyengar comments on a related story: “The further verses indicate that a metallic object eventually landed on earth, leading to earthquakes.” [7]. The EE parallel is the earthquakes before the descent of the goddess.

Conclusions: Most of the phenomena described in the EE are similar to phenomena in the PK. However, they are not copies, only similar. The presence of similar phenomena in unrelated Indian and Japanese records suggest that the phenomena actually did take place substantially as described. A fuller account of the parallels is on the Internet [8]. The phenomena may be comet/meteor related and deserve further investigation.

References: [1] Juhl R. A. 2003. <http://www2.gol.com/users/terukoj/TranslationSeg-2.html> and <http://www2.gol.com/users/bartraj/goddessindex-1.html>. [2] Iyengar R. N. 2004. *Indian Journal of History of Science* 39:11–49. Available as pdf at <http://civil.iisc.ernet.in/~rmi/ancientdisaster.pdf>. [3] Iyengar R. N. 2004. p. 7. [4] Iyengar R. N. 2004. p. 11. [5] Iyengar R. N. 2004. pp. 11 and 16. [6] Iyengar R. N. 2004. p. 16. [7] Iyengar R. N. 2004. p. 22. [8] Juhl R. A. <http://www2.gol.com/users/bartraj/ParallelsWSarasvatiR.html>

5385

ION MICROPROBE REE ANALYSES OF THE YAMATO-983885 LUNAR METEORITE

H. Kaiden^{1,2} and T. Arai¹. ¹Antarctic Meteorite Research Center, National Institute of Polar Research, Tokyo 173-8515, Japan. E-mail: kaiden@nipr.ac.jp. ²Department of Polar Science, School of Multidisciplinary Sciences, The Graduate University for Advanced Studies, Tokyo 173-8515, Japan

Introduction: Yamato (Y-) 983885 is a polymict regolith breccia derived from the Moon [1]. The meteorite contains various lunar crustal rocks such as Mg-rich rocks and a KREEP basalt, which is first reported among the lunar meteorites [2]. Here we report a preliminary ion microprobe REE data for individual minerals from the Y-983885 lunar meteorite and implications for parent melt compositions of the Mg-rich clasts to better understand their connection to KREEP.

Sample and Methods: A polished thin section (PTS) Y-983885,59-2 used in this study is described in detail by Arai et al. [2]. Ion microprobe analyses were carried out on the SHRIMP II at the National Institute of Polar Research, Japan. A modified energy filtering technique [3] was used to discriminate against complex molecular interferences.

Results and Discussion: Y-983885 contains a variety of clasts consisting of a KREEP basalt, a Mg-rich troctolite/norite, a high-Al basalt, a very low-Ti basalt, and a granulite originated from ferroan anorthosite [2]. In this study, we focus on the Mg-rich troctolite, which is composed of Ca-rich plagioclase (59.6 vol%), Mg-rich olivine (23.4 vol%), low-Ca pyroxene (15.5 vol%), and other minor/trace phases [2]. Two spots on plagioclase and three spots on pyroxene in the troctolite were analyzed. Plagioclase is LREE-enriched with La $\sim 10 \times$ chondrite and Lu $\sim 0.5 \times$ chondrite and displays a large positive Eu anomaly. Pyroxene is La $\sim 1 \times$ chondrite and Lu $\sim 20 \times$ chondrite with a negative Eu anomaly. These chondrite-normalized REE abundances of each mineral are broadly consistent with previous ion microprobe studies of Apollo samples [4, 5]. Using these REE abundances with appropriate partition coefficients, we can calculate the parent magma compositions, which can demonstrate a connection between Mg-rich rocks and KREEP basalt.

References: [1] Kaiden H. and Kojima H. 2002. *Antarctic Meteorites* 27. pp. 49–51. [2] Arai T. et al. 2005. *Antarctic Meteorite Research* 18:17–45. [3] Ireland T. R. et al. 1994. *Earth and Planetary Science Letters* 128:199–213. [4] Papike J. J. et al. 1996. *Geochimica et Cosmochimica Acta* 60:3967–3978. [5] Shervais J. W. and McGee J. J. 1998. *Geochimica et Cosmochimica Acta* 62:3009–3023.

5003

DEMONSTRATION OF CRYSTAL FORSTERITE AND STALL STATE GRAIN FORMATIONS

C. Kaito¹, S. Sasaki, Y. Miyazaki, M. Kurumada, A. Kumamoto, H. Suzuki, Y. Kimura, and C. Koike³. ¹Department of Nanophysics in Frontier Projects, Ritsumeikan University, Shiga 525-8577, Japan. E-mail: Kaito@se.ritsumei.ac.jp, ²Laboratory of Physics, Kyoto Pharmaceutical University, Kyoto 607-8414, Japan

Introduction: Astromineralogy has been started due to the presence of crystalline silicate dust by the Infrared Space Observatory and detection of presolar grains [1]. Some experiments based on gas-solid condensation from Mg-Fe-SiO-H₂-O₂ vapors, yielded various phases without olivine or enstatite crystals [2, 3]. We demonstrated the film condensed from vapor phase of SiO and Mg by co-evaporation from different evaporation sources were not mixed at room temperature [4]. Forsterite crystal grains were produced by dropping SiO powder into MgO flame in a mixture gas of Ar and O₂ [5], and/or the coalescence growth of Mg and SiO smokes [6] or MgO and SiO₂ smokes [7]. In the present paper, we showed that the forsterite crystal and stall state grains were produced by the simultaneous flush evaporation technique of different mixture powders of Mg and SiO, i.e., different mixture ration of Mg and SiO vapor was important factor for the formation of amorphous stall and crystal forsterite formation.

Experimental: Mixtures of Mg and SiO powders of different weight ratios were prepared, i.e., Mg: SiO = 1:1, 1:2, 1:3 and 1:4. These mixture powders were dropped on a heated V-shaped Ta boat at 2000 °C in a mixture of Ar (70 Torr) and O₂ (10 Torr) gases. The dropped mixture powders were evaporated before they reached the boat in the mixture gas. Therefore smoke particles were produced.

Results and Discussion: The 1:1 and 1:4 mixture ratio samples showed typical crystal and amorphous grains. Amorphous particles were composed of spherical of 100 nm order. The Mg₂SiO₄ crystal grains showed the polyhedral shape. With the increment of SiO powder, the spherical Mg₂SiO₄ crystal grains were selectively produced. The spherical grains produced from the powder with 1:3 ratio showed the amorphous grains. HRTEM image of this particles showed the existence of microcrystallites with the size of 2 nm order which can be identified as the Mg₂SiO₄ crystallites by HRTEM. The IR spectrum of this sample showed the stall state which was postulated in the paper on the infrared changes observed in magnesium silicates during thermal annealing [8, 9]. The spectrum of 1:3 specimen corresponds to a silicate revolution index (SEI) of 0.78–2.00 of the stall state. The crystalline and amorphous absorption spectra different with the stall state are clearly elucidated.

References: [1] Henning Th. et al. 2002. *Astromineralogy*. [2] Nuth J. A. III. et al. 1988. *Experiments on cosmic dust analogies*. 191 p. [3] Rietmeijer F. J. M. et al. 1999. *The Astrophysical Journal* 527:395. [4] Suzuki N. et al. 2000. *Meteoritics & Planetary Science* 35:269–1273. [5] Kaito C. et al. 1993. *Geomagnetism and Geoelectricity* 45:103. [6] Kaito C. et al. 2003. *Meteoritics & Planetary Science* 38:49–57. [7] Kamitsuji K. et al. 2005. *Astronomy and Astrophysics*. 429:205. [8] Hallenbeck S. L. and Nuth J. A. 1998. *Astrophysics and Space Science* 255:427. [9] Hallenbeck S. L. et al. 2000. *The Astrophysical Journal* 535:247–255.

5193

THE COSMOCHEMICAL Cs PROBLEM

A. P. A. Kallio and T. R. Ireland. Research School of Earth Sciences, Australian National University, Canberra ACT0200, Australia. E-mail: antti.kallio@anu.edu.au

The alkali elements are relatively abundant and highly incompatible, and therefore useful for studying planetary differentiation. Alkali elements are also both volatile and fluid mobile and hence difficult to constrain. The constituents of primitive chondrites have experienced various degrees of hydrous alteration and thermal processing and it is uncertain whether the measured values of Rb and Cs from bulk meteorites represent the solar system. There are no measurements of the Cs content of the Sun and the solar values for Rb are not the same as for CI meteorites [1]. Without a good reference frame from meteorites and solar measurements, it is difficult to model the Rb and Cs abundances in the primitive mantle of the Earth.

A 50% nebular condensation temperature is often used as a measure of volatility for an element. However, condensation temperatures for specific elements are model dependent and can vary a lot. Heating experiments of primitive meteorites show variable fractionations of Rb and Cs so the retentivity of these elements is definitely host dependent and the quantification of volatile behavior is not straight forward. For example, bulk Murchison (CM2) is depleted in volatile elements compared to CIs, but has the same Rb/Cs ratio. The contributions from thermal and aqueous processing in the bulk values are unclear.

To take hydrous alteration out of the equation, olivine-hosted glass inclusions from the Murchison (CM2) meteorite have been analyzed with electron microprobe, SHRIMP and LAICPMS, to study the distribution of Rb and Cs and other trace elements in these primitive materials. CI normalized patterns for refractory elements are flat for both glass inclusions and bulk Murchison. Volatile elements Rb, Cs and Pb are depleted in glass inclusions relative to the refractories, with increasing depletion in that order. The Rb/Cs ratios in the glass inclusions are significantly higher than bulk Murchison (and CI), which could either be inherited from the source of the inclusions or possibly caused by thermal volatilization during formation of the inclusions and their hosts.

References: [1] Asplund M. et al. 2005. In *Cosmic abundances as records of stellar evolution and nucleosynthesis*. San Francisco: Astronomical Society of the Pacific. pp. 1–14.

5180

CATHODOLUMINESCENCE AND RAMAN SPECTROSCOPY OF SHOCKED FELDSPAR WITH PDFs

M. Kayama¹, T. Okumura¹, H. Nishido¹, K. Ninagawa², and A. Gucsik³.
¹Research Institute of Natural Sciences, Okayama University of Science 1-1 Ridai-cho, Okayama, 700-005, Japan. E-mail: kayama@rins.ous.ac.jp.
²Department of Applied Physics, Faculty of Science, Okayama University of Science 1-1 Ridai-cho, Okayama, 700-005, Japan. ³University of West Hungary, Sopron, Hungary

In some of alkali feldspar and plagioclase samples, short and closely spaced planar deformation features (PDFs) are combined with relatively larger and more widely spaced features (deformation band or albite twining) to produce a distinctive ladder texture, which occurs as parallel planar optical discontinuities.

Shock-induced PDFs in feldspar have been less studied and less well characterized than those in quartz because of greater optical and structural complexity. Some of PDFs in feldspar are clearly visible in the CL image, but do not appear in SEM and BSE images. Moreover CL image allows more detail observation of PDFs than optical microscope because of high resolution (~1 μm) by the SEM-CL technique. In this study we have characterized PDFs in feldspar using SEM-CL and 3-D Raman spectroscopy.

Alkali feldspar and plagioclase with PDFs from the Ries crater were selected in polished thin sections under optical microscope. Experimentally shocked synthetic plagioclase (An40) was employed for a reference sample. CL image and spectra were obtained using a CL scanning electron microscopy (SEM-CL), of which system was comprised of SEM (JEOL: JSM-5410) and a grating monochromator (Oxford: Mono CL2). Raman spectra and 3-D Raman map were collected by a microRaman spectrometer (Thermo Nicolet: Almega) with CW laser excitation (532 nm).

CL spectra of plagioclase (An50) from the Ries crater have three broad peaks around at 450, 560 and 700 nm, which can be assigned to defect center, Mn^{2+} activation center and Fe^{3+} activation center, respectively. Alkali feldspar (Or70) from the Ries crater shows a broad CL peak at around 460 nm attributed to defect center. In CL image, PDFs in both shocked alkali feldspar and plagioclase are observed as thin dark lines superimposed on the more brightly luminescence background of the alkali feldspar and plagioclase grains. The thin dark lines correspond to PDFs, which have been recognized under optical microscope.

Experimentally shocked plagioclase at 40 GPa shows two broad peaks around at 450 and 620 nm related to defect and Mn^{2+} activation centers, respectively, whereas Mn^{2+} center in unshocked one is appeared as a broad peak at around 580 nm. PDFs in shocked plagioclase were observed under optical microscope, and also can be detected in CL image, which is similar to that of shocked plagioclase from the Ries crater.

3-D Raman spectral image at 505 cm^{-1} over a sectional area of PDFs in shocked plagioclase from the Ries crater indicates no apparent linear patterns suggesting planar features, whereas experimentally shocked plagioclase at 40 GPa exhibits linear stripe texture in 3-D Raman map, which corresponds to that CL image. Such difference in 3-D Raman map might be at least partly responsible for heating effect at shock event.

5140

CALIBRATION FOR STARDUST CRATERS IN ALUMINUM FOIL: INTERPRETATION OF COMETARY PARTICLE PROPERTIES BY COMPARISON WITH LABORATORY IMPACTS OF MINERAL, POLYMER, AND GLASS GRAINS

A. T. Kearsley¹, M. J. Burchell², P. Wozniakiewicz^{1, 4}, M. J. Cole², G. A. Graham³, R. J. Chater⁴, Z. Dai³, N. Teslich³, F. Horz⁵, and C. Schwandt⁵.
¹Natural History Museum, London, SW7 5BD, UK. ²University of Kent, Canterbury, Kent CT2 7NH, UK. ³LLNL, Livermore, California 94550, USA. ⁴Imperial College of Science, Technology and Medicine, London, SW7 2BP, UK. ⁵NASA Johnson Space Center, Houston, Texas 77058, USA

Introduction: A unique opportunity to study cometary particles has been provided by successful return of Stardust [1]. It is important to understand original grain size, extent of structural damage, and any elemental fractionation suffered by particles during capture, if full interpretation is to be realized. We have simulated impacts on Stardust Al foil, using a suite of mineral powders accelerated by light gas guns [2] to 6.1 kms^{-1} with perpendicular incidence. Our aim has been to produce an accurate comparison by use of well characterized materials with appropriate grain size and composition.

Experimental and Analytical Techniques: 27 buckshot firings onto All1100 foil were performed at the University of Kent and NASA/JSC. Soda lime glass bead samples of narrow size dispersion were used for size calibration. Mineral projectiles were selected to reflect likely and possible species in cometary dust [3] and included olivine, ortho- and clinopyroxenes, calcic feldspar, kamacite, pyrrhotite, magnetite, silicon carbide, corundum, spinel, hibonite, sodalite, calcite, dolomite, breunnerite, gypsum, cronstedtite, lizardite, and saponite. Other projectiles included poly-methyl methacrylate, powdered Orgueil CI chondrite and basalt glass. Soda lime glass craters were measured for a size calibration of cometary dust [4]. Energy dispersive X-ray analyses were performed in situ, and on residue material extracted by focused ion beam microscopy (FIB) techniques [5].

Results and Discussion: The shots yielded thousands of craters on foils. Scanning electron microscopy and FIB revealed abundant residue in the crater interior and rim areas with much of the original projectile retained, mostly melted, yet on occasion preserving some crystalline fragments. A comparison of projectile and residue compositions showed that mineral residues can be identified reliably. Analytical transmission electron microscopy of residue FIB ultrathin sections has shown almost all major elements are retained in substantially original proportions, although there is some depletion of sodium and sulfur. Study of the foil craters will not only provide an accurate measure of flux versus particle size, but will also complement composition studies of particles in aerogel. Samples of our projectile impacts are available on request for further characterization in other laboratories.

References: [1] Tsou P. et al. 2004. *Journal of Geophysical Research* 108:8113 [2] Burchell M. J. et al. 1999. *Measurement Science and Technology* 10:41–50. [3] Rietmeijer F. J. M. 1998. In *Planetary materials*. Washington, D.C.: Mineralogical Society of America. pp. 2-1–2-87. [4] Kearsley A. T. et al. 2006. *Meteoritics & Planetary Science* 41:167–180. [5] Graham G. A. et al. 2006. *Meteoritics & Planetary Science* 41:159–165.

5116

ANALYSES OF NEAR-IR, SPECTROSCOPIC DATA FOR MEMBERS OF ASTEROID FAMILIES WITH MIXED TAXONOMIES

M. S. Kelley¹ and M. J. Gaffey². ¹Department of Geology and Geography, Georgia Southern University, Statesboro, Georgia 30460, USA. E-mail: mkelley@georgiasouthern.edu. ²Department of Space Studies, University of North Dakota, Grand Forks, North Dakota 58202, USA

It is generally accepted that large, taxonomically heterogeneous asteroid families, such as the Koronis and Maria families, are “real” or “genetic.” That is, the members of such a family are derived from a common parent body. This is probably a safe assumption for collisionally young families—those that form dense clusters in orbital element space. But the same is not true for collisionally old families, and particularly those with mixed taxonomies. Not only do dynamical family classification systems disagree on the membership and existence of small families, but in the face of taxonomic, or spectroscopic, heterogeneity such clusters are not considered real in a compositional sense. One should keep in mind that taxonomic homogeneity does not automatically mean genetic reality for an asteroid family. For example, the mineralogical diversity within the S-class asteroids effectively rules out a common origin for all of these objects.

Complete differentiation of a parent body with, for example, an ordinary chondrite starting composition could result in an asteroid with a metallic core, an olivine-dominated mantle, and a basaltic crust. The disruptive collision of such an object could yield asteroid family members in the M, A, and S or V taxonomic classes. This may be a relatively easy scenario to accept since meteorite analogs for each of these classes provide evidence of igneous petrogenesis. It is more difficult to imagine a process that would yield a combination of C-, M-, and R-class asteroids as seen in the Budrosa family. However, there are plausible petrogenetic scenarios based on known classes of meteorites that, although beyond the scope of this presentation, could account for the mix of taxonomies (E, F, and M) in the Nysa-Hertha-Polana region of the mainbelt.

In the present study we use low-resolution near infrared spectroscopic data to examine members of three small- to medium-sized asteroid families that contain an odd mix of taxonomies. The Ceres, Eugenia, and Victoria families each contain S- and G/C-class asteroids. Previously unreleased data for asteroids in these families were obtained with the 52-channel double CVF system at the NASA Infrared Telescope Facility. We will compare these “new” data with existing data for asteroids in these families to begin testing their genetic reality.

5011

SURVIVAL OF METHANOGENS DURING PERIODS OF DESICCATION: IMPLICATIONS FOR LIFE ON MARS

M. G. Kendrick and T. A. Kral. University of Arkansas, Fayetteville, Arkansas, USA. E-mail: tkral@uark.edu

The relatively recent discoveries that liquid water most likely existed on the surface of Mars [1, 2, 3, 4, 5, 6] and that methane currently exists in the Martian atmosphere [7, 8, 9] have fueled the possibility of extant or extinct life on Mars. One possible explanation for the existence of the methane would be the presence of methanogens in the subsurface. Methanogens are microorganisms in the domain Archaea that can metabolize molecular hydrogen as an energy source, carbon dioxide as a carbon source, and produce methane [10]. One factor of importance, and the one that is addressed here, is the arid nature of Mars, at least at the surface. If one is to assume that life exists below the surface, then based on the only example of life that we know, liquid water must be present. Realistically, however, that liquid water may be seasonal just as it is at some locations on our home planet.

Here we report on research designed to determine how long certain species of methanogens can survive desiccation on a Mars soil simulant, JSC Mars-1 [11]. *Methanosarcina barkeri*, *Methanobacterium formicicum*, and *Methanothermobacter wolfeii* were grown on JSC Mars-1, transferred to a desiccator within a Coy anaerobic environmental chamber, and maintained there for varying time periods. Following removal from the desiccator and rehydration in anaerobic culture tubes under ideal growth conditions, gas chromatographic measurements of methane production indicated survival for all three organisms for varying time periods, depending on the organism being tested. *M. barkeri* survived desiccation for 10 days, while *M. formicicum* and *M. wolfeii* were able to survive for 25 days. *M. barkeri* and *M. formicicum* showed reduced methane production with increasing desiccation times, while *M. wolfeii* only showed substantially reduced methane initially following 25 days of desiccation. Methane levels increased rapidly with time, achieving the same methane levels as those desiccated for shorter time periods. Even though all three organisms showed some inhibition in methane production at the longest period of desiccation that allowed for survival, substantial amounts of methane were ultimately attained.

If methanogens are able to exist below the surface of Mars, the existence of liquid water is potentially the most important rate-limiting factor. Results reported here indicate that at least two species of methanogens might be able to survive dry periods for close to a month. Another important factor is temperature. The desiccation experiments reported here were maintained at room temperature. Colder temperatures, such as those observed on Mars, but not cold enough to freeze the subsurface water, might slow down the desiccation damage and lead to even longer survival periods.

References: [1] Christensen P. R. et al. 2004. *Science* 306:1733–1739. [2] Herkenhoff K. E. et al. 2004. *Science* 306:1727–1730. [3] Klingelhofer G. et al. 2004. *Science* 306:1740–1745. [4] Rieder R. et al. 2004. *Science* 306:1746–1749. [5] Squyres S. W. et al. 2004a. *Science* 306:1698–1703. [6] Squyres S. W. et al. 2004b. *Science* 306:1709–1714. [7] Formisano V. et al. 2004. *Science* 306:1758–1761. [8] Krasnopolsky V. A. et al. 2004. *Icarus* 172:537–547. [9] Krasnopolsky V. A. 2005. *Icarus* 180:359–367. [10] Sowers K. R. 1995. In *Methanogens (Archaea: A laboratory manual)*. Cold Spring Harbor Laboratory Press. p. 3. [11] Allen C. C. et al. 1998. In *Space*. pp. 469–478.

5329

THE ANTARCTIC FERRAR DOLERITE AND THE PETROGENESIS OF THE MARTIAN SHERGOTTITES

J. D. Kennedy and R. P. Harvey. Department of Geological Sciences, Case Western Reserve University, Cleveland, Ohio 44106, USA

Introduction: The Ferrar dolerite of East Antarctica has been proposed as a terrestrial analog to Mars because of similarities observed on a variety of scales—from surface weathering features at the outcrop scale [e.g., 1–4] to mineral compositions and textures noted in thin section [1, 2]. Previously, we examined mineralogical changes associated with weathering of the Ferrar. For this study, we investigate the possibility of the Ferrar as a planetary-scale analog to the petrogenesis of the Martian shergottites by establishing a more direct comparison between newly acquired Ferrar thin sections and a thin section of the Martian meteorite Los Angeles.

Mineralogy: *Previous Work:* Previously, we presented analyses from a suite of Ferrar samples that display a range of weathering styles. These data show that the Ferrar's pyroxene, feldspar, and oxide assemblages provide a satisfactory match to the shergottites—especially Zagami and Los Angeles—in terms of both range and average composition. However, there are two significant differences: 1) silica and alkaline-feldspars are prevalent in the Ferrar's mesostasis, while nearly absent in most shergottite lithologies; and 2) the pyroxene-to-feldspar ratio in those Ferrar samples is nearly reversed from that of the shergottites. Both of these observations suggest the Ferrar samples in hand are relatively evolved when compared to most shergottites.

New samples: The shergottites show a range of pyroxene and feldspar compositions representing a range of fractional crystallization stages, with the most evolved samples appear to be Zagami and Los Angeles [5]. Los Angeles, in particular, seems to provide a good comparison for a number of reasons, notably the presence of relatively large (up to 1 mm) silica grains [5]. The Ferrar, as a massive sill (several hundred meters thick) also shows a range of fractional crystallization states. We will present results from a direct comparison between Los Angeles and several newly acquired, well-matched Ferrar samples with much higher modal pyroxene.

Petrogenesis: The Ferrar dolerite is a shallow intrusive exposed along the length of the Transantarctic Mountains. Together with its contemporaneous extrusive counterpart in Antarctica (the Kirkpatrick basalt) and coeval lithologies in Australia and South Africa, they represent one of the largest effusive events in planetary history, the breakup of Gondwanaland in the early- to mid-Jurassic [1, 6, 7]. The tectonic extension and rifting associated with this event is typically considered to be a response to significant mantle upwelling beneath an especially large and insulating continental mass [1, 6, 7]. Similar plumes are commonly cited as the driving force behind large volume Martian magmatism in Tharsis and Elysium [1, 8].

A compelling match between these rocks in modal mineralogy and tectonic setting may also infer analogies between the Martian mantle beneath Tharsis and the pre-breakup terrestrial mantle beneath Gondwanaland. Some isotopic studies suggest a Ferrar origin from very “fertile” mantle, while others prefer a mantle strongly influenced by incorporation of subducted crust [1, 9]. Further analog studies that incorporate isotope data could help clarify this debate.

References: [1] Harvey R. P. 2001. Field Trip and Workshop on the Martian Highlands and Mojave Desert Analogs. LPI Contributions 1101, 25. [2] Allen C. C. and Conca J. L. 1991. Proceedings, 21st Lunar and Planetary Science Conference. pp. 711–717. [3] Rodriguez-Navarro C. 1998. *Geophysical Research Letters* 25:3249. [4] Parsons R. L. and Head J. W. 2005. Abstract #1138. 36th Lunar and Planetary Science Conference. [5] Mikouchi T. 2001. *Antarctic Meteorite Research* 14:1. [6] Encarnacion J. et al. 1996. *GSA Abstracts with Programs* 28:162. [7] Heimann A. et al. 1994. *Earth and Planetary Science Letters* 121:19–41. [8] Wilson L. and Head J. W. 2000. Abstract #1371. 31st Lunar and Planetary Science Conference. [9] Fleming T. H. et al. 1995. *Contributions to Mineralogy and Petrology* 121:217–236.

5021

NONLINEAR SEISMIC PROCESSES ON IMPACT CRATERING: INFORMATION CONTENT

O. B. Khavroshkin and V. V. Tsyplakov. Schmidt Institute of Physics of the Earth, Russian Academy of Sciences, B.Gruzinskaya 10, Moscow 123995 GSP-5, Russia. E-mail: khavole@ifz.ru

Introduction: Historically, craters were first found out element of structure of a surface of the Moon and many other planets.

Parameters of Crater-Forming Processes: Type of an impact body forming a crater may be single or complicated, its density and the form (extent for complicated); speed of a collision for an impact body-surface. Dominant type of seismic waves at the upper structures of heavenly body; Makh numbers M for all stages of wave and integral parameter of nonlinearity of medium and deeper structures.

Seismo-Radiative Stresses or Forces: More correct description of laws of similarity for craters, the conditions of the crater central zone forming demand to account for occurrence and existence of a field of powerful seismo-radiative forces manifesting as acoustic current or pressure in other sections of wave physics. As a result of viscoelastic properties of a crater forming zone and deeper structures instead of acoustic currents it is more correct to consider seismo-radiative forces or pressure (stress). Seismo-radiative stress is proportional to coefficient of nonlinearity n and quadrate of Mach seismic number (M). The record of the stresses was made using radiation of the vibrator for different experimental conditions.

The Mapping of Planet Internal Structure into Structures of Craters and Astroblems:

Conditions of effective mapping are determined by several factors. The following concern to the most essential. An extent and spatial distribution of bodies of crushing impactor, forming one or several long wave train-packages of flat seismic waves with number of Mach $\approx 10^{-2}$ under surface impact. Occurrence of a piston mode of wave trains—bunches of high-frequency seismic waves in an impact zone. For this wave bunch the subsequent preservation of wave train form and conditions $10^{-3} < M < 10^{-2}$ after passage and/or its reflection from geological border of a planet (minus losses). As a direction of vectors of seismo-radiative stresses and a gradient of density of the geological medium are opposite, the occurrence of the central hill is the elementary consequence of this fact. Diameter of the crater with such hill corresponds to the minimal cross section of a wave bunch at a piston mode radiation of seismic waves. Reflected from the removed borders of a planet the wave bunch tests to geometrical divergence because a reflecting surface has a spheroid form. Accordingly, under day surface output seismo-radiative stress or force of wave packages of the reflected beam operates on the area with diameter exceeding an initial crater, and forms an external ring. Thus, the geomorphology of impacted craters and astroblems contains the information about an internal structure of a planet.

5072

THE INTERSTELLAR GAS-DUST STREAMS AS THE INSTRUMENT OF EXOBIOLGY

Oleg B. Khavroshkin and Vladislav V. Tsyplakov. Schmidt Institute of Physics of the Earth, RAS, B Gruzinskay, 10, Moscow, 123995 Russia

Gas-Dust Streams from Double Stars and Lunar Seismicity:

The time series of seismic events were generated as follows: on the ordinate axis the peak amplitudes of events in standard units, on abscissa axis—seismogram durations of the same moonquakes and subsequent time intervals between them were used. Spectrum of the series disclosed time picks on hidden cosmogonical periodicities of lunar seismicity. A part of results (picks) presents orbital periods of double stars nearest to the solar system. The explanation of that results is existing gas-dust streams from binary stars systems and interacting of it with lunar surface.

Genesis of Life: If the solar system is reached by the gas-dust streams from binary stars, then all bodes in space have particles of star dust on their surfaces and/or atmospheres. Solar system has made 8–10 revolutions around galactic center and thus captured dust from many thousands stars. As these stars caught in turn dust particles from other stars, too, then probably our solar system has mainly dust samples from all objects of our galaxy. The age of galaxy and old stars is approximately more than 15 billion years and that of the Earth is only ~4–5 Gyr. Genesis of life for the Earth has not more than 3 billion years. Thus, comparative analysis of simple balance of these times shows that the genesis of life on Earth is the result of galactic processes/objects and not of the solar system, of course. After the formation of the solar system all old and new captured dust particles are first accumulated in the Oort cloud and then they are carried by comets to the planets. The modern state of the Earth has existed for more than 3 billion years, so the opportunities for life to appear were always there. These processes have happened a few times during this period. The sizes of the universe and galaxies at $\tau_0 < 1$ billion years could be much less than modern estimates (for example, up to ~15 times in diameter), that implies the existence of a common gas-dust exchange. The density of physical fields and radiations at the moment τ_0 was many orders of magnitude higher than the density existing now. Disintegration of neutron substance and nucleus of heavy unstable elements have caused constantly existing streams of left polarized electrons which have determined chirality's asymmetry of original organic molecules and thus the chirality the existing biological world. Some types of radiations functionally could replace enzymes during formation of self-reproducing molecular structures. Man uses only 10% of the genetic information contained in human DNA. This illustrates the common total surplus of a genetic material in the biosphere of the Earth. Probably, at the moment τ_0 in unique conditions and with sufficient time for creation, the universal galactic gene was created whose different elements are capable of creating biospheres on planets with the widest set of external conditions and for various stages of development. If the universal uniform galactic genome exists, this universality will appear as redundancy. The universal model of the gene logically contacts the concept of a prediction and a designer, hence, the model of occurrence of life and the Creator is logically more provable.

5122

VARIETY OF REFRACTORY OXIDE GRAINS DEPEND ON FORMATION ENVIRONMENTSY. Kimura^{1, 2} and J. A. Nuth III¹. ¹Code 691, NASA GSFC, Greenbelt, Maryland 20771, USA. ²Ritsumeikan University, Kyoto, Japan. E-mail: ykimura@se.ritsume.ac.jp

Introduction: Almost four decades ago, a 10 μm feature was discovered in evolved stars and silicate grains were suggested as the material responsible [1, 2]. Subsequently, the 10 μm feature has been observed from objects of almost all evolutionary stages, from stars (even some carbon-rich stars) and comets, and is still attributed to silicate grains. Condensation mechanisms for silica and silicate grains have been investigated in both laboratory nucleation experiments and via theoretical calculations. A wide array of grain synthesis experiments have been carried out by several groups [e.g., 3–5]. IR spectra of both amorphous and crystalline silica and silicate grains with various components have been widely observed. The spectral changes in the shape of the 10 μm feature due to thermal annealing of the grains was also investigated as a function of temperature and time. Constraints on the astrophysical environments and formation conditions of circumstellar, interstellar, and interplanetary dust particles have been provided based on comparisons of the observational and laboratory spectra.

Although the correlation between IR spectra and thermal effects has been extensively studied, experiments to observe the effects of changing formation environments are lacking. For example, only a few grain growth experiments have been attempted in magnetic and plasma fields [6, 7]. We assume that their environment can affect grains during formation and growth. Accordingly, it should be important to demonstrate the effects of formation environment during grain formation on the resultant IR spectra. Here we report the IR spectra of iron silicate, iron and silicon oxide particles produced in both electrical discharge and UV irradiation experiments. The average character of the grains will be also presented as analyzed using a transmission electron microscope.

Initial Results: FeSiO particles produced from mixtures of Fe(CO)₅, SiH₄, and O₂ using electrical discharge or UV radiation in flowing H₂ gas have a uniform composition within a probable error of 2% as reflected in their ambient gas atmosphere. SiO and FeO grains have not been observed so far. In contrast, when FeSiO grains were produced by the thermal decomposition of Fe(CO)₅ and SiH₄ within a furnace, the grains were classified into three distinct groups with specific atomic ratios [8].

Silica grains produced by UV irradiation display a very intense feature at 11.3 μm attributed to Si₂O₃. The intensity is as strong as 15% of the simultaneously observed 9.2 μm feature, as compared to the typical intensity of the well-known Si₂O₃ spectrum where the 11.2 μm feature seldom exceeds 5% of the intensity of the strong 9.2 μm peak. These experiments are still progressing. We will show further results and discussion that may provide additional constraints concerning silicate formation conditions.

References: [1] Gillett F. C. et al. 1968. *The Astrophysical Journal* 154: 677–687. [2] Woolf N. J. and Ney E. P. 1969. *The Astrophysical Journal* 155: L181–L184. [3] Brucato J. R. et al. 2002. *Planetary and Space Science* 50: 829–837. [4] Kaito C. 1983. *Japanese Journal of Applied Physics* 22:L432–L434. [5] Nuth J. A. et al. 2002. *Meteoritics & Planetary Science* 37:1579–1590. [6] Withney P. A. and Nuth J. A. 1999. *Icarus* 139:367–373. [7] Sato T. et al. 2003. *Japanese Journal of Applied Physics* 42:5896–5897. [8] Rietmeijer F. J. M. 1999. *Physical Chemistry Chemical Physics* 1:1511–1516.

5119

Fe-Ni METAL AND SULFIDES IN ACFER 094: THERMAL HISTORY OF THE MOST PRIMITIVE CHONDRITE

M. Kimura¹, M. K. Weisberg^{2,3}, and J. N. Grossman⁴. ¹Ibaraki University, Mito 310-8512, Japan. E-mail: makotoki@mx.ibaraki.ac.jp. ²Kingsborough College of the City University of New York, Brooklyn, New York 11235, USA. ³American Museum of Natural History, New York, New York, USA. ⁴U.S. Geological Survey, Reston, Virginia, USA

Introduction: Acfer 094 is a unique carbonaceous chondrite, with properties similar to CO and CM chondrites [1]. The matrix mineralogy [2], abundant presolar grains [1], and primitive features of refractory inclusions [3] indicate that Acfer 094 preserves primordial features that were not modified on the parent body [e.g., 1]. Recently, we showed that Fe-Ni metal is one of the most useful indicators for distinguishing the most primitive chondrites [4]. Here we report the characteristic features of Fe-Ni metal and sulfides in Acfer 094, in order to explore the primitive nature and thermal history of this remarkable chondrite.

Fe-Ni Metal and Sulfides: Fe-Ni metal is fairly abundant in the chondrules and matrix. The texture of Fe-Ni metal in Acfer 094 is almost homogeneous in all occurrences, and shows little plessitic intergrowth. This is in contrast to metal in Semarkona (LL 3.00), which typically shows plessitic texture [4]. In the other type 3 chondrites, Fe-Ni metal generally shows an intergrowth of coarse-grained kamacite and Ni-rich metal [4]. The latter texture is extremely rare in Acfer 094.

The composition of Fe-Ni metal in Acfer 094 depends on the occurrence of the grain: chondrule metal has 4.0–7.4% Ni and 0.16–0.44% Co, whereas matrix metal has 3.8–39.5% Ni and 0.10–1.8% Co. The Ni/Co ratio is generally solar in all occurrences.

Sulfide minerals generally occur as spherical to irregular-shaped grains in the matrix. They generally consist of troilite with pentlandite. Pentlandite contains 16–26% Ni and 0.3–1.8% Co, with solar Co/Ni ratio.

Discussion: Acfer 094 is one of the least metamorphosed chondrites, based on the Cr distribution in olivine [5]. We [4] suggested that the classification of metamorphic grade based on Fe-Ni metal features, especially the texture of plessite, is consistent with the classification by olivine [5]. However, Acfer 094 metal does not show plessitic texture. Alternatively, we suggest that most of Fe-Ni metal in Acfer 094 is martensite, based on texture and Ni content. The metal should have been quenched from high temperature conditions, higher than ~600 °C.

Martensite should transform to plessite during parent body metamorphism under low-temperature conditions [6]. Therefore, presence of martensite strongly indicates that Acfer 094 was hardly subjected to metamorphism on the parent body, and that Acfer 094 seems to be more primitive than Semarkona.

The troilite and pentlandite assemblage may have formed through sulfidation of Fe-Ni metal under low temperatures. The solar Co/Ni ratio of pentlandite supports this idea.

References: [1] Newton J. et al. 1995. *Meteoritics* 30:47–56. [2] Greshake A. 1997. *Geochimica et Cosmochimica Acta* 61:437–452. [3] Krot A. N. et al. 2004. *Geochimica et Cosmochimica Acta* 68:2167–2184. [4] Kimura M. et al. 2006. Abstract #1260. 37th Lunar and Planetary Science Conference. [5] Grossman J. N. and Brearley A. J. 2005. *Meteoritics & Planetary Science* 40:87–122. [6] Reisener R. J. and Goldstein J. I. 1999. Abstract #1868. 30th Lunar and Planetary Science Conference.

5161

OXYGEN ISOTOPES IN MAFIC AND FELDSPATHIC CLASTS FROM POLYMICT UREILITES

N. T. Kita¹, C. A. Goodrich², B. Fu¹, M. J. Spicuzza¹, and J. W. Valley¹. ¹Department of Geology and Geophysics, University of Wisconsin–Madison, Madison, Wisconsin, USA. E-mail: noriko@geology.wisc.edu. ²Department of Physical Sciences, Kingsborough Community College, Brooklyn, New York, USA

Introduction: Polymict ureilites DaG 165 and DaG 319 contain a wide variety of igneous clasts that might be derived from basaltic complements to the ultramafic monomict ureilites [1–2]. In a previous ion microprobe oxygen isotopic study of clasts from DaG 319, most plagioclase bearing clasts were found to plot along the CCAM-line and thus their origin from the ureilite parent body (UPB) was confirmed [1]. However, because of the small number of samples and limited precision of the analyses ($\Delta^{17}\text{O}$ ~1‰), oxygen isotopic systematics among these clasts is not well understood. In this study, the new ion microprobe IMS-1280 [3] was used to perform a systematic survey of 28 new clasts (described by [2, 4]) in DaG 165 and 319, including 20 plagioclase bearing clasts similar to those studied by [1]. In addition, two unusual mafic clasts (olivine with chromite exsolution, and Fe-rich pigeonite containing a melt inclusion) described by [4] and several of the olivine-augite feldspathic clasts described by [2] were studied to clarify their origin.

Ion Microprobe Analyses: The sample was sputtered with focused Cs⁺ primary ions (2–7 nA, 10–15 μm diameter) and oxygen three isotopes were analyzed by 3 Faraday Cup detectors combining mono and multi-collection systems [3]. At least 4–6 repeated analyses were made for each clast in order to obtain <0.3‰ precisions in $\delta^{18}\text{O}$, $\delta^{17}\text{O}$, and $\Delta^{17}\text{O}$. Olivine, pyroxene, and plagioclase standards with matching chemical compositions were used for correction of instrumental mass fractionation.

Results and Discussion: All but one of the feldspathic clasts plot along the CCAM line in the same region as ferroan monomict ureilites ($\Delta^{17}\text{O}$ = –0.5 to –1.4‰). One albitic plagioclase fragment plots on the TF line at $\delta^{18}\text{O}$ ~6‰, similar to enstatite meteorites. The two unusual mafic clasts plot on or slightly above the TF line at $\delta^{18}\text{O}$ ~3‰, indicating a possible link to primitive achondrites or ordinary chondrites. Four olivine-augite bearing feldspathic clasts plot along CCAM, confirming their UPB origin. None of the samples plot in the range of magnesian ureilites ($\Delta^{17}\text{O}$ ~ –2‰ on CCAM), consistent with the previous study [1]. If smelting determined mg#s of monomict ureilites and the UPB had a correlation of $\Delta^{17}\text{O}$ with depth [4], our results indicate a bias toward materials from the deeper source regions (in contrast to the interpretation of [4] that the dominant feldspathic clasts were derived from the shallowest depths). This is likely due to mingling of melts during fractional melt extraction [6], a process that was not recognized in the modeling of [4]. Calcic clasts (An >30) show slightly higher $\Delta^{17}\text{O}$ than albitic clasts (An <30) by 0.3‰. Low degree melts enriched in alkali and other trace elements generated at depth might migrate into shallower region where isotopic mixing with lower $\Delta^{17}\text{O}$ could occur. This is consistent with recent UPB models suggesting that Al-rich melt containing live ²⁶Al concentrated at shallower depths on the UPB [5, 6].

References: [1] Kita N. T. et al. 2004. *Geochimica et Cosmochimica Acta* 68:4213–4235. [2] Cohen B. A. et al. 2004. *Geochimica et Cosmochimica Acta* 68:4249–4266. [3] Kita N. T. 2006. Abstract #1496. 37th Lunar and Planetary Science Conference. [4] Goodrich C. A. et al. 2004. *Chemie de Erde* 64:283–327. [5] Kita N. T. et al. 2005. Abstract #5178. *Meteoritics & Planetary Science* 40. [6] Wilson et al. 2006. #1191. 37th Lunar and Planetary Science Conference.

5299

Hf-W AGES FOR THE ACCRETION OF ORDINARY CHONDRITE PARENT BODIES

T. Kleine¹, A. N. Halliday², H. Palme³, K. Mezger⁴, A. Markowski¹, and M. Touboul¹. ¹Isotope Geochemistry, ETH Zürich, Switzerland. ²Department of Earth Sciences, University of Oxford, UK. ³Institut für Geologie und Mineralogie, Universität zu Köln, Germany. ⁴Institut für Mineralogie, Universität Münster, Germany. E-mail: kleine@erdw.ethz.ch

Introduction: Key issues regarding the early evolution of the solar system include the time scales of accretion, differentiation, and thermal metamorphism of planetesimals. Many of these processes involved metal-silicate fractionations (e.g., core formation, metal formation in ordinary chondrites) and can be dated using ¹⁸²Hf-¹⁸²W chronometry. Hafnium is lithophile, whereas W is siderophile, such that metals have Hf/W~0 and preserve the W isotope composition acquired at the time of their formation. The W isotope compositions of magmatic iron meteorites indicate that their parent bodies differentiated in less than ~1.5 Myr after formation of Allende CAIs [1–3]. Here we present W isotope data for metals from ordinary chondrites to constrain formation intervals between metal segregation in iron meteorite parent bodies and the accretion of ordinary chondrite parent bodies.

Results: Metals from 10 L and 2 H ordinary chondrites were separated and their W concentrations and W isotope compositions determined using methods of [4]. Tungsten contents in the metals continuously increase (with increasing petrologic type) from ~0.3–0.4 ppm in type 3 up to ~1–1.4 ppm in type 6 ordinary chondrites. This range in W concentrations is consistent with results from earlier studies [5]. Despite these variations in W content, all ordinary chondrite metals analyzed so far have similar W isotope compositions ranging from ~-3 to ~-2.5 ε_W (where ε_W is the deviation of ¹⁸²W/¹⁸⁴W from the terrestrial standard value in parts per 10,000). There are no resolvable ε_W differences among metals from type 3, 4, and 5 ordinary chondrites and only type 6 metals appear to be slightly more radiogenic.

Discussion: The increasing W content of metals with increasing petrological type indicates a continuous transfer of W from silicates into metal during thermal metamorphism. This transfer must have occurred rapidly, as indicated by the similarity in W isotope compositions of metals from type 3–5 ordinary chondrites. Thus, W isotopes in metal from type 3 and 4 ordinary chondrites constrain the timing of parent body accretion. Based on the W isotope compositions of metals from Julesburg (L3), Mezö-Madaras (L3), and Saratov (L4) accretion of the L chondrite parent body occurred 3–5 Myr after core formation in the parent bodies of magmatic iron meteorites. Accretion of the H chondrite parent body (based on Hf-W systematics of Ste. Marguerite [6]) would have occurred at 2–4 Myr. These data confirm results that suggested that accretion of chondrite parent bodies postdates differentiation in some asteroids [1, 7]. Additional data, especially for metals from the most primitive ordinary chondrites, are needed to better constrain the effects of parent body processes on the W isotope composition of metals in type 3 ordinary chondrites.

References: [1] Kleine T. et al. 2005. *Geochimica et Cosmochimica Acta* 69:5805–5818. [2] Markowski A. et al. 2006. *Earth and Planetary Science Letters* 242:1–15. [3] Schersten A. et al. 2006. *Earth and Planetary Science Letters* 241:530–542. [4] Kleine T. et al. 2004. *Geochimica et Cosmochimica Acta* 68:2935–2946. [5] Rambaldi E. R. 1976. *Earth and Planetary Science Letters* 31:224–238. [6] Kleine T. et al. 2002. *Nature* 418: 952–955. [7] Bizzarro M. et al. 2005. *The Astrophysical Journal* 632:L41–L44.

5369

PROTOCOL FOR FIRST ORDER PALEOFIELDS ESTIMATION

G. Kletetschka^{1, 2, 3}, P. J. Wasilewski², T. Kohout^{3, 4, 5}, T. Adachi^{1, 2}, and V. Mikula^{1, 2}. ¹Catholic University of America, Washington, D.C., USA. E-mail: Kletetschka@gssc.nasa.gov ²GSFC/NASA, Greenbelt, Maryland, USA. ³Academy of Sciences, Prague, Czech Republic. ⁴Charles University, Prague, Czech Republic. ⁵University of Helsinki, Helsinki, Finland.

Examination Protocol: Our experience from application of normalizing technique to the Murchison and Bjrbole meteorites allows us to develop a list of steps that have to be performed when examining magnetism of an extraterrestrial object.

Protocol for first order paleofield estimation requires decisions with respect to the following questions: Was the sample exposed to geomagnetic field? Does the measurement device produce measurable magnetic field that can partially magnetize the sample (>0.05 mT)? Is the NRM above the noise level of the instrument? Does the REM (NRM/SIRM ratio for all AF steps) curve has significant positive/negative AF slope after the full AF demagnetization of both NRM and saturation isothermal remanent magnetization (SIRM)? Is remanence less than 50% of NRM after sample has been exposed to fields exceeding 0.05 mT? Is there a time dependence of magnetization after putting sample in magnetic vacuum and low temperature (e.g., 77 K). Is NRM after low temperature exposure less than 50? Do sub-samples of meteorite pass conglomerate test?

An example of unusual property of meteorites not often considered is illustrated with the Murchison meteorite. The effect of geomagnetic field exposure and shielding is illustrated in Fig. 1, where the acquired/relaxed component is shown to increase linearly with the logarithm of time. This property is independent of further demagnetization and/or acquisition and thus must be considered when deciphering the extraterrestrial magnetization signature.

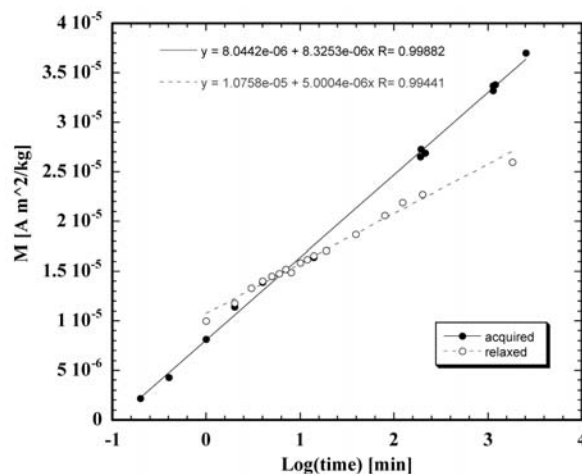


Fig. 1.

5094

THE 2005 ICDP-USGS DEEP COREHOLE IN THE CHESAPEAKE BAY IMPACT STRUCTURE

C. Koeberl¹, G. S. Gohn², W. U. Reimold³, and K. G. Miller⁴. ¹University of Vienna, Department of Geological Sciences, A-1090 Vienna, Austria. E-mail: christian.koeberl@univie.ac.at. ²US Geological Survey, Reston, Virginia 20192, USA. ³Humboldt University (Mineralogy), Invalidenstrasse 43, D-10115 Berlin, Germany. ⁴Rutgers University, Department of Geological Sciences, Piscataway, New Jersey 08854, USA

The late Eocene Chesapeake Bay impact structure is among the largest and best preserved of the known impact structures on Earth, e.g., [1]. In 2004, a multidisciplinary drilling project for this crater, by a research team from 10 countries, had been accepted by the International Continental Scientific Drilling Program (ICDP). Drilling of the joint ICDP and U.S. Geological Survey (USGS) deep corehole into the Chesapeake Bay impact crater began during September 2005 and was completed in early December 2005. This was followed by geophysical logging in the borehole. The drill site is located at Eyreville farm, Northampton County, Virginia, USA, above the near-circular moat structure that surrounds the central uplift of this impact structure. Post-impact marine sediments were cored (starting at the depth of 125 m) above the crater-fill impactite section, which consists (with depth) of sediment-clast breccia, sediment megablocks, a large granitic megablock, smaller sediment blocks, suevite and lithic impact breccia, and a section of only locally brecciated mica schist and pegmatites with rare veining of suevitic and lithic breccia. Overall, core recovery was good to excellent. However, trapped drill rods severely limited the geophysical logging program. Also, a second corehole, 5001-1-B (733 to 1766 m), had to be drilled because the drill bit deviated from the original hole, 5001-1-A (0 to 941 m), during reaming.

Matrix-supported sediment-clast breccia constitutes the uppermost part of the impactite section. This breccia (known from other coreholes in the area and termed "Exmore Breccia") overlies thick sections of Cretaceous sands and clays that probably represent slumped megablocks. An unexpected 275 m thick section of only weakly deformed granitoid underlies the sediment megablocks and probably represents a megablock of target material. The suevitic breccias are coherent, well lithified, and contain clasts of probable impact-melt rock, and fragments of cataclastically deformed metamorphic and igneous target rocks, in an apparently unsorted matrix of similar but finer-grained material. Lithic impact breccias are polymict and resemble the suevite except for a lack of evident impact-melt clasts. The suevitic breccias are underlain by mica schist and granite-pegmatite of the basement. About two dozen scientific teams are working on various geological, mineralogical, geochemical, and geophysical aspects of the borehole and the core samples.

References: [1] Poag C. W., Koeberl C., and Reimold W. U. 2004. *The Chesapeake Bay crater*. New York: Springer. 522 p. [2] Gohn G. et al. 2006. Abstract #1713. 37th Lunar and Planetary Science Conference.

5336

APPLICATIONS OF THE METEORITE PHYSICAL PROPERTIES DATA OBTAINED USING MOBILE LABORATORY FACILITY

T. Kohout^{1, 2, 3}, T. Elbra¹, L. J. Pesonen¹, P. Schnabl^{2, 3}, and S. Slechta^{2, 3}. ¹Division of Geophysics, Faculty of Science, University of Helsinki, Finland. E-mail: tomas.kohout@helsinki.fi. ²Department of Applied Geophysics, Faculty of Science, Charles University in Prague, Prague, Czech Republic. ³Institute of Geology, Academy of Sciences of the Czech Republic, Prague, Czech Republic

Introduction: Physical properties of meteorites provide valuable information about the meteorite history and the meteorite parent bodies—asteroids. Meteorites represent valuable rare material and it is difficult to bring meteorites directly to the laboratory for scientific studies. Thus the mobile laboratory facility was established at the Division of Geophysics, University of Helsinki, in order to make a research tour over the museums and collections in Europe and to measure the physical properties of meteorites in the presence of the curator using harmless, non-destructive methods.

The 2005 European Meteorite Research Tour: The tour was conducted in October 2005 using the mobile laboratory facility. During the tour the 6 member team visited 13 institutions in 8 countries across Europe and measured around 200 individual meteorite samples.

Instruments and Methods: During the meteorite research tour the measurement of bulk physical parameters (magnetic susceptibility, bulk and grain density, porosity, and magnetic remanence) of meteorites was performed.

The Hämäläinen TH-1 portable susceptibility meter with large (12 cm) coil was used for susceptibility measurements of bulk samples. For bulk volume measurements the chemically inert tiny glass beads (20–50 micrometers in diameter) were used to replace liquids used in traditional Archimedean method. The grain volume was measured by Notari portable air pycnometer working at low pressures. The mass was determined using digital balance always calibrated prior the measurements. The magnetic remanence was measured using portable Schoenstedt PSM-1 remanence meter.

Data Application: The results of the project are used to enhance existing database of physical properties of meteorites.

The magnetic susceptibility and density show characteristic values for different meteorite classes and can be used for 1) rapid meteorite classification [1], 2) identification of mislabeled samples, and 3) pairing the samples from meteorite showers.

The porosity data shows wide scatter even among meteorites of the same class. There is a trend in porosity showing decrease with the increasing metamorphic degree as well as with level of terrestrial weathering.

The other applications include solar system history studies, data interpretation of planetary and asteroid space missions, future sample return research, and asteroid mitigation efforts.

References: [1] Terho M. et al. 1993. *Studia Geophysica et Geodaetica* 37:65–82.

5138

AMOEBOID OLIVINE AGGREGATES IN YAMATO-86009 CV CHONDRITE: EVIDENCE FOR IN SITU AQUEOUS ALTERATION

M. Komatsu¹, A. N. Krot², T. Fagan³, M. Miyamoto¹, T. Mikouchi¹, and K. Keil². ¹Department of Earth and Planetary Science, University of Tokyo, Japan. E-mail: mutsumi@um.u-tokyo.ac.jp. ²HIGP/SOEST, University of Hawai'i at Manoa, Honolulu, Hawai'i, USA. ³Department of Earth Sciences, School of Education, Waseda University, Tokyo, Japan

Introduction: Amoeboid olivine aggregates (AOAs) are important refractory components of carbonaceous chondrites (except CH and CB chondrites) and have been interpreted to represent solar nebular condensates that experienced high-temperature annealing, but largely escaped melting [1]. Because AOAs in primitive chondrites are composed of fine-grained minerals that are easily modified during postcrystallization alteration, the mineralogy of AOAs can be used as a sensitive indicator of metamorphic or alteration processes. In order to understand the alteration history of the CV3 chondrites, we performed mineralogical studies of AOAs in the Yamato-86009 CV carbonaceous chondrite.

Samples and Analytical Procedure: Two polished thin sections of Y-86009, 51-1 and 51-2, were studied using optical microscopy, SEM+EDS, and EPMA.

Results and Discussion: AOAs in Y-86009 are irregularly shaped objects, 50–750 μm in size, composed of forsteritic olivine (Fo_{88}), high-Ca pyroxene, anorthite \pm spinel ($\text{FeO} < 1 \text{ wt}\%$). Forsteritic olivine typically shows enrichment in FeO along the cracks and grain boundaries. Anorthite is partly or completely replaced by fine-grained Al-rich phyllosilicates; nepheline is minor. Anhedral grains of hedenbergite occur along grain boundaries in direct contact with phyllosilicates. Euhedral fayalitic olivine grains (Fa_{63-71}) overgrow forsterite and occasionally show inverse compositional zoning. Some forsterite grains are overgrown by euhedral pyroxene ($\text{Wo}_{41}\text{En}_{56}\text{Fs}_3$, $< 10 \mu\text{m}$ in size) along the rim of AOAs. In some cases, enstatite ($\text{Wo}_5\text{En}_{94}$) occurs around the metal-magnetite nodules.

Based on our petrographic observations and the previously reported ¹⁶O-rich compositions of olivine in the Y-86009 AOAs [2], we infer that these AOAs were originally similar to AOAs in the reduced CVs [3] and subsequently experienced low-temperature aqueous alteration. The observed alteration features in Y-86009 are similar to those in CAIs, chondrules, and matrices of the Bali-like oxidized CVs (CV_{oxB}) [4], however, there are some important mineralogical differences as well. The common presence of anorthite in AOAs and rarity of Fa_{100} implies that the degree of aqueous alteration is lower than other CV_{oxB} chondrites. In addition, secondary fayalite in Kaba (CV_{oxB}) rarely shows inverse compositionally zoning and approaches nearly pure fayalite. The presence of nepheline, sodalite, and lath-shaped fayalitic olivine in matrix implies that Y-86009 also experienced higher temperature, and possibly more prolonged aqueous alteration than Kaba. We infer that Y-86009, like MET 00430 [5], is intermediate between CV_{oxA} and CV_{oxB} . Indeed, inverse chemical zoning of individual ferrous olivines are similar to those in MET 00430 [5], suggesting the dissolution of ferrous olivine and precipitation of more forsteritic olivine from a fluid phase during the late-stage thermal metamorphism.

References: [1] Krot A. N. et al. 2004. *Chemie der Erde* 64:185–282. [2] Hiyagon H. and Hashimoto A. [3] Krot A. N. et al. 1995. *Meteoritics* 30: 748–776. [4] Krot A. N. et al. 1998. *Meteoritics & Planetary Science* 33: 1065–1085. [5] Krot A. N. et al. 2003. International Symposium on the Evolution of Solar System Materials. pp. 61–62.

5087

L CHONDRITE ASTEROID BREAKUP TIED TO ORDOVICIAN METEORITE SHOWER BY MULTIPLE ISOCHRON ⁴⁰Ar-³⁹Ar DATING

E. V. Korochantseva^{1,2}, M. Trierloff¹, A. I. Buikin^{1,2}, C. A. Lorenz², M. A. Ivanova², W. H. Schwarz¹, J. Hopp¹, and E. K. Jessberger³. ¹Mineralogisches Institut, Ruprecht-Karls-Universität Heidelberg, Im Neuenheimer Feld 236, D-69120 Heidelberg, Germany. E-mail: trierloff@min.uni-heidelberg.de. ²Vernadsky Institute of Geochemistry, Kosygin St. 19, 119991 Moscow, Russia. ³Institut für Planetologie, Westfälische Wilhelms-Universität, Wilhelm-Klemm-Str. 10, D-48149, Münster, Germany

Radiochronometry of L chondritic meteorites yields a rough age estimate for a major collision in the asteroid belt 500 Ma ago [e.g., 1, 2, 3]. Fossil meteorites from Sweden indicate a highly increased influx of extraterrestrial matter in the Middle Ordovician 480 Ma ago [4]. An association to the L chondrite parent body event was suggested, however, a definite link is precluded by the lack of more precise radiometric ages of L chondrites. Here we report a high precision age value of the L chondrite asteroid breakup obtained by improved ⁴⁰Ar-³⁹Ar dating.

High resolution ⁴⁰Ar-³⁹Ar dating of the L5 chondrite Ghubara (host, chondritic xenolith, impact melt) demonstrated the presence of distinct excess argon components. We identified distinct trapped argon components with lower than terrestrial ⁴⁰Ar/³⁶Ar ratios at medium-high temperature extractions, proving their extraterrestrial origin. In particular, correcting the Ghubara melt age spectrum for trapped excess argon results in an age plateau comprising 24 temperature extractions (~95% ³⁹Ar release) with an age of $465 \pm 4 \text{ Ma}$. This is to our knowledge the first report of non-terrestrial excess argon in asteroidal meteoritic samples identified and corrected for by a multiple isochron approach. Several circumstances favored our discovery: sample selection, high resolution ⁴⁰Ar-³⁹Ar analyses and measures to minimize neutron-induced ³⁸Ar from Cl (Cd shielding, relatively short irradiation time).

We found multiple isochrons also for L-chondrite data of a previous study from the Heidelberg ⁴⁰Ar-³⁹Ar laboratories [5]. The slightly revised ages are consistent, indicating a single asteroid breakup event. The weighted average of the individual results from five L chondrites (Ghubara, Paranaiba, Mbale, Taiban, Bluff) of $469.6 \pm 5.4 \text{ Ma}$ is in perfect agreement with a refined age estimate of the middle Ordovician meteorite shower at $467.3 \pm 1.6 \text{ Ma}$ [6]. Our results link these fossil meteorites directly to the L-chondrite asteroid destruction, rapidly transferred from the asteroid belt and are consistent with the recently demonstrated short transfer time of fossil meteorites [7]. The new age value for the L-chondrite event of $469.6 \pm 5.4 \text{ Ma}$ serves as a precise time marker to calculate the cratering rate before and afterwards, demonstrating that the terrestrial impact crater base [8] displays a significantly increased cratering rate by at least a factor of 4–5.

References: [1] Heymann D. 1967. *Icarus* 6:189. [2] Bogard D. D. et al. 1976. *Journal of Geophysical Research* 32:5664. [3] McConville P. et al. 1988. *Geochimica et Cosmochimica Acta* 52:2487. [4] Schmitz B. et al. 2003. *Science* 300:961. [5] Kunz J. et al. 1997. *Meteoritics & Planetary Science* 32:647–670. [6] Gradstein F. M. et al. 2004. *A geologic time scale*. 589 p. [7] Heck P. R. et al. 2004. *Nature* 430:323. [8] Earth Impact Database. 2003. <http://www.unb.ca/passc/ImpactDatabase>.

5159

SELENIUM AS POSSIBLE INDICATOR OF ASTEROIDAL DIFFERENTIATION

A. Kracher, Ames Laboratory, Iowa State University, Ames, Iowa 50010–3020, USA. E-mail: akracher@iastate.edu

Magmatic iron meteorites are thought to have originated by fractional crystallization of the metallic cores of differentiated asteroids. The crystallization path of a metallic Fe,Ni liquid depends strongly on the initial concentration of non-metals, particularly sulfur. However, the initial sulfur content of the parental melts is poorly constrained. Previous methods have relied on modelling the behavior of metallic trace elements (Ge, Ir, As, etc.) whose partition coefficients are sensitive to melt composition. Here I outline a different way in which the initial sulfur content of the melt might be estimated.

The Se/S ratio of chondritic meteorites is, with few exceptions, remarkably constant [1]. Most magmatic iron meteorites originated in parent bodies that were probably roughly chondritic in bulk composition, e.g., siderophile element abundances in IIIAB irons are similar to those in ordinary chondrites. It can therefore be assumed that the parent bodies of most magmatic iron meteorites had a chondritic Se/S ratio.

Selenium has rarely been determined in the troilite of magmatic irons, but the few analyses that do exist show a Se/S ratio ~30% lower than in chondrites [2]. The abundance of daubréelite, which has a higher Se/S ratio than troilite, is insufficient to account for the missing Se. It is plausible that the remaining Se is present in the metal phase. This is because S behaves as a major element and is saturated in the metallic phase, whereas Se behaves as a dilute solute in both liquid and solid. Hence during fractional crystallization of the core it obeys, at least approximately, Henry's Law. The exact solubility of Se in γ -Fe is not known, but it is sufficiently high to form a $\gamma \leftrightarrow \alpha + \text{FeSe}$ eutectoid at 885 °C, 13° below the α/γ transformation temperature of pure Fe. The Se partition coefficient between melt and solid (Fe,Ni) is likely to be small but not zero.

If the bulk Se content of both sulfide and metal phase can be determined, and a chondritic overall Se/S ratio is assumed, a simple mass balance calculation would yield the relative amounts of sulfide and metal in the original core. Sufficiently precise determination of Se in the metal phase is difficult, especially since a large α/γ segregation is expected from the phase diagram. However, with current analytical methods it should be possible to constrain the S content of the parent melt to within a factor of 2 or less.

References: [1] Dreibus et al. 1995. *Meteoritics* 30:439–445. [2] Kracher et al. 1988. *Microbeam analysis*. 491 p.

5341

DISCOVERY OF THE SUDBURY IMPACT LAYER IN MICHIGAN, USAD. A. Kring¹, J. W. Horton, Jr.², and W. F. Cannon². ¹Lunar and Planetary Laboratory, The University of Arizona, Tucson, Arizona 85721, USA. E-mail: kring@lpl.arizona.edu. ²US Geological Survey, Reston, Virginia 20192, USA

Introduction: We have discovered deposits that contain probable distal ejecta from the 1850 Ma Sudbury impact event in northern Michigan, about 500 km from the center of the impact structure in Ontario. They occur in marine sediments of the Michigamme Formation in the upper Baraga Group of the Marquette Range Supergroup and resemble deposits previously described in Ontario and Minnesota [1]. We are investigating material from five localities in northern Michigan, described here as the Baraga basin, West Dead River, East Dead River, Marenisco, and Republic sites [2]. All of these sites are at or within a few hundred meters above the base of the Baraga Group at a comparable stratigraphic horizon to the Ontario ejecta.

Results: At the Baraga basin site, a 1–2 m thick layer in the lower 10 m of the Michigamme Formation contains well developed accretionary lapilli, chert breccia, and quartz grains that contain single and multiple sets of planar zones of inclusions interpreted to be the metamorphosed relicts of shock-induced planar deformation features (PDFs). The West Dead River site consists of an isolated outcrop of material at least 2 m thick and probably at least 100 m above the base of the Michigamme Formation; it is rich in accretionary lapilli, contains angular chert fragments to about 1 m diameter, and shows strong carbonate replacement. The East Dead River locality is a bed of polymict breccia, about 30 m thick, which contains abundant chert clasts as well as volcanic-like fragments, including sparse accretionary lapilli and relict glass shards that have been replaced by chlorite. The bed is crudely graded with the coarsest clasts at the base. It lies about 300 m above the base of the Michigamme Formation, where it is underlain by banded iron formation and overlain by black pyritic slate. At the Marenisco locality, a 2 m thick bed of coarse sand and conglomerate near the base of the Copps Formation (Michigamme equivalent) contains abundant clasts of Archean granite, less abundant slabs of chert to about 2 m diameter, and quartz grains having possible relict PDFs; it shows strong carbonate replacement. The Republic site is a gravel pit in glacial till, where boulders rich in accretionary lapilli are thought to be locally derived.

Discussion: At this early stage of investigation, we have found accretionary lapilli similar to those at the Ontario locality at five sites. Probable metamorphosed relicts of PDFs are present in quartz at the Baraga basin site and can be found within the cores of lapilli, accreted shells of material, and interstitial matrix. Lapilli are up to 2 cm diameter, are sometimes concentrically zoned, and, rarely, contain lithic cores. Except for the PDFs and the very broad (200–400 km) geographic distribution of the lapilli, they are similar to volcanic lapilli formed in clouds with 15–25 wt% water. The lapilli appear to have been produced in a vapor-charged cloud of impact ejecta that was deposited with sufficient energy, or subsequently reworked, to rip up local lithologies.

References: [1] Addison W. D. et al. 2005. *Geology* 33:193–196. [2] Cannon W. F. et al. 2006. Abstract. Institute on Lake Superior Geology, Annual Meeting.

5331

PHASE RELATIONS IN NA-RICH CHONDRULES

A. Kropf and A. Pack. Institut für Mineralogie, Universität Hannover, Callinstrasse 3, D-30167 Hannover, Germany. E-mail: a.kropf@mineralogie.uni-hannover.de

Introduction: Chondrules are believed to have formed by a brief but intense heating and melting event in the early solar system. We describe two Na- and Al-rich chondrules [1] from UOCs Dar al Gani 369 and 378 [2, 3]. Both chondrules contain ol and glassy mesostasis with <1 wt% MgO and CaO, ~10 wt% Na₂O. Both chondrules are low in FeO [2,4]. We discuss phase relations and with implications for concepts of chondrule precursors and nebular and parent body metasomatism.

Results and Discussion: Crystallization of fo as only liquidus phase in CMAS decreases the MgO-content of the residual melt [7], but can only occur in melts containing >12 wt% MgO. Therefore fo crystallization cannot lead to MgO-contents of <1 wt% as observed in the Na-rich ol-chondrules [4]. Addition of Na₂O to the CMAS system expands the fo stability field towards lower MgO-concentrations in the residual liquid and can explain low MgO in alkali-rich mesostasis. The low MgO values could also be explained by metastable ol crystallization into the fsp or px stability fields or by a combination of presence of alkalis and rapid crystallization.

Dynamic crystallization experiments will be conducted in order to show if metastable fo-crystallization in the fo-ab-an-system can account for the observed low MgO contents.

Low Ca in the chondrules (<1 wt%) may be explained in terms of a precursor that was mainly composed of fo and ab, which would be in agreement with presence of alkalis during chondrule melting and initial chondrule compositions close to the fo-ab eutectic composition. This implies a very brief melting event and/or an environment with high alkali activity. The alkali-rich and Ca-depleted precursor component may have formed by fractional condensation of alkali feldspar at <1000 K [5] or by recycling of Na-rich mesostasis from a previous generation of chondrules [6].

References: [1] Bischoff A. and Keil K. 1984. *Geochimica et Cosmochimica Acta* 48:693–709. [2] Pack A. et al. 2004. *Science* 303:997–1000. [3] Pack A. et al. 2005. *Geochimica et Cosmochimica Acta* 12:3159–3182. [4] Pack A. and Hezel D. 2006. Abstract #1353. 37th Lunar and Planetary Science Conference. [5] Lodders K. 2003. *The Astrophysical Journal* 591:1220–1247. [6] Bischoff A. et al. 1989. *Earth and Planetary Science Letters* 93:170–180. [7] Yoder H. S., Jr. and Tilley C. E. 1962. *Journal of Petrology* 3:342–532.

5061

REFRACTORY INCLUSIONS IN THE METAL-RICH CARBONACEOUS CHONDRITE ISHEYEVO

A. N. Krot¹, M. Chaussidon², G. R. Huss¹, A. A. Ulyanov³, and M. A. Ivanova⁴. ¹HIGP/SOEST, University of Hawai'i at Manoa, Honolulu, Hawai'i, USA. ²CRPG/CNRS, France. ³M. V. Lomonosov Moscow State University, Russia. ⁴Vernadsky Institute of Geochemistry and Analytical Chemistry, Russia

Introduction: Ca,Al-rich inclusions (CAIs) in the metal-rich CH and CB carbonaceous chondrites are characterized by a number of unique mineralogical and isotopic characteristics. For example, CB CAIs analyzed so far are uniformly ¹⁶O-depleted [1] and lack ²⁶Mg* [2]. CH CAIs show a bimodal distribution of O- and Mg isotope compositions: (i) most CAIs are ¹⁶O-enriched; some igneous CAIs are ¹⁶O-depleted [3, 4]; (ii) very refractory, grossite- and hibonite-rich CAIs lack ²⁶Mg*, the inferred ²⁶Al/²⁷Al ratio in less refractory, melilite-rich CAIs is ~5 × 10⁻⁵ [5–7]. Here we describe mineralogy and petrography of CAIs and amoeboid olivine aggregates (AOAs) in the recently discovered metal-rich chondrite Isheyevov [8]; oxygen and magnesium isotope studies of these CAIs are in progress.

Results: Isheyevov contains several lithologies which show mineralogical and chemical affinities to the CH and CB chondrites [8]. Based on the major mineralogy, 159 refractory inclusions found in ~10 cm² of X-ray mapped area of Isheyevov can be divided into hibonite±pyroxene±melilite (37%), grossite-rich (18%), melilite-rich (23%), spinel-rich (16%), pyroxene-anorthite-rich (5%) CAIs, and AOAs (1%). The CAIs and AOAs show no evidence for thermal metamorphism, Fe-alkali metasomatic or aqueous alteration; they are texturally and mineralogically similar to those in the previously studied CH (Acfer 182, ALH 85085, PCA 91467, PAT 91546, NWA 470, 739, and 770) and to a lesser degree to those in CB_b (Hammadah al Hamra 237, QUE 94411) chondrites. As a population of refractory objects, they are distinct from those in CR, CM, CV, CK, CO, and ungrouped carbonaceous chondrites Acfer 094, Adelaide, MAC 87300, and MAC 88107. Most Isheyevov CAIs are very refractory (hibonite- or grossite-rich), rounded or ellipsoidal objects, 20–240 μm in apparent diameter, which appear to have crystallized from rapidly cooling melts and escaped significant interaction with high-temperature nebular gas after solidification (secondary anorthite and Wark-Lovering rims are typically absent), suggesting a short residence time in the high-temperature condensation region. Less refractory CAIs (melilite- and pyroxene-anorthite-rich) and AOAs, 40–300 μm in apparent diameter, appear to have experienced more extensive high-temperature alteration resulting in replacement of melilite and spinel by anorthite and diopside, and formation of Wark-Lovering rims; some CAIs were melted prior to and during chondrule formation. We infer that there are two populations of refractory inclusions in Isheyevov that experienced different thermal histories.

References: [1] Krot A. et al. 2001. *Meteoritics & Planetary Science* 36:1189–1217. [2] Gounelle M. et al. 2006. Abstract #2014. 37th Lunar and Planetary Science Conference. [3] McKeegan K. et al. 2002. *Earth and Planetary Science Letters*. [4] Makide K. et al. 2004. Abstract #9076. Chondrites and the Protoplanetary Disk. [5] Weber D. et al. 1995. *Geochimica et Cosmochimica Acta* 59:803–23. [6] Kimura M. et al. 1993. *Geochimica et Cosmochimica Acta* 57:2329–59. [7] MacPherson G. et al. 1988. *Meteoritics* 24:297. [8] Ivanova M. et al. 2006. Abstract #1100. 37th Lunar and Planetary Science Conference.

5185

DIFFERENCES IN CHONDRULE FORMING ENVIRONMENTS BETWEEN LL AND CO CHONDRITES

E. Kurahashi^{1,2}, N. T. Kita³, H. Nagahara¹, and Y. Morishita². ¹University of Tokyo, Department of Earth and Planetary Sciences, Tokyo, Japan. ²Geological Survey of Japan, AIST, Japan. ³University of Wisconsin–Madison, Madison, Wisconsin, USA. E-mail: erika@eps.s.u-tokyo.ac.jp

The difference in the chondrule forming environments between ordinary (OC) and carbonaceous (CC) chondrites should be investigated in order to clarify the origin of chemical group of chondrites. Petrology of common ferromagnesian chondrules in the least metamorphosed OCs have been well studied [1–3]. Although petrological and isotopic observations on the least metamorphosed CCs have been vigorously carried out recently, systematic investigations of the primitive CCs are limited. Here, we report bulk chemical compositions of individual ferromagnesian chondrules in from CO3.0 Yamato-81020, and compare them to those from LL3.1 Bishunpur and LL3.1 Krymka [4–5].

Bulk major elemental abundances of chondrules measured by EPMA show that elements more refractory than Si are unfractionated for both CO and LL type I chondrules, and volatile elements decrease with volatility. In particular, CO type I chondrules are more depleted in volatiles than LL type I chondrules (average Na abundance; CO 0.11, LL 0.50). Type II chondrules are basically unfractionated for both CO and LL. The bulk compositions of chondrules, CAI and matrix in Y-81020 normalized to those of the bulk chondrite suggest that type I and II chondrules and matrix are depleted and CAIs are enriched in refractory elements, and type Is are richer in refractories than type IIs. Regarding volatiles, type Is are depleted, whereas type IIs are enriched and matrix is more volatile rich. These diversities of chondrules between OC and CC were established in spatially separated regions in the protoplanetary disk, and not by different time, because chondrules of both CO and LL were formed contemporaneously, except CO type IIs [6]. These observations along with non-fractionated pattern of type IIs suggest the following scenario: 1) refractory elements were fractionated at the early stage, of which residues became precursor of chondrules, and 2) type Is were formed from precursor with composition close to type II through evaporative loss of volatile components, and the evaporated fraction added to matrix. In this scenario, matrix is pristine but volatiles were enriched during chondrule formation. As the distribution of Fe is only incompatible with the other volatile elements, we also estimated total Fe abundance in type I and IIs. Type Is in both CO and LL contain less total Fe abundance (3–15 wt%). On the other hand, type IIs in CO have higher Fe abundance (20–27 wt%) than those of LL (12–15 wt%). The significant enrichment of in type II in CO is not explained by only volatility-controlled processes, and another explanation is needed, that is, difference in their precursors which might regard metal/sulfide and silicate fractionation during chondrule formations.

References: [1] Jones R. H. and Scott E. R. D. 1989. Proceedings, 20th Lunar and Planetary Science Conference. pp. 523–536. [2] Jones R. H. 1992. *Geochimica et Cosmochimica Acta* 56:467–482. [3] Huang S. et al. 1996. *Icarus* 122:316–346. [4] Tachibana S. et al. 2003. *Meteoritics & Planetary Science* 38:939–962. [5] Tomomura S. et al. 2004. Abstract #1555. 35th Lunar and Planetary Science Conference. [6] Kurahashi E. et al. 2004. Abstract #1476. 35th Lunar and Planetary Science Conference.

5051

A NEBULAR ORIGIN OF CHLORAPATITE AND SILICATE GLASS IN THE GUIN (UNGR) IRON

G. Kurat¹, E. Zinner², M. E. Varela³, and S. I. Demidova⁴. ¹Institut für Geologische Wissenschaften, Universität Wien, A-1090 Vienna, Austria. ²Laboratory for Space Sciences and Physics Department, Washington University, Saint Louis, Missouri 63130, USA. ³Complejo Astronómico El Leoncito, San Juan, Argentina. ⁴Vernadsky Institute of Geochemistry and Analytical Chemistry, Moscow, 119991, Russia

Silicate inclusions in iron meteorites [1] sample primitive (chondritic) and chemically fractionated parent bodies [2]. Inclusions in IIE irons have extreme fractionations, considered to be due to impact melting and mixing of feldspars and silica from the surface of a highly differentiated parent body [3, 4]. Studies of IIE iron-like inclusions from the Guin (ungr) iron show that they record nebular rather than planetary fractionation processes.

Large silicate inclusions are common [5] and consist of devitrified siliceous glass with or without augite and phosphates. We investigated an elongated oval (2 × 0.5 cm²) devitrified glass inclusion consisting of a fine-grained intergrowth of albite, silica, and low-Ca pyroxene with ilmenite, rutile, FeNi metal, FeS, Cl-apatite, and whitlockite. Albite dominates the composition with (wt%) 70.3 SiO₂, 16.8 Al₂O₃, 0.04 MgO, 1.4 FeO, 1.3 CaO, 8.5 Na₂O, 0.7 K₂O, and 0.17 P₂O₅. Trace element (TE) contents are low (~0.1 × CI) except for Ti, Sr, Zr, and Nb (~10 × CI) and Sc (~1 × CI). The REE contents are low (<0.1 × CI), decreasing from La to Gd (~0.02 × CI) and increasing toward Lu (~0.1 × CI). Eu and Yb have positive anomalies. A chlorapatite co-existing with the devitrified glass has low Ti, V, Zr, and Nb (<0.1 × CI) and high Sr (~20 × CI), REE, and Y (~70–80 × CI) contents with a flat abundance pattern and negative anomalies in Eu and Yb. The complementary TE patterns of Cl-apatite and glass suggest an igneous origin, but compared to experimental TE distribution coefficients between apatite and a siliceous liquid [6], the Guin assemblage is far out of equilibrium, except for Sr. The REE abundance pattern of apatite does not follow the distribution coefficients, but is flat and resembles the group III pattern of CAIs [7] at an abundance similar hibonites [8] and oldhamites [9, 10]. The pattern and abundance level suggest a TE-rich precursor phase for the apatite, oldhamite?, that formed by condensation from nebular gas at low *f*O₂ [11].

The very low TE content of the glass is similar to those of glasses from other IIE irons [4, 12, 13] and does not support derivation from albite as advertised [3, 4] since it is unfractionated. The positive anomalies of Eu and Yb make the pattern very similar to one reported for a glass from the Colomera IIE iron [12] where the anomalies were due to “...melting of silicates under highly reducing conditions, similar to those for enstatite chondrites.” However, the TE pattern of the Guin glass suggests derivation from a nebular reservoir strongly depleted in refractory TE (and Mg!) but not in Eu and Yb. Chlorapatite and devitrified glass in Guin appear to be genetically related, not via an igneous system, but via the solar nebula. The precursors could have been oldhamite and a siliceous liquid that subsequently experienced oxidizing conditions that turned oldhamite into chlorapatite [14, 15]. Metal trapped the products and preserved this primitive matter [16].

References: [1] Bunch T. et al. 1970. *Contributions to Mineralogy and Petrology* 25:297. [2] Wasson D. 1974. *Meteorites*. New York: Springer 316 p. [3] Ruzicka A. et al. 1999. *Geochimica et Cosmochimica Acta* 63:2123. [4] Hsu W. 2003. *Geochimica et Cosmochimica Acta* 67:4807. [5] Rubin A. et al. 1985. *Earth and Planetary Science Letters* 76:209. [6] Green. 1994. *Chemical Geology* 117:1. [7] Martin and Mason B. 1974. *Nature* 249:333. [8] Ireland T. 1988. *Geochimica et Cosmochimica Acta* 52:2827. [9] Kurat G. et al. 1992. *Meteoritics* 26:246. [10] Crozaz G. and Lundberg L. 1995. *Geochimica et Cosmochimica Acta* 59:3817. [11] Lodders K. and Fegley B. 1993. *Earth and Planetary Science Letters* 117:125. [12] Hsu W. et al. 1997. *Meteoritics & Planetary Science* 32:A61. [13] Kurat G. et al. 2005. Abstract #1814. 36th Lunar and Planetary Science Conference. [14] Kurat G. 1988. *Philosophical Transactions of the Royal Society of London A* 325:459. [15] Kurat G. et al. 2002. *Geochimica et Cosmochimica Acta* 66:2959. [16] Kurat G. 2003. Abstract. *Antarctic Meteorites* 65.

5215

DETERMINATION OF ²⁶Al CONTENTS FOR ANTARCTIC METEORITES USING EXTREMELY LOW BACKGROUND γ -RAY COUNTING SYSTEM OF ICRR, UNIVERSITY OF TOKYO

H. Kusuno¹, M. Kobayashi¹, T. Fukuoka¹, and H. Kojima². ¹Department of Environmental Systems, Faculty of Geo-Environmental Science, Risho University, Kumagaya, Saitama 360-0194, Japan. E-mail: tfukuoka@ris.ac.jp. ²Antarctic Meteorites Research Center, National Institute of Polar Research, Itabashi-ku, Tokyo 173-8515, Japan

Introduction: Determination of terrestrial ages of Antarctic meteorites supplies useful informations for the frequency of meteorite fall, mechanism of accumulation of meteorites and the age of ice. ²⁶Al ($T_{1/2} = 7.17 \times 10^5$ yr) is a useful tool for the dating of terrestrial age of meteorite.

Samples and Experimental: ²⁶Al contents in Yamato-791199, -791192, and -791962 meteorites have been determined non-destructively by extremely low background γ -ray counting system of Institute for Cosmic Ray Research, University of Tokyo. The counting system consists of a well type of large volume high pure Ge detector. Absolute counting efficiency of the detector was 1.76% at 1809 keV γ -ray of ²⁶Al. 1.73 to 1.78 g of crushed samples were packed in plastic vials prior to put into the well of detector.

Results and Discussion: The determination results are generally consistent with those of previous work [1–3].

Usually, determinations of ²⁶Al contents for more than 100 g of samples are performed by γ -ray count non-destructively. However, those for small samples such as less than 20 g are very difficult. Recently, accelerator mass spectrometry (AMS) analysis has been applied to determination of ²⁶Al in meteorites. Although the sample amount of AMS analysis is small, this analysis is destructive.

For small size of meteorites which original weights are less than 2 g, non-destructive determination of ²⁶Al content using extremely low background γ -ray counting system has a great advantage, because we can get other informations such as chemical, petrological and mineralogical informations from the same samples after ²⁶Al determination.

References: [1] Fuse and Anders. 1969. *Geochimica et Cosmochimica Acta* 33:653. [2] Komura et al. 1982. The Sixth Proceedings of the Symposium on Antarctic Meteorites. p. 178. [3] Fukuoka et al. 1993. The 18th Symposium on Antarctic Meteorites. p. 152.

5345

METEORITIC MICROFOSSILS IN ELTANIN IMPACT DEPOSITS

Frank T. Kyte¹, Rainer Gersonde², and Gerhard Kuhn². ¹Center for Astrobiology, Institute of Geophysics and Planetary Physics, University of California, Los Angeles, California 90095–1567, USA. E-mail: kyte@igpp.ucla.edu. ²Alfred Wegener Institut für Polar- und Meeresforschung, Postfach 120161, D-27515 Bremerhaven, Germany

Introduction: We report the unique occurrence of microfossils composed largely of meteoritic ejecta particles from the late Pliocene (2.5 Ma) Eltanin impact event. These deposits are unique, recording the only known km-sized asteroid impact into a deep-ocean (5 km) basin. First discovered as in Ir anomaly in sediment cores that were collected in 1965, the deposits contain mm-sized shock-melted asteroidal material, unmelted meteorite fragments (named the Eltanin meteorite), and trace impact spherules. Two oceanographic expeditions by the FS Polarstern in 1995 and 2001 explored ~80,000 km² of the impact region, mapping the distribution of meteoritic ejecta, disturbance of seafloor sediments by the impact, and collected 20 new cores with impact deposits in the vicinity of the Freeden Seamounts (57.3 °S, 90.5 °W). Analyses of sediment cores show that the impact disrupted sediments on the ocean floor, redepositing them as a chaotic jumble of sediment fragments overlain by a sequence of laminated sands, silts and clays deposited from the water column. Overprinted on this is a pulse of meteoritic ejecta, likely transported ballistically, then settled through the water column. At some localities, meteoritic ejecta was as much as 0.4 to 2.8 g/cm². This is the most meteorite-rich locality known on Earth.

Results: Two cores were taken in a basin near the top of the Freeden Seamounts at a water depth of 2.7 km. Sediments in this shallow basin are compositionally different than those at all other sites as they contain abundant calcareous microfossils. In deeper water sites (4 to >5 km depth), higher pressures and CO₂ concentrations cause dissolution of calcite and sediments contain siliceous (opal) microfossils or are barren. An exception to this is a few sites in the immediate vicinity of the seamounts that contain calcareous sediments that flowed off the seamounts after being disturbed by the impact. At the top of the seamounts, sediments with meteoritic ejecta are bioturbated by burrowing organisms. Microfossils of one of these organisms are truly remarkable. These “agglutinated” foraminiferans are unicellular, live in the sediment, and construct their shells from mineral grains in the sediment, which they bind together with an organic cement. The microfossils occur as tubes (up to 7 mm × 3 mm), with a central cavity that the foraminifer inhabited. Interestingly, this particular species of foram is known as a “disaster” species that is quick to re-inhabit an environment after a devastating event, such as a volcanic eruption, or, as we now know, an asteroid impact. On the Freeden seamounts, the most abundant “mineral” grains in these sediments, other than calcareous microfossils, are fragments of meteoritic ejecta. Point counting of 283 grains (25 to 250 μ m) examined by microprobe EDS and WDS in one specimen revealed that 70% of the particles are meteoritic ejecta, primarily vesicular melt rock with lesser pyroxenes and anorthite from the Eltanin meteorite. The other 30% is terrestrial quartz, feldspars, unclassified grains (probably mostly basaltic glass fragments), and a few lithic grains and microfossils.

5107

THE STUDY OF SCHREIBERSITE AND MICRORHABDITE EXTRACTED FROM THE SIKHOTE-ALIN METEORITE

M. Yu. Larionov and V. I. Grokhovsky. Physico-Technical Department, Ural State Technical University, UPI, Ekaterinburg, 620002, Russia. E-mail: lmur2000@rambler.ru; grokh47@mail.ru

Introduction: Iron meteorites contain iron nickel phosphides (Fe,Ni)₃P in the forms of schreibersite and rhabdite. Schreibersite and rhabdite are formed as a result of heterogeneous and homogeneous nucleation mechanisms, respectively [1]. The differences of these phosphides morphology and crystal structure are of interest and, therefore, were studied using various techniques.

Methods: The sample of schreibersite was prepared as a powder using mechanically extracted massive schreibersite from Sikhote-Alin (IIB) meteorite that was treated with HCl to remove kamacite residue. The microrhabdite crystals were extracted electrochemically from Sikhote-Alin (IIB) meteorite. Mössbauer spectra were measured at room temperature using spectrometer SM-2201 with high accuracy, stability and sensitivity in transmission geometry. X-ray diffraction study of microrhabdite and schreibersite was performed with STADI-P diffractometer and VEPP-3 synchrotron equipped by MAR 3450 detector. The Fe, Ni, and P concentrations in extracted phosphide crystals were measured by SEM Philips 30-XL with EDX.

Results and Discussion: The schreibersites with size up to 30 mm were located in α - α grain boundary of Sikhote-Alin meteorite. The extracted microrhabdite look like thin plates about 150 μ m in length and prismatic crystals about 5 μ m in cross section. Mössbauer spectra of schreibersite and microrhabdite samples were different [2]. Mössbauer spectrum of schreibersite was complicated and consisted of at least several magnetic sextets and several quadrupole doublets. Mössbauer spectrum of microrhabdite demonstrated the presence of unresolved magnetic sextet and possibly quadrupole doublet. The unresolved magnetic sextet may be a result of the relaxation processes or fuzzy magnetic phase transition in the sample at room temperature as well as a result of superparamagnetic behavior of microrhabdite particles. X-ray diffraction study of phosphides showed the following parameters of the unit cell: $a_{sch} = 9.049(8)$ Å, $c_{sch} = 4.461(8)$, and $a_{rhab} = 9.029(3)$ Å, $c_{rhab} = 4.461(5)$ for schreibersite and microrhabdite, respectively. The Fe content in schreibersite and microrhabdite was approximately 50 and 38 wt%, respectively, while Ni content was 30 wt% in schreibersite and 40 wt% in microrhabdite. Skála [3] demonstrated that nickel and iron atoms are not distributed equally over three crystallographically non-equal sites of the structure. These results demonstrated the differences of the hyperfine interactions, structural parameters and Fe/Ni content in schreibersite and microrhabdite. It is possible that Ni content increase in microrhabdite correlates with value decrease of unit cell parameter a_{rhab} [4]. Further studies are required to analyze structure, chemistry, and hyperfine parameters mutual relationships for phosphides with different morphologies.

References: [1] Clarke R. S. and Goldstein J. I. 1978. *Smithsonian Contributions to the Earth Sciences* 21. [2] Larionov M. Yu. et al. 2005. Abstract. *Meteoritics & Planetary Science* 40:A89. [3] Skála R. and Cisarova I. 1999. Abstract #1356. 30th Lunar and Planetary Science Conference. [4] Geist V. et al. 2005. *Crystal Research and Technology* 40: 52–64.

5268

DEVELOPMENT OF A NEW RESONANCE IONIZATION MASS SPECTROMETER FOR THE ISOTOPIC ANALYSIS OF Kr AND Xe

B. Lavielle, E. Gilabert, and B. Thomas. CNAB - UMR 5084 CNRS - Le Haut Vigneau, BP 120, 33175 GRADIGNAN Cedex, France. E-mail: lavielle@cenbg.in2p3.fr

A new spectrometer has been built to measure very small abundances of Kr and Xe. This instrument consists of a resonant ionization ion source, a cryogenic sample concentrator, and a time-of-flight mass analyzer. It is based on a similar design than the instrument developed at IRIM, Knoxville, University of Tennessee [1, 2] or than the "RELAX" spectrometer working at University of Manchester [3, 4]. Initially designed for Kr measurements, this new instrument allows Xe analyses by tuning the wavelength for ionization. A two-photon excitation, followed by one-photon ionization at the same wavelength ("2+1" transition), is used. A Kr atom resonantly absorbs two photons with 216.7 nm wavelength, resulting in the electron transition from ground state to $5p[5/2]_2$ state, and then the excited atom subsequently absorbs another photon non resonantly, exceeding the ionization energy level. For Xe, ionization can be achieved following a similar procedure but using a 217.1 nm wavelength ($7d[1/2]_0$ state). Ultraviolet beams are generated by mixing third harmonic of a Nd:YAG laser (1.6J, 10Hz) with a dye laser pumped by the second harmonic of the Nd:YAG laser. Atoms of Kr in the instrument are condensed on a cold trap at 25–35 °K and released after heating by a pulse of an IR NdYAG laser (50 mJ). Ionization and heating lasers are delayed in order to obtain the maximum ionized atoms in the source of the time of flight spectrometer. For now, the detection limit is about several thousands of Kr atoms. Measurements with this new instrument are in progress to determine CRE of iron meteorites by using ⁸¹Kr-Kr dating [4]. Cosmic ray exposure dating in iron meteorites is an important tool for studying variations of galactic cosmic ray in the past and complex irradiation histories of meteorites [5].

Acknowledgements: The CNAB project was financially supported by ANDRA, by the Région Aquitaine (France), by CNRS (GdR FORPRO, Chemistry and SDU-INSU Departments), and by the University Bordeaux I. We thank particularly N. Thonnard (Institute of Rare Isotope Measurement, Knoxville, University of Tennessee) for his very fruitful collaboration and Jamie Gilmour, (SEAES, University of Manchester) for sharing with us his great expertise in the field of RIS-TOF technique.

References: [1] Thonnard N. et al. 1987. *Nuclear Instruments and Method B*29:398–406. [2] Lehmann B. E. et al. 1991. *Applied Geochemistry* 6:419–423. [3] Gilmour J. D. et al. 1991. *Measurement Science and Technology* 2:589–595. [4] Gilmour J. D. 1994. *Review of Scientific Instruments* 65:617–625. [5] Marti K. 1967. *Physical Review Letters* 18:264. [5] Lavielle B. et al. 1999. *Earth and Planetary Science Letters* 170:93–104.

5258

TOF-SIMS ANALYSIS OF CRATER RESIDUES FROM PROJECTILES SHOT ONTO ALUMINUM FOIL

J. Leitner¹, T. Stephan¹, A. T. Kearsley², and F. Hörz³. ¹Institut für Planetologie, Wilhelm-Klemm-Str. 10, 48149 Münster, Germany. E-mail: leitner@uni-muenster.de. ²The Natural History Museum, London, UK. ³NASA Johnson Space Center, Houston, Texas 77058, USA

Introduction: Samples from the Stardust mission offer the first opportunity to analyze cometary matter collected under controlled conditions [1, 2]. In addition to aerogel, Al foils were exposed to the comet as well. These foils were used to facilitate the removal of the aerogel blocks from the collector trays [2].

In this ongoing study [3–5], time-of-flight secondary ion mass spectrometry (TOF-SIMS) is being used for the analysis of crater residues on Al foils from laboratory impacts that employed a variety of well-characterized projectile materials. The major goal of this investigation is to evaluate how well the chemical composition of the projectiles can be reproduced by TOF-SIMS.

Samples and Experimental Procedures: Powdered materials were fired into Stardust-type Al foils with impact velocities ranging from 4.2 to 6.1 km/s. Due to fragmentation in the launch process, a wide range of crater diameters was observed. Initial analyses of projectile residues used powdered CV3 chondrite Allende [3–5], hornblende and coal standards [5]; the present, investigations extended this work to a set of well characterized minerals, including olivine, diopside, pyrrhotite, and bytownite.

After necessary sputter cleaning through Ar ion bombardment, individual craters were rastered with a 0.2 μm ⁶⁹Ga⁺ primary ion beam. From the distribution of secondary ions from major elements, regions of interest were selected for the generation of mass spectra and calculation of element ratios using relative SIMS sensitivity factors derived from glass standards [6].

Results and Discussion: Geometric mean values of most element ratios relative to Si for nearly all examined Allende residues are close to CV element ratios and fit well within the range of ratios observed for Allende chondrules [7].

Due to their greater homogeneity, element ratios in the hornblende residues show significantly less deviations from reference data [8] than the Allende data, as most ratios are within a factor of 1.5 identical to literature values.

Analysis of the coal residues was focused on the behavior of complex molecules. Although Ar sputter cleaning destroys some of the hydrocarbons, they still could be detected in the craters [5].

The analysis of olivine, diopside, pyrrhotite, and bytownite residues is still in progress.

Conclusions: The first results show clearly that rocky material impinging on Al foil at ~6 km/s can be identified by TOF-SIMS analysis. Furthermore, even complex molecules can survive an impact on Al foils under these conditions.

References: [1] Brownlee D. E et al. 2003. *Journal of Geophysical Research* 108:E8111. [2] Tsou P. et al. 2003. *Journal of Geophysical Research* 108:E8113. [3] Stephan T. et al. 2005. Abstract. Workshop on Dust in Planetary Systems. pp. 136–137. [4] Hoppe P. et al. 2006. *Meteoritics & Planetary Science* 41:197–209. [5] Leitner J. et al. 2006. Abstract #1576. 37th Lunar and Planetary Science Conference. [6] Stephan T. 2001. *Planetary and Space Science* 49:859–906. [7] Rubin A. E and Wasson J. T. 1987. *Geochimica et Cosmochimica Acta* 51:1923–1937. [8] Jarosewich E. et al. 1980. *Geostandards Newsletter* 4:43–47.

5190

AMORPHOUS SILICATE HYDRATION IN THE PROTOPLANETARY DISK: AN EXPERIMENTAL APPROACH

H. Leroux. Laboratoire de Structure et Propriétés de l'Etat Solide, Université des Sciences et Technologies de Lille, CNRS-UMR 8008, 59655 Villeneuve d'Ascq, France. E-mail: Hugues.Leroux@univ-lille1.fr

Introduction: In the inner region of the protoplanetary disc, water is found in the form of vapor. If this vapor interacted with silicates at locations where the inner planets and parent bodies of meteorites formed, it could be of primary importance to their evolution [e.g., 1]. Silicates are good candidate to carry on water, in form of hydroxyl bonds. Earlier works showed that hydration of silicates was not kinetically possible on nebular time scales with crystalline silicates as the solid reservoir [2]. However, ISO spectra showed that interstellar silicates are amorphous [e.g., 3], probably irradiated within interstellar shockwaves [4]. Since the protoplanetary disk was formed by interstellar materials, the hydration behavior of amorphous silicates precursors must be examined.

Experimental Procedure: Hydration experiments were performed from room temperature to 200 °C for various reaction times, at 1 atmosphere and saturated water vapor pressure. The silicate materials used were amorphous thin films having a composition close to olivine. The thin films were studied by optical microscopy, scanning electron microscopy (SEM), atomic force microscopy (AFM), and transmission electron microscopy (TEM).

Results: The first modification that appeared in the amorphous thin films consists of extended patches, well visible by optical microscopy. Crystallization of hydrated minerals occurs within these patches, in form of extended needles, nano-scale fibrous texture and well faceted crystals, depending on the experimental conditions. TEM characterization showed that the amorphous phase converted into phyllosilicates, mainly composed of talc, frequently associated with brucite. Kinetics strongly depends on temperature but also on the thin film thickness.

Conclusion: Phyllosilicates are present in the most primitive materials from our solar system (IDPs, micrometeorites, carbonaceous chondrites). In carbonaceous chondrites they display clear evidences for aqueous alteration but the original materials from which they are formed is still largely debated. Recently it was proposed that phyllosilicates can be nebular products [5]. This hypothesis is supported by hydration experiments on magnesiosilica smokes [6]. Our preliminary results confirm that phyllosilicates can be formed from amorphous precursors that simulate interstellar silicates in interaction with water at relatively low temperature.

References: [1] Drake M. J. 2005. *Meteoritics & Planetary Science* 40: 519–527. [2] Prinn R. G. and Fegley B., Jr. 1987. *Annual Review of Earth and Planetary Science* 15:171–212. [3] Kemper F. et al. 2004. *The Astrophysical Journal* 609:826–837. [4] Demyk K. et al. 2001. *Astronomy and Astrophysics* 368:L58–L61. [5] Ciesla F. J. et al. 2003. *Science* 299:549–552. [6] Rietmeijer F. J. M. et al. 2004. *Meteoritics & Planetary Science* 39:723–746.

5068

TITANIUM ISOTOPES IN SOLAR SYSTEM OBJECTS

I. Leya¹, M. Schönbachler², U. Wiechert³, U. Krähenbühl⁴, and A. N. Halliday⁵. Physikalisches Institut, University of Bern, Switzerland. E-mail: ingo.leya@space.unibe.ch. ²Department of Earth Science and Engineering, Imperial College London, UK. ³Institut für Geologische Wissenschaften, Freie Universität Berlin, Germany. ⁴Laboratory for Radiochemistry, University of Bern, Bern, Switzerland. ⁵Department of Earth Sciences, Oxford, UK

Introduction: Isotopic anomalies in solar system objects provide powerful constraints on the origin and evolution of the early solar system. Of particular importance are titanium isotopes in refractory inclusions from primitive meteorites because i) titanium isotopes are important indicators of nucleosynthetic processes contributing to iron group elements and ii) titanium isotopes may also serve as an indicator of possible irradiation processes in the early solar system. Variations in titanium isotopes have been reported for refractory inclusions from Allende (CV3), whereas the type of the anomalies was not well characterized, e.g., [1, 2, 3]. However, while all earlier studies agreed that virtually every Ca-Al-rich refractory inclusion from Allende contains anomalous titanium, the titanium isotopic composition of other meteoritic constituents is still not completely characterized with respect to their nature and extent. Here we present a detailed and consistent database for the titanium isotopic composition in various objects in the solar system.

Experimental: Sample preparation, chemical separation, and data reduction followed the procedures described by [4, 5]. Measurements of isotopic ratios were performed with the high-resolution MC-ICP-MS (Nu 1700) at ETH Zürich.

Results: After correcting for i) mass fractionation (internally via ⁴⁹Ti/⁴⁷Ti), ii) external and plasma specific interferences, and iii) blanks the external reproducibility (2σ) obtained from repeated measurements of terrestrial basalts is 0.36ε, 0.38ε, and 0.28ε, for ⁵⁰Ti/⁴⁷Ti, ⁴⁸Ti/⁴⁷Ti, and ⁴⁶Ti/⁴⁷Ti, respectively. Comparing our data obtained for various standard solutions (synthetic solutions and terrestrial basalts) with literature data clearly indicate that the terrestrial titanium isotopic composition is not well defined. The “standard ratios” used by different groups for normalization differ by up to 15ε-units, making titanium the element with the least known atomic weight among all elements [6].

An unexpected result is the detection of anomalous titanium in ilmenite separates from lunar rocks. New model calculations will enable us to check whether such anomalies are real or whether the effect is simply caused by interactions with galactic cosmic-rays. Most of the meteoritic material analyzed display a normal titanium isotopic composition. For Allende CAIs we confirm an excess of ~10ε in ⁵⁰Ti/⁴⁷Ti. In contrast to earlier studies we found excess ⁵⁰Ti in Allende bulk material (~3ε). Significant anomalies were also found in troilites from Estacado (H6) and in leachates from Allende and Murchison. The new database will be discussed with respect to galactic cosmic-ray interactions, nucleosynthetic processes, and a possible early solar system local irradiation scenario.

References: [1] Heydegger H. et al. 1977. *Meteoritics* 12:257. [2] Niederer F. et al. 1980. *The Astrophysical Journal* 240:L73–77. [3] Niemeyer J. and Lugmair G. 1984. *Geochimica et Cosmochimica Acta* 48:1401–1416. [4] Schönbachler H. et al. 2004. *Analyst* 129:32–37. [5] Leya I. et al. *Analyst*. Forthcoming. [6] Shima M. and Torigoye N. 1993. *International Journal of Mass Spectrometry and Ion Processes* 123:29–39.

5295

OLIVINES IN MAGNESIAN PORPHYRITIC CHONDRULES: MANTLE MATERIAL OF EARLIER GENERATIONS OF DIFFERENTIATED PLANETESIMALS?

G. Libourel¹, A. N. Krot², and M. Chaussidon¹. E-mail: libou@crpg.cnrs-nancy.fr. ¹CRPG-CNRS, UPR2300, BP40, 54501 Vandœuvre les Nancy, France. ²Hawai'i Institute of Geophysics and Planetology, University of Hawai'i at Manoa, Honolulu, Hawai'i 96822, USA

Libourel and Krot [1] reported the discovery of lithic clasts having granoblastic texture and composed of forsterite and Fe,Ni metal within type I chondrules from the CV carbonaceous chondrite Vigarano. They suggested that type I chondrules consist of an inherited, relict component, mainly forsteritic olivine and ±Fe,Ni metal, originated from olivine-dominated (dunite-like) mantle material of earlier generations of differentiated planetesimals, and an igneous component equilibrated with nebular gas—glass, low-Ca pyroxene, high-Ca pyroxene, and ± silica phase. In this scenario, the olivine lithic fragments predate formation of type I chondrules. The chondrule mesostasis, low-Ca and high-Ca pyroxenes are the result of a reprocessing of these olivine clasts in the nebular gas followed by melt infiltration and progressive partial dissolution of the olivines along grain boundaries. The variability in chemical composition observed in the glassy mesostases of type I chondrules results from the progressive addition of a volatile-rich component from the nebular gas [1–3]. If this interpretation is correct, detailed studies of these olivine-rich granoblastic aggregates can help to constrain the main characteristics of these olivine-dominated (dunite-like) mantle material of earlier generations of differentiated planetesimals. We therefore extend our survey to other CV carbonaceous chondrites, including Allende, Efremovka, Leoville, Mokoia, and Vigarano.

From a detailed characterization of the mineralogy and chemistry of these lithic clasts we confirm the occurrence of coarse-grained forsteritic clasts with equilibrium textures inside type I chondrules in all the studied CV chondrites. From their oxygen isotopic composition, we infer that these igneous objects, which are ¹⁶O-enriched [see also 4, 5] in a similar manner as refractory forsterites [6], may be derived from planetesimals that were disrupted (they have a common Δ¹⁷O signature). However, if olivines in the CV magnesian chondrules studied are lithic fragments of pre-existing planetesimals, their Δ¹⁷O values indicate that these planetesimals may not have been sampled yet, since differentiated meteorites have ¹⁷O values >–3‰ [7], at the exception of olivines from a few pallasites such as Eagle Station with Δ¹⁷O = –4.8‰ [8].

References: [1] Libourel G. and Krot A. N. 2006. Abstract #1334. 37th Lunar and Planetary Science Conference. [2] Tissandier L. et al. 2002. *Meteoritics & Planetary Science* 37:1377–1389. [3] Libourel G. et al. 2003. Abstract #1558. 34th Lunar and Planetary Science Conference. [4] Krot A. N. et al. 2005. *Geochimica et Cosmochimica Acta* 70:767–779. [5] Chaussidon M. et al. 2006. Abstract #1335. 37th Lunar and Planetary Science Conference. [6] Pack A. et al. 2005. *Geochimica et Cosmochimica Acta* 68:1135–1157. [7] Krot A. N. et al. *Chemie der Erde*. Forthcoming. [8] Clayton R. N. and Mayeda T. K. 1996. *Geochimica et Cosmochimica Acta* 60:1999–2017.

5102

RECOVERY OF 5354 METEORITES IN GROVE MOUNTAINS, ANTARCTICA, BY THE 22ND CHINESE ANTARCTIC RESEARCH EXPEDITION

Yangting Lin¹, Yitai Ju², Xiabin Xu³, Mingrong Pan⁴, Feixin Huang⁵, Aimin Fang¹, Jinyan Li¹, Xiaobo Liu⁴, Wenjun Pen⁶, Jianmin Hu⁷, and Xiao Cheng⁸. ¹State Key Laboratory of Lithospheric Evolution, Institute of Geology and Geophysics, Chinese Academy of Sciences, China. E-mail: LinYT@mail.igcas.ac.cn. ²China Exploration and Engineering Bureau, China. ³Polar Research Institute of China, China. ⁴China Central Television, China. ⁵Institute of Tibetan Plateau Research, CAS, China. ⁶School of Geodesy and Geomatics, Wuhan University, China. ⁷Institute of Geomechanics, Chinese Academy of Geological Sciences, China. ⁸Institute of Remote Sensing Applications, CAS, China

Introduction: The Grove Mountains are one of the most meteorite-enriched regions in Antarctica, as demonstrated by discovery of a total of 4480 specimens by the 15th, 16th, and 19th Chinese Antarctic Research Expeditions (CHINARE) during 1998–1999, 1999–2000, and 2002–2003 austral summer seasons, respectively [1–3]. In 2005–2006 season, another field party of 11 members explored Grove Mountains again, and found a total of 5354 fragments of meteorites.

Results: Grove Mountains locate east to Amery ice shelf and about 400 km south to the Zhongshan station of China, East Antarctica. There are 64 nunataks in this region, and altitude of the ice fields ranges from 1850 m to 2060 m. On the eastern side, the Gale Escarpment ridge, consisting of three parts, ranges about 50 km in length and in direction of NNE. It blocks the ice sheet flowing from east, with most meteorites stranding along the downstream side of the ridge.

The field party departed from Zhongshan station on December 23, 2005, and returned back on February 18, 2006. It took 17 days on the way, and we had only 41 days on the ice fields in Grove Mountains. Most of the meteorites were collected in the first 20 days, and the rest of time was mainly used for other fieldworks, including geological survey, mapping, and remote sensing flow of the ice sheet.

In the southern part of Gale Escarpment, there was no moraine. All 21 meteorites were found on blue ice, with a total mass of 61 g. 2438 specimens (15.9 kg) were collected in the middle part, and 2144 of them are small fragments found in moraines. These small fragments are heavily weathered, with little fusion crust remained. They are probably fragments from much less number of meteorites. The northern part of Gale Escarpment is the most meteorite-concentrated area in Grove Mountains, with a total of 2847 meteorites (44.2 kg in weight) found in this expedition. Although more than half of the specimens are less than 1 g, many of them have complete fusion crusts and are not fragments broken by weathering. Distribution of meteorites in this area was continuous from moraines to blue ice without clear cutoff. The meteorite collection sites nearly overlaps with those in the 19th CHINARE, indicating continuous coming up of meteorites onto the surface of ice fields.

Acknowledgements: This exploration was organized and supported by Chinese Arctic and Antarctic Administration and Polar Research Institute of China. It was also supported by the Natural Science Foundation of China (Grant no. 40232026).

References: [1] Ju Y. and Liu X. 2000. *Chinese Journal of Polar Research* 12:137–142. [2] Miao B. et al. 2003. *Chinese Science Bulletin* 48: 908–913. [3] Miao B. et al. 2005. *Proceedings of the China Association for Science and Technology* 2: 291–298.

5307

OXYGEN ISOTOPIC COMPOSITIONS IN CM HIBONITE: IMPLICATIONS FOR SOLAR NEBULA HETEROGENEITY

Ming-Chang Liu¹, Kevin D. McKeegan¹, Andrew M. Davis^{2,3}, and Trevor R. Ireland⁴. ¹Department of Earth and Space Sciences, UCLA, Los Angeles, California, USA. E-mail: mcliu@ess.ucla.edu. ²Department of Geophysical Sciences, University of Chicago, Chicago, Illinois, USA. ³Chicago Center for Cosmochemistry, University of Chicago, Chicago, Illinois, USA. ⁴Research School of Earth Sciences, The Australian National University, Canberra, Australia

Introduction: CM hibonite crystals are known to preserve isotope anomalies of large magnitude in Ca, Ti, and O [1–7]. A recent study has also confirmed the existence of apparent deficits in ²⁶Mg in a population of platy hibonite crystals [8]. Unlike the correlation between $\delta^{48}\text{Ca}$, $\delta^{50}\text{Ti}$, and ²⁶Al, oxygen anomalies seem to be independent of hibonite chemistry and morphology [1–7]. We have determined the oxygen isotopic compositions in a suite of Murchison hibonite grains that have been characterized for Mg isotopes [8] in an attempt to better understand the distribution of O isotopic reservoirs in the solar nebula.

Results and Discussion: Oxygen isotope mass spectrometry was performed with the UCLA CAMECA 1270 ion microprobe using the procedures described in [9]. In this session, 6 platy-crystals (PLACs), 6 spinel-hibonite spherules (SHIBs) and 1 blue-aggregate (BAG) were measured. All samples are enriched in ¹⁶O relative to terrestrial values with $\Delta^{17}\text{O}$ ranging from $\sim -15\%$ to -25% , and one extraordinary BAG hibonite with $\Delta^{17}\text{O} = -38\%$. While our results are broadly similar to those found previously [2, 5, 7], the new data show a tendency for PLACs to sample larger oxygen variations than SHIBs. This would be consistent with larger isotopic anomalies generally being associated with PLACs, however there is no apparent quantitative correlation between $\delta^{48}\text{Ca}$ or $\delta^{50}\text{Ti}$ or the presence of Mg isotope anomalies ($\Delta^{26}\text{Mg}^*$ deficits) and the magnitude of the observed ¹⁶O excesses.

Among all the samples, the aggregate ANU-Hib1 is of special interest because it exhibits very heterogeneous Mg isotopic compositions ($\Delta^{26}\text{Mg}^* = 0\%$ and -6% in 2 spots). Two different spots differ by $\sim 50\%$ in both $\delta^{17}\text{O}$ and $\delta^{18}\text{O}$, and plot on a slope 1 trajectory, offset from the CCAM line by $\sim 15\%$. If we assume that the primary oxygen isotope composition of the most ¹⁶O-rich ANU-Hib1 spot evolved off the CCAM line by mass fractionation, similar to what is observed in FUN inclusions [10], we infer a starting composition of ($\delta^{18}\text{O} = -81\%$, $\delta^{17}\text{O} = -80\%$), which is consistent with the most ¹⁶O-rich composition yet observed [11]. Since ANU-Hib1 is an aggregate, the large internal heterogeneity may be ascribed to preservation of distinct oxygen isotope compositions in different hibonite laths. This implies that there must be multiple oxygen reservoirs present in the solar nebula during hibonite formation, although the poorly understood chronology of hibonite formation precludes conclusions regarding possible evolution of those reservoirs.

References: [1] Zinner E. et al. 1986. *The Astrophysical Journal* 311: 103–107. [2] Fahey et al. 1987. *The Astrophysical Journal* 323:91–95. [3] Fahey et al. 1987. *Geochimica et Cosmochimica Acta* 51:329–350. [4] Ireland T. 1990. *Geochimica et Cosmochimica Acta* 54:3219–3237 [5] Sahijpal S. et al. 2000. Abstract #1502. 31st Lunar and Planetary Science Conference. [6] Sahijpal S. et al. 2000. *Geochimica et Cosmochimica Acta* 64:1989–2005. [7] Goswami N. et al. 2001. Abstract #1576. 32nd Lunar and Planetary Science Conference. [8] Liu et al. 2006. Abstract #2428. 37th Lunar and Planetary Science Conference. [9] McKeegan K. et al. 1998. *Science* 280:414–418. [10] Lee et al. 1980. *Geophysical Research Letters* 7: 493–496. [11] Yoshitake and Yurimoto. 2004. Abstract #9049. Workshop on Chondrites and the Protoplanetary Disk.

5359

DIGGING DEEP IN THE SUPERNOVA: TiC AND Fe METAL COMPOSITES IN PRESOLAR GRAPHITE

K. Lodders, Department of Earth and Planetary Science, Washington University, Campus Box 1169, Saint Louis, Missouri 63130, USA. E-mail: lodders@wustl.edu

Introduction: Micron-size presolar graphite of type II supernova (SN) origin can contain numerous inclusions of TiC and Fe,Ni metal up to several hundred nm in size [1]. In most instances, metal is directly attached to TiC subgrains, which [1] interpreted by TiC and metal condensation prior to graphite. Graphite condensation requires a C-rich environment with C/O > 1 but a typical condensation sequence at C/O > 1 in an otherwise solar composition gas is TiC-graphite-SiC-FeSi. So FeSi condenses instead of metal and neither SiC nor FeSi were found in the grains described by [1]. Hence the question how did the TiC-metal-bearing graphites form in SN ejecta?

Condensates in SN Zones were calculated for a 25 solar mass SN using averaged zone compositions from [2]. None of the individual SN zones returns the observed condensate sequence for the grains. Zone compositions with C/O < 1 can be excluded because they yield oxides and silicates. The He-C zone with C/O > 1 favors TiC and graphite, but in addition SiC and FeSi condense. The inner C- and O-poor Si-S and Ni-zones yield metals, sulfides, and exotic refractory silicides for averaged compositions. These exotic condensates appear irrelevant to the observed assemblage; but only the Si-S and Ni zones produce ⁴⁴Ti and ⁴⁹V whose decay products are seen in presolar SN graphites.

Digging Deeper: The ejecta composition of the Ni-zone is quite variable as it depends on the mass-cut and fall back from the SN explosion. A check of the condensates along the compositional gradient of the Ni-zone ejecta shows that titanides such as Ti₅Si₃ and (Fe,Ni)₂Ti also appear. Formation of refractory (Fe,Ni)₂Ti is especially favored if Si and S abundances are reduced. This can be achieved at the innermost ejecta by complete Si-burning with α -rich freeze-out also responsible for ⁴⁴Ti.

Formation of (Fe,Ni)₂Ti is the key to the presolar grain observations [3]. If the Si and S-poor ejecta make it to the C-rich He-C zone, carburization via (Fe,Ni)₂Ti + C = TiC + 2 (Fe,Ni) can explain the observed TiC-metal grains in the presolar graphite. However, the Ni-zone ejecta must cross the Si-S zone and the O-rich O-Si, O-Ne, and O-C zones without mixing before reaching the He-C zone. This may not be a problem if the products of -rich freeze-out are ejected from the core in bipolar jets, which are known to be associated with asymmetric core-collapse SN.

References: [1] Croat T. K. et al. 2003. *Geochimica et Cosmochimica Acta* 67:4705. [2] Rauscher T. et al. 2002. *The Astrophysical Journal* 576: 323. [3] Lodders K. *The Astrophysical Journal*. Forthcoming.

5358

GERMANIUM ISOTOPIC VARIATIONS IN IRON METEORITES

B. Luais¹, CRPG, CNRS-UPR2300, 15, rue Notre-Dame des Pauvres, 54501 Vandoeuvre Cedex, France. E-mail: luais@crpg.cnrs-nancy.fr

Introduction: Magmatic and nonmagmatic iron meteorites have been thought to represent a distinct portion of planetesimals, core and outer part of differentiated bodies, respectively. However, processes by which the nonmagmatic irons (IAB-IICD and IIE groups) are generated, near-surface impact-melt model [1] versus deep origin [2] remain unsolved, especially for the IIE groups. In this respect, germanium which is the most volatile siderophile element is sensitive to processes linked to core formation, such as metal-silicate diffusion and redox process, and to evaporation processes [3]. Ge elemental distribution and Ge isotopic ratios can thus provide informations on the mechanisms of formation and origin of iron meteorites. We present additional Ge isotope data of IIAB, IIIAB, IIC magmatic and IAB-IICD, IIE nonmagmatic iron meteorites, on samples covering a broad range of Ge concentrations.

Methods: Ge isotopes are measured using the Isoprobe Multi-Collector ICP-MS (CRPG-Nancy) with a precision better than 0.06‰ per amu (2 σ total external reproducibility on 11 total replicate analyses of the Magura IAB meteorite, including chemistry, in 7 sessions during 4 years) (% $\delta^8\text{Ge} = ((^{82}\text{Ge}/^{76}\text{Ge})_{\text{sa}}/({}^{82}\text{Ge}/^{76}\text{Ge})_{\text{JMC Std}} - 1) \times 1000$). Germanium was perfectly isolated from the matrix by liquid-liquid chromatography [4, 5].

Results-Discussion: In comparison to previous results, the variations of Ge isotopic ratios have been extended, with a total range of $\delta^{74}\text{Ge}$ from -0.22 to 1.86‰, defining a single mass fractionation line similar to the TMFL [5]. The $\delta^{74}\text{Ge}$ data show a remarkable distinction between magmatic and nonmagmatic groups, without any inter-group correlations with Ge, Ir, Ni contents:

Magmatic groups have similar and high $\delta^{74}\text{Ge}$ values ($\delta^{74}\text{Ge} = +1.35$ to $+1.86$ ‰) for distinct Ge contents. The precision of data even allows distinction between IIA ($\delta^{74}\text{Ge} = 1.77 \pm 0.17$ ‰) and IIB ($\delta^{74}\text{Ge} = 1.35$ ‰) samples.

Nonmagmatic groups have low $\delta^{74}\text{Ge}$ values: high Ge IAB-IICD samples have clustered values around 1.15 ± 0.19 ‰; low Ge IIE samples have lower values with distinction between the Miles group (-0.22 to +0.43‰) and Watson (1.4‰).

Whatever the complex history of magmatic and nonmagmatic irons leading to their Ge-Ir-Ni geochemical trends (e.g., fractional crystallization, trapped liquid, impact melt mixing; [1, 2, 6]), it does not govern the isotopic fractionation of germanium. The data will be discussed as follows: 1) isotopic fractionation in the early stage of formation of these irons, and reflecting the specific redox state of Germanium: either by core segregation for magmatic iron (Ge reduction in metal form, diffusion/reequilibration) or impact melt/gas for nonmagmatic group (formation of volatile Ge oxides enriched in ⁷⁰Ge); 2) more likely, they can also reflect the isotopic composition of their parent body and thus their degree of redox state. In this way, the correlation between $\delta^{74}\text{Ge}$ of a given group of iron (this work) and $\Delta^{17}\text{O}$ of their silicate inclusions and chondritic parent bodies [7] will be discussed.

References: [1] Choi B. G. et al. 1995. *Geochimica et Cosmochimica Acta* 59:593-612. [2] Bogard D. D. et al. 2000. *Geochimica et Cosmochimica Acta* 64:2133-2154. [3] Schmitt W. et al. 1989. *Geochimica et Cosmochimica Acta* 51:4439-4448. [4] Luais B. et al. 2000. *Geoanalysis* 47-48. [5] Luais B. 2003. Abstract. *Meteoritics & Planetary Science* 38:A31. [6] Cook D. L. 2004. *Geochimica et Cosmochimica Acta* 68:1413-1431. [7] Clayton R. N. 1993. *Annual Review of Earth and Planetary Science* 21:115-149.

5273

Rb-Sr ISOTOPE DATA FOR CORE SAMPLES OF THE ICDP BOSUMTWI SCIENTIFIC DRILLING PROJECT, GHANA

S. Luetke^{1, 2}, A. Deutsch^{1, 2}, and A. Sokol¹. ¹Institut für Planetologie, Universität Münster, Wilhelm-Klemm-Str.10, DE-48149 Muenster, Germany. ²ZLG, Münster, Germany. E-mail: luetke.s@uni-muenster.de

Introduction: The 1.07 Ma old Bosumtwi impact structure, Ghana (06°32'N, 01°25'W) is a young and excellent preserved complex crater. As part of the Bosumtwi Core Drilling Project (BCDP) two cores were drilled into impactites (BCDP-7A: annular moat, BCDP-8A: central uplift). In contrast to the broad spectrum of target and impact lithologies found on the crater rim, the drill cores mainly consist of meta-greywackes, phyllites and impact breccias [1, 2]. The goal of this isotope study is to constrain the precursor lithologies of Bosumtwi-related impact glasses (Ivory Coast tektites [IVC] and microtektites).

Samples: We investigated 1) six breccias of cores 7A and 8A, 2) two meta-greywackes (7A), and 3) two shales (7A). (1) consist of mineral (mainly quartz, feldspar, and calcite) and lithic fragments (meta-greywacke and a variety of shales to phyllite) ranging in diameter from 0.1 to 10 cm. The fine grained matrix additionally contains sheet silicates. To estimate the influence of clasts to the whole rock isotope systematics different parts of breccias were separated, i.e., (i) domains exclusively consisting of matrix and clasts ≤ 0.5 cm, (ii) such with matrix and clasts mainly larger than 1 cm, and (iii) single large meta-greywacke clasts (≥ 5 cm). (2) one meta-greywacke is medium grained, the other one phyllitic; (3) the shales are grey to dark grey, very fine grained, and display a foliation; they have a powdery consistence.

Rb-Sr Isotope Data: The breccias from core 8A have $^{87}\text{Sr}/^{86}\text{Sr}$ ratios between 0.703350 ± 14 (2 σ) and 0.708955 ± 12 , those of core 7A higher values from 0.720310 ± 13 to 0.72581 ± 10 . The breccia domains (i), (ii), and (iii) don't display large variation indicating the absence of not yet sampled target lithologies (e.g., granitoids) in the matrix. Two shales of 7A show much higher present day $^{87}\text{Sr}/^{86}\text{Sr}$ ratios (0.728310 ± 13 and 0.750205 ± 14) which is within the range published by [3] for shales, greywackes, and phyllites collected at the rim and in the vicinity of the crater. Reflecting the lower content of micas, greywackes of core 7A yield relatively low $^{87}\text{Sr}/^{86}\text{Sr}$ ratios (0.716423 ± 14 and 0.718968 ± 14), in accordance with our earlier results of core 8A [4]. Respective regression line calculations using the different lithologies result in rather low initial $^{87}\text{Sr}/^{86}\text{Sr}$ ratios of 0.7107 (7A) and 0.7027 (8A); the correspondent age values do not date a so far documented event, their geological relevance is questionable.

Outlook: The current set of isotope data does not allow to correlate specific target rocks with IVC. Therefore further isotope studies (Rb-Sr, Sm-Nd) as well as SEM analyses are in progress.

Acknowledgements: We appreciate support by DFG grant De 401/19. Skillful technical assistance was given by H. Baier, U. Heitmann, and V. Heinrich.

References: [1] Reimold W. U. et al. 2006. Abstract #1350. 37th Lunar and Planetary Science Conference. [2] Deutsch A. et al. 2006. Abstract #1292. 37th Lunar and Planetary Science Conference. [3] Koerberl C. et al. 1998. *Geochimica et Cosmochimica Acta* 62:2179–2196. [4] Luetke S. et al. 2006. Abstract #1811. 37th Lunar and Planetary Science Conference.

5287

ARGON AND NEON IN GENESIS ALUMINUM-COATED SAPPHIRE COLLECTORS FROM REGIME ARRAYS

J. C. Mabry¹, A. P. Meshik¹, C. M. Hohenberg¹, Y. Marrocchi¹, O. V. Pravdivtseva¹, J. Allton², R. Bastien², K. McNamara³, E. Stansbery³, and D. Burnett⁴. ¹Washington University, Physics Department, St. Louis, Missouri 63130, USA. E-mail: jcmabry@wustl.edu. ²Lockheed Martin c/o NASA/JSC, Mail Code KT, Houston, Texas 77058, USA. ³NASA/JSC, Mail Code KA, Houston, Texas 77058, USA. ⁴Geology 100–23, Caltech, Pasadena, California 91125, USA

Introduction: Here we report Ar results from the aluminum on sapphire (AlO₃) bulk regime samples, from which Ne results were obtained [1]. Ar measurements from other regimes are in progress.

Table 1.

Regime	²⁰ Ne fluence, 10 ¹² /cm ²	²⁰ Ne/ ²² Ne	²¹ Ne/ ²² Ne
Bulk	1.23 ± .11	13.96 ± .03	.0346 ± .003
IS	.352 ± .032	13.98 ± .04	.0340 ± .004
CME	.271 ± .024	13.93 ± .04	.0336 ± .004
C-H	.362 ± .032	13.94 ± .04	.0345 ± .004

Method: Since elemental and isotopic abundances of light noble gases in solar wind differ substantially from terrestrial air (usually used for calibration), we used specially tailored calibration procedures. For Ar, we lowered the ion source emission to 50 μA , from our typical 150 μA . Using this procedure, mass discrimination was small and reproducible at less than 0.3%/amu.

The AlO₃ samples were loaded into an extraction cell specially designed to minimize Al sputtering effects, which can contribute significantly to the blank and block the viewport. We rastered areas of 4, 10, 15, and 20 mm² for Ar and 1–2 mm² for Ne, using a Q-switched infrared laser, slightly defocused to optimize the surface energy density and the time needed to complete the raster. The corrections for ¹H³⁵Cl⁺ and ¹H³⁷Cl⁺ interferences at A = 36 and 38 were negligible, as was the ⁴⁰Ar blank ($< 5 \times 10^{-10}$ ccSTP) with observed ⁴⁰Ar/³⁶Ar ratios between 3 and 10.

Ar fluences were calibrated using both an air standard and Springwater olivine grains (mg size), with known amounts of spallogenic ³⁶Ar, ³⁸Ar, ²¹Ne, and ²²Ne [2]. These two calibrations differed by about 8%, which should improve by ongoing interlab calibrations.

Results: The Ar data from all four rastered areas formed a nearly perfect straight line when the ratios of ³⁶Ar/⁴⁰Ar versus ³⁸Ar/⁴⁰Ar were plotted, indicating a mixing of only two distinct components: solar wind and terrestrial atmosphere, no SEP or HCl effects. We calculated fluences (not corrected for backscatter) of $(2.4 \pm 0.2) \times 10^{10}$ ³⁶Ar/cm² and $(4.5 \pm 0.4) \times 10^9$ ³⁸Ar/cm². All four of our ³⁶Ar/³⁸Ar ratios agree to within 5 permil.

Table 2. ³⁶Ar/³⁸Ar ratios (from [3] and this work).

Terrestrial air	5.32
Apollo foils	5.3 ± 0.3
Lunar regolith (Zürich)	5.48 ± 0.05
Lunar regolith (Minnesota)	5.80 ± 0.06
SOHO/MTOF	5.5 ± 0.6
Regime bulk (this work, weighted average)	5.467 ± 0.010

Acknowledgements: Supported by NASA grants NNJO4HI17G and NAG5-12885.

References: [1] Hohenberg C. M. et al. 2006. Abstract #2439. 37th Lunar and Planetary Science Conference. [2] Megrue G. H. 1968. *Journal of Geophysical Research* 73:2027–2033. [3] Weins R. C. et al. 2004. *Earth and Planetary Science Letters* 222:697–712.

5156

STRUCTURAL DOME AT SAO MIGUEL DO TAPUIO, PIAUI, BRAZIL

W. D. MacDonald, A. P. Crósta, J. Francolin

About a dozen known or suspected meteorite impact structures (astroblemes) have been suggested for Brazil (Romano and Crósta 2004). The largest of these is the 40 km-diameter Araguainha dome, of about 245 Ma. Among the suspected impact structures is the dome of São Miguel do Tapuio (e.g., Mariano et al. 2004). Field and laboratory investigations of the structure of the dome were undertaken to evaluate its possible origin by meteorite impact. The dome is defined by a pattern of concentric ridges and depressions approximately 21 km in diameter, with a center near 5°37.6'S, 41°23.3'W. The surrounding country rocks are mainly sandstones of the Cabeças Formation. The dominant lithologies within the structure are quartzose sandstones and quartz-pebble conglomeratic sandstones. Field investigations included several days of examination of outcrops in several transects across and around the structure. Petrographic studies of thin sections of the sandstones and of quartz pebbles isolated from the conglomeratic sandstones were made. These revealed few planar fractures (PFs) and no planar deformation features (PDFs), following the usage of Grieve et al. (1996). These observations are contraindicative of an origin by meteorite impact. Consistent with these observations are 1) the general absence of breccias or breccia-dikes, 2) the absence of shatter-cones, 3) the absence of shock-melt products in outcrop or thin-section, and 4) the absence of other shock-metamorphic indicators. Taken together, the lack of shock features does not support an origin by meteorite impact. Moreover, there are no clear indications of rim-faults or annular half-grabens. What, then, might account for this feature? Although no igneous rocks were found exposed within the structure, evidence of hydrothermal dissolution occurs near the core of the structure. It is possible that heating at depth, perhaps associated with deep-seated intrusion, could mobilize these quartzose strata in a diapiric fashion, resembling that of the Richat structure, Mauritania (Matton et al. 2005), a larger structure 40 km in diameter, for which an association with a deeper alkaline complex has been hypothesized.

References: [1] Grieve R. A. F. et al. 1996. *Meteoritics & Planetary Science* 31:6–35. [2] Mariano R. et al. 2004. *Meteoritics & Planetary Science* 39:A61. [3] Matton G. et al. 2005. *Geology* 33:665–668. [4] Romano R. and Crósta A. P. 2004. Abstract #1546. 35th Lunar and Planetary Science Conference.

5109

LITHIUM ISOTOPE COMPOSITION OF THE INNER SOLAR SYSTEM MATERIALST. Magna^{1,2}, U. Wiechert³, and A. N. Halliday⁴. ¹ETH Zürich, Switzerland. ²University of Genève, Switzerland. E-mail: magna@erdw.ethz.ch. ³Freie Universität Berlin, Germany. ⁴University of Oxford, UK

Introduction: We present a survey of lithium isotopes in rocks from the Earth, Moon, Mars, and Vesta [1]. Spinel lherzolites probably reflect the composition of the upper terrestrial mantle. Olivines contain 80–90% of the Li inventory of spinel lherzolites and thus may be a good first approximation of the Li isotope composition of the Earth's upper mantle. In addition, lunar rocks are analyzed to estimate the lithium isotope composition of the Earth [3].

Results: Terrestrial mantle olivines from a worldwide collection of spinel lherzolites span an extremely narrow range of $\delta^7\text{Li}$ (+3.6 to +3.8‰). $\delta^7\text{Li}$ of pristine whole-rock peridotites is homogeneous at +3.7 to +4.3‰ identical to previously defined $\delta^7\text{Li}$ of the Earth's upper mantle [2]. Lunar mare basalts and picritic glasses show a dramatic variability of $\delta^7\text{Li}$ (+3.4 to +6.4‰) that varies with lithology. A ferroan anorthosite representative of the lunar crust has a $\delta^7\text{Li}$ of +8.9‰ that is not affected by isotopically heavy solar wind due to extremely short exposure (<2 Myr). Two Martian meteorites exhibit slightly different $\delta^7\text{Li}$ values (Zagami +3.9‰; Nakhla +5.0‰). Five eucrites, presumed to be impact-excavated material from asteroid 4 Vesta, yield a $\delta^7\text{Li}$ of +3.7‰. Two chondrites, Allende (CV3) and Bruderheim (L6), are isotopically lighter than the estimated bulk composition of planetary bodies in the inner solar system.

Discussion: Earth's upper mantle seems to have, on average, Li isotope composition of +4.0‰. Three lunar basalts least depleted in Eu (two quartz-normative basalts and a picritic orange glass) constrain a lunar mantle $\delta^7\text{Li}$ mean of $+3.8 \pm 0.4$ ‰. Other mare basalts and picritic glasses are isotopically heavier and correlate with indices of magmatic differentiation (Li/Yb, Ga/Hf, Eu_N/Eu^*). This likely reflects crystallization of olivine and pyroxenes with imposed Rayleigh fractionation during the lunar magma ocean stage. Zagami, a Martian basalt, reflects a source within the Martian mantle and has $\delta^7\text{Li}$ indistinguishable from that of the Earth and Moon. The slightly elevated $\delta^7\text{Li}$ of Nakhla (clinopyroxenite) possibly reflects preferential incorporation of $\delta^7\text{Li}$ into clinopyroxene, an observation in accord with equilibrium intermineral fractionation of Li isotopes in pristine spinel lherzolites ($\delta^7\text{Li}_{\text{ol}} \approx \delta^7\text{Li}_{\text{opx}} < \delta^7\text{Li}_{\text{cpx}}$). Eucrites give a value identical within error to Earth, Moon, and Mars (Zagami).

Conclusions: We provide evidence for homogeneity of mantles of terrestrial planets and a small but significant Li isotope difference between chondrites and planetary bodies in the inner solar system. The difference between primitive and differentiated parent bodies is either established during the planet formation process [4] or reflects water/rock interaction on chondrite parent bodies [5].

References: [1] Magna T. et al. 2006. *Earth and Planetary Science Letters* 243:336–353. [2] Chan L.-H. 2003. *Geochimica et Cosmochimica Acta* 67:A57. [3] Chan L.-H. et al. 2002. *Earth and Planetary Science Letters* 201:187–201. [4] Wiechert U. and Halliday A. N. Forthcoming. *Earth and Planetary Science Letters*. [5] McDonough W. F. et al. 2003. Abstract #1931. 34th Lunar and Planetary Science Conference.

5356

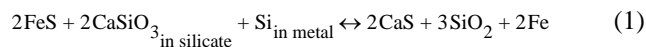
CaS FORMATION FROM A CI COMPOSITION AT HIGH PRESSURE AND TEMPERATURE UNDER LOW OXYGEN FUGACITY

V. Malavergne^{1, 2}, S. Berthet^{1, 2}, and K. Righter³. ¹Lunar and Planetary Institute, Houston, Texas 77058, USA. ²Université de Marne La Vallée, Laboratoire des Géomatériaux, Champs-sur-Marne, 77454 Cedex, France. E-mail: malavergne@lpi.usra.edu. ³NASA Johnson Space Center, Houston, Texas 77058, USA

Introduction: The cubic monosulfide series with the general formula (Mg,Mn,Ca,Fe)S are common phases in the enstatite chondrite (EH) and aubrite meteorite groups. In the Earth's mantle, sulfide minerals are associated with peridotites and eclogites (e.g., [1]). Study of these sulfide mineral systems is of interest for the mineralogy and petrology of planetary mantles. For example, MgS could occur in the primitive Earth [2] and because it remains a low density phase compared to metal, would stay a separate phase during the core formation process, and thus not segregate to the core. (Mg,Ca,Mn,Fe)S sulfides might thus be important phases even in planetary differentiation processes. The importance of such minerals, and their formation, composition, and textural relationships for understanding the genesis of enstatite chondrites and aubrites, has long been recognized [3]. The main objective of this experimental study is to understand the formation and evolution of (Mg,Ca,Mn,Fe)S sulfides, particularly the oldhamite CaS, with pressure and temperature but also with redox conditions because EH and aubrites are meteorites that formed under reduced conditions.

Results: A simplified CI chondritic glass mixed with FeS and Fe-Si alloy were used as starting material. Some trace elements (as U, Nd, and transition elements) were also added. Multi-anvil experiments were performed at the Bayerisches Geoinstitut, Bayreuth, Germany, using a 1200-ton press, up to 20 GPa and 2200 °C. Samples were characterized and analyzed by scanning electron microscopy, Raman spectroscopy and electron microprobe. At 20 GPa and 2200 °C, grains of majorite, which are almost FeO-free, are present with a homogeneous Fe-S-Si alloy, small grains of CaS, and SiO₂.

Discussion: Due to the Si added in the starting material, it was possible to reach highly reduced redox conditions during the experiments. We obtain a minimum relative fO_2 value equal to -6.5 log units below the IW buffer. That means that this sample underwent the same range of fO_2 that prevailed during the formation of EH chondrites. Because of these very low fO_2 it was possible to form some CaS likely through the following reaction:



No silicate melting is thus necessary to crystallize some CaS through process (1). The distribution coefficients of U and Nd between metal and CaS have been measured. Our first results indicate that Nd prefers CaS, even stronger than U does. These observations are in agreement with previous observations done on EH [4, 5]. New piston-cylinder experiments are ongoing to constrain (1) at lower pressure and temperature.

References: [1] Sharp Z. D. 1996. *Nature* 211:402–403. [2] Siebert J. et al. 2004. *Physics of the Earth and Planetary Interiors* 144:421–432. [3] Keil K. 1989. *Meteoritics* 24:195–208. [4] Furst M. J. et al. 1982. *Geophysical Research Letters* 9:41–44. [5] Murrell M. T. and Burnett D. S. 1982. *Geochimica et Cosmochimica Acta* 46:2453–2460.

5181

A COMPARISON OF AN ISLAMIC CONTEMPORARY COMET REFERENCE AND THE *ANGLO-SAXON CHRONICLE* CONTEMPORARY COMET REFERENCE TO HALLEY'S COMET OF 1066 A.D.

A. A. Mardon^{1, 2}. ¹Antarctic Institute of Canada. ²Honourary Professor, Penza State Pedagogical University, P.O. Box 1223, Main Post Office, Edmonton, Alberta T5J 2M4, Canada. E-mail: amardon@shaw.ca

Introduction: The following are two different contemporary written references to Halley's comet of 1066 A.D., one from England and one from the Islamic world. Other comparisons between the *Anglo-Saxon chronicles* records of cometary sightings give the substantiation that the ASC has historical veracity.

Textual References: "In the first tenth of Jumada I if this year a great comet with a long tail appeared in the east. Its width was around three yards and it stretched to the middle of the sky. It stayed until the twenty seventh and then disappeared. Then there appeared at the end of the same month at sunset a heavenly body with light that surrounded it like that of the moon. People were frightened. When the night fell, the heavenly body developed a tail pointing south. It stayed for ten days and then disappeared." Textual contemporary reference from the Islamic Medieval source Ibn al-Jawzi [1].

العشر الأول من جمادى الأولى ظهر كوكب كبير له ذؤابة طويلة يف
بناحية المشرق عرضها نحو ثلاث أذرع وهي ممتدة إلى وسط السماء
وبقي إلى السابع والعشرين من الشهر وغاب ثم ظهر أيضاً آخر الشهر
هليلج هرون رادتس دق بكفوك سمشلا بورغ دن ع روكذملا
هل راص ليللا ملظاً املو اوج عزن او سانلا عاتراف رملك
لحمضا مٹ ماي قرشع يقبو بونجلا وحن بئ اوذ

"Then was over all England such a token seen as no man ever saw before. Some men said that it was the comet-star, which others denominate the long-hair'd star. It appeared first on the eve called 'Litania major,' that is, on the eighth before the calends of May; and so shone all the week." Textual contemporary reference from the *Anglo-Saxon chronicle*.

Acknowledgements: The support of F. Barrage and the Maskukat Collection of Islamic Coins.

References: [1] http://islamiccoins.ancients.info/comets_and_meteorites.htm.

5004

POSSIBLE PLEISTOCENE METEORITE PLACER DEPOSITS ON THE CANADIAN PRAIRIES SIMILAR TO ANTARCTIC METEORITE PLACERS

A. A. Mardon¹, M. Zalcik², J. A. Greenspon³, and E. G. Mardon¹. ¹Antarctic Institute of Canada. E-mail: amardon@shaw.ca. ²Noctilucent Cloud Canadian-American Network. E-mail: bluegrama@shaw.ca. ³Stargate Research Lab. E-mail: jon.a.greenspon@stargateresearch.com

Introduction: In 1988 [1, 2], the first author predicted the possibility that meteorite placer zones might have occurred in North America during the last glaciation. It is possible that similar concentrations of meteorites may be found in North America similar to those that have been found in the Antarctic. In late 2005, it was proposed in the media that the rapid recovery of several meteorites near Winnipeg, Manitoba, Canada, may mean that meteorites could be concentrated there through the same processes that occurred in Antarctica [3, 4].

Analogues to Antarctic Meteorites: Over the later part of the 20th century and the first part of the 21st century, approximately 30,000 separate meteorites have been recovered in the Antarctic by various nations. Is it possible that in formerly glaciated portions of North America there might be meteorite placer deposits that are similar to what has been found in the Antarctic. It should be noted that the author was a junior member of the 1986–1987 USARP team which recovered over 700 separate meteorites in the area of the Antarctic Polar Plateau and the Lewis Cliff Ice Tongue. This area near the source of the Beardmore Glacier has been called from the time of R. F. Scott of the Antarctic as the “Highway to the Pole.” Heavily traversed and overflowed substantially for most of the 20th century, meteorites were not found until W. A. Cassidy led a team to the Lewis Cliff Ice Tongue in the 1980s. We propose that other placers might exist in the Northern Hemisphere, specifically in North America in areas that had similar characteristics of glaciation. Meteorite concentrations in the last glacial period may be similar to the abundance of precious meteorites that have been found in the Antarctic.

Further Research: Other locales around the world in formerly glaciated regions such as Northern Europe and parts of Asiatic Russia should have similar potential Pleistocene deposits to those found in the Antarctic by various nations’ Antarctic meteorite recovery programs [1]. Scientists searching for meteorites may not be looking in locations with analogue glacial characteristics to those meteorite placers that have been found in the Antarctic [5]. If the authors are correct, it might be possible that Pleistocene meteorites placers could be found in North America in the future. Finds on the Canadian prairies might indicate potential meteorites that may be recovered in the future.

References: [1] Mardon A. A. 1988. Abstract. *Meteoritics* 23:286–287. [2] Mardon A. A. 1988. *Meteoritics* 30:5. [3] Mardon A. A. 2005. *The Edmonton Journal*, December 22. [4] Mardon A. A. 2005. *The Lethbridge Herald*, December 28. [5] Hildebrand A. R. 2005. Personal communication.

5248

TRACE ELEMENTS IN PRESOLAR SiC GRAINS: CONDENSATION VERSUS IMPLANTATION

K. K. Marhas^{1,2}, P. Hoppe², and U. Ott². ¹Laboratory for Space Sciences and Physics Department, Washington University, St. Louis, Missouri 63130, USA. E-mail: kkmahas@wuphys.wustl.edu. ²MPI für Chemie, Becherweg 27, D-55128 Mainz, Germany

Introduction: Trace elements in various individual presolar grains serve as a tool to understand the chemical and physical conditions during the formation of presolar grains (in expanding envelope/ejecta of stars). Two scenarios that have been discussed to incorporate trace elements within the forming presolar SiC grains are a) condensation of trace elements as solid solutions [1, 2]. The abundances will be a function of C/O ratio, pressure, volatility and crystal structure; and b) ion implantation of trace elements into the SiC grains. In this case abundances depend on the ionization potential of the respective element [3]. Noble gas data for presolar SiC grains indicate that ion implantation plays an important role. Quantifying the fraction of implanted trace elements might give a better idea on the physical conditions under which SiC condensation takes place.

Experimental: We have measured 32 individual mainstream SiC grains, 7 SiC-agglomerates, and 17 single X-grains from the Murchison and Murray meteorites using the NanoSIMS at the Max Planck Institute for Chemistry at Mainz for Ba isotopes (except ¹³⁰Ba, ¹³²Ba) along with the most abundant isotopes of selected trace elements (Sr, Zr, Cs, La, and Ce) [4].

Results: The trace element characteristics (normalized to Si and Cl) can be summarized as follows: 1) There is a spread of two orders of magnitude for the concentrations of all trace elements except for Cs which varies by seven orders of magnitude. The data obtained for bulk samples of Murchison KJA-KJG grains [1] for Ce, La, Sr, and Zr are compatible with those of the mainstream grains analyzed in this work. 2) There is no systematic difference between the trace element concentrations of the 17 X grain and single mainstream grains and the agglomerates. 3) Normalized Sr abundances are on average lower than Ba by an order of magnitude. 4) Except for Cs and Zr, correlations exist between Ba and the other trace elements, that is, [Ba]-[La], [Ba]-[Ce], and [Ba]-[Sr]. 5) Zr, La, Ba, and Ce are enriched relative to Si and Cl, whereas most of the SiC grains are depleted in Sr. 6) There is a rough negative correlation between concentrations of Ce, Ba, La, and Sr and grain size. This trend even extends to the larger KJH grains (3.4–5.9 microns) studied by [1].

The existence of a negative correlation between grain size and trace element concentration implies that at least some fraction of the Ba and other trace elements were implanted into the mainstream SiC grains. It has been proposed that 60% of the Ba in SiC was trapped by ion implantation [3] and that the rest co-condensed into the SiC grains. The ion implantation scenario is also favored by trace element data from ICPMS measurements on bulk SiC [5]. Clearly, more theoretical work needs to be done in order to get a better understanding on how the trace elements were incorporated in presolar SiC grains.

References: [1] Amari S. et al. 1995. *Meteoritics* 30:679–693. [2] Lodders K. and Fegley B. 1995. *Meteoritics* 30:661–678. [3] Verchovsky A. B. et al. 2004. *The Astrophysical Journal* 607:611–619. [4] Marhas K. K. et al. 2005. Abstract #1855. 36th Lunar and Planetary Science Conference. [5] Yin et al. *The Astrophysical Journal*. Forthcoming.

5195

CHRONOMETRY AND REDOX STATE OF THE ANGRITE PARENT BODY AS INFERRED FROM Hf-W ISOTOPIC DATA

A. Markowski¹, G. Quitte¹, T. Kleine¹, M. Bizzarro², A. J. Irving³, and A. N. Halliday⁴. ¹Institute for Isotope Geochemistry and Mineral Resources, ETH-Zürich, Switzerland. E-mail: markowski@erdw.ethz.ch. ²Geological Institute, University of Copenhagen, Denmark. ³Department of Earth and Space Sciences, University of Washington, Seattle, Washington, USA. ⁴Department of Earth Sciences, University of Oxford, UK

Introduction: The ¹⁸²Hf-¹⁸²W isotopic system is commonly used to date early planetesimal metal-silicate differentiation because it has an appropriate half-life of 8.9 Myr and Hf and tungsten are strongly fractionated during differentiation. Hafnium is strongly lithophile, whereas W is moderately siderophile in a reducing environment. However, the chemical properties of W are different under oxidizing conditions and W becomes more lithophile. According to ²⁶Al-²⁶Mg and U-Pb data [1, 2] angrites are very ancient basaltic achondrites that have differentiated ~3 Myr after the CAIs formation. These achondrites can potentially be used to intercalibrate different chronometers based on short- and long-lived radionuclides (e.g., [3]), because they cooled quickly. They can also be used to study the redox conditions of early planetesimal formation. After the first report on this topic [3], we further investigated the Hf-W isotopic systematics in mineral separates from Sahara 99555 and are in the process of generating pure mineral separates from Northwest Africa 2999.

Chronology: In addition to our previous measurements of Sahara 99555, we obtained Hf-W data for a >230 m fraction which is enriched in feldspars, for fines, and for an acid-washed 80–150 m fraction. We also analyzed a whole rock and fines from another piece of Sahara 99555. All data plot on an isochron with an initial ¹⁸²Hf/¹⁸⁰Hf of $\sim 7.3 \times 10^{-5}$ and an initial ϵ_W of about -2.1. The difference in slopes of Sahara 99555 and Allende CAIs isochrons [4] yields a time interval of ~5 Myr, in good agreement with the ²⁶Al-²⁶Mg age obtained for mineral separates for Sahara 99555 [2, 5, 6], but slightly younger than ²⁶Al-²⁶Mg model ages inferred from whole-rock angrite samples [2]. Average Hf/W ratios obtained for whole-rocks from Sahara 99555 and Northwest Africa 2999 are ~5 and ~3.5, respectively. We thus inferred from Sahara 99555 a model-dependent core formation age for the angrite parent body between 1.7 and 2.8 Myr after Allende CAIs.

Redox Conditions: Using similarity in the bulk silicate solid/liquid distribution coefficients for Th and W, we recalculated the Hf/W ratios of the silicate reservoirs of D'Orbigny (~8), Sahara 99555 (~5), Angra dos Reis (~2), Northwest Africa 2999 (~2) [7, unpublished data]. These Hf/W ratios are lower than those calculated by Halliday [8] for the eucrite parent body, the Earth, and the Moon, suggesting that oxidizing conditions may have prevailed for at least some early planetesimals during core-mantle segregation.

References: [1] Bizzarro M. et al. 2005. *The Astrophysical Journal* 632:L41–L44. [2] Baker J. et al. 2005. *Nature* 436:1127–1131. [3] Markowski A. et al. 2006. Abstract # 2000. 37th Lunar and Planetary Science Conference. [4] Kleine et al. 2005. *Geochimica et Cosmochimica Acta* 69: 5805–5818. [5] Spivak-Birndorf et al. 2005. Abstract #2201. 36th Lunar and Planetary Science Conference. [6] Nyquist et al. 2003. Abstract #1388. 34th Lunar and Planetary Science Conference. [7] Mittlefehldt et al. 2002. *Meteoritics & Planetary Science* 37:345–369. [8] Halliday A. N. 2004. *Nature* 427:505–509.

5130

INVESTIGATING RECOIL LOSS FROM ²²Na DECAY WITHIN NANOGRAINS

E. Marosits and U. Ott. Max-Planck-Institut für Chemie, Abteilung Geochemie, Becherweg 27, D-55128 Mainz, Germany. E-mail: marosits@mpch-mainz.mpg.de

Introduction: Recoil effects may be of importance in the study of presolar grains in a variety of ways. It is essential, e.g., to understand recoil losses in spallation reactions in order to determine presolar cosmic ray exposure ages [1]. Recoil does also occur in radioactive decay, however. For β -decays it is usually a negligible effect, but the situation may be different for grains that are of nm-size, such as the presolar nanodiamonds, where the expected evidence for the former presence of now extinct ²⁶Al and ⁴⁴Ti has not been found [2]. We have started a set of experiments in order to determine whether loss due to recoil may be an explanation for this lack [3].

Experimental: As the next step in our series of investigations we have implanted radioactive ²²Na into both terrestrial detonation nanodiamonds (“K2” supplied by A. P. Koscheev; cf. also [4]) as well as meteoritic nanodiamonds extracted from the Allende and Murchison meteorites using procedures similar to those of [5]. For the implantation radioactive ²²Na as NaCl solution was diluted with stable Na for a ²²Na/²³Na ratio of $\sim 10^{-3}$. Approximately 0.2 μ l solution were put onto a Pt filament together with silica gel, from which they were thermally ionized, accelerated to 1 keV energy and implanted into a nanodiamond layer (~1 mg) deposited on a Cu ribbon. After implantation the diamonds were recovered from the Cu ribbon, washed with HCl to remove surficial Na and kept in NH₃ solution in order to avoid reimplantation of daughter nuclei into neighboring grains. Effective implantation yields were determined by counting the activity of the recovered and washed diamonds and were found to be on the order of 1% ($\sim 6 \times 10^{10}$ atoms) for the terrestrial and ~1‰ ($\sim 5 \times 10^9$ atoms) for the meteoritic diamonds.

Decay and Recoil: Determining recoil loss requires checking the content of the decay product ²²Ne contained in the diamonds after sufficient decays have occurred. The first results for the K2 detonation diamonds will be available by the time of the conference. Results for the Allende and Murchison diamonds will become available later: more complete decay is required because of the smaller amount of implanted ²²Na as well as the rather high background of Ne-HL (cf. [6]).

Acknowledgments: We thank A. P. Koscheev for the K2 diamonds, Ch. Sudek for preparation of the meteoritic residues, and the staff of the mechanical and electronics workshop at MPI for construction of the implantation setup. H. Keller as well as G. Hampel (Institut für Kernchemie, Johannes Gutenberg-Universität Mainz) provided valuable help with handling the radioactive material and made it possible to determine the ²²Na activities of our samples.

References: [1] Ott U. et al. 2005. *Meteoritics & Planetary Science* 40: 1635–1652. [2] Besmehn A. et al. 2000. Abstract #1544. 31st Lunar and Planetary Science Conference. [3] Marosits E. et al. 2005. Abstract. *Meteoritics & Planetary Science* 40:A96. [4] Koscheev A. P. et al. 2001. *Nature* 412:615–617. [5] Amari S. et al. 1994. *Geochimica et Cosmochimica Acta* 58:459–470. [6] Huss G. R. and Lewis R. S. 1994. *Meteoritics* 29:791–810.

5318

INDUCTION HEATING IN ASTEROIDS PART 2: EXPERIMENTAL ANALOGS

C. A. Marsh, D. N. Della-Giustina, J. Giacalone, and D. S. Lauretta. University of Arizona, Lunar and Planetary Laboratory, Tucson, Arizona 85721, USA. E-mail: celinda@lpl.arizona.edu

Introduction: The theoretical background of induction heating of asteroids, as well as recent observations and models of magnetic field strengths are discussed in [1]. We have established a laboratory in which samples can be subjected to magnetic fields and thermal response can be measured. We have conducted a series of experiments to test the effect of induction heating on asteroidal materials. Here we take the parameters from [1] and compare them to our experimental operating procedure and results.

Experimental Methods: The materials used in our experiments are pellets of cutting dust from the Fukang pallasite [3], controlled mixtures of olivine and metal, and pure metal reference materials. Grain sizes and composition are measured in control samples in all cases through optical microscopy and electron microprobe analysis.

Our procedure consists of placing samples in vacuum-sealed silica tubes and heating them using an Ameritherm HotShot radio frequency (RF) induction heating station. This device is designed to heat small objects using frequencies from 150 to 400 kHz with up to 2 kW of power. The calculated maximum magnetic field strength for our experimental configuration is 24 Gauss. Temperature is monitored throughout the experiment using either an Omega IR2 two-color pyrometer or an Omega OS37-10-K pyrometer and DPi32 temperature logging system.

Table 1. Results of induction furnace experiments. Gauss is the magnetic field strength produced by the HotShot.

Sample	Gauss	Temperature
Fukang powder	24 (max)	500 °C
Fe powder	24 (max)	650 °C
Fe foil	24 (max)	750 °C

Conclusions: The results obtained thus far show the dependence of peak temperature reached to both composition and grain size. Considerable heat has been generated at a magnetic field strength below those modeled by [2] as having reached the circumstellar disk. Thus far, we have been able to reproduce the temperatures experienced by type IV and type V ordinary chondrites. We are performing additional experiments on a wide range of asteroidal samples. Additional factors, such as frequency, object size, and duration of heating are needed to extrapolate the experimental system to induction heating on asteroids. As this series of experiments continues, it will provide a critical quantitative constraint on the extent and efficacy of induction heating in asteroids in the early solar system.

References: [1] Della-Giustina D. N. et al. 2006. Abstract #5380. *Meteoritics & Planetary Science* 41. This issue. [2] Favata F. et al. 2005. *The Astrophysics Journal Supplement Series* 160: 469–502. [3] Lauretta D. S. et al. 2006. Abstract #2250. 37th Lunar and Planetary Science Conference.

5204

ISOTOPIC ANALYSIS OF NUCLEOBASES IN THE MURCHISON METEORITE

Z. Martins¹, O. Botta², M. L. Fogel³, M. A. Sephton⁴, D. P. Glavin², J. S. Watson⁵, J. P. Dworkin², A. W. Schwartz⁶, and P. Ehrenfreund^{1, 6}. ¹Astrobiology Laboratory, Leiden Institute of Chemistry, Einsteinweg 55, 2300 RA Leiden, The Netherlands. E-mail: z.martins@chem.leidenuniv.nl. ²NASA Goddard Space Flight Center, Goddard Center for Astrobiology, Greenbelt, Maryland, USA. ³GL, Carnegie Institution of Washington, Washington D.C., USA. ⁴Impacts and Astromaterials Research Centre, Department of Earth Science and Engineering, South Kensington Campus, Imperial College, London, UK. ⁵Planetary and Space Sciences Research Institute, The Open University, Walton Hall, Milton Keynes, UK. ⁶Radboud University Nijmegen, Nijmegen, The Netherlands

Nucleobases are important compounds in modern terrestrial biochemistry, because they are key components of nucleic acids (DNA and RNA), which are the central biopolymers used in the storage, transcription, and translation of genetic information.

Nucleobases have been detected in carbonaceous chondrites by several research groups [1–5]. Because of the fact that significant quantitative and qualitative differences were observed (even within the same meteorite), confirmation of the extraterrestrial origin of these nucleobases is still open to question. In order to address this crucial question, we have performed an extensive analysis that included formic acid extraction of samples of the Murchison meteorite [6], followed by an extensive purification procedure, analysis, and quantification by high-performance liquid chromatography with UV absorption detection and gas chromatography-mass spectrometry. We obtained results that were qualitatively consistent with previous results [3, 4], but showed some significant quantitative differences. Compound specific carbon isotope values for xantine and uracil were obtained, using gas chromatography-combustion-isotope ratio mass spectrometry. We also analyzed a soil sample that was collected in the proximity of the Murchison meteorite fall site, subjecting it to the same extraction, purification, and analysis procedure.

Stable carbon isotope measurements unambiguously confirm that the nucleobases in the Murchison meteorite are indigenous to the meteorite, and clearly differ from the values determined for the terrestrial nucleobases measured in the surrounding fall site soil. These results support the hypothesis that nucleobases were exogenously delivered to the early Earth, contributing to a feedstock of molecules crucial for the origin of life on our planet.

References: [1] Hayatsu R. et al. 1975. *Geochimica et Cosmochimica Acta* 39:471–488. [2] Folsome C. E. et al. 1971. *Nature* 232:108–109. [3] Stoks P. G. and Schwartz A. W. 1979. *Nature* 282:709–710. [4] Stoks P. G. and Schwartz A. W. 1981. *Geochimica et Cosmochimica Acta* 45:563–569. [5] Shimoyama A. et al. 1990. *Geochemical Journal* 24:343–348. [6] Martins Z. et al. 2004. *Meteoritics & Planetary Science* 39:A5145.

5226

SIMULATION OF COSMOGENIC NUCLIDE PRODUCTION IN STONY AND IRON METEORITES

J. Masarik. Department of Nuclear Physics, Komensky University, Mlynska dolina F/1, Sk-842 48 Bratislava, Slovakia. E-mail: Masarik@fmph.uniba.sk

Introduction: Development in the understanding of primary cosmic-ray spectra in the last decade and development in the numerical codes used for simulations of their interaction with matter leads to the changes in theoretical estimates of production rates in meteorites. Influence of these changes on production rates of cosmogenic nuclides is reviewed in this paper. The numerical simulation cosmic-ray particles interactions with matter was done with the LAHET code system (LCS) [1], GEANT [2], and MCNPX [3]. The investigated objects were spheres with various radii that were divided into spherical layers. We used the spectrum of the galactic-cosmic-ray particles corresponding to their long-term averaged value [4]. Two different shapes of differential primary spectra [5, 6] were used in our simulations.

The production rates of nuclides were calculated by integrating over energy the product of these fluxes and cross-sections for the nuclear reactions making the investigated nuclide. For cross-sections, we relied on the values evaluated by us and tested by earlier calculations (e.g., [4]).

Results and Discussion: These spectra depend on the shielding of the sample, i.e., its location inside the object, the object's size, and its chemical composition. The differences in particle fluxes obtained by various codes are minor. There are significant differences between production rate depth profiles in stony and iron meteorites caused by the presence of heavy elements in iron meteorites in much higher concentrations. We found that there are also substantial differences between capture rates for stony and iron meteorites. They are independent of primary spectra. Generally, higher iron content results in lower fluxes of thermal neutrons and therefore also lower capture rates and vice versa.

We can compare our calculations with some cosmogenic nuclide measurements for well studied meteorite, as for example Knyahinya [7]. This study is in progress, and will be presented.

Acknowledgements: This work was supported by Slovak Grant Agency.

References: [1] Prael R. E. and Lichtenstein H. 1989. LA-UR-89-3014. [2] Waters L. S., ed. 1999. MCNPX user's guide, Doc. LA-UR-99-6058. [3] Brun B. et al. 1987. GEANT3 user's guide, Rep. DD/EE/84-1. [4] Masarik J. and Reedy R. C. 1994. *Geochimica et Cosmochimica Acta* 58:5307–5317. [5] Castagnoli G. C. and D. Lal. 1980. *Radiocarbon* 22:133–158. [6] Webber W. R. and Higbie. 2003. *Journal of Geophysical Research* 108:1355. [7] Graf T. et al. 1997. *Meteoritics & Planetary Science* 32:25–30.

5120

CONTINUED SEARCH FOR Q IN DIFFERENT TYPES OF METEORITES BY THE PHYSICAL SEPARATION METHOD

J. Matsuda¹, Y. Matsuo¹, C. Nishimura¹, and S. Amari². ¹Department of Earth and Space Science, Graduate School of Science, Osaka University, Toyonaka, Osaka 560-0043, Japan. E-mail: matsuda@ess.sci.osaka-u.ac.jp. ²Laboratory for Space Sciences and the Physics Department, Washington University, St. Louis, Missouri 63130, USA

Introduction: Meteoritic separates that are enriched in the Q-gases have usually been prepared by the chemical procedure [1]. With Allende (CV3), Matsuda et al. [2] have shown that material that floats on the surface of the water ("floating fraction") during the freeze-thaw disaggregation exhibits the similar isotopic and elemental abundances to those of residues treated with HF-HCl. This method has been applied for a few fragments of Allende and floating fractions enriched in the Q-gases have always been recovered [3, 4].

This physical separation method was also applied for two ordinary chondrites (H/L3.2 and L4-6) [5]. The floating fractions from the two meteorites comprise 0.046 wt% and 0.0057 wt% of the bulk meteorite, respectively. Concentrations of the heavy noble gases (Ar, Kr, and Xe) in the floating fraction from the H/L3.2 meteorite are similar to those of the bulk meteorite, indicating noble gases are not enriched in the floating fraction. Excesses in the heavy noble gases (1–3 orders of magnitude of the bulk meteorite) are observed in the floating fraction of the L4-6 chondrite. However, Xe isotopic ratios of the fraction are identical to those of the air. Obviously, the physical separation method is not applicable to ordinary chondrites to concentrate the fraction enriched in noble gases.

In this study, we applied the physical separation method to Murchison (CM2), a carbonaceous chondrite in a different petrologic type from Allende (CV3).

Results and Discussion: We started from 648.48 mg of a fragment of Murchison. After 120 cycles of the freeze-thaw disaggregation, 0.26 mg of the floating fraction was recovered. This yield (0.004%) is much smaller than the yield (0.068%) obtained after 216 cycles [4], however it is equivalent to the yield (0.004%) after ~120 cycles for Allende [3].

Elemental and isotopic abundances of noble gases in the floating fraction have been analyzed as well as elemental abundances of noble gases in the bulk Murchison. Pronounced enrichment of the heavy noble gases was not observed in the floating fraction from Murchison. Thus, Q in Murchison does not preferentially float on the surface, behaving the same way as the rest of constituents of the meteorite. EDX analysis of the floating fraction with scanning electron microscopy indicates most grains are silicates. This is consistent with the noble gas result and yet illuminates another difference from the Allende floating fractions, where many of the grains are carbonaceous.

It remains to be seen why the physical separation method can be successfully applied only to Allende: a make-up of carbonaceous matter in Allende may favor a preferential separation of Q (and presolar diamond) during the freeze-thaw disaggregation.

References: [1] Lewis R. S. et al. 1975. *Science* 190:1251–1262. [2] Matsuda J. et al. 1999. *Meteoritics & Planetary Science* 34:129–136. [3] Zaizen S. et al. 2000. *Antarctic Meteorite Research* 13:100–111. [4] Amari S. et al. 2003. *Geochimica et Cosmochimica Acta* 67:4665–4677. [5] Nishimura C. et al. 2004. *Meteoritics & Planetary Science* 39:A78.

5209

CATHODOLUMINESCE STUDY OF THE NAKHLITE METEORITES FROM ANTARCTICA

N. Matsuda¹, H. Nishido¹, A. Gucsik², T. Okumura¹, M. Kayama¹, and K. Ninagawa³. ¹Research Institute of Natural Sciences, Okayama University of Science, 1-1 Ridai-cho, Okayama 700-0005, Japan. E-mail: matsuda@rins.ous.ac.jp. ²University of West Hungary, Bajcsy-Zs. E. u. 4., Sopron, H-9400, Hungary. ³Department of Applied Physics, Okayama University of Science, 1-1 Ridai-cho, Okayama 700-0005, Japan

Introduction: The recent discovery of a nakhlite among numerous specimens of the meteorites collected in Antarctica has made many important contributions to its mineralogy, crystallization differentiation, accumulation process, and thermal history. It is noteworthy that hydrated alteration of this meteorite could be estimated from the existence of clay-like materials. In this study we focus on the cathodoluminescence (CL) emitted from the minerals in the nakhlite to investigate their crystal chemistry concerning to lattice defect and trace impurity.

Samples and Methods: Two polished thin sections of Yamato-000593 and Yamato 000749, which are possibly paired, supplied from the National Institute of Polar Research (NIPR) were employed for CL measurements. These meteorites belong to the nakhlite subgroup of the SNC. CL image, which can be compared to optical image under a petrographic microscope, was obtained using a cold-cathode type "Luminoscope" at 15 kV with a cooled CCD camera. A CL image at high magnification and CL spectra were collected using a scanning electron microscope-cathodoluminescence (SEM-CL) composed of SEM: JEOL 5410LV with a grating monochromator: Oxford Mono CL2, where EDS system can be used in combination with SEM-CL. A scanning electron beam of energy 15 kV and current 1.0 nA was adopted in CL analysis.

Results and Discussion: Two samples exhibit a similar petrographic texture with unbrecciated cumuli of mineral grains consisting abundant augite with less olivine, mesostasis, and minor hydrated alteration materials. The texture and mineral paragenesis coincide with the previous description. A systematic survey of all areas by CL imaging reveals that CL emissions with blue, pale pink, yellow, and dark violet colors are apparent in the mesostasis and hydrated alteration zone, whereas narrow streaks of faint emission are recognized in augite and olivine grains. Based on the EDS analysis the outstanding CL of bright blue is emitted only from pure silica grains, which are distributed in the mesostasis with lath-shaped plagioclase or exist as an isolated round shape. CL spectra of these grains indicate a broad peak at around 415 nm, which can be assigned to recombination of self-trapped exciton (STE) and/or E' center characteristic to silica minerals. Usually ordinary quartz shows red to violet CL emission, but not so bright at ambient temperature, with the spectral peak in red color region from 600 to 650 nm. Therefore, the silica minerals with bright blue CL emission might not be identified to quartz. We have been investigating to clarify them using a microRaman spectroscopy. Most plagioclase (An₃₀₋₄₀), which are abundant in the mesostasis, exhibits pale pink CL, of which spectra shows three broad peaks around at 400, 570, and 760 nm corresponding to lattice defect and trace impurities of Mn²⁺ and Fe³⁺, respectively. Yellow and dark violet CL can be detected in glassy "maskelynite" and possibly hydrated alternated zone, but a rare case. In this way a CL method presents unique perspective casting new light on the study of the meteorite.

5247

COMETARY PETROLEUM IN HADEAN TIME?

M. Maurette¹ and A. Brack². ¹CSNSM, Bat. 104, 91405 Orsay-Campus, France. E-mail: maurette@csnsm.in2p3.fr. ²CBM, Rue Charles Sadron, 45071 Orleans Cedex 2, France

Introduction: Kerogens are abundant byproducts of incomplete combustion, pyrolysis, and radiation reprocessing of almost any kinds of organic precursors. In the absence of microorganisms, kerogen is one of the most durable and insoluble organic materials. On Earth, important substances are derived from some parent kerogen. They include petroleum and varieties of activated carbon. We question below whether the constituent kerogen of large, unmelted Antarctic micrometeorites (AMMs), which was identified from C/N ratios measured with a nuclear microprobe [1] might have been involved in the making of abiogenic crude oil in Hadean times, prior to ~4 Ga. As AMMs are probably cometary dust particles [2, 3], this petroleum would have a "cometary" origin.

Delivery of Micrometeorite Kerogen to the Hadean Oceanic Crust:

We predict that a huge mass (~5 × 10²⁴ g) of juvenile micrometeorites (JMMs) was accreted by the Earth, during the first ~200 Ma of the post-lunar period [2]. Recent AMMs flux measurements [4] show that at least ~20 wt% of the micrometeorites survive unmelted upon atmospheric entry [4]. As their kerogen represents about 2.5 wt% of carbon, this amounts to a total mass of kerogen on the early Earth's surface (~2.5 × 10²² g) equivalent to a ~40 m thick global layer. A large fraction of the unmelted JMMs were deposited on the early oceanic crust, which was formed very soon after the formation of the Moon around ~4.4 Ga ago.

A Slow Burial in Deep Sea Sediments That Mimics That of Dead

Plankton: On the Earth, bitumen- and kerogen-rich shales are the source rocks of petroleum. In the biogenic scenario most petroleum exploited today was derived from tiny plants and organisms (i.e., plankton) that thrived in the top layers of the oceans during the Jurassic. When they die they accumulate on the sea floor (like kerogen-rich unmelted micrometeorites), where they get steadily buried in sediments. At depths larger than a few hundreds meters, their residual organics yield kerogen whereas sea sediments are transformed into shales. Then, at larger depths in the "oil window" (between ~0.5–5 km), the heat and pressure break down kerogen to form petroleum.

Surprisingly, kerogen-rich micrometeorites would have followed an *abiogenic* fate that surprisingly well mimics the *biogenic* fate of dead plankton. This led to the abiogenic formation of crude oils at a time of intense impact fracturing, prior to ~4 Ga ago. This likely led to some giant spills of the abiogenic petroleum that could have formed kinds of gigantic mega-films of oil on the oceans, which did capture unmelted micrometeorites and various micrometeoritic "smoke" particles released upon atmospheric entry. Did this "dusty black tide" cosmic machinery open new reaction channels in the prebiotic chemistry of life?

References: [1] Matrajt G. et al. 2003. *Meteoritics & Planetary Science* 38:1585–1600. [2] Maurette M. 2006. *Micrometeorites and the mysteries of our origins*. Berlin: Springer-Verlag. pp. 1–330. [3] Maurette M. and Kurat G. 2006. Abstract #5243. *Meteoritics & Planetary Science* 41. This issue. [4] Duprat J. et al. 2006. Abstract #5239. *Meteoritics & Planetary Science* 41. This issue.

5243

MISSING “CARROTS” IN THE STARDUST AEROGEL

M. Maurette¹ and G. Kurat². ¹CSNSM, Bat. 104, 91406 Orsay-Campus, France. E-mail: maurette@csnsm.in2p3.fr. ²Institut für Geologische Wissenschaften, Universität Wien, Althanstrasse 14, 1090 Vienna, Austria

Introduction: Stardust apparently produced exciting results—as can be deduced from the scarce data available (e.g., NASA Stardust Web site). The conclusions drawn, however, seem to reflect a certain degree of confusion among investigators who either reach the grand conclusion that “the Stardust minerals may have crystallized from melts near other stars” and “at least some comets may have included materials ejected by the early Sun to the far reaches of the solar system.” There is no grand surprise with the mineralogical findings on Wild-2 particles (W2s) as they can be expected from what we know from meteorites, Antarctic micrometeorites (AMMs), and stratospheric IDPs (e.g., [1]). We discuss here our earlier prediction of a possible link between cometary matter and AMMs [2].

Bulbs against Carrots: The W2s recovered at the terminus of about 20 well-visible tracks in the aerogel (with length of up to 12 mm) are made of refractory minerals (forsterite, enstatite, diopside, spinel, anorthite). These tracks have a “bulb” shape very different from the “carrot” shape observed for all projectiles fired into aerogels at speeds similar to that of the W2s (~6 km/s), as to assess their survival during aerogel capture [4]. These spectacular “bulbs” are sprayed with tiny shell-splinters tracks. This bulb shape probably is the result of a powerful microscopic explosion ignited along the track of the W2s.

Saponite-Rich Chondrites without Chondrules: Saponite is the dominant hydrous silicate of IDPs and AMMs. Suppose that it is also the dominant hydrous phase of the W2s before their impact into the aerogel. This mineral contains structural water that starts to be released at a low temperature of ~100 °C. In contrast, the artificially accelerated projectiles included anhydrous minerals, such as those found in chondrules; fragments of the “dry” Allende chondrite; a mineral of the serpentine group (lizardite); and fragments of the Orgueil and Murchison chondrites, where serpentine is the dominant hydrous silicate.

Serpentine-rich projectiles yielded carrot-shaped tracks, probably because serpentine only contains OH groups that are released at a temperature of ~600 °C. Therefore, the dominant bulb shape of the W2s tracks would reflect the explosive release of the constituent water of the W2s saponite as well as a strong depletion of chondrules in the W2s flux. Only the largest refractory phases of the W2 “shrapnel” could continue and form a long track beyond the “bulb.” Surprisingly, the missing raw carrots alone would reveal two major similarities between IDPs, AMMs, and the W2s (i.e., the existence of saponite and a depletion of chondrules). In this case, the chemical and isotopic compositions of the AMMs and W2s olivines should be similar [4].

References: [1] Maurette M. 2006. *Micrometeorites and the mysteries of our origins*. Berlin: Springer-Verlag. pp. 1–330. [2] Maurette M. 1998. In *The molecular origin of life*. Cambridge: Cambridge University Press. [3] Burchell M. J. et al. 2006. *Meteoritics & Planetary Science* 41:217–232. [4] Engrand C. et al. 2006. Abstract #5237. *Meteoritics & Planetary Science* 41. This issue.

5093

THE UNBRECCIATED EUCRITES: VESTA’S COMPLEX CRUST

R. G. Mayne¹, A. Gale², T. J. McCoy², H. Y. McSween Jr.¹, and J. M. Sunshine³. ¹Department of Earth and Planetary Sciences, University of Tennessee, Knoxville, Tennessee 37996–1410, USA. E-mail: rmayne@utk.edu. ²Department of Mineral Sciences, Smithsonian Institution, Washington D.C., 20560–0119, USA. ³Department of Astronomy, University of Maryland, College Park, Maryland 20742, USA

Introduction: 4 Vesta is the largest differentiated asteroid and is critical to understanding the processes that contributed to the evolution of planets in the early solar system history. Gaffey [1] utilized subhemispheric color and spectral variations on the surface of Vesta to produce a lithologic map; however, regolith material blanketing the surface obscured smaller-scale details of the basaltic crust. By examining petrologic and spectral variations in eucrites, we can draw conclusions about the smaller-scale lithologic variations that exist in the upper basaltic crust.

Methodology: Unbrecciated eucrites were selected for study to avoid spectral mixing of different lithologies. The mineral abundances and distributions of 31 thin sections were mapped using the SEM and mineral chemistries analyzed with the electron microprobe. Eleven samples represent the petrologic diversity in the entire group, and their VISNIR spectra were collected at RELAB and modeled using MGM [2, 3].

Discussion: Our ultimate goal is to distinguish different lithologic units, as sampled by eucrites, using their spectra. We must first identify such units petrologically—in terms of textures, mineral chemistries, modes, grain sizes, and cooling rates—and then explore the extent to which they can be spectrally distinguished.

The unbrecciated eucrites are a diverse group of meteorites. To date, we have defined four distinct lithologies for the unbrecciated eucrites using their petrologic characteristics. These units, with an example of each, are: cumulate/slowly cooled (Moore County), partial-cumulate/Mg-rich partial melt (EET 87520), granoblastic (Ibitira), and quenched/quickly cooled (ALHA81001). The primary difference between these is their depth of formation in the crust. The spectra for these types show variations in spectral contrast, band centers, and band widths [4]. Preliminary MGM analyses can distinguish cumulate/slowly cooled from quenched/quickly cooled eucrites. This is possible primarily because quickly cooled eucrites contain only one pyroxene, whereas those that cooled slowly have two. Refined models will test if all four units can be defined by their spectra.

Implications: The basaltic crust on Vesta is complex and eucrites represent our best tool for understanding its formation and diversity, but we require both coordinated spectral/petrologic studies of the lithologic diversity and higher-resolution spectral data for the crust. In addition to continuing our study of eucrites, we intend to apply our laboratory data to the spectra of V-type asteroids [5]. These asteroids are thought to represent km+ sized fragments of the crust of Vesta and, hence, can provide a constraint on the approximate size of lithologic provinces that may occur on Vesta. Ultimately, the DAWN mission will provide the best opportunity to map the basaltic crust of Vesta at the highest spatial resolution.

References: [1] Gaffey M. J. 1997. *Icarus* 127:130–157. [2] Sunshine J. M. 1990. *Journal of Geophysical Research* 95:6955–6966. [3] Sunshine J. M. and Pieters C. M. 1993. *Journal of Geophysical Research* 98:9075–9087. [4] Mayne R. G. et al. 2006. Abstract #1796. 37th Lunar and Planetary Science Conference. [5] Binzel R. P. and Xu S. 1993. *Science* 260:186–191.

5030

FROM GASEOUS GIANTS TO ROCKY PLANETS

M. Mayor, Observatoire de Genève, CH-1290 Sauverny, Switzerland

In the last eleven years, about 200 exoplanets have been detected. Most of these detections have been made with Doppler spectroscopy, looking for the variation of the stellar velocity induced by the gravitational influence of planetary companions. A dozen exoplanets have also been detected by the presence of transits or gravitational microlensing events.

These discoveries have revealed an impressive diversity of exoplanet orbital properties with periods as short as 1.2 days, for example, or orbital eccentricities as large as 0.93. Systems with several planets orbiting the same stars are more and more frequently found, some of them with planets on resonant orbits. Several statistical properties are already emerging and help constraining the formation mechanisms of these systems [1, 2]. These observed statistical properties not only concerns the orbital parameters of planets but also the chemical composition of host stars [3].

The past ten years have also witnessed a remarkable improvement of the precision of radial velocity measurements with a gain of about a factor 100. A precision of the order of 0.5 m/s or better has been achieved (relative Doppler shift of one part in a billion). Planets with masses as small as a few Earth-masses have been detected. The most exceptional system recently discovered includes three Neptune-type planets orbiting a solar-type star with an asteroid belt! [4] The two inner planets have been shown to be mostly rocky by models of planetary formation [5].

Is it possible to expect further significant progresses of Doppler measurements? Such a possibility could be of interest to permit radial velocity follow-up measurements of planetary transit candidates expected from the COROT and KEPLER space missions, the goal being to get a precise determination of mass-radius relations from terrestrial planets to brown dwarfs.

A radial velocity precision at the level of 0.1 m/s does not seem out of reach. With an observing strategy adapted to minimize the influence of the stellar intrinsic variability (magnetic activity, acoustic modes) we should be in position to explore statistical properties of terrestrial planetary systems.

References: [1] Santos N. C., Benz W., and Mayor M. 2005. *Science* 310:251–255. [2] Udry S., Mayor M., and Santos N. C. 2003. *Astronomy & Astrophysics* 407:369–376. [3] Santos N. C. et al. 2003. *Astronomy & Astrophysics* 398:363–376. [4] Lovis C. et al. *Nature*. Forthcoming. [5] Alibert Y. et al. Forthcoming.

5376

LAP 04840: AN AMPHIBOLE-BEARING R-CHONDRITEM. C. McCanta¹, A. H. Treiman¹, and E. Essene². ¹Lunar and Planetary Institute, Houston, Texas 77058, USA. ²Department of Geosciences, University of Michigan, Ann Arbor, Michigan, USA

Introduction: The LaPaz Ice Field 04840 (LAP04840) meteorite is an R chondrite of petrographic grade 6 [1]. It is unique among meteorites, in containing abundant amphibole, and has the second meteoritic occurrence of biotite. If the amphibole is hydrous (as it appears), LAP 04840 must come from deep within a water-rich chondritic asteroid.

Texture: LAP 04840 contains chondrules, chondrule fragments, and mineral grains in a finely crystalline matrix. Chondrules are up to ~3 mm in diameter, and include barred olivine, porphyritic olivine, and porphyritic pyroxene varieties. Many are surrounded by rims of finely crystalline material (~20 μm grain size), which lack larger mineral grains. Matrix among the chondrules and fragments is composed of anhedral grains, also ~20 μm in diameter, in a granulitic, metamorphic texture. Section ,30 shows no signs of deformation or shock after this metamorphism.

Mineralogy: The larger mineral grains (>50 μm) in LAP 04840 are olivine, orthopyroxene, plagioclase, amphibole, Cr-magnetite, and sulfides. Olivine occurs in chondrules and as isolated grains. It is compositionally homogeneous (Fo₆₁Fa₃₉) throughout the meteorite—the same in all analyzed chondrules and mineral grains. The only pyroxene identified is orthopyroxene, which contains abundant inclusions of opaques and other minerals. It has the same composition (Wo₀₁En₆₈Fs₃₁), throughout the meteorite. Amphibole is abundant, ~15%; it is pleochroic in foxy brown colors, and shows strong cleavage at 120° angles. It is magnesiohornblende [1, 2], of nearly constant composition throughout. The amphibole contains little F or Cl, suggesting it is either hydrous or oxy-amphibole. Much of its iron is Fe³⁺ (by normalization). LAP contains no metal. Cr-magnetite is scattered throughout the meteorite, but the largest grains occur with the sulfide phases (pyrrhotite and pentlandite) [1]. It is commonly associated with Cl-bearing apatite. Mg-rich biotite (phlogopite), with little F or Cl, occurs rarely with amphibole, Cr-magnetite, and sulfides.

Metamorphism: The amphibole in LAP 04840 is metamorphic, occurring as anhedral and euhedral scattered through the rock and as replacements of material (glass?) among olivines and pyroxenes in chondrules. By analogy with terrestrial metamorphics, the LAP mineral assemblage (ol-opx-amph) and mineral compositions (e.g., Al in amphibole) suggest upper amphibolite facies conditions: ~600 °C < T < 800 °C, and P(H₂O) > 1 kbar [3, 4]. With this temperature range, olivine-orthopyroxene-spinel equilibria yield fO₂ of QFM + 0.6 (± 0.5) log units, consistent with the high oxidation states of R chondrites and the absence of Fe metal. Pressure of metamorphism is poorly constrained at present. However, water pressure must be high to stabilize this Ti-poor hornblende. For LAP 04840, one must infer that it was metamorphosed deep in a chondritic asteroid, under water-rich conditions.

References: [1] Satterwhite C. and Righter K. 2006. *Antarctic Meteorite Newsletter*. [2] Leake et al. 1997. *American Mineralogist* 82:1019–1037. [3] Robinson P. et al. 1982. *Reviews in Mineralogy* 9B. [4] Spear F. 1993. *Metamorphic phase equilibria and pressure-temperature-time paths*. Washington, D.C.: Mineralogical Society of America.

5082

PYROCLASTIC VOLCANISM ON THE AUBRITE PARENT BODY: EVIDENCE FROM AN Fe,Ni-FeS CLAST IN LAR 04316

T. J. McCoy and A. Gale. Department of Mineral Sciences, Smithsonian Institution, Washington, D.C. 20560-0119, USA

Introduction: A long-standing problem in aubrite petrogenesis has been the absence of basaltic and Fe,Ni-FeS melts, presumed to form during melting of an enstatite chondrite-like protolith, complementary to the enstatite-rich aubrites. A possible solution [1] is that early partial melts were volatile-rich, producing eruption velocities that exceed the escape velocity for asteroids less than ~100 km in radius, and causing these melts to be lost. Pyroclasts produced during such eruptions would range from ~30 μm to ~4 mm in diameter [2]. Samples of these pyroclasts have proven elusive, compromising our ability to fully understand their formation.

Results: Larkman Nunatak (LAR) 04316 is an 1163 g aubrite dominated by a typical enstatite-rich matrix, but containing two cm-sized clasts apparently joined by an igneous contact. One is composed of enstatite+forsterite+glass, similar in size and mineralogy to those described by [3] and interpreted as basaltic vitrophyres extracted at ~1500 °C and “quenched” at 1070–1350 °C. The other is a quench-textured Fe,Ni-FeS clast previously unknown from aubrites. The clast consists of ~60:40 Fe,Ni:FeS by volume (~50:50 by mass) with minor alabandite as grains up to 0.5 mm, corresponding to a metal-sulfide partial melt extracted at ~1300–1350 °C. Fe,Ni forms a dendritic or cellular structure with arm/cell spacings of ~30 microns, implying cooling at 25–30 °C/s [4–6].

Discussion: The co-occurrence of a vitrophyric basaltic clast and an Fe,Ni-FeS clast can provide critical information about the physical setting of formation.

The 25–30 °C/s cooling rate of the Fe,Ni-FeS clast is consistent with “quenching” invoked for the silicate clasts [3]. It was unclear whether cooling occurred during a pyroclastic phase, in a lava flow, or in a conduit. Our cooling rate is consistent with formation of μm - to dm-sized clasts by radiation into space [5, 6] as molten droplets during a pyroclastic phase. Further, they are at the upper range of calculated pyroclast sizes [2], perhaps suggesting agglomeration of smaller pyroclasts during flight. Only their large size allowed retention on the parent body.

It is less clear how the silicate and metal-sulfide clasts came together in the first place. Both would require extraction from a chondritic source at a range of temperatures of ~350–550 °C above the onset of partial melting (~950 °C). It is possible that they were produced essentially contemporaneously at different places in the parent body and were transported together in a complex dike system. Alternatively, they may have only come together during the pyroclastic eruption. If the latter occurred, it is puzzling that these two clasts apparently survived together through 4.5 Ga of impact gardening, suggesting that LAR 04316 might be a particularly ancient regolith breccia.

References: [1] Wilson L. and Keil K. 1991. *Earth and Planetary Science Letters* 104:505–512. [2] Wilson L. and Keil K. 1996. *Earth and Planetary Science Letters* 140:191–200. [3] Fogel R. A. 2005. *Geochimica et Cosmochimica Acta* 69:1633–1648. [4] Scott E. R. D. 1982. *Geochimica et Cosmochimica Acta* 46:813–823. [5] Blau P. J. et al. 1973. *Journal of Geophysical Research* 78:363–374. [6] Blau P. J. and Goldstein J. I. 1975. *Geochimica et Cosmochimica Acta* 39:305–324.

5300

ISOTOPIC COMPOSITIONS OF COMETARY MATTER RETURNED BY THE STARDUST MISSION

K. McKeegan¹, J. Aleon², C. Alexander³, J. Bradley², D. Brownlee⁴, P. Burnard⁵, A. Butterworth⁶, M. Chaussidon⁵, A. Davis⁷, C. Floss⁸, J. Gilmour⁹, Y. Guan¹⁰, C. Hohenberg⁸, P. Hoppe¹¹, I. Hutcheon², M. Ito¹², S. Jacobsen¹³, L. Leshin¹⁴, I. Lyon⁹, K. Marhas⁸, B. Marty⁵, A. Meibom¹⁵, A. Meshik⁸, S. Messenger¹², K. Nakamura¹², L. Nittler³, R. Palma¹⁶, M. Pellin¹⁷, R. Pepin¹⁶, P. Tsou¹⁸, F. Robert¹⁵, D. Schlutter¹⁶, F. Stadermann⁸, R. Stroud¹⁹, A. Westphal⁶, E. Young¹, K. Ziegler¹, and E. Zinner⁸. ¹Department of Earth and Space Sciences, University of California–Los Angeles. E-mail: kdm@ess.ucla.edu. ²IGPP, LLNL. ³DTM, Carnegie Institution of Washington. ⁴University of Washington. ⁵CRPG. ⁶University of California–Berkeley. ⁷University of Chicago. ⁸Washington University. ⁹University of Manchester. ¹⁰Caltech. ¹¹MPI, Mainz. ¹²NASA JSC. ¹³Harvard University. ¹⁴NASA GSFC. ¹⁵Muséum National d’Histoire Naturelle, Paris. ¹⁶University of Minnesota. ¹⁷ANL. ¹⁸NASA JPL. ¹⁹NRL

Introduction: The Stardust spacecraft flew through the coma of comet 81P/Wild-2 on January 2, 2004, at a distance of ~236km and a relative velocity of ~6.1 km/s [1]. Dust particles, which were released from the comet hours before the encounter, were captured in silica aerogel and successfully returned to the Earth on January 15, 2006. Cometary debris was also retained in small impact craters on Al-foil strips adjacent to the aerogel collector cells. A preliminary examination team (PET) of ~150 scientists has been engaged in studying the mineralogy/petrology, chemistry, optical properties, organic materials, fluence, and isotopic compositions of a subset of the returned cometary materials [2, 3]. This report will summarize what has been learned regarding isotopic compositions of select elements by the PET during its six-month investigation.

Goals of PET Isotope Analysis: The PET is designed to provide an initial characterization of the isotope properties of Wild-2 samples, concentrating primarily on major isotope systems (e.g., C, H, O, N) that permit comparison to a larger database of isotope reservoirs found in primitive solar system materials (meteorites and IDPs) and in individual presolar grains. It is hoped that isotopic abundances can help ascertain whether comets are merely mechanical agglomerations of unprocessed presolar materials, or whether their constituents were processed and mixed with other materials in the solar accretion disk. Even if most Wild-2 materials are not distinguishable from the solar system’s matter on the basis of their isotope abundances, it is still possible that the comet could provide an enhanced reservoir of presolar grains with distinct nucleosynthetic histories (i.e., ‘stardust’) which, in principle, could be different than the populations so far identified in meteorites. Coordination with other investigations, especially mineralogy/petrology and organics, can also help decide the nature of specific materials collected by the mission. Additional isotope analyses will be undertaken opportunistically on grains with appropriate mineralogy, e.g., Mg isotopes in refractory grains.

References: [1] Brownlee D. E. et al. 2004. *Science* 304:1764–1769. [2] Brownlee D. E. et al. 2006. Abstract #2286. 37th Lunar and Planetary Science Conference. [3] Tsou P. et al. 2006. Abstract #2189. 37th Lunar and Planetary Science Conference.

5020

RECOGNITION OF ALKALINE ROCKS ON MARS: BASALTS FROM GUSEV CRATER AND NAKHLITES

H. Y. McSween, Jr.¹, K. R. Stockstill², and the Athena Science Team.
¹Department of Earth and Planetary Sciences, University of Tennessee, Knoxville, Tennessee 37996, USA. E-mail: mcsween@utk.edu. ²Hawai'i Institute of Geophysics and Planetology, University of Hawai'i at Manoa, Honolulu, Hawai'i 96822, USA

Introduction: Igneous rocks analyzed by the Spirit rover in Gusev crater [1] include picritic basaltic flows (Adirondack class) on the Plains, a complex variety of float rocks (here we consider only the Wishstone, Backstay, and Irvine classes) on the north face of Husband Hill, olivine-rich outcrops (Algonquin class) on the south face, and volcanoclastic deposits with associated scoria at Home Plate within the Inner Basin. The compositions of all these rocks are mildly alkaline—Gusev volcanics constitute the first alkalic province recognized on Mars. However, reevaluation of nakhlites suggests that they also formed from alkaline parental magma.

Petrogenesis of Gusev Rocks: Highly vesiculated lavas and pyroclastic rocks in Gusev suggest high volatile contents. Calculated liquid lines of descent using MELTS for Adirondack class rocks with 0.5 wt% H₂O at appropriate redox states suggest that the other lithologies encountered in Gusev could have formed by fractional crystallization of the Adirondack class magma at varying depths corresponding to pressures of 0.1–1.0 GPa. This seems plausible because experiments on Adirondack class basalt composition suggest that it is a primitive magma formed by melting the putative Mars mantle assemblage at ~1.0 GPa [2].

Alkaline Nakhlites: A calculated liquid line of descent for the Nakhla parent magma estimated from rehomogenized melt inclusions [3] is also mildly alkaline and resembles low-pressure melts from Gusev. Interstitial liquid compositions in the MIL 03346 nakhlite [4] also demonstrate its alkaline character.

Significance of Alkaline Rocks: In hindsight, it should not be surprising that alkaline igneous rocks occur on Mars. Models for the Martian mantle are enriched in volatiles (including Na₂O and K₂O), and melting of this primitive mantle could produce alkaline magmas. However, SNC meteorites have always been described as subalkaline, as have Mars crustal compositions inferred from orbital remote sensing data. Depleted mantle, the source for most young SNC magmas, had already lost alkalis before these magmas formed, but older magmas such as the nakhlites and Gusev basalts are more likely to have formed from relatively undepleted mantle sources. Small degrees of melting and high pressures have also likely played a role in generating alkaline magmas on Mars [5].

References: [1] Squyres S. W. et al. 2006. *Journal of Geophysical Research* 111:E02S11. [2] Monders A. G. et al. 2006. Abstract #1834. 37th Lunar and Planetary Science Conference. [3] Stockstill K. R. et al. 2005. *Meteoritics & Planetary Science* 40:377–396. [4] Day J. M. D. et al. 1997. *Meteoritics & Planetary Science* 41:581–606. [5] Longhi J. 1991. 21st Lunar and Planetary Science Conference. pp. 695–709.

5077

THE DEEP IMPACT EXPERIMENT: A SMALL-SCALE MOLDAVITE SIMULATION?

H. J. Melosh, Lunar and Planetary Lab, University of Arizona, Tucson, Arizona 85721, USA, and Bayerisches Geoinstitut, Universität Bayreuth, Bayreuth, Germany. E-mail: jmelosh@lpl.arizona.edu

Introduction: On July 4, 2005, the Deep Impact experiment collided a 370 kg spacecraft with comet Tempel 1 at a speed of 10.2 km/sec and an impact angle of about 30° from the horizontal [1]. During the first half-second the Medium Resolution Imaging (MRI) system recorded the rapid expansion of a glowing cloud of molten silicate droplets. Although the Tempel 1 droplets were only about 200 microns in diameter, and probably of mafic composition, the physical circumstances of their formation is a close analog of the formation of Moldavite tektites from the Ries crater (Germany) impact 22 million years ago.

The Deep Impact “Poof”: Within 150 milliseconds after the initial contact, a high velocity, parachute-shaped arc of glowing debris emerged from the impact site. The arc expanded at about 3 km/sec in width and 4.5 km/sec in length, projected on the sky. This plume passed through the slit of the IR instrument, which recorded a spectrum of water vapor, CO₂, HCN, and organic material in emission at temperatures between 1000 and 2000 K. The clear-filter (0.4–1.0 micron) visible MRI images show a bright cloud that cooled in a characteristic log-time cooling curve with a 1/e cooling time of 80 milliseconds, indicating radiation cooling of droplets in the size range of 200 microns. The initial temperature was in the range of 2500–3000 K, where forsterite is molten, but with a low enough vapor pressure that the droplet lifetime against evaporation exceeded the observation time.

Moldavite Formation: Moldavites, in common with other tektites, were created during the impact of a large, high-speed meteoroid with the Earth's surface. Tektites are typically high in SiO₂, although more mafic varieties of microtektites are found in deep sea cores. The sizes of typical tektites are 1–10 cm, with some larger types known. From their distances from their source areas, they were ejected at speeds of a few km/sec and traveled ballistically above the atmosphere before being emplaced downrange of the impact. Many contain vesicles that preserve vacuum, indicating that they cooled in flight, high above the Earth's atmosphere.

Deep Impact as a Moldavite Analog? Both the surface of Tempel 1 and the Moldavite source rocks were probably highly porous accumulations of silicate particles. Most tektites seem to require a target material such as loess, one that is particularly susceptible to melting by shock compression. Tempel 1's bulk density is only about 0.4 gm/cm³, a mixture of silicate and ice dust that is also highly susceptible to melting by shock compression. Modeling of the equations of state of these materials indicate that compression yields hot, molten silicate and vapor that travels at high speed away from the impact site. The difference in scale between typical tektites and the Deep Impact melt droplets may be accounted for by the factor of 100 difference in scales between the two events and the resultant reduction in pressure gradients that tend to reduce melt to small droplets.

References: [1] A'Hearn M. F. et al. 2005. *Science* 310:258.

5083

SOLAR NEON RELEASED FROM GENESIS ALUMINUM COLLECTOR DURING STEPPED UV-LASER EXTRACTION AND STEP-WISE PYROLYSIS

A. Meshik¹, Y. Marrocchi¹, C. Hohenberg¹, O. Pravdivtseva¹, J. Mabry¹, J. Allton², R. Bastien², K. McNamara³, E. Stansbery³, and D. Burnett⁴.
¹Washington University, St. Louis, Missouri 63130, USA. E-mail: am@physics.wustl.edu. ²Lockheed Martin c/o NASA/Johnson Space Center, Mail Code KT, Houston, Texas 77058, USA. ³NASA/JSC, Mail Code KA, Houston, Texas 77058, USA. ⁴Geology 100-23, CalTech, Pasadena, California 91125, USA

Earlier this year we reported results of UV-laser stepped raster extractions of Ne and He from Genesis' Al-collector [1]. Since then, using pyrolysis of a 0.005 cm² fragment of this material left from the earlier study, we have estimated the efficiency of the UV-laser extraction to be at least 95%. We also analyzed Ne released from the Al-collector by means of stepped pyrolysis. Here we compare these new data with stepped UV-laser extraction and the CSSE results [2]. Figure 1 shows the ²⁰Ne/²²Ne ratio extracted from Genesis collectors using these three techniques.

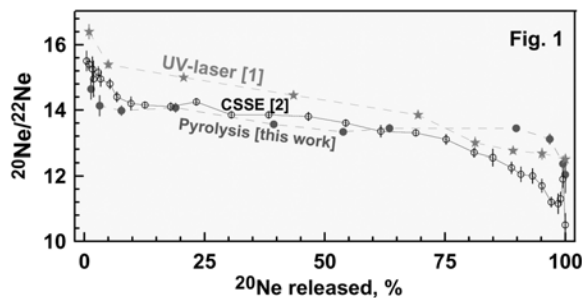


Fig. 1

The common feature in these different extraction methods is the profile of the ²⁰Ne/²²Ne ratios. In the beginning the ratios are elevated, then relatively flat in the middle, and lowest at the end of the extractions. This pattern seems to be due to the different implantation depths for ²⁰Ne and ²²Ne and agrees with isotopic fractionation expected from SRIM calculations [3].

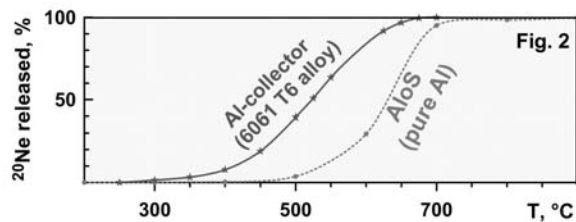


Fig. 2

Comparison of Ne release profiles from the Al-collector and pure Al-coated sapphire (AloS, [4]) reveals significant differences between these materials (Fig. 2), suggesting that AloS may retain noble gases better than the Al-collector. This may explain slightly higher Ne and He fluxes observed in bulk AloS collector [5] relative to those measured in the Al-collector [1].

Acknowledgements: Supported by NASA grants NNJO4HI17G and NAG5-12885.

References: [1] Meshik A. P. et al. 2006. Abstract #2233. 37th Lunar and Planetary Science Conference. [2] Grimberg A. et al. 2006. Abstract #1782. 37th Lunar and Planetary Science Conference. [3] <http://www.srim.org> [4] Meshik A. P. et al. 2000. *Meteoritics & Planetary Science* 35:A109. [5] Hohenberg C. M. et al. 2006. Abstract #2439. 37th Lunar and Planetary Science Conference.

5196

LIFE AFTER SHOCK: THE MISSION FROM MARS TO EARTH

C. Meyer¹, D. Stöffler¹, J. Fritz¹, G. Horneck², R. Möller², C. S. Cockell³, J. P. de Vera⁴, and U. Hornemann⁵. ¹Museum f. Natural History (Mineralogy), Humboldt-University, Invalidenstr. 43, 10115 Berlin, Germany. E-mail: cornelia.meyer@museum.hu-berlin.de. ²DLR, Institute for Aerospace Medicine, Köln, Germany. ³Open University, Milton Keynes, UK. ⁴Institute of Botany, Heinrich-Heine-University Düsseldorf. ⁵Ernst-Mach-Institute, Freiburg im Breisgau, Germany

Introduction: In view of the geological and climatological development of planet Mars, the origin and evolution of life in the first 1.5 billion years of Martian history appears possible. There is also convincing evidence that a significant amount of surface material was ejected from Mars by impact processes and a substantial portion of that transferred to Earth. The minerals of the Martian meteorites collected so far indicate an exposure to shock waves in the pressure range of 5–55 GPa [1]. As terrestrial rocks are frequently inhabited by microbial communities, rocks ejected from a planet by impact processes may carry with them endolithic microorganisms, if microbial life existed/exists on this planet.

Experiment: We produced planar shock waves by an explosive device, which accelerates a planar flyer plate. The plate impacted an Armco iron container, in which the sample, an assemblage of different kinds of microorganisms and rock, was placed parallel to the shock front. Independently of the peak shock pressure predetermined by the dimensions and material properties of the experimental setup, the actual peak shock pressure of the recovered shocked material was controlled by measurement of the refractive indices of plagioclase, based on accurate calibration for shock pressure (e.g., [2]).

Based on the experience with shock recovery experiments at an ambient temperature of 293 K [3], we performed a new set of experiments to extend the temperature conditions to 233 K and 193 K, respectively, in order to better simulate the Martian temperature environment (147–290 K). Considering the detailed knowledge about the composition and constitution of Martian surface rocks and the well-known relation between shock pressure and post-shock temperature for various types of rocks, we used dunite (corresponding to the Martian chassignite meteorites) on the one hand, and sedimentary rock (sandstone) saturated with water and salt on the other hand, as an extension of our earlier work with gabbro [3]. Dunite is the rock of choice because of a relatively low increase of shock and post-shock temperature after shock loading [1]. Sandstone served as an analog of the Martian water-saturated regolith.

Conclusions: The aim of these experiments was to determine the temperature or pressure as the limiting factor for the survival rate of microorganisms during shock loading and to better understand the underlying molecular mechanisms of the survival of microorganisms in an impact and ejection scenario.

References: [1] Fritz J. et al. 2005. *Meteoritics & Planetary Science* 40:1393–1411. [2] Stöffler D. et al. 1986. *Geochimica et Cosmochimica Acta* 50: 889–903. [3] Meyer et al. 2006. *Geophysical Research Abstracts* 8:00554.

5289

POST-SHOCK COOLING HISTORY OF DHOFAR 378 SHERGOTTITE

T. Mikouchi¹, G. McKay², and E. Koizumi¹. ¹Department of Earth and Planetary Science, University of Tokyo, Hongo, Tokyo 113-0033, Japan. E-mail: mikouchi@eps.s.u-tokyo.ac.jp. ²KR, NASA Johnson Space Center, Houston, Texas 77058, USA

Although plagioclase in shergottites is “maskelynite,” Dhofar 378 plagioclase is present as fibrous crystalline phases, which is considered as recrystallization from shock plagioclase melt [1]. Thus, Dhofar 378 is important for assessing a “shock” age of shergottites. This abstract reports results of a mineralogical study of the Dhofar 378 chip that was also used for chronological studies [2, 3], and discusses shock heating and subsequent cooling of Dhofar 378.

Petrography and mineral compositions of the Dhofar 378 sections studied are generally similar to the section that we previously studied [1]. Plagioclase grains are composed of fibrous minute crystalline needles (~100 μm long and <10 μm wide) of An₅₈Or₁ to An₄₀Or₇. Thin K-, Na-rich glass areas (K₂O: 0.5–6.5 wt%, Na₂O: 5–11 wt%) are present near the center of grains. The shock textures of the previously studied section are more extensive than those of sections studied this time, suggesting heterogeneous shock metamorphism even in a small meteorite (15 g total recovered mass).

The presence of both recrystallizing plagioclase rims and the inner K-rich feldspathic glass areas is similar to heated “maskelynite” in Zagami at 900 °C [4]. We performed additional experiments at 1000 and 1100 °C, and found that Dhofar 378 is most similar to the sample heated at 1000 °C for 1–24 hours. The sample heated at 1100 °C contains partial melt between pyroxene and plagioclase. Ca phosphates are absent, and plagioclase grains are clear brown in the sample heated for 24 hours. Thus, the peak temperature of Dhofar 378 during shock would be lower than 1100 °C, probably ~1000 °C. The cooling rate of Dhofar 378 after the shock is difficult to estimate from our present results. However, crystallization experiment of Los Angeles [5], which is nearly identical to Dhofar 378 except for shock degree [1], shows that 2.5 °C/hour cooling could produce similar fayalite textures in Dhofar 378. This cooling rate is comparable to the experimental recrystallization of plagioclase with only small amounts of K-rich glass left, but is very slow for shock environment. We plan to perform cooling experiments of Zagami from 1000 °C and 1100 °C to constrain a post-shock cooling rate of Dhofar 378.

The Ar-Ar age obtained from the same rock chip used for this study gave ~143 Myr, which is interpreted as an earlier impact event rather than the ejection event from Mars [2]. The Sm-Nd result also shows a similar age of 157 Myr [3]. The strong shock metamorphism and slow post-shock cooling observed in Dhofar 378 may record this ~143 Myr event.

References: [1] Mikouchi T. and McKay G. 2003. Abstract #1920. 34th Lunar and Planetary Science Conference. [2] Park J. and Bogard D. D. 2006. *Antarctic Meteorites XXX*. [3] Nyquist L. E. et al. 2006. *Antarctic Meteorites XXX*. [4] Mikouchi T. et al. 2002. *Meteoritics & Planetary Science* 37:A100. [5] Koizumi E. et al. 2005. Abstract #2015. 36th Lunar and Planetary Science Conference.

5315

YOUNG RADIOMETRIC AGES OF SHERGOTTITES: IMPLICATIONS FOR AQUEOUS ALTERATION ON THE MARTIAN SURFACE

K. Misawa¹, H. Kaiden¹, and T. Noguchi². ¹Antarctic Meteorite Research Center, National Institute of Polar Research, Tokyo 173-8515, Japan. E-mail: misawa@nipr.ac.jp. ²Ibaraki University, Mito, Ibaraki 310-8512, Japan

Introduction: Bouvier et al. [1] argued that most radiometric ages of shergottites including lherzolithic were reset recently (i.e., ~180 Ma) by acidic aqueous solutions percolating throughout the Martian surface. Detailed mechanisms of aqueous alteration on the Martian surface are still not well-understood. Grady et al. [2] suggested different flows of water—surface water in contact with Martian atmosphere might be percolating downward from above and precipitation of salts could have occurred. On the other hand, groundwater from melted ice could be circulating from below and alteration of silicates could have occurred.

Results and Discussion: During aqueous alteration elemental fractionations of lithophile trace elements could have occurred. For example, U and Th have similar chemical properties and show tetravalent oxidation state with similar ionic radii. Under oxidizing condition, U forms the uranyl ion which forms compounds easily soluble in water. Therefore, U becomes a mobile element and could be separated from Th which exists only tetravalent state and whose compounds are generally insoluble in water. Large elemental fractionations between U and Th were sometimes observed during acid treatment in laboratories [3–5]. The ²³²Th/²³⁸U (≡ κ) ratios for whole-rock samples of ALH 77005, LEW 88516, and Y-793605 determined by IDMS are constant, i.e., κ = 3.8–4.0 [3–5].

Lherzolithic shergottites are extremely sensitive to addition of mobile lithophile elements (e.g., LREE, Ba, and Sr) during alteration. Variations of Ba/La and Sr/Eu ratios for whole-rock samples of ALH 77005, LEW 88516, Y-793605, and NWA 1950 are small [6–9]. The REE patterns of phosphates and whole-rock samples of ALH 77005, LEW 88516, and GRV 99027 are consistent with closed-system crystallization [10, 11]. Moreover, Ce anomalies, which are recognized as products of aqueous alteration, are not observed.

These facts suggest that abundances of lithophile trace elements were not disturbed, and that the young Rb-Sr, Sm-Nd, and U-Pb ages so far reported could represent crystallization events.

References: [1] Bouvier A. et al. 2005. *Earth and Planetary Science Letters* 240:221–233. [2] Grady M. M. et al. 2005. *Meteoritics & Planetary Science* 40:A59. [3] Chen J. H. and Wasserburg G. J. 1986. *Geochimica et Cosmochimica Acta* 50:955–968. [4] Chen J. H. and Wasserburg G. J. 1993. 24th Lunar and Planetary Science Conference. pp. 275–276. [5] Misawa K. et al. 1997. *Antarctic Meteorite Research* 10:95–108. [6] Shih C.-Y. et al. 1982. *Geochimica et Cosmochimica Acta* 46:2323–2344. [7] Dreibus G. et al. 1992. *Meteoritics* 27:216–217. [8] Misawa K. et al. Forthcoming. *Antarctic Meteorite Research*. [9] Gillet P. et al. 2005. *Meteoritics & Planetary Science* 40:1175–1184. [10] Harvey R. P. et al. 1993. *Geochimica et Cosmochimica Acta* 57:4769–4783. [11] Lin Y. et al. 2005. *Meteoritics & Planetary Science* 40:1599–1619.

5332

GEOCHEMISTRY OF PALLASITE OLIVINES AND THE ORIGIN OF MAIN-GROUP PALLASITES

D. W. Mittlefehldt¹ and D. Rumble III². ¹NASA/Johnson Space Center, Houston, Texas 77058, USA. E-mail: david.w.mittlefehldt@nasa.gov. ²Geophysical Laboratory, Carnegie Institution of Washington, Washington, D.C., USA

Main-group pallasites (PMG) are mixtures of iron-nickel metal and magnesian olivine thought to have been formed at the core-mantle boundary of an asteroid [1]. Some have anomalous metal compositions (PMG-am) and a few have atypically ferroan olivines (PMG-as) [2]. PMG metal is consistent with an origin as a late fractionate of the IIIAB iron core [2]. Most PMG olivines have very similar Fe/Mg ratios, likely due to subsolidus redox reaction with the metal [3]. In contrast, minor and trace elements show substantial variation, which may be explained by either: i) PMG were formed at a range of depths in the parent asteroid; the element variations reflect variations in igneous evolution with depth, ii) the pallasite parent asteroid was chemically heterogeneous; the heterogeneity partially survived igneous processing, or iii) PMG represent the core-mantle boundaries of several distinct parent asteroids [4, 5]. We have continued doing major, minor, and trace elements by EMPA and INAA on a wider suite of PMG olivines, and have begun doing precise oxygen isotope analyses to test these hypotheses.

Manganese is homologous with Fe²⁺, and can be used to distinguish between magmatic and redox processes as causes for Fe/Mg variations. PMG olivines have a range in molar 1000*Mn/Mg of 2.3–4.6 indicating substantial igneous fractionation in olivines with very similar Fe/Mg (0.138–0.148). The Mg-Mn-Fe distributions can be explained by a fractional crystallization-reduction model; higher Mn/Mg ratios reflect more evolved olivines while Fe/Mg is buffered by redox reactions with the metal. There is a positive association between Mn/Mg and Sc content that is consistent with igneous fractionation. However, most PMG olivines fall within a narrow Mn/Mg range (3.0–3.6), but these show a substantial range in Sc (1.00–2.29 µg/g). Assuming fractional crystallization, this Sc range could have resulted from ~65% crystallization of an ultramafic magma. This is inconsistent with formation at the core-mantle boundary of a single asteroid [4].

One alternative is that the PMG are fragments of several asteroids, and these could have had different initial Sc contents, Mn/Mg, and differences in igneous history. Our preliminary O isotope data and those of [6, 7] do not support this, although the coverage of PMG olivines is incomplete.

The PMG-as Springwater is not easily fit in any scenario. Its olivine has among the highest Mn/Mg suggesting it is one of the most evolved, but the lowest Sc content suggesting it is the least evolved. The O isotopic composition of Springwater olivine is the same as that of other PMG. Thus there is no indication that it represents a distinct parent asteroid.

Our preliminary O isotopic data favor a single PMG parent asteroid. In this case, the olivines are more likely melt-residues, and that the parent asteroid was initially heterogeneous in chemical, but not isotopic, composition.

References: [1] Mittlefehldt D. W. et al. 1998. In *Planetary Materials*, edited by Papike J. J. Washington, D.C.: Mineralogical Society of America. [2] Wasson and Choi. 2003. *Geochimica et Cosmochimica Acta* 67:3079–3096. [3] Righter et al. 1990. *Geochimica et Cosmochimica Acta* 54:1803. [4] Mittlefehldt D. W. 1999. Abstract #1828. 30th Lunar and Planetary Science Conference. [5] Mittlefehldt D. W. 2005. *Meteoritics & Planetary Science* 40:A104. [6] Greenwood et al. 2006. Abstract #1768. 37th Lunar and Planetary Science Conference. [7] Ziegler et al. 2006. Abstract #1894. 38th Lunar and Planetary Science Conference.

5292

FERRIC IRON IN Al-BEARING AKIMOTOITE COEXISTING WITH IRON-NICKEL METAL IN A SHOCKED L-6 CHONDRITE

N. Miyajima¹, A. El Goresy¹, C. Dupas², F. Seifert¹, D. Rubie¹, M. Chen³, and X. Xie³. ¹Bayerisches Geoinstitut, Universität Bayreuth, D-95440 Bayreuth, Germany. E-mail: nobuyoshi.miyajima@uni-bayreuth.de. ²Universite des Sciences et Technologies de Lille, Bat C6 F-59655 Villeneuve d'Ascq Cedex, France. ³Guangzhou Institute of Geochemistry, CAS, Wushan, Guangzhou 510640, China

Introduction: Melt veins in many shocked L-6 chondrites contain complex assemblages indicative of formation at high pressures and temperatures during dynamic events on parent asteroids [1–2]. These assemblages include ringwoodite and majorite formed by solid-state phase transformation in addition to the liquidus pair majorite-pyrope_{ss} + magnesiowüstite indicative of crystallization at P < 23 GPa and T ≤ 2000 °C [1–2]. Akimotoite, the ilmenite-structured dense polymorph of (Mg,Fe)SiO₃ pyroxene newly described in shocked chondrites was found to contain variable amounts of Al₂O₃ [3–4]. This raises a question of the possibility of the presence of Fe³⁺ to maintain the charge balance. In order to explore the presence of Fe³⁺, we have examined a shock-melt vein in the Sixiangkou meteorite having high concentrations of akimotoite, using an analytical TEM equipped with electron energy-loss spectrometer (EELS).

Results: In addition to aluminous akimotoite, the vein contains majorite-pyrope_{ss}, ringwoodite, FeNi metal, troilite, and a silicate glass. The glass domains have compositions that are similar to those of synthetic (Mg,Fe)SiO₃ perovskites, low in Al₂O₃. In contrast, the rim of the domains mainly consists of aluminous majoritic garnets [2]. The akimotoite grains far from the domains have appreciable Al contents (1–5 mol% Al₂O₃) and about 5 mol% FeO. The electron energy-loss near-edge structures (ELNES) demonstrate that aluminous akimotoite has high proportions of Fe³⁺ with Fe³⁺/total Fe ratio of 0.30–0.50(5), although it coexists with FeNi metal. This is the first report of Fe³⁺ in natural or synthetic akimotoite. In contrast, the coexisting Fe-rich ringwoodite (Fa_{25–40}), is enriched in Fe²⁺ with the Fe³⁺/total Fe ratio of 0.05(5). The above-mentioned amorphous domains are inferred to be silicate perovskite.

Conclusions: Aluminous akimotoite could contain significant amount of Fe³⁺, even under reducing conditions prevailed during their crystallization. The bulk composition of the melt vein is chondritic [2]. The MgSiO₃ glass (perovskite?)-majorite-akimotoite-ringwoodite assemblages are not predicted as a stable liquidus assemblage deduced from high-pressure experiments of chondritic bulk composition [1]. The texture is, however suggestive of resulting from crystallization of a melt and its partial reaction with olivine- and pyroxene-fragments at pressures expected in static high-pressure experiments.

References: [1] Agee C. B. et al. 1995. *Journal of Geophysical Research* 100:17,725–17,740. [2] Chen M. et al. 1996. *Science* 271:1570–1573. [3] Tomioka N. and Fujino K. 1999. *American Mineralogist* 84:267–271. [4] Sharp T. G. et al. 1997. *Science* 277:352–355.

5225

EVOLUTIONARY TRENDS OF ACAPULCOITES: NEW EVIDENCES FROM CHEMICAL, MINERALOGICAL AND PETROLOGIC DATA ON PRIMITIVE, TYPICAL AND TRANSITIONAL ACAPULCOITES

V. Moggi-Cecchi¹, G. Pratesi^{2, 3}, and L. Mancini¹. ¹Museo di Scienze Planetarie, Provincia di Prato, Via Galcianese, 20/h, I-59100 Prato, Italy. E-mail: v.moggi@pratoricerche.it. ²Museo di Storia Naturale, Università degli Studi di Firenze, I-50121 Florence, Italy. ³Dipartimento di Scienze della Terra, Università di Firenze, Via La Pira, 4, I-50121, Florence, Italy. E-mail: gpratesi@unifi.it

Introduction: NWA 1052 and NWA 1054 are two primitive acapulcoites whose main masses weigh 22 and 86 g, respectively [1, 2]. Dho 290 is a typical acapulcoite with a main mass of 62 g [3]. NWA 3008 is a transitional acapulcoite with a main mass of 157 g [4]. The NWA 3008 and Dho 290 thin sections have been kindly provided by J. Schlüter (Mineralogical Museum, University of Hamburg) and by M. Nazarov (Vernadsky Institute of Moscow).

Description: NWA 1052 and 1054 display a granular fine-grained texture with olivine and orthopyroxene phenocrysts and relic RP and POP/PP chondrules ranging in size from 400 to 1400 μm set in a feldspathic matrix. Dho 290 has a granoblastic texture with ipidiomorphic crystals of silicates (ranging from 100 to 300 μm in size), chromite and phosphates (<100 μm) mixed with troilite and metal (both >200 μm). NWA 3008 has a granoblastic texture with grains in the range of 100–300 μm . The areal distributions of silicates, metal, and troilite have been measured in all the samples with a Zeiss Axioplan 2 optical microscope equipped with the Axiovision 4.1 software: NWA 1052 and NWA 1054 show a finer-grained texture, (91 and 86% of silicates in the 0–25,000 μm^2 range), while Dho 290 and NWA 3008 display a more coarse-grained texture (63 and 66% of silicates in the 0–25,000 μm^2 range). The comparative study of the modal mineralogy of these samples showed a decreasing amount of opaque phases (troilite and metal) going from NWA 1052–NWA 1054 (15% of the total volume) to Dho 290 (12%) and NWA 3008 (10%). For what concerns the chemical characteristics both Na and Cr contents of diopside and Fo-Fs molar contents of olivine and orthopyroxene have been detected by EMPA in all the samples. The increasing Cr contents and Fo-Fs distributions suggest a trend going from NWA 1052 to NWA 3008 (Fig. 1).

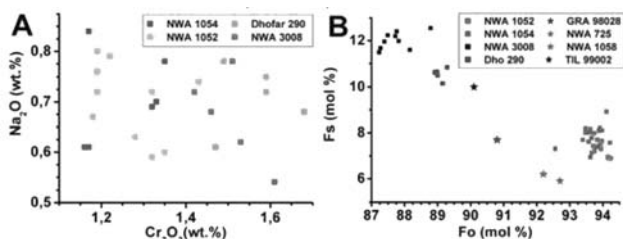


Fig. 1. a) Plot of Na versus Cr contents of diopside in NWA 1052, NWA 1054, Dho 290 and NWA 3008; b) plot of Fs versus Fo contents of olivine and orthopyroxene for the same samples compared with literature data (star) from [5].

Conclusions: Both textural, mineralogical, and chemical data suggest a rather clear and coherent evolutionary trend going from the more primitive NWA 1052 and NWA 1054 acapulcoites to the more evolved ones, Dho 290 and NWA 3008, in good agreement with the trend indicated by [6].

References: [1] Moggi-Cecchi V. et al. 2005. Abstract # 1808. 36th Lunar and Planetary Science Conference. [2] Russel S. et al. 2005. *Meteoritics & Planetary Science* 40:A210 [3] Russel S. et al. 2002. *Meteoritics & Planetary Science* 37:A157–A184 [4] Russel S. et al. 2004. *Meteoritics & Planetary Science* 39:A233 [5] Patzer A. et al. 2004. *Meteoritics & Planetary Science* 39:61.

5390

STUDY OF NORTHWEST AFRICA 4269: A METAL-RICH LIKE “EUCRITE” BASALTIC ACHONDRITE

B. N. Moine¹, A. Seddiki², C. Renac¹, J. Bascou¹, and J. Y. Cottin¹. ¹Laboratoire de Pétrologie-Géochimie UMR CNRS 6524, “Magmas et Volcans,” Université Jean Monnet, Saint-Etienne 42023, France. E-mail: moineb@univ-st-etienne.fr. ²Laboratoire de Magmatisme et Géodynamique des Bassins Algériens, Université d’Oran Essenia, Oran 31000, Algeria

NWA 4269 is a highly metamorphic basaltic monomict breccia from southern Algeria. This meteorite presents microstructure variations characterized by both coarse-grained regions with magmatic relict (subophitic texture) constituted by pigeonite and plagioclase minerals and fine-grained recrystallized regions, which contain α -quartz, low- and high-Ca pyroxenes, plagioclase, troilite, Fe metal, with Ca-phosphate ilmenite, spinel in minor proportion. In recrystallized regions, pyroxenes (low-Ca: Fs_{63-66} , high-Ca: Fs_{31-33}) are equilibrated at 900 °C. The mean FeO/MnO atomic ratio in pyroxenes is 28, with very low variations. Fe metal is abundant in this sample (more than 1%). Metals display a low Ni content (<0.1 wt%) and is located only in recrystallized regions in small inclusions of low-Ca pyroxene or in/around quartz grains. However, it can also occur as millimeter-sized elongated grains. Sulfide is abundant and occurs only as low-Ni pyrrhotite. Metal abundance in eucrite is often interpreted as reduction of Fe-rich orthopyroxene during thermal event by reaction with sulfide, as described in Camel Donga eucrite or in some lunar rocks.

Trace-element pattern of whole-rock normalized to CI is flat ($15 \times \text{CI}$) except for highly volatile elements (Rb, Pb) that are depleted and for Ba, U, and Nb that show slight enrichment. In situ trace element analyses of pyroxene and plagioclase obtain by laser ablation coupled with an ICP-MS also display similar La/Y and Sm/Yb ratio with highly metamorphosed noncumulate eucrites.

Petrographic, petrologic, and geochemical characteristics of this meteorite are very similar to metamorphosed noncumulate eucrite and Ibitira achondrite; however, oxygen stable-isotope composition measured on this sample shows a higher $\Delta^{17}\text{O}$ (0.136, $\delta^{18}\text{O} = 3.27$ and $\delta^{17}\text{O} = 1.84$) than this of HED group and nearby from $\Delta^{17}\text{O}$ of Ibitira.

This $\Delta^{17}\text{O}$ deviation from HED group could reflect intrinsic heterogeneities in the HED parent body due to incomplete mixing at an early stage, or, it is conceivable that there was more than one parent body for eucrite-like basaltic achondrites.

5135

DUST FROM COLLISIONS IN CIRCUMSTELLAR DISKS: SIMILARITIES TO METEORITIC MATERIALS?

A. Morlok^{1, 2}, M. Köhler³, M. Anand⁴, C. Kirk², and M. M. Grady⁴.
¹Department of Earth and Planetary Sciences, Kobe University, Nada, Kobe 657-8501, Japan. E-mail: morlok70@kobe-u.ac.jp. ²The Natural History Museum, Cromwell Road, SW7 5BD, London, UK. ³Institut für Planetologie, Wilhelm-Klemm Str. 10, 48149 Münster, Germany. ⁴The Open University, Walton Hall, Milton Keynes MK7 6AA, UK

Introduction: There is growing evidence from astronomical observations that dust is produced in later stages of circumstellar disks by collisions of larger bodies or planetesimals (e.g., [1, 2]). The bodies involved probably have characteristics similar to the planetesimals in our own young solar system. In the form of meteorites we have remnants of these bodies available for measurements. For the interpretation of astronomical infrared spectra of dust, a comparison with infrared spectra of material from such meteorites should be useful.

Samples and Techniques: Material from matrix and CAI was separated from polished samples, powdered to a submicron powder, and measured using a Perkin Elmer AutoImage FTIR microscope (e.g., [3]). For chondrules and bulk measurements of achondrites and Martian samples, infrared spectra were obtained from KBr pellets using the Perkin Elmer Spectrum One workbench (e.g., [4]). For the comparisons and calculations here, all transmission/absorption spectra were calculated to a spectral resolution of 4cm^{-1} in the range from 8 to $16\ \mu\text{m}$.

Discussion: If the population of planetesimals collided in the observed circumstellar discs is as diverse as in our own solar system, the astronomical infrared spectra show probably a mixture of many types of sources, both primitive and differentiated. Thus also mixtures of laboratory meteorite spectra were calculated and compared with typical astronomical spectra of circumstellar disks, where accretion (and thus collisions) possibly already took place. First preliminary results are presented below.

Single Meteorite Samples: Matrix material from Kakangari (K3) has very similar band positions to HD 179218 (~1.25 My [5]) and Hen 3-600 (1–10 Myr [5]), although with different relative band intensities. Material from bulk Ureilites (Hajmah-A) is similar to that of HD 100546 (>10 Myr [5]) [4].

Meteorite Mixtures: Spectra like that of Herbig stars HD 142527 (~1 Myr [5]) and HD 104237 (~2 Myr [5]) can be reproduced with a 1:2 mixture of olivine rich matrix from a CO chondrite (Ornans) and tektite (representing impact melt glasses). A 3:3:5 mixture of ureilites, chondrules, and tektite also shows a good similarity, like a 1:2 mixture of Kakangari matrix and olivine-rich chondrules.

The spectra of Herbig star HD 163296 (~5 My [5]) has similarity to a 1:2:1.5 mixture of CI1 (Alais) matrix, olivine-rich chondrules, and HED bulk material. Also a mixture of chondrule material and tektites gives good results.

Some results make more sense in an early solar system environment than others. This will be discussed in the presentation.

References: [1] Tesesco et al. 2005. *Nature* 433:133–136. [2] Okamoto et al. 2004. *Nature* 431:660–663. [3] Morlok et al. 2005. Abstract # 1644. 36th Lunar and Planetary Science Conference. [4] Morlok et al. 2006. Abstract #1519. 37th Lunar and Planetary Science Conference. [5] Van Boekel et al. 2005. *Astronomy & Astrophysics* 437:189–208.

5041

DETERMINING THE EFFECTS OF AQUEOUS ALTERATION ON THE DISTRIBUTION OF OXYGEN ISOTOPES IN CARBONACEOUS CHONDRITES

A. A. Morris, I. A. Franchi, L. Baker, J. Watson, and I. P. Wright. Planetary and Space Sciences Research Institute, The Open University, Milton Keynes, MK7 6AA. E-mail: a.a.morris@open.ac.uk

Background: Carbonaceous chondrites (particularly the CI, CM, and CR meteorites) have the most diverse range of high and low temperature mineral phases, and display the widest range of oxygen-isotopic compositions [1, 2]. There are then inherent problems when trying to interpret early solar system history. One is identifying the isotopic signature of oxygen from specific component compounds in a complex mixture of materials that existed in the solar nebular, and deconvoluting this from signatures developed during parent body processing, of which aqueous alteration is the most widespread. Models to account for the variations in oxygen-isotopic compositions in carbonaceous chondrites (e.g., [3, 4]) generally involve mixing of a solid anhydrous silicate component, with an isotopic composition enriched in ^{16}O , with liquid water depleted in ^{16}O along with mass-dependent isotopic fraction between various phases at low temperature [5]. Isotopic evolution of the fluids involved in these reactions would be expected to lead to significant isotopic heterogeneity within the components (e.g., [4]).

Research: We have employed a number of approaches to better determine the distribution of oxygen isotopic components within these complex meteorites. Much of our work has been involved with characterizing the products from artificial hydrothermal alteration of olivine. Olivine was reacted with neutral, acidic and alkaline solutions at $330\ ^\circ\text{C}$ and 50 bar pressure with the aim of producing phyllosilicates of serpentine composition (lizardite, chrysotile, and antigorite); the products were characterized using Raman spectroscopy, SEM, XRD, and thermal analysis. Stepped heating extraction to liberate water and structural $(\text{OH})^-$ has also been undertaken [6]; this technique permits isotopic measurements of resolved components, the identification of which has been established by detailed study of the thermal release temperature of water $(\text{OH})^-$ components and a range of terrestrial analogues. This method has been used to trace the location of different oxygen reservoirs as alteration proceeds in further artificial hydrothermal alteration reactions of olivine using isotopically labeled water. Stepped heating extraction of water and $(\text{OH})^-$ have also been used to characterize the oxygen isotopic composition of liberated, indigenous, water $(\text{OH})^-$ from a range of carbonaceous chondrites (CI, CM2, CR2).

Summary: The initial stepped heating experiments for carbonaceous chondrites revealed considerable variation in $\delta^{18}\text{O}$ [5]. Much of our new work has been aimed at determining the extent of isotopic fractionation associated with the formation of the common phyllosilicates found in meteorites, and identifying the specific minerals liberating $(\text{OH})^-$ at each temperature. This will be used ultimately to better constrain the isotopic composition of the fluids involved in the alteration process on carbonaceous chondrite parent bodies.

References: [1] Clayton R. N. and Mayeda T. K. 1999. *Geochimica et Cosmochimica Acta* 63:2089–2104. [2] Brearley A. J. and Jones R. H. 1999. In *Planetary Materials*, edited by Papike J. J. Washington, D.C.: Mineralogical Society of America. pp. 3-01–3-370. [3] Clayton R. N. and Mayeda T. K. 1984. *Earth and Planetary Science Letters* 67:151–161. [4] Young E. D. et al. 1999. *Science* 286:452–455. [5] Franchi et al. 2001. *Philosophical Transactions of the Royal Society of London A* 359:2019–2035. [6] Baker et al. 2002. *Analytical Chemistry* 74:1665–1673.

5255

SPATIAL DISTRIBUTION OF DEUTERIUM HOT-SPOTS IN THE INSOLUBLE ORGANIC MATTER: A NANOSIMS STUDY

S. Mostefaoui¹, F. Robert¹, S. Derenne², and A. Meibom¹. ¹LEME, CNRS-Muséum, Paris, France. E-mail: robert@mnhn.fr. ²LCBOP-BioEMCO, CNRS-ENSC, Paris, France

Introduction: Because of a systematic enrichment in deuterium, the insoluble organic molecules (IOM) of the carbonaceous meteorites are generally considered to represent interstellar materials. However, the D/H ratios in IOM remain much lower than those measured by spectroscopy in the organic molecules of the interstellar gas phase (ISM). Since no plausible process has been proposed to account for this discrepancy, a straight heritage of the IOM from ISM remains uncertain. Recently, NanoSIMS data have yielded new information that may provide a solution to this pending issue.

The Heterogeneous Distribution of Deuterium in IOM: It has been recently shown [1, 2] that organic species with low C/H ratio (1.2 ± 0.2) are embedded in the IOM and exhibit much higher δD values (δD up to +7000‰) than the bulk IOM value ($\delta D = +1000 \pm 200$ ‰). This “material” (D hot-spots) exhibits highly variable D/H ratios, compared with the more invariable D/H ratio of the enclosing IOM. Based on a correlation between the D/H ratio and the binding energy of the organic H [3], it was proposed that the radical-rich regions of the IOM are the carriers of these D hot-spots [4]. Indeed, the presence of paramagnetic organic radicals (with unpaired electron orbitals) has been observed by EPR spectroscopy in the IOM [5]. Micrometer regions of the IOM are characterized by high concentration of free radicals. These radical-rich regions must be regarded as “survivals” of the parent body hydrothermalism, likely because they were embedded in minerals or too deeply embedded in the bulk IOM to be reached and destroyed by circulating water.

Testing the Hypothesis: According to EPR data, the abundances of these free radicals relative to bulk IOM, vary from Murchison to Orgueil to Tagish Lake; that is: 4%, 17%, and 50%, respectively. Thus, if the deuterium is indeed concentrated in free radicals-rich regions, it should be possible to correlate the surface density of D hot-spots obtained through NanoSIMS image analyses with the relative abundances of free radicals. We will present these new results along with IOM extracted from an unequilibrated enstatite meteorite.

References: [1] Nittler L. R. et al. 2005. Abstract #5215. *Meteoritics & Planetary Science* 40:A114. [2] Young A. F. et al. 2004. Abstract #2097. 35th Lunar and Planetary Science Conference. [3] Remusat et al. 2006. *Earth and Planetary Science Letters* 243:15–25. [4] Robert et al. 2006. Abstract #1301. 37th Lunar and Planetary Science Conference. [5] Binet L. et al. 2002–2004. *Geochimica et Cosmochimica Acta* 66:4177–4156 and 68:881–891.

5064

NITROGEN IN INDIVIDUAL CHONDRULES FROM ORDINARY, ENSTATITE, AND CARBONACEOUS CHONDRITES

S. V. S. Murty and J. P. Das. Physical Research Laboratory, Ahmedabad 380009, India

Introduction: Isotopic composition of nitrogen ($\delta^{15}N$) shows distinct grouping for ordinary (O), enstatite (E), and carbonaceous (C) chondrites, similar to $\Delta^{17}O$ values that are due to differences in their formation environment [1, 2]. On the other hand, the differences between $\Delta^{17}O$ of chondrules from their respective parent chondrites signify the precursor differences [3]. A systematic investigation of trapped nitrogen and noble gases in individual chondrules from O, E, and C chondrites has been undertaken with the objective of understanding the nature of chondrule precursors as well as the chondrule formation environment and processes.

Samples: We have only selected petrologic class 3 and 4 for OC, 3 for EC, and 2 and 3 for C chondrites, to minimize effect of parent body processes. We have analyzed a total of 77 chondrules coming from 10 chondrites belonging to O (6), E (2), and C (2). Splits for 27 of these chondrules that are >1 mg have been analyzed by EPMA for chemical and mineralogical characterization. FeO contents suggest that 13 of these belong to type I, while 14 are from type II. N and noble gases have been analyzed by laser heating gas extraction [4]. $\delta^{15}N$ of total measured N has been corrected for cosmogenic contribution, based on ^{21}Ne [5], to derive $\delta^{15}N$ of trapped N.

Results and Discussion: Among ordinary chondrites, while the N contents are comparable or higher, the $\delta^{15}N$ of individual chondrules show a wide range (generally more positive) as against the narrow range for bulk UOC. The trend for individual chondrites (Dhajala and Björbole from which a large number of chondrules have been analyzed) is same as that for all UOC together. Among C chondrites, though the N contents in chondrules are very low as compared to the parent chondrite, the $\delta^{15}N$ values are more positive, similar to the trend in OC. However, for E chondrites the $\delta^{15}N$ of chondrules overlap those of bulk chondrites. These observations possibly suggest that EC chondrules formed from same precursors as their parent chondrites.

Among chondrules from all chondrites, the spread in $\delta^{15}N$ is more among type II (FeO-rich) chondrules as compared to type I (FeO-poor). When only UOC are considered, the same trend is clearly displayed. The process by which type I chondrules are derived from type II [6], results in homogenization of $\delta^{15}N$. There is narrowing in the range of $\delta^{15}N$ as the % melt (represented by feldspar content) increases. $\delta^{15}N$ variations among individual chondrules are mostly of primary nature, but in some cases, could have been modified by secondary processes (both nebular and parent body origin). Those of primary origin indicate the differences in precursor materials. The narrowing in the $\delta^{15}N$ with lower FeO and higher melt proportion suggest that the melting, which brought about these changes, is due to a secondary heating event in the nebula, resulting in the homogenization of N components from an ensemble of precursors making up the primary chondrule.

References: [1] Kung C. and Clayton R. N. 1978. *Earth and Planetary Science Letters* 38:421–435. [2] Clayton R. N. 1993. *Annual Review of Earth and Planetary Sciences* 21:115–149. [3] Clayton R. N. et al. 1991. *Geochimica et Cosmochimica Acta* 55:2317–2337. [4] Mahajan R. R. and Murty S. V. S. 2003. *Proceedings of the Indian Academy of Sciences: Earth and Planetary Sciences* 112:113–127. [5] Mathew K. J. and Murty S. V. S. 1993. *Proceedings of the Indian Academy of Sciences: Earth and Planetary Sciences* 102:415–437. [6] Sears D. W. G. et al. 1996. In *Chondrules and the protoplanetary disk*. Cambridge: Cambridge University Press. pp. 221–232.

5118

MELT CONDENSATION FOR THE ORIGIN OF CHONDRULES IN ORDINARY CHONDRITES INFERRED FROM BULK CHEMICAL COMPOSITION AND MASS-DEPENDENT OXYGEN ISOTOPIC FRACTIONATION

H. Nagahara¹, K. Ozawa², and N. T. Kita³. ¹Department of Earth and Planetary Science, University of Tokyo, Hongo, Tokyo 113-0033, Japan. E-mail: hiroko@eps.s.u-tokyo.ac.jp. ²Department of Earth and Planetary Science, University of Tokyo, Japan. ³Department of Geology and Geophysics, University of Wisconsin, Madison, Wisconsin, USA

Introduction: Although chondrule formation by melting of precursor materials has been favored, the model has a fundamental disadvantage because it does not explain the diversities of bulk compositions well (e.g., [1]).

Key Question: A precise and comprehensive study of chondrule compositions for primitive ordinary chondrites revealed the refractory element abundances being constant and less than the solar value, while a large Mg/Si fractionation exists on both higher and lower sides than the solar ratio, which could not be an inheritance from the precursors, but is explained by kinetic condensation of silicate melt in dust-enriched systems [2]. Another important observation is that the oxygen isotopic composition for chondrules from ordinary chondrites are mass-dependent fractionated, where type I chondrules are lighter with wide variation, whereas type IIs are heavier with a limited range [3]. It is known that all metallic elements do not show notable mass-dependent isotopic fractionation, and therefore, oxygen is the only element that shows mass-dependent isotopic fractionation. A question arises: which process is responsible for and which conditions are necessary to generate the chemical and isotopic characteristics of chondrules?

Model: The model by [2, 4] was modified to investigate the conditions where chemical diversity of bulk compositions with oxygen isotopic variations for type I and II chondrules are formed through evaporation and condensation of melt droplets.

Results and Discussion: Mass-dependent isotopic fractionation is the direct evidence for the role of evaporation/condensation in the formation of chondrules. Type I chondrules are explained by rapid condensation of silicate melt from the gas with the solar compositions with dust enrichment by more than about a hundred. The presence of more oxygen in the gas than metallic elements formed chondrules with light oxygen compositions. The oxygen isotopic variation among type I chondrules was caused by rapid chemical isolation of chondrules from the residual gas. The fairly low Mg/Si composition and homogeneous and heavier oxygen isotopic compositions of type II chondrules are explained by condensation of residual gas to melt droplets after type I chondrule isolation, which kept chemical and isotopic equilibrium during condensation to lower temperatures, and which eventually got volatile components with almost the solar ratios.

References: [1] Jones R. H. et al. 2005. In *Chondrites and the protoplanetary disk*. San Francisco: Astronomical Society of the Pacific. pp. 251–285. [2] Nagahara H. et al. 2005. In *Chondrites and the protoplanetary disk*. San Francisco: Astronomical Society of the Pacific. pp. 456–468. [3] Kita N. T. et al. 2006. Abstract #1496. 37th Lunar and Planetary Science Conference. [4] Ozawa K. and Nagahara H. 2001. *Geochimica et Cosmochimica Acta* 65:2171–2199.

5218

COMPLEX EXPOSURE HISTORY OF VACA MUERTA MESOSIDERITE INFERRED FROM NOBLE GASES

K. Nagao and K. Bajo. Laboratory for Earthquake Chemistry, Graduate School of Science, University of Tokyo, Bunkyo-ku, Tokyo 113-0033, Japan. E-mail: nagao@eqchem.s.u-tokyo.ac.jp

Introduction: Vaca Muerta is classified as a mesosiderite, which suggests collision event(s) between differentiated asteroidal bodies for its formation. Several compositionally different clasts are found in the meteorite. Sm-Nd ages of 4.4–4.5 Ga [1] and ³⁹Ar-⁴⁰Ar ages of 3.8–4.0 Ga [2] have been reported. Cosmic-ray exposure age determined for metal phase is 133 Ma [3].

Experimental: Bulk sample (0.2086 g) and chips (0.4844 and 0.4829 g) from a eucritic pebble in the Vaca Muerta mesosiderite were measured for noble gases with stepwise heating method: eight and 13 temperature steps from 400 to 1800 °C. The concentration of ⁸¹Kr and cosmogenic Kr isotopic composition were also determined for a chip (0.2129 g) from the eucritic pebble.

Results and Discussion: Ar isotopic ratios at low temperatures are plotted close to the atmospheric value in a plot of ⁴⁰Ar/³⁶Ar versus ³⁸Ar/³⁶Ar. At the middle temperatures, however, the ratios plot in a narrow area (³⁸Ar/³⁶Ar = 1.53 and ⁴⁰Ar/³⁶Ar = 87), then go downward to cosmogenic Ar (³⁸Ar/³⁶Ar = 1.54 and ⁴⁰Ar/³⁶Ar ~ 0). The Ar component (hereafter “VM-component”) at the middle temperature range must be a mixing product between radiogenic ⁴⁰Ar and cosmogenic Ar. Bulk sample shows clear excess in ⁴⁰Ar compared with the VM-component, which would be an in situ produced radiogenic ⁴⁰Ar after formation of the VM-component. The observed Ar isotopic feature can be explained as: 1) noble gases had been well degassed from differentiated parent bodies prior to a collision, 2) collision of the differentiated asteroids produced the mesosiderite breccia at 4.4–4.5 Ga [1], 3) cosmogenic and radiogenic Ar accumulated in the breccia were mixed at the thermal event which reset K-Ar system (4 Ga determined by ³⁹Ar-⁴⁰Ar method [2]), and 4) cosmic-ray irradiation during the transit from a Vaca Muerta parent body to the Earth.

Based on the above described model, the transit time is calculated as about 30 Myr, while the period of cosmic-ray exposure at the breccia formation (4.4–4.5 Ga) must be longer than 90 Myr. ⁸¹Kr-Kr exposure age of 180 Myr obtained for the eucritic pebble suggests >150 Myr for the early irradiation period.

If K-Ar age of 4 Ga [2] is adopted for our samples, K concentration in the eucritic pebble should be as low as 2–7 ppm, while 240 ppm is calculated from radiogenic ⁴⁰Ar concentration for the bulk sample. Noticeable amount of excess ¹²⁹Xe from ¹²⁹I could not be detected in the samples, which indicates that volatile degassing occurred or continued until the ¹²⁹I extinction in the mesosiderite parent body.

References: [1] Stewart B. W. et al. 1994. *Geochimica et Cosmochimica Acta* 58:3487–3509. [2] Bogard D. D. and Garrison D. H. 1998. *Geochimica et Cosmochimica Acta* 62:1459–1468. [3] Begemann F. et al. 1976. *Geochimica et Cosmochimica Acta* 40:353–368.

5265

MINERALOGY AND OXYGEN ISOTOPE SIGNATURES OF THE ASUKA-881020 CH CHONDRITE

T. Nakamura¹, T. Noguchi², and T. Akaki¹. ¹Department of Earth and Planetary Sciences, Kyushu University, Fukuoka, Japan. E-mail: tomoki@geo.kyushu-u.ac.jp. ²Department of Materials and Biological Sciences, Ibaraki University, Ibaraki, Japan

Asuka-881020 is the first CH chondrite found in the Japanese Antarctic meteorite collection [1]. It consists mainly of CH chondrite host and minor amounts of phyllosilicate-rich clasts [1]. The host is a mixed material of chondrules, fragmented mineral aggregates (~80%), and FeNi metallic grains (~20%). The chondrules are mostly cryptocrystalline or glassy type and range in size typically from 50 to 100 μm but occasionally up to 200 μm . Overall mineralogical signatures of the host are similar to other CH chondrites (e.g., [2, 3]). Oxygen isotope analysis was performed on 24 chondrules using an ion probe Cameca 6f at Kyushu University. The results show that oxygen compositions of most chondrules distribute along but slightly (~5 permil in $\delta^{17}\text{O}_{\text{SMOW}}$) above the CCAM line in a range from -10 to +5 permil in $\delta^{17}\text{O}_{\text{SMOW}}$; the range of compositions is similar to chondrules in other carbonaceous chondrites.

The phyllosilicate clasts occupy ~3% of the whole areas of the meteorite investigated. The size of the clasts is variable from 20 to 500 μm across. Pyrrhotite plates and magnetite framboids commonly occur in the clasts. Dolomite crystals with sizes from 20 to 80 μm are also contained. Synchrotron X-ray diffraction analysis of several clasts indicates that dominant phyllosilicates vary between clasts: one is rich in serpentine and the other is rich in saponite. In both serpentine- and saponite-rich clasts, prism reflections, which are resulted from stacking disorder of tetrahedron sheets, are clearly observed. Major element compositions of phyllosilicate-rich portions in the clasts were obtained using an analytical TEM. In the (Si+Al)-Mg-Fe ternary diagram, compositions of a serpentine-rich clast are plotted between serpentine and low-Ca pyroxene solid solution, while those of a saponite-rich clast are clustered between saponite and low-Ca pyroxene solid solution. The differences in both mineral and chemical compositions between serpentine- and saponite-rich clasts suggest that they are alteration products formed under different physico-chemical conditions. The two types of hydrous clasts were incorporated during/after formation of the CH chondrite parent body. The preservation of serpentine indicates that the temperature during formation of this meteorite has never exceeded 600 °C.

References: [1] Noguchi T. et al. 2004. *Antarctic Meteorites* 28:62–63. [2] Grossman J. N. et al. 2002. *Earth and Planetary Science Letters* 91:33–54. [3] Krot A. N. et al. 2004. *Meteoritics & Planetary Science* 37:1451–1490.

5034

ESTIMATION OF SHOCK PRESSURE EXPERIENCED BY EACH ORDINARY CHONDRITE WITH AN X-RAY DIFFRACTION METHOD

Y. Nakamura¹, S. Yamada², and K. Yoshida³. ¹Kyushu University Museum, Kyushu University, Japan. E-mail: nakamura@museum.kyushu-u.ac.jp. ²NTT Dokomo Chugoku, Japan. ³NTT Data, Japan

Introduction: Shock metamorphism is pervasively recognized in meteorites, and it is an important subject to estimate the degree of shock experienced by each meteorite. Chondrites have been classified into six degrees based on the intensity of shock that was recorded as shock textures on olivine [1]. However, the classification is qualitative one in order to know shock pressures.

It is experimentally suggested that the crystal lattice of olivine has been strained by shock and the maximum strain estimated by an X-ray diffraction method linearly increases with the increase of the pressure loaded on it [2]. In this study, we determined apparent strains of olivines in ordinary chondrites by an X-ray method and try to draw the relation line between the maximum strain and shock pressure applicable to ordinary chondrites.

Experimental Method: We analyzed eight ordinary chondrites showing variable degrees of shock. The polished thin sections of the eight chondrites were observed under a microscope and shock stages for each chondrite were determined referred to [1]. Four to eight olivine grains of about 50 μm in size, being confirmed to be homogeneous in their chemical compositions, were taken out of the polished thin sections. Their X-ray powder diffraction patterns were obtained by a Gandolfi camera. The position and the integral breadth of each X-ray reflection were precisely determined by applying a profile-fitting technique with a pseudo-Voigt type shape function. The maximum strains of olivine crystals were determined based on the equation, $\beta = 4e \tan \theta$, where e , β , and θ are the maximum strain, the broadening due to the strain and the half of the angle between incident and diffraction beams, respectively [3]. The maximum strain e is equal to $\Delta d/d$, where Δd is the maximum deviation of the interplanar spacing d due to distortion of a crystal.

Results and Discussion: The maximum strains of olivine crystals for each chondrite are obtained as follows: 0.033–0.044% for Great Bend (S1), 0.037–0.064% for Y-790752 (S2), 0.040–0.092% for Mulga (north) (S2), 0.061–0.108% for Leedeey (S3), 0.083–0.122% for Dhurmsala (S3), 0.098–0.160% for Ohuma (S3), 0.107–0.170% for Arcadia (S3), and 0.136–0.190% for Bruderheim (S4). The maximum strains for each chondrite vary by about 0.01% for Great Bend (S1), by about 0.03% for Y-790752 (S2), and by about 0.06% for others. The variation may reflect inhomogeneous stress on each olivine when the chondrite was shocked due to a heterogeneous petrographic texture of a chondrite. Then, the maximum values of the maximum strains for each chondrite are taken as a measure of shock pressure. The maximum strain of olivine is experimentally found to increase linearly with shock pressure [2] and also nonlinearly with shock duration time. Then, the relationship between the maximum strain and shock pressure applicable to chondrites was estimated from the shock-pressure ranges for each shock stage of [1]. The result was also compared to experimentally determined ones of different shock duration time.

References: [1] Stöffler D. et al. 1991. *Geochimica et Cosmochimica Acta* 55:3845–3867. [2] Uchizono A. et al. 1999. *Mineralogical Journal* 21: 15–23. [3] Wilson A. J. C. 1962. *X-ray optics*. New York: John Wiley and Sons.

5136

SEARCH FOR EXTINCT ^{36}Cl IN ALLENDE CAIS: THE PINK ANGEL

D. Nakashima, U. Ott, and P. Hoppe. Max-Planck-Institut für Chemie, Becherweg 27, D-55128 Mainz, Germany. E-mail: ott@mpch-mainz.mpg.de

Introduction: Radioactive ^{36}Cl ($T_{1/2} = 0.3$ Ma) has long been suspected to have been present in the early solar system. Its actual detection, however, has proven to be difficult. Part of the problem is that Cl-rich phases such as sodalite tend to be alteration rather than primary phases and that the decay of ^{36}Cl primarily leads to volatile ^{36}Ar . Search for ^{36}Ar excesses due to decay of extinct ^{36}Cl in sodalite-rich CAIs from the Allende meteorite (e.g., [1, 2]) have been negative, while a reported excess in bulk Efremovka [3] has shown to be an analytical artifact [4].

Decay to ^{36}S : Although only 1.9% of decays lead to ^{36}S , search in S may be advantageous because of the much lower volatility as compared to Ar [5]. Lin et al. [5] found ^{36}S excesses correlating with Cl/S in sodalites from a CAI in Ningqiang, corresponding to $^{36}\text{Cl}/^{35}\text{Cl} \sim 5 \times 10^{-6}$ at the time of sodalite formation. A similar ratio was found in sodalites in the Allende Pink Angel by [6]. On the other hand, we found no evidence for extinct ^{36}Cl in our study of another fine-grained Allende CAI [7].

New Measurements: Using the Mainz NanoSIMS, we performed measurements on a thin section of the Pink Angel that was kindly supplied by G. J. Wasserburg in order to confirm the results of [6]. Procedures were as described in [7], but there was a problematic background that required subtraction of 90% of the signal at ^{36}S , much more severe than in [7], where the correction typically amounted to some 30%.

Results: Our results basically confirm the observations of [6] in that ^{36}S is enhanced. A weighted fit to our data yields $(^{36}\text{Cl}/^{35}\text{Cl})_0 = (4.2 \pm 1.4) \times 10^{-6}$, compatible with the initial $^{36}\text{Cl}/^{35}\text{Cl} \sim 4 \times 10^{-6}$ of [6]. However, because of the background problem, our errors are somewhat large and it is possible that we are in fact dealing with a disturbed system.

Discussion: A late irradiation origin for ^{36}Cl has been favored by [6], similar to the case of ^{10}Be . However, unlike the latter, which appears to be present in roughly equal abundance in all studied CAIs, ^{36}Cl appears to be variable. Critical in the interpretation is when and where the alteration processes occurred that led, among others, to the formation of sodalite [8]. Absence of sodalite from the matrix of their sample has been interpreted by [6] as indication that alteration happened in the nebula rather than on the Allende parent body. We have, however, observed sodalites in Allende matrix, and sodalites have been found in the matrix of many CV3 meteorites [8]. Clearly the possibility of multiple alteration episodes needs to be considered.

Acknowledgments: We thank Jerry Wasserburg for the Pink Angel sample, Joachim Huth for work on the SEM, and Ahmed El Goresy for valuable advice and discussions.

References: [1] Villa I. et al. 1981. 12th Lunar and Planetary Science Conference. pp. 1115–1117. [2] Göbel R. et al. 1982. *Geochimica et Cosmochimica Acta* 46:1777–1792. [3] Murty S. V. S. et al. 1997. *The Astrophysical Journal* 475:L65–L68. [4] Rai V. K. et al. 2003. *Geochimica et Cosmochimica Acta* 67:4435–4456. [5] Lin Y. et al. 2005. *Proceedings of the National Academy of Sciences* 102:1306–1311. [6] Hsu W. et al. 2006. *The Astrophysical Journal* 640:525–529. [7] Plagge M. et al. 2006. Abstract #1287. 37th Lunar and Planetary Science Conference. [8] Krot A. N. et al. 1995. *Meteoritics* 30:748–775.

5137

NOBLE GASES IN THE ISHEYEVO METEORITED. Nakashima¹, S. P. Schwenzer¹, L. Franke¹, U. Ott¹, M. A. Ivanova², A. I. Buikin², J. Hopp³, E. V. Korochantseva^{2, 3}, and M. Trierloff³. ¹Max-Planck-Institut für Chemie, Germany. E-mail: naka@mpch-mainz.mpg.de. ²Vernadsky Institute of Geochemistry and Analytical Chemistry, Russia. ³Mineralogisches Institut, Ruprecht-Karls-Universität Heidelberg, Germany

Introduction: The recently discovered metal-rich carbonaceous chondrite Isheyevu [1] consists of at least two lithologies: a fine-grained, metal-poor (<20 vol%) lithology (CH-like) and a coarse-grained, metal-rich (~70 vol%) lithology (CB_b-like) [2]. Isheyevu should provide a clue for the genetic relationship between CB and CH chondrites. Here we report results of stepwise noble gas analyses of Isheyevu meteorite samples.

Results and Discussion: The trapped $^{36}\text{Ar}/^{132}\text{Xe}$ ratio (~900) is higher than that of Q gases, suggesting that Isheyevu has Ar-rich gases and/or solar noble gases. Isotopic ratios of He and Ne show that Isheyevu contains solar and cosmogenic noble gases. This suggests that Isheyevu is a regolith breccia. The solar $^4\text{He}/^{20}\text{Ne}$ ratio is about 252, which is comparable to the typical value for solar wind implanted species (258, lunar soil ilmenites 12001, [3]). The trapped $^{20}\text{Ne}/^{36}\text{Ar}$ ratio (8.2) is lower than that for lunar soil ilmenites 12001 (26.8, [3]). If solar ^{20}Ne is lost, even more solar ^4He would be lost. The solar $^4\text{He}/^{20}\text{Ne}$ ratio is expected to be lower. It is likely that the low $^{20}\text{Ne}/^{36}\text{Ar}$ ratio is due to enrichment of trapped ^{36}Ar , i.e., Ar-rich gases. Such Ar-rich gases also have been seen in CH and CB chondrites [4, 5].

Xe isotopic ratios show that the dominant component is Xe-Q, while minor components are cosmogenic Xe and atmospheric Xe in the lowest temperature fraction (600 °C). Solar Xe can not be clearly observed. Kr isotopic ratios show the presence of cosmogenic Kr as well as a hint of neutron-induced Kr from Br. The presence of neutron-induced Kr suggests that the preatmospheric size of Isheyevu is larger than 22 cm in radius [6], assuming that the neutron-induced Kr was produced during exposure of the meteoroid.

Cosmogenic ^{21}Ne concentrations vary from sample to sample. The shortest possible cosmic-ray exposure age is 45 Ma, which is calculated from the lowest cosmogenic ^{21}Ne concentration, the production rate given by [7], the bulk chemical composition and the assumption that the meteorite was exposed to cosmic rays with 4π geometry and with average shielding. The estimated exposure age is comparable to our previous result (~36 Ma, [2]).

Assuming that measured ^{40}Ar is totally radiogenic in origin, the gas retention age is calculated as 4.4 Ga from concentrations of K (45 ppm) and ^{40}Ar (3.2×10^{-6} cm³/g). The estimated gas retention age is longer than our Ar-Ar dating results of <3.5 Ga [2], which may result from different degrees of partial loss of radiogenic ^{40}Ar .

References: [1] Ivanova M. A. et al. 2005. *Meteoritics & Planetary Science* 40:A74. [2] Ivanova M. A. et al. 2006. Abstract #1100. 37th Lunar and Planetary Science Conference. [3] Eberhardt P. et al. 1972. 3rd Lunar Science Conference. pp. 1821–1856. [4] Lewis R. S. 1985. *Meteoritics* 20: A698. [5] Weber H. W. et al. 2001. *Meteoritics & Planetary Science* 36: A220. [6] Eberhardt P. et al. 1963. *Earth Sciences and Meteoritics* 143–168. [7] Schultz L. and Freundel M. 1985. In *Isotopic ratios in the solar system*. Toulouse: Cepadues-Editions. pp. 27–33.

5310

ORDINARY CHONDRITES: AN IRON ISOTOPE STUDY

A. W. Needham^{1,2}, D. Porcelli¹, and S. S. Russell². ¹Department of Earth Sciences, University of Oxford, Oxford, UK. E-mail: andrewn@earth.ox.ac.uk. ²Department of Mineralogy, Natural History Museum, London SW7, UK

Introduction: The properties of iron—its abundance, relative volatility, sensitivity to redox conditions, and occurrence as metal, sulfide, and silicate phases—make it an important element to study in ordinary chondrites. High-precision Fe-isotope analyses have only become possible within the past decade due to advances in multi-collector plasma-source mass-spectrometry. Previous studies (e.g., [1, 2, 3]) have focused on differentiated meteorites and carbonaceous chondrites, with only a handful of ordinary chondrite analyses yet reported. This is the first extensive study of Fe-isotope fractionations in ordinary chondrites, including analyses of bulk meteorite, chondrules, matrix, metal, and sulfide phases.

Method: Polished blocks of bulk chondrites were analyzed by SEM prior to micro-drilling (accurate to <100 μm). A wide range of chondrules, chondrule rims, metal, sulfides, and matrix samples were extracted, digested, and processed by anion-exchange columns. The Fe solutions were then analyzed by MC-ICP-MS, with a precision (2σ) of ± 0.06‰ on δ⁵⁶Fe; see [4] for details of MC-ICP-MS technique. Results are reported relative to the IRMM-14 standard. The same procedures, excluding SEM and micro-drilling, were performed for whole-rock analyses.

Samples: To date, the sample set comprises 16 ordinary chondrites, representing H, L, and LL groups, from petrologic type 3.4 to 6. Analyses of more highly-unequilibrated (<3.4) ordinary chondrite samples are pending. A similarly extensive study of carbonaceous and enstatite chondrites is also underway.

Results: The range in Fe-isotope compositions of bulk samples is −0.18‰ to +0.01‰. H, L, and LL samples plot throughout this range, though there is a slight bias towards isotopically lighter LL samples. Metal phases range from −0.24‰ up to +0.3‰; low-Ni metal tends to be heavier, with only high-Ni metal found to be isotopically lighter than the standard. Sulfide phases have been found to be isotopically light, ranging from 0 to −0.37‰. Chondrules in type III chondrites exhibit a wide range of compositions, from −0.28‰ to +0.26‰. Some chondrules in types IV–VI chondrites have equally large fractionations, but on average are less fractionated than in type III.

Analyses of almost 100 mineral-separates and bulk samples have revealed a wide and complex range of Fe-isotope compositions in ordinary chondrites. Relationships with other chemical and mineralogical features provide constraints on the processes (evaporative losses, etc.) controlling Fe distribution.

References: [1] Zhu et al. 2001. *Nature* 412:311–313. [2] Poitrasson F. et al. 2005. *Earth and Planetary Science Letters* 234:151–164. [3] Mullane E. et al. 2005. *Earth and Planetary Science Letters* 239:203–218. [4] Belshaw N. et al. 2000. *International Journal of Mass Spectrometry* 197: 191–195.

5320

CLUES TO CHICXULUB DEPOSITIONAL HISTORY FROM Mg AND K SIGNATURES IN THE YAX-1 IMPACTITES

M. J. Nelson and H. E. Newsom. University of New Mexico, Institute of Meteoritics, Department of Earth and Planetary Sciences, Albuquerque, New Mexico 87131, USA. E-mail: MEL14@unm.edu

Introduction: The ICDP Yaxcopoil-1 drill core, in the annular trough of the Chicxulub crater, exhibits layered impactites consisting of upper suevite and lower impact melt breccia [1]. Impactites are Mg- and possibly K-rich in certain units [2, 3, this work]. Models that explain these Mg and K signature signatures can be divided into two categories: 1) Chicxulub impactites are the result of a silicate melt later altered by some kind of fluid [3, 4], or 2) impactites were initially Mg-, and/or K-rich from primary melt composition [2, 5], or some combination thereof. Each model has substantial implications for the dynamics of impactite deposition, and hydrothermal processes.

Methods and Results: Microprobe and X-ray diffraction analyses were conducted to determine textural and chemical relationships of melt clasts, the origin of Mg and K signature, and if the impactites contain hydrothermal minerals. We found the K and Mg signatures are spatially decoupled. In the melt breccias, K-enrichment exists only on angular, silicate melt clast rims, while the matrix material consists of a separate Mg-, calcite-rich phase with no K-enrichment. The upper suevite also contains these two phases: An Mg-, calcite-rich phase, and an Si-, Al-, sometimes K-rich phase, but both phases comprise the groundmass and schlieren melt clasts. The results of this study support a sequence as follows: 1) Dolomite and granite were melted and ejected during transient crater formation. 2) Granitic melt was quenched, brecciated, and enriched in potassium by seawater. 3) Transport and deposition followed, the nature of which was somewhat different for melts at depth than from those above. At depth, the granitic melt was rapidly permeated by Mg-rich dolomitic melt immediately before or upon deposition, during the lateral surge associated with the collapse of the transient crater. Above, starting at Unit 3 [1], dolomite and granite melt textures appear to be consistent with simultaneous ballistic transport, and the two melts were likely in contact longer. Lower in the section, melts were then deposited as melt breccia, consisting of angular silicate melt clasts and dolomitic melt matrix, while melts above were deposited as suevite, consisting of schlieren dolomite and silicate melts. This study found no evidence for extensive hydrothermal alteration at the Yax-1 site, although silicate melt in upper suevite does appear to have been altered by dolomite melt, and possibly seawater.

Acknowledgements: Yaxcopoil-1 core samples were obtained from CSDP team. Research funding was provided by NASA Planetary Geology and Geophysics program and MFRP (H. Newsom, P.I.).

References: [1] Dressler B. O. et al. 2003. *Eos* 84:125–130. [2] Tuchscherer et al. 2004. *Meteoritics & Planetary Science* 39:955–978. [3] Ames D. E. et al. 2004. *Meteoritics & Planetary Science* 39:1145–1168. [4] Zürcher L. and Kring D. A. 2004. *Meteoritics & Planetary Science* 39: 1199–1222. [5] Dressler B. O. et al. 2004. *Meteoritics & Planetary Science* 39:857–879.

5355

IN SITU IDENTIFICATION OF A PRESOLAR SiC X GRAIN, PRESOLAR SILICATES AND ¹³C-RICH GRAINS IN THE ALLAN HILLS 77307 METEORITE

A. N. Nguyen, L. R. Nittler, and C. M. O'D. Alexander. Department of Terrestrial Magnetism, Carnegie Institution of Washington, Washington, D.C., USA. E-mail: nguyen@dtm.ciw.edu

Introduction: Presolar grains have traditionally been identified by the measurement of single grains from acid residues or size-separated matrix grains [1]. Whereas the analysis of these samples allows for more isolated studies of specific mineral phases or grain sizes, the analysis of polished meteorite sections is well-suited for surveying the relative abundances of different presolar phases in a sample that has undergone less laboratory processing, and for investigating petrologic relations (if any) between presolar grains and surrounding meteoritic materials.

Raster ion imaging in the NanoSIMS ion microprobe has been employed in the identification of very small isotopically anomalous silicate grains in IDPs [2, 3], meteorites [4, 5], and micrometeorites [6]. Exploiting the enhanced capabilities of the new Carnegie NanoSIMS 50L, we analyzed a polished section of the CO3.0 meteorite ALHA77307 by simultaneous ion imaging of the O and Si isotopes. For some areas, we imaged the O and C isotopes, as well as ²⁸Si. With this experimental setup, anomalous silicates, oxides, SiC, and C-rich grains can be identified.

Results: We measured a total area of ~2700 μm² and identified 13 presolar silicate grains, all of which are smaller than 300 nm. Most of these grains have O isotopic compositions consistent with Group 1 presolar oxides [7], but two of the silicate grains fall into Group 3 and one grain is a Group 4. The Si isotopic compositions of five of these grains were determined, and fall in the range seen for mainstream SiC grains and other presolar silicate grains [5, 8]. We also identified a <200 nm grain having depletions in both ²⁹Si and ³⁰Si ($\delta^{29}\text{Si} = -280 \pm 54$, $\delta^{30}\text{Si} = -387 \pm 61$), similar to those typically seen in SiC X grains originating from type II supernova. The NanoSIMS ²⁸Si/¹⁶O ratio of this grain is high relative to the surrounding matrix grains, most of which are silicates, suggesting that it is indeed a SiC. The abundance of SiC X grains in bulk meteorite samples is only ~100 ppb, compared to ~110 ppm for presolar silicate grains. The detection of this grain demonstrates that even very rare presolar grain types can effectively be identified with the experimental technique employed. We plan to measure the C and N isotopic compositions of this grain.

Two grains having slight enrichments in ¹³C ($\delta^{13}\text{C} = 67 \pm 5$; 78 ± 8) were also identified. SEM-EDX analyses (5 kV) of these grains show peaks for C and O. It is possible that these grains are organic in nature. We will measure the N and H isotopes in the NanoSIMS to more fully characterize these grains.

References: [1] Zinner E. K. 2004. In *Meteorites, planets, and comets*. Oxford: Elsevier-Perigamon. pp. 17–39. [2] Messenger S. et al. 2003. *Science* 300:105–108. [3] Floss C. et al. 2006. *Geochimica et Cosmochimica Acta* 70: 2371–2399. [4] Nguyen A. N. and Zinner E. 2004. *Science* 303:1496–1499. [5] Mostefaoui S. and Hoppe P. 2004. *The Astrophysical Journal* 613:L149–L152. [6] Yada T. et al. 2006. Abstract #1470. 37th Lunar and Planetary Science Conference. [7] Nittler L. R. et al. 1997. *The Astrophysical Journal* 483:4715–495. [8] Nguyen A. N. et al. 2005. Abstract #2196. 36th Lunar and Planetary Science Conference.

5063

AN EXPERIMENTAL STUDY OF THALLIUM PARTITIONING AND ISOTOPE FRACTIONATION DURING PLANETARY CORE FORMATION PROCESSES

S. G. Nielsen¹, B. J. Wood², M. Rehkämper³, and A. N. Halliday¹. ¹Department of Earth Sciences, University of Oxford, Parks Road, Oxford, OX1 3PR, UK. E-mail: snielsen@els.mq.edu.au. ²Department of Earth and Planetary Sciences, Macquarie University, 2109 NSW, Australia. ³Department of Earth Science and Engineering, Imperial College, London SW7 2AZ, UK

In a recent study [1], it was proposed on the basis of thallium (Tl) isotope variations in iron meteorites that the short-lived radioactive nuclide ²⁰⁵Pb, which decays to ²⁰⁵Tl with a half-life of 15 Myr, was present in the early solar system. A caveat of the ²⁰⁵Pb-²⁰⁵Tl decay system is that Tl only has two isotopes (²⁰³Tl and ²⁰⁵Tl) and it is therefore difficult to distinguish between Tl isotope variations from the decay of ²⁰⁵Pb and stable isotope fractionation. Specifically, it was concluded that the troilite nodules of iron meteorites contain Tl that is isotopically fractionated relative to the metal phase. These are therefore not suitable as indicators of ²⁰⁵Pb decay.

Modeling of terrestrial accretion and core formation furthermore implies that either the Earth's core is highly enriched in Tl compared to iron meteorites or most of the original terrestrial Tl budget was lost to space, for example, during the putative Moon-forming giant impact. The latter is mechanistically difficult. The partitioning behavior of Tl between metal, silicate, and sulfide is, however, unknown. It is therefore currently not possible to predict the amount of Tl present in the core and compare it with that required by isotopic mass balance modeling.

In order to investigate the behavior of Tl during core formation and crystallization processes, we experimentally reacted mixtures of silicate, sulfide, and metal in a piston-cylinder apparatus at 2 GPa and 1750 °C. Preliminary results on Tl partitioning between liquid metal and silicate indicate a $D^{\text{met/sil}} < 1$, which would result in a silicate Earth with a much higher Tl concentration than is observed today. As Tl is relatively chalcophile, it is not surprising that $D^{\text{met/sil}}$ is dependent on the sulfur concentration of the liquid metal, whereby the highest partition coefficients are observed for pure liquid sulfide ($D^{\text{sul/sil}} > 150$). However, the partition coefficient for Tl at a sulfur concentration similar to that of the Earth's core (about 1.7%, [2]) is still too low to extract sufficient Tl from the silicate mantle.

An alternative mechanism for placing additional Tl in the core is offered by the late addition of pure sulfide, a process recently revisited by Wood and Halliday [3]. If the $D^{\text{sul/sil}}$ value determined here is representative for sulfide segregation from the mantle, then <0.8% (by weight) of the mantle would have to precipitate as sulfide in order to balance the Tl budget of the bulk Earth. This does not appear unrealistic, as the giant impact would have contributed a significant amount of sulfur to the Earth [3].

Additional experiments will be performed to determine if any Tl isotope fractionation occurs during core formation or crystallization and to obtain more detailed information on the Tl partitioning during metal-sulfide-sulfide segregation.

References: [1] Nielsen S. G., Rehkämper M., and Halliday A. N. 2006. *Geochimica et Cosmochimica Acta* 70:2643–2657. [2] Dreibus G. and Palme H. 1998. *Geochimica et Cosmochimica Acta* 60:1125–1130. [3] Wood B. J. and Halliday A. N. 2005. *Nature* 437:1345–1348.

5173

THERMOLUMINESCENCE STUDY IN THE JAPANESE ANTARCTIC METEORITES COLLECTION: ASUKA ORDINARY CHONDRITES

K. Ninagawa¹, N. Imae², H. Kojima², K. Yanai³, and A. J. T. Jull⁴.
¹Department of Applied Physics, Okayama University of Science, Okayama 700-005, Japan. E-mail: ninagawa@dap.ous.ac.jp. ²National Institute of Polar Research, Tokyo 173-8515, Japan. ³Department of Civil and Environ., Iwate University, Morioka 020-8551, Japan. ⁴NSF-Arizona AMS Laboratory, University of Arizona, Tucson, Arizona 85721, USA

Introduction: Induced thermoluminescence (TL), the response of a luminescent phosphor to a laboratory dose of radiation reflects the mineralogy and structure of the phosphor and provides valuable information on the metamorphic and thermal history of meteorites. Especially the sensitivity of the induced TL is used to determine petrologic subtype of unequilibrated ordinary chondrites [1]. Natural TL, the luminescence of a sample that has received no irradiation in the laboratory, reflects the thermal history of the meteorite in space and on Earth. Natural TL data thus provide insights into such topics as the orbits of meteoroids, the effects of shock heating, and the terrestrial history of meteorites [2]. Natural TL properties also can be applied to find paired fragments [3].

Primitive Ordinary Chondrites: We measured induced and natural TL properties of ninety Asuka unequilibrated ordinary chondrites (LL: 16, L: 27, H: 47) from the Japanese Antarctic meteorite collection from the D1, D2, and D3 sites near the Sør Rondane Mountains. Most of the chondrites had TL sensitivities over 0.1, corresponding to petrologic subtype 3.5–3.9. Six chondrites, A-881244 (L3), A-87319 (L3), A-881607 (LL3), A-881328 (LL3), A-9043 (L3), and A-881408 (LL3), were revealed to be primitive ordinary chondrites under petrologic subtype 3.2. They are particularly significant in understanding the nature of primitive material in the solar system.

Pairing: Natural and induced TL properties were also applied to find paired fragments, and we found 26 TL potential paired fragments, nine groups in the Asuka samples [4, 5]. A group of H3 at D1 site comprises a chain of paired fragments. An H3 chondrite might be shower near the Sør Rondane Mountains. We will determine terrestrial ages for ten chondrites by cosmic produced nuclides, ¹⁴C and ¹⁰Be, and we will get information not only for assurance of TL pairing but also for glaciological setting near the Sør Rondane Mountains.

Acknowledgements: This work was carried out in part under the Visiting Researcher's Program of the Research Reactor Institute, Kyoto University.

References: [1] Sears et al. 1991. 21st Lunar and Planetary Science Conference. pp. 493–512. [2] Benoit et al. 1991. *Icarus* 94:311–325. [3] Ninagawa et al. 1998. *Antarctic Meteorite Research* 11:1–17. [4] Ninagawa et al. 2002. *Antarctic Meteorite Research* 15:114–121. [5] Ninagawa et al. 2005. *Antarctic Meteorite Research* 18:1–16.

5105

3-D RAMAN SPECTROSCOPY OF THE PDFs IN QUARTZ FROM THE RIES IMPACT STRUCTURE

H. Nishido¹, A. Gucsik², K. Ninagawa¹, and T. Okumura¹. ¹Okayama University of Science, Department of Applied Physics, Ridai-cho 1-1, Okayama, 700-0005, Japan. ²University of West Hungary, Bajcsy-Zs. u. 4., Sopron, H-9400, Hungary. E-mail: ciklamensopron@yahoo.com

Introduction: The study of Raman properties of unshocked and experimentally shock-deformed minerals (e.g., quartz) has the potential to provide a tool that can be used in shock barometry to supplement the methods available so far (mainly optical microscopy; also birefringence and density measurements of shocked quartz are rarely done; cf. [1]). MicroRaman spectroscopy is by now a fairly routine technique that is not too complicated in its use (unlike, e.g., the NMR technique of [2]), and the identification of a Raman spectroscopic method that would allow to a) identify shocked minerals, and b) give information on the shock pressure would be useful for the identification and study of impact structures.

Experimental Procedure: Raman spectra were obtained with an Almega: confocal microRaman spectrometer with a 20 mW at 532 nm with Nd:YAG laser excitation system.

Results and Discussion: Raman spectra of quartz have been described in great detail by previous scientists (e.g., [1]). They found changes in frequency and line-width of the 206 and 464 cm⁻¹ A₁ Raman modes of quartz, which were determined over temperatures from 23 to 800 °C and simultaneously at pressures between 0.1 MPa and 2.1 GPa, using a hydrothermal diamond-anvil cell (HDAC). The positions and widths of peaks in the Raman spectra of our measurements are in good agreement with these previous studies. Raman spectra of the coesite as a high-pressure polymorph of quartz have been reported by (e.g., [2]). On the other hand, in laser-heated diamond cell experiments, found that coesite exhibits three relatively strong Raman bands at 489, 552, and 790 cm⁻¹ and stishovite shows a strong peak at 790 cm⁻¹ [3]. These authors concluded that stishovite was converted to coesite at 10 GPa and 2330 °C. Raman spectra of planar deformation features (PDFs) in the shocked quartz from the Ries impact structure exhibit a pronounced peak at around 455 cm⁻¹, which can be assigned to Si-O stretching vibration, whereas typical low-quartz has a sharp and intense peak at 464 cm⁻¹. This frequency shift might be related to a distortion of structural configuration caused by shock-metamorphism. 3-D Raman imaging analysis using this Raman peak reveals a striped image comprised of high and low crystalline parts. This 3-D Raman image corresponds to the optical image of PDFs. Consequently, Raman spectroscopy is a potentially useful tool that can be used to characterize PDFs (as most important mineralogical criteria of presence of shock metamorphism) of quartz from impactites. These results also give new insight into the structural changes that occur in quartz during shock metamorphism, and the pressures associated with these changes.

Acknowledgements: This work has been partly supported by the Hungarian Space Office (TP-293). Authors express grateful thanks to A. Osada for Raman spectroscopy in Himeji Analysis and Evaluation Center (Japan).

References: [1] Schmidt C. and Ziemann A. M. 2000. *American Mineralogist* 85:1725–1734. [2] Boyer H. et al. 1985. *Physics and Chemistry of Minerals* 12:45–48. [3] Serghiou et al. 1995. *Geophysical Research Letters* 22:441–444.

5368

CONSTRAINING THE NUMBER OF LUNAR AND MARTIAN METEORITE FALLS

K. Nishiizumi¹ and M. W. Caffee². ¹Space Sciences Laboratory, University of California–Berkeley, Berkeley, California 94720–7450, USA. E-mail: kuni@ssl.berkeley.edu. ²Department of Physics, Purdue University, West Lafayette, Indiana 47907–1396, USA

Introduction: Extensive searches in Antarctica and in other arid environments for extraterrestrial materials are increasing the number of lunar and Martian meteorites to our collections. However, in many instances the meteorite is paired with other fragments from the same object that impacted Earth. Identification of these pairs is a critical component of the studies of source objects, impact events, and orbital dynamics of those meteorites. Chemical and petrographic properties are useful criteria for distinguishing individual falls for both lunar and Martian meteorites, however, this information alone is not always sufficient for all objects, especially lunar meteorites. Cosmogenic nuclide studies of lunar and Martian meteorites have contributed significantly to our understanding of these objects. The specific goals of these measurements are to constrain or set limits on the following shielding or exposure parameters: 1) the depth of the sample at the time of ejection from the Moon or Mars, 2) the transition time from ejection off the lunar or Martian surface until capture by the Earth, and 3) the terrestrial residence time. The ejection age in conjunction with the sample depth on the Moon or Mars can then be used to model impact and ejection mechanisms. We have measured cosmogenic nuclides in 48 (33 individual) lunar and 37 (30) Martian meteorites; a summary of new measurements is presented below.

New Measurements: Although the data are still preliminary, we measured cosmogenic nuclides in 10 new lunar and seven new Martian meteorites since our last report [1].

Lunar Meteorites: Among 11 Dhofar meteorites we studied, we found seven individual falls. Dhofar 489/908/911/1085 are paired. Our measurements indicate that they were ejected from $>1100 \text{ g/cm}^2$ on the Moon and the transition time from Moon to Earth is $4 \pm 1 \text{ kyr}$; the terrestrial age is $\sim 300 \text{ kyr}$. Dhofar 081/280/910 are paired and were ejected from a depth of $200\text{--}230 \text{ g/cm}^2$ on the lunar surface. The preliminary ^{10}Be 4π exposure age of Dhofar 1084 is $0.32 \pm 0.06 \text{ Myr}$. We identified 6–7 individual falls of NWA meteorites using cosmogenic nuclide. ^{10}Be and ^{26}Al results indicate: 1) NWA 3160 is possibly paired with NWA 773, 2) NWA 2200 and 3136 were ejected from a depth of $50\text{--}100 \text{ g/cm}^2$ on the lunar surface, and 3) NWA 3163 was ejected from a depth of $300\text{--}320 \text{ g/cm}^2$. The ^{10}Be 4π exposure age of NEA 001 is $0.44 \pm 0.08 \text{ Myr}$. Conclusive exposure histories will be obtained after ^{36}Cl and ^{41}Ca measurements.

Martian Meteorites: New exposure ages of shergottites are consistent with previously identified exposure age clusters. The preliminary ^{10}Be exposure age of NWA 1195, 2046, and 2626 are $1.1 \pm 0.2 \text{ Myr}$. The exposure ages of NWA 1068, 1110, 1460, 2646, 3171, and GRV 99027 are in the range of $2.5\text{--}3.1 \text{ Myr}$. ^{36}Cl and ^{41}Ca terrestrial age measurements are in progress.

Acknowledgements: We thank ENSL, MN-Berlin, NAU, NSM-Tokyo, Polar Research Institute of China, SWML, U. Münster, U. Washington, Vernad, Gregory, Hupe, and Nelson for providing meteoritic samples.

References: [1] Nishiizumi K. 2004. *Meteoritics & Planetary Science* 39:A77.

5296

CORRELATED MICROANALYSIS OF PRESOLAR MATERIALS

L. R. Nittler. Department of Terrestrial Magnetism, Carnegie Institution of Washington, Washington, D.C., 20015, USA. E-mail: lrn@dtm.ciw.edu

Introduction: Presolar grains and organic matter in extraterrestrial materials are samples of stars and molecular clouds available for study in terrestrial laboratories [1–3]. As such, they provide new insights, not obtainable by other means, into a wide variety of astrophysical processes and environments. However maximizing the information obtained requires correlated multi-analytical techniques on the same samples. Fortunately, the explosion of nanoscience in recent years has led to the development of many new techniques enabling high-sensitivity, multi-technique analysis of micro-scale materials.

Presolar Grains: Presolar grains are tiny (2 nm to 20 μm) pristine samples of stardust preserved in meteorites and interplanetary dust particles (IDPs) [1]. Their isotopic compositions are used to determine stellar sources (e.g., red giant, supernova) and to constrain stellar evolution and nucleosynthesis models. Their microstructures (e.g. crystal structure, defects, etc.) provide insights into the physical and chemical conditions of grain condensation in stars and dust processing in the interstellar medium [4, 5]. Ideally, a complete picture of a presolar grain includes both multi-element isotopic data and microstructural data, but obtaining correlated data on the same grains has been difficult due to the necessity of thin ($\sim 100 \text{ nm}$) samples for structural studies and thicker samples for isotopic measurements. The development of high sensitivity, high spatial resolution secondary ion mass spectrometry (NanoSIMS) and focused-ion-beam (FIB) sample preparation has greatly enabled combined isotope-structural presolar grain studies. For example, correlated submicron isotopic and structural data for individual graphite and SiC grains from supernovae [6–8] provide an unprecedented view of dust condensation within supernovae.

Presolar Organic Matter: Both meteorites and IDPs contain organic matter with H and N isotopic signatures indicating an origin in interstellar space prior to solar system formation [2, 3]. The organics are not well characterized, especially at microscales, and correlated analyses are essential for maximizing the yield of information. Using SIMS isotopic measurements to identify isotopically anomalous materials, traditional ultramicrotomy and/or FIB techniques can be used to extract samples for additional analyses by, e.g., transmission electron microscopy, synchrotron X-ray and infrared spectroscopy, and microRaman analysis [9–11]. Such correlated analyses have indicated both some common features of primitive organic matter and strong variations on small spatial scales, indicating a diversity of formation processes and subsequent evolution.

References: [1] Nittler L. R. 2003. *Earth and Planetary Science Letters* 209:259–273. [2] Messenger S. 2000. *Nature* 404:968–971. [3] Busemann H. et al. 2006. *Science* 312:727–730. [4] Bernatowicz T. J. et al. 1996. *The Astrophysical Journal* 472:760–782. [5] Stroud R. M. 2005. In *Chondrites and the protoplanetary disk*. San Francisco: Astronomical Society of the Pacific. p. 645. [6] Croat T. K. et al. 2003. *Geochimica et Cosmochimica Acta* 67:4705–4725. [7] Stroud R. M. et al. 2004. *Meteoritics & Planetary Science* 39:A101. [8] Stadermann F. J. et al. 2005. *Geochimica et Cosmochimica Acta* 69:177–188. [9] Keller L. P. et al. 2004. *Geochimica et Cosmochimica Acta* 68:2577. [10] Floss C. et al. 2004. *Science* 303:1355–1358. [11] Busemann H. et al. 2006. Abstract #2005. 37th Lunar and Planetary Science Conference.

5316

EXTREME ^{13}C AND ^{15}N ENRICHMENTS IN A MURCHISON PRESOLAR SiC GRAIN

L. R. Nittler, C. M. O'D. Alexander, and A. N. Nguyen. Department of Terrestrial Magnetism, Carnegie Institution of Washington, Washington, D.C., 20015, USA. E-mail: lrn@dtm.ciw.edu

Although the stellar sources for most presolar SiC grains are well established, the origin of grains with extreme ^{13}C , ^{15}N , and ^{30}Si excesses is controversial. Originally attributed to novae [1], isotopic data for some of these grains are better explained by supernovae [2]. We report isotopic data for presolar SiC grains from Murchison, one of which has the largest ^{13}C and ^{15}N excesses yet measured in presolar grains.

We used the ims-6f ion probe to automatically analyze C and Si isotopes in 1550 0.5–5 μm SiC grains from a new residue prepared using the CsF technique [3]. The Si data are shown in Fig. 1. The abundances of subgroups are in the ranges of previous studies, with the exception of the supernova-derived X grains, which are present at 2 \times higher abundance than previously observed. Since X grains are apparently more disordered than other SiC grains [4], the higher abundance might indicate that they preferentially survive the CsF chemistry, relative to the standard HF/HCl treatment. Two highly unusual grains were also identified. Grain 505-1 has \sim solar $^{29}\text{Si}/^{28}\text{Si}$, a huge ^{30}Si excess ($^{30}\text{Si} = 850\%$), and light C ($^{12}\text{C}/^{13}\text{C} = 150$). Grain 240-1 has excesses in both ^{29}Si and ^{30}Si , but lies to the right of the mainstream correlation line, and has $^{12}\text{C}/^{13}\text{C} = 1.04 \pm 0.01$. A preliminary measurement with the new Carnegie NanoSIMS 50L indicates $^{14}\text{N}/^{15}\text{N} \leq 5$ for this 800 nm grain. SEM-EDX analysis indicates a very high Al concentration (>10 wt%) and we estimate [N]>2 wt% from the NanoSIMS CN $^-$ /C $^-$ ratio.

Both the $^{12}\text{C}/^{13}\text{C}$ and $^{14}\text{N}/^{15}\text{N}$ ratios of grain 240-1 are lower than previously reported for any presolar grain and are consistent with pure nova ejecta with white dwarf masses of \sim 1.0–1.2 M [5]. A supernova origin is unlikely since the nonexplosive H burning in such stars cannot produce such low $^{12}\text{C}/^{13}\text{C}$. Grain 505-1 is similar to a previously-reported grain, M26a-454-3 [3]. Its ^{13}C depletion rules out a nova origin. Additional NanoSIMS isotopic measurements (e.g., Al-Mg, Ti, Ca) for both unusual grains will help unravel their origins.

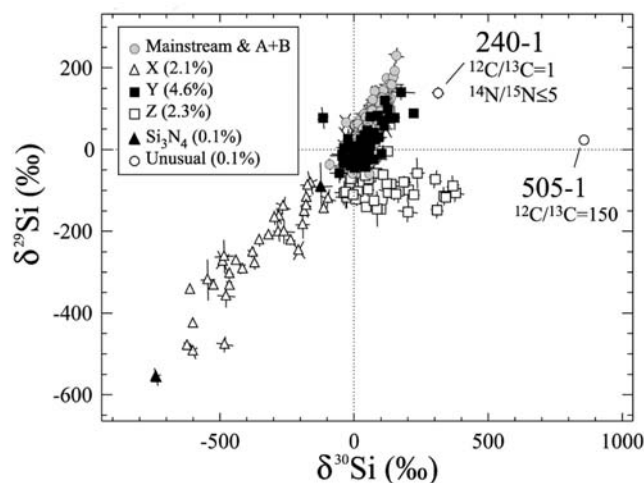


Fig. 1.

References: [1] Amari S. et al. 2001. *The Astrophysical Journal* 551: 1065–1072. [2] Nittler L. R. and Hoppe P. 2005. *The Astrophysical Journal* 631:L89–L92. [3] Nittler L. R. and Alexander C. M. O'D. 2003. *Geochimica et Cosmochimica Acta* 67:4961–4980. [4] Stroud R. M. et al. 2004. *Meteoritics & Planetary Science* 39:A101. [5] José J. et al. 2004. *The Astrophysical Journal* 612:414–428.

5154

TRAPPING NOBLE GASES IN FULLERENES

Joseph A. Nuth¹, Luann Becker², Robert J. Poreda³, and Frank T. Ferguson^{1,4}. ¹Code 691, NASA GSFC, Greenbelt, Maryland 20771, USA. E-mail: Joseph.A.Nuth@NASA.gov. ²Department of Geological Sciences, Institute of Crustal Studies, University of California–Santa Barbara, Santa Barbara, California 93106, USA. ³Department of Earth, New York 14627, USA. ⁴Chemistry Department, The Catholic University of America, Washington, D.C. 20064, USA

Introduction: The possible role of natural fullerenes as a carrier of planetary noble gases is under debate. Research on synthetic fullerenes, such as produced by carbon-arc evaporation and soot deposition, suggests that the encapsulation of the noble gases in C60 and C70 is proportional to the partial pressure of the gas at the time of fullerene formation [1, 2].

Experiments: Graphitic smokes (GS) are made by electrically heating a 5 cm long graphite rod thinned to increase its electrical resistance. For each experiment the graphite rod was heated quickly to produce a “hot cylinder” of carbon vapor in a premixed noble gas atmosphere. The condensed smoke formed a deposit on an aluminum plate positioned in the condensation chamber 15.2 cm above the continuously heated graphite rod. This thin graphite rod allows carbon to condense more uniformly in comparison to the arc-discharge evaporation process typically used in fullerene synthesis [4, 5].

Kimura et al. [6] used the arc-discharge technique for the preferential production of higher fullerenes that were also produced by Rotundi et al. [5] wherein soot contained higher fullerenes [4]. The arc-discharge process is nonlinear in comparison to the simple evaporative heating method [3] that we have adapted for our studies of synthetic noble gas carbon carriers. Previous investigations of the bulk GS sample that was analyzed for Xe yielded values as high as 13.7×10^{-6} cm³ STP/gm of ¹³²Xe (3). This value is \sim 2 orders of magnitude greater than typical ¹³²Xe amounts for other synthetic carbon residues [7]. While this result was exciting, the origin of the carrier for GS bulk material remained unknown. We obtained GS soot material synthesized in a noble gas mixture of 49% Ne, 49% Ar, 1% Xe, and 1% Kr with the balance provided from He for a 300 torr atmosphere maintained during GS soot condensation [3].

For previous fullerene investigations [8–10] we developed a two-step extraction method for isolating fullerenes from natural samples: first, Toluene extraction that separated predominately C60, C70 up to C100, and a second extraction with high boiling solvent (1,2,4 trichlorobenzene or 1,2,3,5 tetramethylbenzene) to separate higher fullerenes in the C100–C300 range. We will report the results of these studies at the meeting.

References: [1] Saunders et al. 1993. *Science* 259:1428–1431. [2] Giblin et al. 1997. *Journal of the American Chemical Society* 119:9883–9890. [3] Olsen et al. 2000. Abstract #1479, 31st Lunar and Planetary Science Conference. [4] Krätschmer et al. 1990. *Nature* 347:354–357. [5] Rotundi et al. 1998. *Astronomy & Astrophysics* 329:1087–1096. [6] Kimura et al. 1995. *Chemical Physics Letters* 246:571–576. [7] Ott et al. 1981. [8] Becker et al. 2000. *Proceedings of the National Academy of Sciences* 97:2979–2983 [9] Becker et al. 2001. *Science* 291:1530–1533. [10] Poreda and Becker. 2003.

5143

INITIAL ISOTOPIC HETEROGENEITIES IN ZAGAMI: EVIDENCE OF A COMPLEX MAGMATIC HISTORY

L. E. Nyquist¹, C.-Y. Shih², and Y. D. Reese³. ¹NASA Johnson Space Center, Houston, Texas 77058, USA. E-mail: laurence.e.nyquist@nasa.gov. ²ESCG Jacobs-Sverdrup, Houston, Texas 77058, USA. ³Mail Code JE-23, ESCG/Muniz Engineering, Houston, Texas, 77058, USA

Introduction: Interpretations of Zagami's magmatic history range from complex [1, 2] to relatively simple [3]. Discordant radiometric ages led to a suggestion that the ages had been reset [4]. In an attempt to identify the mechanism, Rb-Sr isochrons were individually determined for both fine-grained and coarse-grained Zagami [5]. Ages of ~180 Ma were obtained from both lithologies, but the initial ⁸⁷Sr/⁸⁶Sr (I_{Sr}) of the fine-grained lithology was higher by $8.6 \pm 0.4 \epsilon$ -units. Recently, a much older age of ~4 Ga has been advocated [6]. Here we extend our earlier investigation [5].

Rb-Sr Data: In [5] we applied identical, simplified procedures to both lithologies to test whether a grain-size dependent process such as thermally driven subsolidus isotopic reequilibration had caused age-resetting. Minerals were separated only by density. In the present experiment, purer mineral separates were analyzed with improved techniques. Combined Rb-Sr results give ages (T) = 166 ± 12 Ma and 177 ± 9 Ma and $I_{Sr} = 0.72174 \pm 9$ and 0.72227 ± 7 for the coarse-grained and fine-grained lithologies, respectively. I_{Sr} in the fine-grained sample is thus higher than in the coarse-grained sample by $7.3 \pm 1.6 \epsilon$ -units. The results for the coarse-grained lithology are in close agreement with $T = 166 \pm 6$ Ma, $I_{Sr} = 0.72157 \pm 8$ for an adjacent sample [7] and $T = 178 \pm 4$ Ma, $I_{Sr} = 0.72151 \pm 5$ [4, adjusted] for a separate sample. Thus, fine-grained Zagami appears on average to be less typical of the bulk than coarse-grained Zagami.

Conclusions: Fine-grained Zagami was suggested to have inherited more numerous pyroxene cores from an earlier magma chamber than coarse-grained Zagami [1]. Higher I_{Sr} in the finer-grained parts may in part be inherited from radiogenic Sr from old pyroxenes in the magma reservoir. However, most LIL elements in Zagami probably were derived from a crustal reservoir. Thus, higher I_{Sr} in the finer-grained lithology also could have come from a greater contribution from an old, crustal, high Rb/Sr component. Failure to achieve isotopic equilibrium throughout the magma suggests rapid, complex, magmatic processes, perhaps initiated by sudden injection of a metasomatic fluid. Variations in the initial abundance of pyroxene cores plus early crystallization of pyroxene may have caused the magma to "choke," freezing isotopic differences into different volumes. These effects probably affected most of the ~175 Ma shergottites contributing to ambiguities in interpreting their isotopic data.

References: [1] McCoy T. M. et al. 1992. *Geochimica et Cosmochimica Acta* 56:3571–3582. [2] McCoy T. M. et al. 1995. 26th Lunar and Planetary Science Conference. pp. 925–926. [3] Treiman A. H. and Sutton S. R. 1992. *Geochimica et Cosmochimica Acta* 56:4059–4074. [4] Shih C.-Y. et al. 1982. *Geochimica et Cosmochimica Acta* 46:2323–2344. [5] Nyquist L. E. et al. 1995. 26th Lunar and Planetary Science Conference. pp. 1065–1066. [6] Bouvier A. et al. 2005. *Earth and Planetary Science Letters* 240:221–233. [7] Borg L. E. et al. 2005. *Geochimica et Cosmochimica Acta* 69:5819–5830.

5249

MICROCHONDRULES WITHIN A TROILITE-RICH RIM AROUND A CHONDRULE IN THE YAMATO-790448 LL3 CHONDRITE

R. Okazaki and T. Nakamura. Department of Earth and Planetary Sciences, Faculty of Science, Kyushu University, Hakozaki, Higashiku-ku, Fukuoka 812-8581, Japan. E-mail: okazaki@geo.kyushu-u.ac.jp

Introduction: Many small spherical silicates have been recognized in ordinary chondrite [1–3]. Silicate spherules with <40 μ m diameter were arbitrarily defined as "microchondrules," compared to normal-sized chondrules that are larger than several hundred micrometers. Microchondrules have been found in FeO-rich matrices or chondrule rims so far. Here we report the presence of microchondrules in a sulfide-silicate-metal rich rim surrounding a chondrule in Yamato (Y)-790448 LL3.2 [4] chondrite.

Methods: Polished thin sections prepared from Y-790448 were investigated with an optical microscope and an SEM. Chemical compositions were determined with an EMPA.

Results and Discussion: A POP chondrule (800 μ m in diameter) in Y-790448 has a rim (up to 150 μ m in thickness) consisting of troilite, silicates, and metal. Pyroxene and olivine compositions of the chondrule are typically Fs_{16} and Fa_{20} , respectively. The silicates in the rim consist dominantly of low-Ca pyroxene. There are two kinds of morphology for the pyroxene: round (microchondrules with 5–25 μ m in diameter) and fragmental (irregular and blade-like). The fragmental pyroxenes, probably chondrule fragments, show chemical zoning: at a point 3 μ m inside from the edge of pyroxene fragments the composition is slightly enriched in FeO (Fs_{20}) compared to the further inner part (Fs_{16}). In contrast, chemical compositions of pyroxene microchondrules are homogeneous within each of them and moderately higher in FeO (up to Fs_{25}) than those in the enclosed host chondrule.

Troilite and Fe-Ni metal fill clacks in the microchondrules and the interstices between pyroxene fragments and microchondrules, which suggests that opaque minerals have been melted. The Co content in kamacite in the rim is in the range of those in chondrules and matrix in Bishunpur [5]. This is unlike S-rich chondrule rims where Co enrichments were observed and thought to result from oxidation and sulfuration with the nebular gas [6]. Thus, the kamacite composition in the sulfide-silicate-metal rich rim in Y-790448 implies that heating occurred in an environment separated from nebular gas, i.e., in the parent body. If we assume that both of the pyroxene fragments and microchondrules have formed from the host chondrule pyroxenes, their FeO variations could be due to different duration and/or peak temperature of the heating event. Such heterogeneous heating effects might be caused by impact shock in the parent body.

References: [1] Rubin R. E. et al. 1982. *Geochimica et Cosmochimica Acta* 46:1763–1776. [2] Krot A. N. et al. 1997. *Geochimica et Cosmochimica Acta* 61:463–473. [3] Krot A. N. and Rubin A. E. 1996. In *Chondrules and the protoplanetary disk*. Cambridge: Cambridge University Press. pp. 181–184. [4] Ninagawa K. et al. 1998. *Antarctic Meteorite Research* 11:1–17. [5] Kojima T. et al. 2003. *Geochimica et Cosmochimica Acta* 67:3065–3078. [6] Rambaldi E. R. and Wasson J. T. 1981. *Geochimica et Cosmochimica Acta* 45:1001–1015.

5189

CATHODOLUMINESCENCE AND RAMAN SPECTROSCOPIC CHARACTERIZATION OF SHOCKED QUARTZ FROM THE BARRINGER AND RIES IMPACT CRATERS

T. Okumura¹, A. Gucsik², H. Nishido¹, and K. Ninagawa³. ¹Research Institute of Natural Sciences, Okayama University of Science, 1-1 Ridai-cho, Okayama 700-0005, Japan. E-mail: okumura@rins.ous.ac.jp. ²Department of Soil Science, University of West Hungary, Bajcsy Zs. E. u. 4., Sopron, H-94000, Hungary. ³Department of Applied Physics, Okayama University of Science, 1-1 Ridai-cho, Okayama 700-0005, Japan

Introduction: We discuss an effect of shock metamorphism on quartz from impact craters by means of cathodoluminescence (CL) and 3-D Raman spectrometry. Cathodoluminescence microscopic and spectroscopic methods are useful techniques which enable easily characterization of planar microstructure in quartz [1–3]. MicroRaman spectroscopy is a technique that provides information on lattice vibration from a microscopic area.

Samples and Methods: The samples employed here are twenty quartz grains at various shock stages from the impact craters, the Ries crater and the Barringer meteor crater. They were prepared as polished thin sections using nonluminescent epoxy resin and coated with 20 nm-thick carbon. The planar microstructures, planar deformation features (PDFs), and planar fractures (PFs) were observed in several quartz grains under a petrographic microscope. Raman spectra were obtained with a confocal microRaman spectrometer at 20 mW on Nd:YAG laser (532 nm) excitation system. CL spectral measurements were carried out using a SEM-CL (SEM combined with a grating monochromator) with an accelerating voltage of 15 kV. The sample temperature was controlled in the range from –192 to 25 °C using a cryostage.

Results and Discussion: Raman spectra of shocked quartz exhibit a pronounced peak at around 455 cm⁻¹, which can be assigned to Si-O stretching vibration, whereas typical low-quartz has a sharp and intense peak at 464 cm⁻¹. This frequency shift might be related to a distortion of structural configuration caused by shock-metamorphism. 3-D Raman imaging analysis using this Raman peak reveals a stripe pattern suggesting lamination layer comprised of high and low crystalline parts. This 3-D Raman image corresponds to the optical image of PDFs. Furthermore, SEM-CL imaging of some shocked quartz gives apparent features related to PDFs, which can be clearly observed under polarized microscope.

CL spectra of shocked quartz exhibit a doublet peak in the range from 450 to 500 nm. Upon heating the CL intensity rapidly decreased. The decay of CL intensity in low-quartz is well known as a temperature quenching effect. Activation energy in temperature quenching process was evaluated by assuming Mott-Seitz model. Arrhenius plot leads to activation energy (E) of 0.068 ~ 0.085 eV in the range from –180 to –30 °C for shocked quartz. On the other hand, unshocked ordinary quartz exhibits two temperature quenching processes, where the E is 0.03 eV up to –110 °C and 0.235 eV above –110 °C. Therefore, the effect of shocked-metamorphism might affect to electronic transition process in defect centers correlated to CL emission.

References: [1] Marshall D. J. 1988. *Cathodoluminescence of geological materials*. Boston: Unwin Hyman. 146 p. [2] Hayward C. L. 1998. In *Modern approaches to ore and environmental mineralogy*. Mineralogical Association of Canada. pp. 269–325. [3] Boggs S. et al. 2001. *Meteoritics & Planetary Science* 36:783–793.

5101

IDENTIFICATION OF M1 AND M2 SITES IN OLIVINE AND PYROXENE BY MÖSSBAUER SPECTROSCOPY OF ORDINARY CHONDRITES

M. I. Oshtrakh and E. V. Zhiganova. Faculty of Physical Techniques and Devices for Quality Control, Ural State Technical University–UPI, Ekaterinburg, 620002, Russian Federation. E-Mail: oshtrakh@mail.utnet.ru, evgeniya@dpt.ustu.ru

Introduction: It is well known that both olivine and pyroxene contain two crystallographically nonequivalent octahedral sites M1 and M2. These sites are occupied by Fe²⁺ and Mg²⁺ ions. The contrast of M1 and M2 sites geometry in olivine is less than that in pyroxene. The Fe-Mg distribution between two sites is of interest due to its possible application for minerals cooling history determination. Mössbauer spectroscopy was successfully used to distinguish M1 and M2 sites in pure synthetic and natural olivines, orthopyroxenes and clinopyroxenes [1–4]. Ordinary chondrite is a mixture of olivine, pyroxene, troilite, metal and iron oxides. Therefore, its Mössbauer spectra contain superposition of several components that increases difficulties to distinguish subspectra corresponded to M1 and M2 sites in. In this work we demonstrate the possibility to reveal sites M1 and M2 for olivine and pyroxene in ordinary chondrites using Mössbauer spectroscopy with high velocity resolution.

Methods: Samples of ordinary chondrites Farmington L5 (1), Kunashak L6 (2), Vengerovo H5 (3), and Zvonkov H6 (4) were prepared as a powder. All samples were measured at room temperature using high stable and sensitive Mössbauer spectrometer SM-2201 in transmission geometry with moving absorber. Mössbauer spectra were measured with registration in 4096 channels with further presentation in 1024 channels by summation of neighbor channels.

Results: Mössbauer spectra of ordinary chondrites were fitted using seven or eight components, including four components related to M1 and M2 sites in olivine and pyroxene. Some results are given in Table 1. Higher values of quadruple splitting were related to higher octahedral site distortion.

Table 1

Sample	M1		M2		M1/M2
	δ , mm/s	ΔE_Q , mm/s	δ , mm/s	ΔE_Q , mm/s	
Olivine					
1	1.207	2.982	1.119	2.876	1.09
2	1.195	3.023	1.162	2.836	1.20
3	1.209	2.986	1.133	2.902	1.29
4	1.209	3.000	1.131	2.922	1.39
Pyroxene					
1	1.256	2.672	1.165	2.078	0.18
2	1.221	2.485	1.182	2.070	0.21
3	1.202	2.540	1.169	2.084	0.12
4	1.212	2.576	1.177	2.087	0.26

Experimental error is ± 0.014 mm/s.

Conclusions: Using Mössbauer spectroscopy with high-velocity resolution the M1 and M2 sites in olivine and pyroxene of ordinary chondrites were identified and compared with [1–4].

References: [1] Van Alboom A. et al. 1993. *Physics and Chemistry of Minerals* 20:263–275. [2] Eeckhout S. G. et al. 2000. *American Mineralogist* 85:943–952. [3] Wang L. et al. 2005. *Geochimica et Cosmochimica Acta* 69: 5777–5788. [4] Morozov M. et al. 2005. *European Journal of Mineralogy* 17: 495–500.

5114

STUDY OF CH/CB METEORITE ISHEYEVO BY MÖSSBAUER SPECTROSCOPY

M. I. Oshtrakh, V. I. Grokhovsky, and K. A. Uimina. Faculty of Physical Techniques and Devices for Quality Control, Ural State Technical University –UPI, Ekaterinburg, 620002, Russian Federation. E-mail: oshtrakh@mail.utnet.ru, grokh47@mail.ru

Introduction: Carbonaceous chondrites CH and CB enriched with Fe(Ni,Co,Cr) metal phases are the most primitive meteorites. The meteorite bencubbinite Isheyevo was recently found in Russia. This unique meteorite contains zones with different lithology [1]. Metal grains in these zones had the same size (0.1–0.3 mm) and similar structural variety. Meteorites of CR clan were not studied by Mössbauer spectroscopy yet. Therefore, in this work the first study of bencubbinite Isheyevo by Mössbauer spectroscopy was made.

Methods: Two samples of surface and internal regions of meteorite Isheyevo fragment were prepared as powders. Samples were measured at room temperature using high stable and sensitive Mössbauer spectrometer SM-2201 in transmission geometry with moving absorber. Mössbauer spectra were measured with registration in 4096 channels with further presentation in 1024 channels by summation of neighbor channels.

Results: Mössbauer spectra of Isheyevo samples of surface and internal regions (Fig. 1) consisted of the main asymmetrical sextet and several minor components. Asymmetrical sextets in both samples were better fitted as superposition of four sextets: 1) α_2 -Fe(Ni) ($H_{\text{eff}} = 346$ kOe), 2) α -Fe(Ni) ($H_{\text{eff}} = 334$ kOe), 3) α -Fe(Ni) ($H_{\text{eff}} = 333$ kOe), and 4) γ -FeNi ($H_{\text{eff}} = 312$ – 314 kOe). Other spectral components were different for the samples of external and internal regions. In case of external region (Fig. 1a), two different models with the same χ^2 values were used. Small quantities of olivine (5), pyroxene (6), and unknown high-spin ferrous compound (7) were the same in both models. The first model showed the presence of two singlets whose parameters were close to taenite γ -Fe(Ni) and niningerite (see [2]) while the second model assumed the presence of ~9% ferric oxide, whose subspectrum is represented by one doublet (8), as in ordinary chondrites [3]. In the spectrum of internal region small quantities of olivine (5), unknown high spin ferrous compound (6) and ~3% ferric oxide (7) were found.

Conclusions: The first Mössbauer study of CH/CB meteorite Isheyevo revealed several metal phases and different minor components in external and internal regions. However, further study by various techniques is required for clarification.

References: [1] Ivanova M. A. et al. 2006. Abstract # 1100. 37th Lunar and Planetary Science Conference. [2] Dunlop R. A. 1997. *Hyperfine Interactions* 110:209–215. [3] Zhiganova E. V. et al. *Hyperfine Interactions*. Forthcoming.

5322

REFRACTORY LITHOPHILE ELEMENT FRACTIONATION IN ISHEYEVO SILICATES

A. Pack¹, B. Hattendorf², and D. Günther². ¹Institut für Mineralogie, Universität Hannover, Callinstrasse 3, D-30167 Hannover, Germany. E-mail: a.pack@mineralogie.uni-hannover.de. ²Laboratorium für Anorganische Chemie, ETH Hönggerberg, HCI, CH-8093 Zürich, Germany

Introduction: We have conducted an LA-ICPMS study of refractory lithophile elements (RLEs) in order to trace high-T gas/solid fractionation in Isheyevo silicates (chondrules and CAIs).

Results: REEs are largely unfractionated in cryptocrystalline, metal-poor and -rich chondrules with <1 – 7 CI, resembling those in other metal-rich chondrite chondrules [1]. One exception (IV, metal-rich PO chondrule) shows distinct ultrarefractory REEs [2]. Three of six CAIs show volatility-controlled group II REE patterns [3], with the remaining three having largely unfractionated REEs. Isheyevo chondrules define $Y/Ho = 24$, which is close to the solar ratio of 26.2 ± 0.4 [4]. Chondrule IV has a Y/Ho ratio of only 10.4, opposite to what is expected for an object enriched in the ultrarefractory component [4]. This suggests that REEs in IV may have condensed after removal of the very first condensates with high Y/Ho . Two of three CAIs with group II patterns have subchondritic Y/Ho (7 and 11). Isheyevo chondrules have $Zr/Hf = 36$, which is close to the chondritic value of 34.3 ± 0.3 [5]. Only IV deviates from that ratio with $Zr/Hf = 46$, which we relate to fractional condensation (i.e., $Tc(Zr) > Tc(Hf)$ [6]). CAIs show variable Zr/Hf with those CAIs with chondritic Y/Ho also having chondritic Zr/Hf . Nb/Ta shows a larger scatter than Y/Ho and Zr/Hf with an average ratio of 18 in Isheyevo chondrules, which is similar to the chondritic value of 19.9 ± 0.6 [5]. Chondrule IV has $Nb/Ta = 9$ that is explained by $Tc(Ta) > Tc(Nb)$ [6]. Nb/Ta in CAIs varies from 12.2 to 24.5.

Discussion: Unfractionated REEs suggest formation of the majority of Isheyevo chondrules from *primitive* material, i.e., that has not undergone major nebular or parent body chemical fractionation. The same conclusion is drawn from near chondritic Y/Ho , Zr/Hf , and Nb/Ta ratios. Chondrule IV shows evidence for incorporation of an ultrarefractory component that formed by high-T fractional condensation. Fractionated Y/Ho in IV suggests effective isolation of dust at the high-T end of the condensation sequence. Volatility-controlled REEs that are known from other carbonaceous [7–11] and ordinary chondrite [12] chondrules are interpreted by incorporation of CAI-like material into chondrule IV. CAIs in Isheyevo have REE patterns that are well known for decades from carbonaceous chondrite CAIs [3] and are explained in terms of volatility-controlled chemical fractionation in an H_2 -rich nebular gas [13]. Our data are not supportive for an origin of Isheyevo chondrules different from chondrules of other chondrites, i.e., though a late impact [14].

References: [1] Krot A. N. et al. 2001. *Science* 291:1776. [2] Boynton W. V. and Frazier R. M. 1980. 11th Lunar and Planetary Science Conference. p. 103. [3] Mason B. and Martin P. M. 1977. *Smithsonian Contributions to the Earth Sciences* 19:84. [4] Pack A. et al. *Geochimica et Cosmochimica Acta*. Forthcoming. [5] Münker C. et al. 2003. *Science* 301:84. [6] Lodders K. 2003. *The Astrophysical Journal* 591:1220. [7] Misawa K. and Nakamura N. 1988. *Geochimica et Cosmochimica Acta* 52:1699. [8] Misawa K. and Nakamura N. 1988. *Nature* 334:47. [9] Misawa K. and Nakamura N. 1996. In *Chondrules and the protoplanetary disk*. Cambridge: Cambridge University Press. p. 99. [10] Russell S. S. et al. 2002. *Geochimica et Cosmochimica Acta* 66:A658. [11] Ash R. D. et al. 2003. Abstract #1907. 34th Lunar and Planetary Science Conference. [12] Pack A. et al. 2004. *Science* 303:997–1000. [13] Boynton W. V. 1989. In *Geochemistry and mineralogy of rare earth elements*. Washington, D.C.: Mineralogical Society of America. [14] Krot A. N. et al. 2005. *Nature* 436:989.

5366

THE CHONDRITE PARADOX

H. Palme. University of Cologne, Institute of Geology and Mineralogy, Zulpicher Str. 49b, 50674 Cologne, Germany. E-mail: herbert.palme@uni-koeln.de

One of the most perplexing aspects of primitive chondritic meteorites is the narrow range and solar-like bulk chemical and isotopic composition of centimeter-sized samples in contrast to the large compositional variations of their individual mg-sized components: chondrules, inclusions, fragments, matrix.

Chondrules in ordinary chondrites (OC) and in carbonaceous chondrites (CC) show a wide range of chemical compositions, including variable degrees of oxidation and a large range of oxygen isotope ratios of individual chondrules (e.g., [1]). Components of primitive chondrites are in apparent thermodynamic disequilibrium with each other. Curiously, we assume that the stronger the disequilibrium, the more primitive is the meteorite. A simple nebular model would predict the opposite. The chaotic mixture of chondrules, fragments, metal, and matrix accreted to a meteorite with a very simple bulk composition, when scaled to average solar system abundances. The Na/Mn ratio is solar in bulk OC and CC chondrites [2]; OC even have solar Na/Mg ratios. The Na/Mn ratio varies widely among individual chondrules, fractionates strongly during evaporation and condensation, and is extremely redox sensitive.

The source of the material of the inner solar system is the extremely well-mixed interstellar matter (ISM). New results on Os [3] and Zr [4] isotopes demonstrate that physically separable nucleosynthetic components are present in chondritic meteorites, excluding total evaporation, isotopic homogenization, and recondensation of matter at the beginning of the solar system. Uniform isotopic composition of solar system material is achieved by sampling the extremely well mixed ISM, which on melting, evaporation, and condensation, produces coarse-grained chondrule precursors. Random sampling of these components leads to the observed uniform and solar-like bulk meteorite compositions.

Accretion of chondrites occurred from chemically fractionated materials homogeneously distributed in the nebula on a very local scale. A large compositional stratification and gross deviations from the solar-like average chemistry of the nebula can be excluded, except for a general depletion of volatiles. Fragments from destroyed differentiated planetesimals of earlier generations [5] do not contribute to chondritic bulk compositions. Compositional similarities of the Earth and CV chondrites suggest a huge CV-like reservoir and small OC reservoirs [6].

References: [1] Jones R. H. et al. 2005. In *Chondrites and the protoplanetary disk*. San Francisco: Astronomical Society of the Pacific. pp. 251–285. [2] O'Neill H. St. C. and Palme H. 1998. In *The Earth's mantle: Structure, composition and evolution*. Cambridge: Cambridge University Press. pp. 3–126. [3] Brandon A. D. et al. 2005. *Science* 309:1233–1236. [4] Schönbachler M. et al. 2005. *Geochimica et Cosmochimica Acta* 69:5113–5122. [5] Kleine T. et al. 2005. *Geochimica et Cosmochimica Acta* 69:5805–5818. [6] Palme H. 2001. *Philosophical Transactions of the Royal Society of London A* 359:2061–2075.

5142

Ar-Ar AGE OF SHERGOTTITE DHOFAR 378: FORMATION OR EARLY SHOCK EVENT?

J. Park and D. D. Bogard. ARES code KR, NASA Johnson Space Center, Houston, Texas 77058, USA. E-mail: jisun.park1@jsc.nasa.gov

Introduction: Martian shergottite Dhofar 378 (Dho 378) is from Oman, weighs 15 g, and possesses a black fusion crust [1]. The plagioclase in other shergottites has been converted to maskelynite by shock, but Dho 378 experienced even more intense shock heating, estimated at 55–75 GPa [2]. Dho 378 plagioclase (~43 modal%) melted, partially flowed and vesiculated, and then partially recrystallized [3]. Here we report ^{39}Ar - ^{40}Ar dating of K-enriched phases of Dho 378. We suggest that the determined age may date the intense shock heating event this meteorite experienced, but not the later impact that initiated the CRE age.

Ar-Ar Results: The ^{39}Ar - ^{40}Ar data for 16 stepwise temperature extractions of mixed mesostasis plus plagioclase show the following major characteristics. Changes in the K/Ca ratio and in the differential rate of ^{39}Ar release with extraction temperature suggest three distinct, but overlapping Ar diffusion domains: <13%, 13–45%, and >45% cumulative ^{39}Ar release. The youngest Ar-Ar age, ~162–165 Myr, is observed at ~28–40% ^{39}Ar release, which we attribute primarily to the mesostasis. Extractions releasing >45% ^{39}Ar , probably from plagioclase, suggest older Ar-Ar ages and indicate release of trapped Martian ^{40}Ar . An isochron plot for eight extractions, releasing 3–45% of the ^{39}Ar and corrected for $^{36}\text{Ar}_{\text{cos}}$ using directly measured $^{36}\text{Ar}_{\text{cos}}$, gives an Ar-Ar age of 143 ± 4 Myr (where the \pm ignores the uncertainty in applying a correction for $^{36}\text{Ar}_{\text{cos}}$). Applying a correction assuming only one-half of the measured $^{36}\text{Ar}_{\text{cos}}$ gives an age of 159 ± 2 Myr. Correcting for $\text{cos-}^{36}\text{Ar}$ using the minimum measured $^{36}\text{Ar}/^{37}\text{Ar}$ ratio gives a minimum possible age of 138 ± 5 Myr. All of these ages are within combined uncertainties of the Sm-Nd age of 157 ± 24 Myr [4]. The trapped $^{40}\text{Ar}/^{36}\text{Ar}$ ratio obtained from the isochron is largely defined by the highest [K] data.

Conclusions: We suggest that the ~143 Myr Ar-Ar age determined from the Dho 378 isochron may not date the impact that ejected the meteorite into space ~3 Myr ago, but a much earlier impact at ~143 Myr. The relationship between the similar Ar-Ar and Sm-Nd ages is not clear. Diffusion data for ^{39}Ar examined in thermal models for post-shock cooling of Dho 378 indicate that total loss of ^{40}Ar from the low-temperature phase but only partial loss of trapped ^{40}Ar from the high-T phase are consistent with inferred cooling rates. For the Ar-Ar isochron not to have been reset ~3 Myr ago would seemingly require: 1) the mesostasis was not heated above ~500 °C, in spite of the observation that plagioclase was melted; or 2) K-rich phases heated to melting cooled so rapidly, on the order of seconds, such that ^{40}Ar diffusive loss did not occur; or 3) the Ar-Ar age dates only feldspar and not mesostasis, in spite of high (~1) K/Ca ratios observed.

Acknowledgements: We thank H. Takeda for supplying the Dho 378 sample, C.-Y. Shih for separating the plagioclase analyzed, D. Garrison for lab support, and T. Mikouchi, G. McKay, L. Nyquist, and F. Hörz for helpful discussions.

References: [1] Russell S. S. et al. 2002. *Meteoritics & Planetary Science* 37:A157–A184. [2] Ikeda et al. Forthcoming. *Antarctic Meteorite Research*. [3] Mikouchi T. and McKay G. 2003. Abstract #1920. 36th Lunar and Planetary Science Conference. [4] Nyquist et al. 2006. Abstract. *Antarctic Meteorites* 30.

5184

MONOMICT IMPACT BRECCIA FROM DHALA STRUCTURE, ARCHEAN BUNDELKHAND CRATON, CENTRAL INDIA: MACRO- AND MESOSCOPIC IMPACT-INDUCED DEFORMATION

J. K. Pati¹, M. Nadeem¹, R. Kundu¹, R. Bhusan¹, and W. U. Reimold².
¹Department of Earth and Planetary Sciences, Nehru Science Centre, University of Allahabad, Allahabad-211 002, India. E-mail: jkpati@yahoo.co.in. ²Museum of Natural History (Mineralogy), Humboldt University in Berlin, Invalidenstrasse 43, D-10115 Berlin, Germany. E-mail: uwe.reimold@museum.hu-berlin.de

Introduction: The Dhala impact structure centered at 25°17'59.7"/78°8'3.1", with an estimated diameter of ~15 km, is located in the westernmost part of the Bundelkhand craton, Shivpuri District, Madhya Pradesh State, India [1]. The presence of unequivocal and diagnostic shock metamorphic features, extensive macro-deformation, and a large impact melt breccia dyke has already been reported [2]. The Dhala structure has a well-defined central uplift surrounded by largely eroded multiple breccia rings. The breccia rings are separated by crater-fill sediments and suevite deposits. Monomict impact breccia outcrops occur as elliptical bodies with maximum elevation of 360 m. The present study reports the data from the field study of monomict granitoid breccia outcrops and IRS-1D (PAN+LISS-III) hybrid geocoded analog data.

Results: A total of 98 presently exposed breccia outcrops occur around the central uplift with highly variable characteristics. The clasts are very angular, vary in size, and show varied orientation. The average aspect ratios of clasts from one outcrop to another vary. Brittle structures (like joints and faults) and melt (±breccia) veins of varied length and width are observed. About 657 joint data and 55 fault trends have been collected from the breccia rings of Dhala structure. The faults show sinistral as well as dextral offset. The study of satellite data reveals the presence of a strong regional E-W fabric on both the northern ("Raksa Shear Zone," [3]) and the southern ("Bundelkhand Tectonic Zone," [4]) sides of the crater structure. Radial and concentric fractures are observed in and around the central uplift up to a distance of about 10 km from the center. The central uplift has undergone faulting. The regional E-W trending mylonitic fabric (steeply dipping due N) shows a gentle swerving to the ESE around the Dhala structure. Giant quartz veins with nearly NE-SW trend and relatively lighter appearance in the satellite data are the most conspicuous linear structures with positive relief in the environs of the crater. Mafic intrusives can be identified as linear outcrops with a darker appearance and with a NW-SE trend. Quartz veins as well as mafic dykes show offset and fracturing at the outcrop scale, in the vicinity of the Dhala structure. The brittle structures in areas covered by alluvium are basically identified by abruptly (90°) changing stream trends.

Discussion: The distribution and density of brittle structures observed in breccia outcrops are variable. Apparent melt veins at the mm to cm scale in the monomict breccia are oriented parallel to important fracture directions. Joint analysis shows a radial pattern with slight complication due to preexisting fabric elements (giant quartz veins, mafic dykes, and the "Bundelkhand Tectonic Zone"). The presence of brittle structures in giant quartz veins and mafic intrusives and swerving of the mylonitic foliation in diorite suggest that the impact event postdates these respective events.

References: [1] Pati J. K. 2005. *Meteoritics & Planetary Science* 40: A121. [2] Pati J. K. et al. 2006. 1st International Conference on Impact Cratering in the solar system. [3] Senthianappan M. 1981. *Geological Survey of India Special Publication* 3:73–76. [4] Pati J. K. 1999. *Geological Survey of India Record* 131:95–96.

5286

MINERAL ASSEMBLAGE IN TARGET ROCKS OF THE ARAGUAINHA IMPACT CRATER AND SHOCK PRESSURE ESTIMATION

M. Paulo-Rodriguez¹, R. Romano¹, W. U. Reimold², and C. Lana¹.
¹Department of Geology, UFOP, Brazil. E-mail: munyke@gmail.com.
²Museum of Natural History (Mineralogy), Humboldt University, Invalidenstrasse 43, 10115 Berlin, Germany

Introduction: The Araguinha impact structure is a well preserved, 40 km diameter, complex impact crater, situated within the northeastern part of the Parana Basin, straddling the border between Mato Grosso and Goias states, central Brazil. The impact structure has a central uplift of ~6 km diameter. This work presents the results of the petrographic study of 120 thin sections from different sampling areas from the NE to the SW across the structure. The rocks affected by the impact include the Precambrian to Ordovician crystalline basement, exposed at the center of the uplifted core, and Permian to Ordovician sedimentary units (Furnas, Ponta Grossa, and Aquidauana formations), occurring in ring structures around the central uplift [1].

Petrology: The core of the central uplift consists of a quartz-syenite with cm sized subhedral K feldspar phenocrysts, exhibiting planar deformation features (PDFs) in up to three crystallographic orientations per grain, as well as diaplectic K feldspar glass. The other main constituents are plagioclase, quartz, amphibole, biotite, and accessory minerals (carbonate and zircon). Plagioclase is coarse-grained, subhedral, exhibiting polysynthetic twinning, with areas of maskelynite and up to two directions of PDFs. Quartz crystals are fine-grained, anhedral, exhibit undulatory extinction and well-developed, generally decorated PDFs, with up to three directions per grain, as well as planar fractures. Amphibole is medium-grained and subhedral. Biotite is fine-grained and subhedral, and has abundant kink bands, as well as inclusions of zircon that show one or two directions of shock features. Impact melt breccia was sampled at a location close to the center of the structure. It contains subrounded to rounded clasts of medium-grained quartz, coarse-grained K feldspar, and fine-grained muscovite, carbonate, and zircon. The matrix has a fluidal texture with finest-grained quartz and K feldspar microliths, and voids filled by secondary quartz. The texture is indicative of rapid cooling. Sandstone from the Furnas, Ponta Grossa, and Aquidauana formations consists of rounded or subrounded quartz, plagioclase, K feldspar, muscovite, biotite, chlorite, epidote, zircon, and magnetite. The grain sizes range from medium-grained (quartz, plagioclase, and K feldspar) to fine-grained (muscovite, biotite, chlorite) and very fine-grained (epidote, zircon, and magnetite). Sandstones from a radial distance of ~5 km from the core only display undulatory extinction and deformation bands in quartz that are not diagnostic shock deformation.

Conclusions: Intense pressure produced during the impact induced characteristic shock metamorphism in the rocks of the central uplift, but not beyond. Planar deformation features in quartz, K feldspar, and plagioclase, and occurrence of diaplectic glass in K feldspar and plagioclase (maskelynite) indicate that the quartz-syenite of the central uplift experienced shock pressures between 20 and 35 GPa. In the sandstones, however, the absence of characteristic shock effects indicates that the rocks in the outer part of the central uplift through to the outer rim of the structure were affected by pressures of no more than 8 GPa.

References: [1] Lana C. et al. 2006. *Geology* 34:9–12.

5290

Hf-W CHRONOMETRY OF AUBRITES

M. Petitat, T. Kleine, M. Touboul, B. Bourdon, and R. Wieler. Institute of Isotope Geochemistry and Mineral Resources, ETH Zürich, Switzerland. E-mail: mpetitat@student.ethz.ch

Introduction: Aubrites are achondrites that formed under highly reducing conditions. They contain different silicate lithologies that formed during igneous processes on the parent body. They also contain small amounts of metal. The depletion of siderophile elements in aubrites indicates segregation of metal in the parent body [1]. The time scales of metal formation and igneous differentiation in the aubrite parent body can be most effectively studied using ^{182}Hf - ^{182}W chronometry. Here we present the first Hf-W data for aubrites.

Results: Hf-W data were obtained for metals from Norton County and two silicate-rich fractions from Norton County and Peña Blanca Spring. Analytical methods are similar to those described in [2]. The W concentrations in the two silicate-rich fractions are only a few ppb, reflecting the strong depletion of siderophile elements in aubrites. Metal from Norton County contains ~400 ppb W and has a radiogenic W isotope composition of $\sim 5.5 \epsilon_{\text{W}}$ (where ϵ_{W} is the deviation of $^{182}\text{W}/^{184}\text{W}$ from the terrestrial standard value in parts per 10,000). The silicate-rich fractions, despite having elevated Hf/W, exhibit W isotope compositions similar to that of the Norton County metal. Owing to the low W content in these silicate-rich fractions, however, their W isotope data have high uncertainties, such that with more precise analyses ϵ_{W} differences between different fractions might eventually become resolvable.

Discussion: The radiogenic W isotope composition of Norton County indicates a high Hf/W in the mantle of the aubrite parent body, consistent with Hf-W fractionation due to metal segregation (i.e., core formation). Additional Hf-W fractionation might have occurred during silicate melting in the mantle. The radiogenic W isotope composition of the Norton County metal requires a late mobilization of radiogenic W from silicates into the metal. Calculating an age for metal formation requires knowledge of Hf/W in the reservoir from which the metal formed. Although this is currently not known, the similarity in W isotope composition of the Norton County metal and silicate-rich fractions suggest that the last W isotope equilibration between metal and silicates occurred late (after a few half-lives of ^{182}Hf). This is consistent with equilibrated Cr isotopes in Norton County [3] and with relatively young Mn-Cr and I-Xe ages for the aubrite Bishopville [4, 5]. Determining precise Hf-W ages for aubrites needs to take into account potential cosmogenic ^{182}W -production by neutron-capture of ^{181}Ta during prolonged exposure to cosmic rays. These effects are restricted to silicates and do not affect the W isotope composition of the Ta-free metals, indicating that the elevated ϵ_{W} of the Norton County metal can be interpreted to chronological significance. The similarity of W isotope compositions of metals and silicates in Norton County suggests that cosmogenic ^{182}W additions in the silicates were small and did not exceed ~ 3 – 4ϵ units.

References: [1] Lodders K. et al. 1993. *Meteoritics* 28:538–551. [2] Kleine T. et al. 2004. *Geochimica et Cosmochimica Acta* 13:2935–2946. [3] Hsu W. et al. 1997. Abstract. 28th Lunar and Planetary Science Conference. pp. 609–610. [4] Shukolyukov A. and Lugmair G. W. *Geochimica et Cosmochimica Acta* 68:2875–2888. [5] Podosek F. A. 1970. *Geochimica et Cosmochimica Acta* 34:341–365.

5071

LIGHTSCATTERING STUDIES OF COMETS AND METEORITES WITH T-MATRIX METHOD

D. Petrov and Yu. Shkuratov. Astronomical Institute of Kharkov National University, 35 Sumskaya Street, Kharkov, 61022, Ukraine. E-mail: petrov@astron.kharkov.ua

Introduction: Cometary dust exhibits negative branches of polarization of light scattered at small phase angles [1]. This feature gives an opportunity to estimate physical parameters of the dust. To make such estimates, one needs to use a light scatter theory for small particles with irregular shapes. There are several methods of light scatter calculations for such particles. One of them is the T-matrix method [2]. Recently, we modified the T-matrix method, which allows us to calculate photometric and polarimetric properties of irregularly shaped particles comparable with the light wavelengths very rapidly [3]. This T-matrix modification is now the most prospective for any light scatter calculations, in particular for light scatter studies of celestial bodies, including comets.

Model: The particle shape is presented by an angular dependence of the distance from the particle center to its surface $r(\theta, \varphi)$. As a model of cometary particles we used particles of random Gaussian shapes [4]. The cometary particles are suggested to be silicate with the refractive index $m = 1.6 + 0.005i$.

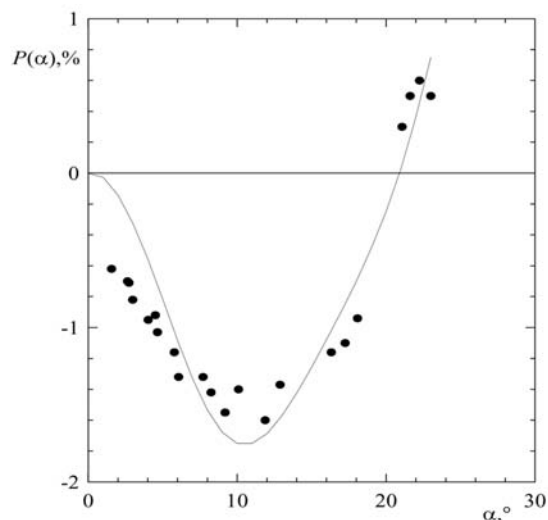


Fig. 1.

Results and Discussion: The dark points in Fig. 1 present the measured negative polarization branch of light scattered by comet Halley [1]. The solid line in Fig. 1 presents results of our simulation for the cometary particles calculated with the modified T-matrix method. Model particles were averaged over both orientation and size parameter in a range of $X = 0.5 \dots 6.5$ with the power law of probability density $\rho = Ar^{-2.4}$, where $A = 0.546$ is the normalizing factor. As one can see, our calculations reproduce both the depth and inversion angle of the branch and qualitatively describe its shape. The difference at small phase angles could be explained with the influence of another mechanisms of negative polarization, e.g., with the coherent backscatter effect that may contribute to polarization at these phase angles [5].

References: [1] Kiselev N. N. and Chernova G. P. 1981. *Icarus* 48:473–481. [2] Mishchenko M. et al. 1996. *Journal of Quantitative Spectroscopy & Radiative Transfer* 55:535–75. [3] Petrov D. et al. *Journal of Quantitative Spectroscopy & Radiative Transfer*. Forthcoming. [4] Petrov D. et al. 2005. Abstract #M42_56. 42nd International Microsymposium on Comparative Planetology. [5] Shkuratov Yu. et al. 1994. *Earth, Moon, and Planets* 65:201–246.

5349

SEARCH FOR ^{58}Fe ANOMALIES IN ORGUEIL AND ALLENDE METEORITES

Franck Poitrasson and Rémi Freydisier. LMTG-CNRS, 14, av. E. Belin, 31400 Toulouse, France. E-mail: Franck.Poitrasson@lmtg.obs-mip.fr

Introduction: Iron is the second most abundant element in terrestrial planets after oxygen. Hence, any nucleosynthetic effect revealed by its isotopic composition will likely apply to a large fraction of the matter involved in planet formation. However, with the exception of the early finding of mass-independent ^{58}Fe variations in three refractory inclusions from the Allende meteorite [1], subsequent searches could not confirm this result [2, 3]. The three other stable isotopes of iron, ^{54}Fe , ^{56}Fe , and ^{57}Fe , were found to show only mass-dependent isotopic variations [4–6]. Presolar grains might be an exception to this rule [7], although this finding was subsequently challenged [8]. To evaluate whether anomalous abundances of the neutron-rich ^{58}Fe isotope actually occur in early solar system material, we developed a new analytical approach based on high-resolution MC-ICP-MS.

Material and Methods: A step-leaching procedure, derived from [9, 10], was employed to extract selectively Fe from different mineral fractions of the Orgueil chondrite (from MHN, Toulouse). Chondrules and refractory inclusions were handpicked from a crushed chip of Allende (from USNM, Washington). We developed a high mass resolution MC-ICP-MS protocol involving desolvating nebulization after enhanced Fe purification to measure $\delta^{57}\text{Fe}$ and $\delta^{58}\text{Fe}$ with a similar level of precision per amu. The reproducibility estimated so far on $\delta^{58}\text{Fe}$ is $<0.3\%$ (2SD).

Results: Leaching solutions from Orgueil show large mass-dependent variations (range: 1.6‰) in $\delta^{58}\text{Fe}$, depending on the nature of the phase being dissolved relating to the temperature, length, and acid strength of a given leaching step. In contrast, no mass-independent ^{58}Fe enrichment or depletion could be detected within $\pm 0.1\%$. Similarly, Allende components show several permil mass-dependent Fe-isotope variations, as previously observed [4, 6], but again, no ^{58}Fe anomalies have been found yet.

Conclusions: We have been so far unable to reproduce the mass-independent ^{58}Fe variations found by [1] in the Allende meteorite. This conclusion was previously reached on different material [2, 3], though it is based here on high mass resolution MC-ICP-MS analysis. Additional measurements are needed on inclusions of Allende and other meteorites to strengthen this conclusion. If confirmed, this would restrict the inference of an initial mass-independent isotopic heterogeneity of elements, excluding oxygen, to a limited fraction of the matter making up terrestrial planets.

References: [1] Völkering J. and Papanastassiou D. A. 1989. *The Astrophysical Journal* 347:L43–L46. [2] Khem K. et al. 2003. *Geochimica et Cosmochimica Acta* 67:2879–2891. [3] Dauphas N. et al. 2004. *Analytical Chemistry* 76:5855–5863. [4] Zhu X. K. et al. 2001. *Nature* 412:311–313. [5] Poitrasson F. et al. 2005. *Earth and Planetary Science Letters* 234:151–164. [6] Mullane E. et al. 2005. *Earth and Planetary Science Letters* 239:203–218. [7] Davis A. M. et al. 2002. 33rd Lunar and Planetary Science Conference. [8] Marhas K. K. et al. 2004. 35th Lunar and Planetary Science Conference. [9] Rotaru M. et al. 1992. *Nature* 358:465–470. [10] Podosek F. A. et al. 1997. *Meteoritics & Planetary Science* 32:617–627.

5040

PARTIALLY EQUILIBRATED NITROGEN IN THE HAMMADAH AL HAMRA 237 METEORITE

K. V. Ponganis and K. Marti. Department of Biochemistry and Chemistry, University of California–San Diego, La Jolla, California 92093–0317, USA. E-mail: kmarti@ucsd.edu

The Hammadah al Hamra 237 (HaH 237) meteorite contains about 60–70 vol% Fe,Ni-metal [1, 2]. Metal occurs exclusively outside chondrules and often is enclosing silicate inclusions.

A sample of HaH 237 has been studied by stepped combustion [3]. Since the separation of a clean metal phase is very difficult because of the intergrown texture of this meteorite, it is useful to compare data obtained by stepwise pyrolysis with those obtained by combustion.

The metal phase is often combusted before silicates release the bulk of the gases. We added two combustion steps at 750 °C and 850 °C after the 1000 °C pyrolysis step. The results obtained by the two complementary techniques are shown in Fig. 1.

The nitrogen signatures in the low-temperature release of both techniques are similar and increase to a maximum close to $\delta^{15}\text{N} = +200\%$, which indicates that combustion of the metal phase apparently does not significantly affect the overall signature. Similarly, the later pyrolysis release steps are uniform, suggesting isotopic equilibration. However, the later combustion steps reveal the presence of a lighter nitrogen component, which is duplicated in the added combustion steps of the pyrolysis experiment, indicating the existence of a phase that was only partially equilibrated.

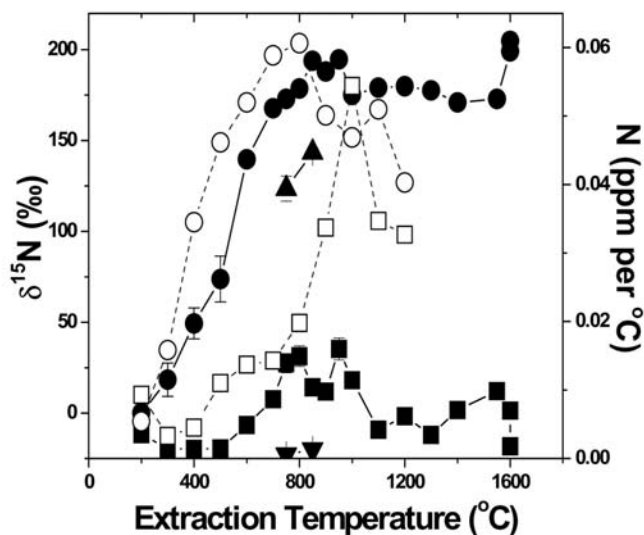


Fig. 1. A comparison of nitrogen signatures in HaH 237 obtained by combustion and by pyrolysis. Solid symbols are from this study, open symbols from Sugiura et al. [3]. All circles are $\delta^{15}\text{N}$. All squares are normalized N concentrations (ppm per °C). The right side up black triangle is $\delta^{15}\text{N}$ from combustion, this study. The upside down black triangle is normalized N from combustion, this study.

References: [1] Zipfel J., Wlotzka F., and Spettel B. 1998. Abstract #1417. 29th Lunar and Planetary Science Conference. [2] Krot A. N., Meibom A., Weisberg M. K., and Keil K. 2002. *Meteoritics & Planetary Science* 37:1451–1490. [3] Sugiura N., Zashu S., Weisberg M., and Prinz M. 2000. *Meteoritics & Planetary Science* 35:987–996.

5092

IMPACT CRATERS: EJECTION OF LARGE ROCK BLOCKS AS MEASURED FROM MARTIAN IMPACT CRATER CLUSTERSOlga Popova¹, William K. Hartmann², and Ivan Nemtchinov¹. ¹Institute for Dynamics of Geospheres, Moscow, Russia. ²Planetary Science Institute, Tucson, Arizona, USA

For some years, we have been studying clusters of craters on Mars. We identified one category of isolated “small clusters” (10 m-scale craters spread over a few hundred meters) that match our predicted parameters for primary stone meteoroids fragmenting in the present Martian atmosphere [1]. We also found scattered “large clusters” (700 m-scale craters spread over 5–10 km), which we concluded must be created by breakup of very large secondary blocks (500 m-scale) ejected from large (≥ 10 s km) primary craters [2]. We visualize weak (perhaps prefractured) blocks breaking up during launch, with fragments spreading at few m/s during the ½ hour flight out of atmosphere, through space, and back through the atmosphere. The size-frequency distribution (SFD) of the fragments (and craters in the cluster) has an unusual bell shape, rather than the “traditional” power law. Ivanov (private communication) has suggested this SFD may fit a Weibel distribution, characteristic of one-time breakup events. Recent work by W. K. Hartmann has found a similar SFD in discrete clusters with rays from crater Gratterri, albeit at a smaller scale (80 m-scale craters spread over 1 km). This confirms for the first time an observational link (in SFD) between the scattered “large clusters” and clusters known to come impact crater secondary ejecta. Large impacts may launch larger semi-coherent blocks than have been commonly modeled.

References: [1] Popova O. et al. 2003. *Meteoritics & Planetary Science* 38:905–925. [2] Popova O. et al. *Icarus*. Forthcoming.

5302

NEW I-Xe DATA FOR CHONDRULES FROM THE L4 BJURBÖLE METEORITE

O. V. Pravdivtseva, A. P. Meshik, and C. M. Hohenberg. McDonnell Center for the Space Sciences and Physics Department, Washington University, CB 1105, Saint Louis, Missouri 63130, USA. E-mail: olga@wuphys.wustl.edu

I-Xe studies of chondrules sometimes provide more questions than answers. Iodine host phase is difficult to identify when chondrules are small and separation of pure mineral phases is not possible. In these cases the interpretation of I-Xe ages is difficult, since chondrules potentially contain multiple iodine-carrier phases. Nevertheless, age information from different mineral components in chondrules or other complex samples [1] can be successfully resolved if, during stepwise heating, radiogenic xenon from different components is released at different temperatures. Thus, among 43 LL chondrules studied so far, 10 have yielded two well-resolved distinct isochrones, with higher temperature releases corresponding to older apparent I-Xe ages. Lower temperature I-Xe ages generally reflect postformational alteration. Not only do LL chondrules tend to be younger with increasing metamorphic grade, but the spread between high- and low-temperature ages increases also, suggesting longer or multiple alteration events for higher metamorphic grade meteorites [2].

A similar trend is observed for H4 NWA 267 [3] and H5 Richardton. Our recent study of 3 Elenovka L5 chondrules demonstrates the presence of two distinct iodine carrier phases in one of the samples, with an age difference between the high- and low-temperature phases of 27 ± 10 Ma. I-Xe studies of 2 Saratov L4 chondrules yield ages that differ by 12 Ma [4].

Earlier studies of L4 Bjurböle chondrules [5] provided 13 high precision I-Xe ages without indication of multiple iodine host phases. With the refined absolute normalization of the internal standard Shallowater [6], absolute ages of the Bjurböle chondrules cluster at 4564.8–4563.3 Ma, 2.4 Ma after formation of CAIs, the estimated time of the chondrule formation [7].

A new I-Xe study of six other Bjurböle chondrules is under way to explore the possible presence of low-temperature iodine carrier phases. The lower temperature isochrons may have been overlooked since earlier stepwise heating extractions have been done with 200 °C incremental temperature steps. The first chondrule yielded relative I-Xe age of 0.0 ± 0.7 Ma. Low temperature peaks on the release profiles of radiogenic ¹²⁹Xe and ¹²⁸Xe correspond to the experimental points that form a correlation line of the same slope that the major apparent isochron, but require a different subplanetary trapped Xe component [8].

Acknowledgements: Supported by NASA grant NAG5-12776. We thank University of Missouri Reactor staff for the irradiation of samples.

References: [1] Pravdivtseva O. V. et al. 2003. Abstract. *Meteoritics & Planetary Science* 38:A140. [2] Pravdivtseva O. V. et al. 2005. Abstract #2534. 36th Lunar and Planetary Science Conference. [3] Pravdivtseva O. V. et al. 2005. *Meteoritics & Planetary Science* 40:A124. [4] Pravdivtseva O. V. et al. 2006. Abstract #2418. 36th Lunar and Planetary Science Conference. [5] Caffee M. W. et al. 1982. 13th Lunar and Planetary Science Conference. pp. A303–A317. [6] Gilmour J. D. et al. 2006. *Meteoritics & Planetary Science* 41:19–31. [7] Amelin Yu. et al. 2002. *Science* 297:1678–1683. [8] Hohenberg C. M. et al. 2004. *Geochimica et Cosmochimica Acta* 68:4745–4763.

5044

MICROBIAL STRUCTURES IN HYDROTHERMAL DEPOSITS AS BIOMARKERS FOR MARS

L. J. Preston, M. J. Genge, and R. Ghail. Impact and Astromaterials Research Centre (IARC), Imperial College London and The Natural History Museum, Exhibition Road, London SW7 2AZ, UK. E-mail: louisa.preston@imperial.ac.uk

Introduction: Hydrothermal systems may potentially provide microbial habitats on Mars. We have investigated silica sinters with green microbial layers, from Waitotapu, New Zealand, in order to characterize the nature of microbial structures that could be used as potential biomarkers. This study will be extended to examine microbial activity in basaltic hydrothermal deposits.

Samples and Methods: The sample was obtained from an extinct sinter deposit 1 m from an acidic (pH 2.6), hot (40–41 °C) stream that flows into a crater lake [1]. The textures and mineralogy of the samples were determined using backscattered electron and secondary electron imaging with chemical analyses by energy dispersive spectroscopy.

Results: The host sinter is primarily a fine-grained porous aggregate of aluminous oxyhydroxides and amorphous silica composed of compositionally distinct parallel fibers >10 nm across. Pores include submicron interfiber spaces within the fine-grained matrix to larger (>100 µm) irregular voids resulting in a variable porosity.

A variety of irregular clasts (<21 µm–1.5 mm in size) are present within the host sinter and comprise ~50 vol% of the samples. Lithic and crystal clasts are the most abundant and are dominated by irregular silica grains showing zoning, with subordinate clasts of partially altered potassic feldspathic glass. Clasts of feldspathic glass are banded and exhibit preferential dissolution of certain bands and deposition of amorphous silica. Rare zircon grains are also present.

Pore spaces and cracks consisting of highly porous (>70 vol%) botryoidal threadworks of amorphous silica are also observed. Threadworks consist of subparallel, interlinked sheets of amorphous silica (<2.6 µm thick). Botryoidal overgrowths of amorphous silica occur often only on one side of the silica sheets but sometimes between them suggesting this was a fluid pathway. Areas of threadwork having no clear truncated margins, that may have formed in situ, are observed in the fine-grained matrix. In a few areas, sinuous layers of titanium oxide (<2 µm in width) were observed coating the silica sheets.

The green layer within the sinter differs primarily from the surrounding matrix in its high concentration of spherical meshwork structures, possibly indentations of spinose plant spores [2]. Highly eroded silica filaments may represent preserved microorganisms.

Discussion: Threadwork structures observed in the sinters are most abundant within and in proximity to the inferred microbial layer and may have formed by microbial deposition; however, an inorganic origin through the dissolution of silica is also possible. The presence of titanium oxide layers within the silica threadworks, however, is significant since HFSE are highly insoluble. Mobilization of Ti^{3+} by microbial action may, therefore, have occurred and provide an easily identifiable biomarker.

References: [1] Jones B., Renault R. W., and Rosen M. R. 2000. *PALAIOS* 15:450–475. [2] Herdianita N. R., Browne P. R. L., Rodgers K. A., and Campbell K. A. 2000. *Mineralium Deposita* 35:48–62.

5267

HIGH-PRECISION W ISOTOPE MEASUREMENTS OF IRON METEORITES

L. Qin^{1, 2, 4}, N. Dauphas^{1, 2, 3, 4}, M. Wadhwa^{2, 4}, P. E. Janney⁴. ¹Origins Laboratory, The University of Chicago, Chicago, Illinois 60637, USA. ²Department of the Geophysical Sciences, The University of Chicago, Chicago, Illinois 60637, USA. ³Enrico Fermi Institute, The University of Chicago, Chicago, Illinois 60637, USA. E-mail: qinlp@uchicago.edu. ⁴Department of Geology, The Field Museum, Chicago, Illinois 60605, USA

The ^{182}Hf - ^{182}W system ($t_{1/2} \sim 8.9$ Myr) is very useful for dating metal-silicate differentiation in the parent bodies of iron meteorites relative to the beginning of the solar system (with initial $\epsilon^{182}\text{W}$ of -3.47 ± 0.20 defined by a CAI isochron [1]). Accurate age determinations may help us better constrain accretion and differentiation time scales, planetesimal sizes, and possible heat sources. Cosmogenic effects have been documented for W isotopes, which may limit the usefulness of this chronometer for dating early solar system processes [2–4]. Indeed, the variations measured in $\epsilon^{182}\text{W}$ cannot be totally ascribed to the decay of ^{182}Hf . A major challenge is to find a proper way to correct for these effects. In preliminary work, we reported resolvable deficits in $\epsilon^{184}\text{W}$ for two iron meteorites with high exposure ages (Tlacotepec, IVB and Deep Springs, ungrouped) [5, 6]. We report here new high-precision W measurements of a larger set of iron meteorites from groups IAB, IIAB, IIIA, IVAB, and IID.

$\epsilon^{182}\text{W}$: All the magmatic iron meteorites with low exposure ages show a narrow range of $\epsilon^{182}\text{W}$, from -3.35 ± 0.06 to -3.58 ± 0.05 , indicating that metal-silicate segregation was contemporaneous or slightly postdated the formation of CAIs (within ~2 Myr). The nonmagmatic iron meteorite BoHumilitz (IA) has more radiogenic $\epsilon^{182}\text{W}$ of -3.02 ± 0.09 . Except for Skookum (IVB), iron meteorites with long exposure ages all show deficits in $\epsilon^{182}\text{W}$ (-3.77 ± 0.04 to -4.25 ± 0.05) relative to the inferred initial solar system value. This most likely resulted from exposure to cosmic radiation, a conclusion that agrees with recent studies [4, 7–8].

$\epsilon^{184}\text{W}$: Except for IVB iron meteorites and Deep Springs, all other samples have values undistinguishable from the NIST standard. All IVBs, with both low and high exposure ages, show similar depletions ($\sim -0.1 \epsilon$) in $\epsilon^{184}\text{W}$. This cannot be explained by cosmic irradiation because one would expect to see a correlation with $\epsilon^{182}\text{W}$. It may instead be the imprint of nucleosynthetic effects as has been observed for Mo and Ru isotopes [9–11]. At this stage, no correction of cosmogenic effects on $\epsilon^{182}\text{W}$ can be made based on $\epsilon^{184}\text{W}$ measurements.

References: [1] Kleine T. et al. 2005. Abstract #1431. 36th Lunar and Planetary Science Conference. [2] Leya I. et al. 2003. *Geochimica et Cosmochimica Acta* 67:529–541. [3] Masarik J. 1997. *Earth and Planetary Science Letters* 152:181–185. [4] Markowski A. et al. 2006. *Earth and Planetary Science Letters* 242:1–15. [5] Qin L. et al. 2005. *Meteoritics & Planetary Science* 40:A124. [6] Qin L. et al. 2006. Abstract #1771. 37th Lunar and Planetary Science Conference. [7] Lee D.-C. 2005. *Earth and Planetary Science Letters* 237:21–32. [8] Schersten A. et al. 2005. *Earth and Planetary Science Letters* 241:530–542. [9] Chen J. H. et al. 2003. Abstract #1789. 34th Lunar and Planetary Science Conference. [10] Chen J. H. et al. 2004. Abstract #1431. 35th Lunar and Planetary Science Conference. [11] Dauphas N. et al. 2004. *Earth and Planetary Science Letters* 226:465–475.

5305

METAMORPHIC HISTORY OF PRISTINE CHONDRITES AS REVEALED BY ORGANIC MATTER: A NEW PETROLOGIC CLASSIFICATION

E. Quirico¹, L. Bonal¹, M. Bourot-Denise², and G. Montagnac³. ¹Laboratoire de Planétologie de Grenoble Université Joseph Fourier Grenoble Cedex 9, France. E-mail: eric.quirico@obs.ujf-grenoble.fr. ²Muséum National d'Histoire Naturelle, Paris, France. ³Laboratoire de Sciences de la Terre ENS-Lyon, France

Recently a new approach to determine the degree of metamorphism of pristine chondrites has been successfully applied to series of unequilibrated ordinary chondrites (OCs), carbonaceous CV, and CO chondrites [1–3]. Its principle is that the structure of organic matter (OM) trapped in the matrix is irreversibly transformed by thermal metamorphism, and thus reflects the metamorphic grade. This transformation is independent of the mineralogical context and aqueous alteration. Thus it does not suffer from artifacts and is valid regardless of the chondrite chemical class. OM maturity is provided through Raman spectroscopy [4]. Here we present a synthesis of extended measurements collected on ~40 chondrites, and we discuss further the interpretation of OM maturity in terms of thermal history as well as several implications.

We suggest that OM maturity, as derived from Raman spectroscopy, reflects the temperature of the metamorphism peak (TMP). For the most metamorphosed chondrites (PT > 3.7), a geothermometer calibrated using terrestrial rocks may even be used [5]. A TMP of 330 ± 30 °C is estimated for Allende (CV3), consistently with earlier independent mineralogical indicators (e.g. [6]). The petrologic types derived from this approach thus exhibit an unambiguous signification and allow comparison of objects belonging to different chemical classes. Another advance is the high sensitivity of this approach to weak metamorphism grades. In particular, the results show that Semarkona (LL3.0) cannot be further considered as the metamorphism onset as it experienced some metamorphism. Unfortunately, Raman spectroscopy is not sensitive to very weak metamorphic grade, and the actual metamorphism onset has not been determined. Some Antarctic chondrites were found to exhibit some metamorphism grade ranging between Semarkona and type 3.1 as Bishunpur and Krymka, but no objects were found ranging between type 1/2 (CM/CI/CR) and Semarkona. For this reason, we propose to establish a new petrologic scale using the FWHM-D Raman parameter normalized to Semarkona. In such a framework, Semarkona's PT is 1, all objects investigated in our study do have a PT > 1, and the actual metamorphism onset is equal to 0 (but practically speaking it is not accurately located). For the most metamorphosed objects, a temperature of metamorphism peak is provided along with PT. Furthermore, aqueous alteration should be considered as an independent geological process, characterized by another scale, as objects may have experienced high degrees of both metamorphism and aqueous alteration [2].

We would recommend this approach for classifying objects in collections. The technique is fast, easy to implement, can be performed on raw rocks, and Raman microprobes are a widespread analytical tool.

References: [1] Quirico E. et al. 2003. *Meteoritics & Planetary Science* 38:795. [2] Bonal et al. 2006. *Geochimica et Cosmochimica Acta* 70:1849–1863. [3] Bonal et al. 2005. Abstract #1699. 36th Lunar and Planetary Science Conference. Also Forthcoming. *Geochimica et Cosmochimica Acta*. [4] Quirico et al. 2005. *Spectrochimica Acta A* 61:2368–2377. [5] Beyssac et al. 2002. *Journal of Metamorphic Geology* 20:859–871. [6] Weinbruch et al. 1994 *Geochimica et Cosmochimica Acta* 58:1019–1030.

5236

NICKEL ISOTOPES IN ANGRITES: CHRONOLOGICAL INTERPRETATION VERSUS NUCLEOSYNTHETIC ANOMALIES?

G. Quitté¹, M. Bizzarro², A. Markowski¹, and C. Latkoczy³. ¹IGMR, ETH Zürich, Switzerland. E-mail: quitte@erdw.ethz.ch. ²Geological Institute, University of Copenhagen, Denmark. ³Laboratory for Inorganic Chemistry, ETH Zürich, Switzerland

Introduction: Angrites are rapidly cooled differentiated meteorites that formed very early in the solar system history [1, 2]. Angrites are thus critical samples when trying to intercalibrate different chronometers. Al-Mg and Pb-Pb ages for Sahara 99555 have been recently determined, and the measurements of W [3, 4] and Ni isotopes are currently underway to broaden the number of chronometers used on this meteorite. Sahara 99555 is of particular interest because of its pristine nature, which may suggest that the Fe-Ni system remained undisturbed, even if Ni is very sensitive to metamorphism. ⁶⁰Fe decays to ⁶⁰Ni with a short half-life of 1.49 Myr, and this chronometer can thus be used to precisely date planetary accretion and evolution. Moreover, Ni isotopes can provide strong constraints on the nucleosynthetic events that occurred shortly before the start of the solar system. All Ni isotopes are indeed produced by a statistical equilibrium process (e-process), but ⁶²Ni and ⁶⁴Ni are preferentially produced in a neutron rich environment (e- or r-process), whereas an excess of ⁶¹Ni reflects a major contribution from an s-process.

Analytical Procedure: Mineral separates and whole rock samples for Sahara 99555 have been analyzed in two different laboratories and results have been compared and combined. In both cases, Ni has been separated from the matrix elements using ion exchange procedures. At ETH Zürich, an additional liquid-liquid extraction has been performed. The Ni isotopic composition has been determined using a MC-ICPMS (Axiom in Copenhagen and the new large geometry and high resolution Nu1700 in Zürich).

Results and Discussion: Whole rock samples and mineral separates display a range of Fe/Ni ratios varying from ~1500 to ~11,000. When normalizing the isotope data to the ⁶²Ni/⁵⁸Ni ratio, only one pyroxene fraction with elevated Fe/Ni ratio shows a resolvable ⁶⁰Ni-excess of 87 ± 30 ppm, although a broad correlation between ⁶⁰Ni/⁵⁸Ni and the Fe/Ni ratio is observed when combining all fractions. The slope of this regression corresponds to a ⁶⁰Fe/⁵⁶Fe of $\sim 2 \times 10^{-9}$. If we interpret this line as an isochron, Sahara 99555 seems to have formed >10 Myr after CAIs, which is inconsistent with results obtained from absolute and other short-lived chronometers. Furthermore, the intercept of this regression is identical to the terrestrial standard, which is inconsistent with late reequilibration of the Fe-Ni systematics. When normalizing the isotope data to the ⁶¹Ni/⁵⁸Ni ratio, we note the presence of ⁶²Ni-deficits ranging from 30 to 100 ppm in some of the samples, and no resolvable excesses in ⁶⁰Ni. This discrepancy may be attributed to the presence of variable nucleosynthetic effects on the normalizing isotopes (⁶¹Ni and ⁶²Ni) and/or large uncertainties associated with the measurements of the ⁶¹Ni/⁵⁸Ni ratio. It is not clear from these preliminary results whether or not resolvable ⁶⁰Ni, ⁶¹Ni, or ⁶²Ni anomalies are present in these fractions. More replicate measurements and analysis of other fractions are underway.

References: [1] Bizzarro M. et al. 2005. *The Astrophysical Journal* 632:L41–L44. [2] Baker J. et al. 2005. *Nature* 436:1127–1131. [3] Markowski A. et al. 2006. Abstract #2000. 37th Lunar and Planetary Science Conference. [4] Markowski et al. 2006. Abstract #5195. *Meteoritics & Planetary Science* 41. This issue.

5229

CORRELATED EXCESSES OF ^{60}Ni AND ^{62}Ni IN REFRACTORY INCLUSIONS

G. Quitté¹, A. N. Halliday², B. Meyer³, A. Markowski¹, C. Latkoczy⁴, and D. Günther⁴. ¹IGMR, ETH Zürich, Switzerland. E-mail: quitte@erdw.ethz.ch. ²Department of Earth Sciences, Oxford University, UK. ³Department of Physics and Astronomy, Clemson, USA. ⁴Laboratory for Inorganic Chemistry, ETH Zürich, Switzerland

Introduction: Calcium-aluminium-rich inclusions (CAIs)—considered to be the first objects that formed in the solar system—commonly show nucleosynthetic heterogeneities. The origin of these anomalies may be linked to the production of the short-lived nuclides that were also present in the early solar system. Short-lived nuclides can be generated by irradiation and spallation during an active phase of the young sun or by nucleosynthetic events in stellar environments. The determination of their initial abundances thus enables one to test different models. Iron-60 decays to ^{60}Ni ($t_{1/2} = 1.5$ Myr) and is of particular interest because it cannot be produced locally in the solar system by irradiation.

Technique and Results: We analyzed six CAIs from Allende and one CAI from Efremovka. Nickel has been extracted from the sample with a three-step chemical procedure. Following a first ion exchange, a liquid-liquid extraction was performed. The Ni fraction was further purified on a second ion exchange resin. The Ni isotopic composition has been measured using a high-resolution MC-ICPMS (Nu 1700 instrument) at a mass resolution of 2600. The external reproducibility for a standard is about 0.3ϵ and 0.6ϵ for the $^{60}\text{Ni}/^{58}\text{Ni}$ and $^{61}\text{Ni}/^{58}\text{Ni}$ ratios respectively. Each sample has been measured up to 13 times in different sessions. Most CAIs show an excess of ^{62}Ni when data are normalized relative to $^{61}\text{Ni}/^{58}\text{Ni}$. This excess translates into a deficit of ^{61}Ni when normalizing to $^{62}\text{Ni}/^{58}\text{Ni}$ and is interpreted as a nucleosynthetic anomaly.

Discussion: The CAIs display correlated anomalies of ^{60}Ni and ^{62}Ni coupled with effects on ^{96}Zr . Iron-60 is produced in significant amounts together with ^{62}Ni and ^{96}Zr in a stellar environment, but not ^{60}Ni . Therefore, the ^{60}Ni excess is more likely to result from decay of ^{60}Fe . The effects show the signature of neutron-burst nucleosynthesis in a massive star. Such a neutron burst is plausibly responsible for the abundance of many short-lived radioactivities present in the early solar system.

A two-point internal isochron for an Allende CAI showing no nucleosynthetic anomaly yields a slope of 3.4×10^{-7} corresponding to a lower limit for the initial $^{60}\text{Fe}/^{56}\text{Fe}$ of the solar system. However, based on the mineralogy of this CAI, the Fe-Ni system has probably reequilibrated. An independent estimate can be derived from two bulk CAIs with no nucleosynthetic anomaly and characterized by the same $^{26}\text{Al}/^{27}\text{Al}$ initial ratio. An initial $^{60}\text{Fe}/^{56}\text{Fe}$ higher than 1.8×10^{-6} is inferred if both CAIs formed from the same isotopically homogeneous reservoir. This is higher than previous estimates and consistent with the results of the nucleosynthetic modeling. It would also indicate that ^{60}Fe played a major role as a heat source to melt planetesimals. However, more data are needed to demonstrate that such an inference from two CAIs is correct.

5036

FORMATION INTERVAL OF THE LUNAR MANTLE FROM HIGH-PRECISION Nd-ISOTOPE MEASUREMENTS OF SIX LUNAR BASALTS #5035

K. Rankenburg¹, A. D. Brandon¹, and C. R. Neal². ¹NASA Johnson Space Center, Mailcode KR, 2101 Nasa Road One, Houston, Texas 77058, USA. E-mail: kai.rankenburg1@jsc.nasa.gov. ²Department of Civil Engineering and Geological Sciences, University of Notre Dame, Notre Dame, Indiana 46556, USA. E-mail: neal.1@nd.edu

Introduction: If the Moon has superchondritic $^{142}\text{Nd}/^{144}\text{Nd}$ identical to the Earth, as suggested by available data [1, 2], then the giant impact must have occurred into an already differentiated Earth, predominantly sampling the LREE-depleted reservoir. In order to test this hypothesis, Nd-isotope ratios were obtained on a Thermo-Finnigan Triton TIMS for six lunar basalts that span the compositional range of lavas from the Moon: 15555, LAP 02205: low-Ti; 70017, 74275: high-Ti; 15386, SAU 169: KREEP basalts. The lunar samples have crystallization ages of 3.15–3.9 Ga and preserve a range of present-day $\epsilon^{142}\text{Nd}$ from -0.30 ± 0.07 (2σ) to $+0.07 \pm 0.05$ when corrected for the effects of neutron irradiation.

The evolution of the lunar mantle is modeled assuming formation from material with average chondritic composition with present-day $\epsilon^{143}\text{Nd} = 0$ and $\epsilon^{142}\text{Nd} = -0.2$ [1]. The $\epsilon^{143}\text{Nd}$ and $\epsilon^{142}\text{Nd}$ of the evolving lunar mantle is calculated using a two-stage model [2]. Self-consistent values of $(^{147}\text{Sm}/^{144}\text{Nd})_{t_1}$ and t_1 are calculated for each sample by simultaneously solving the equations for the evolution of ^{142}Nd and ^{143}Nd . The best fit to the data yields a source formation age of all basalt samples of $215 + 23, -21$ Myr (2σ) after solar system formation, and an intercept at the chondritic $^{147}\text{Sm}/^{144}\text{Nd}$ of -0.19 ± 0.02 (MSWD = 0.99), consistent with contemporaneous formation of the source regions represented in this study from a LMO with a present day $\epsilon^{142}\text{Nd} = -0.19$.

A model in which the Moon was formed from material that predominantly sampled the Nd-depleted reservoir of an already differentiated Earth and/or impactor, is not consistent with the data. Because both Earth and Moon likely formed in the same region of the solar nebula, the Earth should also have a chondritic bulk composition. In order to mass balance the Nd budget, these constraints require that a complementary reservoir with lower $^{142}\text{Nd}/^{144}\text{Nd}$ resides in the Earth's mantle.

References: [1] Boyet M. and Carlson R. W. 2005. *Science* 309:576. [2] Nyquist L. E. et al. 1995. *Geochimica et Cosmochimica Acta* 59:2817.

5224

GENTNER—A MINIATURIZED LIBS/RAMAN INSTRUMENT FOR THE COMPREHENSIVE IN SITU ANALYSIS OF THE MARTIAN SURFACE

I. Rauschenbach¹, V. Lazić², E. K. Jessberger¹, and the GENTNER Team.
¹Institut für Planetologie, Westfälische Wilhelms-Universität Münster, Germany. E-mail: irausch@uni-muenster.de. ²ENEA, Frascati (RM), Italy

We introduce a novel instrument to determine in situ rapidly and with relatively high sensitivity (down to 10 ppm) the concentrations of many elements in Martian rock, coarse fine and soil samples with a lateral resolution of <1 mm. At the same time the instrument will provide information on possible organic components as well as mineralogical information. Detection of the life-related elements like H, C, N, O, P, S, and Fe and investigation of their 3-D distributions as well as their occurrences in the various Martian materials may be indicative of biological activity [1].

The proposed instrument is a combination of laser-induced breakdown spectroscopy (LIBS) and Raman spectroscopy. It is named GENTNER honoring the German physicist and cosmochemist Wolfgang Gentner (1906–1980). GENTNER meets the requirements concerning advanced in situ analytical tools, like short measurement duration; high sensitivity; high repetition rate; high reproducibility; low mass, size, and resource needs; and high flexibility with respect to type, shape, and size of sample material. This innovative instrument, the combination of LIBS with Raman, greatly profits from synergetic effects, sharing the optical spectrometer, the lasers, and onboard data reduction facilities [2]. It also gains from recent developments in miniaturization and from front-line laser research.

The basic GENTNER concept consists of one or more small, light-weight sensor heads mounted on an arm and/or near the tip of a drill, and an instrument module (pump lasers, spectrometer, electronics, etc.) installed on a rover. Optical fibers connect the sensor heads and instrument module. An essential feature is the nonprerequisite of sample preparation. GENTNER will perform hundreds of individual chemical, mineralogical, and “organic” analyses of all sample types within reach at all geologic sites visited. Distant geologic units are accessible through the analysis of wind- and impact-transported individual coarse fines (~1 mm) samples. These analyses will not be obstructed by dust coverage since the instrument allows depth profiling for up to 2 mm. At the same time GENTNER shall serve to grossly characterize samples prior to GC-MS and isotopic studies in order to preselect interesting samples for these experiments [3].

However, the variability of the environmental conditions on Mars and the differences of the physical-chemical characteristics of the expected samples, require extensive studies of LIBS and Raman spectroscopy under Martian conditions. To obtain reliable quantitative LIBS results and to optimize the LIBS system performance we studied in a first step the influence a) of sample temperature and b) of physical status—rock or powder.

References: [1] Bertrand R., Del Bianco A., Jessberger E. K., Mann I., Peuser P., Rost D., Schneider K., Stephan T., and Weber I. 2003. Flight Model Instrument Concept, LIRAMIS-TN22-03, issue 1.0, ESTEC Contract No.: 16475/02/NL/HB. [2] Bertrand R., Del Bianco A., Jessberger E. K., Mann I., Peuser P., Rost D., Schneider K., Stephan T., and Weber, I. 2003. LIRAMIS Instrument Definition Document. LIRAMIS-TN4-10c, Issue 1.0. [3] Bertrand R., Del Bianco A., Jessberger E. K., Mann I., Peuser P., Rost D., Schneider K., Stephan T., and Weber, I. 2001. Technical Data Package. ESTEC Contract no. 14866/00/NL/LVH.

5346

UPDATES OF PROTON CROSS-SECTIONS FOR PRODUCING COSMOGENIC RADIONUCLIDES

R. C. Reedy¹ and K. J. Kim². ¹Institute of Meteoritics, University of New Mexico, Albuquerque, New Mexico 87131, USA. E-mail: reedy@unm.edu. ²NSF-Arizona AMS Laboratory, Physics Building, University of Arizona, Tucson, Arizona 85721, USA

Introduction: Good models are needed to interpret concentrations of cosmogenic nuclides measured in samples of solar-system matter. Theoretical calculations are usually used to get production rates to compare with measurements. Important inputs to these theoretical calculations are cross-sections for making the nuclide of interest from its major target elements. Protons make almost all nuclides produced by solar energetic particles and a fraction of the nuclides made by galactic-cosmic-ray (GCR) particles [1]. Most GCR-produced nuclides are made by neutrons, and cross-sections for proton reactions are often used for neutrons or as a basis for estimating neutron cross-sections.

Proton Reactions Making Cosmogenic Radionuclides: Many cross-sections for proton-induced reactions have been measured in the last decade and were included in these evaluations of cross-sections for making cosmogenic nuclides. As the first phase of a project to update the cross-sections used for our theoretical models, we are doing the major radioactive cosmogenic nuclides ¹⁰Be, ²⁶Al, and ³⁶Cl, which are major radionuclides made both by solar protons and GCR particles.

Many cross-sections for making these radionuclides for a range of targets and for energies from threshold to ~1 GeV were published in the late 1990s by R. Michel and co-workers (e.g., [2]) and by J. Sisterson and colleagues (e.g., [3, 4]). We also compiled cross-sections from earlier works and searched several archives for additional measurements.

Evaluation: The compiled cross-sections for these radionuclides were plotted as a function of energy for each major target element. An evaluated set of cross-sections as a function of energy was generated. Often the data from the two major groups were in good agreement. Occasionally, there was some spread in their cross-sections for an energy. If there were no other measurements, a smoothed curve that was roughly an average of the different measurements was adopted.

Summary: Revised cross-sections as a function of energy have been evaluated for the main proton reactions making ¹⁰Be, ²⁶Al, and ³⁶Cl. These cross-sections will be used to reinterpret profiles of these radionuclides measured in the top centimeter or so of lunar rocks, such as 64455 [5]. Proton cross-sections for other nuclides will be compiled and evaluated. These proton cross-sections will also be used as starting points for estimating improved cross-sections for neutron-induced cross-sections.

References: [1] Reedy R. C. and Arnold J. R. 1972. *Journal of Geophysical Research* 77:537–555. [2] Michel R. et al. 1997. *Nuclear Instruments and Methods B* 129:153–193. [3] Sisterson J. M. et al. 1997. *Nuclear Instruments and Methods B* 123:324–329. [4] Sisterson J. M. et al. 1997. *American Institute of Physics Conference Proceedings* 392:811–814. [5] Nishiizumi K. et al. 1995. 26th Lunar and Planetary Science Conference. pp. 1055–1056.

5062

RADIOGENIC AND STABLE THALLIUM ISOTOPE VARIATIONS IN IRON METEORITES

M. Rehkämper¹, S. G. Nielsen², H. M. Williams², M. Schönbacher¹, and A. N. Halliday³. ¹Department of Earth Science and Engineering, Imperial College, London SW7 2AZ, UK. ²Department of Earth and Planetary Sciences, Macquarie University, 2109 NSW, Australia. ³Department of Earth Sciences, University of Oxford, Oxford OX1 3PR, UK

The short-lived radionuclide ²⁰⁵Pb decays to ²⁰⁵Tl with a half-life of 15 Myr. Evidence for the presence of live ²⁰⁵Pb in the early solar system was provided by a recent Tl isotope study [1], which established a ²⁰⁵Pb-²⁰⁵Tl isochron for seven metal fragments from the IAB irons Toluca and Canyon Diablo. Five troilites from the same meteorites do not conform to the isochron relationships exhibited by the metal samples. In particular, four of the sulfides exhibit Tl isotope compositions that are significantly less radiogenic than the coexisting metals. In studies of extinct radionuclides, it has been standard practice to use the least radiogenic isotope ratio measured as the best approximation of the solar system initial. This assumption is questionable for the ²⁰⁵Pb-²⁰⁵Tl decay system, however, because it is difficult to account for the large isotopic contrast between metals and sulfides (up to about 5‰) by radiogenic decay of ²⁰⁵Pb alone.

Mass dependent isotope fractionations provide an alternative explanation for the troilite data and such stable isotope effects have recently been identified in iron meteorites for Fe [2] and Ni [3]. Sulfides from various irons have a mean Fe isotope composition that is isotopically lighter than the metal by $0.5 \pm 0.2\%$ (1sd) for ⁵⁷Fe/⁵⁴Fe, and this offset is most readily explained by equilibrium fractionation. This suggests that the much larger Tl isotope differences between metals and troilites are unlikely reflect equilibrium isotope effects. Rather, they are thought to be due to kinetic fractionations that were generated by diffusion.

This interpretation follows from studies of the extinct ¹⁰⁷Pd-¹⁰⁷Ag chronometer. Such investigations showed that the troilites of IVA irons exhibit large (up to ~20%) excesses of radiogenic ¹⁰⁷Ag. These excesses were thought to be caused by the diffusion of radiogenic Ag from the metal phase (with very high Pd/Ag) to associated sulfide inclusions (with low Pd/Ag), either during slow cooling or secondary heating [4]. Such a scenario is realistic because metal fragments from IVA irons are known to display ¹⁰⁷Ag excesses of up to ~800% and these can dominate the composition of the sulfides. The isotopic systematics are different for Tl because radiogenic ingrowth did not generate such extreme variations in isotope compositions. The unradiogenic Tl isotope ratios of the troilites may thus reflect diffusion of Tl with preferential transport of the lighter ²⁰³Tl isotope, as would be expected for kinetic isotope fractionation.

Using reasonable values for the relative abundances of Tl in sulfides and metal, it can be demonstrated that diffusion can generate troilites depleted in ²⁰⁵Tl without significantly disturbing the isotope composition of coexisting metal. The proposed fractionation model can be tested, but this is difficult because this requires, for example, analyses of Tl diffusion profiles at metal—sulfide grain boundaries or the quantification of kinetic isotope fractionations for troilite—metal pairs using reasonable analog elements.

References: [1] Nielsen S. G. et al. *Geochimica et Cosmochimica Acta*. Forthcoming. [2] Williams H. M. et al. 2004. *Eos* 85:F1251. [3] Quitte G. et al. 2005. Abstract #P41E-02. *Eos* 86. [4] Chen J. H. and Wasserburg G. J. 1990. *Geochimica et Cosmochimica Acta* 54:1729-1743.

5233

MILTON PALLASITE AND THE SOUTH BYRON IRON TRIO: A GROUPELLET FORMED BY OXIDATION AND FRACTIONAL CRYSTALLIZATION

V. S. Reynolds¹, T. J. McCoy¹, and W. F. McDonough². ¹Department of Mineral Sciences, Smithsonian Institution, Washington, D.C. 20560-0119, USA. ²Department of Geology, University of Maryland, College Park, Maryland 20742, USA

Introduction: Among pallasites, only main group pallasites (PMG) show geochemical affinities to a group of irons (IIIAB), suggesting formation on the same parent body [1]. Additional links would greatly expand our understanding of core-mantle relationships. The Milton pallasite is ungrouped due to its high Ni and Ir concentrations, anomalous oxygen isotope signature, and FeO-rich olivine [2]. The metal composition of Milton is similar to the high-Ni irons South Byron, ILD 83500, and Babb's Mill (Troost's Iron), grouped as the South Byron trio [3]. We examined the metallographic structures and siderophile element abundances of these meteorites to determine whether they originated from the same parent asteroid and understand its formation.

Results: As high-Ni irons, the structures of all four are similar and dominated by plessite. South Byron and ILD 83500 contain sub-mm spindles of kamacite, as do larger plessitic areas of Milton. Rare sulfides and chromites are present, as are minute schreibersites that are associated with the kamacite spindles. The heat-treated Babb's Mill (Troost's Iron) lacks kamacite spindles. Milton also exhibits swathing kamacite surrounding silicates and oxides.

CI chondrite-normalized siderophile element patterns for Milton, South Byron and ILD 83500 are remarkably similar. Refractory siderophiles are enriched at ~10–100 × CI. Volatile siderophiles exhibit smaller enrichments at ~1–10 × CI. Milton and South Byron show depletions in elements readily oxidized (W, Mo, Fe, Cr, and P). Finally, as observed by [3], we show differences in platinum group elements (e.g., Re, Os, Ir) are consistent with fractional crystallization.

Discussion: The shared characteristics of Milton and the South Byron trio are consistent with formation on the same parent body, suggestive of a different history for these meteorites from other pallasite and high-Ni irons. In most high Ni irons (e.g., IVA, IVB, Tishomingo), high-T condensation had a significant role, forming a Ni-enriched, volatile-depleted siderophile element pattern [4, 5]. If condensation played a significant role in the formation of Milton-South Byron, these meteorites would be volatile siderophile depleted; however, they are not. While condensation processes may have a role in determining the bulk Ni concentration of this group, the uniform depletions of redox sensitive elements suggests that oxidation was a dominant process. We propose that oxidation controlled core formational processes on the parent body, as evidenced by the presence of Fe-rich silicates, chromite, and phosphate [2]. Evidence for fractional crystallization is apparent in siderophile and PGE abundances, as suggested for the South Byron trio [3]. Unlike the pallasite in the PMG-IIIAB grouping [1], the pallasite in the Milton-South Byron grouplet appears to represent an early crystallizing solid.

References: [1] Mittlefehldt D. W. et al. In *Planetary materials*. Washington, D.C.: Mineralogical Society of America. [2] Jones R. H. et al. 2003. Abstract #1683. 34th Lunar and Planetary Science Conference. [3] Wasson J. T. et al. 1989. *Geochimica et Cosmochimica Acta* 53:735–744. [4] Corrigan C. M. and McCoy T. J. 2005. Abstract #7023. Oxygen in Asteroids and Meteorites. [5] Campbell A. J. and Humayun M. 2005. *Geochimica et Cosmochimica Acta* 69:4733–4744.

5364

MINERALOGY AND PETROLOGY OF THE MARE BASALT-RICH BRECCIA MET 01210

K. Righter¹ and B. Bussey². ¹NASA-JSC, Mailcode KT, 2101 NASA Parkway, Houston, Texas 77058, USA. E-mail: kevin.righter-1@nasa.gov. ²Planetary Exploration Group, Space Department, JHU/APL, 11100 Johns Hopkins Road, MP3-E169, Laurel, Maryland 20723, USA

Introduction: Meteorite Hills (MET) 01210 was announced as a 22.8 g anorthositic breccia based on the examination of one thin section [1]. Subsequent studies [2–6] have revealed the presence of many basaltic lithologies in addition to anorthositic. In some cases, basalt dominates by a 3:1 ratio (e.g., [4]). We have undertaken a petrographic study of MET 01210 and compare our results to other sections, thus giving a more comprehensive view of this interesting piece of the Moon.

Petrography and Mineralogy: The section studied (.34) contains ten large clasts (> 500 μm), including five coarse-grained gabbros, two fine-grained feldspathic, two fine-grained basaltic (Fig. 1), and one symplectitic textured lithic clasts. Also present are numerous finer-grained (< 500 μm) single mineral fragments, including many (5) large silica grains. Clasts make up approximately 15% of the mode, whereas the balance is made of either the finer mineral and lithic fragments and/or glassy matrix. Given this mixture of clast material and similar ratios apparent among the finer materials, this section also is consistent with a “mingled” breccia, as suggested by [6].

Discussion: The diverse clast types indicate an origin from a region that is proximal to both deep units such as the coarse-grained gabbros and the fayalite-hedenbergite symplectites (also consistent with fine, extensive exsolution lamellae, [5]), and shallower units as the finer-grained basaltic and anorthositic clasts. It is most similar in petrography to other mingled breccias such as Asuka-881757/Yamato-793169 (also noted by [3]).

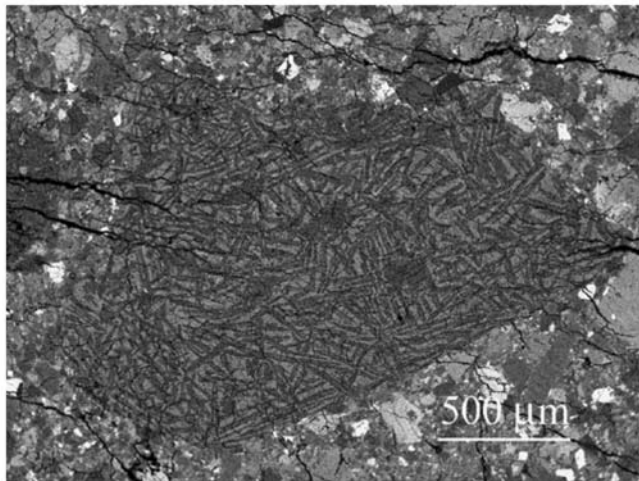


Fig. 1. A melt clast containing laths of nearly pure anorthitic plagioclase (dark) in a glassy matrix of basaltic composition (lighter). Width is 2.0 mm.

References: [1] Satterwhite et al. 2004. *Antarctic Meteorite Newsletter* 27(1). [2] Patchen A. D. et al. 2005. Abstract #1411. 36th Lunar and Planetary Science Conference. [3] Arai T. et al. 2005. Abstract #2361. 36th Lunar and Planetary Science Conference. [4] Zeigler R. A. et al. 2005. Abstract #2385. 36th Lunar and Planetary Science Conference. [5] Huber H. and Warren P. H. 2005. Abstract #3512. 36th Lunar and Planetary Science Conference. [6] Korotev R. L. and Irving A. J. 2005. Abstract #1220. 36th Lunar and Planetary Science Conference.

5363

THE GREAT DIVERSITY OF PLANETARY MATERIALS RETURNED FROM THE QUEEN ALEXANDRA RANGE, ANTARCTICA

K. Righter¹, R. P. Harvey², J. Schutt², C. Satterwhite³, K. M. McBride³, T. J. McCoy⁴, and L. Welzenbach⁴. ¹NASA-JSC, Mailcode KT, 2101 NASA Parkway, Houston, Texas 77058, USA. E-mail: kevin.righter-1@nasa.gov. ²Department of Geology, Case Western Reserve University, Cleveland, Ohio 44106–7216, USA. ³ESCG, Jacobs-Sverdrup, NASA-JSC, Houston, Texas 77058, USA. ⁴Department of Mineral Science, NHB119, Smithsonian Institution, Washington, D.C. 20560, USA

Introduction: The Queen Alexandra Range (QUE) has yielded 3444 meteorites over six ANSMET collecting seasons. This huge number compares with 2186 from the Elephant Moraine, 1870 from Lewis Cliffs, 1600 from Allan Hills, and 1130 from the Meteorite Hills regions. Although it is clear that many of the samples from this region are from a large ordinary chondrite fall, there is a great diversity of interesting samples.

Chondrites: Several chondrites found in the QUE range have contributed to the recognition of new chondrite groups. The metal-rich chondrites (QUE 94411, 94627, and 99309) are all now recognized to be part of the CB group [1]. Additionally, nine CK chondrites have been found in the QUE region, and made a significant contribution to the great number of CKs overall that have come from Antarctica (~70%). QUE 97008 is recognized to be a rare low-grade type III chondrite [2]. The region has also yielded 24 CM, one CO, two CR, seven CV, and five each of EH and EL chondrites.

Achondrites: A large range of valuable achondrites has come from this region, including three lunar meteorites (QUE 93069, 94269, and 94281), a shergottite (QUE 94201), 24 HEDs, three ureilites, an ungrouped achondrite (QUE 93148), a winonaite (QUE 94535), and an unusual 2.4 kg ungrouped enstatite meteorite (QUE 94204 and seven paired masses from the 97 and 99 seasons). Two of the lunar meteorites are paired but are feldspathic regolith breccias [3], whereas the third (94281) is a glass-rich, anorthositic-rich, feldspathic regolith breccia [4]. These samples have provided new insight into the history and origin of the Moon. The 12 g basaltic shergottite is very unusual in that it is P-rich and contains up to 5% modal apatite, and as a result has provided age and petrologic information complementary to other shergottites [5]. The unusual achondrite QUE 93148 appears to be linked to pallasites [6]. The QUE region has also yielded one pallasite, 12 mesosiderites, and one enormous iron—22 kg QUE 99001. The paucity of irons in Antarctica has been emphasized by [7], but this is a welcome anomaly.

Summary: The return of these samples, as well as the detailed studies that followed illustrates the potential of even a single Antarctic region to advance our knowledge and understanding of planetary materials.

References: [1] Weisberg M. K. et al. 2001. *Meteoritics & Planetary Science* 32:401–418. [2] Grossman J. N. and Brearley A. J. 2005. *Meteoritics & Planetary Science* 40:87–122. [3] Korotev R. L. et al. 1996. *Meteoritics & Planetary Science* 31:909–924. [4] Arai T. and Warren P. H. 1999. *Meteoritics & Planetary Science* 34:209–234. [5] McSween H. Y. et al. 1996. *Geochimica et Cosmochimica Acta* 60:4563–4569. [6] Goodrich C. A. and Righter K. 2000. *Meteoritics & Planetary Science* 35:521–535. [7] Cassidy W. 2003. *Meteorites, ice and Antarctica*. Cambridge: Cambridge University Press. 349 p.

5377

REVISITING THE DECOMPRESSED DENSITY OF MERCURY

M. A. Riner^{1,2}, C. R. Bina², and M. S. Robinson^{1,2}. ¹Center for Planetary Sciences, Northwestern University, Evanston, Illinois, USA. E-mail: mariner@earth.northwestern.edu. ²Department of Geological Sciences, Northwestern University, Evanston, Illinois, USA

Introduction: Mercury is unique among the terrestrial planets in terms of its low mass (3.302×10^{23} kg) and high average density (5.427 g/cc) that together imply an iron-rich composition relative to Venus, Earth, Mars, and the Moon. Typically planetary bulk density is converted to decompressed density to allow meaningful interplanetary comparisons. The methodology used to calculate planetary decompressed density is not well documented in the scientific literature. Meaningful interpretations of decompressed density values require a clear elucidation of assumptions and methodology. In this abstract we present a detailed calculation of decompressed density for Mercury along with an analysis of the sensitivity of the method and implications for scientific interpretations of Mercury's decompressed density.

Method: The model uses a second-order Birch-Murnaghan equation of state to calculate Mercury's self compression, assuming an adiabatic temperature profile within the mantle and core (e.g., [1]). The temperature difference at the core mantle boundary is represented by the difference between the mantle and core adiabats extrapolated to zero pressure, ΔT_k . We assume a constant thermal expansion coefficient ($\alpha = 2.5 \times 10^{-5} \text{ K}^{-1}$).

The model is constrained by the observed total mass and total radius. Unfortunately the moment of inertia of Mercury is poorly constrained because Mercury rotates so slowly that nonhydrostatic contributions to the second degree gravitational potential coefficient, J_2 , are larger than the hydrostatic contribution (e.g., [2]). The model was applied to 1300 random scenarios using the range of values shown in Table 1. The parameter values for the core are selected to cover a range of compositions (Fe and FeS) and phase (liquid and solid) [3].

Table 1. From left to right the columns indicate the range of values for mantle density, core density, bulk moduli of mantle and core, (all at zero-pressure and 300 K) core radius, and the temperature difference between the mantle and core adiabats extrapolated to zero pressure.

	ρ_m^o	ρ_k^o	K_{Sm}^o	K_{Sk}^o	R_k	ΔT_k
	g/cc	g/cc	GPa	GPa	km	K
Values	3.35	6.4	180	170	2000	500
	± 0.25	± 1.4	± 30	± 40	± 400	± 500

Results: Model scenarios with the lowest mass errors ($\pm 10^{19}$ kg) have decompressed densities between 5.19 and 7.38 g/cc. The larger values for decompressed density correspond to larger core radii counterbalanced, to match the total mass, by low core densities, high core bulk moduli, and/or hot core adiabats. Restricting the core radius to <2200 km (rather than <2400 km) results in decompressed density values between 5.19 and 6.38 g/cc.

Conclusions: Due to the uncertainty in the moment of inertia factor, core size, and the core and mantle density for Mercury, accurate calculation of the decompressed density is not possible at this time. Thus the commonly held assumption that, due to its small mass, the decompressed density of Mercury is well constrained at 5.3 g/cc is still open to question. However, application of this model to the Earth indicates that the decompressed density of the Earth is well constrained (0.1 g/cc), even with variations in the mantle and core density and core size, as long as the total mass, total radius, and moment of inertia factor constraints are met. Measurement of the moment of inertia for Mercury would better constrain the decompressed density.

References: [1] Stacey F. D. 1992. *Physics of the Earth*. Brookfield Press. [2] Ness N. F. 1978. *Space Science Reviews* 21:527–553. [3] Harder H. and Shubert G. 2001. *Icarus* 151:118–122.

5339

VARIATIONS IN LUNAR OPAQUE PHASE AND GRAIN SIZE: IMPLICATIONS FOR REMOTE SENSING OF TiO₂

M. A. Riner¹, M. S. Robinson¹, P. G. Lucey², and D. S. Ebel³. ¹Center for Planetary Sciences, Northwestern University, Evanston, Illinois 60208, USA. E-mail: mariner@earth.northwestern.edu. ²Hawai'i Institute of Geophysics and Planetology, SOEST, University of Hawai'i, Honolulu, Hawai'i, USA. ³American Museum of Natural History, New York, New York, USA

Introduction: Many workers have shown a correlation between visible color and TiO₂ abundance of lunar samples. However, nagging uncertainties remain in the universal applicability of visible color differences to accurate prediction of TiO₂ abundance from remote sensing observations (e.g., [1, 2]). Here we investigate two potentially important controls on UVVIS color of lunar soils that may hinder accurate TiO₂ estimates: presence of opaque mineralogy other than ilmenite, and opaque grain size variations.

Methods: Reflectance spectra of samples of powdered natural basalt, synthetic ilmenite (FeTiO₃) and synthetic ulvöspinel (Fe₂TiO₄) were measured (Ocean Optics HR2000CG-UV-NI, 200–1100 nm at near zero phase angle (α) and/or RELAB 300–2800 nm at $\alpha = 30^\circ$ [3]). Reflectance spectra of mixtures of these components were modeled using radiative transfer methods [4]. Preliminary assessment of the mixture modeling was confirmed by spectral measurements of four mixtures of ilmenite and basalt.

Results: The 415/750 nm color ratio of ulvöspinel is 4% lower than ilmenite (Table 1), which reduces to <1% in the modeled mixtures of the opaque minerals with basalt (Table 1). Some of the ratio change may be due to grain size distribution variations between the two samples. Decreasing the grain size of ilmenite from 20–63 μm to <20 μm decreases the 415/750 ratio by 9%.

Table 1. Relative color of measured mineral separates at varying grain sizes ($\alpha = 0^\circ$), model mixtures from end-member spectra measured at $\alpha = 30^\circ$.

Measured samples	415/750	Modeled mixtures	415/750
Ilmenite (<63 μm)	0.984	20% ilmenite	0.832
Ulvöspinel	0.947	40% ilmenite	0.865
Ilmenite (20–63 μm)	1.020	20% ulvöspinel	0.829
Ilmenite (<20 μm)	0.931	40% ulvöspinel	0.857

Discussion: Ulvöspinel on the lunar surface is spectrally indistinguishable from ilmenite from the 415/750 nm ratio alone. Since a given mass of ulvöspinel has one third less mass of TiO₂ than ilmenite, its occurrence results in a TiO₂ overestimate using this ratio. The change in the 415/750 nm ratio caused by variations in the ilmenite grain size fractions considered here is twice as large as the difference between ulvöspinel and ilmenite (Table 1). Decreasing the grain size of a mineral (e.g., ilmenite) in a mixture tends to increase its apparent abundance. Thus mixing systematics indicate that decreasing ilmenite grain size will increase the 415/750 nm ratio while spectral changes have the opposite effect. The magnitude of these competing effects is unknown. The spectral changes due to particle size variation must, therefore, be considered in addition to the mixing systematics.

Conclusions: If some areas of the lunar regolith carry ulvöspinel as the dominant opaque mineral, estimates of TiO₂ abundance could be in error up to several weight percent. Spectral changes due to grain size variations in ilmenite affect the UVVIS ratio by ~9% for the size separates considered here. The effect on TiO₂ estimates also depends on the competing effect of mixing systematics. Actual variations in particle size distributions on the lunar surface may be smaller than those shown here, resulting in less dramatic variations in UVVIS ratio. Further work to assess the relative magnitudes of the competing effects of ilmenite grain size on UVVIS color is necessary.

References: [1] Elphic R. C. et al. 2002. *Journal of Geophysical Research* 107:10.1029/2000JE001460. [2] Gillis et al 2003. *Journal of Geophysical Research* 108:5009. [3] Pieters C. M. 1983. *Journal of Geophysical Research* 88:9534–9544. [4] Clark B. E. et al. 2001. *Meteoritics & Planetary Science* 31:1617–1637.

5259

THE MOLECULAR STRUCTURE AND ISOTOPIC COMPOSITIONS OF THE INSOLUBLE ORGANIC MATTER IN CHONDRITES

F. Robert¹ and S. Derenne². ¹LEME, CNRS-Muséum, Paris, France. E-mail: robert@mnhn.fr. ²LCBOP-BioEMCo, CNRS, ENSC, Paris, France

The interstellar origin (ISM) of the insoluble organic matter (IOM) extracted from CCs was originally supported by two independent observations: 1) its infrared spectrum mimics the interstellar spectrum around 3.3 microns [1], and 2) its hydrogen is enriched in Deuterium relative to clay minerals [2]. To better constraint a model accounting for its organo-synthesis, the details of the molecular structure of the IOM were investigated since 1999. Several interesting discoveries have been made during the course of these studies involving pyrolysis GC-MS, MNR and infrared spectroscopy, GC-iRMS and NanoSims imaging.

(1) The origin of the Universal 3.3 micron feature is now better understood: it results from the statistical distribution of C and H to form all the possible substitutions of the -CH₂ and -CH₃ bounds in aliphatic chains [3].

(2) The PAHs that constitute the largest moieties of fused benzene rings are formed by a number of cycles (three on average in 2-D), markedly lower than the PAHs detected in interstellar grains [4]. This may result from the photodissociation of the smaller aromatic units by UV radiations. This is most likely the signature of a protosolar process rather than ISMs.

(3) The benzene rings have a unique signature attesting of their extraterrestrial origin: they contain di-radilcoids [5]. Although predicted by quantum theory, these di-radilcoids were never observed in natural substances. As water circulation and/or parent body metamorphism would have erased these di-radicals, such a feature was likely established during the condensation of the IOM from the gas.

(4) Since no amine is present in the IOM (at a detection limit $\leq 7\%$), amino acids are not the by-products of the hydrolysis of a precursor polymer common to the soluble and the IOM [6].

(5) The planetary noble gases are mechanically trapped in the organic polymer and not in the benzenic molecules or in the leftover oxides associated with acid extracts [7].

(6) The D/H ratios of the three main organic bounds (aliphatic, aromatic, benzylic) exhibit a systematic D enrichment in the weaker organic hydrogen bounds. Therefore, the enrichment in Deuterium was acquired after the formation of the IOM and, in this respect, IOM cannot be regarded as an interstellar heritage.

References: [1] Ehrenfreund P., Robert F., and D'Hendecourt L. 1991. *Astronomy & Astrophysics* 252:712–717. [2] Robert F. and Epstein S. 1982. *Geochimica et Cosmochimica Acta* 46:81–95. [3] Gardinier A., Derenne S., Robert F., Behar F., Largeau C., and Maquet J. 2000. *Earth and Planetary Science Letters* 184:9–21. [4] Derenne S., Rouzaud J.-N., Clinard C., and Robert F. 2005. *Geochimica et Cosmochimica Acta* 69:3911–3918. [5] Binet L., Gourie D., Derenne S., Robert F., and Ciofini I. 2004. *Geochimica et Cosmochimica Acta* 68:881–891. [6] Remusat L., Derenne S., Robert F., and Knicker H. 2005. *Geochimica et Cosmochimica Acta* 69:3919–3932. [7] Marrocchi Y., Derenne S., Marty B., and Robert F. *Earth and Planetary Science Letters* 236:569–578. [8] Remusat et al. 2006. *Earth and Planetary Science Letters* 243:15–25.

5001

A CATALOG OF LARGE METEORITE SPECIMENS FROM CAMPO DEL CIELO METEORITE SHOWER, CHACO PROVINCE, ARGENTINA

M. C. L. Rocca. Mendoza 2779-16A, Ciudad de Buenos Aires, (1428DKU), Argentina. E-mail: maxrocca@hotmail.com

Introduction: The Campo del Cielo meteorite field in Chaco Province, Argentina, (27°30'S, 61°42'W) consists of at least 20 meteorite craters with an age of about 4000 years.

The area is composed of sandy-clay sediments of Quaternary-recent age. The impactor was an iron-nickel Apollo-type asteroid (Octahedrite meteorite type IA) and plenty of meteorite specimens survived the impact. The impactor's diameter is estimated at 5–20 meters. The impactor came from the SW and entered the Earth's atmosphere in a low angle of about 9°. As a consequence, the asteroid broke in many pieces before creating the craters. The first meteorite specimens were discovered during the time of the Spanish colonization. Craters and meteorite fragments are widespread in an oval area of 18.5 × 3 km (SW-NE), thus Campo del Cielo is one of the largest meteorite crater fields known in the world.

Crater #3, called "Laguna Negra," is the largest (115 m in diameter). Inside crater #10, called "Gómez" (~25 m in diameter), a huge meteorite specimen called "El Chaco," of 37.4 tons, was found in 1980. Inside crater #9, called "La Perdida" (25 × 35 m in diameter), several meteorite pieces were discovered weighing in total about 5200 kg.

The following is a catalog of large meteorite specimens (more than 200 kg) from this area as of 2005. Information given is the name of the meteorite, its weight, date of discovery, and current location.

Catalog: [1] El Abipon: 460 kg. 1936. Museo Argentino de Ciencias Naturales, (MACN), Buenos Aires City, Argentina. [2] El Chaco: 37.4 tons. 1980. Gancedo, Chaco, Argentina. This specimen is the second-heaviest known meteorite in the world. [3] El Mataco: 998 kg. 1937. Museo Provincial, Rosario, Santa Fe, Argentina. [4] El Mocovi: 732 kg. 1925. MACN, Buenos Aires City, Argentina. [5] El Patio: 350 kg. Found before 1960. Estancia El Taco, Chaco, Argentina. [6] El Taco: 1998 kg. 1962. Main mass at National Museum of Natural History, Smithsonian Institution, Washington, D.C., USA; 600 kg. at Planetarium of Buenos Aires City, Argentina. [7] El Toba: 4210 kg. 1923. MACN, Buenos Aires City, Argentina. [8] El Tonocote: 850 kg. 1931. Planetarium, Buenos Aires City, Argentina. [9] La Perdida(1): 1625 kg. 1965. Planetarium, Buenos Aires City, Argentina. [10] La Perdida(2): 3370 kg. 1965. Still in the crater. [11] Meson de Fierro: 15 tons. 1576. Lost. [12] Runa Pocito: 750 kg. 1803. British Museum, London, UK. [13] No Name: 10 Tons. 1997. Near its find site, Chaco, Argentina. [14] La Sorpresa: 7–10 tons. 2005. Still in the crater.

Acknowledgements: This work was funded by The Planetary Society, Pasadena, California, USA.

5002

TWO NEW POTENTIAL METEORITE IMPACT SITES IN CHUBUT PROVINCE, ARGENTINA

M. C. L. Rocca, Mendoza 2779-16A, Ciudad de Buenos Aires, (1428DKU), Argentina. E-mail: maxrocca@hotmail.com

Site One: A remarkable site of a possible new large meteorite impact craters field has been studied by the examination of Landsat and aerial photographs (Instituto Geografico Militar).

More than 100 small possible simple-type craters are widespread over an area of 27×15 km located at Meseta Filu-Co, Bajada del Diablo, Chubut Province, Argentina ($42^{\circ}45'S$, $67^{\circ}30'W$). The largest crater's diameter is 1 km. Most of these craters show clear evidences of having raised rims. Fourteen craters have diameters between 300 and 1000 meters.

Craters are mainly located on areas where fluvial sedimentary deposits (conglomerates) of Tertiary and Quaternary age are exposed, but many craters are also located on several different geologic terrains like, e.g., small basaltic plateaux and pyroclastic rocks.

Areas exposing recent fluvial sediments show no crater, so the impact event was not very recent [1]. No doubt, many craters have been erased by the recent fluvial erosion processes and what we see today is just a fraction of the original population of craters.

When meteorite showers reach the ground, they distribute themselves into a strewn field that usually defines an elliptical-shaped area called the dispersion ellipse. The long axis is coincident with the direction of motion of the swarm and the most massive fragments normally fall at the far end of the dispersion ellipse [2].

There is no evidence for those patterns in the case of Bajada del Diablo craters. Medium to large craters are randomly distributed all over the whole area of the craters field. No clear dispersion ellipse is visible in the images.

Most probably, this crater field is the result of the impact of a 100–200 m wide, rubble-pile type asteroid that was broken in hundreds of fragments by the force of the Earth's gravity shortly before entering the atmosphere. The swarm of fragments then created the crater field.

Site Two: Meseta del Canguel, Chubut Province, ($44^{\circ}28'S$, $68^{\circ}35'W$).

Three possible simple-type impact craters are located in an Y-shape configuration on a olivine-basalt plateau. Craters show raised rims.

Diameters: 1.3, 0.8, and 0.6 kilometers.

Age is estimated in less than 20 Ma [3].

Acknowledgements: This work was funded by The Planetary Society, Pasadena, California, USA.

References: [1] Corbella H. 1987. *Revista Asociación Mineralogía, Petrología y Sedimentología* 18:67. [2] Krinov E. 1966. *Giant meteorites*. New York: Pergamon Press. [3] Ardolino A. et al. 1999. *Anales SEGEMAR* 29:579–612.

5191

MAGNETIC CLASSIFICATION, WEATHERING, AND TERRESTRIAL AGES OF ANTARCTIC ORDINARY CHONDRITES

P. Rochette¹, L. Folco², J. Gattacceca¹, C. Berteloot¹, and C. Suavet¹. ¹CEREGE University of Aix-Marseille 3, France. ²Museo Nazionale Antartide, Siena, Italy

Magnetic susceptibility (χ) provides a means to discriminate rapidly between LL, L, and H falls [1]. This method allows rapid scan of collections without sample preparation and with portable instruments [2]. However, the classification abilities are hampered by weathering: for example, a weathered H chondrite can yield the same susceptibility as a fresh L chondrite. The three well-separated Gaussian distributions for fresh LL, L, and H falls [1] are skewed and partially merged by the weathering effect. The use of density measurements [3] does not really help to solve the ambiguity. In order to delineate this effect, we propose a simple mathematical model using the $\log\chi$ versus terrestrial age function as input data. To constrain the model $\log\chi$ versus terrestrial age function, we can use meteorites with cosmogenic isotopes-derived ages. We will present data on Antarctic meteorites (from the PNRA and ANSMET collections), showing a rather significant correlation for H and L, at odds with the literature contention that terrestrial age is independent of weathering grade in Antarctic meteorites. This contradiction likely arises from the fact that the weathering grade adopted for Antarctic meteorites (WG) is a sort of color index, that does not represent correctly the amount of metal oxidized in nonmagnetic phase (akagaenite, goethite, paramagnetic Fe^{3+}), which is actually what $\log\chi$ measures. We will discuss the dispersion observed in the correlation in terms of uncertainties in terrestrial age and log determination, as well as in terms of different weathering processes depending on the story of the meteorite on or in the ice. As a perspective the calibration curve can be used to predict the terrestrial age distribution of a given collection for which $\log\chi$ measurements are available.

References: [1] Rochette P. et al. 2003. *Meteoritics & Planetary Science* 38:251–268. [2] Folco L. et al. 2006. *Meteoritics & Planetary Science* 41:343–353. [3] Consolmagno G. J. et al. 2006. *Meteoritics & Planetary Science* 41:331–342.

5074

MAGNETIC CLASSIFICATION OF C, E, K, R, AND UNGROUPED CHONDRITES

P. Rochette¹, J. Gattacceca¹, L. Sagnotti², L. Folco³, G. Consolmagno⁴, and M. Denise⁵. ¹CEREGE CNRS University of Aix-Marseille 3, France. ²INGV Roma, Italy. ³Museo Nazionale Antartide, Siena, Italy. ⁴Specola Vaticana, Vatican City. ⁵MNHN, Paris, France

Magnetic susceptibility (χ) provides a means to discriminate rapidly between LL, L, and H falls [1]. We expand this work to C, E, K, R, and ungrouped chondrites, based on a previously published database [2, 3] and new data. The complete database corresponds to more than 400 different meteorites (and 700 samples) from 21 large collections around the world. A preliminary summary was included in [4]. Once weathering effect is isolated (mostly visible for metal-rich material: E, CR, CH), most groups, except CM and CV, yield well-grouped $\log\chi$ values, indicative of a rather restricted variation of the amount of magnetic minerals (metal, magnetite, or pyrrhotite).

One can distinguish three categories: weakly magnetic R (mean $\log\chi$ of 3.2), moderately magnetic CO, K, CK, and CI ($\log\chi$ from 4.5 to 4.9, i.e., similar to L) and strongly magnetic CR, CH, and E ($\log\chi$ from 5.1 to 5.4, i.e., similar to H). On the other hand, a wide range of values are observed for CM and CV, from 3.3 to 4.9, i.e., a factor 40 range in magnetic mineral amount (wt%), while the total iron amount is much less variable. No tendency for a grouping toward a specific value is observed, although one may distinguish a "grouplet" of strongly magnetic CM, already pointed out as anomalous: Bells, Essebi, Niger, MAC02606, MET01177. The corresponding range of redox conditions encountered in CM and CV should be discussed in terms of metamorphism on the parent bodies, but it seems that larger values (near 4.9) are observed for less metamorphosed meteorites. This large range allows to propose pairing hypothesis for Antarctic CV and CM. Among the ungrouped C2 to C4 a somewhat similar range is observed although a tendency toward values near 4.9 (case of, e.g., Tagish Lake, Coolidge) is somehow visible.

Other ungrouped, anomalous meteorites are tentatively compared to some groups based on their $\log\chi$ value. For example, Kaidun fits with an average CI magnetic content, Taffafaset with a CR magnetic content.

References: [1] Rochette P. et al. 2003. *Meteoritics & Planetary Science* 38:251–268. [2] Rochette P. et al. 2001. *Quaderni di Geofisica*. [3] Smith et al. 2006. *Meteoritics & Planetary Science* 41:355–374. [4] Folco L. et al. 2006. *Meteoritics & Planetary Science* 41:343–353.

5282

SRTM INVESTIGATION OF THE ARAGUAINHA IMPACT CRATER, CENTRAL BRAZIL

R. Romano¹, G. R. Cooper², and W. U. Reimold^{2,3}. ¹Department of Geology, Federal University of Ouro Preto, Minas Gerais, 35400-000 Brazil. E-mail: rromano@gmail.com. ²Impact Cratering Research Group, School of Geosciences, University Witwatersrand, Johannesburg, RSA. ³Museum für Naturkunde (Mineralogie), Humboldt-Universität, Berlin, Germany

The 40 km diameter Araguainha impact structure (at 16°47'S, 52°59'W) was excavated ~245 Ma ago in flat-lying Permian to Devonian sediments of the intracratonic Paraná Basin, central Brazil. The impact origin for the structure is based on the presence of shatter cones and bona fide shock deformation of minerals from throughout the central parts of the structure. The structure is characterized by an ~8 km wide central uplift surrounded by a 10–15 km wide zone of annular rings formed by vertical and lateral movements of the target rocks during the collapse stage [1].

In this study, we analyzed three arc second Shuttle Radar Topography Mission (SRTM) data and enhanced thematic Mapper (ETM+) Landsat images for the region around Araguainha. Several enhancement methods for circular structures were applied to the SRTM data, such as radial sunshading [2].

Color composite Landsat ETM+ with RGB 7-4-2 bands, sharpened with the panchromatic band, shows a structure comprising a 6 km wide, near-circular central uplift, open to the southeast, surrounded by an apparently flattish depression of about 5 km width, with a ~7.5 km radius intermediate ring feature, followed by the outer rim at 20–22 km from the center. The structure appears to be very well-preserved in the N and NW sectors, where it was not affected by erosion by the Araguaia River, which cuts the structure across the SW and NE sectors.

The SRTM raw data for the area of the structure provide a detailed representation of the annular and concentric drainage pattern. The sunshading filters provide a much clearer image of the structure than the Landsat imagery. As in the Landsat image, the SRTM data show a structure with prominent annular rings in the N and NW sectors. The radial average filter applied gives more detail about the ring features. A central topographic low is observed with a radius of 2.1 km, followed by an outer central ring of 3.6 km and an annular trough of ~3.4 km radius. The first intermediate ring appears as a narrow feature at 7 km. The second intermediate ring, at 12.2 km, is the most prominent one, with an average elevation of 100 m compared to the annular trough. A third intermediate ring appears at 14.6 km from the center, followed by the outer rim at 18.5 km.

The Landsat and SRTM data provide a powerful tool for detailed observations of structure and morphology of impact structures. These data indicate that the Araguainha structure comprises a complex peak-ring structure. Comparing these features with other similar impact structures on Earth could provide fundamental information with regard to the identification of such structures and for the understanding of cratering mechanisms.

References: [1] Lana et al. 2006. *Geology* 34:9–12; [2] Cooper G. R. J. 2003. *Computers and Geosciences* 29:941–948.

5164

THE NATURE OF THE LITHIUM-RICH PHASE FOUND IN MIL 03346 MESOSTASIS

D. Rost¹, E. P. Vicenzi¹, M. Fries², and A. Steele². ¹Smithsonian Institution, Department of Mineral Sciences, Washington, D.C. 20560, USA. E-mail: rostd@si.edu. ²Geophysical Laboratory, Carnegie Institution of Washington, Washington, D.C. 20015, USA

Introduction: Martian meteorite MIL 03346 putatively originates from an upper stratum of the nakhlitic lava flow(s) [1]. The recent discovery of Li-rich grains in its mesostasis [2] is important for understanding the preterrestrial aqueous alteration processes in nakhlites, since a readily dissolvable Li host phase is a likely source for the Li enriched in secondary clay minerals found in Nakhla and Lafayette [3, 4], by way of percolating fluids. Here we present additional spectroscopic information regarding the nature of the Li-enriched phase in MIL 03346.

Methods: Polished thin sections were used for ToF-SIMS analyses (IONTOF TOF-SIMS IV), confocal Raman examination (WITec α -SNOM), and EDX measurements (Thermo Electron NSS on both a JEOL 840A and an FEI Nova NanoSEM 600).

Results: The MIL 03346 mesostasis contains small grains (10–50 μm) with compositions that suggest fayalite, i.e., $\sim(\text{Fe}_{0.91}\text{Mg}_{0.06}\text{Mn}_{0.03})_2\text{SiO}_4$ if cast into the olivine formula, and high Li contents ranging from 44 to 100 ppm. However, Raman spectroscopic analysis identified fayalite only in the cores of a few grains. The majority of the grains are not olivine as their distinctive Raman spectrum is incompatible with common mafic silicates, e.g., olivine and pyroxene. The Li concentrations in both phases are indistinguishable. An $\sim 50 \mu\text{m}$ thick rim of phenocrystic olivine in contact with the mesostasis turned out to be this unknown phase as well, and is similarly rich in Li.

Small deviations in the composition of the unknown phase relative to the fayalite (Fe depletion and O enrichment) suggest the ferriolivine laihunite, $\text{Fe}^{2+}\text{Fe}^{3+}_2(\text{SiO}_4)_2$. This is supported by similar Raman spectra taken from our National Museum of Natural History's laihunite mineral specimen.

Discussion: Oxidizing conditions and temperatures of $\sim 700^\circ\text{C}$ convert olivine (fayalite) into ferriolivine (lahunite) and other reaction products, e.g., hematite and magnesioferrite [5–7]. In MIL 03346, no such additional oxides have been observed in connection with the assumed laihunite. Therefore, it is difficult to speculate on the conditions of laihunite formation in MIL 03346.

The high Li concentrations might be the result of a general trend of Li enrichment in the nakhlitic parental melt as it is also documented in increasing bulk meteorite contents of Li (see overview in [2]) at supposed shallower stratigraphic levels [8, 1]: Eventually, the olivine in the MIL 03346 mesostasis was the least unsuitable phase to incorporate Li.

The Li concentrations in these grains are comparable to those in secondary clays [3, 4] and could represent the original siting of Li, before it was mobilized by penetrating fluids.

Outlook: Analyses of other laihunite samples are planned to corroborate its presence in MIL 03346. EMPA will be employed to confirm our current microanalytical observations.

References: [1] Mikouchi T. et al. 2005. Abstract #1944. 36th Lunar and Planetary Science Conference. [2] Rost D. et al. 2006. Abstract #2362. 37th Lunar and Planetary Science Conference. [3] Rost D. and Vicenzi E. P. 2004. *Meteoritics & Planetary Science* 39:A92. [4] Rost D. et al. 2005. Abstract #2306. 36th Lunar and Planetary Science Conference. [5] Kondoh S. et al. 1985. *American Mineralogist* 70:737–746. [6] Iishi K et al. 1997. *Physics and Chemistry of Minerals* 25:8–14. [7] Khisina N. R. et al. 1998. *European Journal of Mineralogy* 10:229–238. [8] Mikouchi T. et al. 2003. Abstract #1883. 34th Lunar and Planetary Science Conference.

5241

METAMORPHIC CONTROL OF NOBLE GAS ABUNDANCES IN PRISTINE CHONDRITES

J.-N. Rouzaud¹, L. Bonal², and E. Quirico². ¹Laboratoire de Géologie–ENS, 24, rue Lhomond 75231 Paris Cedex 5, France. ²Laboratoire de Planétologie de Grenoble, UJF, Bât. D de Physique 38041 Grenoble Cedex 9, France. E-mail: lydie.bonal@obs.ujf-grenoble.fr.

One of the most enduring enigmas of meteoritics is the nature of the Q (or P1) phase carrier with its associated trapped “planetary Q-gases” (He, Ne, Ar, Kr, and Xe). Much evidence suggests that the Q-phase carrier is carbonaceous, but the location of noble gas atoms in the carbon network has not been yet identified. Many studies suggest that the abundance of the Q phase in pristine chondrites is controlled by thermal metamorphism (TM) [1, 2], and that this parameter should be used as a petrologic indicator. But, this general trend was established using petrologic types (PT) derived by induced thermoluminescence, which may be erroneous [3], and in any case does not provide direct information on the structure of OM where the Q-phase is sited. In this study, the structure and texture of chondritic OM was studied by HRTEM in Kaba, Leoville, Mokoia, Allende, and Tieschitz. HRTEM provides de-averaged structural information at the nanometric scale, and clues on the microtexture. The metamorphic grade and PT of these objects were previously evaluated [3], based on the structural grade of OM, attempted by Raman spectroscopy. Using noble gas abundances available in literature, we have revisited the question of the metamorphic control of the Q (P1), P3, and P6 components and the carrier of the Q phase.

Discussion: HRTEM results point out that within the series of chondrites studied, the microtexture is controlled by (TM): for Allende (>3.6), the aromatic layers are the longest (until a few nm, with a mean value of 0.9 nm), and the best stacked (55% of unstacked layers, stacks formed by 3–6 layers, with a mean value of 2.4 and the mean interlayer spacing is here 0.40 nm); the layer length varies between 0.8 and 0.9 for Leoville (3.1–3.4) and between 0.7 and 1 nm for Mokoia (~3.6). Using the Raman tracer FWHM-D [3], P3 appears as well correlated to the metamorphic grade. This confirms the result of [4]. But, P6 is not correlated, consistently with the fact the P6-carrier sited in nanodiamonds is released at very high temperatures (in agreement with [4]). Our results demonstrate that the Q (=P1) abundance is not well correlated with the metamorphism grade. That is in disagreement with the study of [2]. This parameter should not be used as a petrologic indicator for deriving low petrologic types. This last result questions the nature of the carrier of the Q (P1) phase. As lamellar and onion-like structures are the result of TM, they cannot be this carrier as suggested by [5]. Our results are however consistent with a very complex siting, in contrast with a single carrier for the P3 component (surface of nanodiamonds), for which the release pattern is simple. This multiple carrier might include the interlayer space sitings [6], but the complex metamorphic control suggest other carriers.

References: [1] Busemann H. et al. 2000. *Meteoritics & Planetary Science* 35:949–973. [2] Huss G. et al. 1996. *Geochimica et Cosmochimica Acta* 60:3311–3340. [3] Bonal L. et al. 2006. *Geochimica et Cosmochimica Acta* 70:1849–1863. [4] Huss et al. 1994. *Meteoritics & Planetary Science* 29:811–829. [5] Vis R. D. et al. 2002. *Meteoritics & Planetary Science* 37: 1391–1399. [6] Marrochi Y. et al. 2005. *Earth and Planetary Science Letters* 236:569–578.

5271

OXIDATION STATE AND O-ISOTOPIC COMPOSITIONS OF EQUILIBRATED H CHONDRITES

Alan E. Rubin. Institute of Geophysics, University of California–Los Angeles, Los Angeles, California 90095–1567, USA. E-mail: aerubin@ucla.edu

Equilibrated members of the H-L-LL sequence show a correlation between mean group oxidation state (as represented by olivine Fa) and mean group O-isotopic composition (indicated by $\Delta^{17}\text{O}$): H4–6 (Fa 18.8 mol%, $\Delta^{17}\text{O} = 0.73\text{‰}$), L4–6 (Fa 24.7 mol%, $\Delta^{17}\text{O} = 1.07\text{‰}$), LL4–6 (Fa 29.4 mol%, $\Delta^{17}\text{O} = 1.26\text{‰}$) [1, 2]. The correlation is not restricted to the group means, but also occurs among 14 H-chondrite falls [3]. I have analyzed olivine in six additional H4–6 falls for which O-isotopic compositions were previously determined [2]: Ambapur Nagla, H5 (Fa 18.2 ± 0.1 , $n = 28$; $\Delta^{17}\text{O} = 0.75\text{‰}$); Charsonville, H6 (Fa 17.6 ± 0.2 , $n = 22$; $\Delta^{17}\text{O} = 0.65\text{‰}$); Forest City, H5 (Fa 18.0 ± 0.2 , $n = 27$; $\Delta^{17}\text{O} = 0.75\text{‰}$); Kernouvé, H6 (Fa 18.6 ± 0.2 , $n = 26$; $\Delta^{17}\text{O} = 0.78\text{‰}$); Pantar, H5 (Fa 18.3 ± 0.5 , $n = 27$; $\Delta^{17}\text{O} = 0.56\text{‰}$); Weston, H4 (Fa 18.3 ± 0.3 , $n = 23$; $\Delta^{17}\text{O} = 0.88\text{‰}$). (At this point, 20 of the 22 H-chondrite falls for which O-isotopic data are available have been analyzed; electron microprobe analyses of the two remaining H chondrites, H5 Leighton and H6 Cape Girardeau, are pending.) The correlation between olivine Fa and $\Delta^{17}\text{O}$ is significant: $r = 0.574$, $n = 20$, $2\alpha = 0.008$, significant at the 99.2% confidence level. However, three samples (Pantar, Weston, Tysnes Island) are solar-gas-rich regolith breccias; the first two of these are outliers. Because regolith breccias contain exotic clasts of different chondrite groups [4, 5], their bulk O-isotopic compositions are not representative of pristine H-chondrite material. If these breccias are omitted from the correlation, its significance increases: $r = 0.725$, $n = 17$, $2\alpha = 0.001$, 99.9% confidence level.

There are also correlations between olivine Fa and $\Delta^{17}\text{O}$ among H-chondrite falls of the same petrologic type (again omitting the regolith breccias): H5 ($r = 0.825$, $n = 5$, $2\alpha = 0.09$, 91% confidence level); H6 ($r = 0.832$, $n = 7$, $2\alpha = 0.02$, 98% confidence level). However, the H4 correlation is not significant: $r = 0.569$, $n = 5$, $2\alpha = 0.36$, 64% confidence level.

It is likely that the correlations between oxidation state and O-isotopic composition in OC were established in the solar nebula. Rubin [3] proposed that a single component (^{17}O -rich phyllosilicate) was acquired by OC during agglomeration; H chondrites acquired the lowest abundance and became the most reduced OC with the lightest O isotopes. Different amounts of this component were incorporated into individual batches of H-chondrite material irrespective of their future parent-body thermal histories.

Equilibrated L- and LL-chondrite falls show no intragroup correlations between Fa and $\Delta^{17}\text{O}$ [3]; the appreciable scatter in the L data and even greater scatter in the LL data may be caused by the presence in these rocks of an additional, heterogeneously distributed, O-bearing component that is more abundant in LL chondrites. One candidate is the set of coarse silica-rich clasts in LL3.6 Parnallee that have $\Delta^{17}\text{O}$ values of 1.5–3.0‰ [6]. Even during metamorphism to petrologic-type-VI levels, these clasts would not have completely equilibrated their O isotopes [7].

References: [1] Rubin A. E. 1990. *Geochimica et Cosmochimica Acta* 54:1217–1232. [2] Clayton R. N. et al. 1991. *Geochimica et Cosmochimica Acta* 55:2317–2337. [3] Rubin A. E. 2005. *Geochimica et Cosmochimica Acta* 69:4907–4918. [4] Noonan A. F. and Nelen J. A. 1976. *Meteoritics* 11: 111–130. [5] Keil K. and Fodor R. V. 1980. *Chemie de Erde* 39:1–26. [6] Bridges J. C. et al. 1995. *Meteoritics* 30:715–727. [7] Olsen E. J. et al. 1981. *Earth and Planetary Science Letters* 56:82–88.

5274

SHOCK AND ANNEALING IN EL CHONDRITES

Alan E. Rubin. Institute of Geophysics, University of California–Los Angeles, Los Angeles, California 90095–1567, USA. E-mail: aerubin@ucla.edu

Shock has affected the structure, texture, and mineralogy of EL chondrites of all petrologic types.

EL3: Shock stages range from S2–S5; many samples are foliated. Impact deformation caused foliations in OC [1]; it is likely that EL3 foliations also formed by impact. Extensive shock melting is precluded by the presence of excess ^{53}Cr in EL3 sphalerite [2].

EL4: The three rocks I studied are impact-melt breccias (IMBs) of shock-stage S2. QUE 94368 contains euhedral enstatite grains protruding into kamacite and euhedral graphite laths surrounded by metal and silicate; these features are characteristic of enstatite-chondrite IMBs (e.g., EH Abee [3]). QUE 94368 contains euhedral grains of sinoite ($\text{Si}_2\text{N}_2\text{O}$) that probably crystallized from the melt [4]. Grein 002, which was partly impact-melted, contains euhedral grains of enstatite, graphite, and sinoite [5]. MAC 02747 contains euhedral grains of enstatite and graphite.

EL5–EL6: Nearly all of these rocks are S2, but many EL6 chondrites have features suggesting much higher shock levels at an earlier period. Blithfield is a chondrule-free IMB with large sulfide-rich, kamacite-poor clasts, a metal-rich matrix, and cm sized metal veins. Hvittis is a fragmental breccia with impact-melt-rock clasts. Atlanta contains a sulfide-rich, kamacite-poor clast and cm long metal veins. NWA 2213 has euhedral grains of enstatite and graphite, kamacite grains with small troilite blebs, and troilite grains with small kamacite blebs. Forrest 033, GRO 95626, and QUE 97462 contain euhedral grains of enstatite and graphite. Other EL6 chondrites also contain euhedral enstatite grains. Euhedral grains of sinoite occur in Forrest 033, Hvittis, Jajh deh Kot Lalu, Pillistfer, Ufana, Yilmia, ALHA81021, LEW 88714, EET 90102, and Neuschwanstein. Diopside is present in EL3 MAC88136 [6], EL4 Grein 002 [5], EL6 EET90102 [7], and EL6 NWA 2213. Diopside is probably a primary phase in EL3 chondrites. In EL4–6 chondrites, diopside may have formed by reaction of oldhamite and enstatite at high temperatures followed by quenching [7]. The brecciated and melted textures of some EL6 chondrites and textural and mineralogical similarities to the impact-melted portions of EL4 chondrites (including the presence of sinoite, diopside, euhedral enstatite and euhedral graphite) suggest that at least some EL6 chondrites are annealed IMBs. The EL4–6 chondrites may have formed from EL3 chondrites by variable degrees of impact heating, burial beneath insulating regolith material, and annealing. Annealing in the EL4–6 chondrites erased shock effects in pyroxene, producing grains with sharp optical extinction. Subsequent impacts caused undulose extinction to develop in pyroxene, changing the rocks' shock-classifications to stage S2. It is unclear to what extent the decay of short-lived radionuclides contributed to EL-chondrite metamorphism. About 60% of EL6 chondrites have similar ^{21}Ne CRE ages (27 ± 6 Ma) [8, 9], suggesting that these rocks were in the same location on their parent asteroid and likely experienced similar shock and thermal histories.

References: [1] Sneyd D. S. et al. 1988. *Meteoritics* 23:139–149. [2] El Goresy A. et al. 1992. 23rd Lunar and Planetary Science Conference. pp. 331–332. [3] Rubin A. E. and Scott E. R. D. 1997. *Geochimica et Cosmochimica Acta* 61:425–435. [4] Rubin A. E. 1997. *American Mineralogist* 82:1001–1006. [5] Patzer A. et al. 2004. *Meteoritics & Planetary Science* 39:1555–1575. [6] Lin Y. T. et al. 1991. 22nd Lunar and Planetary Science Conference. pp. 811–812. [7] Fogel R. A. 1997. *Meteoritics & Planetary Science* 32:577–591. [8] Crabb J. and Anders E. 1981. *Geochimica et Cosmochimica Acta* 45:2443–2464. [9] Patzer A. and Schultz L. 2001. *Meteoritics & Planetary Science* 36:947–961.

5091

AL-26 IN SEMARKONA (LL3.0) CHONDRULES: ONSET AND DURATION OF CHONDRULE FORMATION

N. G. Rudraswami¹, B. K. Chattopadhyay², B. K. Bandopadhyay², and J. N. Goswami¹. ¹Physical Research Laboratory, Ahmedabad-380009, India. ²Geological Survey of India, Kolkata-700016, India. E-mail: gowda@prl.res.in

Al-Mg isotope records have been studied in Semarkona (LL3.0) chondrules to further our understanding of the onset and duration of chondrule formation. The extremely low degree of thermal metamorphism suffered by this meteorite in its parent body is expected to preserve the pristine records of Al-Mg isotope system in the analyzed chondrules. An earlier study of ²⁶Al records in Semarkona chondrules [1] suggested onset of chondrule formation about 2 Ma after CAI and a short duration of chondrule formation. Studies of chondrules from other UOCs support late formation of chondrules but argue for an extended duration of chondrule formation of >2 Ma [2-4].

A polished thin section of Semarkona was mapped using SEM and EPMA to identify chondrules containing Al-rich phases (glassy mesostasis and rare plagioclase). A Cameca ims-4f ion microprobe was used for isotopic studies of a dozen selected chondrules. The presence of Mg-rich microcrystallites within the Al-rich glassy phases makes it difficult to carry out meaningful isotopic study in many chondrules. However, we could detect well-resolved ²⁶Mg excess (from ²⁶Al decay) in four of the chondrules where we could conduct meaningful isotopic analysis. The data yielded well-behaved isochrones and we infer initial ²⁶Al/²⁷Al ratio of $(1.24 \pm 0.26) \times 10^{-5}$, $(1.14 \pm 0.27) \times 10^{-5}$, $(1.10 \pm 0.12) \times 10^{-5}$, and $(5.4 \pm 0.2) \times 10^{-6}$, respectively, for these chondrules.

The initial ²⁶Al/²⁷Al values obtained in this study reinforce the suggestion that formation of CAIs preceded chondrules formation by at least 1.5 Ma. Further, three of the chondrules have very similar initial ²⁶Al/²⁷Al that suggests a short duration of chondrule formation in the early solar system. However, the fourth chondrule, which has a large spread in Al/Mg ratio and a very well-behaved Al-Mg isotope systematic, has an initial ²⁶Al/²⁷Al ratio lower than the other chondrules. Low initial ²⁶Al/²⁷Al ratios of $(4 \text{ to } 8) \times 10^{-6}$ have also been reported earlier [5] for Semarkona and Bishunpur (LL3.1) chondrules. These data argue for an extended duration of chondrule formation unless we invoke thermal metamorphism of these chondrules in a pre-parent body setting. Both the proposition of an extended duration of chondrule formation and thermal metamorphism in a pre-parent body environment require isolation of CAIs and chondrules for significant durations of more than 3 Ma before their mixing and accretion to form the chondritic parent bodies. This is in contrast to the fact that accretion, differentiation and crust formation in the case of parent bodies of differentiated meteorite was complete within 3-5 Ma following the formation of CAIs (see, e.g., [6-9]).

References: [1] Kita N. T. et al. 2000. *Geochimica et Cosmochimica Acta* 64:3913-3922. [2] Russell S. S. et al. 1996. *Science* 273:757-762. [3] Huss G. R. et al. 2001. *Meteoritics & Planetary Science* 36:975-997. [4] Mostefaoui S. et al. 2002. *Meteoritics & Planetary Science* 37:421-438. [5] McKeegan K. et al. 2000. Abstract # 2009. 31st Lunar and Planetary Science Conference. [6] Srinivasan G. et al. 1999. *Science* 284:1348-1350. [7] Kleine et al. 2002. *Nature* 418:952-955. [8] Yin Q. et al. 2002. *Nature* 418:949-952. [9] Kleine et al. 2005. *Geochimica et Cosmochimica Acta* 69:5805-5818.

5080

NWA 2999 AND OTHER ANGRITES: NO COMPELLING EVIDENCE FOR A MERCURIAN ORIGIN

A. Ruzicka and M. Hutson. Cascadia Meteorite Laboratory, Department of Geology, Portland State University, 17 Cramer Hall, 1721 SW Broadway, Portland, Oregon 97207, USA

Introduction: NWA 2999 is the tenth known angrite and contains disequilibrium textural features, which recently led to the suggestion that it and other angrites were derived from Mercury [1, 2]. These features include diopsidic-augitic clinopyroxene (cpx) + spinel (sp) symplectites around plagioclase (plag), and discontinuous coronas of plag around sp. The textures were interpreted by Irving et al. [1, 2] as having formed by crossing the olivine (ol) + plag = sp + orthopyroxene (opx) + cpx reaction boundary twice, with the symplectites forming by transition to higher pressure (>6.7 kb), and the plag coronas forming upon pressure release. We suggest instead that these textures were more likely produced during low-pressure crystallization.

Melting and Crystallization in Angrite Systems: Partial melts of carbonaceous chondrite precursors under relatively oxidizing conditions at 1 bar produce angrite-like melt compositions and mineralogies [3, 4]. The low-pressure liquidus phase diagrams of Longhi [4] show that sp and plag can either appear or disappear as temperature is changed under relatively oxidizing conditions. For an Allende (CV3) oxidized composition with no Fe removed, initial melting begins at ~1130 °C with coexisting ol, cpx, and sp. Plag forms and cpx disappears after ~4% melting at ~1162 °C and plag disappears after 19% melting at ~1248 °C. For an Allende composition with 10% Fe removed, ol + cpx + plag + sp coexist with the first melt, sp disappears after ~1% melting, cpx disappears after ~1.7% melting at ~1166 °C, and after 22% melting plag disappears and sp reappears. We suggest that plag coronas around sp in NWA 2999 formed as temperature dropped to ~1250 °C when plag began to crystallize. Cpx + sp symplectites around plag probably formed as temperature dropped to ~1165 °C, when both cpx and sp were stable. Thus, cooling during crystallization can explain the disequilibrium textures. Pressure changes and large planetary bodies are not required.

Angrites from Mercury? In contrast to Irving and co-workers [1, 2], we find no compelling evidence that angrites were derived from Mercury. Arguments against a Mercurian origin for angrites were given previously [5] and include their old crystallization ages (4.56 Ga) and ferrous compositions. In particular, the ferrous compositions and reflectance spectra of angrites are completely at odds with spectral data for Mercury [6, 7]. The minimal shock and metamorphic effects experienced by most angrites are also inconsistent with their derivation from a large body [8]. Finally, NWA 2999 contains ~8% metal [2], unlike what one would expect for Mercury's crust or mantle.

References: [1] Irving T. et al. 2005. *Eos* 86(52). [2] Kuehner S. M et al. 2006. Abstract #1344. 37th Lunar and Planetary Science Conference. [3] Jurewicz A. et al. 1993. *Geochimica et Cosmochimica Acta* 57:2123-2139. [4] Longhi J. 1999. *Geochimica et Cosmochimica Acta* 63:573-585. [5] Love S. and Keil K. 1995. *Meteoritics* 30:269-278. [6] Burbine T. et al. 2002. *Meteoritics & Planetary Science* 37:1233-1244. [7] Burbine T. et al. 2001. Abstract #1857. 32nd Lunar and Planetary Science Conference. [8] Mittlefehldt D. et al. 2002. *Meteoritics & Planetary Science* 37:345-369.

5266

TRACE-ELEMENT COMPOSITIONS OF NORMAL, DUSTY, AND CLEAR OLIVINE IN CHAINPUR CHONDRULES

A. Ruzicka¹, C. Floss², and M. Hutson¹. ¹Department of Geology, 17 Cramer Hall, 1721 SW Broadway, Portland State University, Portland, Oregon 97207, USA. ²Laboratory for Space Sciences, Washington University, Saint Louis, Missouri 63130, USA

Introduction: As part of a continuing study of trace-element compositions of olivine in chondrules from UOCs such as Sahara-97210 (LL3.2) and Chainpur (LL3.4) [1], we have obtained the first trace element data for dusty olivine and coexisting clear olivine, in addition to normal igneous olivine, in chondrules from Chainpur. Dusty olivine contains micron-sized Ni-poor metal dust and is widely agreed to have formed by FeO-reduction of olivine during chondrule formation [2, 3].

Dusty and Clear Olivines: We analyzed two porphyritic-pyroxene-olivine (PPO) chondrules that contain dusty-metal-bearing olivine and clear olivine. The clear olivine shows normal Fe-Mg zoning. The dusty and clear grains have the lowest concentration of Ni (10–22 and 16–34 $\mu\text{g/g}$, respectively) of all olivine analyzed to date, much lower than in normal igneous olivine from Chainpur ($124 \pm 35 \mu\text{g/g}$, $N = 13$). Co contents are also low in both dusty and clear olivine (~6–12 and ~5 $\mu\text{g/g}$, respectively) compared to normal igneous olivine in Chainpur (25–130 $\mu\text{g/g}$). Low Ni and Co contents in dusty olivine were found despite analyzing metal dust with SIMS (~2 wt% overall in the dusty olivines, as inferred from EMPA data), indicating the olivine must be highly depleted in these elements. The P content of clear olivine (14–26 $\mu\text{g/g}$) is significantly lower than in coexisting dusty olivine (130–230 $\mu\text{g/g}$), and lower than in normal igneous grains (range 25–1000 $\mu\text{g/g}$, mean ~300 $\mu\text{g/g}$).

Formation of the PPO Chondrules: Clear olivine probably formed by igneous crystallization from melts that were produced during the reheating event that caused metal dust to exsolve in dusty olivine. Similar, and low, abundances of Ni and Co in the dusty and clear olivine implies that they equilibrated with melt under reducing conditions sufficient to cause metal saturation and low $D^{\text{ol/melt}}$ values, corresponding to $f\text{O}_2$ values less than 3.9 log units below the CCO and NNO buffers [4]. This is consistent with the observed Fa contents of olivine (Fa_{4-9}) in the chondrules. Evidently, normal olivine crystallized with higher $D^{\text{ol/melt}}$ and $f\text{O}_2$ values, leading to higher Ni and Co contents. The low P content in clear olivine is also attributed to formation under low $f\text{O}_2$, but evidently P in the dusty olivine was out of equilibrium with the chondrule melt. Heating during chondrule formation must have been sufficiently long to allow Ni and Co to diffuse out of the dusty olivine, but not so long as to allow P to diffuse out. Based on Ni and Co diffusion data [5] and the size of the dusty relicts, this heating duration is estimated as about a few hours.

References: [1] Ruzicka A. and Floss C. 2004. Abstract #1422. 35th Lunar and Planetary Science Conference. [2] Leroux H. et al. 2003. *Meteoritics & Planetary Science* 38:81–94. [3] Jones R. H. and Danielson L. R. 1997. *Meteoritics & Planetary Science* 32:753–760. [4] Ehlers K. et al. 1992. *Geochimica et Cosmochimica Acta* 56:3733–3743. [5] Morioka M. 1981. *Geochimica et Cosmochimica Acta* 45:1573–1580.

5106

SEM-CL STUDY OF QUARTZ FROM MT. OIKEYAMA—EVIDENCE OF A POSSIBLE IMPACT STRUCTURE IN JAPAN

M. Sakamoto¹, H. Nishido², A. Guccik³, K. Ninagawa¹, and T. Okumura¹. ¹Neba Elementary School, 80 Neba Village, Nagano, 395-0701, Japan. ²Okayama University of Science, Department of Applied Physics, Ridai-cho 1-1, Okayama, 700-0005, Japan. ³University of West Hungary, Bajcsy-Zs. u. 4., Sopron, H-9400, Hungary. E-mail: ciklamensopron@yahoo.com

Introduction: The origin of the Mt. Oikeyama structure in central Japan has been debated for many decades. The purpose of this study is to provide new information about scanning electron microscope cathodoluminescence (SEM-CL) data of planar microdeformations in quartz samples to determine whether this area was formed by tectonic, regular geological processes, or shock metamorphic events.

Experimental Procedure: SEM-CL imaging and CL spectral analyses were performed on selected polished thin sections coated with a 20 nm thin film of carbon in order to avoid charge build-up. SEM-CL images were collected using a scanning electron microscope (SEM), JEOL 5410LV, equipped with a CL detector, Oxford Mono CL2, which comprises an integral 1200 grooves/mm grating monochromator attached to reflecting light guide with a retractable paraboloidal mirror.

Results and Discussion: Gratz et al. [1] distinguished shocked quartz from tectonically deformed quartz by SEM on the HF-etched quartz, and reported differences between glass-filled planar deformation features (PDFs—"pillaring" texture) and glass-free tectonic deformation arrays. These similarities of the shock-related pillaring texture and tectonic-related arrays in a quartz sample from Mt. Oikeyama are visible in the secondary image followed HF-etching. This indicates that the presence of glass-filled micro-cracks such as wide planar transformation lamellae might be related to the shock-metamorphic processes [1]. Seyedolali et al. [2] and Boggs et al. [3] revealed that planar microstructures in shocked quartz resulted from meteorite or cometary impact that can be discriminated from other similar features by SEM-CL image. Typical CL image of PDFs described by [3] is characterized by fine, dark streaks with 1–2 μm thickness in bright luminescent background and sufficient parallelism of dark streaks with 5–20 μm spacing, where the texture of CL image is favorably compared with planar microstructures illustrated in petrographic optical image. Overwhelming parallel dark streaks observed in CL image of Oikeyama quartz are quite narrow in thickness of 1–2 μm or less near to effective resolution of CL imaging, whereas several broad dark bands with 5–10 μm thick can be recognized. The spacings of dark streaks are predominant in 3–5 μm . According to the verification by [3] parallel dark streaks in CL image of Oikeyama quartz could be unambiguously led to the evidence of PDFs. Consequently, all arguments of an impact origin of Mt. Oikeyama and related rocks are based on interpretation of selected SEM-CL observations.

Acknowledgements: This work has been partly supported by the Hungarian Space Office (TP-293).

References: [1] Gratz A. J. et al. 1996. *Earth and Planetary Science Letters* 142:513–521. [2] Seyedolali A. et al. 1997. *Geology* 25:787–790. [3] Boggs S. et al. 2001. *Meteoritics & Planetary Science* 36:783–793.

5228

CHICXULUB EJECTA PLUME FORMATION AND THE LINK WITH THE GLOBAL K-P BOUNDARY

T. Salge, L. Hecht, and D. Stöfler. Museum of Natural History (Mineralogy), D-10099 Berlin, Germany. E-mail: tobias.salge@rz.hu-berlin.de

Introduction: The Chicxulub target was composed of 1) an ~3 km thick sedimentary sequence, resulting in an extremely volatile-rich target, and 2) a crystalline silicate basement. A petrographic and chemical study of samples from the marine K-P site of El Guayal [1] ~520 km SE of Chicxulub and of selected samples from the UNAM-7 borehole near the crater rim [2] has been carried out.

El Guayal: An ~40 m thick carbonate megabreccia documents the failure of the Yucatán platform due to impact-induced earthquakes [1]. The overlying ~10 m thick suevite-like sequence contains shocked minerals and altered (to clay minerals) silicate melt particles. Spherulitic carbonate melts are similar to rapidly quenched feathery calcite of the Y6 crater suevite [3]. Fusion of silicate melt with carbonate-induced calcite recrystallization at >750 °C. CO₂ release is indicated by voids in silicate melt at the contact to the calcite. Accretionary lapilli <2 cm in size occur at the base of an upper 2.5 m thick subunit. They contain mainly <150 μm sized shocked and molten particles and were formed during a late stage of plume evolution in a turbulent steam-condensing environment. Multiple laminations, each with decreasing grain size, document recurring heat increase [4]. In the clay unit on top of the suevite, a PGE-enriched impactor component was deposited together with shocked quartz and carbonate melt spheroids. This provides evidence linking the Chicxulub impact with the global K-P boundary.

UNAM-7: Into the suevite of UNAM-7 307.85 m [2], altered (to clay) silicate melt particles were deposited in the liquid state as shown by reaction rims against matrix. Seawater interaction is indicated by Br, Cl, and Sr enrichment of silicate melt particles. The underlying polymict sedimentary breccia of UNAM-7 381.40 m contains polygonal to interlobate calcite spheroids indicative for deposition in a molten state. The matrix is composed of microcrystalline calcite and microcrystalline to larger/euhedral anhydrite and shows a schlieren-like flow texture. Calcite degassing is indicated in anhydrite clasts by thin schlieren of microcrystalline calcite associated with voids. These observations suggest matrix formation by exothermic reaction of decomposed calcite (CaO) with water (slaking) and subsequent back-reaction with CO₂. Hence, anhydrite precipitated from sulfate-rich fluids heated >350 °C by slaking and from silicate melt particles, analogous to processes related to VHMS deposits.

Conclusions: The following sequence of processes is suggested: 1) Vapor release by decomposition of water-saturated sediments changed ejecta distribution from ballistic to flow-like transport. 2) Ejecta plume collapse separated suevite from impactor material that had been lifted into the stratosphere. 3) Fusion of the different target components initiated hot gas-driven lateral transport in a basal flow. 4) Accretionary lapilli formed in a coherent turbulent ash cloud.

Acknowledgements: This work is part of T. S.'s Ph.D. thesis. T. S. kindly thanks P. Claeys for providing samples, R. Tagle for PGE analyses, and H. Stosnach for introduction to TXRF analyses.

References: [1] Grajales J. M. et al. 2000. *Geology* 28:307–310. [2] Urrutia-Fucugauchi J. et al. 1996. *Geofísica Internacional* 35:125–133. [3] Claeys P. et al. 2003. *Meteoritics & Planetary Science* 38:1299–1317. [4] Moore J. G. and Peck D. L. 1962. *The Journal of Geology* 70:182–193.

5206

ON PLANETESIMAL MELTING AND CHRONOLOGY

I. S. Sanders. Department of Geology, Trinity College, Dublin, Ireland. E-mail: isanders@tcd.ie

Basaltic meteorites, from their Al-Mg whole-rock model ages, were produced in a brief period between 3 and 4 million years (Myr) after CAIs [1, 2]. Since two basaltic meteorites, Sahara 99555 and Asuka-1394, have precise Pb-Pb ages of 4566.2 and 4566.5 Ma, respectively [1, 3], the popular Pb-Pb age of 4567.2 Ma for CAIs [4] poses a conundrum. Also puzzling is the ¹⁸²W anomaly in iron meteorites, which suggests that metal cores formed <1 Myr after CAIs [5].

Thermal modeling offers insights into the timing of melting. The model of [6] modified with initial ²⁶Al/²⁷Al, ⁶⁰Fe/⁵⁶Fe, and decay energies used by [2] shows the dominant effect of accretion time on the melting of a planetesimal's insulated interior. If accretion happened within about 1 Myr of CAIs, heating would have outstripped melt percolation and led to wholesale meltdown and turbulent convection in all but the outer crust [6]. Sooner rather than later, a dense iron core would have separated, with its ¹⁸²W deficit. Little evidence of this early melting survives in meteorites other than irons, possibly because the molten silicate fraction was recycled by planetesimal disruption into chondrules [7]. Where accretion happened between about 1 and 1.5 Myr after CAIs, it is likely that the rate of heating was slow enough to let basaltic partial melt segregate and reach the planetesimal surface between 3 and 4 Myr after CAIs, in agreement with the whole-rock Al-Mg ages. If accretion was 1.5–2 Myr after CAIs then heat loss would confine any melting to the planetesimal's deep interior and accretion after 2 Myr would preclude melting. By then the unspent radioactivity would have fallen below the 1.6 kJ/g needed to melt dry primitive rock [7].

Basalt production is proposed here as a new anchor for the Al-Mg, Pb-Pb, and Mn-Cr chronometers. In this case, the two Pb-Pb ages of 4566 Ma [1, 3] date eruption, making CAIs 4569.5 Ma, as shown by [1]. Also, the eucrite whole-rock Mn-Cr isochron of [8] is taken to date eruption at 4566 Ma, making "absolute" Mn-Cr ages based on the angrite anchor, LEW 86010, 1.5 Myr too young. This realignment of ages suggests that the 4567.2 Ma CAI age [4] was reset after CAI formation, and that the Pb-Pb and Mn-Cr systems in LEW 86010 may record different stages during cooling. However, the basalt anchor improves I-Xe ages [9] (Shallowater becomes 4564.8 Ma due to the 1.5 Myr shift in Mn-Cr ages) and, pleasingly, the Hf-W age of CAIs shifts by 1.5 Myr to 4569.5 Ma [5].

Finally, could some iron cores predate CAIs as hinted at by [5]? One speculative option to explore is that CAIs themselves may have a planetary origin. Could they be condensates from a large early runaway that exploded catastrophically while heating and accreting? Could the vapor pressure in its superheated, totally molten center have grown to exceed the pressure of its younger, thick, and still cool overburden?

References: [1] Baker J. et al. 2005. *Nature* 436:1127–1131. [2] Bizzarro M. et al. 2005. *The Astrophysical Journal* 632:L41–L44. [3] Amelin Y. et al. 2006. Abstract #1970. 37th Lunar and Planetary Science Conference. [4] Amelin Y. et al. 2002. *Science* 297:1678–1683. [5] Kleine T. et al. 2005. *Geochimica et Cosmochimica Acta* 69:5805–5818. [6] Hevey P. J. and Sanders I. S. 2006. *Meteoritics & Planetary Science* 41:95–106. [7] Sanders I. S. and Taylor G. J. 2005. In *Chondrites and the protoplanetary disk*. San Francisco: Astronomical Society of the Pacific. pp. 915–932. [8] Lugmair G. W. and Shukolyukov A. 1998. *Geochimica et Cosmochimica Acta* 62:2863–2886. [9] Gilmour J. D. et al. 2006. *Meteoritics & Planetary Science* 41:19–31.

5277

THERMAL OUTGASSING OF ORDINARY CHONDRITIC MATERIAL—II. SENSITIVITY STUDIESL. Schaefer¹ and B. Fegley, Jr.² Washington University, Saint Louis, Missouri, USA. ¹E-mail: laura_s@wustl.edu. ²bfegley@wustl.edu

Introduction: We modeled outgassing of ordinary chondritic (OC) material. Results for our nominal model are described in our companion abstract [1]. In this abstract, we describe the sensitivity of our nominal results to (1) variations in P and T, (2) variable volatile (H, C, N, O, S) abundances, (3) kinetic inhibition of solid solutions, (4) solubility of C and N in metal, and (5) open (versus closed) system behavior.

Methods: Our nominal model is described in [1]. In our sensitivity studies (1–4), we varied only one parameter at a time with all other parameters kept at their nominal values. Study (1): P varied from 1 to 5000 bars at constant T, and T from 100 to 1600 K at constant P. Study (2): Volatile abundances varied within the range observed in OCs. Study (3): Equilibrium calculations were allowed to produce either pure phases or ideal solid solutions. Study (4): Amounts of C and N dissolved in Fe metal were calculated. Study (5): An open system is modeled to first approximation as sequential equilibration of outgassed volatiles within a layer, removal to a higher, cooler layer, and reequilibration.

Results:

(1) At low temperatures ($T < 600$ K), variation of pressure has little effect on major gas chemistry. At higher temperatures, the CH_4 abundance decreases with decreasing pressure, whereas H_2 increases. At high T (1200 K), $\text{CO} > \text{CH}_4$ for pressures less than 10 bars. While the major gas changes with pressure, oxygen fugacity is independent of total pressure.

(2) H was varied as both H and H_2O with no difference in effect. For large H abundances, the major gas is H_2 , followed by CH_4 and H_2O . For very small H abundances, the total gas abundance drops (carbon forms graphite and/or carbides), and the major gas is N_2 . Large C abundances do not change the overall gas chemistry, but at small C abundances, methane is only important for $T < 500$ K, with H_2 and H_2O more abundant at $T > 500$ K. Variable N abundances only affected N_2 and NH_3 abundances. Varying the S abundance had no effect on gas chemistry. There was no change in gas chemistry for O = 32–38 wt%. At lower O abundances, CH_4 and H_2 were the only abundant gases, and mineral assemblages were very reduced (e.g., CaS, MgS, $\text{Si}_2\text{N}_2\text{O}$).

(3) Calculation of solid phases as either pure phases or ideal solid solutions did not effect the equilibrium gas composition.

(4) N solubility in metal was neglected in the nominal runs. When allowed, solubility of nitrogen in Fe metal is only significant at higher temperatures, where ~9% of total N_2 dissolves in γ -Fe. Even less N dissolves in Fe-Ni alloy. Roaldite (Fe_4N) did not form in any models. The amount of C dissolved in Fe metal is consistent with that observed in ordinary chondrites. When C solubility was not allowed ϵ -carbide (Fe_2C) formed instead.

(5) Outer layers of the parent body were highly enriched in volatiles in the open system calculations and hydrous phases such as mica, serpentine, talc formed. The equilibrium gas composition did not change significantly during open system outgassing.

Acknowledgements: Supported by the NASA Astrobiology, Origins, and Outer Planets Research Programs. We thank K. Lodders for helpful discussions.

References: [1] Fegley B., Jr. and Schaefer L. 2006. Abstract #5275. *Meteoritics & Planetary Science* 41. This issue.

5023

COMPARISON OF HSE IN EARTH AND MOON

G. H. Schmidt. Institute of Nuclear Chemistry, University of Mainz, Germany. E-mail: gerhard.schmidt@uni-mainz.de

The Moon can provide insight into the early development of the Earth, where the direct record of early evolution was destroyed by geological activity. Ages of polymict impactite samples show that the majority of the craters on the Moon's surface are at least 3.9 Ga old [1, 2]. During solidification of the Earth's crust, the surface was exposed to a similar flux of impacting asteroidal fragments as the Moon, adding highly siderophile elements (HSE: Os, Ir, Ru, Pt, Rh, Pd) into the crust. The abundances of the HSE Ir, Ru, and Pd in the Earth's upper continental crust (UCC) derived on impact melt sheets and impactites are about 14 ± 8 pg/g Ir, 1.0 ± 0.6 ng/g Ru, and 2.0 ± 0.5 ng/g Pd. Elemental ratios of HSE and Ni in the upper crust are highly fractionated in comparison to the Earth's mantle [3]. The abundance distribution indicates two groups of elements; 1) Os and Ir and 2) Ru, Pt, Rh, Pd, and Ni. The fractionation pattern from IIIAB iron meteorites and pallasites are comparable with a compilation of the present UCC data suggesting that the young UCC probably preserves an imprint of some of the major fractionation processes which have occurred in magmatic iron meteorites or pallasites.

The content of Ru in the UCC is in the same range as the indigenous content of 2.01 ± 0.72 ng/g Ru derived from regression in Apollo 17 aphanitic impact melt rocks [4]. Palladium in the Earth's UCC is in the same range than the indigenous content of 2.86 ± 0.94 ng/g Pd in poikilitic lunar melt rocks. It is assumed that HSE in these Apollo rocks were added from the impactor that formed the Serenitatis basin. The "indigenous" HSE components in these rocks should have been added by >3.9 Ga impact event(s). Probably the nature of the materials that have bombarded the Moon (>3.9 Ga) was similar to the material that added these elements into the crust (magmatic iron meteorites and/or pallasites?).

In comparison to the Earth's mantle, Apollo 17 impact melt rocks show different noble metal patterns (see Fig. 1) than the "late accreted materials" on Earth (e.g., Ru/Ir in the Earth's mantle is 2.01 ± 0.12 [3], in lunar melt rocks, uncorrected for indigenous Ru, the Ru/Ir ratio is 1.68 ± 0.09 [5]).

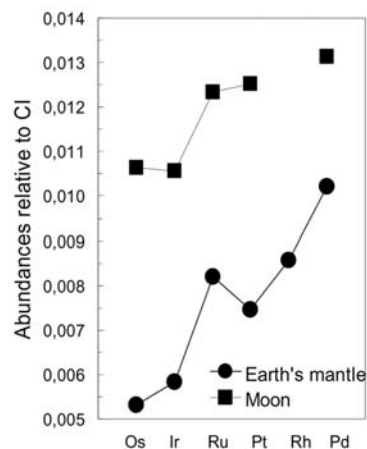


Fig. 1.

References: [1] Kirsten T. et al. 1973. Proceedings, 4th Lunar Science Conference. pp. 1757–1784. [2] Neukum G. et al. 1975. Proceedings, 6th Lunar Science Conference. pp. 2597–2620. [3] Schmidt G. 2004. *Meteoritics & Planetary Science* 39:1995–2007. [4] Puchtel I. S. et al. 2006. Abstract #1428. 37th Lunar and Planetary Science Conference. [5] Puchtel I. S. et al. 2005. Abstract #1707. 36th Lunar and Planetary Science Conference.

5052

THE DISRUPTION OF THE L CHONDRITE PARENT BODY AND THE GREAT ORDOVICIAN BIODIVERSIFICATION EVENT

Birger Schmitz. Department of Geology, Lund University, SE-22362 Lund, Sweden. E-mail: birger.schmitz@geol.lu.se

Evidence is growing in favor of that the disruption of the L chondrite parent body ~470 Ma led to a two orders of magnitude increase in the flux of extraterrestrial material to Earth during ~10–30 Myr [1–3]. Frequent impacts of large L chondritic asteroids during this period may have spurred one of the most important species diversification events in the history of life.

The most compelling evidence for an enhanced flux of extraterrestrial material is the high abundance of fossil meteorites (1–20 cm in diameter) in mid-Ordovician marine limestone in southern Sweden [1]. The meteorites are accompanied by abundant extraterrestrial chromite grains (>0.06 mm) dispersed throughout the limestone [2–3]. The stratigraphic distribution of the chromite can be reproduced in sections over 350 km distance in Sweden, and tentatively also in sections from central China. Petrographic studies of the fossil meteorites and the chemistry of meteorite-enclosed and sediment-dispersed chromite grains indicate an L chondritic origin. Cosmogenic isotopes in the chromite support an origin of the meteorites from an asteroid break-up event [4].

Considering that meteorites struck the Earth at an enhanced rate, it is likely that the same applies for large asteroids. Support for this comes from an overrepresentation in the geological record of impact craters with a mid-Ordovician age [1]. For example, of 17 known craters on the Balto-Scandian shield, four have been dated with great confidence by chitinozoan stratigraphy to the middle or early late Ordovician. The recent discovery that the resurge deposits of the Lockne impact crater are extremely enriched in L chondritic chromite [5] shows that at least one of the four mid-Ordovician craters may be related to the disruption event. This is consistent with model simulations that indicate an enhanced flux of objects to Earth during 2–30 million years after major disruption events in the asteroid belt [6].

The so-called Great Biodiversification Event during the mid- to late-Ordovician is one of the most important events in the history of life [7]. The biodiversity of invertebrates increased dramatically from a low in the Cambrian and early Ordovician to levels more similar to the present in the late Ordovician. Frequent bombardment of Earth by asteroids may have spurred these evolutionary changes. Repeated impacts created pressure on species to adapt to environmental perturbations. Previously, mid-Cenozoic faunal turnovers have been proposed to be related to a comet or asteroid shower [8], but although several craters of this age are known, there is no support from meteorite K-Ar gas retention ages for an asteroid shower of the same magnitude as in the mid-Ordovician. That impacts can have profound effects on life is obvious from the sequence of events at the Cretaceous-Paleogene boundary.

References: [1] Schmitz B. et al. 2001. *Earth and Planetary Science Letters* 194:1–15. [2] Schmitz B. et al. 2003. *Science* 300:961–964. [3] Schmitz B. and Häggström T. 2006. *Meteoritics & Planetary Science* 41: 455–466. [4] Heck P. R. et al. 2004. *Nature* 430:323–325. [5] Alwmark C. and Schmitz B. 2006. Abstract #5056. *Meteoritics & Planetary Science* 41. This issue. [6] Zappala V. et al. 1998. *Icarus* 134:176–179. [7] Webby B. D. et al. 2004. *The Great Ordovician biodiversification event*. Cambridge: Columbia University Press. 496 p. [8] Tagle R. and Claeys P. 2004. *Science* 305:492.

5330

THE Pd-Ag CHRONOMETER AND EARLY PLANETARY DIFFERENTIATIONM. Schönbächler^{1, 2}, R. W. Carlson¹, and E. H. Hauri¹. ¹Department of Terrestrial Magnetism, Carnegie Institution of Washington, 5241 Broad Branch Road, NW, Washington, D.C. 20015, USA. ²Department of Earth Sciences and Engineering Imperial College London, SW7 2AZ, UK. E-mail: marias@imperial.ac.uk

Introduction: The extinct ¹⁰⁷Pd-¹⁰⁷Ag isotope system can be used as a chronometer for the accretion and subsequent chemical differentiation of planetary bodies in a similar way as has been done with the ¹⁸²Hf-¹⁸²W system. In contrast to the refractory elements Hf and W, there is a distinct difference in volatility between more refractory Pd and moderately volatile Ag. This offers the potential not only to track metal-silicate differentiation processes but also volatility-related events.

Defining the initial ¹⁰⁷Pd abundance of the solar system is crucial for the application of the Pd-Ag system. Internal isochrons determined for iron meteorites yield initial ¹⁰⁷Pd/¹⁰⁸Pd ratios in the range of $1.5 - 2.5 \times 10^{-5}$ [1]. Whether these results reflect the initial abundance of ¹⁰⁷Pd in the solar system is unclear, because the absolute age corresponding to these internal isochrons is unknown. More recent studies suggest that the initial ¹⁰⁷Pd abundance might be up to an order of magnitude higher [2, 3]. Further work is required to solve this issue.

A complication for the Pd-Ag chronometer is that Ag has only two isotopes, which makes it difficult to correct for chemically induced mass-dependent fractionation. Mass fractionation effects in ¹⁰⁷Ag are clearly displayed in ordinary chondrites, some of which show correlated Ag and Cd [4] isotopic variation. In contrast to ordinary chondrites, the CI, CM, and oxidized CV chondrites possess the same Cd isotope composition as the Earth. In addition, carbonaceous chondrites show a considerable spread in Pd/Ag ratios (up to a factor 3) that could provide the opportunity to define a “whole rock” Pd-Ag isochron that represents a good estimate of both the initial ¹⁰⁷Pd abundance and ¹⁰⁷Ag/¹⁰⁹Ag of the solar system. By comparison with the Ag isotopic composition of the Earth, the Pd-Ag system has the potential to provide chronological constraints on the Earth's core formation.

Results: We have analyzed various chondrites including ordinary, enstatite, and carbonaceous chondrites. Six different dissolutions of Allende (CV3) yield an $\epsilon^{107}\text{Ag}$ of -0.6 ± 0.5 (2σ) relative to the NIST Ag standard. We will present additional data from CI, CM, and oxidized CV chondrites whose analysis is in progress now. The comparison of Allende with the terrestrial Ag isotope composition determined from a variety of terrestrial basalts yields—depending on the model assumption—an age for an instantaneous Earth core formation of between 10 and 29 Myr after the start of the solar system. This is consistent with evidence from the Hf-W system.

References: [1] Chen J. H. and Wasserburg G. J. 1996. In *Earth processes: Reading the isotopic code, geophysics monograph '95*, pp. 1–20. [2] Carlson R. W. and Hauri E. H. 2001. *Geochimica et Cosmochimica Acta* 65:1837–1848. [3] Woodland S. J. et al. 2005. *Geochimica et Cosmochimica Acta* 69:2153–2163. [4] Wombacher F. et al. 2003. *Geochimica et Cosmochimica Acta* 67:4639–4654.

5285

A STONY METEORITE DISCOVERED BY THE MARS EXPLORATION ROVER OPPORTUNITY ON MERIDIANI PLANUM, MARS

C. Schröder¹, R. Gellert², B. L. Jolliff³, G. Klingelhöfer¹, T. J. McCoy⁴, R. V. Morris⁵, D. S. Rodionov¹, P. A. de Souza, Jr.⁶, A. S. Yen⁷, J. Zipfel⁸, and the Athena Science Team. ¹Inst. Anorg. und Analyt. Chemie, Johannes Gutenberg-Universität, Mainz, Germany. E-mail: schroedc@uni-mainz.de. ²University of Guelph, Ontario, Canada. ³Washington University, Saint Louis, Missouri, USA. ⁴Smithsonian Institution, Washington, D.C., USA. ⁵NASA JSC, Houston, Texas, USA. ⁶CVRD Group, Rio de Janeiro, Brazil. ⁷JPL/Caltech, Pasadena, California, USA. ⁸Forschungsinstitut und Naturmuseum Senckenberg, Frankfurt/Main, Germany

Introduction: The Mars Exploration Rover Opportunity is exploring the Meridiani Planum terrain of Mars. The area is characterized by a sulfate-rich bedrock largely covered by windblown basaltic sand and a hematite lag [1, 2]. Only two large rocks (Bounce Rock and Heat Shield Rock) have been observed; they are interpreted as ejecta from a distant crater and an iron meteorite, respectively. However, numerous cobbles (here, rock fragments >1 cm) are scattered across the surface of Meridiani Planum [3]. Here we make the case for the possible meteoritic origin of one of these cobbles.

Results and Discussion: On sol 121 of its mission, Opportunity investigated an ~3 cm sized cobble at the rim of Endurance crater. The cobble named FigTree_Barberton was analyzed in situ by the Microscopic Imager (MI), the Alpha Particle X-ray Spectrometer (APXS), and the Mössbauer (MB) spectrometer. Barberton was too small to be brushed or abraded. Hence, the APXS spectra and, to a lesser degree, the MB spectra are contaminated by a thin dust covering. Owing to mission constraints, integration times for both spectrometers were limited. After subtraction of a dust component, APXS reveals a composition rich in Mg and Ni and poor in Al and Ca unlike any other material analyzed by Opportunity. The Fe-bearing mineralogy revealed in MB spectra is dominated by the mineral olivine and contains metallic Fe in the form of kamacite. Nanophase ferric oxide may be attributed to dust contamination or alteration after deposition of the rock on the surface of Mars. The presence of kamacite suggests crystallization below the IW buffer. This makes a Martian origin of Barberton unlikely, since SNC meteorites crystallized at or slightly below the QFM buffer and lack metallic Fe (e.g., [4]). Compared to a range of meteorites [5], Barberton is similar in Mg/Si, Ca/Si, and Al/Si ratios to howardites and diogenites, but enriched in S/Si, Fe/Si, and Ni and depleted in O. Mesosiderites provide a good match because they have a howardite-like silicate composition with additional metal and sulfide. Mesosiderites typically do not contain abundant olivine, although olivine diogenites are known. Imperfections in the dust correction may allow for other possibilities. In any case, it appears likely that Barberton is the first stony meteorite discovered on the surface of Mars.

References: [1] Squyres S. W. et al. 2004. *Science* 306:1698–1703. [2] Klingelhöfer G. et al. 2004. *Science* 306:1740–1745. [3] Jolliff B. L. et al. 2006. Abstract #2401. 37th Lunar and Planetary Science Conference. [4] Herd C. D. K. et al. 2001. *American Mineralogist* 86:1015–1024. [5] Nittler L. R. et al. 2004. *Antarctic Meteorite Research* 17:231–251.

5293

LARGE W-182 EXCESSES IN SILICATE INCLUSIONS OF IAB IRON METEORITES

T. Schulz^{1, 2, 3}, C. Muenker², K. Mezger³, and H. Palme¹. ¹Institut für Geologie und Mineralogie, Universität zu Köln, Zùlpicher Str. 49b, 50674 Köln, Germany. ²Mineralogisch-Petrologisches Institut, Universität Bonn, Poppelsdorfer Schloss, 53115 Bonn, Germany. ³Zentrallabor für Geochronologie, Institut für Mineralogie, Universität Münster, Corrensstr. 24, 48149 Münster, Germany

The formation of nonmagmatic iron meteorites during metal-silicate fractionation may have occurred during condensation in the solar nebula [1] or in the interior of planets and planetesimals (e.g., [2–4]). Nonmagmatic iron meteorites with silicate inclusions like the IAB-IIICD group are particularly interesting for the application of the Hf/W system as a chronometer for silicate-metal fractionation events during the early history of the solar system.

We have recently shown that silicate inclusions of four IAB iron meteorites display a very different W isotope composition than matrix and inclusion metals [6]. Both metals have ϵ_W values of around -3 and the corresponding silicates have excesses of about $+6$. One possibility to interpret the similar W-182 excesses but variable Hf/W ratios in the four silicate inclusions was to postulate a separate late stage thermal metamorphic event that reequilibrated the silicate inclusions. This event must have taken place after Hf-182 was extinct. Further analyses of separated silicates were done to evaluate whether the uniform value of $+6\epsilon$ records a maximum W-182 excess or if there are still reservoirs with higher W-182 that were not equilibrated.

The measured matrix- and inclusion metals of the IAB meteorites Lueders, Landes, and Campo del Cielo are indistinguishable from each other and range from -3.5 to $-3 \epsilon_W$ units. Newly prepared silicate separates of extremely high purity from the meteorite Campo del Cielo and Caddo County, however, yield highly radiogenic ϵ_W values of $\sim+10$ and $\sim+30$, respectively, similar to values obtained for eucrites. We suspect that these values represent Hf-182 decay in clinopyroxene, the major host phase of Hf in these inclusions.

Altogether the new results confirm that there is no complete equilibration between matrix metals and silicate inclusions in IAB iron meteorites. In some cases, the silicate inclusions may have internally equilibrated after Hf-182 was extinct, yielding less radiogenic ϵ_W . The inclusions that were not equilibrated preserved their highly radiogenic ϵ_W , thus providing time constraints on the parent body of the inclusions. Due to the very low exposure age of Caddo County (~ 5 Myr) a cosmic ray effects can be neglected.

References: [1] Wasson. 1972. Proceedings, 24th International Geological Congress. pp. 161–168. [2] Wasson et al. 1980. *Zeitschrift für Naturforschung* 35a:781–795. [3] Choi et al. 1995. *Geochimica et Cosmochimica Acta* 59:593–612. [4] Kelly et al. 1977. *Geochimica et Cosmochimica Acta* 41:93–111. [5] Kleine et al. 2005. *Geochimica et Cosmochimica Acta* 69:5805–5818. [6] Schulz et al. 2006. Abstract #1401. 37th Lunar and Planetary Science Conference.

5132

NEW DATA ON THE COOLING HISTORY OF THE H CHONDRITE PARENT BODY

W. H. Schwarz¹, M. Tieloff¹, E. V. Korochantseva^{1, 2}, and A. I. Buikin^{1, 2}.
¹University of Heidelberg, Institute of Mineralogy, Im Neuenheimer Feld 236, D-69120 Heidelberg, Germany. E-mail: Winfried.Schwarz@min.uni-heidelberg.de. ²Vernadsky Institute of Geochemistry, Kosygin St. 19, 119991 Moscow, Russia

Introduction: In the early solar system, ~4.6 Ga ago, the formation of asteroidal-sized solid bodies took place in less than 10 Ma, including the parent bodies of chondritic meteorites. Their early thermal histories have been constrained using various radiochronometer, in order to reconstruct heating mechanisms of thermal metamorphism, and structure and cooling history of their parent bodies (e.g., [1–6]).

⁴⁰Ar-³⁹Ar dating: Eight H chondrites with complete (U-Pb [5], Ar-Ar, and ²⁴⁴Pu fission track [6], MTCR [4]) chronologies indicate undisturbed cooling in a parent body heated by ²⁶Al. Here we present new ⁴⁰Ar-³⁹Ar data for different H chondrites to complement previously published ²⁴⁴Pu fission track data [6]. Repeat analyses of Guarena (H6) yielded 4428 ± 10 Ma, Mt. Browne (H6) 4486 ± 5 Ma. Dhofar 323 (H5; host and xenolith) is 4510 ± 7 Ma, the H4 chondrites Ankober, Beaver Creek, Quenggouk, and Ochansk are between 4448 ± 7 and 4526 ± 6 Ma old (constants by [7]).

Discussion: Pu fission track cooling rates and densities in merrillite and orthopyroxene correlate with the Ar-Ar age of the meteorites (in principal higher for H4 chondrites and lower for H6 chondrites), as expected for cooling models of an onion shell layered body [1, 2, 5, 6]. This conclusion holds for Guarena, Mt. Browne, Dhofar 323, Ochansk, and Beaver Creek. H6 Mt. Browne and H4 Beaver Creek were likely located close to the H6/H5 and H4/H5 boundaries. However, two H4 chondrites (Ankober and Quenggouk) have lower-than-expected absolute Pu FT densities and Ar-Ar ages, though both metallographic and Pu FT cooling rates are fast as for other H4 chondrites. We conclude that these meteorites were affected by an early impact on the parent body, thereby resetting the K-Ar clock and the Pu FTs, and subsequent fast cooling. Apparently, only part of the H4 material was affected and not redeposited into deep layers (in this case cooling would have been slow).

Conclusions: If the H chondrite parent body has been completely fragmented and reassembled affecting the interior H6 core [4], there should be meteorites with petrographic type H6, high metallographic and Pu cooling rates, and at least very high (H4-like) Ar-Ar ages. This is not the case yet, and thus it is not necessary to postulate fragmentation and reassembling of the whole parent body. Instead, the “simple” cooling of a large asteroid (with several impacts on its surface affecting only part of the H4 layer) is a viable explanation for all data presented here and in the literature (e.g., [4–6]).

References: [1] Herndon J. M. and Herndon M. A. 1977. *Meteoritics* 12:459–565. [2] Miyamoto M. et al. 1981. Proceedings, Lunar and Planetary Science Conference. pp. 1145–1152. [3] Grimm R. E. 1985. *Journal of Geophysical Research* 90:2022–2028. [4] Taylor et al. 1987. *Icarus* 69:1–13. [5] Göpel C. et al. *Earth and Planetary Science Letters* 121:153–171. [6] Tieloff M. et al. 2003. *Nature* 422:502–506. [7] Steiger R. H. and Jäger E. 1977. *Earth and Planetary Science Letters* 36:359–362.

5013

NITROGEN AND NOBLE GASES IN ALHA77005, A SMALL MARTIAN METEORITE FROM ANTARCTICA

S. P. Schwenger, S. Herrmann, and U. Ott. Max-Planck-Institut für Chemie, Joh.-J. Becherweg 27, D-55128 Mainz, Germany. E-mail: schwenze@mpch-mainz.mpg.de

ALHA77005 is a small (482.5 g) Martian meteorite found in the 1977–1978 field season in Antarctica [1] and is—also in its noble gas patterns—most closely related to LEW 88516 [2]. Its exposure age is ~3 Ma (mean of data given in [3, 4]), its terrestrial residence age (190 ± 70) ka [3]. Besides its pristine petrography, alteration assemblages (observed by [5] and most likely of terrestrial origin) are noteworthy in the discussion of its noble gas inventory. To our knowledge, no nitrogen data have been reported so far. Literature data on noble gases are: a complete set of He, Ne, and Ar data as well as concentrations of ⁸⁴Kr and ¹³²Xe are reported by [6, 7]; Kr and Xe data by [8]; and ³⁶Ar, ⁸⁴Kr, and ¹³²Xe by [9]. He, Ne, Ar, and Kr data are given by [10]; [11] focus on neon; [12] measured the whole set of 23 noble gas isotopes; and [13–15] performed Ar-Ar analyses.

Results: We measured nitrogen and noble gases on a pyroxene (26.7 mg) and an olivine (45.8 mg) separate, and report He and Ne data for a bulk sample (43.2 mg).

Helium: Comparable concentrations of ⁴He were found in all three samples: (33 ± 3) × 10⁻⁸ ccSTP/g (bulk), (29 ± 1) × 10⁻⁸ ccSTP/g (olivine), and (28 ± 6) × 10⁻⁸ ccSTP/g (pyroxene). The ratio ⁴He/³He is ~4.6, indicating the presence of cosmogenic Helium only and the complete loss of any radiogenic component.

Neon: As for ⁴He, amounts of ²²Ne agree within error in all three samples: (1.33 ± 0.10) × 10⁻⁸ ccSTP/g (bulk), (1.19 ± 0.01) × 10⁻⁸ ccSTP/g (olivine), and (1.16 ± 0.01) × 10⁻⁸ ccSTP/g (pyroxene). Our ²¹Ne/²²Ne ratios fall into the range given in the literature, but are lower than predicted from theoretical calculations for GCR neon using the production rates as function of chemistry of [16]. Following [11] we consider contributions from SCR neon as the most likely explanation.

Nitrogen: Our preliminary data give 10.0 ± 0.5 ppm of N₂ and 5.3 ± 0.3 ppm in olivine and pyroxene, respectively.

Heavy Noble Gases: In the 1600 °C step of our olivine separate, we found the highest ¹²⁹Xe/¹³²Xe ratio measured in this meteorite so far: 1.87 ± 0.05. It is accompanied by high (cosmogenic corrected) ⁴⁰Ar/³⁶Ar of 1790 ± 76. While whole rock samples seem to be compromised by elementally fractionated air contamination (cf. also [12]), our results for the mineral separates agree well with the data found for pyroxenes and olivine by [9].

References: [1] McSween H. Y. et al. 1979. *Science* 204:1201–1203. [2] Treiman A. H. et al. 1994. *Meteoritics* 29:581–592. [3] Schultz L. and Freundel M. 1984. *Meteoritics* 19:310. [4] Meyer C. 2001. *Mars meteorite compendium 2001*. [5] Smith J. V. and Steele J. M. 1984. *Meteoritics* 19:121–133. [6] Bogard D. D. et al. 1984. *Geochimica et Cosmochimica Acta* 48:1723–1739. [7] Nagao K. 1987. 12th Symposium on Antarctic Meteorites. [8] Swindle T. D. et al. 1986. *Geochimica et Cosmochimica Acta* 50:1001–1015. [9] Bogard D. D. and Garrison D. H. 1998. *Geochimica et Cosmochimica Acta* 62:1829–1835. [10] Eugster O. et al. 2002. *Meteoritics & Planetary Science* 37:1345–1360. [11] Garrison D. H. et al. 1995. *Meteoritics* 30:738–747. [12] Miura Y. N. et al. 1995. *Geochimica et Cosmochimica Acta* 59:2105–2113. [13] Jessberger E. K. et al. 1981. *Meteoritics* 16:331–332. [14] Schaeffer O. A. and Warasila R. 1981. Proceedings, 7th Lunar Science Conference. pp. 932–942. [15] Bogard D. D. and Garrison D. H. 1999. *Meteoritics & Planetary Science* 34: 451–473. [16] Leya I. et al. 2000. *Meteoritics & Planetary Science* 35:259–286.

5353

METEORITICAL AND DYNAMICAL CONSTRAINTS ON FORMATION MECHANISMS FOR ASTEROIDS AND PLANETS

Edward R. D. Scott. HIGP, University of Hawai'i at Manoa, Honolulu, Hawai'i 96822, USA. E-mail: escott@hawaii.edu

How, when and where did asteroids form? Recent advances in integrating radiometric ages from long and short-lived isotopes [1] and thermal modeling [2] provide a new framework for understanding planetesimal formation and suggest that the thermal histories of meteorite parent bodies are closely linked to their formation times and locations. Chondrule ages and properties show that chondrites accreted intermittently from diverse batches of chondrules and other materials over a 4 Myr period starting 1 Myr after CAI formation [3, 4]. Iron meteorites and achondrites come from bodies that accreted earlier, when ^{26}Al was more abundant [5, 6]. Two different accretion mechanisms have been offered to account for the long time scale of chondrule formation. 1) Chondrules accreted to the surface of preexisting bodies (e.g., [7]). 2) Differentiated and chondritic parent bodies formed in separate locations at different times. The latter is more consistent with meteorite evidence and requires a revision in the starting conditions inferred for dynamical models of planet formation to allow planetesimal formation to last 5 Myr. Formation of differentiated and chondritic bodies in separate locations can be accommodated if most irons formed inside 2 AU, as Bottke et al. [8] proposed; rare C-rich differentiated meteorites like ureilites and IAB irons may have formed simultaneously beyond 3 AU. Chondrite parent bodies formed subsequently in the gap between these two locations. If planetary embryos formed in under 1 Myr at 1 AU, they would have excited nearby planetesimals and prevented late-forming bodies from accreting near early-formed bodies.

Formation of Jupiter: Dynamical models suggest that asteroids could not have accreted in the main belt if Jupiter formed before the asteroids, as some chondrule-formation models imply [7, 9]. Jupiter therefore reached its current mass >3–5 Myr after CAIs formed. This precludes formation of Jupiter via a gravitational instability <1 Myr after the solar nebula formed [9], and strongly favors core accretion models for the giant planets.

Other Planetary Systems: Extrasolar planets have unusual orbits compared to solar giant planets, which may reflect differences in formation times. Planets that form quickly could interact gravitationally with more massive disks and migrate faster and further. In addition, early formed planets would be more susceptible to orbital perturbations caused by close approaches of sibling protostars, as these become less frequent over time.

References: [1] Kita N. T. et al. 2005. In *Chondrites and the protoplanetary disk*. San Francisco: Astronomical Society of the Pacific. pp. 558–587. [2] Hevey P. J. and Sanders I. S. 2006. *Meteoritics & Planetary Science* 41:95–106. [3] Amelin Y. et al. 2002. *Science* 297:1678–1683. [4] Krot A. N. et al. 2005. *Nature* 436:989–992. [5] Kleine T. et al. 2005. *Geochimica et Cosmochimica Acta* 69:5805–5818. [6] Bizzarro M. et al. 2005. *The Astrophysical Journal* 632:L41–L44. [7] Weidenschilling S. J. et al. 1998. *Science* 279:681–684. [8] Bottke W. F. et al. 2006. *Nature* 439:821–824. [9] Boss A. P. and Durisen R. H. 2005. *The Astrophysical Journal* 621:L137–L140.

5251

THE MAGMATISM ON MARS INFERRED FROM CHEMICAL COMPOSITIONS OF MARTIAN METEORITES

N. Shirai and M. Ebihara. Department of Chemistry, Graduate School of Science, Tokyo Metropolitan University, Hachioji, Tokyo 192-0397, Japan. E-mail: shirai@comp.metro-u.ac.jp

Introduction: Martian meteorites are divided into four major groups; shergottites, nakhlites, chassignites, and ALH 84001. An idea that Martian meteorites were derived by remelting a common mantle source at different times is controversial [1]. To understand the linkage among Martian meteorites should provide us insights in considering the petrogenetic processes and magmatism on Mars. We conducted a chemical study of Martian meteorites to place constraints on the petrogenesis for Martian meteorites based on their chemical compositions.

Analytical Procedures: We used three nuclear analytical methods (PGA, INAA, and IPAA) and ICP-MS to determined major, minor, and trace elements in Martian meteorites.

Result and Discussion: La/Th ratios are found to increase with decreasing La/Yb ratios among shergottites. However, nakhlites and chassignites are not on this observed trend. Given bulk partition coefficients for dominant minerals of the Martian mantle (olivine, pyroxene, and garnet) [2], igneous processes involving such dominant minerals cannot produce the chemical characteristics for nakhlites and chassignites. Shirai and Ebihara [3] suggest that igneous processes involving apatite, epidote, and/or zircon control the fractionation of La/Th and La/Yb for nakhlites and chassignites.

Using a multi-stage evolution model proposed by [4], we reported that majorite is responsible for chemical characteristics (Hf/Sm and La/Yb ratios) in Martian meteorites [5]. However, La/Th ratios for nakhlites cannot be produced by igneous process involving majorite. To overcome such a difficulty, we constructed the following petrogenetic processes based on a multi-stage evolution model. At the first stage, the majorite cumulate formed during the differentiation of Martian magma ocean at 4.553 Ga, only 13 Ma after the solar system formation. At the second stage, the majorite cumulate was partially melted and the produced melt crystallized at 4.0 Ga. At the nakhlites' crystallization age (1.26–1.37 Ga), partial melting of the crystallized melt formed at 4.0 Ga occurred. The produced melt and residue represent nakhlites and shergottites (QUE 94201, Y-980459, DaG 476, SaU 005, and Dho 019), respectively. Assuming that majorite was the only mineral present until 4.0 Ga and that clinopyroxene and an accessory mineral (zircon, epidote, and apatite) constituted the precursor material for Martian meteorites at the subsequent igneous process, we calculated chemical compositions of the melt and the solid (residue) produced at each stage. Our results suggest that zircon is responsible for the fractionation of La and Th in nakhlites. However a multi-stage evolution model doesn't explain chemical compositions of olivine-phyric shergottites. Thus, being different the inference from Nd isotopic compositions, chemical compositions of Martian meteorites support an idea of distinct multiple mantle sources.

References: [1] McSween H. Y. 2002. *Meteoritics & Planetary Science* 37:7–25. [2] Longhi et al. 1992. *Mars* 184–208. [3] Shirai N. and Ebihara M. Forthcoming. [4] Shih. C.-Y. et al. 1999. *Meteoritics & Planetary Science* 34:647–655. [5] Shirai N. and Ebihara M. 2005. *Meteoritics & Planetary Science* 40:A140.

5057

AIRBURSTS IN THE EARTH'S ATMOSPHERE: APPLICATION TO THE 1908 TUNGUSKA EVENT

V. V. Shuvalov. Institute for Dynamics of Geospheres RAS, Leninsky pr. 38-1, 119334 Moscow, Russia. E-mail: shuvalov@idg.chph.ras.ru

The Tunguska event [1] that occurred in 1908 was the largest aerial burst induced by asteroidal (or cometary) impact and recorded in human history. The term “aerial burst” defines a variety of impacts which do not produce craters, but produce strong atmospheric (radiation, shock waves, acoustic-gravity waves) and possibly surface (devastations and fires) effects. There are good reasons to believe that Tunguska-like and much larger aerial bursts continuously occurred during geological history.

Three types of air bursts can be considered: surface impact (when a hot jet or fireball touches the ground), Tunguska-like phenomena (when a jet or fireball does not reach the ground but produces fires and devastation), and meteor-like phenomena (when there is a bright flash but no surface effects). The purpose of this work is to study numerically the influence of impact angle and projectile properties (velocity and density) on the processes accompanying aerial burst.

I modeled the impacts of spherical stony and cometary projectiles of different sizes (from 20 to 1000 m) at velocities $U = 50$ and 20 km/s. Impact angles were 90 , 45 , 30 , 15 , and 5 degrees (to horizon).

To perform numerical simulations, I used the model developed by Shuvalov and Artemieva [2]. For all trajectory angles α , I numerically solved a 2-D problem with effective atmospheric scale height $H/\cos(\alpha)$, where H is the normal atmospheric scale height. Initial altitude (at $t = 0$) was 70 km.

Numerical simulations show that in all the cases under consideration the projectile begins to deform under increasing aerodynamic loading forming a typical pancake-like structure, then it transforms into a debris jet consisting of meteoroid vapor, fragments, and shock-compressed air. After total evaporation of projectile debris, a gaseous jet consisting of vapor and hot air is formed. An important feature is that the disruption and total evaporation of a projectile occurs at a high velocity which is close to the pre-entry velocity. This scenario is typical for both cometary and stony meteoroids.

The impact velocity very slightly influences the altitude of projectile disruption and deceleration. The influence of projectile density is much stronger. A 100 m diameter cometary projectile with a density of 0.9 g/cm³ produces approximately the same effect as a 100 m diameter stony projectile with a density of 3.5 g/cm³. The impact angle is also an important parameter. Solid fragments of cometary meteoroids with initial diameter exceeding 70 m reach the ground in a vertical impact whereas a 1000 m diameter comet burns totally in the atmosphere in a very oblique 5° impact.

Numerical simulations show that 30 – 45° oblique impacts of both a 60 m diameter stony meteoroid and a 100 m diameter cometary meteoroid produce effects similar to those observed in the 1908 Tunguska event.

Acknowledgements: This publication is based on work supported by Award No. RUG-2655-MO-05 of the U.S. Civilian Research and Development Foundation.

References: [1] Vasilyev N. A. 1998. *Planetary and Space Science* 46: 129–150. [2] Shuvalov V. V. and Artemieva N. A. 2002. *Planetary and Space Science* 50:181–192.

5240

STATISTICAL ASSESSMENT OF MAJOR ELEMENT COMPOSITION OF MOLDAVITES FROM THE CHEB BASIN

R. Skála. Institute of Geology, Academy of Sciences of the Czech Republic, Rozvojová 269, CZ-16500 Praha 6, Czech Republic. E-mail: skala@gli.cas.cz

Introduction: The Tertiary and Quaternary sediments of the Cheb Basin are known as one of the sites where Central European tektites are found in a considerable amount. Up to now, between 1200 and 1500 individual pieces were found there. This constitutes the third most prominent source of moldavites known. The areas in and around the Cheb Basin can be considered a separate subfield. This subfield is the closest one to the source crater of moldavites—the Ries impact structure.

Samples and Data Processing: For the current study, a total of 24 moldavites from the Cheb Basin were selected. As a reference, a set of 12 moldavites from three different South Bohemian localities and three Moravian moldavites were chosen. All these samples were prepared as polished (thin) sections and analyzed with an electron microprobe for major elements. Later multivariate statistical tests allowed to exclude outliers. The data with outliers left out were subsequently processed with the statistical packages SYSTAT (version 11).

Factor Analysis was carried out separately for the data collected for the samples from the Cheb Basin and those for South Bohemian and Moravian moldavites. Both groups of moldavites, applying the Keiser criterion, produce two-dimensional factor loading plots with three distinct clusters. These three components accounted for 84% of the total variance in the case of Cheb moldavites and for 82% in the case South Bohemian and Moravian samples. Individual clusters for the samples from the Cheb Basin consist of: (1) SiO₂, (2) TiO₂, Al₂O₃, FeO, and Na₂O, and (3) CaO, MgO, and K₂O. For other group of samples, however, the results differ: factor loadings are somewhat rotated and, more importantly, K₂O groups with cluster (2) instead of (3); which is identical to the data given in [1].

Cluster Analysis provided a few relatively well-defined and separated groups. The largest distance from remainder of the data was recorded for three samples (Chlum, Jankov, and Štěpánovice). Other samples are well clustered with very small mutual distances—one of the clusters contains almost exclusively the samples from the Cheb Basin whereas the remaining samples are mixed in other cluster.

Conclusions: Factor analysis showed striking difference between the chemical composition of Cheb moldavites and moldavites from remaining part of the moldavite strewn field on the Czech Republic territory. It possibly reflects different composition of the source material. Simultaneously, cluster analysis revealed that some of the Cheb moldavites are chemically close to those from South Bohemia.

Acknowledgements: This work was funded by the grant of the Czech Science Foundation (GAČR) No. 205/05/2593 and falls within the research plan AV0 Z30130516 of the Institute of Geology AS CR.

References: [1] Delano J. W. et al. 1988. *Proceedings, 2nd International Conference on Natural Glasses*. pp. 221–230.

5238

“THE CURATOR’S DILEMMA” REVISTED—CHALLENGES FOR METEORITE COLLECTIONS IN THE 21st CENTURY

C. L. Smith¹ and L. C. Welzenbach². ¹Department of Mineralogy, The Natural History Museum, Cromwell Road, London, SW7 5BD, UK. E-mail: C.L.Smith@nhm.ac.uk. ²Department of Mineral Sciences, National Museum of Natural History, Smithsonian Institution, Washington, D.C. 20560-0119, USA

Introduction: The article “The Curator’s Dilemma” was published in *Meteoritics* nearly 30 years ago [1]. With the advent of new investigative techniques, new avenues of research, and important new curatorial methods, it is timely to restate the challenges faced by meteorite curators. M. H. Hey [1] described the greatest challenge of collection curation as “two diametrically opposed duties: On the one hand, [the curator] must make material available for research and study, and on the other, he must preserve the material in his care for enjoyment and study by future generations.” He goes on to outline seven criteria in order to strike a balance, all of which are still appropriate and applicable today.

The Challenges: *The cost of doing business:* For more than 100 years, our collections have been providing meteorites to the scientific community. Evolving technology, new areas of research, and the sheer number of scientific investigations place significant demands on dwindling or even nonexistent museum resources, especially for collections that are very small relative to most museum populations. Those same new research fields may impact storage practice and accessibility. For example, samples stored in a Teflon bag may affect C isotope studies in astrobiological investigations. More research is needed to identify the effects of storage practices on the meteorites. Ideally we would apply clean room models for storage and handling, but must consider accessibility as well as cost. A solution may be to use limited clean room storage for samples where terrestrial contamination is the most detrimental to scientific studies, e.g., SNCs, carbonaceous chondrites.

Acquisition of new meteorites has also evolved from a century ago. We now compete against a large population of collectors for smaller amounts at greater expense. More meteorites on the market enables us to broaden the range of meteorite types in our collections, but smaller quantities require a more detailed approach to sample allocation. First we direct the investigator to institutions with main masses. We use our broad understanding of the different investigative methods and techniques used to ensure that allocation of rare and limited material is resolving a fundamental problem. Although modern techniques allow for detailed information (e.g., about single isotopes or unique compounds) to be gathered from small fragments of material, the curator would like to see coordinated studies, allowing for as much information to be gathered from the material as possible.

Information management has become one of the foremost tools used for accountability, strategic planning, and collections management. The NHM and NMNH manage the meteorite inventory and publication information with the “EMU” database system. The power and flexibility of EMU allows us to develop new policies and procedures that help us address our diametrically opposed duties as well as streamlining requirements of accountability and providing us with quick reference to information for the increasing number of diverse and complex requests.

References: [1] Hey M. H. 1969. *Meteoritics* 4:253–255.

5042

SIMULTANEOUS ACCRETION OF DIFFERENTIATED OR METAMORPHOSED ASTEROIDAL CLASTS AND CHONDRULES

A. K. Sokol and A. Bischoff. Institut für Planetologie, Wilhelm-Klemm-Str. 10, 48149 Münster, Germany. E-mail: sokola@uni-muenster.de

The idea that certain meteorites represent samples of “second-generation” parent bodies (daughter asteroids) formed after collisional destruction of “grandparent” planetary bodies has been discussed earlier (e.g., [1–3]). Recent high-precision Hf-W and Al-Mg isotopic studies on differentiated meteorites indicate that differentiation on planetesimals occurred early, within ~3 Ma of the start of the solar system (e.g., [4–6]). Thus, accretion of differentiated planetesimals predated that of undifferentiated planetesimals. Chondrites derive from relatively late formed planetesimals that may have formed by reaccretion of debris produced during collisional disruption of first-generation planetesimals.

Increasing evidence is found for accretion of metamorphosed or differentiated planetesimal clasts with chondrules at a time, when chondrite parent bodies formed. In the case differentiated and metamorphosed “precursor” asteroid were destroyed prior to chondrites parent body formation, fragments of these earlier bodies may have been mixed with later formed chondrules and should exist in type III or other primitive chondrites.

In some of the most primitive chondrites (Krymka, Adrar 003, Acfer 094), we have found unusual fragments, which seem to have suffered thermal metamorphism. They look like typical type VI lithologies, having 120° grain boundary junctions. In contrast to their host rocks all these inclusions show a homogeneous composition of minerals. They are chemically equilibrated. Most of them also contain coarse-grained plagioclases.

Some other observed clasts have igneous textures. Granitoid and andesitic fragments in the ordinary chondrites Adzhi-Bogdo and Study Butte [7, 8] indicate mixing of achondritic fragments and chondritic components. Also, the dark inclusions in CR and CH chondrites may be excellent witnesses to document formation of the final parent body by secondary accretion [3, 9].

The existence of phases with high Al/Mg ratios in the observed inclusions offers a possibility for dating the time difference between the formation of these clasts and chondrules or CAIs using the Al-Mg chronometer. This work is in progress.

References: [1] Hutchison R. 1996. In *Chondrules and the protoplanetary disk*. Cambridge: Cambridge University Press. pp. 311–318. [2] Bischoff A. 1988. *Meteoritics & Planetary Science* 33:1113–1122. [3] Bischoff A. and Schultz L. 2004. *Meteoritics & Planetary Science* 39:A15. [4] Bizzarro M. et al. 2005. *The Astrophysical Journal* 632:L41–L44. [5] Baker et al. 2005. *Nature* 436:1127–1131. [6] Kleine T. 2005. *Geochimica et Cosmochimica Acta* 69:5805–5818. [7] Bischoff A. et al. 1993. *Meteoritics* 28:570–578. [8] Fredriksson K. et al. 1989. *Zeitschrift für Naturforschung* 44a:945–962. [9] Bischoff A. et al. 2006. In *Meteorites and the early solar system II*. Tucson, Arizona: The University of Arizona.

5179

PERCOLATION OF Fe-FeS MELTS THROUGH AN OLIVINE MATRIX. A STUDY WITH A CENTRIFUGING PISTON CYLINDER

G. Solferino¹, N. Bagdassarov², and M. W. Schmidt¹. ¹Institute for Mineralogy and Petrology, ETH Zurich, Switzerland. E-mail: solferino@erdw.ethz.ch. ²Institut fuer Geowissenschaften, J. W. Goethe Universitaet

Theories about the formation of the Earth's core postulate the segregation of molten iron-sulfide material through solid silicates [1]. The efficiency of this mechanism has not yet been proved and is still under discussion. The present study aims to establish the percolation threshold [2] for a simplified composition representative of the Earth's core and silicate mantle and to verify whether and under which conditions buoyancy-driven segregation of such melts is a feasible process. Starting materials are iron-sulfide powder (on the eutectic composition of the Fe-FeS system) mixed with natural (S. Carlos) olivine powder. Experiments were performed in a standard end-loaded piston cylinder and in the newly developed centrifuging piston cylinder. With the centrifuging piston cylinder it is possible to spin a small press (standard 14 mm diameter, salt-pyrex assembly) to a maximum speed of 2900 rpm (equivalent to an acceleration of 3000 g) at experimental conditions to 1.5 GPa and 1300 °C.

A series of static and centrifuge experiments were performed using iron-sulfide plus olivine mixtures in double Pt-Graphite capsules (highly reducing conditions). No oxygen was detected in the melt pools (EDS measurements performed with an EMPA, Jeol JXA-8200) after the experiments. BSE images of quenched samples show interconnection of the melt in samples with 20 vol% of iron-sulfide, whereas at 10 vol% the melt is located in isolated pockets and in triple junctions. Centrifuge experiments were performed with mixtures containing 20 vol% of melt in an olivine matrix and an additional thin layer of pure iron-sulfide on top of the olivine-melt. No sign of a melt displacement towards the bottom of the capsule was observed, although theory predicts melt segregation velocities of about 40 mm/h at 100 g [3]. A reason for this behavior could be a high surface tension of the metallic-anionic melt that hinders its mobility in the inter-grain space. In a different series of centrifuge experiments, on olivine plus silicate melt, we have shown, that melt segregates (towards the top of the capsule), proving that the experimental set-up is proper to study percolation in partially molten systems. Thus, the absence of segregation for the iron-sulfide melt cannot be ascribed to an experimental flaw.

In conclusion, percolation of metallic-rich melts through a solid silicate matrix does not seem a plausible mechanism for core formation in terrestrial planets (at least in absence of shear deformation) at reducing conditions.

References: [1] Ringwood A. E. 1990. In *Origin of the Earth and Moon*. pp. 101–134. [2] von Bagen N. and Waff H. S. 1986. *Journal of Geophysical Research* 91:9261–9276. [3] McKenzie D. 1989. *Earth and Planetary Science Letters* 95:53–72.

5165

THE GLUE THAT BINDS: CONSOLIDATION PROCESSES FOR PLANETARY MATERIALS

J. G. Spray. Planetary and Space Science Centre, Department of Geology, University of New Brunswick, 2 Bailey Drive, Fredericton, New Brunswick, E3B 5A3, Canada. E-mail: jgs@unb.ca

Introduction: On Earth, the transformation of unconsolidated sediment (e.g., sand) to rock (sandstone) occurs via the process of lithification. Lithification typically occurs via burial within the upper crust at <150 EC, at depths <5 km in the presence of liquid H₂O. Liquid H₂O is critical to the process of lithification because it is the transporting medium for dissolved and suspended ions and mineral species, which eventually precipitate as a cement that binds the unconsolidated grains. Lithification also applies to sedimentary deposits formed by precipitation of minerals from aqueous solutions at surface, or near-surface, conditions (e.g., to generate sulfate or carbonate-rich evaporite rocks). However, for many planetary bodies in our solar system, there are no large sources of liquid H₂O to facilitate the lithification process. Despite the absence of water on such bodies, the development of consolidated fragmental material is commonplace. This material, typically in the form of breccias, is a relatively coherent rock, yet the nature of the “glue” that binds the fragments is not well understood. Clearly, other processes are responsible for the lithification that we take for granted in the sedimentary rocks developed on our wet planet. This work explores these processes.

Ices and Melts: For certain planetary bodies, unconsolidated material may be bound by ices, such that it possesses rock-like properties in terms of strength and behavior. In the absence of H₂O, unconsolidated semi-molten material can be lithified by welding and compaction (e.g., certain pyroclastic discharges that fall and accumulate to form ignimbrites). This requires the production of hot volcanogenic or impact ejecta.

Consolidation Processes: In this work, we explore the nature of the binding medium in different types of lunar breccia collected during the Apollo 15, 16, and 17 missions, in meteorites of the howardite, eucrite, and diogenite (HED) class and in laboratory-shocked lunar regolith samples [1, 2]. Analytical scanning electron microscopy (SEM) and field emission SEM are used to explore the microstructures. The samples are grouped as: 1) being primarily derived from unconsolidated lunar regolith; 2) impact melt rocks, and 3) samples that were primarily derived from solid rock that were impact brecciated. There is a significant overlap between these groups. Features that affect the cohesiveness and coherence of the rock are given particular attention. For this study, bridges are necks between grains, intergranular melts are melts that have between grains, fused grains are grains that are joined at a contact interfaces with no visible neck, and annealed fractures are fractures that have been partially or totally closed by either diffusion across the fracture or melting either side of the fracture. The various mechanisms of lithification are explored and discussed. Localized shock heating appears to be the dominant welding process.

References: [1] Schaal R. B. et al. 1979. Proceedings, 10th Lunar and Planetary Science Conference. pp. 2547–2571. [2] Schaal R. B. and Hörz F. 1980. Proceedings, 11th Lunar and Planetary Science Conference. pp. 1679–1695.

5123

ANALOGOUS EXPERIMENTS ON CHONDRULE FORMATION USING RAPID IR-LASER HEATING

T. Springborn¹, T. Poppe¹, C. Güttler¹, J. Blum¹, and J. Wasson². ¹Institute für Geophysik und extraterrestrische Physik, Technische Universität Braunschweig, Mendelssohnstr. 3, 38106 Braunschweig, Germany. E-mail: t.springborn@tu-bs.de. ²Institute for Geophysics and Planetary Physics, University of California–Los Angeles, 405 Hilgard Avenue, Los Angeles, California 90095–1567, USA

Introduction: Chondrules witnessed an energetic process that a large fraction of solar system material underwent in the time of planet formation. The chondrule precursors were porous dust aggregates composed of micrometer-sized major silicate and minor grains together with recycled chondrules. Chondrules formed by rapid melting by an unknown process in free space followed by rapid cooling. To investigate the formation conditions of first-generation chondrules, we have started an experimental study aiming at the transformation of porous dust samples to melt spherules via IR-laser irradiation. We use dust samples of micrometer-sized grains of iron, SiO₂, obsidian, albite, fayalite, and peridot, and mixtures thereof. The samples, which have a typical mass of 2 mg, are irradiated for up to 10 seconds by a 30 W IR laser at ambient air pressures between 1 bar and 10⁻⁵ mbar. In some experiments the samples cooled in free fall.

First Results: A few samples (SiO₂) were not transformed because too little radiation was absorbed and some samples exploded. In most samples, 10–80% of the initial material was thermally processed. In about 50 experiments, spherules of chondrule size were formed, after some experiments even several spherules were found. We embedded some samples in epoxy resin and sectioned them, prior to microscopy. The samples analyzed so far are often porous, some contain large bubbles, and mostly, melting had not been complete but occurred to a varying extent. Assuming that roughly 2 kJ/g are required for melting [1], a first estimate of the energetic efficiency (energy consumed for melting/heating energy) is in the order of 1%.

Conclusions: For the first time, we produced chondrule-sized melt spherules from aggregates of micrometer-sized dust grains by electromagnetic radiation heating under conditions relevant for the formation of first-generation chondrules. However, unlike chondrules, most spherules produced up to now are porous or contain large bubbles. The experimental study is still in progress, and a final assessment will only be possible after further experiments.

References: [1] Wasson J. T. 1996. In *Chondrules and the protoplanetary disk*. Cambridge: Cambridge University Press. pp. 45–54.

5338

THE DISTRIBUTION OF INCLUSIONS IN A SINGLE LARGE PRESOLAR SILICON CARBIDE GRAIN

F. J. Stadermann¹, T. Stephan², A. S. Lea³, and C. Floss¹. ¹Laboratory for Space Sciences, Washington University, Saint Louis, Missouri 63130, USA. E-mail: fjs@wustl.edu. ²Institut für Planetologie, Universität Münster, 48149 Münster, Germany. ³Pacific Northwest National Laboratory, Richland, Washington 99352, USA

The Murchison LS+LU presolar grain separation fraction contains large SiC grains with sizes above 2 μm [1]. A previous study of this SiC size fraction found two morphological types: irregular to round grains and blocky grains with flat surfaces [2]. We have performed detailed elemental and isotopic characterizations of a single 15 μm × 20 μm SiC grain of the latter type. We used complementary imaging techniques of SEM, NanoSIMS, ToF-SIMS, and Auger spectroscopy to determine the types and distributions of various inclusions in this unusually large SiC grain.

An initial NanoSIMS bulk C and N isotopic measurement of this particle identifies it as a likely mainstream type of SiC grain (e.g., [3]) with ¹²C/¹³C = 54.1 ± 0.1 and ¹⁴N/¹⁵N = 447 ± 26. Subsequent O imaging yielded a low secondary ion signal, but indicated a heterogeneous distribution of numerous submicrometer spots with elevated O signals. These spots were clearly correlated with minute inclusions that were brought to the surface and then rapidly consumed by the primary ion beam sputtering. The O isotopic compositions of all spots, as well as the integrated composition of the remainder of the SiC are normal within errors. This indicates that the measured O may not be indigenous to the particle and that the O yield in the vicinity of inclusions may be artificially enhanced, similar to what has been observed in studies of internal grains within presolar graphites [4].

In an effort to determine the nature of the inclusions, we examined the particle with ToF-SIMS, in both positive and negative secondary ion modes, and with scanning Auger spectrometry. The latter technique for high spatial resolution elemental imaging is an ideal complement to NanoSIMS isotopic imaging measurements, because the volume of material analyzed by both techniques is virtually identical [5–7].

Imaging of the surface of the SiC grain showed Ti-V hotspots, which are likely to be TiC inclusions, as has been observed elsewhere [8]. We also observed hotspots of Al and of (not spatially correlated) Ca. Some of the inclusions appear to be correlated with steps or boundaries within the SiC grain structure. We will continue with another round of NanoSIMS measurements to determine the isotopic composition of the inclusions.

Acknowledgements: Some of the Auger measurements were performed with the PHI 700 demonstration instrument at Physical Electronics in Chanhassen, Minnesota.

References: [1] Amari S. et al. 1994. *Geochimica et Cosmochimica Acta* 58:459–470. [2] Virag A. et al. 1992. *Geochimica et Cosmochimica Acta* 56:1715–1733. [3] Meyer B. S. and Zinner E. 2006. In *Meteorites and the early solar system II*. Tucson, Arizona: The University of Arizona Press. [4] Stadermann F. J. et al. 2005. *Geochimica et Cosmochimica Acta* 69:177–188. [5] Stadermann F. J. et al. 2005. *Meteoritics & Planetary Science* 40: 146. [6] Stadermann F. J. et al. 2006. Abstract #1663. 27th Lunar and Planetary Science Conference. [7] Floss C. et al. 2006. *Geochimica et Cosmochimica Acta* 70:2371–2339. [8] Stroud R. M. and Bernatowicz T. J. 2005. Abstract #2010. 26th Lunar and Planetary Science Conference.

5344

MINERALOGY AND PETROLOGY OF COMET WILD-2 NUCLEUS SAMPLES—FINAL RESULTS OF THE PRELIMINARY EXAMINATION TEAM

Stardust Mineralogy/Petrology Subteam: Michael Zolensky¹, Phil Bland², John Bradley³, Adrian Brearley⁴, Sean Brennan⁵, John Bridges⁶, Donald Brownlee⁷, Anna Butterworth⁸, Zurong Dai³, Denton Ebel⁹, Matt Genge², Matthieu Gounelle¹⁰, Giles Graham³, Jeff Grossman²⁸, Lawrence Grossman¹¹, Ralph Harvey¹², Hope Ishii³, Anton Kearsley¹³, Lindsay Keller¹, Alexander Krot¹⁴, Falko Langenhorst²⁷, Antonio Lanzirotti¹⁵, Hugues Leroux¹⁶, Graciela Matrajt⁷, Keiko Messenger¹, Takashi Mikouchi¹⁷, Tomoki Nakamura¹⁸, Kazumasa Ohsumi¹⁹, Kyoko Okudaira²⁰, Murielle Perronnet¹, Frans Rietmeijer⁴, Steven Simon¹¹, Thomas Stephan²¹, Rhonda Stroud²², Mitra Taheri²², Kazu Tomeoka²³, Alice Toppani³, Peter Tsou²⁴, Akira Tsuchiyama²⁵, Michael Velbel²⁹, Iris Weber²¹, Mike Weisberg²⁶, Andrew Westphal⁸, Hajime Yano²⁰, and Thomas Zega²². ¹NASA JSC. E-mail: michael.e.zolensky@nasa.gov. ²Imperial College. ³Lawrence Livermore National Laboratory. ⁴University New Mexico. ⁵SLAC. ⁶Open University. ⁷University of Washington. ⁸University of California–Berkeley. ⁹American Museum of Natural History. ¹⁰Muséum National D'Histoire Naturelle. ¹¹University of Chicago. ¹²Case Western Reserve University. ¹³Natural History Museum. ¹⁴University of Hawai'i. ¹⁵Brookhaven National Lab. ¹⁶University Sciences et Technologies de Lille. ¹⁷University of Tokyo. ¹⁸Kyushu University. ¹⁹Inst. Materials Structure Science-KEK, 20JAXA-ISAS. ²¹University Münster. ²²Naval Research Lab. ²³Kobe University, 24JPL. ²⁵Osaka University. ²⁶Kingsborough Community College. ²⁷Inst. für Geowissenschaften. ²⁸US Geological Survey. ²⁹Michigan State University

Introduction: The sample return capsule of the Stardust spacecraft was successfully recovered in northern Utah on January 15, 2006, and its cargo of coma grains from Comet Wild-2 has now been the subject of intense investigation. This presentation will present the “final” results from the mineralogical and petrological analyses that will have been performed.

Mineralogy/Petrology: Although one month does not appear to be much time, it has been sufficient to permit numerous analyses (E-beam, Synchrotron XRD, spectroscopy, etc.) to have been performed to permit some understanding of the following fundamental sample issues:

1. Comet nucleus mineralogy and petrology, and grain physical properties
2. Sample variability
3. Type and degree of sample alteration by the collection process, and subsequent sample handling
4. Sample documentation and handling procedures
5. Comparisons to what was reported by the Deep Impact Mission to Comet Temple 1

Future of the Samples: Following the close of sample preliminary examination, Stardust samples will be made available to the larger community as are lunar samples, IDPs, and Antarctic meteorites. A sample “catalog” will be available at the JSC Curation website (<http://curator.jsc.nasa.gov/stardust/index.cfm>). A dedicated peer review committee will consider all sample requests. The Stardust interstellar tray is being scanned in the Cosmic Dust Laboratory; when this operation is complete (~Christmas 2006) the Cosmic Dust Laboratory will be reopened for business.

5139

TIME-DEPENDENT ENRICHMENT OF URANIUM IN OMAN DESERT CHONDRITES

Ch. Stenger¹, U. Krähenbühl¹, and B. A. Hofmann². ¹Department of Chemistry and Biochemistry, University of Bern, Freiestr. 3, 3012 Bern, Switzerland. E-mail: ch_stenger@students.unibe.ch. ²Natural History Museum Bern, Bernastr. 1, 3005 Bern, Switzerland

Introduction: Surfaces of chondritic meteorites collected in the deserts of Oman in 2001–2003 are exposed to the often much higher concentrations of elements of interest in the desert soils. In the case of uranium, the abundance levels for the soils are about 500 times higher than the one measured for chondrites. The enrichment of this element found on the surface on meteorites and its diffusion into the interior are investigated.

Experiments: Three H chondrite finds of similar size were studied for their uranium concentrations showing different degrees of weathering (W1, W2, W4) and having terrestrial ages of 5500, 18,700, and >50,000 years, respectively. A slice of 10 mm was cut out of the meteorites. Out of these slices, rods were cut and the rods divided into pieces. Pieces making up about 1 g were ground in a tungsten carbide ball mill and sieved to a size fraction finer 25 µm. The finest dust (<12 µm) was removed by sedimentation in acetone. Of the resulting size fractions 200 mg were contacted with 0.6 ml 40% nitric acid for 1 hour. The measurement of the released uranium by leaching the powder fractions were performed with a quadrupole ICP-MS.

Results: From each meteorite three positions were analyzed for U enrichments:

- surface exposed to air
- surface in contact to soil
- an interior chip

For the oldest investigated meteorite, the sample in contact with the ground was the highest in U contamination; for the two younger meteorites, the surface sample exposed to the air was highest. The interior samples were lowest in U concentrations for all meteorites. In Table 1, the values for the surface concentration in air minus the volume concentrations are given for the samples together with the measured carbon 14 ages and the calculated terrestrial ages, taking the age of the meteorite JaH 078 as a basis.

Table 1. U enrichment on the surface of meteorite [1].

Sample	¹⁴ C age measured [2]	U surface enrichment	Calculated terrestrial age
SaU 001	5500 ± 1300	2.46 ppb	6890 ± 2300
JaH 078	18,700 ± 1300	6.67 ppb	18,700
Dho 005	> 50,000	27.18 ppb	76,200 ± 16,100

Conclusions: Weathering of meteorites influencing their composition in hot deserts is controlled by temperature regime, humidity, and local composition of the soil and the duration of all these processes. But the uptake of uranium is dominated by the duration of the transfer of U from soil to the meteorite surface leading to a proportionality of surface enrichment of U and terrestrial residence time. In contrast to carbon 14 ages the “U enrichment ages” are not limited to 50,000 years of exposure.

References: [1] Christian Stenger. 2006. Master's Thesis. University of Bern, Bern, Switzerland. [2] Al-Kathiri et al. 2005. *Meteoritics & Planetary Science* 40:1215–1239.

5171

TERRESTRIAL ANALOGS FOR METEORITIC POROSITY MEASUREMENTS

M. M. Strait¹, G. J. Consolmagno, S. J.², and D. T. Britt³. ¹Alma College, Alma, Missouri 48801, USA. E-mail: straitm@alma.edu. ²Specola Vaticana, V-00120, Vatican City State. ³University of Central Florida, Orlando, Florida, USA

Introduction: Porosity is an important parameter in studying the evolution of bodies in the solar system. We have been measuring the porosity of meteorites for a number of years using two methods: hand sample measurements using helium pycnometry [1] and thin section measurements using backscatter scanning electron microscopic images and a computer measurement program [2]. For most meteorite types measured, there is good agreement between the two methods; however, the hand sample method must have the pore spaces empty of weathering products and accessible to the helium and the thin section method must have the porosity visible within the resolution of the imaging system [3]. Both methods can reliably measure porosities within the limitations of each method.

Ordinary chondrites and achondrites show agreement between the two methods within $\pm 5\%$ [4], however, carbonaceous chondrites show significantly more porosity in the hand samples. This difference is still being explored and may be due to the complex texture of the fabric obscuring the porosity, or it could be in the nature of the minerals present in these meteorites.

Results: Here we report another validation of our methodology. A suite of typical terrestrial rocks covering a wide range of rock classes and porosities has been measured using both methods. The rocks being measured include igneous rocks (porphyry, gneiss, gabbro, basalt, basalt breccia, and anorthosite), metamorphic rocks (quartzite, schist, marble, chert breccia, and slate) and sedimentary rocks (limestone, ferruginous sandstone, siliceous sandstone, shale, and siltstone). Thin sections were made from the same hand samples on which measurements were made. The porosities of the terrestrial rocks chosen match the range of porosities observed in the meteorites that have been measured. The metamorphic rocks show the lowest porosities ranging from 0.5% in quartzite to 2.3% in the schist. The igneous rocks were a fair amount of overlap with the metamorphic rocks, ranging from 0.7% in gneiss to 3.9% in anorthosite. Sedimentary rocks porosities are significantly higher, ranging from limestone at 3.7% to siltstone at 28%.

Appearances in the terrestrial samples tend to be similar to like porosities in meteorites. However, carbonaceous chondrites measured using hand samples show porosities ranging up to 25%, although the pore space is not as evident as that exhibited in terrestrial samples with porosities this high. In fact, thin section porosities and appearances of carbonaceous chondrites appear similar to the very low porosity samples such as quartzite.

Texture in terrestrial rocks is cleaner than that seen in meteorites and shows none of the weathering that fills in pore spaces in some meteorites. Published values for porosities in the suite measured here agree within the error ranges we have determined.

References: [1] Britt D. T. and Consolmagno G. J. 2003. *Meteoritics & Planetary Science* 38:1161–1180. [2] Strait M. M. et al. 1996. 27th Lunar and Planetary Science Conference. pp. 1285–1286. [3] Strait M. M. and Consolmagno G. J. 2004. *Meteoritics & Planetary Science* 39:A100. [4] Strait M. M. and Consolmagno G. J. 2005. Abstract #2073. 36th Lunar and Planetary Science Conference.

5360

SUPERNOVA NIERITE (α - Si_3N_4) FROM MURCHISON

R. M. Stroud¹, L. R. Nittler², and C. M. O'D. Alexander². ¹Code 6360, Naval Research Laboratory, Washington, D.C. 20375, USA. E-mail: stroud@nrl.navy.mil. ²Department of Terrestrial Magnetism, Carnegie Institution of Washington, Washington, D.C. 20015, USA

Introduction: Meteoritic Si_3N_4 includes both solar and presolar grains. Silicon nitride grains found in enstatite chondrites, e.g., Qingzhen (EH3) [1], Indarch (EH4) [2], are almost exclusively solar in origin, whereas those from ordinary and carbonaceous chondrites, e.g., Murchison (CM2), Tieschitz (H3.6), have isotopic signatures similar to SiC X grains, indicating an origin in type II supernovae [3–6]. Two crystalline polytypes of meteoritic Si_3N_4 have been identified, nierite (α - Si_3N_4) and β - Si_3N_4 [7], however, no structural data on supernova grains are yet published. We report here results from transmission electron microscopy (TEM) investigations of Si_3N_4 from Murchison, which indicate that the X-grain associated Si_3N_4 takes the nierite form.

Methods: We analyzed the CsF residue of Murchison of [4] using an EDAX particle analysis system on a JEOL 6500F SEM to identify SiC and Si_3N_4 grains on two mounts. We identified seven Si_3N_4 grains, ranging in size from 0.4 to 1.5 μm . Although isotopic data are not yet available, based on the previous studies on the same residue [4], we can be fairly certain that these are presolar supernova grains. Two of the new grains have an elongated, needle-like morphology, while the others appear blocky in the SEM. Sections for TEM studies were prepared using in situ focused-ion-beam (FIB) lift-out with a FEI Nova 600 FIB. The TEM studies were performed with a JEOL 2200FS microscope, equipped with a Noran System Six energy dispersive spectroscopy (EDS) system and Gatan Ultrascan CCD.

Results: The $\text{Si}_3\text{N}_4/\text{SiC}$ ratio of 10^{-3} is consistent with the results of [4] and with isotopic results on a new Murchison residue [8]. This is about $3\times$ higher than was previously found for residues prepared by HF/HCl [3, 6], suggesting that Si_3N_4 better survives the CsF treatment. Bright-field TEM imaging and diffraction studies of one of the sectioned grains reveal that it consists of two distinct, well-ordered crystals: one 150 nm \times 100 nm and one 125 nm \times 220 nm; both with the nierite structure (trigonal, $a = 0.7758$ nm, $c = 0.5623$ nm). The composition of the crystals measured by EDS is stoichiometric Si_3N_4 .

Discussion: The formation of Si_3N_4 in type II supernovae is poorly understood. The observed grain morphologies suggest formation under equilibrium condensation conditions, however calculations [9] indicate that Si_3N_4 is unstable with respect to SiC, TiN, and AlN. Isotopic measurements to confirm the supernova origin of this grain and structural studies of additional Si_3N_4 grains are planned in order to better constrain the circumstellar condensation conditions.

References: [1] Lin Y. T., Amari S., and Pravdivtseva O. 2002. *The Astrophysical Journal* 575:257–263. [2] Russell S. S. et al. 1995. *Meteoritics* 30:399–404. [3] Nittler L. R. et al. 1995. *The Astrophysical Journal* 453: L25–L28. [4] Nittler L. R. and Alexander C. M. O'D. 2003. *Geochimica et Cosmochimica Acta* 67:4961–4980. [5] Zinner E. et al. 2003. *Meteoritics & Planetary Science* 38:5106. [6] Hoppe P. et al. 1996. *Geochimica et Cosmochimica Acta* 60:883–907. [7] Lee M. R. et al. 1995. *Meteoritics* 30: 387–398. [8] Nittler L. R., Alexander C. M. O'D., and Nguyen A. 2006. *Meteoritics & Planetary Science* 41. This issue. [9] Lodders K. and Fegley B. 1995. *Meteoritics* 30:661–678.

5065

NUMERICAL MODELING OF TEKTITE ORIGIN IN VERTICAL IMPACTS

V. V. Svetsov. Institute for Dynamics of Geospheres, Russian Academy of Sciences. E-mail: svetsov@idg.chph.ras.ru

Introduction: Geochemical arguments show that tektites are derived from sedimentary layers at the Earth surface [1–3]. Numerical simulations of ejecta motion after impacts [4] suggest that the Ries-moldavite strewn field could have been created by an oblique impact at angles 30–50° to the horizontal with a velocity of 20 km/s. In this case, the melt of an upper 40 m thick layer is ejected downrange, moves through the atmosphere in a cloud of heated gas, and lands at some distance from the crater as tektites. However, this is not the only way to explain the origin of tektites. It has been speculated that tektites can be produced in vertical impacts and move through a wake left by an impactor in the atmosphere [5]. Another possible mechanism (at least for layered Australasian tektites) is the melting of soils by radiant heating from aerial bursts [6]. In this study numerical simulations of ejecta motion were made for near-vertical impacts.

Numerical Approach: The modeling of impacts was based on hydrodynamic equations which were solved numerically by the SOVA method [7]. Tillotson equation of state was used for target materials and a tabulated equation of state for heated air. Tektites were treated as particles moving with melted materials after ejection from a growing crater and as small objects moving individually through the atmosphere at the later stage. The approach was in general similar to that used in [4]. It was assumed that the impact occurs at some small angle to the vertical but the flow was simulated approximately as axially symmetrical.

Results: The motion of a molten surface layer at relatively low impact velocities has some specific features. A sandy layer melts near the impact point and is ejected to the wake. The melt particles move at the top of a low-velocity (2–3 km/s) ejecta curtain along trajectories close to vertical. From altitudes above ~50 km they move ballistically through the wake filled by air heated to some thousands Kelvins and then through the upper atmosphere. This tektite-forming material spreads in the direction opposite to the impact direction (in contrast to oblique impacts) and lands in some area with a shape depending on the impact velocity and angle. Some selected impact parameters give the best fit to the size of the tektite strewn field and its distance from the Ries crater. The calculated mass of tektites is of the order of the mass obtained by geological estimates.

Conclusions: The simulations show that the moldavite strewn field could originate from impacts of asteroids about 1 km in size at angles 10–20° to the vertical with velocities from 11.2 km/s to about 13 km/s. Near-vertical impacts with higher velocities can produce more extensive tektite strewn fields.

Acknowledgments: This publication is based on work supported by Award No. RUG-2655-MO-05 of the U. S. Civilian Research and Development Foundation.

References: [1] Barnes V. E. 1990. *Meteoritics* 25:149–159. [2] Glass B. P. 1990. *Tectonophysics* 171:393–404. [3] Koeberl C. 2001. GSA Special Paper 293. pp. 133–151. [4] Stöffler D. et al. 2002. *Meteoritics & Planetary Science* 37:1893–1907. [5] Svetsov V. 2001. 6th ESF-Impact Workshop. pp. 127–128. [6] Wasson J. T. 2003. *Astrobiology* 3:163–179. [7] Shuvalov V. 1999. *Shock Waves* 9:381–390.

5117

Ar-Ar DATING OF SHOCK-MELTED H CHONDRITES

T. D. Swindle, D. A. Kring, C. Isachsen, E. K. Olson, and J. R. Weirich. Lunar and Planetary Laboratory, University of Arizona, 1629 E. University Boulevard, Tucson, Arizona 85721-0092, USA. E-mail: tswindle@u.arizona.edu

As a part of our ongoing project to study shocked and shock-melted ordinary chondrites, we have used the ^{40}Ar - ^{39}Ar technique to analyze 12 samples from three H chondrites. Our two main goals are to determine when major recent (<1 Ga) events happened and how the early impact history compares with that of the Moon, for which a cataclysmic bombardment ~4 Ga ago has been proposed.

For Gao-Guenie, a chondrite with impact melt veins, three of the six samples studied have four- or five-point low-temperature isochrons of 305 Ma to 360 Ma, and a fourth has a minimum apparent age of 310 Ma (the other two samples do not have any apparent ages that low). We interpret this as incomplete degassing in an impact event 310 ± 25 Ma ago. At least three other H chondrites (of a total of 19 studied) contain evidence for an impact event between 270 Ma and 390 Ma [1, 2]. LaPaz Icefield 02240, an impact-melt breccia, has clearly been partially degassed in an event <1100 Ma ago, but there are no apparent low-temperature isochrons or plateaus. Northwest Africa 2058, a meteorite that is >90% impact melt, also suffered an event in the last 500 Ma, but it is impossible to pin it down more precisely than that with the present data, even though we analyzed three samples.

As previously reported [3], all three samples of LAP 02240 have apparent plateau ages of ~4000 Ma (average of 3914 ± 36 Ma), consistent with the lunar cataclysm, and roughly consistent with three other H chondrites. Gao-Guenie is the only other sample of those reported here that might contain information about early impacts. One sample appears to have a plateau at ~4300 Ma, which would make it a rare sample with a shock age between 4000 Ma and 4400 Ma. However, on closer inspection, the apparent ages in the “plateau” systematically rise, from ~4200 Ma to ~4400 Ma, suggesting a phase that was only partially degassed in the 300 Ma event [4].

References: [1] Bogard D. D. 1995. *Meteoritics* 30:244–268. [2] Folco L. et al. 2004. *Geochimica et Cosmochimica Acta* 68:2379–2397. [3] Swindle T. D. et al. 2006. Abstract #1454. 37th Lunar and Planetary Science Conference. [4] McDougall I. and Harrison T. M. 1999. *Geochronology and thermochronology by the $^{40}\text{Ar}/^{39}\text{Ar}$ method*. New York: Oxford University Press.

5294

EXPERIMENTAL STUDY ON KINETIC CONDENSATION OF METALLIC IRON UNDER CONTROLLED SUPERSATURATION

S. Tachibana, Y. Ikeda, H. Nagahara, K. Ozawa, and M. Yamada. Department of Earth and Planetary Science, University of Tokyo. E-mail: tachi@eps.s.u-tokyo.ac.jp

Introduction: Condensation is a fundamental process to form solids under low-pressure conditions as in the primitive solar nebula. The condensation rate from vapor is proportional to $(\alpha_c p - \alpha_e p^{eq})$, where p is a vapor pressure near the substance, p^{eq} is the equilibrium vapor pressure, and α_c and α_e are called the condensation and evaporation coefficients that express kinetic hindrances for evaporation and condensation ($0 < \alpha_c, \alpha_e \leq 1$), respectively. It is important to determine α_c and α_e as a function of temperature and p in order to understand time scales and physical conditions for condensation of solid objects in the early solar system. A previous study on evaporation of metallic iron, a major Fe-bearing phase in the early solar system, under controlled p showed that α_c and α_e are dependent on both temperature and p in the undersaturated conditions [1]. In this study, we have performed condensation experiments of metallic iron on a substrate under controlled p and condensation temperature in order to examine growth kinetics of metallic iron and its dependence on physical conditions for condensation such as p and temperature.

Experiments: A metallic iron pellet, put in the end of an alumina tube, was evaporated at ~ 1270 °C for 6–48 hours, and the evaporated iron gas was condensed onto a molybdenum or metallic iron substrate, of which temperature was ~ 960 °C. The alumina tube was used to collimate the evaporated iron gas escaping from the tube and to increase the incoming flux onto the substrate. The weight changes of the evaporation source and the substrate were measured by an electric microbalance, and condensates were examined by FE-SEM equipped with EDS.

Results and Discussion: Metallic iron was condensed on the substrate under the supersaturation ratio (S) of < 10 , which was estimated from the weight change of the evaporation source and the kinetic theory of gases escaping from the alumina tube. No other iron-bearing phase such as iron oxides was condensed. Condensation steps with the interval of < 100 nm were observed at the surface of metallic iron, indicating that lateral growth of metallic iron occurred under relatively low supersaturation conditions and that kinetics of surface atomistic processes should thus be taken into account to understand the growth kinetics. Our preliminary results showed that the actual condensation flux, obtained from the weight change of the substrate, was not significantly smaller than the ideal net condensation flux at 960 °C and S of < 10 . Although further detailed experimental work is needed, this implies that the kinetic hindrance of condensation of metallic iron under relatively low supersaturation conditions may not be significantly large.

References: [1] Tachibana S. et al. 2001. Abstract #1767. 32nd Lunar and Planetary Science Conference.

5269

A NEW FIREBALL IN EARLY APRIL: A POSSIBLE ASSOCIATION WITH THE PŘÍBRAM RADIANT

Gonzalo Tancredi. Depto. Astronomía–Fac. Ciencias. Uruguay. E-mail: gonzalo@fisica.edu.uy

Introduction: On 6:50 TU April 4, 2004, a very bright fireball was observed in the southern part of Uruguay (South America). After interviewing more than 30 witnesses, we were able to reconstruct the trajectory of the bolide. In order to compute the trajectory in the atmosphere, we have developed a variant of the method of intersection of planes [1]. For each witness we obtained a plane in the space where he viewed the bolide; different weights could be assigned to each witness. The common intersection of the planes is computed by solving two overdetermined system of linear equations with the single value decomposition method.

Conclusions: We reached the following conclusions:

- The peak absolute magnitude was $M \sim -18$, corresponding to a meteoroid with a mass over 1 ton.
- We obtained a set of solutions depending on the distributions of weights assigned to the observations. Assuming a velocity at infinity of 18 km/s, we obtain the following geocentric radiants:
 - For equal weights: RA = 184°; Dec = 8°
 - For weights proportional to the maximum height respect to the horizon observed by the witness: RA = 190°; Dec = 21°

The large difference between the two solutions expresses the bad quality of the visual data. Nevertheless, it is interesting to point out that the second solution is quite close to the radiants of the Příbram meteorite [2], the first meteorite recovered by the European Fireball Network in April 7, 1959 (Czech Republic), which it is proposed to be associated with the Neuschwanstein meteorite [3] also recovered by the EFN in April 6, 2002 (Austria).

We also investigate other fireballs observed in early April and the distribution of incoming material from the near Earth asteroid population for those days.

References: [1] Ceplecha Z. 1987. *Bulletin of the Astronomical Institute of Czechoslovakia* 38:222–234. [2] Ceplecha Z. 1961. *Bulletin of the Astronomical Institute of Czechoslovakia* 12:21–45. [3] Spurný P., Oberst J., and Heinlein D. 2003. *Nature* 423:151–153.

5205

COSMIC RAY FLUX VARIATION DURING MID-19th CENTURY REVEALED BY LOW ⁴⁴Ti ACTIVITY IN ALLEGAN METEORITE

C. Taricco¹, N. Bhandari², P. Colombetti¹, N. Verma¹, and G. Vivaldo¹.
¹Dipartimento di Fisica Generale, Università di Torino, Via P. Giuria 1, 10125 Torino, and Istituto di Fisica dello Spazio Interplanetario (IFSI), INAF, Corso Fiume 4, 10133, Torino, Italy. ²Basic Sciences Research Institute, Navrangpura, Ahmedabad, India

Introduction: We have shown that the activity of cosmogenic radioisotope ⁴⁴Ti ($T_{1/2} = 59.2$ yr) is a good index of centennial scale modulation of galactic cosmic ray (GCR) flux by heliospheric magnetic field [1, 2] and, compared to the conventional studies based on atmospheric ¹⁴C and ¹⁰Be in terrestrial archives, has the basic advantage that terrestrial influences, due to climatic changes in deposition rate variations, etc., are completely avoided. The measurements in 19 chondrites show that the GCR flux decreased by about 43% over the past 235 years [1] and, superimposed on this declining trend, the ⁴⁴Ti activity also shows a ~87 year oscillations, in phase with the Gleissberg cycle of solar activity. Since ⁴⁴Ti activity in meteorites integrates the production over a few decades before the fall, our calculations indicate a phase difference of a few decades between the cosmic ray intensity variations and time of fall of the meteorites. Thus the centennial solar cycle predicts GCR flux minima during the middle of 19th and 20th centuries, reflected in the observed ⁴⁴Ti activity minima around 1900 and 2000. In order to confirm these minima with better accuracy, we have now set up an improved gamma-ray spectrometer and measured the ⁴⁴Ti activity of a ~250 g fragment of H5 chondrite Allegan, which fell on July 10, 1899, in Michigan (USA).

Experimental System: The new set-up is a highly specific and selective spectrometer located at the underground (70 m.w.e.) Research Station of Monte dei Cappuccini in Torino (Italy). The main detector is a high-purity large Ge diode (about 3 kg) with high resolution (2 keV at 1332 keV) and relative efficiency (150%), surrounded by an active shield of NaI(Tl) of about 90 kg. The passive shield consists of 20 cm thick high-purity lead and 5 cm oxygen-free, high-conductivity copper. The electronic chain has been tailored for the measurement of 1157 keV γ -ray from ⁴⁴Ti(⁴⁴Sc) in coincidence with annihilation photons from β^+ decay.

Results: Using this detector, we have measured ⁴⁴Ti activity of the Allegan meteorite for about three months, obtaining a net counting rate of (0.0008 ± 0.0001) cpm. This value is significantly above the background of the system. This value, corrected for the target elemental (Fe + Ni) abundances and shielding effects based on cosmic ray tracks, gives a ⁴⁴Ti activity of (4.84 ± 0.61) dpm/kg (Fe + Ni). This activity is lower than the values measured in Alfanello (date of fall: 1883) and Bath (1892), which fell before Allegan, and Olivenza (1924) which fell afterwards, but similar to the values obtained in Lancon (1897) and Holbrook (1912) which fell within a few years of Allegan. These results confirm the centennial modulation of the GCR flux and its minimum during mid-19th century.

References: [1] Taricco et. al. *Journal of Geophysical Research*. Forthcoming. [2] Bonino et al. 1995. *Science* 270:1648–1650.

5183

IRON SPHERULES WITH SILICATE CORES AND A CHONDRITIC AGGREGATE SPHERE FROM DEEP SEA SEDIMENTS

Y. Tazawa¹ and T. Fukuoka². ¹Department of Physics, Graduate School of Science, Kyoto University, Kyoto 606-8502, Japan. E-mail:tazawa@cr.scphys.kyoto-u.ac.jp. ²Department of Environmental Systems, Faculty of Geo-Environmental Sciences, Risho University, Kumagaya 360-0194, Japan

Introduction: Spherules from deep-sea sediments (DSSs) usually have metallic cores consisting of Fe, Ni, Co, and/or platinumoid elements (e.g., [1, 2]). The cores are thought to be formed from ablation droplets by heating and quenching during the atmospheric entry of meteoroids.

Here we report six deep sea spherules proved to be of extraterrestrial origin by their high abundances of siderophile elements (SPE: e.g., Ni, Co, Ir, Os, Au, etc.) and chondritic compositions of lithophile elements (LPE: e.g., Mg, Al, Sc, V, Cr, Mn, Fe), especially two iron spherules have silicate (glassy?) cores so far unknown in anywhere. They have been studied on their chemical and petrological features by INAA, EPMA, SEM/EDX, and XDP.

Samples: Spherules analyzed here are three iron spherules (IS) and three stony spherules (SS) extracted from sediments dredged from 4700 m deep floor at the Central Pacific Ocean (9°30'N, 174°18'W ~ 9°31'N, 174°17'W) [3], which were provided by late Prof. K. Yamakoshi, and K. Nogami.

Results:

- One of IS, whose bulk composition assayed by INAA is: Fe 67.6%; Ni 4.50%; Co 0.18%; and Ir 2.34 ppm, and also by XDP is: spotty patterns of magnetite ($d \approx 8.43\text{\AA}$) and wüstite ($d \approx 4.28\text{\AA}$), has a mantle of Ni, Co rich Fe oxide (i.e., Fe 69.60%; Ni 4.06%; Co 0.35%; O 25.30%) and an eccentric spherical core of Ni, Fe rich silicate (i.e., SiO₂ 35.2%; NiO 31.8%; FeO 19.1%; Al₂O₃ 6.6%; MnO 3.2%).
- Another IS, whose bulk composition is: Fe 67.0%; Ni 1.59%; Co 0.24%; and Ir 0.41 ppm and also magnetite ($a \approx 8.43\text{\AA}$), wüstite ($a \approx 4.30\text{\AA}$), has also a mantle of Ni, Co rich Fe oxide (i.e., Fe 71.09%; Ni 1.46%; Co 0.40%; O 25.62%) and an "amoeboidal" (or a walnut-shape) silicate (glassy?) core consisting of Si, Fe, Al, Mg, and K (i.e., SiO₂ 64.9%; FeO 17.4%; Al₂O₃ 10.9%; MgO 3.7%; K₂O 2.1%). These kinds of silicate or glassy cores have never been observed in IS.
- The rest IS, whose bulk composition is: Fe 66.0%; Ni 5.16%; Co 0.18%; and Ir 3.97 ppm and also magnetite ($a \approx 8.34\text{\AA}$), wüstite ($a \approx 4.28\text{\AA}$), is a homogeneous brick work of μm -sized grains of magnetite and wüstite (i.e., Fe 66.4%; Ni 5.1%; Si 1.2%; Co 0.3%; Cr 0.2%; O 26.6%) except voids or glassy grains in the central region.
- A SS is an fragile and porous aggregate of $\mu\text{-sized}$ grains of mafic silicates, oxides, and sulfides, and shows an XDP pattern of faint and broaden lines of magnetite ($a \approx 8.51\text{\AA}$), wüstite ($a \approx 4.25\text{\AA}$), and olivine ($d_{130} \approx 2.75\text{\AA}$, $a \approx 4.86\text{\AA}$, $b \approx 10.01\text{\AA}$, $c \approx 6.02\text{\AA}$). These features harmonize well with the bulk composition (i.e., Mg 20.3%, Fe 20.1%, Ni 1.27%, Al 0.46%, Cr 0.20%, Mn 0.10%, Co 484 ppm, V 89 ppm, Sc 4.91 ppm, Os 1.9 ppm, Ir 0.51 ppm, and Au 0.42 ppm) quite similar to C1 (except for higher Os, Au, and Mg and lower Al and Mn contents).

References: [1] Brownlee D. E. 1985. *Annual Review on Earth and Planetary Science* 13:147–173. [2] Blanchard M. B. et al. 1980. *Earth and Planetary Science Letters* 46:178–190. [3] Yamakoshi K. 1994. In *Extraterrestrial dust. Laboratory studies of interplanetary dust*. Tokyo: Terra Scientific Publishing Co. 203 p.

5186

CHEMICAL COMPOSITIONS OF ANTARCTIC MICROMETEORITES AND THEIR TYPES

Y. Tazawa¹, T. Fukuoka², N. Hoshi², Y. Fukushi^{2,6}, Y. Saito³, T. Noguchi⁴, and T. Yada⁵. ¹Department of Physics and Astrophysics, Graduate School of Science, Kyoto University, Kyoto 606-8502, Japan. E-mail: tazawa@cr.scphys.kyoto-u.ac.jp. ²Department of Environmental Systems, Faculty of Geo-Environmental Science, Rissho University, Kumagaya 360-0914, Japan. ³Radio Isotope Laboratory, College of Science and Engineering, Aoyama Gakuin University, Sagami-hara 229-8551, Japan. ⁴Department of Materials and Biological Science, Ibaraki University, Mito 310-8512, Japan. ⁵Department of Earth and Planetary Science, University of Tokyo, Tokyo 113-0033, Japan. ⁶Present address: Department of Earth and Planetary Science, Tokyo Institute of Technology, Tokyo 152-8551, Japan

Microparticles of extraterrestrial origin that survived heating during atmospheric entry and weathering after settling on Earth have been collected in large quantities from Antarctica (e.g., [1–4]). Called “Antarctic micrometeorites” (AMMs), they have been investigated widely in recent years because of primitive and/or unknown grains that have been expected to be found (e.g., [5–8]). Instrumental neutron activation analysis (INAA) is the most advantageous means of measuring abundances of many elements of individual microscopic samples (\geq sub- μ g in weight) in quantitative, simultaneous, and nondestructive ways. So far, we have investigated chemical features of individual AMMs by means of INAA [9–11]. We report here recent results of AMMs.

Forty-one individual AMMs collected from Dome Fuji Station (77°19'S, 39°42'E; water tank deposit) [2], Point K-5 near Kuwagata Nunatak (72°06'S, 35°15'E; bare ice), and Point MY-3 near Minami-Yamato Nunataks (72°26'S, 35°20'E; bare ice) around Yamato Mountains [3], and Point N-7 near Tottuki Point (68°55'S, 39°51'E; bare ice) on the Soya Coast [4], have been confirmed as those well-preserved chondritic compositions, though one third of them were fully melted in appearance: (1) abundance patterns normalized to CI and Mg (LPEs and REEs), and CI and Fe (SPEs) are classified into six types. Seven MMs show the patterns parallel to CI within 0.2–5 times of CI (type I), 14 MMs show the patterns similar to the type I except Ir or Co lowered to 0.1 (type II), seven MMs show the patterns with Na (0.002–0.1), Ir (0.1–0.6), and Au (\leq 0.5) depletions (type III), seven MMs show Cr (0.1–0.3), Na (\leq 0.7), Ir (0.8–0.5), Co (\leq 0.7) and Au (\leq 0.4) depletions and Mn (2–6) enrichments (type IV). Five of the six other MMs show LPE patterns similar to achondrite or scatter ones and absent of REEs (type V). The last one is an iron type MM.

References: [1] Maurette M. et al. 1991. *Nature* 351:44–47. [2] Nakamura T. et al. 1999. *Antarctic Meteorite Research* 12:183–198. [3] Yada T. and Kojima H. 2000. *Antarctic Meteorite Research* 13:9–18. [4] Iwata N. and Imae N. 2002. *Antarctic Meteorite Research* 15:25–37. [5] Noguchi T. and Nakamura T. 2000. *Antarctic Meteorite Research* 13:285–301. [6] Nakai I. et al. 2000. *Antarctic Meteorite Research* 302–310. [7] Osawa T. et al. 2000. *Antarctic Meteorite Research* 322–342. [8] Yada T. et al. 2005. *Antarctic Meteorites* 29:94–95. [9] Fukuoka T. et al. 2000. *Antarctic Meteorites* 25:10–11. [10] Tazawa Y. et al. 2003. International Symposium: Evolution of Solar System Materials. pp. 138–139. [11] Tazawa Y. et al. 2005. *Antarctic Meteorites* 29:84–85.

5025

RECORDS OF IMPACT EVENTS IN THE ELGA (IIE) IRON

S. N. Teplyakova. Vernadsky Institute of Geochemistry and Analytical Chemistry, Russian Academy of Sciences. E-mail: svun2002@mail.ru

Introduction: Previous investigations of silicate inclusions (SI) in IIE irons suggested that SI probably were formed by the partial melting of H-chondrite precursors, or by condensation of minerals and metals from the solar nebula [1–5]. Here we report results on mineralogy, petrology, and mineral chemistry of eleven SI and the host metal of the Elga (IIE) meteorite. It was shown that chemically SI are similar to those of the Miles (IIE) and that some of SI after their formation were melted as a result of local heating during impact metamorphism.

Results: The silicate inclusions consist of euhedral pyroxene crystals ($\text{Wo}_{37-44}\text{En}_{44-50}$; Cr_2O_3 1.5 wt%; $\text{Fe/Mn} = 15-31$) enclosed in a SiO_2 -rich feldspathic glass ($\text{Ab}_{72-92}\text{Or}_{7-26}$ to $\text{Ab}_{38-43}\text{Or}_{53}$). Mineral modes are (vol%): pyroxene 22–34; glass 66–78. Minor phases include bronzite, chromite, schreibersite, phosphate, troilite, kamacite, and taenite. Locally, some glass contains FeNi metal as well metal-sulfide and silicate globules. Fe-Ni-P inclusions are in both the Elga metal and in SI. Objects within metal are rounded, but objects in SI are irregularly shaped. All Fe-Ni-P inclusions have an unusual, dendritic-like texture. The bulk composition of SI silicate portion is (wt%): SiO_2 65.8; TiO_2 0.27; Al_2O_3 12.71; Na_2O 6.24; K_2O 1.71; CaO 5.28; MgO 4.69; MnO 0.1; FeO 2.81; Cr_2O_3 0.36. Elga host metal shows plastic deformation, while the SI show brittle deformation.

Discussion: The mineral assemblage of the Elga SI is similar to other IIE irons [6]. Fe/Mn ratios and Cr_2O_3 content of pyroxenes from the Elga SI are similar to those of other IIE inclusions, primitive achondrites, and ureilites. The Elga SI are enriched in K, Na, and Al compared to SI IIE iron and H chondrites, indicating of the high abundance of feldspar component. Chemically, SI resemble the cryptocrystalline inclusions of the Miles (IIE) [1]. Ca phosphate surrounds the SI, indicating reduction reactions between metal and silicate due to thermal metamorphism, after impact event. Some SI are similar to the melt pockets observed in shocked chondrites. Such structures may have formed due to impact melting and mixing of silicate and metal melts, followed by rapid cooling. In iron meteorites, dendritic Fe-Ni-P objects have not previously been found coexisting with silicate melts. We believe that the dendritic structure of these objects is the result of rapid cooling. Deformed Widmanstätten pattern throughout the sample, SI which are similar to the melt pockets, and coexisting lamellar and the dendritic schreibersite objects suggests local heating and may reflect varying temperatures across the shock wave front. Brittle deformation of some SI also supports the impact hypothesis for the origin of the melts after the metal and silicate material had already been combined in a body.

References: [1] Ikeda Y. et al. 1997. *Antarctic Meteorite Research* 10: 355–372. [2] Meibom A. and Clark B. E. 1999. *Meteoritics & Planetary Science* 34:7–24. [3] Hsu W. et al. 1997. *Meteoritics & Planetary Science* 32: A61–62. [4] Ruzicka A. 1999. *Geochimica et Cosmochimica Acta* 63:2123–2143. [5] Rao A. S. P. 1985. 16th Lunar and Planetary Science Conference. pg. 683R. [6] Mittlefehldt D. W. et al. 1998. In *Planetary materials*. Washington, D.C.: Mineralogical Society of America. pp. 4–195.

5129

ION MICROPROBE U-Pb DATING OF PHOSPHATES IN VERY LOW-TI BASALTIC BRECCIA

K. Terada¹, Y. Sasaki¹, and Y. Sano². ¹Department of Earth and Planetary Systems Science, Hiroshima University, Higashi-Hiroshima 739-8526, Japan. E-mail: terada@sci.hiroshima-u.ac.jp. ²Center for Advanced Marine Research, Ocean Research Institute, The University of Tokyo, Nakano-ku 164-8639, Japan

Abstract: The lunar meteorites have valuable information for understanding the evolution of the Moon's crust, since each meteorite may potentially provide a new insight into the thermal history of unexplored regions of the Moon. In spite of their scientific interests, chronological studies of very low-Ti (VLT) basaltic meteorites have not been well understood, since the most VLT basalt meteorites are brecciated and consist of mixtures of materials with different origins. In this paper, we summarize our recent studies of in situ U-Pb dating of VLT meteorites.

An ion microprobe analyses of mare-origin's phosphates in Yamato-981031 resulted in a total Pb/U isochron age of 3535 ± 170 Ma in the $^{238}\text{U}/^{206}\text{Pb}$ - $^{207}\text{Pb}/^{206}\text{Pb}$ - $^{204}\text{Pb}/^{206}\text{Pb}$ 3-D space (95% confidence limit), while those of QUE 94281 resulted in a total Pb/U isochron age of 3401 ± 170 Ma and 65 ± 300 Ma (95% confidence limit). These formation ages of phosphates are consistent with each other and also agree with previous studies of 3569 ± 100 Ma for EET 96008 [1] and 3521 ± 138 Ma for EET 87521 [2], whose basaltic components are also classified into VLT mare basalt. This result indicates that there is no chronological impediment to the hypothesis that these meteorites have originated from the same place on the Moon and were launched by a single impact, which has been proposed based on the similarity of launching ages, mineralogical and geochemical signatures [3–5].

Recent global and high-resolution mappings of chemical composition and mineralogical composition on the Moon observed by Clementine and Lunar Prospector enable us to discuss on the ejection sites of some lunar meteorites [6–8]. Assuming the scenario for Yamato-981031 [8], our data suggest that the formation age of northern parts of mares of near-side of Moon (possibly, Mare Frigoris or Lacus Somniorum or Lacus Mortis) might be about 3.5 Ga. Thus, our in situ dating techniques of lunar brecciated meteorites coupled with the higher-resolution remote-sensing data may provide a radiometric (not based on the crater density) chronological assessment of unexplored regions on the Moon.

References: [1] Anand M. et al. 2003. *Geochimica et Cosmochimica Acta* 67:3499–3518. [2] Terada K. et al. 2005. *Geophysical Research Letters* 32:L20202. [3] Arai T. and Warren P. H. 1999. *Meteoritics & Planetary Science* 34:209–234. [4] Warren P. H. and Ulf-Møller F. 1999. Abstract #1450. 30th Lunar and Planetary Science Conference. [5] Korotev R. L. et al. 2003. *Antarctic Meteorite Research* 16:152–175. [6] Fagan T. J. et al. 2002. *Meteoritics & Planetary Science* 37:371–394. [7] Gnos E. et al. 2004. *Science* 305:657–659. [8] Sugihara T. et al. 2004. *Antarctic Meteorite Research* 17:209–230.

5340

Lu-Hf SYSTEMATICS OF THE ANGRITE SAH 99555

K. Thrane¹, J. N. Connelly^{1, 2}, M. Bizzarro¹, L. Borg³, and D. Ulfbeck¹. ¹Geological Institute, University of Copenhagen, Denmark. E-mail: kthrane@geol.ku.dk. ²Department Geological Sciences, University of Texas at Austin, Texas, USA. ³Institute of Meteoritics, University of New Mexico, New Mexico, USA

Introduction: Estimates of the ^{176}Lu decay constant derived from terrestrial and meteoritic (chondrites and eucrites) samples have differed significantly and correspond to $1.87 \times 10^{-11} \text{ yr}^{-1}$ [1, 2] and $1.93\text{--}1.98 \times 10^{-11} \text{ yr}^{-1}$ [3–6], respectively. More recently, Amelin's [7] internal isochron from a 4557 Ma meteorite using phosphate minerals yielded an estimate of the ^{176}Lu decay constant compatible with the terrestrial value.

Objectives: We use the 4566.18 Ma [8] angrite SAH 99555 to derive an internal isochron using silicate phases to further evaluate both the ^{176}Lu decay constant and the initial $^{176}\text{Hf}/^{177}\text{Hf}$ ratio of the solar system.

Method: We dissolved carefully picked olivine, pyroxene, and plagioclase mineral fractions (two each) from SAH 99555 as well as two whole-rock samples. HFSEs and REEs were first separated from the bulk matrix using cation resin after which Hf and Lu/Yb were further purified using TODGA and RE-spec resins, respectively [9]. Lu and Hf were analyzed on the Axiom MC-ICP-MS in Copenhagen. Sm and Nd from the LMREE cuts from the RE-spec step were further purified using methylactic columns and were analyzed on the VG Sector 54 TIMS at the University of New Mexico.

Results: In the Lu-Hf system, the two pyroxene, two olivine, and two whole-rock fractions define a line with slope and intercept of 0.09516 ± 0.00100 and 0.279682 ± 0.000030 . The slope corresponds to ages of 4874 ± 48 Ma and 4584 ± 45 Ma using the meteoritic- [6] and terrestrial-derived decay constants, respectively. Two plagioclase fractions plot slightly above the line. In the Sm-Nd system, the two pyroxene and two whole-rock fractions define a line corresponding to an age of 4591 ± 49 Ma. The olivine and plagioclase fractions plot above the WR-pyroxene line.

Discussion: Concordance between the WR-pyroxene Pb-Pb age [8] and our WR-pyroxene Sm-Nd age demonstrate both isotopic systems were undisturbed in these components. The line defined in Lu-Hf space by replicate WR-pyroxene-olivine fractions indicates that Lu-Hf in these components also behaved as a closed system. The slope of this internal isochron infers that ^{176}Lu decayed at a rate or in a manner comparable to that determined for chondrites [6]. The derivation of this internal isochron for a differentiated basalt precludes accelerated ^{176}Lu decay via formation of the short-lived isomer ^{176m}Lu ($t_{1/2} = 3.7$ h) by γ -ray irradiation [10] prior to accretion of the angrite parent body. Instead, any formation of the isomer ^{176m}Lu caused by γ -ray irradiation requires this energy to have been derived internally after angrite crystallization, which implies short-lived nuclides served as a possible energy source.

References: [1] Scherer E. et al. 2001. *Science* 293:683–687. [2] Söderlund U. et al. 2004. *Earth and Planetary Science Letters* 219:311–314. [3] Patchett P. J. and Tatsumoto M. 1980. *Nature* 288:571. [4] Tatsumoto M. et al. 1981. [5] Blichert-Toft et al. 2002. [6] Bizzarro M. et al. 2003. *Nature* 421:931–933. [7] Amelin Y. 2005. *Science* 310:839–841. [8] Baker J. et al. 2005. *Nature* 436:1127–1131. [9] Connelly J. N. et al. *Chemical Geology*. Forthcoming. *Chemical Geology*. [10] Albarède F. et al. 2006. *Geochimica et Cosmochimica Acta* 70:1261–1270.

5086

TIMING OF DIFFERENTIATION OF PALLASITE PARENT BODIES: EVIDENCE FROM Al-Mg SYSTEM

T. Tomiyama¹, M. Bizzarro², A. N. Krot¹, G. R. Huss¹, and T. E. Bunch³.
¹HIGP/SOEST, University of Hawai'i at Manoa, Honolulu, Hawai'i 96822, USA. E-mail: tomi@higp.hawaii.edu. ²Geological Institute, University of Copenhagen, DK-1350, Denmark. ³ARC Desert Research Field Station, Prescott, Arizona 86301, USA

Introduction: Pallasites probably sample the core-mantle boundaries of parent bodies that experienced extensive melting and differentiation due to decay of ²⁶Al ($\tau_{1/2} \approx 0.73$ Myr). Both the Al-Mg and metal-silicate fractionation recorded by pallasites can be potentially dated using short-lived isotope systematics. Precise bulk Pb-Pb and Al-Mg isotope analyses suggest that the accretion and differentiation of planetesimals occurred within ~1 Myr of formation of CAIs [1, 2]. Based on differences in chemistry, mineralogy, and O-isotopic compositions, several pallasite groups may exist [3]. We have initiated a high-precision Al-Mg isotopic study of several groups of pallasites to understand the time scale for their differentiation.

Experiments: Microdrilled powders and chipped fragments of pallasite, olivine, and pyroxene were dissolved with HF-HNO₃ and Mg was purified by cation exchange chemistry. Magnesium isotope ratios were measured by MC-ICPMS, and $\delta^{26}\text{Mg}^*$ values are reported relative to the mean mass-bias-corrected ²⁶Mg/²⁴Mg obtained on bracketing terrestrial standards (DSM-3 or mantle olivine). Samples are analyzed at least eight times.

Results: Analysis of the J-11 mantle olivine yielded of $-0.004 \pm 0.008\%$, i.e., identical to the terrestrial standard, while silicates from four pallasites representative of different (sub)groups exhibit resolvable ²⁶Mg* deficits (average of $-0.022 \pm 0.008 \%$; Table 1), in agreement with previous reports [4].

Table 1. ²⁶Mg* deficits in pallasites.

Sample	Group	Mineral	$\delta^{26}\text{Mg}^*$ (‰)	Error (2 σ)
Omolon	Main group (M.G.)	ol	-0.025	0.009
Huckitta	M.G. anom met. [5]	ol	-0.021	0.006
Springwater	M.G. anom sil. [5]	ol	-0.028	0.012
Zinder	Pyroxene pal	opx	-0.017	0.008

Discussion: In a model where ²⁶Al was homogeneous in the early solar system, the present solar ²⁶Mg/²⁴Mg ratio represents addition of ²⁶Mg* to an initial ²⁶Mg/²⁴Mg ratio. If Al-Mg fractionation decreased the Al/Mg ratio relative to solar while ²⁶Al was alive, deficits of $\delta^{26}\text{Mg}^*$ will result. All pallasites we measured have $\delta^{26}\text{Mg}^*$ deficits, indicating formation within the lifespan of ²⁶Al. Assuming an initial ²⁶Al/²⁷Al ratio of $\sim 5.85 \times 10^{-5}$, based on bulk CAIs [6, 7], and a solar ²⁷Al/²⁴Mg ratio of ~0.1, we calculate an initial $\delta^{26}\text{Mg}^*$ of ~ -0.042 . If a pallasite parent body had a solar bulk Al/Mg ratio, the time necessary to raise the initial $\delta^{26}\text{Mg}^*$ to ~ -0.022 , when the pallasites differentiated, would be ~0.8 Myr. This result is highly model-dependent reflecting choices of Al/Mg, initial $\delta^{26}\text{Mg}^*$, and details of differentiation.

References: [1] Baker J. et al. 2005. *Nature* 436:1127-1131. [2] Bizzarro M. et al. 2005. *The Astrophysical Journal* 632: L41-L44. [3] Jones R. H. et al. 2003. Abstract #1683. 34th Lunar and Planetary Science Conference. [4] Baker J. and Bizzarro M. 2005, Abstract #8612. Protostars and Planets V. [5] Wasson J. T. and Choi B.-G. 2003. *Geochimica et Cosmochimica Acta* 67:3079-3096. [6] Bizzarro M. et al. 2004. *Nature* 431: 275-278. [7] Thrane K. et al. *The Astrophysical Journal*. Forthcoming.

5313

Hf-W CONSTRAINTS ON THE FORMATION AND THERMAL METAMORPHISM OF ACAPULCOITES

M. Touboul¹, T. Kleine¹, B. Bourdon¹, J. Zipfel², and A. J. Irving³. ¹Institute for Isotope Geochemistry and Mineral Resources, ETH Zürich, Switzerland. E-mail: touboul@erdw.ethz.ch. ²Forschungsinstitut und Naturmuseum Senckenberg, Frankfurt am Main, Germany. ³Department of Earth and Space Sciences, University of Washington, Seattle, Washington, USA

Introduction: Acapulcoites are primitive achondrites that have modal mineral abundances similar to ordinary chondrites and exhibit broadly chondritic bulk compositions. Their formation probably involved thermal metamorphism and melting at the Fe,Ni-FeS cotectic. Their textures reflect extensive solid-state recrystallization [1]. However, there is evidence from metal inclusions in pyroxene and in few olivine cores that partial melting of silicates occurred [2]. ¹⁸²Hf-¹⁸²W chronometry is well suited to constrain the time scales of thermal metamorphism (and melting) in the acapulcoite parent body and here we present the first Hf-W data for acapulcoites.

Results: Metals separated from the acapulcoites Dhofar 125 and NWA 2627 are enriched in W (~800-900 ppb) and have ϵ_W values of ~ -3 (ϵ_W is the deviation of ¹⁸²W/¹⁸⁴W from the terrestrial standard value in parts per 10,000). Whole-rock analyses for NWA 2627 (~600 mg) and Dhofar 125 (~150 mg) yield Hf/W ratios of ~0.6 and ~1.6 and ϵ_W values of ~ -2 and ~ -1.5 , respectively.

Discussion: The Hf-W systematics of the NWA 2627 and Dhofar 125 whole-rocks are consistent with a chondritic bulk composition for the acapulcoites. Differences in Hf/W and ϵ_W between NWA 2627 and Dhofar 125 might reflect sample heterogeneities but may also be due to differences in the chemical composition of acapulcoites. The chondritic Hf-W systematics of NWA 2627 and Dhofar 125 indicate that, if partial melting occurred, these melts were not extracted. The enrichment of W in the acapulcoite metal is similar to that observed for metals in equilibrated ordinary chondrites, indicating transfer of W from silicates into metal during thermal metamorphism. Tungsten model ages for the NWA 2627 and Dhofar 125 metals are 5 ± 2 Myr after formation of Allende CAIs (using $\epsilon_W = -1.9 \pm 0.1$ for carbonaceous chondrites [3] and initial $\epsilon_W = -3.47 \pm 0.20$ [4]). These ages are similar to Hf-W ages obtained for equilibrated ordinary chondrites, indicating similar time scales of metamorphism on the acapulcoite and ordinary chondrite parent bodies. The W model ages for the NWA 2627 and Dhofar 125 metals are older than a Pb-Pb age for phosphates [5] and a Mn-Cr age for oxides and silicates from Acapulco [6]. If the latter are representative for all acapulcoites, then these age differences could reflect different closure temperatures for Hf-W and Pb-Pb/Mn-Cr. Alternatively, Hf-W ages might date the onset of metamorphic heating whereas Pb-Pb and Mn-Cr ages might reflect cooling from peak metamorphic temperatures (as suggested by [7] for ordinary chondrites).

References: [1] McCoy T. J. et al. 1996. *Geochimica et Cosmochimica Acta*. 60:2681-2708. [2] Zipfel J. et al. 1995. *Geochimica et Cosmochimica Acta*. 59:3607-3627. [3] Kleine T. et al. 2004. *Geochimica et Cosmochimica Acta* 68:2935-2946. [4] Kleine T. et al. 2005. *Geochimica et Cosmochimica Acta* 69:5801-5815. [5] Göpel et al. 1992. *Meteoritics* 27:226. [6] Zipfel et al. 1996. *Meteoritics & Planetary Science* 31:A160. [7] Humayun M. and Campbell A. J. 2002. *Earth and Planetary Science Letters* 198:225-243.

5084

EARLY SOLAR SYSTEM CHRONOLOGY IN THE ASTROPHYSICAL CONTEXT

M. Trierloff¹ and H. Palme². ¹University of Heidelberg, Institute of Mineralogy, D-69120 Heidelberg, Germany. E-mail: trierloff@min.uni-heidelberg.de. ²University of Cologne, Institute for Mineralogy and Geochemistry, Zùlpicherstrasse 49b, 50674 Kùln, Germany

Radioisotope chronologies from both long-lived nuclides (^{238,235}U-^{206,207}Pb, ⁴⁰K-⁴⁰Ar [1, 2]) and short-lived radionuclides (¹²⁹Xe from ¹²⁹I; $T_{1/2} = 16$ Myr [3], excess ²⁶Mg from ²⁶Al; $T_{1/2} = 0.73$ Myr [4], ⁵³Cr from ⁵³Mn; $T_{1/2} = 3.7$ Myr [5], ¹⁸²Hf from ¹⁸²W; $T_{1/2} = 9$ Myr [6, 7]) provide a framework for the formation of solids in the early solar system. We present an early solar system chronology based on the calibration of short-lived isotope chronometries to several tie points (CAIs, H chondrites, Acapulco), and planetesimal heating in the early solar system [2, 8]. Conditions of formation of the first solids in the solar nebula varied—most probably due to p,T differences imposed by the early Sun—with radial distance and/or time, and caused the compositional variety of planetesimals concerning refractory and volatile elements, metals, and Mg-rich silicates [8, 9].

Radiometric dating and chemical composition suggest that individual planetesimals grew rapidly in the asteroid belt (within <1 Myr), but different planetesimals formed over a time interval of 4 million years [2, 7, 8], well within the lifetime of protoplanetary dust disks in extrasolar systems [10, 11]. Early planetesimals were heated to varying degrees by decay heat of short-lived nuclides (primarily ²⁶Al) [2]. This caused melting and differentiation in early (within <2 Ma after CAIs) formed planetesimals and led to the formation of iron cores and basaltic rocks, while chondritic planetesimals that accreted later remained undifferentiated [2, 7, 8]. As most chondrules were immediately consumed in accreting planetesimals, they were only preserved in unmelted chondritic parent bodies and their age distribution is biased to the formation time interval of chondrites 2–3 Ma after CAIs [8]. The formation of solids in the early solar system (CAIs, chondrules, planetesimals, and terrestrial planets) are still insufficiently linked to astrophysically constrained processes like early protostellar activity, disk dissipation, formation and migration of gas planets interacting with young disks [10, 11]. Models of Earth and Mars formation based on ¹⁸²Hf-¹⁸²W core formation ages estimate the presence of planetary embryos of 60% the size of Mars after 2–4 Ma. This requires the early presence of Jupiter to effectively prevent the formation of a proto-planet in the asteroid belt. Planetesimal formation in the asteroid belt and the terrestrial planet formation zone at <3 Ma after CAIs was likely accompanied by inner disk clearing permitting solar wind irradiation (and possibly volatile element depletion) of terrestrial—and partly asteroidal—precursor planetesimals [12].

References: [1] Amelin Y. et al. 2002. *Science* 297:1678–1683. [2] Trierloff M. et al. 2003. *Nature* 422:502–506. [3] Gilmour J. D. et al. 2006. *Meteoritics & Planetary Science* 41:19–31. [4] Bizzarro M. et al. 2004. *Nature* 431:275–278. [5] Lugmair G. W. and Shukolyukov A. 1998. *Geochimica et Cosmochimica Acta* 62:2863–2886. [6] Kleine T. et al. 2002. *Nature* 418, 952–955. [7] Kleine T. et al. 2004. *Geochimica et Cosmochimica Acta* 68:2935. [8] Trierloff M. and Palme H. In *Planet formation*. Cambridge University Press. Forthcoming. [9] Palme H. 2001. *Philosophical Transactions of the Royal Society of London A* 359:2061–2074. [10] Haisch K. E. et al. 2001. *The Astrophysical Journal* 553:L153–L156. [11] Briceno C. et al. 2001. *Science* 291:93–96. [12] Trierloff M. et al. 2000. *Science* 288: 1036–1038.

5381

ALUMINUM-RICH CHONDRULES AND TYPE C CAIs: AN EXPERIMENTAL COMPARISON OF FORMATION CONDITIONS

E. J. Tronche¹, R. H. Hewins^{1, 2}, and G. J. MacPherson³. ¹Laboratoire d'Etudes de la Matière Extraterrestre, MNHN and CNRS-UMS2679 61 rue Buffon, 75005 Paris, France. ²Department of Geological Sciences, Rutgers University, 610 Taylor Road, Piscataway, New Jersey 08854, USA. ³Department of Mineral Sciences, MRC NHB-119, National Museum of Natural History, Smithsonian Institution, Washington, D.C. 20560, USA

Introduction: Aluminum-rich chondrules are a compositional link between ferromagnesian chondrules and plagioclase-rich (type C) CAIs [1]. However, whereas Al-rich chondrules are compositionally and texturally very diverse, type C CAIs are a much more restricted group of objects. We previously [2] reported dynamic crystallization experimental results that demonstrate the relationship between bulk composition, mineralogy, texture, maximum melting temperature (T_{max}), and cooling rate for four different Al-rich chondrule bulk compositions. Here we more thoroughly contrast those results (for the two most plagioclase-normative compositions only: PL-1 and PL-2; see [2]) with experiments on a type C CAI synthetic bulk composition in order to constrain whether or not the two groups of objects formed under similar conditions (thermal histories). The experimental techniques and starting compositions were reported in [1].

Results: As expected, first order differences exist because of differing bulk compositions. The type C CAI melt yields liquidus spinel, followed successively by anorthite, aluminous diopside, and melilite. The two Al-rich chondrule compositions are less spinel-normative and have forsterite as a late-crystallizing phase. Type C CAIs can be formed at subliquidus temperatures (1400–1450 °C), a little bit higher than for type B chondrules [3], but similar to Al-rich chondrules of PL1 and PL2 compositions. Cooling rates for this type of composition and those temperatures do not change textures much and no estimation can be made. We cannot say that the type C CAI and the two Al-rich chondrule compositions have different thermal histories.

Discussion: Natural type C CAIs usually have ophitic textures, but the anorthite lath sizes can vary enormously from one type C CAI to another. Also they seem to have a wide range of oxygen isotopic compositions [4] and ²⁶Mg excesses [4–5], that could lead to the idea of different formation processes for this group of objects. Hence, a quantitative study of textures, mineral zonation, and melilite abundance in primitive and remelted C-CAI might prove instructive. Peak temperatures probably increased from type B CAIs to ferromagnesian chondrules, but C-CAI may include objects with CAI-like and chondrule-like heating-cooling conditions.

References: [1] MacPherson G. J. and Huss G. R. 2005. *Geochimica et Cosmochimica Acta* 69:3099–3127. [2] Tronche E. J., Hewins R. H., and MacPherson G. J. 2006. Abstract #1640. 37th Lunar and Planetary Science Conference. [3] Stolper E. and Paque J. M. 1986. *Geochimica et Cosmochimica Acta* 50:1785–1806. [4] Imai and Yurimoto. 2000. Abstract #1510. 31st Lunar and Planetary Science Conference. [5] Kita et al. 2004. Abstract #1471. 35th Lunar and Planetary Science Conference.

5178

CHROMIUM ISOTOPIC STUDY OF UREILITE

T. Ueda¹, K. Yamashita², and N. Kita³. ¹Graduate School of Science and Technology, Kobe University, 1-1 Rokkoudai-cho, Nada, Kobe 657-8501, Japan. E-mail: 058s402n@stu.kobe-u.ac.jp. ²Institute for the Study of the Earth's Interior, Okayama University, Yamada 827, Misasa, Tottori 682-0193, Japan. ³Department of Geology and Geophysics, University of Wisconsin–Madison, 1215 W. Dayton Street, Madison, Wisconsin 53706–1692, USA

The Mn-Cr chronometer is an ideal tool to unravel the age of igneous activities in the early solar system. However, recent discovery of isotope anomaly on ⁵⁴Cr in differentiated meteorites (e.g. [1, 2]) makes the isotopic investigation of ⁵⁴Cr/⁵²Cr also very important. In this study, we have measured the Cr isotopic signature of three monomict ureilites, ALHA77257, Y-791538, and META78008. All measurements were made using Finnigan MAT262 mass spectrometer in a single collector peak-jumping mode [2]. In order to minimize the effect of residual mass fractionation, a relatively large number of repeated measurements were made for each sample (>40 sets of 300 ratios).

The results of the three samples show that their ⁵³Cr vary from +0.04 to +0.29, and ⁵⁴Cr from -0.73 to -1.16. These values are correlated on a ⁵³Cr versus ⁵⁴Cr diagram (Fig. 1), and the slope of the linear trend is similar to that of the terrestrial standards. Such correlation may indicate that the effect of residual mass fractionation has not been fully eliminated for these samples. However, it is also difficult to reject the possibility at this point that the three samples are from isotopically different reservoir.

If we assume that they are from a single reservoir, we can calculate the ⁵⁴Cr value of the ureilite parent body (UPB) by taking the average of all the ⁵⁴Cr values determined so far. Our current best estimate calculated using this procedure is ⁵⁴Cr = -0.93 ± 0.23. This value is in good agreement with our earlier work [2], as well as the value recently reported by Shukolyukov and Lugmair [3]. While the number of data is still limited, the currently available data clearly indicate that the Cr isotopic signature of the UPB is different from those of carbonaceous chondrites (⁵⁴Cr > 0) and Earth (⁵⁴Cr = 0).

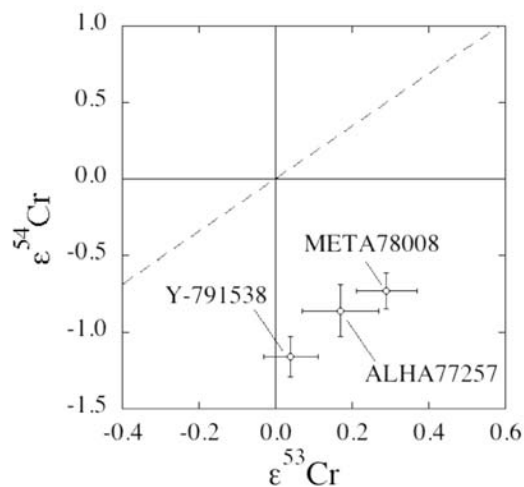


Fig. 1. Results of the Cr isotopic analysis.

References: [1] Trinquier A. et al. 2005. Abstract #1259. 36th Lunar and Planetary Science Conference. [2] Yamashita K. et al. 2005. Antarctic Meteorites 28:100–101. [3] Shukolyukov A. and Lugmair G. W. 2006. Abstract #1478. 37th Lunar and Planetary Science Conference.

5232

MICROSCOPIC MAGNETIC FIELD DISTRIBUTIONS OF UNEQUILIBRATED ORDINARY CHONDRITES

M. Uehara and N. Nakamura. Division of Geoenvironmental Science, Tohoku University, Sendai 980-8578, Japan. E-mail: syok@dges.tohoku.ac.jp

Introduction: Unequilibrated ordinary chondrites preserve metallic phases formed during solar nebular processes [1–3]. The metallic phase of Fe-Ni grains appear to simultaneously preserve a magnetic environment of the early solar nebula as a natural remanent magnetizations (NRMs). An experimental study suggested that abundant submicron-sized kamacite grains in a reduced “dusty” olivine acquire magnetically stable pre-accretional NRMs when the chondrules were formed [4]. Lauretta et al. [2] suggested that silicon-bearing Fe-Ni grains in the matrix of Bishunpur (LL3.1) were formed in the reducing environment of chondrule melts. It implies that such Fe-Ni grains in the matrix also acquired pre-accretional NRMs. Furthermore, if these metal grains were magnetized before incorporation into chondrules, their NRMs should be randomly oriented. Hence, the correlation between magnetic grains and their NRMs is interesting, because it provide constraints on the thermal, chemical and magnetic environment of the solar nebula, and the acquisition process of NRMs in the nebula. However, there is no study focused on NRM of these Fe-Ni grains in the unequilibrated ordinary chondrites. Here, we report spatial distributions of NRMs in unequilibrated ordinary chondrites using a custom-made scanning MI (magneto-impedance) magnetic microscope.

Method: We examine two 3 mm thick slices of NWA 1756 (LL3.0/3.2) and NWA 2632 (LL3.2). Images of the out-of-the-page component of the magnetic field 300 μm above the sample were obtained by a scanning MI magnetic microscope that has a resolution and sensitivity of 500 μm, 360 nT, respectively. The measurements were made in a three-layered mu-metal magnetic shield.

Results and Discussion: Magnetic images of the NWA 1756 sample reveal a spatially heterogeneous pattern of magnetization showing eight distinct magnetized points, suggesting pre-accretional NRMs. A comparison with the magnetic minerals shows that magnetized points are associated with kamacite in the matrix, which is often surrounded by FeS, and also shows that large (~300 μm) kamacite grains were strongly magnetized. Although a chondrule contains dusty olivine grains, we detect only a slight magnetic signature from this chondrule. In contrast, magnetic images of the NWA 2632 sample shows homogenized pattern of magnetization. It is supposed that one large dipole moment exists in the piece of the sample, suggesting that the NWA 2632 sample is dominated by a post-accretional NRM. These preliminary results suggest that the scanning MI magnetic microscopy is able to decide the NRM carriers in the unequilibrated ordinary chondrites.

References: [1] Rambaldi E. R. and Wasson J. T. 1981. *Geochimica et Cosmochimica Acta* 45:1001–1015. [2] Lauretta D. S. et al. 2001. *Geochimica et Cosmochimica Acta* 65:1337–1353. [3] Lauretta D. S. and Buseck P. R. 2003. *Meteoritics & Planetary Science* 38:59–79. [4] Uehara M. and Nakamura N. *Earth and Planetary Science Letters*. Forthcoming.

5172

A POSSIBLE ORIGIN FOR THE DEPLETION OF SIDEROPHILE ELEMENTS IN CHONDRULES

M. Uesugi¹ and M. Sekiya². ¹Japan Synchrotron Radiation Research Institute (JASRI) 1-1-1 Kouto, Sayo-cho, Sayo-gun, Hyogo 679-5198, Japan. ²Department of Earth and Planetary Sciences, Faculty of Sciences, 33 Kyushu University, Hakozaki, Fukuoka, 812-8581, Japan

Introduction: Chondrules have a distinctive feature that they are depleted in siderophile elements relative to the solar elemental abundance [1]. Several processes, such as ejection of iron component by high-speed rotation of chondrules during their formation and fractionation in the condensation of chondrule precursor materials from hot nebular gas, are considered to be possible reasons of the iron-chondrule separation [2]. Separation due to physical fission of chondrule and metallic iron part is one of the most probable reasons for the depletion. The fission could occur at the time of chondrule formation, so, if the physical fission is responsible to the depletion of siderophile elements in chondrules, we can obtain important information of chondrule formation processes by investigating the feature. We propose a new viewpoint for the study of this process, based on the theoretical calculation of the separation of melted chondrule and iron sphere at the time of the chondrule formation.

Basics: We calculated total surface energy of a melted chondrule, a melted iron sphere, and their interface for the cases those an iron sphere is on the surface (hereafter, we call this condition as ON), inside (IN), and outside (OUT) of a melted chondrule. At first, we estimate the interfacial energy between the melted iron and chondrule by calculating the equilibrium shape for ON state and comparing it with the natural chondrules. In the calculations, we use 1830 erg cm⁻² for the interfacial energy, which is the average of the result from three chondrules, and 400 and 1700 erg cm⁻² for the surface energies of melted chondrule and Fe, respectively.

Results and Discussion: Our calculation shows that the total surface energy for OUT condition is lower than that for IN condition. This means that once a melted iron sphere which initially inside of a melted chondrule reaches the surface during the chondrule formation process, the iron sphere is immediately ejected to the outside of the melted chondrule. And also, it is difficult that a melted iron sphere which initially outside of a melted chondrule penetrates into the melted chondrule, because strong surface tension prevents the penetration. On the other hand, the total surface energy for ON condition is lower than any other conditions. This means that if a melted iron sphere initially on the surface of a melted chondrule, the iron sphere is strongly bound on the surface by the surface tension. Thus, our calculations show that iron spheres being inside of melted chondrules are easily ejected to the outside of the chondrules, if they reach the surface of melted chondrules during the chondrule formation. If a melted chondrule has some amount of angular momentum, iron spheres are transported to the surface of melted chondrules, and immediately leave from the surface of chondrules. Thus, the ejection of iron sphere due to surface tension would play important role for the origin of the contents of siderophile elements in chondrules.

References: [1] Gooding J. L. 1983. In *Chondrules and their origins*. pp. 61–87. [2] Grossmann J. N. and Wasson J. T. 1985. *Geochimica et Cosmochimica Acta* 49:925–940.

5045

THE TYPE IA SUPERNOVA AND ORIGIN OF THE SOLAR SYSTEM

G. K. Ustinova. Institute of Geochemistry and Analytical Chemistry, RAS, Moscow. E-mail: ustinova@dubna.net.ru

Introduction: Because of the absence of the *r*-process products among the extinct radionuclides with the short intervals of generation, the last supernova before the formation of the solar system was the type Ia supernova (the so-called carbon-detonation supernova), which could not survive the carbon explosive burning and was fully disrupted [1]. The injection of its specific matter (especially, large amounts (0.4–0.6 M_⊙) of iron [2]) into the protosolar nebula created the initial large-scale chemical heterogeneity of the accreting matter, which led to the initial (before condensation!) metal-silicate separation of the matter in the conditions of the supersonic turbulence in the collapsing nebula [3]. Both the factors ranged the consequence of events in the formation of the solar system bodies, which is recently derived from the Hf-W chronometry [4, 5].

Drafts of Scenarios: The large quantity of synthesized and shock wave accelerated iron nuclei were among the first ones that penetrated into the collapsing protosolar nebula and, being captured by supersonic turbulence, they created some iron-rich regions of various scale, so that the further condensation and accumulation in those regions formed the iron planetesimals and iron parent bodies. In some cases of especially huge vortices the captured iron laid the metallic core embryos of some planets, which were built up further due to magmatic differentiation. This fact promoted the rapid formation of the planets, which follows from the ¹⁸²Hf-¹⁸²W data [4, 5]. The intermediate and light nuclei of the type Ia supernova also reached the accreting system and rather later were captured gradually by the especially huge vortices, which still were not dissipated. They had played the key role in formation of the earth group planets under the reducing conditions being typical for the corresponding heliocentric distances. When practically all the injected iron was caught by the turbulence, the new developed vortices captured the intermediate-mass explosion products. Depending on the distance from the protosun, and, therefore, from the different PT-conditions of condensation, the different types of stony bodies of various scale were created, whose accumulation led later to the formation of stony planetesimals and the parent bodies of stony meteorites of different types. Certainly, all the possible cases of the blended matter could occur. The most part of the unburned C and O of the type Ia supernova was accreted at the conclusive stage of accretion in the various conditions of low temperatures and free gravitation that provided the formation of carbonaceous chondrites of different types. The giant planets were apparently formed by the giant vortices in the main matter of the protosolar molecular nebula at the distances which had not been reached by the exploded matter of the type Ia supernova.

Summary: The thorough development of the above frame models will substitute the chondrite models of the solar system.

References: [1] Ustinova G. K. 2002. *Doklady RAS* 382:242–245; Abstract #1015. 33rd Lunar and Planetary Science Conference. [2] Gamezo V. N. et al. 2003. *Science* 299:77–81. [3] Ustinova G. K. Abstract #1070. 37th Lunar and Planetary Science Conference. [4] Yin Q. et al. 2002. *Nature* 418: 949–952. [5] Kleine T. et al. 2002. *Nature* 418:952–955.

5160

THE SURFACE ELEMENTAL COMPOSITION OF 4 VESTA BASED ON HED METEORITES: PROSPECTIVE STUDY FOR INTERPRETATION OF GAMMA-RAY AND NEUTRON SPECTRA FOR THE DAWN MISSION

T. Usui and H. Y. McSween, Jr. Planetary Geosciences Institute, Department of Earth and Planetary Sciences, University of Tennessee, Knoxville, Tennessee 37996, USA. E-mail: tusui@utk.edu

Asteroid 4 Vesta, believed to be the parent body of the voluminous howardite, eucrite, and diogenite (HED) achondrites [1–3], will be investigated by the Dawn orbiting spacecraft [4]. Dawn carries a gamma-ray and neutron detector (GRaND) that will measure and map some major and trace element abundances [5]. Drawing on HED geochemistry, we propose a quantitative mixing model that uses element ratios (determined more precisely than absolute elemental abundances) appropriate for the interpretation of GRaND data.

Because the spatial resolution of GRaND is relatively coarse, analyzed chemical compositions on the surface of Vesta will likely reflect mixing of three end-member components: diogenite, cumulate eucrite, and basaltic eucrite. Reliability of the mixing model is statistically investigated based on published whole-rock data for HED meteorites (N = 48). We demonstrate that the mixing model can accurately estimate the abundances of all the GRaND-analyzed major elements, as well as minor elements (Na, Cr, and Mn) not analyzed by this instrument. We also show how a similar mixing model can determine the modal abundance of olivine, and we compare estimated and normative olivine data for olivine-bearing diogenites.

This study provides a way to leverage the large geochemical and mineralogical database on HED meteorites as a tool for interpreting chemical analyses by GRaND of mapped units on the surface of Vesta. Therefore, this study should help constrain the geologic context for HED meteorites and provide new insights into the structure and igneous evolution of Vesta.

References: [1] Binzel R. P. and Xu S. 1993. *Science* 260:186–191. [2] Keil K. 2002. In *Asteroids III*. Tucson, Arizona: The University of Arizona Press. pp. 573–584. [3] McCord T. B. et al. 1970. *Science* 168:1445–1447. [4] Russell C. T. et al. 2004. *Planetary and Space Science* 52:465–489. [5] Prettyman T. H. et al. 2003. *IEEE Transactions on Nuclear Science* 50:1190–1197.

5230

THE STRUCTURE AND ORIGIN OF METAL IN ISHEYEVO CB/CH METEORITE

K. A. Uymina and V. I. Grokhovsky. Ural State Technical University–UPI, Ekaterinburg, 620002, Russia. E-mail: ksenia_uimina@mail.ru, grokh47@mail.ru

Introduction: The unique mineralogical, chemical, and textural data of the CR chondrite clan meteorites is poorly understood and widely discussed [1–4]. The recently discovered metal-rich Isheyev meteorite contains several lithologies with different contents (7–70 vol%) of Fe-Ni metal and genetically links CH and CB of carbonaceous chondrites [5]. Zoned metal grains with striking components distribution are the most interesting. Both nebular and asteroidal models have been proposed to explain this distribution [6]. Here we report the results of optical microscopy observations after etching, accompanied with results of SEM/EDX analysis, and Mössbauer spectroscopy, and discuss the possible origin of metal structure.

Results: We observed a variety of metal microstructures. The metal clasts are polycrystalline, boundaries marked by secondary minerals make grains to look sharp. Part of coexisting metal grains is zoned with kamacite structure. These grains were found in both metal-rich and metal-poor lithology, have size up to 1 mm, and contain 12–4 wt% of Ni, 0.7–0.3 wt% of Cr. It was found that the gradient of Ni concentration is orientation-dependent: in zoned metal grains we observed the anisotropy of Ni, Cr gradients. Moreover, zoned metal grains contain numerous small spherical inclusions of another phase with Cr and S near the boundary area. These inclusions increase in size while approaching the hydrated boundary.

The neighboring grains can have different metal distribution and different texture. The unzoned kamacite grains with almost constant Ni 7.5–7.85 wt% and Cr 0.19–0.26 wt% were observed. Zoneless plessite grains with average Ni 7.5 wt% were found, along with few populations of metal-sulfide aggregates, including “kamacite (Ni 5.1 wt%, Cr 0.22 wt%, P 0.46wt%) with Neumann bands - troilite enriched in Cr,” “kamacite (Ni < 7.8wt%) - taenite (44.9 wt%) - troilite,” and “kamacite (Ni 4.7wt%) - martensite (13.2 wt%) - troilite.” The Mössbauer spectroscopy confirmed the heterogeneous structure of Fe-Ni alloys and showed four main components in metal part of spectrum [7].

Discussion: The primitive meteorite Isheyev meteorite has complex multistage history. Despite the fact that CALs [8] and osbornite [9] of very refractory nature in the Isheyev carbonaceous are nebular products, we argue that unusual metal grain zoning may be connected with the process of secondary diffusion. We assume that the so-called “internal oxidation” took place within the metal grains starting from hydrated grain boundary sources, and produced the observed metallography features. Small inclusions located in the by-boundary areas of most zoned metal grains, and anisotropy of chemical gradients can prove this suggestion. The existence of “puzzle-shape” formed by zoned and unzoned metal grains can not be explained using nebular models.

References: [1] Meibom A. et al. 2000. *Science* 288:839–841. [2] Krot A. N. et al. 2005. *Nature* 436:989 – 992. [3] Perron C. et al. 2000. *Meteoritics & Planetary Science* 39:A82. [4] Krot A. N. et al. 2006. Abstract # 1224. 37th Lunar and Planetary Science Conference. [5] Ivanova M. A. et al. 2006. Abstract #1100. 37th Lunar and Planetary Science Conference. [6] Righter K. et al. 2003. Abstract #1373. 34th Lunar and Planetary Science Conference. [7] Oshtrakh M. I. et al. 69*AMSM*. Forthcoming. [8] Krot A. N. et al. 2006. Abstract #1226. 37th Lunar and Planetary Science Conference. [9] Grokhovsky V. I. 69*AMSM*. Forthcoming.

5203

WEATHERING OF ORDINARY CHONDRITES FROM THE ATACAMA DESERT, CHILE: FIRST RESULTS FROM MÖSSBAUER SPECTROSCOPY

E. M. Valenzuela¹, Y. Abdu², R.B. Scorzelli², J.B. de Campos³, M. Duttine^{2*}, and D. Morata¹. ¹Dep. de Geología, Universidad de Chile, Santiago, Chile, E-mail: edvalenz@cec.uchile.cl. ²Centro Brasileiro de Pesquisas Físicas (CBPF/MCT), RJ, Brazil. E-mail: scorza@cbpf.br. ³Instituto Nacional de Tecnologia (INT/MCT), RJ, Brazil. *On leave from Centre de Recherches en Physique Appliqué à l'Archéologie (CRPAA), Bordeaux, France

Introduction: We report the first quantitative results of the study of 21 meteorites from the Atacama Desert, northern Chile. The meteorites are ordinary chondrites (OC) and include the three chemical groups (H, L, and LL). The goals of this study are the identification and quantification of the weathering products of these meteorites, in order to understand the weathering processes acting in the Atacama Desert, one of the oldest and driest deserts of the world, and compare these first results with samples from other deserts. As recently fallen equilibrated OC contain iron only as Fe⁰ (kamacite and taenite) and Fe²⁺ (olivines, pyroxenes, and troilite), the abundance of ferric iron is directly related to the level of terrestrial weathering [1]. In this way, the characterization of weathering products of these samples using Mössbauer spectroscopy, X-ray diffraction (XRD), and magnetic properties [2] allow us to have a complete picture of iron oxide/hydroxides nature and behavior.

Results: As Mössbauer spectroscopy is extremely sensitive to changes in Fe valence state, the technique, complemented by XRD, allows the recognition and quantification of all the Fe-bearing phases. The percentage of these phases was obtained for the primary minerals: olivine, pyroxene, troilite, and Fe-Ni metal, and for the ferric alteration products which gives the percentage of oxidation of the samples. The subspectra arising from the presence of Fe³⁺ are generally fitted with a paramagnetic doublet and a magnetic sextet(s). The doublet can be associated with the paramagnetic phases: akaganéite, lepidocrocite, and/or small-particle goethite, while the sextet(s) are due to the magnetically ordered phases: magnetite, maghemite, hematite, and large-particle goethite.

From the Mössbauer absorption areas of these oxides, the terrestrial oxidation of the Atacama OC was found to range from ~5% to ~60%. The amounts of silicates as well as the opaque phases (troilite and Fe-Ni metal) were found to decrease in a constant rate with increasing oxidation level. A histogram of percentage oxidation versus frequency shows a peak at ~30–35% similar to that observed in the Sahara Desert OC [3]. Akaganéite, the first product of Fe-Ni oxidation [4], is present only in some samples, deduced from XRD data.

Further low temperature Mössbauer measurements are in progress in order to better resolve the individual components of the oxide phases, especially the paramagnetic phases. The MS and XRD results will be correlated with the terrestrial ages of these weathered meteorites.

References: [1] Bland P. A. et al. 2002. *Hyperfine Interactions* 142: 481. [2] Valenzuela M. E. et al. 2006. Abstract. *Desert Meteorite Workshop*. [3] Bland P. A. et al. 1998. *Geochimica et Cosmochimica Acta* 62:3169. [4] Buchwald V. F. and Clarke R. S. Jr. 1989. *American Mineralogist* 74:656–667.

5253

MAGNETIC ANISOTROPY OF CARBONACEOUS CHONDRITES AND ACHONDRITES

M. van Ginneken^{1,2}, J. Gattacceca¹, and M. Gounelle^{2,3}. ¹CEREGE, CNRS/University of Aix-Marseille 3, France. E-mail: gattacceca@cerege.fr. ²LEME, Muséum National d'Histoire Naturelle, Paris, France. E-mail: gounelle@mnhn.fr. ³IARC, Natural History Museum, London, UK

Magnetic anisotropy has been shown to be a good proxy to the petrofabric of meteorites [1]. In particular the degree of magnetic anisotropy of ordinary chondrites increases with shock stage [2], indicating that hypervelocity impacts are the main phenomenon responsible for the foliation of ordinary chondrites.

The principal scope of the present work is to discuss the origin of the petrofabric in carbonaceous chondrites, using anisotropy of magnetic susceptibility (AMS) as a proxy to the petrofabric. Is the foliation of carbonaceous chondrites related to impacts as for ordinary chondrites? Can accretion and/or metamorphism be responsible for the foliation?

The data set of AMS measurements on carbonaceous chondrites was until now rather limited (33 measurements including only 11 falls [2, 3]). We measured the AMS of an additional 51 carbonaceous chondrites from the MNHN in Paris, including 27 falls. After discussing the experimental limitations of such measurements (in particular the effect of shape anisotropy), the total data set will be interpreted in relation with porosity, shock stage, metamorphism, petrographic observations, and magnetic mineralogy.

The significance of AMS data obtained on Rumuruti chondrites (characterized by very low degree of anisotropy) and achondrites (HED, SNC, aubrites, ureilites) will also be discussed in the light of new measurements.

References: [1] Sneyd D. S. et al. 1988. *Meteoritics* 23:139–149. [2] Gattacceca J. et al. 2005. *Earth and Planetary Science Letters* 234:351–368. [3] Smith D. L. et al. 2006. *Meteoritics & Planetary Science* 41:355–373.

5050

A UNIVERSAL METEORITE FORMATION PROCESS

M. E. Varela¹ and G. Kurat². ¹Complejo Astronómico El Leoncito (CASLEO), Av. España 1512 sur, J5402DSP, San Juan, Argentina. ²Institut für Geologische Wissenschaften, Universität Wien, Althanstrasse 14, A-1090 Vienna, Austria

Our study of glasses in several types of meteorites show that all glasses have a common source, the solar nebula [1]. Glasses are the remnants of the liquid that facilitated growth of well-ordered crystals from the gas phase by the VLS growth process. The chemical (major and trace element) composition of all glasses have a surprising property: they do not show the signature of crystallization of the minerals they are associated with. Our key observation is that glasses do not have the composition of the residual melt from which the crystals (documented by glass inclusions), or aggregates and chondrules (documented by mesostasis glass), or the whole rock (documented by glasses that fills open spaces in achondrites) were formed [2–3]. These observations led us to develop The Primary Liquid Condensation (PLC) model [4] that utilizes the ability of dust-enriched solar nebular gas to directly condense a silicate liquid (e.g., [6]). Once a stable CMAS liquid nucleus is formed and growth into a droplet, an olivine crystal can nucleate from the liquid. If the quantity of liquid is low, the crystal nucleus will continue growing where it is covered by the liquid. In this way a single crystal can be formed. Increasing the liquid/crystal ratio can create olivine aggregates and droplets of crystal-liquid mush, PO chondrules [7]. If condensation of liquid is faster than nucleation of an olivine crystal, a chondrule-sized droplet is formed, which at a high degree of undercooling will homogeneously or heterogeneously nucleate an olivine crystal. Instantaneously, a plate dendrite can be formed, the barred olivine (BO) texture. We have estimated the composition of the initial liquid droplet for such chondrules to be: SiO₂: 46.1 wt%, MgO: 38.5 wt%, Al₂O₃: 8.4 wt%, CaO: 7.1 wt%. The primary condensate liquid from which BO chondrules could be formed will condense in regions with a dust/gas ratio enhanced over the solar value by $\sim 700 \times$ CI dust—at $T \sim 1700$ °C and $p \sim 10^{-3}$ atm [8]. Variation in the chemical composition of, e.g., the mesostasis glasses, is achieved by continuing communication of the glass with the cooling nebula that will result in a variety of elemental exchanges. This way an infinite amount of individual chemical compositions for chondrules and other chondrite constituents is created—as it is observed.

A liquid of similar composition and origin also formed the olivine-anorthite intergrowth of angrites [9] and a chemically slightly modified liquid—increased Si/Mg but similar TE abundance—crystallized the eucrites [10].

Also, radiating pyroxene (RP) chondrules could form as droplet liquid condensates directly from a nebular gas [11]. Enstatite becomes a stable liquidus phase in a $800 \times$ CI dust-enriched nebular gas at a p^{out} of 10^{-3} atm., after about 72% of the originally present Mg was removed (as forsterite?) from the system.

In conclusion, the PLC model describes a universal process that can create all major chondrule types, PO, BO, and RP, omnipresent in all chondrites, in the same region of the solar nebula. In addition, it can also create some common achondrites (e.g., ureilites, angrites, eucrites) directly in the solar nebula and does neither need parent bodies nor reheating events. The PLC model describes chondritic constituents and their infinite chemical variability as well as the most common achondrites as consequent products of just a single-step cooling solar nebula.

References: [1] Varela and Kurat. 2004. *Meteoritics & Planetary Science* 39:A109. [2] Varela et al. 2002. *Geochimica et Cosmochimica Acta* 66:1663–1679. [3] Varela et al. 2003. *Geochimica et Cosmochimica Acta* 67:5027–5046. [4] Varela et al. 2005. *Icarus* 178:553–569. [6] Ebel and Grossman. 2000. *Geochimica et Cosmochimica Acta* 64:339–366. [7] Kurat et al. 2004. *Meteoritics & Planetary Science* 39:A57. [8] Varela et al. *Icarus*. Forthcoming. [9] Varela et al. 2005. *Meteoritics & Planetary Science* 40:409–430. [10] Varela et al. 2005. EGU05-A-07425. [11] Ebel et al. 2003. Abstract #2059. 34th Lunar and Planetary Science Conference.

5219

AQUEOUS CORROSION TEXTURES ON WEATHERED CHAIN SILICATE SURFACES AS POSSIBLE TERRESTRIAL ANALOGS OF PYROXENE ALTERATION IN MARS METEORITES

M. A. Velbel¹ and S. J. Wentworth². ¹Department of Geological Sciences, Michigan State University, East Lansing, Michigan 48824–1115, USA. E-mail: Velbel@msu.edu. ²ESCG, Mail Code JE23, Johnson Space Center, Houston, Texas 77058, USA

Denticulated margins (also known in older literature as “sawtooth,” “cockscorn,” or “hacksaw” terminations) are a common feature of pyroxenes and amphiboles. Large, well-developed denticles are visible in transmitted-light microscopy of grain mounts and thin-sections; smaller denticles are visible using scanning and transmission electron microscopy. Denticles are commonly the remnants of undissolved material that formerly constituted the walls between elongate etch pits (the characteristic aqueous-dissolution form of chain-silicate minerals) [1]. Similar processes create similar ranges of dissolution forms and dimensions on minerals of both pyroxene and amphibole groups [1]. Denticles are best expressed where a grain boundary, transmineral fracture, or dislocation array transects the crystal at a high angle to the z-axis [1]. Denticles occur widely in terrestrial near-surface materials that have experienced low-temperature aqueous alteration, including chemically weathered regoliths, soils, sediments and sedimentary rocks [1]. Denticles in these materials are commonly tens of microns in length [1, 2]. Denticles are much less common at the surfaces of chain-silicate crystals altered by aqueous solutions at higher temperatures.

Microdenticles microns rather than tens of microns long are developed on the lateral surfaces of larger “classic” denticles on hornblende from a weathered regolith in the southern Appalachian mountains (North Carolina, USA). Microdenticles share the shape and orientation of the larger more typical denticles, suggesting similar crystallographic controls on the corrosion process. However, because the elongate pointed forms are on surfaces closer in orientation to prism faces than to (001) termini of the chain silicate crystals, these arrays of microdenticles more closely resemble a surface covered with imbricate pointed scales than a sawtooth margin. The arrays of imbricate microdenticles are formed by aqueous alteration during weathering chain-silicates; they are later-stage corrosion forms on surfaces of chain-silicate minerals that show larger-scale evidence of typical weathering [3]. Furthermore, the scaly, imbricate microdenticles of the weathered terrestrial chain silicate are very similar in size, shape and distribution to micron-scale features reported from pyroxenes in several Mars meteorites [4, 5]. The close similarity of these demonstrably aqueous weathering-related terrestrial chain-silicate microdenticles with only slightly smaller microdenticles on pyroxenes in several Mars meteorites supports previous proposals of a low-temperature aqueous origin of the Mars meteorites microdenticles [4, 5].

References: [1] Velbel M. A. In *Heavy minerals in use*. Elsevier. Forthcoming. [2] Mikesell et al. 2004. *Quaternary Research* 62:162–171. [3] Velbel M. A. 1989. *Clays and Clay Minerals* 37:515–524. [4] Wentworth et al. 2005. *Icarus* 174:382–395. [5] Wentworth et al. 1998. 29th Lunar and Planetary Science Conference. pp. 1793–1794.

5325

WHOLE-ROCK OXYGEN ISOTOPE COMPOSITIONS ARE UNRELATED TO DEGREE OF AQUEOUS ALTERATION IN CM2 CHONDRITES

M. A. Velbel¹, E. K. Tonui², and M. E. Zolensky³. ¹Department of Geological Sciences, Michigan State University, East Lansing, Michigan 48824-1115, USA. E-mail: velbel@msu.edu. ²Department of Earth and Space Sciences, University of California-Los Angeles, Los Angeles, California, USA. ³Astromaterials Research and Exploration Science Office, NASA Johnson Space Center, USA

Introduction: This paper reexamines published whole-rock oxygen isotope data for CM2 chondrites [1], including nine non-Antarctic falls and 25 Antarctic finds, and revisits previously published relationships between whole-rock oxygen isotope compositions and aqueous alteration of CM chondrites [2].

Oxygen Isotope Compositions of Antarctic CM2 Finds: Antarctic CM2 finds and non-Antarctic CM2 falls plot on the same mixing line (slope 0.70) on an oxygen three-isotope plot [1]. If oxygen isotopes of Antarctic CM2 finds were affected by terrestrial weathering, then 1) their pre-weathering compositions would have plotted off the mixing line, and 2) the composition of each Antarctic find would have been shifted from its preterrestrial composition, along a line with a slope corresponding to mass-dependent fractionation, to its present composition on the mixing line. Furthermore, this would have had to have happened for each Antarctic CM2 on the mixing line, by precisely and only the amount required to move each sample's plot from its preterrestrial composition to its measured composition. A simpler scenario is that 1) Antarctic CM2s plot (like their counterpart non-Antarctic CM2 falls) on the mixing line before arrival in Earth's environment, and 2) the oxygen isotope compositions of Antarctic CM2 chondrites [1] are their preterrestrial compositions, unmodified by terrestrial weathering.

Oxygen Isotope Composition and Degree of Aqueous Alteration: Non-Antarctic CM2 falls Murray and Murchison, and Antarctic CM2 finds QUE 93005 and ALH 83100, all have nearly identical oxygen isotope compositions [1]. Murchison and Murray are two of the least-altered CM2 chondrites known [2]; ALH 83100 [3] and QUE 93005 [4-6] are among the most-altered CM2s known. The wide range in degree of alteration exhibited by four CM2 chondrites [2-6] with nearly identical oxygen isotope compositions [1] suggests that oxygen isotopes do not reflect the degree of aqueous alteration of these CM2 chondrites.

Conclusions: Distribution of oxygen isotope compositions of Antarctic CM2 finds and non-Antarctic CM2 falls along the same preterrestrial mixing line on an oxygen three-isotope plot suggests similar (pre-terrestrial) controls on oxygen isotope compositions of both non-Antarctic CM2 falls and Antarctic CM2 finds. Whole-rock oxygen isotope compositions of CM2 chondrites do not reflect mass-dependent effects of pre-terrestrial aqueous alteration, and therefore are not related to other previously suggested measures of aqueous alteration [2].

References: [1] Clayton R. L. and Mayeda T. K. 1999. *Geochimica et Cosmochimica Acta* 63:2089-2104. [2] Browning L. B. et al. 1996. *Geochimica et Cosmochimica Acta* 60:2621-2633. [3] Zolensky M. E. et al. 1997. *Geochimica et Cosmochimica Acta* 61:5099-5115. [4] Rubin A. E. et al. 2005. *Meteoritics & Planetary Science* 40:A131. [5] Velbel M. A. et al. 2005. Abstract #1840. 36th Lunar and Planetary Science Conference. [6] Velbel M. A. et al. 2005. *Meteoritics & Planetary Science* 40:A161.

5245

ISOTOPE ANALYSES OF THE COARSEST GRAIN-SIZE FRACTIONS OF ORGUEIL NANODIAMONDS

A. B. Verchovsky¹, A. V. Fisenko², L. F. Semenova², and I. P. Wright¹. ¹Open University, Milton Keynes, UK. E-mail: a.verchovsky@open.ac.uk. ²Vernadsky Institute RAS, Moscow, Russia

Introduction: The best evidence of the existence of several populations of meteoritic nanodiamonds has been obtained by separating them into grain-size fractions using centrifugation [1]. The diamond fractions of Efremovka CV3, Boriskino CM2, and Krymka LL3.1 are systematically different in ¹³C with a total range from -22 to -40‰ with the lowest values corresponding to the coarsest fractions [2]. Using model calculations for a mixture of two diamond populations with different average grain sizes it is possible to calculate isotopic compositions of the end-member carbon components [2, 3]. In order to substantiate the efficiency of the modeling procedure it is clearly desirable to try and obtain the coarsest diamond fraction possible. In this study we have separated and analyzed the coarsest grain-size fractions of nanodiamond from the Orgueil CI meteorite.

Separation Procedures: Colloidal diamonds from 46 g of bulk Orgueil sample have been obtained using standard procedures [4]. The coarse materials, such as spinel and SiC, have been separated from the colloid by prolonged centrifugation. An additional long-duration centrifugation of the colloid allowed us to obtain a sediment fraction which seems to contain nanodiamonds originated from AGB stars [5]. The residual colloid has been treated to centrifugation at 13,500 g in four steps, with durations from 1 to 6 hours. It allowed us to obtain 4 coarse fractions which we analyzed for C, N, Ne, Ar, and Xe isotopes and concentrations and He concentration simultaneously using the Finesse machine [6]. We have not directly measured the grain size of the fractions, however their relative sizes can clearly be deduced from the sequence of the centrifugations.

Results: Our isotope data undoubtedly suggest that in this separation we obtained the coarsest fraction of nanodiamonds produced so far. It follows from the carbon isotopic compositions of the fractions and the noble gas (particularly for Xe-P3 and Xe-HL) concentrations which are known to show significant variations in the grain-size fractions due to implantation effects [1]. Interestingly, the highest concentration of Xe is observed, not in the coarsest fraction, but in the one previous to this in the centrifugation sequence. This means that the average grain size of the coarsest fraction is larger than the implantation range of Xe. The highest concentration of Xe obtained in the study is 8.2×10^{-6} cc/g which is 15 times higher than for the bulk Orgueil diamonds [7]. The overall ¹³C of the coarsest fraction is -50‰, but is as low as -55‰ in certain temperature steps. A diamond population with such a light carbon isotopic composition is supposed to be a carrier of P3 noble gases and formed in the protosolar nebula [8]. And the carbon isotopic composition of the population is well within the range evaluated for the Sun [9].

References: [1] Verchovsky A. B. et al. 1998. *Science* 281:1165. [2] Verchovsky A. B. et al. 2004. Abstract #1673. 35th Lunar and Planetary Science Conference. [3] Fisenko A. V. et al. 2005. Abstract #2304. 36th Lunar and Planetary Science Conference. [4] Amary S. et al. 1994. *Geochimica et Cosmochimica Acta* 58:459. [5] Verchovsky A. B. et al. 2005. Abstract #2285. 36th Lunar and Planetary Science Conference. [6] Verchovsky et al. 1998. *Meteoritics & Planetary Science* 32:A131. [7] Huss G. R. and Lewis R. S. 1994. *Meteoritics* 29:791. [8] Gilmour J. D. et al. 2005. *Geochimica et Cosmochimica Acta* 69:4133. [9] Wiens R. C. et al. 2004. *Earth and Planetary Science Letters* 222:697.

5075

ASTEROID COLORS: A NOVEL TOOL FOR MAGNETIC FIELD DETECTION? THE CASE OF VESTA

P. Vernazza¹, R. Brunetto^{2,3}, G. Strazzulla³, M. Fulchignoni¹, P. Rochette⁴, N. Meyer-Vernet¹, and I. Zouganelis¹. ¹LESIA, Observatoire de Paris, France. ²Dipartimento di Fisica, Università di Lecce, Lecce, Italy. ³INAF-Osservatorio Astrofisico di Catania, Italy. ⁴CEREGE Aix en Provence, France. ⁵Space Sciences Laboratory, University of California at Berkeley, Berkeley, California, USA

Vesta's surface is surprisingly pristine. Although its basaltic surface is roughly similar to the lunar surface, which is intensely space-weathered, its surface remains unaltered. It has been shown recently that solar-wind irradiation dominates asteroidal space weathering with a time scale on the order 10^4 – 10^6 yr. Recent ion irradiation experiments on pyroxenes have shown significant reddening and darkening of the collected spectra with progressive irradiation [1]. Since pyroxene is a major surface component of Vesta as determined by spectroscopy, we aimed to test whether the solar wind irradiation alters significantly the optical properties of the surface of Vesta. Consequently, we performed an ion irradiation experiment (using Ar ions with 400 keV energy) on an eucrite meteorite (Bereba), which characterizes the surface of Vesta well, in order to simulate the solar wind irradiation on this asteroid. Using an irradiation typical for a solar irradiation over a 10^4 – 10^5 yr time scale we found an IR spectra typical for the lunar surface but strongly reddened with respect to the Vesta surface spectra. On the contrary, present Vesta spectra match perfectly the fresh Bereba spectra [2].

Our result implies that if solar wind ions had reach the surface of Vesta since at least 10^4 – 10^5 yr, its reflectance spectrum should be much redder and its albedo lower. Explaining this lack of irradiation record by an impact resurfacing in statistically highly unlikely considering the time scale and the need for resurfacing the near totality of Vesta surface. In particular the very large polar impact invoked for Vesta is much too old to have played a role [3]. The only mechanism left is the presence of a magnetic field (throughout present time) shielding the surface from solar wind ions. This magnetic field should be produced by the remanent magnetization recording a now extinct dynamo (functional at 4.5 Ga, while the metallic core was liquid). Important paleofields (about 10 μ T) recorded in eucrite and howardite support this assumption [4]. This is the first remote detection of the magnetic field of an asteroid based on its color.

References: [1] Brunetto R. and Strazzulla G. 2005. *Icarus* 179:265. [2] Vernazza P. et al. *Astronomy and Astrophysics*. Forthcoming. [3] Bottke W. F. et al. 2005. *Icarus* 175:111. [4] Gattacceca J. and Rochette P. 2004. *Earth and Planetary Science Letters* 227:377.

5016

A SOURCE OF THE POPIGAI IMPACT FLUIDIZITES: DATA ON TRACE ELEMENTS

S. Vishnevsky¹ and S. Simakin². ¹Inst. of Mineral. and Petrol., Novosibirsk-90, 630090, Russia. E-mail: svish@uiggm.nsc.ru. ²Inst. of Microelectronics and Informatics, Yaroslavl-7, 150007, Russia. E-mail: simser@mail333.com

Introduction: The Popigai impact fluidizite dykes originate by jetting of hot volatile+melt mixtures (VMMs) at ~ 0.8 – 3.3 GPa residual shock pressure [1–4]. They made up of water-rich (1.11–8.97 wt% of H₂O) glass particles, fragments of host gneisses, and crypto-grain matrix. Three types of the glasses are found: type I—homogeneous similar to target gneisses in terms of bulk geochemistry; type II—heterogeneous, (fine banding of “femic,” “salic,” and type I glasses); type III—“salic” glasses, rich in Si, K, and Na. The VMMs were derived from complex Archean basement rocks [4] but their source is still open. In order to solve the question, the trace (TE) and rare earth (REE) elements were studied in individual particles of the fresh glasses by means of ion probe (20 runs, namely: 14 type I glass particles, SiO₂ 57.2–60.14 wt%; 1 type II glass particle, including 1 “salic” K-Na-Ca band, and two type I glass bands, SiO₂ 58.61 and 58.83 wt%; three type III glass particles: lechatelierite (L), and two high-silica (HS) particles, SiO₂ 88.71 and 89.94 wt%). All data are in ppm \pm st. dev. Data on TE are reported here; data on REE are in [5].

Observations: TEs in type I glasses are found as (16 runs): V 138 \pm 10.03; Zr 188 \pm 23.4; Rb 91 \pm 5.5; Sr 224 \pm 26.3; Ba 783 \pm 107; Ta 1.29 \pm 0.23; Nb 13.74 \pm 0.93; Hf 5.25 \pm 0.68; Y 34.1 \pm 7.4; Th 14.9 \pm 2.45; U 1.61 \pm 0.27 and Cr 165 \pm 16.8 for 13 similar runs; in three others Cr is detected as 365, 1166, and 2404 ppm). Most of TEs in “salic” K-Na-Ca glass show poor amounts: V 39, Zr 0.65, Ta 1.59, Nb 0.22, Hf 0.37, Y 1.13, Th 0.02, U 0.09 and Cr 19; but feldspar-isomorphic TEs are higher: Rb 172, Sr 468, Ba 3730. TE amounts in HS-glasses are varying: V 26 and 99.7, Zr 4.8 and 33.5, Rb 32 and 73, Sr 21 and 41, Ba 58 and 220, Ta 0.2 and 0.4, Nb 4.8 and 11.9, Hf 0.2 and 0.8, Y 2.4 and 2.6, Th 0.6 and 0.7, U 0.07 and 0.3, Cr 17 and 101. Lowest amounts are in L: V 2.2, Zr 0.8, Rb 1.6, Sr 1.5, Ba 3.7, Ta 0.08, Nb 0.19, Th 0.05, U 0.01, and Cr 4.

Conclusions: Compared to data by [6], type I glasses are very similar to both the granulites of Khapchan series and diaphthorites of amphibolite facies derived from them, in amounts of Th, U, and their ratio, Th/U = 9.33 \pm 0.94. Our REE data [5] also support the same source of the glasses. Khapchan granulites are very “dry” (L.O.I. = 0.36 \div 1.31 after [6]), so diaphthorites derived from the granulites were the most possible source rocks for the VMMs. Amounts of V, Zr, and Nb in type I glasses are also similar to those found [6] for Khapchan rocks. Compared to data by [6] for the granulites, higher amounts of Sr, Ba, and Nb in the glasses are, probably, caused by diaphthoresis; data on Hf and Y are absent in [6]. Amounts of TEs in K-Na-Ca and L-glasses are similar to those for quartz and feldspars. Intermediate TE amounts in HS-glasses are explained by mixing. Anomalously high Cr amount in type I glasses is probably related to projectile.

Acknowledgements: RFBR grant #04-05-64127 is acknowledged for this study.

References: [1] Vishnevsky S. et al. 2005. Abstract #1145. 36th Lunar and Planetary Science Conference. [2] Vishnevsky S. et al. 2005. *Meteoritics & Planetary Science* 40:A162. [3] Vishnevsky S. et al. 2006. Abstract #1268. 37th Lunar and Planetary Science Conference. [4] Vishnevsky S. et al. *Geologia i Geofizika*. Forthcoming. [5] Vishnevsky S. and Simakin S. 2006. Abstract #5107. *Meteoritics & Planetary Science* 41. This issue. [6] Rosen O. M. et al. 1988. *Archean of the Anabar Shield and early evolution of Earth*. Moscow: Nauka Press. 253 p. In Russian.

5017

A TARGET SOURCE OF THE POPIGAI IMPACT FLUIDIZITES: DATA ON REE

S. A. Vishnevsky¹ and S. G. Simakin². ¹Institute of Mineralogy and Petrology, Novosibirsk-90, 630090, Russia. E-mail: svish@uiggm.nsc.ru. ²Institute of Microelectronics and Informatics, Yaroslavl-7, 150007, Russia. E-mail: simser@mail333.com

Introduction: The Popigai impact fluidizite glasses and their ion probe studies are described in [1]. Below the data on REE (all in ppm) are reported for the fresh glass particles of the rocks.

Observations: REE spectra in type I glasses including their bands in type II particle are very similar and show the next features (see Fig. 1): i) REE totals are $186.4 \div 305.9$; ii) fractionation degree, LaN/YbN, is average ($6.5 \div 9$) or relatively high ($9 \div 12.25$); the “heavy” (Gd-Yb) spectra are semi-horizontal, whereas the “light” (La-Sm) ones are more steep (LaN/SmN $4.23 \div 5.46$), showing the enrichment for La-Sm; iii) the “light” versus “heavy” REE totals ratio is $10.05 \div 12.33$; iv) 13 runs show weak/moderate negative Eu-anomaly ($\text{Eu}/\text{Eu}^* = 0.58 \div 0.88$); three other runs show weak positive anomaly ($\text{Eu}/\text{Eu}^* = 1.08 \div 1.15$). REE spectrum of K-Na-Ca glass band in type II particle is complex, with low total (7.83), but high fractionation degree ($\text{La}_N/\text{Yb}_N = 39.17$); the “light” versus “heavy” REE totals ratio is 3.28; Eu shows strong positive anomaly ($\text{Eu}/\text{Eu}^* = 10.5$). REE spectrum of lechatelierite (L) is complex with low total; the spectra of high-silica glasses (HS) are slightly higher and coordinate with type I glass spectra.

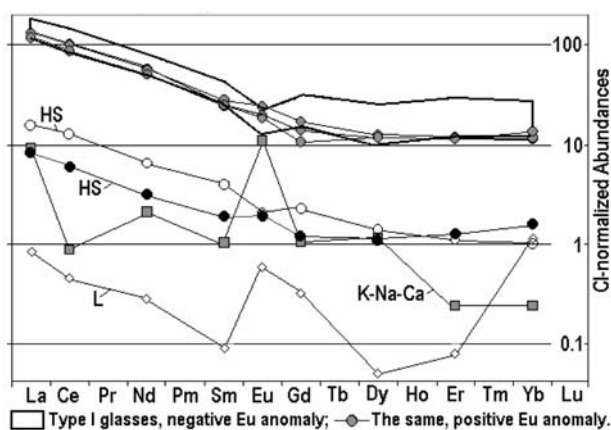


Fig. 1.

Conclusions: Following to our data, type I glasses with negative Eu-anomaly are rather similar to clinopyroxene gneisses of the Khapchan series (carbonate Archean granulites of the Anabar shield, [2]), but type I glasses with positive Eu-anomaly are similar to hypersthene plagiogneiss layers occurred within Khapchan strata. In both the cases, using the data by [2], no REE fractionation had taken place during the shock origin of the volatile+melt mixtures of the fluidizites. The spectrum of K-Na-Ca glass band is similar to feldspar ones, but higher REE-totals and presence of Fe (1.21 wt%) and Mg (1.45 wt%) show imprint of the type I melt. Negative Ce-anomaly ($\text{Ce}/\text{Ce}^* = 0.37$) in the glass differs from those of typical feldspars and could be related to pre-Cambrian diaphthoresis of the source granulites. REE-spectrum of L-glass is similar to typical quartz ones. Higher REE amounts in HS-glasses and similarity of their spectra to type I glasses can be explained by impurity of type I melt.

Acknowledgements: RFBR grant #04-05-64127 is acknowledged for this study.

References: [1] Vishnevsky S. A. and Simakin S. G. 2006. Abstract #5016. *Meteoritics & Planetary Science* 41. This issue. [2] Rosen O. M. et al. 1988. *Archean of the Anabar Shield and the Early Evolution of Earth*. Moscow: Nauka Press. 253 p. In Russian.

5211

REEVALUATION OF HIGH RESOLUTION $^{40}\text{Ar}/^{39}\text{Ar}$ AGES OF PLAGIOCLASE SEPARATES FROM IAB SILICATE INCLUSIONS AND IMPLICATIONS FOR THE THERMAL HISTORY OF THE IAB PARENT BODY

N. Vogel^{1,2} and P. R. Renne¹. ¹Berkeley Geochronology Center, California 94709, USA. E-mail: nvogel@space.unibe.ch. ²Present address: Institute of Physics, Space Research and Planetary Sciences, University of Berne, Switzerland

Introduction: In order to contribute to the understanding of the formation and thermal evolution of the IAB parent body, we present Ar-Ar ages of silicate inclusions from Caddo County (CC), Campo del Cielo (CdCl, 2), Landes (L), and Ocotillo (O). From each inclusion plagioclase separates of different grain sizes (l, m, s) were produced to monitor their influence on the age of a sample and to minimize complexity of the Ar-Ar age spectra.

Results: Figure 1 shows the ages of all separates. While ages within one inclusion vary significantly, all inclusions show one common age information around 4.43 Ga (shaded area). CC and L show additional higher ages, whereas CdCl and 2 also show clear evidence for a later event around 4.3 Ga, probably local impact reheating. Highest ages within one inclusion are not necessarily correlated with largest grains as expected from diffusion theory. We assume that during thermal events small amounts of plagioclase-rich melt formed within parts of the inclusions. These larger younger plagioclase grains were probably separated from smaller older plagioclase by our grain size sorting.

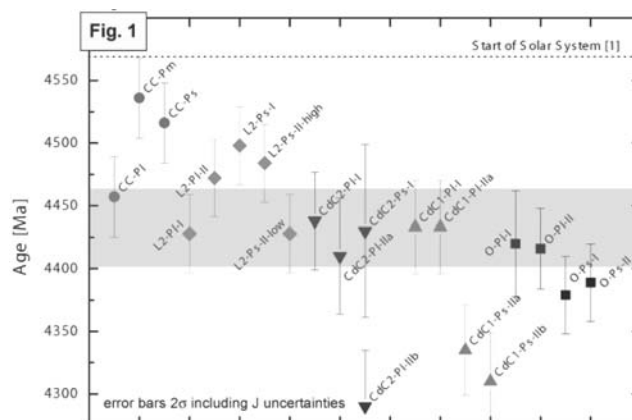


Fig. 1.

Discussion: A thermal event ~4.45 Ga erased all previous K-Ar age information from CdCl, 2, and O, whereas L and in particular CC were less affected and parts of them preserved higher ages. Thus, the temperature during this event cannot have been exceedingly high, in agreement with the fact that Rb-Sr, Sm-Nd, and I-Xe ages were not reset at this time (e.g., [2]). Since separation of high- and low-age plagioclase is not quantitative, “endmember ages” are probably more extreme than our actual ones. The CC age of 4536 ± 32 Ma is thus a lower limit for K-Ar closure after the thermal event dated also by Rb-Sr, Sm-Nd, and I-Xe. This might have been the mixing of metal and silicates by impact(s) few Ma after the start of the solar system [3, 4]. Taking into account the 2σ uncertainty of our highest CC age, the discussed K-Ar age bias of old meteorites cannot be larger than ~50 Ma and is almost certainly distinctly smaller.

References: [1] Amelin et al. 2002. *Science* 297:1678–1683. [2] Bogard et al. 2005. *Meteoritics & Planetary Science* 40:207–224. [3] Benedix et al. 2000. *Meteoritics & Planetary Science* 35:1127–1141. [4] Wasson and Kallemeyn. 2002. *Geochimica et Cosmochimica Acta* 66:2445–2473.

5194

CHARACTERIZATION OF PRESOLAR SILICATE GRAINS BY COMBINED NANOSIMS/TEM STUDIES

C. Vollmer¹, P. Hoppe¹, F. E. Brenker², R. M. Stroud³, and C. Holzzapfel⁴.
¹Max-Planck-Institut für Chemie, D-55020 Mainz. E-mail: cvollmer@mpch-mainz.mpg.de. ²JWG-Universität, D-60054 Frankfurt, Germany. ³Naval Research Laboratory, Washington, D.C. 20375, USA. ⁴Universität des Saarlandes, D-66041 Saarbrücken, Germany

Introduction: Silicates condense in the outflows of evolved O-rich stars or supernova ejecta and are detected as presolar grains in primitive solar system materials by high resolution mass spectrometry (e.g., [1, 2]). Detailed mineralogical information of this type of presolar grains obtained by transmission electron microscopy (TEM) is rare due to their small size and required elaborate extraction methods and is available for only seven grains to date [2–6]. Here we report on our continued search for presolar silicates in the matrix of Acfer 094 and the successful lift out of two of these grains for further investigation by TEM.

Methods: Anomalous silicate grains have been identified by NanoSIMS ion imaging described in [7]. To produce electron transparent sections the focused ion beam method (FIB) with an in situ nano manipulator has been used [8, 9]. The ~100 nm thin sections were then investigated by TEM (200 kV) applying bright and dark field techniques and EDX analysis.

Discussion: A total of 17 presolar silicate grains have been detected in Acfer 094 giving a matrix normalized abundance of ~140 ppm based on the size in the SEM. One ~1 µm large silicate described already in [7] encloses a subgrain of presumably Al₂O₃. Theoretically nucleation seeds of Al₂O₃ or TiO₂ are predicted for silicate condensation [10] and there is also spectroscopical evidence for composite grains [11]. The O isotope composition of the silicate and the subgrain are different even within error ranges, which might shed new light on isotopic heterogeneity in the disks of evolved stars. The FIB section of this grain revealed no large extension in depth pointing to a flat ellipsoidal shape. Research on this section is still in progress. The occurrence of this composite grain underlines furthermore the unique primitive nature of Acfer 094. TEM investigation of a second presolar silicate (~350 nm, O isotope group I) yielded a glass of non-stoichiometric composition containing abundant specks of a crystalline Fe-rich phase, which could be seen in dark-field imaging mode. Broad beam EDX analysis of a large part of the grain showed an S content in the percentage range indicating a GEMS-like composition. Confirmation of this grain to be indeed the presolar grain identified in the initial NanoSIMS search has to be confirmed in a further NanoSIMS measurement.

References: [1] Mostefaoui S. and Hoppe P. 2004. *The Astrophysical Journal* 613:L149–152. [2] Messenger S. et al. 2005. *Science* 309:737–741. [3] Messenger S. et al. 2003. *Science* 300:105–108. [4] Nguyen A. 2005. Ph.D. thesis. Washington University, Saint Louis, Missouri, USA. [5] Yada T. et al. 2005. Abstract #1227. 36th Lunar and Planetary Science Conference. [6] Floss C. et al. 2006. *Geochimica et Cosmochimica Acta* 70:2371–2399. [7] Vollmer et al. 2006. Abstract #1284. 37th Lunar and Planetary Science Conference. [8] Zega T. and Stroud R. M. 2006. Abstract #1441. 37th Lunar and Planetary Science Conference. [9] Holzzapfel C. et al. 2005. Microscopy Conference. p. 96. [10] Gail H.-P. and Sedlmayr E. 1999. *Astronomy and Astrophysics* 347:594–616. [11] Dijkstra C. et al. 2005. *The Astrophysical Journal* 633: L133–136.

5155

MELTED-REDUCED PIGEONITE, VERMICULAR SILICA, SI-RICH GLASSES, AND OTHER IMPACT-SMELTING PRODUCTS IN THE LAR 04315 UREILITE

Paul H. Warren and Alan E. Rubin. Institute of Geophysics, University of California–Los Angeles, Los Angeles, California 90095, USA

Our studies indicate that the anomalous LAR 04315 ureilite [1] formed by intense shock, including pyroxene-localized shock melting, of an otherwise normal ureilite. The late, post-decompression (post-parent-body disruption?) “smelting” process that affected all ureilites, mainly by reduction of olivine rims [2], primarily affected shock-melted pyroxene in LAR 04315.

Later annealing made the final state of the 1–2 mm pyroxenes crystalline, but recovery from shock-melt is indicated by, inter alia, scattered small voids in almost all of the pyroxene [1]. These voids are typically 40 × 20 µm, but curved and in some cases vermicular. They comprise ~20 vol% of the space within pyroxene, or 10 vol% of the rock. Isolated patches of little-altered, void-free pyroxene are usually <<0.1 mm across. However, one 0.9 × 0.7 mm low-shock pyroxene consists mainly of large ~100 × 100 µm void-free patches. During cooling, coarse twins developed in pyroxene, probably as the grains transformed from protoenstatite to pigeonite. Pyroxene compositions are unusually diverse, with random, void-rich pyroxenes showing effects of FeO loss (reduction). But the most FeO-rich analyses, all from the 0.9 × 0.7 mm low-shock pyroxene, are tightly clustered in the normal ureilite fashion at Wo_{10.3}, mg ~ 81.8. Isolated small void-free patches tend to resemble the low-shock remnant in composition. The voids within pyroxene may not be completely empty. In X-ray maps, they show locally higher Ca, Mg, and O, and lower C, than empty (crack) voids.

The original 1–2 mm olivines now consist of mosaics of small (usually <<0.5 mm), often angular pieces [1], indicating that they were strongly shocked, shattered, and subsequently welded together by (presumably) the same annealing process that recrystallized the pigeonites. Even so, the olivine avoided pervasive reduction. Tiny metal grains are common between olivine subgrains, but amount to only ~1% of the volume within any original olivine; and although subtle differences between subgrains are apparent in BSE images, these differences are difficult to detect quantitatively. The average olivine core composition, Fo_{81.9}, is nearly identical in mg to the intact pigeonite. For comparison, in 12 other ~Fo₈₂ ureilites (literature data), olivine-core mg is lower, but only by 1.6 ± 1.0 mol%, than pigeonite mg. In some places, clusters of rounded olivine remnants are surrounded by interstitial pyroxene, typically of relatively high-Ca composition.

In some ferroan ureilites, post-decompression reduction of minor interstitial basaltic melt appears to have locally generated Si-Al-rich melts [2]. A similar process resulted in relatively significant proportions of Si-Al-rich glass in LAR04315, and also long (up to ~100 × 5 µm) vermicular grains of a silica phase, with typically ~99.0 wt% SiO₂, 0.4% Al₂O₃ and 0.2% FeO.

The phase oxidized during the smelting of LAR04315 was presumably, as generally assumed for ureilites, solid C. From the extent of reduction of pigeonite, a remarkably high yield of CO/CO₂ gas is implied: ~0.7 wt% of the rock. The rock probably did not remain a totally closed system during the smelting. Maintenance of the observed moderate (~10%) porosity as CO/CO₂ gas would require an end-stage P of ~500 bar, far too high for oxidation of C at the low *f*O₂ implied by the high-mg silicates.

References: [1] McCoy T. et al. 2005. *Antarctic Meteorite Newsletter* 28(2). [2] Warren P. H. and Huber H. 2006. Abstract #2400. 37th Lunar and Planetary Science Conference.

5379

GASP! GAS-ASSOCIATED SPHEROIDAL PRECIPITATES RELATED TO HASP, FOUND IN ANORTHOSITIC APOLLO 14 REGOLITH BRECCIA 14076

Paul H. Warren, Eric Tonui, and Edward D. Young. Institute of Geophysics, University of California—Los Angeles, Los Angeles, California 90095, USA

The 14076 regolith breccia constitutes roughly half of a 2.0 g pebble. It is far more aluminous (30 wt% Al_2O_3) than any other Apollo 14 rock [1]. 14076 is extraordinarily rich in spheroidal HASP (high-Al, Si-poor) glasses (and devitrification products) that formed as residues from fractional evaporation of superheated highland impact-melt splashes [1, 2]. An issue not yet addressed regarding HASP, is the ultimate fate of the SiO_2 , FeO, and MgO, after evaporation removed them from the flying superheated melt droplets. During a compositional survey of ~60 regolith glass spheroids in 13 mm² thin section 14076.5, it became evident that a significant component of the spheroid population is distinctively tiny, and also distinctive in composition. The 30 spheroids smaller than 5 μm are preponderantly the opposite of HASP: nearly pure SiO_2 (the only two exceptions have apparent $D = 4\text{--}4.5 \mu\text{m}$). The vast majority of these Si-rich spheroids are ~2 μm across—not quite large enough to quantitatively analyze. Only the two largest, 4–5 μm across (the next largest has $D = 3 \mu\text{m}$), yielded good analyses, indicating 96–99 wt% SiO_2 . However, the problem with the analyses of the smaller spherules is often not so much beam overlap onto outside solids, but overlap onto adjacent regolith porosity, such that the analyses suffer more from low sums than from inaccurate element:element ratios, and the high-Si nature of the true composition is nonetheless manifest. In the intermediate size range (18 spheroids with apparent D between 5 and 15 μm), HASP compositions are especially common; e.g., 10 of the 18 have <35 wt% SiO_2 , and of these, seven have <24 wt% SiO_2 . The 13 spheroids larger than ~15 μm (apparent D) are preponderantly either “normal” in SiO_2 or mildly HASP.

As a name for this new type of lunar regolith spheroid, we have chosen GASP, for gas-associated spheroidal precipitates. It seems highly probable that these materials represent condensates of the mainly SiO_2 -gas component that was fractionally evaporated out of the associated HASP spheroids.

Besides HASP and the distinctively Si-rich variety of GASP, 14076.5 also contains at least three spheroids ($D = 7\text{--}12 \mu\text{m}$) of distinctively FeO-rich composition, 30–38 wt% FeO. The high FeO is accompanied by high SiO_2 (56–63 wt%) and not by high TiO_2 (undetectable to 0.04 wt%), so it is hardly likely to represent melt splashes of a mare surface material. The FeO-rich spheroids display quench textures, with constituent minerals far too small for quantitative analysis, but probably dominated by an Fe-rich low-Ca pyroxene (or pyroxenoid) and Si-rich glass. Probably these spheroids also represent condensates of the SiO_2 - and FeO-rich gas component that was fractionally evaporated out of the associated HASP spheroids. No MgO-rich GASP spheroids were found. Possibly Mg (as the MgO would have evaporated), with an atomic weight of just 24, was less efficiently recondensed than Si and Fe, and instead mainly lost by hydrodynamic escape.

The presence of three different forms of HASP-GASP spheroidal materials all in a single regolith sample (and not, so far, found together anywhere else) suggests that the impact that produced these distinctive materials was relatively small (i.e., not basin-scale).

References: [1] Jerde E. et al. 1990. *Earth and Planetary Science Letters* 98:90–108. [2] Vaniman D. T. and Bish D. L. 1990. *American Mineralogist* 75:676–686.

5387

EVIDENCE OF DIFFERING LIQUID REGIMES IN METALLIC MAGMAS

John T. Wasson. Institute of Geophysics and Planetary Physics, University of California, Los Angeles, California 90095–1567, USA. E-mail: jtwasson@ucla.edu

Introduction: The magmatic iron meteorites formed by fractional crystallization in kilometer-size bodies of magma. On plots of Ir versus Au the left envelope of the scatter field defines the location of the solid crystallization track. The liquid crystallization track can be inferred because some members of each group formed as mixes of equilibrium solids and trapped melt [1]. The equation currently used to model the crystallization is simplified version of eq. (8) of Chabot and Jones [2]:

$$\log D = \log D_0 - \beta \cdot \log [(1 - 2X_S - 3X_P)/(1 - X_S - X_P)] \quad (1)$$

The key terms are D , the solid/liquid distribution ratio and β , the slope showing the change in D with changing nonmetal content of the magma; X_S and X_P are mole fractions.

Wasson et al. [3] recently noted that, in order to obtain good fits to the data sets they needed very different values of the intercepts D_0 . For groups such as IID and IVA with low nonmetal contents they require D_0 values for Ir are around 1.7; for groups with moderately high nonmetal contents (IIAB and IIIAB) the D_0 values for Ir are near 4.5.

Here we call attention to the rapid change in slope within group IVA; at a Au content of about 1.6 $\mu\text{g/g}$ corresponding to ~60% crystallization of the magma the slope changes within a small range in Au contents. At this point the S and P contents of the magma had increased by factors of ~2.5.

We suggest that this large change reflects the transition between two melt regimes; at low S and P concentrations the nonmetals seem to have relatively minor effects on D values, but at the higher values (above Au = 1.6 $\mu\text{g/g}$) the liquid enters a different chemical-physical regime in which the change in D value is much more pronounced. In Fig. 1, we show two solid tracks and one liquid track; the second liquid track is off scale.

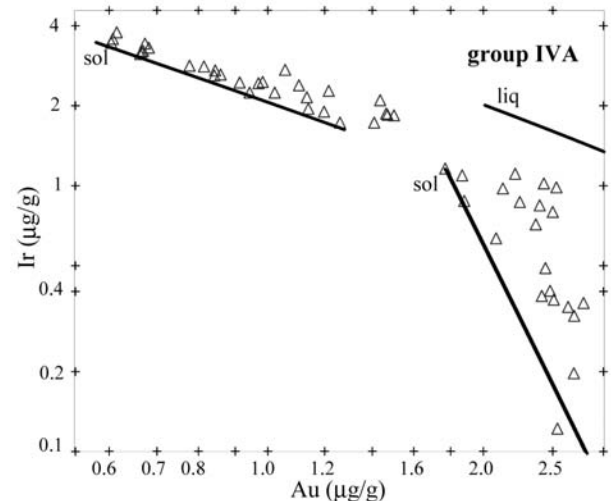


Fig. 1.

References: [1] Wasson J. T. 1999. *Geochimica et Cosmochimica Acta* 59:115; [2] Chabot N. L. and Jones J. H. 2003. *Meteoritics & Planetary Science* 38:1425. [3] Wasson J. T., Huber H., and Malvin D. J. *Geochimica et Cosmochimica Acta*. Forthcoming.

5343

NEBULAR FINES, PRESOLAR GRAINS, AND COLLATERAL DAMAGE DURING CHONDRULE FORMATION

John T. Wasson. Institute of Geophysics and Planetary Physics, University of California, Los Angeles, California 90095-1567, USA. E-mail: jtwasson@ucla.edu

Introduction: Paul Pellas once said that St. Mesmin was not a meteorite but a meteorite collection. Many of the chondrules in LL3.0 Semarkona and other primitive chondrites are not just chondrules, they contain so many relict grains that they could be called chondrule collections. Each relict grain is a fragment of an earlier chondrule, and frequently different chondrule precursors are represented. This and other evidence shows that (at least in the ordinary chondrite formation region) chondrule matter experienced several flash-heating events that raised temperatures high enough to melt chondritic silicates. The mechanism that formed chondrules is still not known, but there is little doubt that it heated both the chondrule precursors and the associated gas and dust to create a plasma with a temperature in excess of 2000 K, high enough to permit rapid heat conduction into 10 μm grains. It is important to determine if nebular fines ("matrix") experienced the same number of high-temperature events, and how this relates to the composition of the fines and the observed abundance of presolar grains.

Vaporization versus Survival of Presolar Grains: Wasson [1] noted that the temperature at which olivine vaporizes is ~1300 K, >600 K lower than that achieved in the chondrule-melting plasmas. Because evaporation occurs one layer at a time, tiny matrix grains will evaporate even though the chondrules lose relatively trivial mass fractions.

A reasonable working assumption is that 90% of nebular fines have passed through a hot plasma; in these parcels micrometer-size olivine and more volatile silicates evaporated. A key question is then what happened to presolar grains. The abundance of presolar diamonds and SiC in Semarkona and other low-type-III ordinary chondrites is ~100 $\mu\text{g/g}$ [2]. Is it reasonable that this is a remnant population, and that ~90% of the original inventory has been destroyed? The two possible answers are 1) yes, and 2) no, these refractory grains are more resistant to evaporation.

Late versus Early Presolar Matter: The nebula was continuing to accrete during the period of chondrule formation; accretion powered the turbulence that hindered the formation of planetesimals and led to grain-gas segregations of the sort recorded in the metal-silicate fractionation within the ordinary-chondrite suite. It seems likely that nebular fines within primitive chondrites are themselves a mixture of a) late arriving presolar matter, most of which has not been immersed in a chondrule-forming plasma; and b) a much larger fraction which largely consisted of smoke-like particles that formed by flash evaporation and rapid condensation during chondrule formation.

Alexander [3] inferred that chondritic fines consist of slightly modified interstellar matter that is very closely related to the matter in CI chondrites. My view is very different. I suspect that CI chondrites are not grail-like, but samples of largely recycled fines from one particular nebular time and place.

References: [1] Wasson J. T. 1996. *Chondrules and the Protoplanetary Disk* 45. [2] Huss G. R. and Lewis R. S. 1995. *Geochimica et Cosmochimica Acta* 59:115. [3] Alexander C. 2005. *Meteoritics & Planetary Science* 40: 973.

5317

SULFIDE-METAL NODULES IN EH3 CHONDRITES

M. K. Weisberg^{1, 2}, H. C. Connolly^{1, 2}, D. S. Ebel², and M. Kimura³. ¹Department of Physical Sciences, Kingsborough College CUNY, Brooklyn, New York 11235, USA. E-mail: mweisberg@kbcc.cuny.edu. ²Department of Earth and Planetary Sciences, American Museum Natural History, New York, New York 10024, USA. ³Ibaraki University, Mito 310-8512, Japan

Introduction: The enstatite chondrites (EC) have highly reduced mineral assemblages (e.g., [1]) that likely formed in equilibrium with a reducing vapor. Another intriguing aspect of the EC is that they appear to share the same oxygen isotopic reservoir as the Earth and Moon [2, 3]. A wide variety of sulfide-metal assemblages in EC record primary and secondary processes [4]. Here we focus on the origin of sulfide-metal nodules in Sahara 97096 and Kota Kota (both EH3) in relation to chondrule formation and nebular condensation under reduced conditions. We previously described sulfide-metal nodules in Sahara 97096 [5].

Results: Sahara 97096 and Kota Kota are among the most primitive EH3 chondrites, based on modal abundances (>6 vol%) and compositions (>0.2 wt% Cr₂O₃) of their olivine [6]. Sulfide-metal nodules are roughly circular in thin section with sharp, well-defined boundaries. Nodule sizes range from ~50 to 300 μm , slightly smaller than the chondrules (up to ~700 μm). Sulfide-metal nodules contain a wide variety of sulfides including troilite \pm oldhamite (CaS), \pm Niningerite [(Mg,Fe,Mn)S], \pm ferroan sphalerite [(Zn,Fe)S], \pm djerfisherite [(K,Na)₆(Cu,Fe,Ni)₂₅S₂₆Cl], in association with Si-bearing kamacite \pm schreibersite, \pm perryite [(Ni,Fe)_x(Si,P)_y]. Many of these sulfides are also present in EH3 chondrules. Troilite is generally the most common sulfide in the nodules \pm exsolution of daubreelite [(Fe,Cr)₂S₄]. Schreibersite generally occurs as small inclusions in oldhamite or niningerite and occasionally in troilite. Nodules generally contain ubiquitous grains of silica and enstatite. Some have small amounts of graphite. One unusual nodule in Kota Kota contains 7 vol% ferroan sphalerite and small grains of a Na-rich feldspathic component. Some nodules have concentric layered structures with oldhamite or niningerite cores, as previously reported [7].

Discussion and Conclusions: Sulfide-metal nodules are sensitive indicators of metamorphism of E3 chondrites. Oldhamite is predicted to be the highest-temperature Ca-bearing phases to condense from a cooling solar gas under reducing conditions [8], consistent with its occurrence in the cores of some layered nodules [7] and its enriched REE abundances [9]. Sulfide-metal nodules may be the equivalent of refractory inclusions under reducing conditions. Alternatively, the nodules formed as immiscible sulfide-metal liquids during chondrule formation.

References: [1] Keil K. 1968. *Journal of Geophysical Research* 73: 6945-6976. [2] Clayton R. N. and Mayeda T. K. 1984. *Journal of Geophysical Research* 89:C245-C249. [3] Javoy M. 1995. *Geophysical Research Letters* 22:2219-2222. [4] El Goresy A. et al. 1988. *Proceedings of the NIPR Symposium Antarctic Meteorites* 1:65-101. [5] Weisberg M. K. and Prinz M. 1998. Abstract #1741. 29th Lunar and Planetary Science Conference. [6] Weisberg M. K. et al. 2005. Abstract #1420. 36th Lunar and Planetary Science Conference. [7] Lin Y. and El Goresy A. 2002. *Meteoritics & Planetary Science* 37:577-599. [8] Larimer J. W. and Bartholomay M. 1979. *Geochimica et Cosmochimica Acta* 43:111-120. [9] Crozaz G. and Lundberg L. L. 1995. *Geochimica et Cosmochimica Acta* 59:3817-3831.

5350

COSMOGENIC RADIONUCLIDES IN A WEATHERED, 2.8 MILLION YEAR OLD H CHONDRITE FOUND ON TOP OF FRONTIER MOUNTAIN, ANTARCTICA

K. C. Welten¹, K. Nishiizumi¹, L. Folco², and M. W. Caffee³. ¹Space Sciences Laboratory, University of California–Berkeley, Berkeley, California 94720, USA. E-mail: kwelten@berkeley.edu. ²Museo Nazionale dell'Antartide, 53100 Siena, Italy. ³PRIME Lab, Purdue University, West Lafayette, Indiana 47907, USA

Introduction: In 2001, a small (1.5 g) chondrite was found on top of Frontier Mountain (FRO) during a geomorphological survey by a PNRA team. The meteorite was found on a glacially eroded bedrock surface at an altitude of 2775 m (i.e., ~600 m above present-day ice level). The meteorite, FRO 01149, is an H4 chondrite [1], and shows almost complete oxidation of the metal and sulfides. Preliminary cosmogenic ¹⁰Be and ⁴¹Ca results indicated a terrestrial age >0.5 Myr and possibly >2 Myr [2]. However, the lack of metal and possible contamination of the meteorite with terrestrial (“meteoric”) ¹⁰Be and ³⁶Cl made the interpretation of these results difficult. We therefore carried out leaching experiments to remove the weathering products, and measured ¹⁰Be, ²⁶Al, and ³⁶Cl in the leached silicate grains.

Experimental: After crushing the meteorite to <0.5 mm, we leached ~150 mg in 6N HCl. After leaching for 10 min. at ~25 °C, we dissolved 31 mg of the residue (R1) for radionuclide analysis. The remaining fraction was then leached for 30 min in 6N HCl at ~50 °C. The residue was rinsed and two aliquots, of 27 mg (R2, <125 μ) and 4 mg (R3, <125 μ), and a duplicate sample of 18 mg (R4) were dissolved for radionuclide analysis by AMS.

Results and Discussion: Chemical analysis of the four samples shows that leaching at ~25 °C removed only half of the oxidized FeNi-metal (R1), whereas leaching at ~50 °C (R2–R4) removed >99% of the weathering products. The latter was confirmed by microprobe analyses and BSE imaging of the leached grains. The ¹⁰Be and ²⁶Al concentrations in R2–4 show average values of 6.2 ± 0.2 and 3.8 ± 0.2 dpm/kg, respectively. These concentrations and the average ²⁶Al/¹⁰Be ratio of 0.61 ± 0.02 correspond to a terrestrial age of 2.82 ± 0.10 Myr. The average ³⁶Cl concentration of 0.057 ± 0.013 dpm/kg in two leached samples (R2, R4) only yields a minimum age of ~2 Myr, since part of the ³⁶Cl is due to in situ production on Earth, which is estimated at ~0.03 dpm/kg (15 atoms/g/year) at an altitude of 2775 m [3].

The ²⁶Al/¹⁰Be ratio of ~0.41 in the bulk sample is ~30% lower than in the leached samples. This low value is due to contamination with ~2.4 dpm/kg of meteoric ¹⁰Be, which was incorporated in the meteorite upon oxidation of the metal. Similarly, the high ³⁶Cl concentrations of ~0.8 dpm/kg in the bulk sample and ~0.5 dpm/kg in R1 are also due to “meteoric” ³⁶Cl. The terrestrial ¹⁰Be and ³⁶Cl components correspond to a ¹⁰Be/³⁶Cl ratio of ~7.4, within the range of 5–20 found in polar ice samples.

Conclusions: With a terrestrial age of ~2.8 Myr, FRO 01149 is the oldest stony meteorite found on Antarctica [4, 5]. Its location of find and high degree of weathering suggests it is a local fall and constrains the last overriding of Frontier Mountain. Preliminary results of in situ ¹⁰Be in quartz from the granitic bedrock surface show a minimum exposure age of ~1.2 Myr.

References: [1] Russell S. et al. 2002. *Meteoritics & Planetary Science* 37:A157–A182. [2] Folco L. et al. 2004. *Meteoritics & Planetary Science* 39:A40. [3] Gosse J. and Phillips F. 2001. *Quaternary Science Review* 20:1475–1560. [4] Scherer P. et al. 1997. *Meteoritics & Planetary Science* 32:769–773. [5] Welten K. et al. 1997. *Meteoritics & Planetary Science* 32:775–780.

5382

THE COMPLEX EXPOSURE HISTORY OF A LARGE L6 CHONDRITE SHOWER FROM OMAN

K. C. Welten¹, K. Nishiizumi¹, D. J. Hillegonds², and M. W. Caffee³. ¹Space Sciences Laboratory, University of California–Berkeley, Berkeley, California 94720, USA. E-mail: kwelten@berkeley.edu. ²CAMS, Lawrence Livermore National Laboratory, Livermore, California 94550, USA. ³PRIME Lab, Purdue University, West Lafayette, Indiana 47907, USA

Introduction: Most of the large chondrites, like Bur Gheluai, Gold Basin, Jilin, QUE 90201, and Tsarev reveal complex exposure histories with a first stage on the parent body and a second stage of 0.4–20 Myr in space. Recently, a large L6 chondrite strewn field, JaH 073, was found in Oman [1]. This well-documented shower contains ~3000 fragments with a total mass of ~550 kg. Preliminary noble gas results show low ²²Ne/²¹Ne ratios and a factor of 15 variation in the ²¹Ne concentration, indicating a large pre-atmospheric size and possibly a complex exposure history [2]. To investigate its cosmic-ray exposure history in more detail we measured cosmogenic ¹⁰Be, ²⁶Al, and ⁴¹Ca in ten fragments of this shower.

Experimental Methods: We crushed the meteorite samples and leached silicate grains >0.25 mm for 30 min in 6N HCl to remove weathering products. The leached samples were then rinsed and dissolved in HF/HNO₃ for radionuclide analysis. Concentrations of ¹⁰Be and ²⁶Al were measured at Purdue, those of ⁴¹Ca were measured at LLNL.

Results and Discussion: Concentrations of ⁴¹Ca range from 6 to 35 dpm/kg. The high ⁴¹Ca contents in the JaH 073 samples are due to neutron-capture ⁴¹Ca contributions, which range from ~0.2 to 1.8 dpm/gCa. The maximum value of 1.8 dpm/gCa can only be acquired in objects with radii of 50–200 cm, thus confirming the large pre-atmospheric size of JaH 073 [1, 2].

The ¹⁰Be and ²⁶Al concentrations range from 7.6–12.8 dpm/kg and 45–64 dpm/kg, respectively, while the ²⁶Al/¹⁰Be ratio ranges from 4 to 6. Interestingly, the ²⁶Al/¹⁰Be ratio is inversely correlated with the ¹⁰Be concentration (Fig. 1). This trend is similar to the one observed in Jilin and suggests a complex exposure history with a long exposure on the parent body, followed by a relatively short exposure (~1.0 Myr) as a large object in space. This scenario corroborates the trend that many large chondrites were exposed on their parent body before ejection into space.

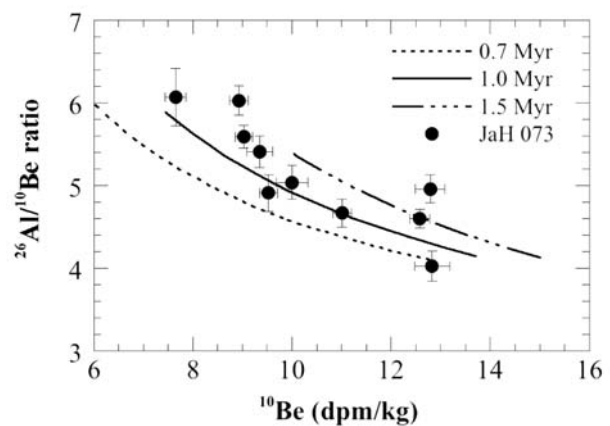


Fig. 1. Measured ²⁶Al/¹⁰Be versus ¹⁰Be in JaH 073, compared to calculated values for second-stage exposure times of 0.7–1.5 Myr.

References: [1] Gnos E. et al. 2003. *Meteoritics & Planetary Science* 38:A31. [2] Huber L. et al. 2006. Abstract #1628. 37th Lunar and Planetary Science Conference.

5018

IMPACT-RELATED DEFORMATION IN THE COLLAR ROCKS OF THE VREDEFORT DOME, SOUTH AFRICA

Frank Wieland, Roger L. Gibson, and Wolf Uwe Reimold. Impact Cratering Research Group, School of Geosciences, University of the Witwatersrand, Private Bag 3, P.O. Wits 2050, Johannesburg, South Africa. E-mail: fwieland@ix.urz.uni-heidelberg.de

Introduction: The Vredefort Dome represents the deeply eroded remnant of the eroded central uplift of the world's oldest (2.02 Ga) and largest (ca. 300 km) known impact structure [1]. It comprises an ~40 km wide core of Archean basement gneisses and an ~20 km wide collar of subvertical to overturned Late Archean to Paleoproterozoic supracrustal strata. We report on the results of a detailed structural geological study of the supracrustal strata of the inner collar of the Dome.

Results: Contrary to the findings about shatter cones of some earlier workers in the Vredefort structure [2, 3], the Vredefort cone fractures do not show uniform apex orientations at any given outcrop. The model of simple back-rotation of the strata to a horizontal pre-impact position does not lead to a uniform centripetal-upward orientation of the cone apices. Striation patterns on the cone surfaces are variable, ranging from typically diverging, i.e., branching off the cone apex, to subparallel to parallel on almost flat surfaces and striation angles do not increase with distance from the crater center, as suggested previously [4]. Pseudotachylitic breccias in the collar rocks occur as up to several centimeter-wide veins with variable orientations to the bedding and as more voluminous pods and networks in zones of structural complexity, such as the hinges of large-scale folds and along large-scale faults. This study revealed a highly heterogeneous internal structure of the collar involving folds, faults, fractures and melt breccia occurrences that are interpreted as the product of shock deformation and central uplift formation during the Vredefort impact event. Broadly radially-oriented symmetric and asymmetric folds, with wavelengths from tens of meters to kilometers, and conjugate radial to oblique faults with strike-slip displacements of, typically, tens to hundreds of meters accommodated tangential shortening of the collar of the dome that decreased from ~17% at a radial distance from the dome center of 21 km, to <5% at a radial distance of 29 km.

In addition to shatter cones, quartzite units show two other fracture types—a centimeter-spaced rhomboidal to orthogonal type that may be the product of shock-induced deformation and related to the formation of shatter cones, and later joints accomplishing tangential and radial extension.

Conclusions: Based on these results, it is possible to establish a temporal sequence of deformation events. Shatter cones and related, closely spaced fractures were formed during the shock phase of the cratering process. The formation of, at least some, shock-induced pseudotachylitic breccia also belongs into this phase. Large-scale folds and faults, and friction-generated melts can be related to the initial formation of the central uplift, and formation of extensional joints to the subsequent collapse of the central uplift.

References: [1] Gibson R. L. and Reimold W. U. 2001. *Memoir '92, Council for Geoscience*. [2] Manton 1962a. MSc. thesis. University of Witwatersrand, Johannesburg, South Africa. [3] French B. 1998. *Traces of catastrophe*. Houston: Lunar and Planetary Institute. [4] Sagy et al. 2004. *Journal of Geophysical Research* 109:B10209.

5067

WHAT ARE THE CONSEQUENCES IF THE "SEP" SOLAR NOBLE GAS COMPONENT DOES NOT EXIST?

R. Wieler, A. Grimberg, and V. S. Heber. ETH Zürich, Isotope Geology, NW C84, CH-8092 Zürich, Switzerland. E-mail: wieler@erdw.ethz.ch

Lunar dust grains appear to contain a solar noble gas component isotopically heavier than the solar wind (SW) and implanted to larger depths. This component was attributed to solar particles implanted at considerably higher energies than the SW [1, 2], and dubbed "SEP" for Solar Energetic Particles [2]. Supportive evidence came from analyses of solar energetic particles from coronal mass ejections, which also suggested $^{20}\text{Ne}/^{22}\text{Ne}$ on average possibly to be lower than the SW value [3]. However, it has been difficult to reconcile the high apparent abundance of SEP in lunar samples with the very low measured flux of solar energetic particles, hence the suspicion that "SEP" may be an artifact caused by isotope-dependent penetration depths or diffusion (e.g., [4, 5]).

Data from a metallic glass exposed on the Genesis mission now seem to have clarified this conundrum [6]. The depth profile of $^{20}\text{Ne}/^{22}\text{Ne}$ in the glass is very similar to that predicted for an isotopically uniform SW component implanted with the velocity distribution measured by Genesis. Thus, the gases at larger depths in all probability do not represent an isotopically distinct component.

Here we discuss some implications of this finding in geo- and cosmochemistry. In many cases, consequences are not dramatic. Often, measured isotopic compositions of solar gases heavier than the pure SW, rather than implying a prominent contribution of SEP, now indicate a relative enrichment of (isotopically heavy) fractionated SW from larger depths, due to, e.g., loss of outermost grain layers. Further work will have to clarify whether young lunar grains in sputter-saturation equilibrium conserve the true SW isotopic composition at the very surface, as postulated [7], but first Genesis data [8] appear to confirm previous SW compositions based on lunar samples. The isotopic composition of Ne in the Earth's mantle has been interpreted to reflect grains containing a mixture of SW-Ne and SEP-Ne added to the accreting Earth [9]. Now, as in the lunar regolith, this putative "Ne-B" would be reinterpreted as enrichment of fractionated SW-Ne due to partial grain surface erosion. A similar enrichment now seen in deeper layers in lunar grains [7] will not necessarily affect the alternative interpretation of these data by [10], who suggest that some volatiles in the lunar regolith originate from the Earth's atmosphere. Oxygen lighter than the terrestrial atmosphere in lunar metal grains has been interpreted as representing SEP-oxygen [11]. Being viewed now as high-speed SW-oxygen instead, the inference by [11] about the isotopic composition of solar-nebula O would not need to be revisited, because the depth-dependent fractionation of SW species remains identical to the previously supposed fractionation between SW and SEP.

References: [1] Black D. C. and Pepin R. O. 1969. *Earth and Planetary Science Letters* 6:395–405. [2] Wieler R. et al. 1986. *Geochimica et Cosmochimica Acta* 50:1997–2017. [3] Leske R. A. et al. 1999. *Geophysical Research Letters* 26:2693–2696. [4] Frick U. et al. 1988. 18th Lunar and Planetary Science Conference. pp. 87–120. [5] Mewaldt R. A. et al. 2001. AIP Conference Proceedings 598:393–398. [6] Grimberg A. et al. 2006. Abstract #1782. 37th Lunar and Planetary Science Conference. [7] Heber V. S. et al. *The Astrophysical Journal* 597:602–614. [8] Meshik A. P. et al. 2006. Abstract #2433. 37th Lunar and Planetary Science Conference. [9] Tieloff M. et al. 2000. *Science* 288:1036–1038. [10] Ozima M. et al. 2005. *Nature* 436:655–659. [11] Hashizume K. and Chaussidon M. 2005. *Nature* 434:619–622.

5207

THE EFFECT OF ATMOSPHERIC ENTRY HEATING ON MICROMETEORITE VOLATILE COMPOSITION

R. C. Wilson, V. K. Pearson, I. A. Franchi, I. P. Wright, and I. Gilmour. Planetary and Space Sciences Research Institute, Open University, Milton Keynes, UK. E-mail: r.c.wilson@open.ac.uk

Introduction: With estimates of present day mass flux of $40,000 \pm 20,000$ t/yr [1], micrometeorites (MMs) may have served as a substantial contributor of volatiles and biologically significant molecules to the early Earth (or other young planetary surfaces). These particles have high relative velocities, which dissipate their energy during atmospheric entry. This study investigates the effect of heating during atmospheric entry, on the survival and modification of organic material in MMs, and their involvement in prebiotic organic chemistry.

Experimental Techniques: Due to the micrometer-sized nature of MMs and their low availability for analysis, compositionally analogous materials are required to represent unmelted MM particles. In this case, 9 mg aliquots of the powdered carbonaceous chondrite Murchison are used.

The samples were heated in air to peak temperatures between 400 and 1000 °C for the short durations of 5, 10, and 20 seconds using a platinum filament fitted to a CDS 1000 pyroprobe. A thermocouple was embedded in the sample to quantify the peak temperature experienced by the sample. The heating range is comparable to the peak temperatures experienced by unmelted MMs [2, 3]. Fractions of the heated sample were examined using elemental and thermo-gravimetric (TG) analyzers, to assess the percentage carbon loss and volatile and organic survival.

Results: Elemental analysis demonstrates that the shorter the heating duration, the higher the percentage of total carbon surviving any peak entry heating temperature. A minimum of 5% total carbon remains in samples heated to ~900 °C for 20 s, corresponding to carbonate minerals. A minimum of 30% total carbon remains in samples heated to a similar peak temperature for 5 s. The remaining carbon is dominated by carbonate minerals with detectable quantities of organics.

A greater abundance and broader range of organic material survives in samples exposed to higher entry heating temperatures at shorter heating durations. As TG CO₂ profile peaks corresponding to organics are very broad, it is not possible to identify individual organic components. Alternative techniques are required to determine the nature of surviving organic material.

Similarly, at shorter heating durations, a greater abundance of adsorbed and structurally bound water was able to survive, when exposed to higher entry heating temperatures. The structural water peaks are consistent with cronstedtite [4], a dominant phyllosilicate present in Murchison [5].

Implications: The results demonstrate that organic molecules and other volatile components can withstand certain atmospheric entry heating conditions. It is therefore plausible that micrometeorites may have made a contribution to the organic inventory of the early Earth, prior to the evolution of life.

References: [1] Love S. G. and Brownlee D. E. 1993. *Science* 262:550–553. [2] Toppani A. et al. 2001. *Meteoritics & Planetary Science* 36:1377–1396. [3] Love S. G. and Brownlee D. E. 1991. *Icarus* 89:26–43. [4] Morris A. A. et al. 2005. Abstract #1925. 36th Lunar and Planetary Science Conference. [5] Buseck P. R. and Hua X. 1993. *Annual Review of Earth and Planetary Sciences* 21:255–305.

5078

IMPLICATIONS FOR THE CHICXULUB FIREBALL DERIVED FROM A SYSTEMATIC ANALYSIS OF ITS DEPOSITS

A. Wittmann, D. Stöffler, L. Hecht, and T. Kenkmann. Museum für Naturkunde, Mineralogie, Invalidenstr. 43, 10115 Berlin, Germany. E-mail: axel.wittmann@museum.hu-berlin.de

Introduction: A continuous record of the Chicxulub fireball deposits is intersected in the ICDP-Chicxulub Yaxcopoil-1 (Yax-1) drilling that is located in the structure's annular moat, ~60 km SSE' from the crater's center [1]. Systematic, image analysis-based study of this 100 m sequence of suevite-like rocks was conducted on photographs of half-cores and thin sections of ~40 samples to reconstruct emplacement conditions of these impact breccias.

Samples and Methods: Modal abundance of components and particle shape parameters were determined for the lapilli particle size range recorded in the half-cores. Bulk chemical compositions were derived from EMP analyses of 90 impact melt particles (MP).

Results: Five MP types were distinguished. The first type was rapidly quenched and is only abundant in the uppermost units and in dike breccias. The second type is variably quenched, rich in vesicles, and exhibits shard morphologies, thus indicating airborne transport. This MP type only occurs in the upper four units that are interpreted as airfall suevites. The third MP type is thoroughly crystallized with Pl and Cpx phenocrysts and is the most abundant MP type in the three basal units that overlie sedimentary megablocks. In these units, shape parameters of these MP indicate thermal softening and some corroded rims, suggesting post-depositional temperatures >~700 °C [2]. The fourth MP type bears abundant Fe-O crystals and is only abundant in the airfall suevites. This suggests fO_2 conditions in excess of the FMQ-buffer for the formation of this MP type [3]. The variation in bulk chemical compositions of the MP is more pronounced on the unit-level than between particle types. This could suggest a homogenized impact melt that underwent compositional differentiation due to alteration and variable degrees of quenching. Carbonate target clasts in the lower airfall suevites and the impact melt unit indicate contact metamorphism. Below the impact melt unit, carbonate occurs with melt textures [1]. Particle size distributions in the uppermost unit agree with models for condensation from an impact vapor plume [4]. Distinct sorting is only indicated in the uppermost unit. Alignments of MP indicate increasing turbulence with depth and melt injections in dikes.

Conclusions: Petrologic characteristics of MP in Yax-1 suggest variable fO_2 and T-t conditions during their formation: Shape parameters indicate sorting processes, alignments and modifications of MP. Indications for thermal alteration of the MP above ~700 °C and reworking features suggest the presence of a hot region of the fireball that collapsed with an erosive surge after the deposition of a melt unit that capped a ground-surg ed ejecta curtain deposit. Melt textures indicate that degassing of anhydrite and carbonate was inhibited below the melt unit.

References: [1] Stöffler D. et al. 2004. *Meteoritics & Planetary Science* 39:1035–1067. [2] von Engelhardt et al. 1995. *Meteoritics & Planetary Science* 30:279–293. [3] Frost B. R. 1991. *Reviews in Mineralogy* 25:1–9. [4] de Niem, D. 2002. GSA Special Paper #356. pp. 631–644.

5049

STEPWISE CHEMICAL DISSOLUTION OF CARBONACEOUS CHONDRITES: CORRELATIONS BETWEEN VOLATILE TRACE ELEMENTS AND MAJOR/MINOR MINERAL CONSTITUENT ELEMENTS

S. F. Wolf. Department of Chemistry, Indiana State University, Terre Haute, IN 47809-5901. E-mail: wolf@indstate.edu

Introduction: In an effort to gain a greater understanding of the distribution and cosmochemical affinity of volatile trace elements (VTEs) within primitive meteorites we are performing stepwise chemical dissolution of homogenized bulk samples of the carbonaceous chondrites Allende (CV3) and Murchison (CM2). Previously we reported preliminary results from these experiments examining fractional releases of the highly VTEs Cd, Bi, Tl, and In [1]. Here we examine releases for the complete dissolution experiment for these highly VTEs, several additional VTEs (Cu, Ag, Ga, Rb, Cs, Se, Te, Zn, and Pb) and correlations between releases of these elements and the releases of major/minor mineral constituent elements (Na, Mg, Al, Si, P, S, K, Ca, Ti, Cr, Mn, Fe, Co, and Ni). We use multivariate factor analysis and cluster analysis to determine whether or not there are correlations in the release patterns of the VTEs and the major/minor mineral constituent elements. Afterward, we interpret these correlations as indirect evidence of the identity of the VTE-containing host phase or phases.

Methods: We use a modified dissolution procedure based on the method of Podosek et al. [2] in which 1 g aliquots of powdered homogenized samples of each meteorite were treated with increasingly aggressive reagents: H₂O, 9 M CH₃COOH, 4 M HNO₃, 6 M HCl, HF/HCl, HNO₃/HCl, and HClO₄. Leachates were analyzed by ICPMS and fractional releases relative to bulk concentrations were calculated as described in [1].

Results: Measured releases of major/minor elements are consistent with non-stoichiometric dissolution of a complex mixture of mineral phases. Releases of VTEs indicate that as a group they are dispersed heterogeneously with respect to their host phases. Releases of the highly VTEs Pb, Cd, Bi, Tl, and In are consistent with the presence of multiple volatile-rich, chemically fractionated, low-temperature phases. Factor analysis of elemental releases show that five factors account for 91% of the variance of the elemental release data. Analysis of factor loadings reveal clusters of elements possessing correlated fractional releases, resulting presumably from dissolution of the same mineral phase or suite of mineral phases. The largest cluster loaded on factor F1 comprising major/minor elements Na, Mg, Al, K, Ca, Mn, and Fe. This cluster apparently represents lithophile behavior. Included in this group of lithophiles are the highly VTEs Cd and In. The second significant cluster loaded primarily on Factor F2 and comprised siderophiles Ni and Co along with the VTEs Cu, Te, Pb, Bi, and Tl. Chalcophile elements including S and Se clustered on Factor F3. Fractional release patterns for S were consistent with multiple S-containing phases including a water-soluble sulfate phase (in Murchison), a HNO₃-soluble phase and a HNO₃/HCl-soluble phase (in both Allende and Murchison). Further partial-dissolution experiments are in progress to determine whether the highly VTEs are preferentially sited on the exterior of grain boundaries. Together, our data should help elucidate some of the complex cosmochemical processes that led to the final distribution of VTEs in primitive meteorites.

References: [1] Wolf S. F. 2005. *Meteoritics & Planetary Science* 40: A169. [2] Podosek F. A. et al. 1997. *Meteoritics & Planetary Science* 32: 617-627.

5076

ANALYSIS OF RESIDUES RESULTING FROM MAFIC SILICATE IMPACTS INTO ALUMINIUM 1100

P. J. Wozniakiewicz^{1,2}, A. Kearsley¹, M. J. Burchell³, M. J. Cole³, and P. A. Bland². ¹IARC, Department of Mineralogy, The Natural History Museum, London SW7 5BD, UK. E-mail: p.wozniakiewicz@nhm.ac.uk. ²IARC, Department of Earth Sciences and Engineering, Imperial College London, South Kensington Campus, London SW11 3RA, UK. ³School of Physical Sciences, University of Kent, Canterbury, Kent CT2 7NR, UK

Introduction: The Al 1100 foils on the Stardust spacecraft had the primary function of securing the aerogels in place, however they also provided an extra surface totaling 153 cm² [1] upon which cometary materials may be examined, in the form of impact residues. Their collection will provide flux information for particles $\leq 1 \mu\text{m}$ in size that cannot easily be found and extracted from aerogel, as well as compositional information on a wide size range of impacting particles.

Earlier work [2] suggests that residues should be plentiful from impacts at Stardust encounter velocities ($\sim 6.1 \text{ km/s}$); however, little is known about how the materials will have changed during impact. Fully exploiting this unique opportunity requires that we understand the impact process occurring on the foils; and in particular, whether it is possible to distinguish the most important minerals expected within cometary materials.

Experimental Methodology: For this study, a series of light gas gun shots were conducted at the University of Kent, firing magnesium silicate minerals into Stardust foils. An Mg-rich olivine, enstatite, diopside, and lizardite were chosen as representative of minerals likely to be contained within comets [3]. Residues from five craters for each of these magnesium silicates were then analyzed using SEM EDS at the Natural History Museum. As the residue thickness and geometry (a thin sheet on a sloping interior crater wall) differ from the form of conventional microanalysis standards, creating a relatively short matrix absorption pathway, it was not considered appropriate to use the matrix correction routines used for normal quantitative electron microprobe analyses. The raw magnesium and silicon counts were therefore compared against those for their precursor projectiles. The Mg to Si ratio was chosen for comparison as it provides an excellent, but simple means by which to distinguish between these important cometary dust components.

Results and Discussion: A small but systematic increase in Mg counts relative to Si is seen for all residues when compared to projectile compositions. However, in our graphical plots, the minerals remain distinct from one another in both projectile and residue composition. We conclude that the main groups of anhydrous mafic silicates should be easily and reliably distinguishable in EDS analyses taken from within Stardust foil craters, suggesting that a valuable additional collection of cometary materials is available to researchers. We are now extending our study to recognition and in situ analyses of other silicate, sulfide, carbonate and oxide minerals of importance in extraterrestrial samples.

References: [1] Tsou P., Brownlee D. E., Sandford S. A., Hörz F., and Zolensky M. E. 2003. *Journal of Geophysical Research* 108: 8113, 10.1029/2003JE002109. [2] Bernhard R. P. and Hörz F. 1995. *International Journal of Impact Engineering* 17:69-80 [3] Hanner M. S. 2003. In *Astromineralogy*. pp. 171-188.

5115

PLANETESIMAL FORMATION INDUCED BY PHOTOPHORESIS AT THE INNER EDGE OF THE SOLAR NEBULA

G. Wurm¹, O. Krauss¹, and H. Haack². ¹Institut für Planetologie, Wilhelm-Klemm-Str. 10, D-48149 Münster, Germany, E-mail: gwurm@uni-muenster.de. ²Natural History Museum of Denmark, Øster Voldgade 5-7, DK-1350 Copenhagen K, Denmark

Introduction: Studies of ²⁶Al in eucrites and mesosiderites show that large planetesimals accreted shortly after the solar nebula formed, probably in much less than 1 Myr and before chondrite parent bodies formed [1]. Recent dynamical studies and interpretations of observations of asteroids suggest that differentiated bodies in the main asteroid belt originally formed closer to the sun and were scattered into the main belt [2]. No differentiation occurred for small planetesimals which formed in the asteroid belt as they formed too late to be melted.

However, this idea is currently motivated by the assumption that planetesimals can accrete faster closer to the sun due to an enhanced density of the nebula. While this is certainly true in general terms, this is probably not important for time scales of planetesimal formation. In a typical nebula and typical aggregation model planetesimal formation only needs 2000 yr at 1 AU [3]. Also cometesimals forming at 30 AU from the sun do so quickly in less than 300,000 yr [3]. Both time scales are relatively short compared to the suggestion that the small difference of 1 AU between the terrestrial planet region and the main asteroid belt should make a difference of 1 Myr in accretion. Therefore, some mechanisms are needed to delay planetesimal formation with respect to a typical aggregation model and trigger it somehow at a location moving slowly away from the sun.

Inner Edges of Protoplanetary Disks and Photophoresis: Recently a number of protoplanetary disks have been observed which clearly show evidence for a sharply truncated inner edge at several AU distance from their stars, TW Hya being one example [4]. Still gas is accreting in some of these objects [5]. This means that the inner clearing is mostly devoid of small dust and transparent to sunlight but the disks still contain significant amounts of gas. As outlined in our earlier work photophoresis inevitably acts on solid particles in such environments [6, 7]. We find that photophoresis can push the inner edge outwards on time scales of 1 Myr/1 AU and does not allow particles smaller than ~10 cm to move inwards [8].

We suggest that photophoresis concentrated material at the inner edge of the solar nebula at an early stage leading to rapid accretion of asteroids and planetary embryos in the inner solar system. Presence of ²⁶Al in these bodies caused all of these early accreted bodies to differentiate. Planetesimals continue to form as the edge moves outwards to the asteroid belt but at that time heating by ²⁶Al is no longer sufficient to differentiate these planetesimals.

References: [1] Bizarro M. et al. 2005. *The Astrophysical Journal* 632: L41–L44. [2] Bottke W. F. et al. 2006. *Nature* 439:821–824. [3] Weidenschilling S. J. 2000. *Space Science Review* 92:281–296. [4] Calvet N. et al. 2002. *The Astrophysical Journal* 568:1008–1016. [5] Rettig T. W. et al. 2004. *The Astrophysical Journal* 616:L163–L166. [6] Krauss O. and Wurm G. 2005. *The Astrophysical Journal* 630:1088–1092. [7] Wurm G. and Krauss O. 2006. *Icarus* 180:487–495. [8] Krauss O. and Wurm G. Forthcoming.

5026

HIGH-PRESSURE MINERAL ASSEMBLAGES IN SHOCK MELT VEINS OF SUIZHOU METEORITE

Xiande Xie^{1, 2}, Ming Chen², and Deqiang Wang². ¹Guangdong Provincial Academy of Sciences. E-mail: xdxie@gzb.ac.cn. ²Guangzhou Institute of Geochemistry, Chinese Academy of Sciences

The Suizhou meteorite was classified as a shock-vein-bearing L6 chondrite, and was evaluated by previous investigators as a weakly shock-metamorphosed (S2 to S3) meteorite. At first glance, metal and troilite in Suizhou show almost no change (S2), and olivine and pyroxene show a few sets of shock-induced fractures (S2-S3) [1], indicating that its shock stage of S2 to S3 was reasonable according to the principles of Stöffler's classification for shocked chondrites. However, our recent studies revealed that the Suizhou is an unique chondrite with specific and unusual shock-related mineralogical features: 1) most of the plagioclase grains in the Suizhou unmelted chondritic rock were melted and transformed into maskelynite during the shock event, implying that plagioclase experienced strong compression (S5), and two morphological types of maskelynite were identified, namely, thetomorphic and allomorphic maskelynites; 2) the very thin shock melt veins in Suizhou are filled with abundant various shock-produced high-pressure mineral phases, and no glassy phases have ever been identified in veins, indicating that this part of meteorite was very strongly shocked (S6); and 3) the melt veins consist of two high-pressure mineral assemblages [1–8]. One is a coarse-grained assemblage of minerals that occur as individual monomineralic or multiminerallitic grains, and it includes ringwoodite, majorite, akimotoite, devitrified perovskite, hollandite-structured NaAlSi₃O₈, tuite (γ -Ca₃(PO₄)₂), and two post-spinel phases—the CaFe₂O₄- and CaTi₂O₄-type polymorphs of chromite. The other assemblage is a fine-grained mineral assemblage that occurs as the matrix of the melt veins that has been totally crystallized into different mineral phases: idiomorphic garnet of majorite-pyroxene composition (in solid solution), irregular magnesiowüstite, and microcrystalline ringwoodite in interstices of garnet and magnesiowüstite grains. Therefore, the shock features listed above match a wide range of shock stages, namely, from S2 to S6, and hence, covered a wide range of shock-produced high pressures and temperatures from 5 to >45–90 GPa and 600–1750 °C. However, on the basis of our recent analyses, we come to a conclusion that the actual shock level of the Suizhou meteorite could be evaluated as S3-S4, and the unmelted chondritic rock of the meteorite experienced a shock pressure and temperature of up to 20–22 GPa and 1000–1100 °C, respectively. Locally developed thin shock melt veins in the meteorite were formed at the same or a bit higher pressure (up to 22–24 GPa) but at an elevated temperature of 2000–2200 °C. The higher temperature in veins than that in unmelted chondritic rock was achieved by local shear-friction stress along the vein-stretching directions during the shock event.

References: [1] Xie X. et al. 2001. *European Journal of Mineralogy* 13:1177–1190. [2] Xie X. et al. 2001. *Chinese Science Bulletin* 46:1121–1126. [3] Xie X. et al. 2002. *Geochimica et Cosmochimica Acta* 66:2439–2444. [4] Xie X. et al. 2003. *European Journal of Mineralogy* 15:1001–1005. [5] Chen M. et al. 2004. *Meteoritics & Planetary Science* 39:1797–1808. [6] Chen M. et al. 2003. *Geochimica et Cosmochimica Acta* 67:3937–3942. [7] Chen M. et al. 2004. *Proceedings of the National Academy of Science* 100: 14,651–14,654. [8] Xie X. et al. 2005. *Science in China, Series D* 48:815–821.

5386

ALKALINE COPPER OXIDE DEGRADATION OF INSOLUBLE ORGANIC MATTER IN CARBONACEOUS CHONDRITES

H. Yabuta, G. D. Cody, and C. M. O'D. Alexander. Carnegie Institution of Washington, Washington, D.C., USA. E-mail: hyabuta@ciw.edu

Introduction: Recently, it has been revealed that hydrothermal treatment of insoluble organic matter (IOM) in CM chondrite markedly reduced oxygen-linked alkyl carbon components (O-CHx) then produced a variety of discrete organic molecules including prebiotic compounds such as dicarboxylic acids and benzimidazoles, as well as polycyclic aromatic hydrocarbons (PAHs) [1]. Comparative study of IOM structures in different types of chondrites [2] has also suggested that the partial conversion of O-CHx and CHx could have yielded some discrete organic molecules by aqueous alteration on the parent body. These results indicate that O-CHx in IOM could be a key structure in chemical evolution of chondritic organic matter during parent body processing. In this study, we have conducted alkaline CuO degradation of IOM for the purpose to elucidate the building blocks of the O-CHx structure and their abundances in molecular level by cleaving ether-linkages (C-O-C) in IOM selectively.

Experimental: The reaction of alkaline CuO degradation cleavages ether linkages of the molecule selectively and oxidizes the ether groups into carboxyl or hydroxyl groups [3]. A Teflon bomb (23 ml) was loaded with 2 mg of Murchison IOM, 10 mg CuO powder, 1 mg of ammonium iron (II) sulfate hexahydrate $[\text{Fe}(\text{NH}_4)_2(\text{SO}_4)_2 \times 6\text{H}_2\text{O}]$ and 2.5 ml of 2M NaOH solution. The bomb was sealed and heated at 170 °C for 3 h. After the bomb had cooled down, the sample liquid was acidified to pH < 1, and extracted with ethyl acetate. The extract was dried under N₂ flow, derivatized with 100 ul of N,O-bis-(trimethylsilyl) trifluoro-acetamide (BSTFA) at 80 °C for 3 h, and analyzed by GC-MS.

Results and Discussion: Forty-seven compounds have been identified to date at 0.01–1 pmol/mg IOM level. They included 15 dicarboxylic acids (C₂–C₆), 11 hydroxy acids (C₂–C₆), two hydroxydicarboxylic acids (C₄), 14 aromatic acids, and five other compounds. Among these compounds, all hydroxy- and hydroxydi-acids were seen for the first time as products of Alkaline CuO degradation of Murchison IOM, compared to the past study [3]. Succinic and benzoic acids were the most abundant (1.55 and 1.08 pmol/mg IOM, respectively). These results show that alkyl chains from C₂ to C₇ and one or two alkyl substituted aromatics (mainly benzene ring) were ether-linked in the IOM structure. Most of dicarboxylic, hydroxy-, and hydroxydicarboxylic acids reported in this study have been identified from an aqueous extract of Murchison meteorite [4]. In addition, abundance of these acids declined with increasing carbon number, which is known to be a typical pattern for prebiotic synthesis of the compounds. These soluble acids in Murchison may be derived from the IOM during aqueous alteration. Residual IOM after oxidation was 60–75% of the original weight, which were roughly consistent with aromaticity of Murchison IOM (61.7–65.7%) [2]. The residual portion is probably composed of aromatic and carbonyl carbons that were not reacted in the degradation.

References: [1] Yabuta H. et al. Forthcoming. [2] Cody G. D. and Alexander C. M. O'D. 2005. *Geochimica et Cosmochimica Acta* 69:1085–1097. [3] Hayatsu R et al. 1980. *Science* 207:1202–1204. [4] Cronin J. R. et al. 1993. *Geochimica et Cosmochimica Acta* 57:4745–4752.

5202

MINERALOGICAL STUDY OF AUGITE-BEARING LODRANITE, NWA 2235 AND IMPLICATION FOR ITS ORIGINA. Yamaguchi¹, H. Takeda², and M. Kusakabe³. ¹National Institute of Polar Research, Tokyo 173-8515, Japan. E-mail: yamaguch@nipr.ac.jp. ²Chiba Institute of Technology, Chiba 275-0016, Japan. ³Institute for Study of the Earth's Interior, Okayama University, Misasa, Tottori 682-0913, Japan

Introduction: Lodranites and acapulcoites belong to a subgroup of primitive achondrites, and possess recrystallized textures and modified chondritic mineralogy. The primitive achondrites experienced variable degrees of partial melting and melt migration. We performed a mineralogical study of a new augite-bearing lodranite, NWA 2235. We examined a PTS of NWA 2235 optically and with EPMA.

Results: The PTS of NWA 2235 shows a coarse-grained aggregate with abundant 120° triple point junctures, composed of olivine (55 vol%) (Fa_{9.4–13.8}), orthopyroxene (17%) (Ca_{2.0}Mg_{46.1}), augite (7%) (Ca_{44.3}Mg_{50.5}), FeNi metal (8.5%), troilite (1%), chromite, Ca-phosphates and weathering products. No plagioclase is observed in the PTS. Olivine grains contain small glass inclusions (~30–40 μm) rich in K₂O and Na₂O (~5–6 wt%). The grains of orthopyroxene (~4 mm) and augite (~2.6 mm) are very large, poikilitically enclosing surrounding minerals. Compositions of silicate minerals are within the ranges of lodranites and acapulcoites.

Although oxygen isotopic composition of NWA 2235 ($\delta^{17}\text{O} = 1.62$, $\delta^{18}\text{O} = 4.94$) is slightly outside the range of lodranites, the $\Delta^{17}\text{O} (= -0.96)$ is similar to those of common lodranites. Coupled with the textural and mineralogical data, we classified NWA 2235 into a lodranite.

Discussion: Unlike other lodranites, NWA 2235 contains large grains of augite and orthopyroxene. These pyroxene grains were likely formed during grain coarsening with minor amounts of melt [1]. The Na and K-rich glass inclusions in olivine could be trapped melt, indicating the presence of minor amount of partial melts. NWA 2235 experienced a strong thermal metamorphism, minor melting and recrystallization.

Mineral abundances of lodranites vary significantly [2]. Different degrees of partial melting and melt migration (local segregation of partial melts), grain coarsening with minor amount of melts could explain the varying abundances. To explain the properties of lodranites, collisional heating has been suggested for the heat source for the metamorphism [1]. However, in the case of relatively small asteroids, impact heating is not effective heat source [3]. Yamaguchi et al. [4] suggested that moderate shock metamorphism at high temperatures near the solidus causes partial melting. We suggest that impacts occurred on the lodranite parent body which had been heated internally (e.g., by ²⁶Al). Different degrees of heating, brecciation and melting inside the parent body may explain the heterogeneous textures [1] of lodranites.

References: [1] Takeda H. et al. 1994. *Meteoritics* 29:830–842. [2] Yugami K. et al. 1998. *Antarctic Meteorite Research* 11:49–70. [3] McCoy T. et al. 1996. *Geochimica et Cosmochimica Acta* 60:2681–2708. [4] Yamaguchi A. et al. 2002. In *High-pressure shock compression of solids V*. pp. 29–45.

5337

TEMPERATURE DEPENDENCE ON THE EFFECTS OF AQUEOUS ALTERATION ON MINERALOGY AND NOBLE GAS COMPOSITIONS IN CARBONACEOUS CHONDRITE NINGQIANG

Y. Yamamoto¹, T. Nakamura², T. Noguchi³, and K. Nagao¹. ¹Laboratory for Earthquake Chemistry, University of Tokyo, Japan. E-mail: y-yamam@eqchem.s.u-tokyo.ac.jp. ²Department of Earth and Planetary Sciences, Kyushu University, Japan. ³Department of Materials and Biological Science, Ibaraki University, Japan

Introduction: Aqueous alteration is thought to be the earliest chemical reaction occurred in their parent bodies. Carbonaceous chondrites that experienced aqueous alteration might have changed mineralogy and noble gas compositions. In earlier work, we revealed that a major part of primordial noble gases in the Ningqiang carbonaceous chondrite lost during experimental aqueous alteration [1]. In order to understand the temperature dependence of mineralogical and noble gas compositional changes during aqueous alteration, we performed aqueous alteration experiments on Ningqiang at 100, 150, and 200 °C. Powdered Ningqiang weighing 0.6 g was kept in liquid water at these temperatures for 20 days. Mineralogy and noble gases in natural and altered Ningqiang were analyzed.

Results and Discussion: In the sample altered at 100 °C, mineralogical changes are minor and could not be detected by XRD analyses. In contrast, 150 and 200 °C altered samples greatly changed its mineralogical compositions. Olivine, low-Ca pyroxene, and iron sulfide, which are main components of Ningqiang, were decomposed, and serpentine and hematite were formed. Serpentine appears to have formed from the elements supplied by the decomposition of olivine and pyroxene. It was confirmed by the electron microscopic observation that serpentine grown around olivine and pyroxene grains.

The aqueous alteration experiment also shows compositional change of trapped noble gases. The 100 °C altered sample lost 6–20% of trapped ³⁶Ar, ⁸⁴Kr, and ¹³²Xe compared with those in natural Ningqiang. Significant depletions of trapped noble gases occurred at higher temperatures, i.e., 56–65% and 83–94% at 150 and 200 °C, respectively. These results indicate that trapped Ar, Kr, and Xe can be easily removed from their carrier phase in the temperature higher than 100 °C. The (³⁶Ar)_{trap}/¹³²Xe and ⁸⁴Kr/¹³²Xe ratios in the 200 °C altered sample were reduced to 85 and 1.2, respectively (natural Ningqiang: 235 and 1.4, respectively). Calculated (³⁶Ar)_{trap}/¹³²Xe ratio of trapped noble gases removed through the alteration at 100°C is 68. Those in the sample altered at 150 and 200 °C are 259 and 263, respectively. The (³⁶Ar)_{trap}/¹³²Xe ratios removed at 150 and 200 °C are higher than that in the 100 °C sample and are in the range of Ar-rich gas in enstatite chondrites [2] and ureilites [3]. These results suggest that the Ar-rich gas in the Ningqiang is removed through the decomposition of olivine and pyroxene at temperatures higher than 100 °C. Our results lead that both mineralogical and noble gas compositional changes by aqueous alteration are greatly dependent on its temperature.

References: [1] Yamamoto Y. et al. 2006. *Meteoritics & Planetary Science* 41:541–552. [2] Crabb J. and Anders E. 1981. *Geochimica et Cosmochimica Acta* 45:2443–2464. [3] Wacker J. F. 1986. *Geochimica et Cosmochimica Acta* 50:633–642.

5146

EVOLUTION OF DIFFERENTIATED ASTEROIDS AS INFERRED FROM COOLING RATES OF MAGMATIC IRON METEORITES

J. Yang¹, J. I. Goldstein¹, and E. R. D. Scott². ¹Department of Mechanical and Industrial Engineering, University of Massachusetts, Amherst, Massachusetts 01003, USA. E-mail: jiyang@ecs.umass.edu. ²Hawai'i Institute of Geophysics and Planetary, University of Hawai'i, Honolulu, Hawai'i 96822, USA

Introduction: Magmatic iron meteorites are generally thought to come from metallic cores of differentiated parent bodies that cooled slowly inside silicate mantles. Our new cooling rate data are incompatible with this model and imply that some cores and mantles were separated before the Widmanstätten pattern formed.

Cooling Rates: The metallographic cooling rates for both the IIIAB and IVA magmatic iron groups are correlated with bulk Ni content in each group [1, 2]. For IVA irons, cooling rates increase from 90 to 7000 K/Myr with decreasing Ni. For IIIAB irons, the cooling rate variation is smaller, 60–340 K/Myr. Even allowing for variations in nucleation mechanism and temperature, the cooling rate ranges in IIIAB and IVA are inconsistent with cooling in a core surrounded by a silicate mantle.

Discussion: The cooling rates of irons from the core of an asteroid with a silicate mantle should be the same [3]. Our cooling rates for the IIIAB and IVA irons are incompatible with such a model. We argue that their parent bodies experienced impacts that removed almost all of their silicate mantles before kamacite formed. For IIIAB irons, the impact produced a metallic core covered by some remaining silicate or regolith. For IVA irons, the impact left little or no silicate on the metallic core. Our cooling rate and thermal modeling suggest that at the time of the mantle-stripping impact, the temperature of the metallic core was 850–1200 °C, i.e., the core and mantle may both have been partly molten. As a result, the metal cores then cooled faster near the surface and much slower near the center of the cores. If iron meteorites came from bodies that formed at 1–2 AU and were scattered into the asteroid belt by planetary embryos [4], the primary IVA and IIIAB bodies could have had their silicate mantles removed by tidal effects and impacts with embryos [5]. The very early separation of mantle materials from metallic cores may be the reason for the “missing” olivine meteorites [4].

Conventional thermal models imply that iron meteorite parent bodies had diameters of 24–130 km [6] or 4–200 km [7], but we infer that the metallic core of the IVA irons was around 300 km across and comparable in size to 16 Psyche, the largest known M class asteroid, which is 260 km across.

Our model also implies that the IIIAB and IVA cores crystallized inwards [8] not outwards [9] so high-Ni irons formed at the center.

References: [1] Yang J. and Goldstein J. I. *Geochimica et Cosmochimica Acta*. Forthcoming. [2] Yang J. et al. *Geochimica et Cosmochimica Acta*. Forthcoming. [3] Haack H. et al. 1990. *Journal of Geophysical Research*. 95B:5111–5124. [4] Bottke et al. 2006. *Nature* 439: 821–824. [5] Asphaug E. et al. 2006. *Nature* 439:155–160. [6] Haack H. and McCoy T. J. 2003. In *Meteorites, comets and planets: Treatise on geochemistry*, vol. 1. Amsterdam: Elsevier. [7] Chabot N. L. and Haack H. In *Meteorites and the early solar system II*. Forthcoming. [8] Haack H and Scott E.R.D. 1992. *Journal of Geophysical Research*. 97:14727–14734. [9] Wasson J. T. 1985. *Meteorites: Their record of early solar system history*. New York: W.H. Freeman Press.

5108

FRACTAL DIMENSION ANALYSIS OF HELLAS BASIN: THE MARTIAN IMPACT CRATER MIGHT BE ANCIENT LAKES/SEAS

Guo Yangrui. Taiyuan No. 5 High School, China. E-mail: G2COM@126.com

Introduction: Some Martian impact craters are considered to be ancient lakes or seas, e.g., Hellas and Rabe. Parker proposed the Martian shoreline in Northern Plain in 1989, and the shoreline has two different levels [6, 7]. It aroused many controversies on whether early Mars had oceans and whether the topography was formed by wave or wind. Fractal analysis allows quantification of natural objects that appear to be in a statistical scene self-similarity. Bernard Sapoval pointed out wave erosion was main power to form coastline fractal [3]. Terrestrial coastlines show dimensions between 1.13 and 1.25 [1, 2]. Wind erosion is nonfractal, which has fewer dimensions. This study proposed fractal method in order to analyze erosion process in Hellas.

Hellas impact basin is one of the most prominent topographic features in the southern hemisphere of Mars. Hellas basin is about nine kilometers deep. The main basin rim is about 2300 km in diameter. Below -5800 m, large impact craters are not apparent in Hellas; between -5800 and -1800 m, large craters are present but are degraded [4, 5]. I used U.S. Geological Survey Mars Global Digital Elevation Model, based on Mars Orbiter Laser Altimeter data at scale 1:10,000,000, clipped out the Hellas region. The contours at elevations -3000 m, -3500 m, -4000 m, -4500 m, -5000 m, -5500 m, and two proposed shorelines at elevations -3100 m and -5800 m were drawn automatically using a geographic information system (GIS) software package. All contours are closed-curves. An image-processing program HarFa 5.1 via box-counting method calculated the fractal dimensions. The fractal dimension is the slope of the straight line Black and White. The eight results show a fractal dimensions ranging from 1.147 to 1.235, and mean is 1.182.

Conclusions: The contours are fractal, so the topography must be created by fractal geologic process. If the topography were formed by wave erosion, they might keep some original features. Therefore, the result of analyze of Hellas shoreline/lakeshore fall within terrestrial results that can be interpreted as strong evidence of Hellas as a lake/sea on Mars. Scientists used rules of thumb in order to deduce the climate on early Mars. The fractal analysis can provide a new way for understanding Martian histories. As the water in Hellas slowly disappeared, the sea level decreased and wave actions continued, so all the results could be kept in a certain range. Water decelerated and prevented small meteorites from falling into Hellas. The degraded impact craters might be eroded by wave actions; some small-integrated craters might be formed after the water disappeared.

References: [1] Cull S. C. 2003. Abstract #1100. 34th Lunar and Planetary Science Conference. [2] Mandelbrot B. B. 1967. *Science* 156:636–638. [3] Sapoval B. et al. 2004. Abstract #NG11A-06.2004 Joint Assembly. [4] Crown D. A. et al. 2005. Abstract #2097. 36th Lunar and Planetary Science Conference. [5] Moore J. M. et al. 2001. Abstract #1446. 32nd Lunar and Planetary Science Conference. [6] Parker T. J. et al. 1989. *Icarus* 82: 111–145. [7] Carr M. H. and Head J. III. W. 2003. *Journal of Geophysical Research* 108:1–8.

5250

SUPERNOVA MIXTURES REPRODUCING ISOTOPIC RATIOS OF LOW DENSITY GRAPHITE GRAINS

T. Yoshida. National Astronomical Observatory of Japan, Tokyo 181-8588, Japan. E-mail: takashi.yoshida@nao.ac.jp

Introduction: Low-density graphite grains are believed to be originating from supernovae [1]. They have excesses of ^{28}Si and ^{18}O , and some of them have evidence for the original presence of ^{44}Ti [1, 2]. Recently, their isotopic ratios have been compared quantitatively with those deduced from supernova nucleosynthesis calculations [3, 4]. In order to reproduce the isotopic and elemental signatures, large-scale heterogeneous mixing of supernova ejecta should be taken into account. In this study, we seek mixtures of supernova ejecta reproducing isotopic ratios of low density graphite grains. We also investigate the mixing ratios and compositions of the mixtures.

Supernova Mixing Models: We use the abundance distributions of the supernova ejecta of 3.3, 4, 6, and $8 M_{\text{solar}}$ He star models corresponding to 13, 15, 20, and $25 M_{\text{solar}}$ zero-age main sequence stars [4]. We divide the supernova ejecta into seven layers; the Ni, Si/S, O/Si, O/Ne, C/O, or O/C, He/C, and He/N layers. Then, we seek mixtures reproducing Niso isotopic ratios of individual graphite grains using χ^2 -value evaluation. We seek the minimum χ^2 -value and the corresponding mixing ratios. When the χ^2 -value of a mixture corresponding to a grain is smaller than $4 N_{\text{iso}}$, we consider that the mixture reproduces N_{iso} isotopic ratios of the grain.

Results: We pick up 26 low-density graphite grains in [3] and seek mixtures reproducing $^{12}\text{C}/^{13}\text{C}$, $^{14}\text{N}/^{15}\text{N}$, $^{16}\text{O}/^{17}\text{O}$, $^{16}\text{O}/^{18}\text{O}$, $^{26}\text{Al}/^{27}\text{Al}$, $^{29}\text{Si}/^{28}\text{Si}$, and $^{30}\text{Si}/^{28}\text{Si}$ of the individual grains. For three grains, $^{44}\text{Ti}/^{48}\text{Ti}$ is also compared. We find mixtures reproducing six isotopic ratios for 20 individual graphite grains. The mixtures are classified into three groups. The mixtures in the first group reproduce the isotopic ratios except $^{14}\text{N}/^{15}\text{N}$. The main component of the mixtures is the He/N layer. Most of the mixtures indicate the mixing ratios of the He/N layer larger than 0.8. The mixtures also indicate $^{14}\text{N}/^{15}\text{N}$ much larger than the measured one. The mixtures in the second group reproduce the isotopic ratios except $^{12}\text{C}/^{13}\text{C}$, which is much larger than the measured ratios. The main component is the He/C layer so that $^{14}\text{N}/^{15}\text{N}$ and the excesses of ^{18}O in the grains are well reproduced. The second main component is the He/N layer and its mixing ratio is of order 0.1 in most cases. The mixtures in the third group reproduce both $^{12}\text{C}/^{13}\text{C}$ and $^{14}\text{N}/^{15}\text{N}$ but show large $^{26}\text{Al}/^{27}\text{Al}$. The main component is the Ni layer; the mixing ratio is larger than 0.9 for most cases. For one grain of which $^{44}\text{Ti}/^{48}\text{Ti}$ has been measured, we find mixtures reproducing six isotopic ratios including $^{44}\text{Ti}/^{48}\text{Ti}$. The mixing ratios of the mixtures are similar to those in the first group. The C/O ratios in most of the mixtures are larger than unity. Elemental composition of the mixtures will be constrained by the formation theory of presolar grains from supernovae.

References: [1] Amari S., Zinner E., and Lewis R. S. 1995. *The Astrophysical Journal Letters* 447:L147–L150. [2] Nitter L. R. et al. 1996. *The Astrophysical Journal Letters* 462:L31–L34. [3] Travaglio et al. 1999. *The Astrophysical Journal* 510:325–354. [4] Yoshida T., Umeda H., and Nomoto K. 2005. *The Astrophysical Journal* 631:1039–1050.

5174

O-ISOTOPIC DISTRIBUTION OF PORPHYRITIC AND NONPORPHYRITIC CHONDRULES IN ACFER 214, CH CHONDRITE

M. Yoshitake¹ and H. Yurimoto². ¹Department of Earth and Planetary Sciences, Kobe University, 1-1 Rokkoudai-cho, Nada, Kobe 657-8501, Japan. E-mail: miwa@kobe-u.ac.jp. ²Natural History Sciences, Hokkaido University, Sapporo 060-0810, Japan

Introduction: Chondrules are one of the major components in chondrites. Clayton et al. [1] reported that O-isotopic compositions of 23 chondrules in the Allende meteorite. Porphyritic type chondrules have more ¹⁶O-rich compositions than barred olivine chondrules in the Allende meteorite. These O-isotopic distributions can be explained by interaction between a solid precursor (¹⁶O-rich) and a nebular gas (¹⁶O-poor) during the chondrule-forming events [1, 2]. The range and frequency of the distribution reflect the degree of equilibrium of the exchange or O-isotopic composition of nebula gas at chondrule fraction.

On the other hand, previous study revealed that a CH chondrite contains a chondrule extremely enriched in ¹⁶O [3]. This result suggests that chondrules in CH chondrites may retain its original O-isotopic composition.

Results and Discussion: We identified chondrules in Acfer 214 CH chondrite, and classified into porphyritic olivine (PO, 19.2%), porphyritic olivine pyroxene (POP, 25.8%), porphyritic pyroxene (PP, 4.6%), granular olivine pyroxene (GOP, 3.3%), cryptocrystalline (C, 37.1%), and barred olivine (BO, 9.9%) chondrules by backscattered electron images using SEM-EDS. Oxygen isotopic compositions in 151 chondrules of the Acfer 214 chondrite were analyzed by secondary ion mass spectrometry using the CAMECA ims 1270.

All O-isotopic compositions of chondrules were plotted along the CCAM line. The O-isotopic compositions in these chondrules distributed from -20 to +15‰ ($\delta^{18}\text{O}$) except a chondrule reported by [3]. This is consistent with previous reports [3, 4, 5]. These results indicate that O-isotopic distribution of chondrules in CH chondrite is wider than that of Allende [1, 2]. Moreover, O-isotopic compositions of non-porphyritic (C and BO) chondrules distributed from -19 to +12‰ ($\delta^{18}\text{O}$). This distribution is wider than that of porphyritic type (PO, PP, POP, and GOP) chondrules. This trend of O-isotopic compositions between non-porphyritic and porphyritic types chondrules differs from the case of Allende meteorite [2, 6]. In this case, O-isotopic exchange process was not caused O-isotopic compositions of chondrules in Acfer 214. These results indicate that chondrule precursors had different O-isotopic compositions one another or chondrule formation occurred in various environments with different O-isotopic compositions.

References: [1] Clayton R. N. et al. 1983. In *Chondrules and their origins*. pp. 37–43. [2] McSween H. Y. Jr. 1985. *Meteoritics* 20:523–540. [3] Kobayashi S. et al. 2003. *Journal of Geochemistry* 37:663–669. [4] Krot A. N. et al. 2000. Abstract #1459. 31st Lunar and Planetary Science Conference. [5] Jones et al. 2005. Abstract #1813. 36th Lunar and Planetary Science Conference. [6] Clayton R. N. et al. 1993. *Annual Review of Earth and Planetary Science* 21:115–149.

5007

POSSIBLE HEIGHTENED NOCTILUCENT CLOUD ACTIVITY NEAR STRONG PERSEID MAXIMA

M. Zalcik¹ and A. A. Mardon². ¹Noctilucent Cloud Canadian-American Network. E-mail: bluegrama@shaw.ca. ²Antarctic Institute of Canada, P.O. Box 1223, MPO, Edmonton, AB, Canada T5J 2M4. E-mail: amardon@shaw.ca

Introduction: Noctilucent clouds (NLC) are ice clouds that form in Earth's mesosphere at heights of 80–85 km [1]. The accretion nuclei of NLC are thought to include meteoric particles as well as hydrated ions [2]. It has been argued that significant intrusions of meteor dust resulting from major meteoric events could increase the availability of nuclei, rendering more and/or brighter displays, the most compelling example being a bright display of NLC immediately following the Tunguska, Russia (60.9N, 101.9E), fireball of June 30, 1908 [3]. To see if heightened activity by the Perseid meteor shower in 2004 as reported by the International Meteor Organization [4] and predicted by P. Brown [5] had any effect on NLC during the Perseid peak dates of August 11–12, we examined NLC observations at the Rankin Inlet, Canada, NU Flight Service Station (62.4N, 92.1W) and the Baker Lake, Canada NU Community Aerodrome Radio Station (64.2N, 96.1W), participants in the NLC CAN AM NLC observing network. Table 1 lists the results for the years 2003 to 2005 inclusive. There were two nights with NLC in 2004 as seen from Baker Lake, but, compared with the other years in the study, there does not seem to have been a substantial increase in activity around the dates of the Perseid peak. The inherent interference by tropospheric clouds, which prevent (the farther away) NLC from being seen, makes any conclusions somewhat shaky. Indeed, of the six sightings listed in the Table 1, only two of these were made under ideal tropospheric conditions themselves.

Table 1. Comparison of Perseid Peak dates from two years compared with observations of noctilucent clouds in two Northern Canadian NLC CAN AM NLC observing sites in 2003, 2004, and 2005.

Rankin Inlet, Canada					Baker Lake, Canada				
Aug	10/ 11	11/ 12	12/ 13	13/ 14	Aug	10/ 11	11/ 12	12/ 13	13/ 14
2003	–	–	–	Y	–	Y	–	–	Y
2004	–	–	–	–	Y	–	–	–	Y
2005	–	Y	–	–	–	–	–	–	–

Y = yes, NLC seen; – = interference by tropospheric clouds

Conclusions: NLC activity as seen from Rankin Inlet, NU and Baker Lake, NU around the time of the strong Perseid meteor shower peak in 2004 was no higher than NLC activity at the same sites and dates in 2003 and 2005. Hence, perhaps a higher flux of shower meteors does not render heightened NLC activity. Interference by tropospheric clouds at both sites makes any conclusions difficult to support.

References: [1] Gadsden M. and Schroeder W. 1989. *Noctilucent clouds*. Springer Verlag. [2] Turco R. P., Toon O. B., Whitten R. C., Keesee R. G., and Hollenback D. 1982. *Planetary and Space Science* 30:1147–1181. [3] Vestine E. H. 1934. *Journal of the Royal Astronomical Society of Canada* 28: 249–272, 303–317. [4] International Meteor Organization. 2004. www.imo.net/news/perseids2004-4. [5] Brown P. 2006. Personal communication.

5383

SOME APPLICATIONS OF THE CHONDRITE OXYGEN MIXING MODEL

B. Zanda^{1, 2} and R. H. Hewins². ¹MNHN-CNRS UMS2679, 75005, Paris, France. E-mail: zanda@mnhn.fr. ²Geological Sciences, Rutgers University, Piscataway, New Jersey 08855, USA

Introduction: Abundances of the petrographic constituents of chondrites (type I and type II chondrules, refractory inclusions, metal and matrix) correlate within chondrite groups, indicating that these groups were generated by the mixing of a limited number of simple reservoirs, hereafter called “primary mixes” [1]. The abundances of petrographic constituents also correlate with oxygen isotope signatures across chondrite groups and this allowed us to extract the oxygen isotopic signatures associated with the five petrographic constituent pure poles at the time of isolation of the chondritic reservoirs [2].

Applications: *Oxygen Isotopic Signatures of Chondrite Classes:* Based on those of the pure poles, we derived the oxygen isotopic signatures associated to the primary mixes: these allow to precisely describe the oxygen isotopic signatures of all the chondrites groups. For example, CM and CO chondrites are known to lie on a slope 0.7 line in the 3-isotope plot [3] which is very accurately predicted by this model.

Other Mixing Trends: Other mixing trends appear obvious in the oxygen 3-isotope plot. For example, pallasites lie on a 1.3 slope line in the 3-isotope plot with $R_2 = 0.99$, a trend unexplained so far, but on which some light can be shed from the primary mixes lying close to the end-members of the trend.

Chemical and Petrological Information: The C concentration of chondrites exhibits a weak correlation with their matrix abundance. The correlation between C concentration and $\Delta^{18}\text{O}$ is much stronger because $\Delta^{18}\text{O}$ is actually a more integrative measurement of matrix abundance in a chondrite than measurements done by point counting. As various achondrites also plot on the C versus $\Delta^{18}\text{O}$ correlation, this indicates that they initially contained matrix similar to that of chondrites and allows to derive the abundance of that matrix

Conclusions: The chondrite oxygen mixing model is a powerful tool which allows to understand the relationship between all the chondrite groups. Applied to primitive achondrites and differentiated meteorites it can be used to make inferences on their initial petrography and chemistry.

References: [1] Zanda B. and Hewins R. H. 2006. Abstract #2199. 37th Lunar and Planetary Science Conference. [2] Zanda B. et al. *Earth and Planetary Science Letters*. Forthcoming. [3] Clayton R. N. 2005. *Treatise of Geochemistry* 1:129–142.

5375

COORDINATED STRUCTURE-ISOTOPE STUDIES OF PRESOLAR HIBONITES

T. J. Zega¹, R. M. Stroud¹, L. R. Nittler², and C. M. O'D. Alexander². ¹Naval Research Laboratory, Code 6360, 4555 Overlook Ave. SW, Washington D.C., 20375, USA. ²Department of Terrestrial Magnetism, Carnegie Institution of Washington, 5241 Broad Branch Rd NW, Washington D.C., 20015, USA. E-mail: zega@nrl.navy.mil

Introduction: Hibonite (CaAl_2O_9 , S.G: $P6_3/mmc$) is predicted to be the second major oxide to condense from a gas of solar composition [1]. It is a major constituent of calcium- and aluminum-rich inclusions in chondritic meteorites, and it has been identified in the infrared spectra of planetary nebulae [2]. Thus, information on the structure and composition of hibonite is important for constraining the conditions of circumstellar environments and providing ground-truth for observational astronomy. [3] used transmission electron microscopy to provide the first structural confirmation and characterization of presolar hibonite. Here we expand on those efforts and report results from two additional grains.

Methods: An acid-residue of Krynka meteorite was analyzed using a Cameca IMS 6f and nanoSIMS 50 secondary ion microprobes (SIMS), and the presolar grains were identified on the basis of their O isotope values [4]. We used the focused-ion-beam scanning-electron microscope (FIB-SEM) to create, thin, and extract, in situ, electron-transparent sections [5] for further investigation with a transmission electron microscope (TEM). The FIB section was analyzed using a 200 keV JEOL 2200FS TEM equipped with an energy-dispersive spectrometer, in-column energy filter, and bright- and dark-field detectors.

Results and Discussion: SIMS analysis reveals that both grains are ^{18}O depleted and fall in the Group 2 category for presolar oxides, suggesting that they formed in low-mass asymptotic giant branch stars that experienced cool-bottom processing [6]. Grain KR-1-83-2 has $\delta^{17}\text{O} = 722 \pm 30\text{‰}$ and $\delta^{18}\text{O} = -888 \pm 19\text{‰}$, whereas grain KR3B-92-11 has $\delta^{17}\text{O} = 2064 \pm 95\text{‰}$ and $\delta^{18}\text{O} = -768 \pm 8\text{‰}$.

Measurements on selected-area electron-diffraction patterns acquired from the grains confirm the identity and crystallinity of the hibonite. TEM bright-field and high-angle annular-dark-field imaging reveals that both grains have uniform contrast, verifying that they are single crystalline with no evidence of subgrains. High-resolution TEM imaging on KR1-83-2 reveals that lattice fringes are discontinuous in some areas, suggesting minor amorphization, possibly due to pre-accretionary radiation processing. Energy-dispersive spectroscopy shows that grain KR1-83-2 contains abundant Al and Ca with minor Ti and Fe, whereas grain KR3B-92-11 contains abundant Al, Ca, Ti, and minor Mg. These results are generally consistent with equilibrium condensation predictions and the previous report by [3] of a Group 1 hibonite grain.

References: [1] Lodders K. 2003. *The Astrophysical Journal* 591: 1220–1247. [2] Hofmeister A. M. et al. 2004. *Geochimica et Cosmochimica Acta* 68:4485–4503. [3] Stroud R. M. et al. 2005. *Meteoritics & Planetary Science* 40:A148. [4] Nittler L. R. et al. 2005. Abstract #2200. 36th Lunar and Planetary Science Conference. [5] Zega T. J. and Stroud R. M. 2006. Abstract #1441. 37th Lunar and Planetary Science Conference. [6] Wasserburg G. J. et al. 1995. *The Astrophysical Journal Letters* 447:L37–40.

5235

PAIRING AND PETROGENETIC RELATIONSHIPS AMONG BASALTIC LUNAR METEORITES FROM NORTHWEST AFRICA

R.A. Zeigler¹, R. L. Korotev¹, B. L. Jolliff¹, T. E. Bunch², and A. J. Irving³.
¹Department of Earth and Planetary Sciences, Washington University, Campus Box 1169, Saint Louis, Missouri 63130, USA. E-mail: zeigler@levee.wustl.edu. ²Department of Geology, Northern Arizona University, Flagstaff, Arizona 86011, USA. ³Department of Earth and Space Sciences, University of Washington, Seattle, Washington 98195, USA

Several lunar meteorite stones discovered in northwestern Africa since 2000 are fragments of a single, complex, coarse-grained basaltic breccia from the Moon. The stones, about 1.2 kg in total mass, include previously studied NWA (Northwest Africa) 773 [1, 2] and more recently discovered NWA 2700, NWA 2727, NWA 2977, NWA 3160 [3, 4], and at least one other yet-to-be described stone.

As a whole, the meteorite consists of several lithologies, but the breccia is sufficiently coarse grained and the stones sufficiently small that individual stones each contain only a subset of the lithologies. The meteorite is best described as a fragmental breccia consisting mainly of clasts, some greater than 1 cm in size, of porphyritic olivine basalt, (most prominent in stones 2727 and 3160) and cumulate olivine gabbro (most prominent in 773, 2700, and 2977) [1]. NWA 773 also contains regolith breccia that is finer grained than the fragmental breccia and which itself contains a minor component of nonmare material [1, 2]. NWA 2727 contains a minor component of ferrogabbro [4].

We conclude that the stones are paired on the basis of their compositional and textural similarity to each other and their uniqueness as whole compared to other lunar samples. The olivine basalt is a VLT (very-low-Ti) lunar basalt [1]. On the basis of mineral composition and bulk sample composition (INAA [5]), the same basalt occurs in all the stones. Similarly, the olivine cumulate is compositionally distinct. Both lithologies share several key trace-element characteristics that show they are petrogenetically related to each other and together distinct from any other basaltic lunar meteorite and any basalt from the Apollo and Luna collection. These features are relative enrichment in LREE, high Th/REE, and very low concentrations of the 'plagiophile' elements Na₂O, Sr, and Eu. This fingerprint suggests a common source region for the different lithologies, one that is different from that of nearly any previously studied lunar basalt.

For NWA 773, Jolliff et al. [2] argued for a shallow intrusive setting for crystallization of the olivine cumulate and derivation from a melt of composition similar to Apollo 14 VLT volcanic glass, with modest assimilation of a KREEP component. Moreover, the breccia associated with the olivine cumulate may be dominated by extrusive VLT basalt related to the shallow intrusive. We will test this and other scenarios for petrogenetic relationships using data from the new NWA meteorites.

Acknowledgements: This work was supported by NASA grant NNG04GG10G.

References: [1] Fagan T. J. et al. 2003. *Meteoritics & Planetary Science* 38:529–554. [2] Jolliff B. L. et al. 2003. *Geochimica et Cosmochimica Acta* 67:4857–4879. [3] Zeigler R. A. et al. 2006. Abstract #1804. 37th Lunar and Planetary Science Conference. [4] Bunch T. E. et al. 2006. Abstract #1375. 37th Lunar and Planetary Science Conference. [3] Zeigler et al. 2006. *Antarctic Meteorites* 30.

5170

PETROGRAPHIC AND MINERALOGICAL STUDIES OF THE LUNAR METEORITE DHOFAR 1180

Aicheng Zhang and Weibiao Hsu. Purple Mountain Observatory, Nanjing, 210008, China. E-mail: aczhang@pmo.ac.cn

Introduction: Lunar meteorites provide important clues to better understand the formation and evolution of the Moon. Up to now, near 40 lunar meteorites were identified, and most were found in cold- and hot-deserts [1]. Dhofar 1180 is a newly recovered lunar breccia from Oman in 2005. Here, we present petrographic and mineralogical studies of this new lunar meteorite.

Results: Dhofar 1180 is a polymict breccia that contains lithic clasts of gabbro, anorthositic gabbro, granulite, subophitic basalt, troctolite, Ti-rich clast (olivine and pyroxene grains set in Ti-rich glass), microporphyritic crystalline impact melt breccia, and gabbroic anorthosite. They usually occur as angular fragments ranging in size from 0.1 to 1 mm. Individual mineral fragments of pyroxenes, olivine, and anorthite are abundant in the matrix, as well impact glass with various sizes. They range in size from 0.1 to 1 mm. Some pyroxene grains display fine exsolution. Most large mineral fragments show undulose extinction.

Mineral chemistry varies from clast to clast. Olivine usually has a Fa value of 31–69. In the Ti-rich clast, the value in olivine varies from 54 to 98. For olivine grains with MnO > 0.10 wt%, the molar FeO/MnO ratio varies from 70 to 110 with an average of 93, which falls within the range of typical lunar olivines [2]. Pyroxene also shows extensive chemical variation among clasts. Pyroxene mainly occurs as pigeonite (En_{24–66}Fs_{23–59}Wo_{6–24}), augite (En_{11–41}Fs_{23–59}Wo_{28–38}), and pyroxferroite (En_{1–9}Fs_{65–86}Wo_{14–26}). The molar FeO/MnO ratio of pyroxene varies from 50 to 70 with an average of 63. Anorthite is highly enriched in Ca and shows a small compositional variation (An_{91–99}) among clasts. Chromite-spinel-ulvöspinel solid solution and ilmenite were also found in clasts. The impact glass has a composition of anorthite and contains several per cents of MgO and FeO.

Discussion: Whole rock compositions of Dhofar 1180 bear many characteristics of lunar meteorites [3]. It was classified as a fragmental or regolith breccia. Petrography and mineral chemistry of plagioclase, olivine and pyroxene are consistent with a lunar origin [4, 5]. The existences of anorthositic clasts and pyroxferroite further confirm the conclusion.

Among well-defined lunar meteorites, Dhofar 1180 has Al₂O₃ (23 wt%) and FeO (9.2 wt%) contents similar to those of Yamato-983885 and Calalong Creek [1, 3]. However, its Th concentration (0.9 ppm) is significantly lower than that of Yamato 983885 (2 ppm) and Calalong Creek (4 ppm) [3]. Our data shows that KREEP basalt that occurred in both Yamato-983885 and Calalong Creek is absent in Dhofar 1180. In Dhofar 1180, Ti-rich clast and impact glass are abundant, but are absent in Yamato-983885 and Calalong Creek although low-Ti basalt clast was reported in Calalong Creek [4, 6]. The above distinction among Dhofar 1180, Yamato-983885, and Calalong Creek suggests that Dhofar 1180 probably represent a unique lunar breccia.

References: [1] Korotev R. L. 2005. *Chemie der Erde* 65:297–346. [2] Papike J. J. 1998. *Planetary Materials*. Washington, D.C.: Mineralogical Society of America. [3] http://epsc.wustl.edu/admin/resources/moon_meteorites.html. [4] Arai T. et al. 2005. *Antarctic Meteorite Research* 18:17–45. [5] Kaiden H. and Kojima H. 2002. Abstract #1598. 33rd Lunar and Planetary Science Conference. [6] Hill D. H. and Boynton W. V. 2003. *Meteoritics & Planetary Science* 38:595–626.

5100

STUDY OF METAL EXTRACTED FROM TZAREV L5 CHONDRITE BY MÖSSBAUER SPECTROSCOPY AND METALOGRAPHY

E. V. Zhiganova and M. I. Oshtrakh. Faculty of Physical Techniques and Devices for Quality Control, Ural State Technical University–UPI, Ekaterinburg, 620002, Russian Federation. E-mail: evgeniya@dpt.ustu.ru, oshtrakh@mail.utnet.ru

Introduction: Mössbauer spectra of ordinary chondrites consist of several components related to metal, troilite, olivine, pyroxene, and iron oxides. The area of metal subpeaks does not exceed 20% and this value is related to the metal iron content. Usually chondrite metal contains more than one metal phase, but they cannot be resolved in complicated Mössbauer spectrum of chondrite sample [1, 2]. Therefore, metal extraction from meteorite matter is necessary for detailed study by Mössbauer spectroscopy.

Methods: A sample of metal extracted from ordinary chondrite Tzarev L5 was prepared as powder and glued on pure aluminum foil. Extraction was performed by several steps: powdering, levigation in acetone followed by the separation in strong and weak magnetic fields, then drying and etching by weak HF, and final selection with binocular loupe from silicates. Mössbauer spectrum was measured at room temperature using spectrometer SM-2201 with high accuracy, stability, and sensitivity in transmission geometry with moving absorber. Sections of Tzarev L5 for metallography were polished with diamond paste and etched by Nital (2 vol% HNO₃, balance ethyl alcohol). Chemical composition of metal was obtained by microanalysis EDAX realized on SEM.

Results: Mössbauer spectrum of metal from Tzarev L5 was measured with high velocity resolution using 4096 channels and then presented in 1024 channels for fitting. The results of the spectrum better fit demonstrated the presence of three sextets with the hyperfine field values related to kamacite α -Fe(Ni,Co), martensite α_2 -Fe(Ni,Co) and kamacite α' -Fe(Ni,Co), one doublet related to residue olivine, and one singlet related to taenite γ -Fe(Ni,Co). The result of the metal grains metallography demonstrates the presence of various metal phases: α -Fe(Ni,Co), α_2 -Fe(Ni,Co), and both α' -Fe(Ni,Co) and γ -Fe(Ni,Co) in plessite.

Conclusions: Study of extracted metal from Tzarev L5 by Mössbauer spectroscopy permitted us to reveal four different metal phases and determine its hyperfine parameters and relative areas. These results were in good agreement with metallography data.

References: [1] E. V. Zhiganova et al. 2005. *Meteoritics & Planetary Science* 40:A174. [2] E. V. Zhiganova et al. *Hyperfine Interactions*. Forthcoming.

5144

SI AND C ISOTOPIC RATIOS IN AGB STARS: SiC GRAIN DATA, MODELS, AND THE GALACTIC EVOLUTION OF THE SI ISOTOPES

E. Zinner¹, L. R. Nittler², R. Gallino^{3, 7}, A. I. Karakas⁴, M. Lugaro⁵, O. Straniero⁶, and J. C. Lattanzio⁷. ¹Washington University, Saint Louis, Missouri 63130, USA. E-mail: ekz@wustl.edu. ²Carnegie Institution of Washington, NW Washington, D.C. 20015, USA. ³Università di Torino, Italy. ⁴McMaster University, Hamilton, Ontario, L8S 4M1, Canada. ⁵University of Utrecht, 3508 TA Utrecht, The Netherlands. ⁶INAF, Osservatorio Astronomico di Teramo, Italy. ⁷Monash University, Victoria 3800, Australia

Presolar grains of the mainstream, Y and Z type are believed to have an origin in carbon stars. We compared the C and Si isotopic ratios of these grains [1] with the results of theoretical models for the envelope compositions of AGB stars. Two sets of models (FRANEC, Monash) use a range of stellar masses (1.5 to 5 M_⊙), metallicities, different prescriptions for mass loss, and two sets of neutron-capture cross-sections for the Si isotopes [2, 3]. They predict that the shifts in Si isotopic ratios and the increase of ¹²C/¹³C in the envelope during third dredge-up are higher for higher stellar mass, lower metallicity, and lower mass loss rate. The Guber et al. [3] cross-sections result in larger shift in the ³⁰Si/²⁸Si ratios and smaller shifts in the ²⁹Si/²⁸Si ratios than the Bao et al. [2] cross-sections. Because the ²²Ne neutron source dominates Si nucleosynthesis, the effect of the ¹³C source is negligible.

Comparison of the model predictions with grain data confirms an AGB origin for mainstream, Y, and Z grains, with the first type coming from stars with solar metallicity [4], the rest from stars with lower-than-solar metallicity [1, 5, 6]. The Si isotopic ratios of the Z grains favor the more recent Guber et al. [3] cross-sections. The ¹²C/¹³C ratios of low-metallicity models are much higher than those found in Z grains and cool bottom processing [7] must be invoked to explain the grains' C isotopic ratios. The high predicted C/O ratios in low-metallicity stars not experiencing this process might have prevented the formation of SiC and led to the condensation of graphite instead [8]. By combining Z grain Si data with the models we determined the evolution of the ²⁹Si/²⁸Si ratios in the Galaxy as function of metallicity Z (Fig. 1). At Z < 0.01 this ratio rises much faster than current Galactic evolution models [9] predict and suggest an early source of the heavy Si isotopes not considered in these models, which are mainly based on type II supernova nucleosynthesis.

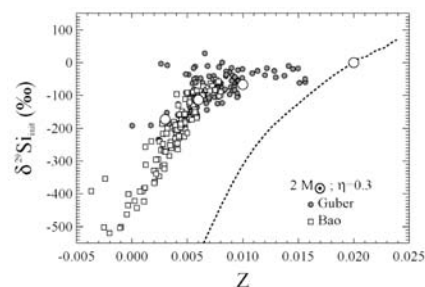


Fig. 1. Predicted evolution of ²⁹Si/²⁸Si as function of metallicity based on Z grains and the FRANEC models of a 2 M_⊙ star with Reimers mass loss η of 0.3 and two sets of Si cross-sections. This evolution is compared with the GCE model of Timmes and Clayton [9] (dotted line). The large open circles are the ratios assumed in our theoretical models.

References: [1] Nittler L. R. and Alexander C. M. O'D. 2003. *Geochimica et Cosmochimica Acta* 67:4961. [2] Bao Z. Y. et al. 2000. *Nucl. Data Tables* 76:70. [3] Guber K. H. et al. 2003. *Physical Review C* 67: 062802-1. [4] Hoppe P. and Ott U. 1997. In *Astrophysical implications of the laboratory study of presolar materials*. New York: AIP. p. 27. [5] Hoppe P. et al. 1997. *The Astrophysical Journal* 487:L101. [6] Amari S. et al. 2001. *The Astrophysical Journal* 546:248. [7] Nollett K. M. et al. 2003. *The Astrophysical Journal* 582:1036. [8] Jadhav M. et al. *New Astronomy Reviews*. Forthcoming. [9] Timmes F. X. and Clayton D. D. 1996. *The Astrophysical Journal* 472:723.

5321

Fe-ISOTOPIC FRACTIONATION IN CB CHONDRITES

J. Zipfel¹ and S. Weyer². ¹Senckenberg Forschungsinstitut und Naturmuseum, Senckenberganlage 25, 60325 Frankfurt am Main, Germany. E-mail: jzipfel@senckenberg.de. ²Institut für Mineralogie, J. W. Goethe-Universität Frankfurt, Germany

Introduction: CB group meteorites share many properties with carbonaceous chondrites, such as presence of refractory inclusions, chondrules or chondrule fragments, high and unfractionated refractory element abundances. Yet some of their properties are unusual: extremely high FeNi-metal abundances, absence of hydrated matrix, and extreme depletions of moderately volatile lithophile and siderophile elements. In addition, chondrules in CB chondrites are ~5 Myr younger than calcium-aluminum-rich inclusions (CAIs) in CV3 chondrites [1, 2], and CAIs and chondrules don't show any evidence for the existence of live ²⁶Al at time of formation [3]. However, ⁵³Mn-⁵³Cr systematics of HaH 237 follows the general trend defined by CI, CM, CO, and CV carbonaceous chondrites and plots on an isochron of ~4568 Myr, which is interpreted to indicate a general event of moderately volatile element loss, e.g. of Mn, at the start of the solar system [4, 5]. The low ⁵³Cr/⁵⁴Cr ratio in HaH 237 is inconsistent with volatile loss 5 Myr later during a separate event, such as vaporization in a giant impact cloud [6].

Evidence for a condensation origin of metal in HaH 237 is provided by chemically zoned metals with fractionated Fe isotopes. In these metals, lighter Fe is concentrated in Ni-rich cores and heavier Fe in Ni-poor rims [7]. Iron isotopes of metal-rich "bulk samples" of HaH 237 and Isheyevo, which both contain zoned metal grains [6], plot on a mass-dependent fractionation line. Isheyevo contains the lightest Fe ($\delta^{56}\text{Fe} = -0.443\text{‰}$) and HaH 237 slightly heavier Fe ($\delta^{56}\text{Fe} = -0.297\text{‰}$), indicating that the fraction of light Fe which is probably sited in metal, is slightly higher in Isheyevo. Gujba does not contain any chemically zoned metal and a large metal aggregate separate that was analyzed has normal Fe isotope composition ($\delta^{56}\text{Fe} = 0.025\text{‰}$) [6]. We have analyzed additional metal and silicate separates of the same meteorites plus samples from Bencubbin. The Fe composition of a second metal-rich Isheyevo sample is identical to our earlier findings. Preliminary data of silicates in Isheyevo have heavier Fe ($\delta^{56}\text{Fe} = -0.032\text{‰}$). A separate of Gujba enriched in fine-grained metal shows significantly lighter Fe compositions ($\delta^{56}\text{Fe} = -0.363\text{‰}$) than the previously analyzed coarse metal aggregate. This Fe isotope composition is similar to that of the HaH 237 and Isheyevo samples and indicates that fine grained metal in Gujba, although being chemically unzoned, must be derived from a source with similar Fe isotope composition.

References: [1] Krot A. N. et al. 2005. *Nature* 436:989–992. [2] Kleine T. et al. 2005. *Geochimica et Cosmochimica Acta* 69:5805–5818. [3] Gounelle M. 2006. Abstract #2014. 37th Lunar and Planetary Science Conference. [4] Shukolyukov A. and Lugmair G. W. 2001. *Meteoritics & Planetary Science* 36:A188–A189. [5] Palme H. 2001. *Philosophical Transactions of the Royal Society of London A* 359:2061–2075. [6] Zipfel J. and Weyer S. 2006. Abstract #1902. 37th Lunar and Planetary Science Conference. [7] Alexander C. M. O'D. and Hewins R. H. 2004. *Meteoritics & Planetary Science* 39:A13.